# Optical Coherence Tomography for Monitoring Plants' Responses to Biotic Stressors

**Ghada Sasi**

**BSc (Hons), MSc, AFHEA**

A thesis submitted in partial fulfilment of the requirements for the degree of

Doctor of Philosophy

The University of Sheffield

School of Mathematical and Physical Sciences

Subject: Bioimaging and Biophotonics

September 2025

**Acknowledgement**

I would like to sincerely thank my dear mother, Zina Omar, for her unwavering support, love, encouragement, and help throughout my life. I am also deeply grateful to my brother, Dr. Walid Sasi, and my sister, Dr. Sahar Sasi, for their support, and care. I deeply miss the presence of my beloved father, Dr. Salem Sasi, whose memory continues to inspire and guide me every day.

I am grateful to the Embassy of Libya and The University of Sheffield for their generous funding.

My heartfelt thanks go to my supervisor, Dr. Adrien Chauvet, Department of Chemistry, University of Sheffield, for his continuous guidance, patience, motivation, and immense knowledge. His invaluable support throughout my PhD studies, research, publications, and thesis writing has been instrumental.

I am also grateful to Professor Stephen Rolf, School of Biosciences, and Professor Stephen Matcher, Electrical and Electronic Engineering (EEE), University of Sheffield, for providing essential materials, scientific guidance, and valuable discussions during our monthly meetings.

I would like to thank the Grantham Centre for Sustainable Futures team for their exceptional training program, which has equipped me with vital skills and knowledge for my future career.

In this academic journey, the guidance, kindness, and belief from all these individuals have been essential to reaching this milestone. Thank you from the bottom of my heart.

## Abstract

This project explores Optical Coherence Tomography (OCT) as a potential new imaging technique to detect early signs of infection in plants. OCT can be applied to deliver cross-sectional and three-dimensional images of plant's microstructures non-invasively, in vivo, and in real-time. This puts forward a very exciting potential methodology for boosting our understanding of plant's response to stressors, plant health, and disease management. OCT traditionally finds wide application in medical imaging, particularly in ophthalmology, to image the retina with high resolution. This research project aims to adapt this technology to the realm of botany. More specifically, the objective is to monitor the response of wheat plants when infected by *septoria*. In this aim, OCT provides detailed images of inner structures without affecting the plant, which enables continuous monitoring without altering the growth and development of the plant. Specifically, the study monitors the response of wheat plants infected by *Septoria*. This project thus corresponds to a proof-of-concept which demonstrate the detection of early signs of infection before any external signs are visible.

The principal strength of OCT lies in its ability to provide detailed internal images without damaging the plant, allowing continuous monitoring of growth and disease progression. This non-invasive capacity is crucial for pathogen detection, which in turn maximizes crop survival and minimizes chemical treatment use. In my study, OCT was benchmarked against advanced techniques such as confocal microscopy, epifluorescence microscopy, and scanning electron microscopy (SEM), alongside manual analysis using FIJI and MATLAB, confirming its reliability.

However, OCT also presents certain limitations. Compared with established imaging methods, its penetration depth in dense plant tissues is limited, which can result in blurry images. In addition, interpretation of OCT images requires specialized expertise and dedicated software to extract meaningful data. In this study, collaboration with a software company enabled the development of customized machine learning based segmentation software. This tool allows rapid, automated OCT image analysis, producing immediate quantitative results and significantly enhancing the efficiency of plant research.

The OCT analyser software, based on machine learning (ML), applies masks to the inner structure of leaves to enable gap thickness measurements and extract meaningful data. However, the current version of the software was trained on only one variety (AxC169). To improve its robustness, it will need to be trained on additional varieties. The gap thickness measurements, whether performed manually or through automated approaches, are provided in this study to ensure availability for other researchers.

Overall, the integration of OCT with ML is highly promising and has the potential to open new opportunities for agricultural applications

## Publications

Copies of the two publications are included in the appendices for reference, and the official published versions can also be accessed online via the following links:

1- Part of Chapter I of this thesis has been published as:

Sasi, G. S., & Chauvet, A. A. P. (2025). Using Optical Coherence Tomography in Plant Biology Research: Review and Prospects. Sensors, 25(8), 2467. https://doi.org/10.3390/s25082467

2- Chapter VI of this thesis has been published as:

Sasi, G.S., Matcher, S.J. & Chauvet, A.A.P. Optical coherence tomography for early detection of crop infection. Plant Methods 21, 92 (2025). https://doi.org/10.1186/s13007-025-01411-7

## Declaration

I, Ghada Salem Youssef Sasi, confirm that this Thesis is my own work. I am aware of the University's Guidance on the Use of Unfair Means (www.sheffield.ac.uk/ssid/unfair-means). This work has not been previously presented for an award at this, or any other university.

## List of Content

**List of Tables**



**List of Figures**

## Abbreviations and Acronyms

| | |
|---|---|
| AHDB | Agriculture and Horticulture Development Board |
| AxC | Avalon and Cadenza variety |
| bOCT | Biospeckle OCT |
| CWS | calcofluor white stain |
| DME | diabetic macular edema |
| dOCT | Dynamic OCT |
| DOPU | Degree of polarization uniformity |
| FD-OCT | Fourier-domain OCT |
| FF-OCT | Full-field OCT |
| GFP | Green Fluorescent Protein |
| GS | Growth Stage |
| HSI | Hyperspectral imaging |
| ISOCT | Inverse Spectroscopic OCT |
| LIF | Laser-induced fluorescence |
| ML | Machine learning |
| MRI | Magnetic resonance imaging |
| NIR | Near-infrared |
| OCT | Optical Coherence Tomography |
| PCR | polymerase chain reaction |
| PDB | Potato Dextrose Broth |
| PS-OCT | Polarization-sensitive OCT |
| R gene | Resistance gene |
| ROI | region of interest |
| SEM | Scanning Electron Microscopy |
| SI | Supplementary Information |
| SLD | Superluminescent diode |
| S-OCT | Spectroscopic OCT |
| SS-OCT | Swept-source OCT |
| STB | Septoria tritici blotch |
| TD-OCT | Time-domain OCT |
| TSP | Total soluble protein |
| UMRAS | Universal multiple angle Raman spectroscopy |
| XCT | X-ray tomography |

## Thesis outline

1. General Objectives

The goal is to use Optical Coherence Tomography (OCT) as a novel imaging tool to provide cross-sectional and three-dimensional monitoring of plant microstructures in vivo, non-invasively, and in real time for the detection of early pathogenic infections.

The project consists of:

1. Selecting adequate crop (i.e. wheat)
2. Growing the selected plant
3. Selecting the appropriate fungus (i.e. *Septoria tritici*)
4. Growing the selected fungus
5. Developing effective inoculation methods
6. Monitoring development of infection using epifluorescence, confocal and SEM microscopy
7. Monitoring progression of infection at various stages (Days 0-14 after inoculation) by performing daily OCT scans using the Lumedica system.
8. Compare OCT data (control and infected leaves) with data obtained from epifluorescence, confocal and SEM microscopy.
9. Perform manual segmentation analysis on OCT data for both control and infected plants at each time point (Days 0-7 after inoculation) using FIJI image software.
10. Perform automated segmentation analysis on OCT data for both control and infected plants at each time point (Days 0–7 after inoculation) using custom software developed specifically for this project.

2. Chapter organization

This thesis is organized into the following chapters:

**Chapters I** provide a general introduction, including a review of relevant literature and the fundamental concepts underlying this research. It includes the general concepts of OCT, a comparison between OCT and alternative imaging techniques used for similar purposes, as well as a description of the selected crop (wheat) and its stressor (*septoria* infection).

**Chapter II** discusses the methodologies employed throughout the thesis. This chapter included a detailed introduction to OCT image calibration using FIJI System software, as well as an

overview of the Lumedica OCT system and the microscopy techniques utilized in the research. It also includes the methodology of plant growth and the inoculation protocol of *Septoria tritici* fungus.

**Chapter III** corresponds to a comparative study between OCT imaging and SEM at different stages of wheat plant development, from germination to seed formation. This analysis illustrates the strengths and limitations of OCT as an imaging tool in botany.

**Chapter IV** corresponds to a comparative study between OCT imaging and SEM at different stages of wheat (variety AxC169) infections by *Zymoseptoria tritici*, causing *Septoria tritici* blotch (STB). This analysis illustrates the strengths and limitations of OCT as an imaging tool in monitoring the development of infection. This study serves as a proof of concept that infection can be related to structural changes within the mesophyll.

**Chapter V** corresponds to a detailed analysis of OCT images taken daily, from day 0 to 7 after inoculation (before any visible signs appear). The analysis is based on manual image segmentation that focusses on the apparent gap thickness as marker of infection. This chapter further explores the potential of automating such an analysis using a bespoke machine learning software.

# Chapter I: Introduction

## 1. OCT: concepts, popularity and advantages

Visualizing the microscopic structure of plants in vivo, non-invasively, and in real-time is the holy grail of botany. Optical coherence tomography (OCT) has all the characteristics necessary to achieve this feat. Indeed, OCT provides volumetric images of the internal structure of plants without the need for histological preparation. With its micrometric resolution, OCT is commonly used in medicine, and in ophthalmology primarily. But its use in the field of botany is seldom. The aim of the present work is thus to review the latest technical development in the field of OCT and to highlight its current use in botany, in order to promote the technique and further advance research in the field of botany.

### a) Coming of age

Optical coherence tomography (OCT) is, at its core, an interferometric imaging technique. One of the first uses of low-coherence interferometry induced by backscattering within soft tissues was by Fercher et al. in the 1980s [1]. In this pioneering work, Fercher et al. succeeded in measuring the optical length of the human eye in vivo. After nearly a decade of technical development, the first OCT setup was demonstrated in 1991 [2-5] by Fujimoto et al. In comparison to Fercher's single-point imaging, OCT provides cross-sectional and three-dimensional imaging of soft tissues while remaining noninvasive [6]. Five years later, the first commercial OCT instrument was launched [7] and was rapidly implemented for healthcare applications. Today, in light of its imaging capabilities and practicality, OCT is routinely used by ophthalmologists to examine patients [8]. However, using OCT imaging as a non-invasive and real-time technique to investigate plants tissue remains rare. Its first use in the field of botany was reported by Sapozhnikova et al. in 2004 [9]. In this work, the team described their ability to directly visualize the dehydration and rehydration dynamics of *Tradescantia pallida* (Rose) leaves. The penetration depth was about 1–2 mm and the spatial resolution was about 15 μm [9]. OCT techniques have, since then, greatly improved in terms of scan rates, contrast, sensitivity, and phase-stability [2, 10]. For example, from an initial~400 axial scans (A-scans) per second [11], OCTs are now commonly running at hundreds of kHz [12], thus improving spatial and time resolution. These improvements in acquisition speed and precision are paving the way for real time functional imaging in all scientific fields.

Time-domain OCT (TD-OCT), which was the first type of system, was using a moving reference mirror to capture images, but it was slow and had limited resolution. Fourier-domain OCT (FD-OCT), which was later developed, instead uses Fourier transformation, thus improving speed and image quality. The development of swept-source OCT (SS-OCT), in particular, further enhanced imaging depth and speed by making use of novel tunable lasers. All these advancements make OCT ready for agricultural applications, such as effective plant health monitoring and food quality assessment [11, 13-15].

b) Concepts and characteristics of OCT

The common feature of OCT systems is their ability to generate non-invasive, high-resolution, depth-resolved images of soft tissue solely by collecting backscattered light [16, 17]. This backscattered light is then made to interfere with a reference light originating from the same initial light source to produce an interferogram, be it a fixed wavelength laser, a swept-source laser, or a superluminescent diode [18]. And since backscattering is the result of a variation in refraction index between differing intrinsic structural components, analysis of the interferogram allows the retrieval of this depth-resolved structural information.

In comparison to the narrow light sources and long coherence lengths typically used in Michelson interferometry [19], OCT benefits from spectrally broadband light sources with low temporal coherence and high spatial coherence, which improves the depth resolution of the resulting images [14]. The sample arm of this low coherence interferometer is often extended via an optic fiber for hand-held applications. This feature enables the OCT systems to be adapted to target samples, which is advantageous for in vivo biological applications.

OCT can be performed either in the time or spectral domain. On the one hand, as introduced earlier, TD-OCT produces tomographic images by oscillating a reference arm mirror of the interferometer to create temporal interferences. On the other hand, Fourier-domain OCT (FD-OCT) generates the spectral interferogram by mixing the broadband backscattered light from the sample with the reference light without changes in the reference arm length [20]. Because the core of FD-OCT is devoid of moving parts and because Fourier analysis of spectral interferogram is fast, the technique has the advantage of being ~100 times faster than TD-OCT [21, 22] while being more robust for in-field applications. The FD-OCT family includes both the Spectral domain OCT (SD-OCT) as well as SS-OCT. While SD-OCT still uses a spectrometer with a dispersive element and a relatively slower detector array, the SS-OCT benefits from an optical source which rapidly sweeps a narrow linewidth over a broad range of wavelengths. In SS-OCT, each wavelength is then detected sequentially during each sweep by a high-speed photodetector.

This technical feat allows SS-OCT to reach hundreds of kHz in image acquisition rates, thus increasing in reliability when monitoring moving objects [23]. Note that when it comes to scanning speed, typical TD- and SD-OCT still requires scanning of either the reference mirror or of the excitation wavelength, respectively, to produce an entire b-scan. This scanning requirement can be bypassed in "single-shot" OCT systems, which can acquire full b-scan at every shot by using a broad light source and a diffracting element to record each wavelength separately and simultaneously via photodetector arrays [24]. However, even if each b-scan is taken virtually instantaneously, the processing of each scan might take up to 140 ms [25].

In terms of image quality, the axial resolution (Z-axis) typically depends on the bandwidth of the OCT light source; the lateral resolution (X-Y plane) is usually given by the numerical aperture of the microscope objective used, as depicted in Figure 1. Resolutions of both axis are typically in the order of 1–10 µm in OCT systems [26, 27]. The sensitivity, on the other hand, is related to a combination of factors, including laser power (typically in the µW range to avoid damaging the tissues), scattering [28, 29] (which can be enhanced with contrast agents), and scanning speed (of up to MHz for FD-OCTs).

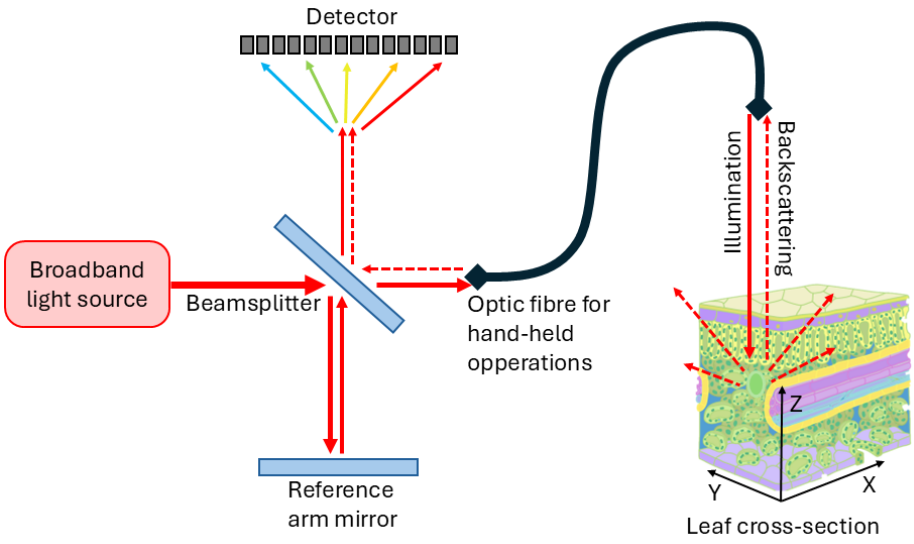


Figure 1: Principle of interferometry with beam propagation through optic fiber for hand-held applications. The sample is scanned laterally (X-Y) through sets of galvanometers.

Overall, OCTs are technically simple, compact, robust, and adaptable to various environments, which make them ideally suitable for biological applications.

c) Popularity of OCT in botany

Owing to its many advantages, OCT has been extensively utilized in the medical field for various health applications and, more specifically, in ophthalmology, cardiology, and dermatology. The widespread adoption of OCT is illustrated by the ever-increasing number of publications pertaining its use in the medical field, numbering in the tens of thousands every year, as shown in Figure 2. In comparison, following the same metric, the use of OCT in botany is about fifty times less prevalent. This wide disparity between the use of OCT in the medical field and in botany is actually surprising given the comparable suitability and potential impact this technique has on both fields.

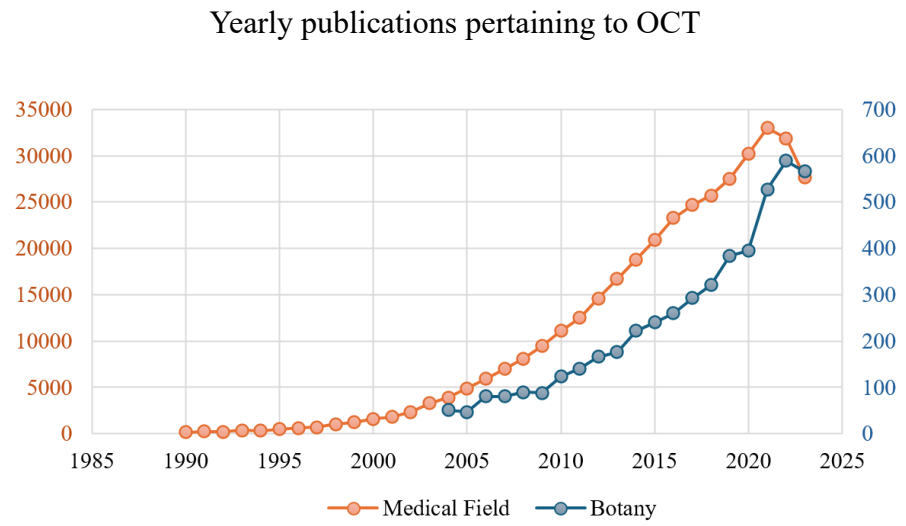


Figure 2: Annual number of OCT-related publications (blue) compared to the number of publications specific to the field of OCT applied to botany (In medical field: using keyword search: "optical coherence tomography" OR medical field. In botany: using keyword search: "optical coherence tomography" botany OR plant OR leaf OR seed OR plant's root).

d) Comparison with alternative techniques

To better appreciate the potentialities of OCT in plant biology research, it is useful to compare it with common imaging techniques that are readily used in the field of study. And beyond the various technical characteristics of each imaging tool, the following discussion also includes practicality and ease of access, which is where OCT's primary strengths reside.

1. High-resolution microscopy [54], and genetic testing, such as polymerase chain reaction (PCR) [30]. These techniques are the most cumbersome given the necessity to process the sample beforehand and the need to access large-scale facilities.
2. RGB Imaging [31], more practical and field-applicable techniques often suffer from lower precision, can be useful for plant health studies but is generally insensitive to early-stage infections [32].

3. The highest resolution technique available is X-ray tomography (XCT). This system provides 3D rendering of the internal structures of plant tissue with nanometric resolution [33, 34]. Samples can be as large as a whole plant (e.g., 40 cm tall), depending on the size of the sample chamber, but it is not field-applicable [35]. Furthermore, high X-ray dose causes ionization, which disrupts and damages the plant [36-38].
4. Hyperspectral imaging (HSI), which includes UV reflectance imaging [39, 40], serves as a non-invasive and efficient tool for studying plants and whole crops. Although such spectroscopic method is in theory diffraction limited, HSI' resolution is typically low given the sensor size and its distance from the object [41]. Although HSI typically has the lowest spatial resolution [42], it is the most practical for field application, offering insights into the health, physiology, and interactions of plants with their environment.
5. Raman microscopy is often used as a convenient and non-invasive way to monitor the presence of specific molecules in tissues. Molecules are categorized by the vibrational signature of their functional groups [43]. For this technique, no sample preparation is needed; it is non-destructive and is highly sensitive, which makes it field applicable. The past decade has seen the development of universal multiple angle Raman spectroscopy (UMRAS) for monitoring functional groups of embedded molecules, thus paving the way for 3D Raman imaging [44, 45]. But to characterize tissues solely based on the functional groups of its constituting molecules is not at all trivial, in addition, difficult to obtain replicate measurements due to weak Scattering [46].
6. Laser-induced fluorescence (LIF) is commonly used, like HSI, to remotely assess whole leaves, plants, and even crops [47]. It allows for real-time imaging and is non-invasive [48]. LIF typically gives information about the presence of chlorophyll via its induced fluorescence [48]. Consequently, LIF is restricted to monitoring chlorophyll and other highly fluorescent molecules within tissues, without revealing direct information about the tissue's internal structure.
7. Magnetic resonance imaging (MRI) is another non-invasive [49], non-destructive imaging technique, which also provides three-dimensional images. It also allows for whole plant investigation [50]. However, MRI has a typical axial resolution of 1.5–2.0 mm [18, 51] and is not field-applicable.
8. Ultrasound imaging is another 3D imaging technique which uses sound instead of radiation. It can be used to investigate plant tissue and water movement within it [52]. Ultrasound imaging benefits from a significantly higher penetration depth compared to OCT, typically up to several centimeters depending on the frequency used. However, it

has lower axial and lateral resolution compared to OCT [53], often around 10 to 100 times lower, ranging from about 50 μm to 500 μm [54] while OCT's axial resolutions typically range from 1 to 15 μm [52-54]. Ultrasounds have been shown to directly affect plants, albeit in a positive way by promoting seed germination, improving nutrient uptake, and increasing useful chemical production. [55].

Hence, in light of the conventionally used imaging techniques, it is understood that OCT represents a powerful compromise between resolution and practicality, bringing 3D imaging into the field for real-time analysis.

## 2. OCT variants

The suitability and potential impact of OCT in the field of botany can be further appreciated by exploring the different types of OCT systems that have already been employed in botany. Benefiting from its technical simplicity (compared to alternative imaging systems) OCT is highly suitable for a range of multimodal imaging techniques:

### a) Polarization-sensitive OCT

Polarization-sensitive OCT (PS-OCT) benefits from the ability of fibrous structures in altering the polarization of light. Because different tissues alter the polarization of light differently, this system provides an added layer of contrast, that of polarization, on top of the typical grey-scale OCT images. For example, it allows differentiation between distinct cellular layers that would otherwise appear as the same grey-shade [56]. More specifically, it measures birefringence, which reflects tissue organization by assessing how light slows differently along specific axes, with the fast axis orientation indicating the preferred direction of light propagation within the tissue, and the degree of polarization uniformity (DOPU) helping identify regions with uniform or disrupted polarization properties.

PS-OCT can be further extended by applying the Mueller matrix method to capture diattenuation, which describes how tissue differentially absorbs or transmits polarized light. This provides additional contrast for distinguishing subtle tissue characteristics [57].

### b) Full-field OCT

Full-field OCT (FF-OCT) is a technique that differs from time-domain and frequency-domain OCT by producing tomographic images without scanning a light beam using galvanometer scanners [58, 59], similar to the "single-shot" OCT system discussed earlier [24, 25]. Instead, the entire sample is illuminated with a light of extremely short coherence. The tomographic

images are thus obtained in the en-face orientation (orthogonal to the optical axis) by a Linnik-type interferometer. Accordingly, full-field OCT is also called en-face OCT or, more commonly, full-field optical coherence microscopy (OCM). The transverse resolution of full-field OCT is similar to that of conventional microscopy (~1 μm) but has the advantage of being non-invasive and not requiring any histological treatments. The axial resolution, determined by the spectral properties of the illumination source, is also of the order of 1 μm [60].

c) Spectroscopic OCT

Spectroscopic OCT (S-OCT) differs from standard OCT by further analyzing the spectrum of the backscattered light [61, 62]. Analogous to the PS-OCT, S-OCT provides additional contrasts which consist of the spectral blue- or red-shift of the backscattered light's maximum amplitude. Accordingly, by monitoring the spectrum of the scattered light, structures that selectively absorb part of the incident light can thus be distinguished.

d) Biospeckle OCT

Biospeckle imaging consists of analyzing the backscattered light from a coherently illuminated object. Typically, for static objects, the backscattered rays interfere with themselves and create a speckle pattern that is unique to the object's surface and internal structure (depending on the penetration depth of the light used). If the objects are biological samples, the flow of their constituent parts (e.g. flow of red blood cells through veins [63]) will generate a continuously evolving speckle pattern called biospeckle. Biospeckle OCT (bOCT) is also known as "dynamic OCT" [64], as well as "OCT angiography" or "optical coherence angiography" [65]. Monitoring biospeckles over time helps assess the level of physiological activity of the sample. Thus, in comparison to OCT, bOCT provides an additional contrast which consists of the physiological activity of the sample.

e) Dynamic OCT

A recent study demonstrates that dynamic OCT (dOCT) is a powerful imaging technique capable of high-contrast, label-free, real-time 3D visualization of plant pathogens, such as fungal hyphae, within living tissues [66]. However, its application in real field is currently limited due to the complexity of data interpretation in plant research. dOCT requires advanced software for image processing and segmentation to extract meaningful insights into the dynamic processes occurring within plant cells and tissues. While dOCT offers improved contrast and the ability to monitor cellular dynamics, traditional OCT remains advantageous in

certain scenarios due to its simplicity, faster data acquisition, and ease of interpretation making it suitable for rapid, large-scale assessments [64, 66].

f) Inverse Spectroscopic OCT

In this variant of OCT, the signals are further analyzed to extract depth-dependent absorption and scattering parameters [67]. Indeed, attenuation in OCT describes the weakening of the light signal as it passes through tissue, caused by both absorption and scattering. The more attenuation there is, the weaker the OCT signal becomes, which can affect the clarity and quality of the resulting images [68]. Thus, by monitoring the changes in scattering intensities, it then becomes possible to infer about the concentration and size of the scattering particles at various depths.

While many more types of OCT are currently employed in healthcare, the few that have been selected here are among those that have been demonstrated in botany in only the last decades, showing that the field is fast developing.

## 3. Use of OCT in botany

As already alluded to, the use of OCT in ophthalmology has grown to the point where it is now an indispensable tool in the field. But OCT's abilities to investigate in real-time soft tissues without histological preparations, and without incurring radiation damages, are equally suited for botany. Plants, like skin and retinae, are comprised of soft tissues that can be subject to the exact same type of investigations, as demonstrated subsequently.

a) OCT for non-invasive investigation of crops

Because OCT uses scattered light to probe the internal structure of tissues, the depth and overall quality of the images depend on the type of tissues investigated. For example, while OCT can image the whole cross section of a soft *Arabidopsis* leaf [69-71], the same equipment is barely able to image the first cell layer of a sturdy tomato leaf due to insufficient light penetration [72]. Indeed, the denser the sample, the greater the absorption and the less scattered light is collected from the sample's internal structures. This phenomena is illustrated in J.C. Clements' work on thick lupin seeds [73]. In this study, although OCT was used to distinguish between different species by looking at differences in hull thicknesses, as shown in Figure 3, the penetration depth was limited to ~200 μm with no discernable structural element within specific layers.

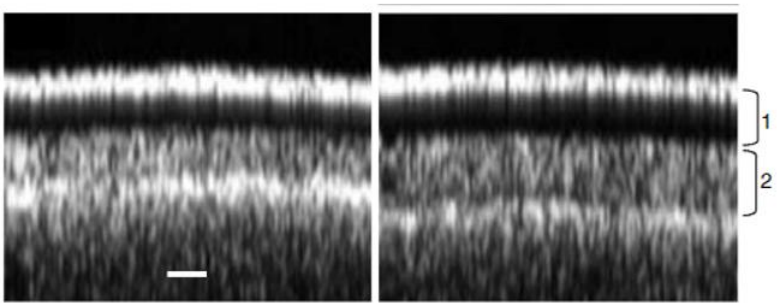


Figure 3: OCT images show the layers of lupin seed (1) is the first palisade layer. (2) is the second palisade layer. The scale bar is 50 μm. Figures were adapted from [73].

On the other hand, water-rich samples, such as onions [74], kiwi, and orange fruits, [71] allow the visualization of individual vacuoles up to 1 mm under the surface, as depicted in Figure 4. It is, however, important to note that penetration depth within tissues is wavelength dependent. But overall, near-IR is ideally suited for plant investigations [75].

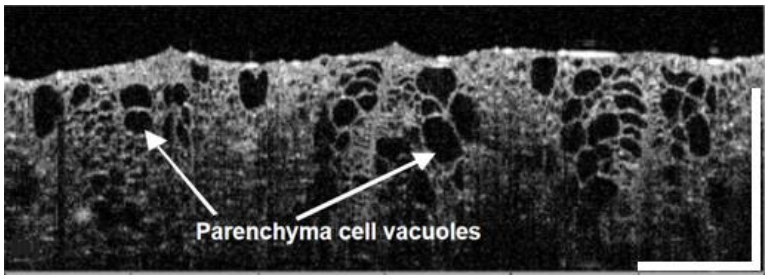


Figure 4: An OCT image of the kiwifruit parenchyma cell vacuoles. Figure adapted from [71]. Scale bars are 1 mm.

In another example, OCM has been used to investigate the wax layer of apple [76] and the soft Arabidopsis plant [77]. Along with the vacuoles, OCT was successful in visualizing other subcellular structures such as the trichomes' nuclei and organelles. OCT was similarly successful in distinguishing distinct stages in the senescence of leaves by monitoring texture changes at differing yellowing stages [78].

Although dense samples typically yield limited imaging depth, complementary image processing can help circumvent the limited resolution and extract additional information such as particle size and concentrations. For example, ISOCT has been used to estimate depth-resolved concentrations of chlorophylls in corals [79].

Overall, by providing details of internal structures, OCT has been demonstrated to be a fast and reliable tool to investigate and differentiate between crop types.

b) OCT to study plant's responses to biotic stresses

Although OCT's typical micrometric resolution does not allow for direct visualization of fungi, it can still be used to differentiate between infected and non-infected crops whenever the infection alters the plant's overall internal structure. For example, OCT has been used to study the morphological changes in response to Anthracnose [80], a fungal disease that typically causes dark lesions on leaves [81]. It has been used to follow the development of a progressive rind breakdown disorder in 'Nules clementine' mandarin [69-71] via the progressive collapse of oil glands. Similarly, OCT has been used to detect pathological infections such as *Venturianashicola*, which causes pear scab disease [82-84]. It has also been used to investigate the gray leaf spot disease in *Capsicum annuum* leaves [85], to diagnose *marssonina* blotch disease in apple leave [86], to detect melon seeds infected with the Cucumber green mottle mosaic virus [87, 88], to investigate fungal (*Botrytis allii*) and bacterial (*Pseudomonas* sp.) infection in onions [86, 89], to detect Anthracnose fungus-infected tomato seeds [90], to investigate virus-infected orchid plant leaves [91, 92], and to detect defects and rot in onions [84, 89]. Considering these various applications, OCT has demonstrated to be an ideal diagnostic tool for the quality control of crops, allowing for early treatment and reducing waste. While OCT does not directly identify the exact pathogen, it can detect structural changes in tissues caused by infection, including tissue degradation, swelling, or abnormal patterns.

c) OCT to study plant's responses to abiotic stress

Beyond the visualization of plants' morphological changes induced by infections, OCT can effectively monitor the effects of environmental changes, as these abiotic stresses can alter cell structure, tissue thickness, and water content. For example, OCT was used to study the effect of drought and rehydration on leaf morphology [93], as well as to study the effect of ozone stress on Chinese chives (*Allium tuberosum*) leaves [94]. Similarly, the advantages of OCT over more advanced techniques, such as confocal microscopy and micro-CT, were further demonstrated while monitoring the effects of preharvest fertilization treatments and of fruit storage on fruits such as apples [95] and kiwi [96].

These last examples illustrate that OCT is also suited to studying the effects of environmental factors incurred through urbanization and industrialization.

d) OCT for investigation of live responses

Since OCT measurements are non-invasive, successive measurements can be performed at the same location without altering the plant's metabolism and physiological functions. This

characteristic enables the investigation of time-resolved dynamics of structural changes within a specific section of the plant. And given the fast acquisition speed of OCT, the time lapse between measurements can be easily adjusted to the process under investigation.

In this manner, the internal changes induced by the rotting of apples could be followed over the course of 25 days [84]. The spread of rot was evidenced by a gradual increase of the infected region in a lateral direction and a gradual disappearance of the cuticle, wax, epidermis, and hypodermal layers. In another instance, OCT was successfully used to monitor the emergence of roots from switchgrass seeds over a lap of 21 h [97, 98]. Similarly, the effect of ozone on the internal cell structure of Chinese chives leaves was investigated via bOCT [99, 100]. The technique was effective in distinguishing changes only a few hours after ozone exposure.

In faster timescales, OCT was also used to monitor modifications in the distribution and structure of chloroplasts in tobacco, only minutes after inoculation of the bacterial elicitor harpin protein [101].

Finally, through continuous monitoring, OCT was used to investigate signaling mechanisms in real time. It was then possible to follow the propagation of slow wave potential, induced by laser burn, across a young tomato plant [102] .

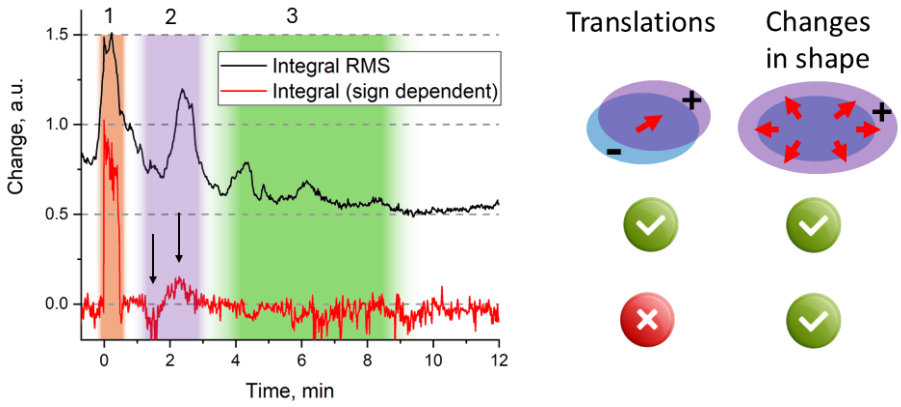


Figure 5: Time-resolved integrated A-scans difference image of a tomato leaf after laser burn. The red curve represents the integral accounting for changes in sign (normalized), while the black curve indicates the magnitude of the squared root of the integral (normalized and adjusted vertically for clarity). Each integral corresponds to specific cellular changes depicted to the right. The feature observed between 0 and 0.5 min is partially attributed to light scattering caused by a 30 s wounding laser pulse (zone 1). The shaded purple area (zone 2, black arrows) denotes the anticipated changes in the shape of the adjacent leaf. The shaded green area (zone 3) denotes the translational relaxation of the leaf. Adapted from [102].

## 4. The prospects of OCT in botany

Although the vast majority of research involving OCT still pertains to the medical field, this brief review demonstrates the suitability of OCT in botany as well. In comparison to current imaging tools, OCT suffers from a resolution which seems limited to ~1 µm, regardless of the

equipment type. The technique, however, hugely benefits from its simplicity, real-time acquisition, and non-invasiveness. OCT is thus prone to develop in research fields that require site-specific, systematic and/or real-time monitoring. As such, OCT is ideal for systematic screening of fruits and vegetables for quality control purposes. It is also ideally suited for real-time monitoring of responses to biotic and abiotic stresses. It is noted that across the board, the quality of OCT images is often speckled, which is a common issue in coherence-based imaging techniques [103]. Fortunately, with the advent of machine learning algorithms, while speckle noise can be treated directly [104], further qualitative information can be more efficiently and effectively extracted by automated image processing such as registration and segmentation [105]. Given the simplicity and robustness of the equipment, it is a matter of time until OCT is applied for field experiments and finds its place in a farmer's toolbox for direct crop screening. Hand-held OCT are currently being developed [97, 98, 106]. The impact of a portable OCT is huge and is attracting attention, as illustrated by the funding of projects aimed at its development. However, adoption by farmers will depend on cost, ease of use, and proven benefits. Devices must also be durable and fit seamlessly into existing farm practices [107], even if the vast majority of these projects are still dedicated to clinical purposes.

## 5. Wheat and STB

This chapter provides an overview of the biological and agricultural context relevant to research on *Septoria tritici* blotch (STB) in wheat. It is divided into two main parts. The first part introduces the wheat crop, including its global significance, growth stages (with a focus on the Zadoks system), leaf structure, and the specific wheat varieties used in the experiments. The second part focuses on STB, detailing its impact on wheat, life cycle, genetic variability, and morphological characteristics. Additionally, different plant pathology visualization techniques are compared, with particular emphasis on OCT. The chapter concludes with a summary of the key points that establish the context for the following chapters.

### 1. Wheat

#### a) Global impact

Wheat is cultivated in about 122 countries, with China, India, and the USA being major producers [108-110]. In the UK, wheat constitutes 58% of crops grown and yields approximately 15 million tons annually [111-113]. Its rich nutritional content makes it a key source of protein, carbohydrates, and fibers, forming the basis of foods like bread, pastries, and pasta [109, 114-117]. Wheat is, however, vulnerable to various diseases amongst which the

most potent are the wheat blast, *Fusarium* Head Blight, *Zymoseptoria tritici*, rusts, powdery mildew, and various root diseases [118-121]. The latter especially is a devastating fungus which can cause up to 40% yield loss in wheat crops [122]. *Septoria* is thus a major concern for agriculture in the UK and Europe. Furthermore, this fungus propagates rapidly under favorable humid conditions, which is specifically relevant to the UK and continental Europe. Global efforts to help farmers anticipate *Septoria* outbreaks are being actively developed. These measures focus on both prophylactic and curative strategies. For example, Agriculture and Horticulture Development Board (AHDB) [123] and UK Crop Science [124], which conducts thorough research on *Septoria*, already provides with clear guidelines on how to prevent and how to treat *Septoria* outbreak. Such outbreaks is commonly controlled using fungicides[121]. However, the key to successful fungicide treatment is the timeliness of the treatment. Delaying the treatments until external symptoms are visible can significantly decrease their efficacy [125]. Yield recovery may be limited to 10–30% compared to preventative treatment, which can save up to 70–90% of potential yield [126-128]. With respect to preventive treatments, it has been shown that triazole-based products, for example, are sustainable and effective when applied before infection. But the overuse of such prophylactic strategies nevertheless results in a decline in treatments efficacy from 90% to 60% [127]. It thus becomes crucial to detect and treat the infection as early as possible so as to limit the overuse of fungicides [129].

b) Classification of wheat developmental stages

Following the Agriculture and Horticulture Development Board (AHDB) wheat growth guide and the Wheat Training website [130], there are four types of staging systems:

- **Zadoks**: Provides detailed, two-digit coding for growth stages (e.g., GS00–GS99).
- **Haun**: Focuses on leaf production.
- **Feekes-Large**: Identifies main stages but lacks detailed subdivisions.
- **Waddington**: Covers spike development in barley and wheat, especially before the opening of a flower.

Understanding these stages, as summarized in Table 1, is crucial for effective timing of treatments like fertilizer, pesticides, and irrigation. The GS (Growth Stage) numbers refer to stages within the Zadoks Growth Scale, a system used to describe the development of cereal crops like wheat. This scale provides a two-digit code to specify each growth stage, The first

digit (0–9) represents the main growth stage (e.g., germination, tillering, heading). The second digit provides subdivisions of that stage, offering a more precise indication of the plant's progress within each main stage. For example: GS00: Dry seed (start of germination stage), GS99: harvestable stage. This coding system helps researchers and agronomists identify exact stages for optimal crop management activities.

Table 1: Summary with key notes about the main wheat growth stages and staging systems according to Zadoks system.

| **Growth Stage** | **Description** | **Key Points** |
|---|---|---|
| GS00–GS19 | Germination and Seedling Growth starts with the dry kernel's germination (kernel is individual grain or seed) and proceeds to leaf formation | Emergence date is when 50% of seedlings appear. Sowing depth and seed viability impact successful emergence. |
| GS20–GS29 | Lateral shoots (tillers) grow from the plant base | Tillers affect yield potential; ear development and stem elongation also begin here. |
| Stem Elongation (GS30–GS39)<br>Booting (GS40–GS49)<br>Heading (GS50–GS59) | Final spikelet formation, stem elongates, flag leaf emerges, and the ear is pushed through the flag leaf sheath | Terminal Spikelet: labour-intensive to identify.<br>Heading Date: measured when 50% of spikes emerge from the sheath. |
| Flowering (GS60–GS69) | Anthers release pollen; a gradient in flowering across the spike is common | Highly sensitive to temperature; flowering time varies along the spike. |
| Milk and Dough Development (GS70–GS89) | Early kernel formation (milk stage), followed by rapid kernel size and dry weight increase (dough stage) | Hard dough stage is physiological maturity; kernels reach 30% moisture. |
| Ripening (GS90–GS99) | Kernel moisture decreases to 13–14%, suitable for harvest | Marks the final growth stage for harvest readiness. |
| Generation Times in Greenhouse | Varies by wheat type: winter wheat takes 6–8 months, spring varieties need 3–4 months | Vernalization required for winter wheat; "speed breeding" can accelerate growth using extended daylight. |

The elongation phase in wheat plants, also known as stem elongation GS 31 in the Zadoks system, is a specific growth stage in cereal crops, particularly wheat. During this phase, the plant begins to grow taller as the stem elongates [131]. It is a critical stage because the crop is susceptible to diseases such as STB [132]. It is important to note that monocots are sometimes referred to as seed leaves, as they are part of the seed or embryo of the plant. However, the subsequent leaves, known as true leaves, begin developing later and play a role in photosynthesis [133].

There are various strategies to inoculate plants with fungus, such as smearing it on leaves or spraying. Since *Septoria* spreads through the air [124], spraying is a suitable inoculation method. In this case, the second newest leaves were selected for the inoculation.

c) General structure of a plant leaf

In summary, plant leaves contain two layers which known as photosynthetic tissue: the palisade and spongy mesophyll. While the palisade mesophyll comprises of tightly packed columnar cells, the structure of the spongy mesophyll remains less defined and is frequently regarded as a random assembly of irregularly shaped cells [134].

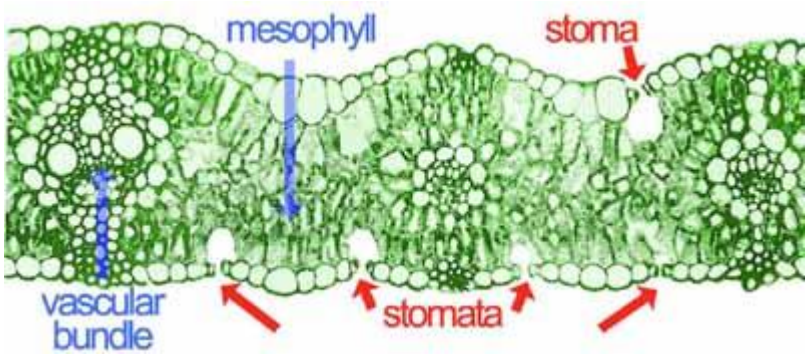


Figure 6: The figure shows the structure (cross-section) of wheat leaf. Figure adapted from [135]

The development of wheat plant trichomes, small hair-like structures on the plant surface, begins in the early stages of the plant's life cycle but not during the embryonic stage. Trichome formation occurs later as the plant matures and responds to environmental factors such as light, temperature, and stress. Increased light exposure, for example, can lead to greater trichome size and density, as trichomes help shield the plant from harmful UV radiation [136-140]. Moreover, trichome characteristics can act as stress indicators, with their size and density reflecting environmental conditions [141]. However, excessive stress may negatively impact plant leaf health.

d) Wheat varieties

There are different wheat types, e.g., AABBDD bread wheat and AABB durum wheat. Within these types, varieties such as Avalon (A) and Cadenza (C) differ in susceptibility to *Septoria tritici*, with Avalon being relatively more susceptible and Cadenza carrying resistance traits. Researchers aim to improve wheat resistance to *Septoria* by crossing Avalon (susceptible) with Cadenza (resistant) to create the Avalon × Cadenza (AxC) mapping population [142]. Hundreds of varieties are cultivated in the UK, including AxC22, AxC53, AxC169, and AxC157 [143, 144]

2. *Septoria tritici* blotch STB

a) Impact and classification of STB

*Septoria tritici* blotch STB is a disease caused by fungus and one of the most devastating foliar diseases of wheat in the European Union [145] and causes major damage to UK winter and spring wheat [122].

The pathogen was first described as the causal agent of *Septoria tritici* blotch (STB) in 1842 by Desmazieres [146] and later classified as *Mycosphaerella graminicola* (Fuckel) J. Schröt. It was first recorded in New Zealand in 1927 by Cunningham [147]. Initially considered less important, its significance increased in 1948 when a rise in the spread of lesions on both upper and lower leaf surfaces was observed. These lesions appeared as areas covered with golden-brown to black spots on wheat crops. Since 1953, the disease has been widespread each year, particularly during periods of cool, wet weather. It has since become common globally and is of considerable economic importance in many countries [147].

Wheat is deeply affected by abiotic stress such as the ones induced by climate change [148, 149] and affected by biotic stress such as fungus [150]. It is typically the most common disease affecting wheat [118, 151]. This study will focus on the biotic stressor *Septoria.*

The germination of *Septoria* occurs in two steps:

- *Asexual Reproduction or formation of spores*

STB is characterized by the production of conidia-fungal spores at the tip of hyphae, within pycnidia-fruiting bodies, due to asexual sporulation, that is, the process or formation of spores [152].

- *Sexual Reproduction*

These fruiting bodies or asci are dark brown and about 68-114 µm in diameter. The asci containing ascospores are approximately 11-14 x 30-40 µm and develop within lesions [146]. The fungus has a mating system for producing fruiting bodies that would develop beneath the host's epidermis. Spore germination typically occurs within 12 hours of contacting a leaf when humidity levels are high [146]. Both sexual (ascospores) and asexual (conidia) spores can germinate on the leaf surface, independent of the wheat plant’s resistance or susceptibility. The symptoms show up, more commonly in leaves, within two to three weeks of infection in the

form of yellow spots that turn brown [153, 154]. This can, in subsequent time, lead to necrosis of leaves and of the whole plant, which causes a huge loss in yield annually [151, 155].

b) *Septoria tritici* life cycle

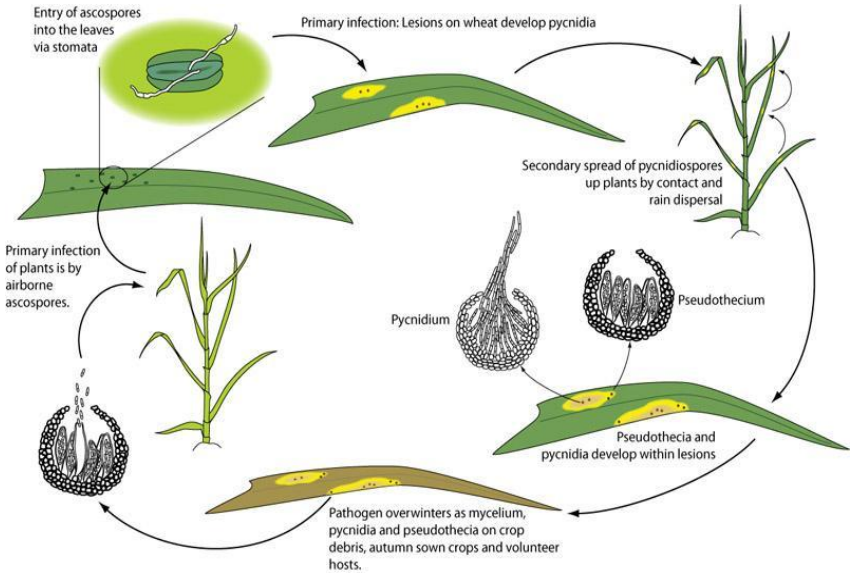


Figure 7: Disease cycle of *Septoria* in wheat. This figure adapted from [156].

*Septoria tritici* is classified as Ascomycota or as septate fungi. Septate means that the hyphae are divided into cells and all septa has little spores [157].

According to [158], the *Septoria* fungus cell structure consists of 1. Hyphae, which branch out in all directions to secrete enzymes to break down organic matter and then absorb small molecules formed. 2. Septum: or a wall between individual cells. It is very vital in the compartmentalization of the cells and thus facilitates damage control and selective transport of organelles and nutrients from one cell to another without interfering with the integrity of the cells. Each *Septoria* spore typically has 3-7 indistinct septa and *Septoria* size measures approximately 2.6 x 62.5 µm. All septa can be carried by the wind, moving from one plant to another, from one crop to the next. The initial symptoms which are characterized by necrotic spots of STB on the leaves can be seen after seedlings or the young leaves of wheat were infected. 3. Vacuole: that plays an important role in storing nutrients and waste products.

The life cycle of *Septoria* was discussed by [156, 159], the damp and moist conditions of the UK provide an ideal breeding ground for STB. In such conditions, STB spores germinate and form a germ tube (~2 µm in diameter [160]) which penetrates the interior leaf through stomata.

Following detection of pathogen, the plant's immune response and cell death mechanisms developed, enabling the hyphae to grow within the plant tissue [161]. Spore germination occurs after at least 20 hours of high relative humidity (Figure 8).

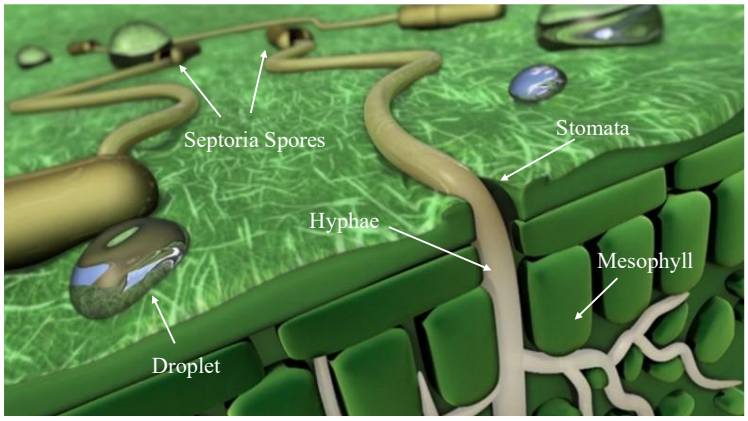


Figure 8: The diagram shows the extent of *Septoria* within the mesophyll. Captured image from [*Septoria* Life Cycle], YouTube channel [162].

After 24-48 hours of pathogen attachment, the fungus grows in the spaces between the mesophyll cells. During this time, the disease is not visible to the naked eye, and the young plant still looks green and healthy. Macroscopic disease symptoms generally do not appear until 7–12 days after the pathogen inoculation. Within the leaf, the fungal mycelium is developing (i.e. the vegetative part of a fungus that consists of branching called thread-like hyphae).

After 2–8 days of contact, the hyphae extend within the mesophyll tissue and acquire nutrients from the plant apoplast. During this biotrophic phase, the infection is typically symptomless, as the host cells remain largely intact. The mesophyll cells begin to die rapidly, and visible symptoms (yellow lesions) usually appear around 11–18 days after infection. The next phase of the infection cycle is referred to as “necrotrophic”, in which extensive cell death and tissue necrosis occur, contrasting with the earlier symptomless biotrophic stage.

14-28 days after inoculation, we monitor the formation of pycnidia with conidia in substomatal cavities of senescent tissue. As they remove water, the spores swell. In dry weather conditions, the surrounding tissues shrink at a faster rate than the developing spores, which forces them to move from pycnidia onto the surface of decaying leaves. The impact of further rainfall causes the spores to break up and spread. The spores are thus carried in the rain and splashed onto other leaves in the surrounding crops, and the cycle begins again.

As described, the first symptoms of infection are typically noticed when the plant is already in chlorotic stage, the yellow spots on the leaf tissue, due to the pathogen's effect on the plant's ability to produce chlorophyll, which is needed for photosynthesis [163]. This stage is very critical for the early diagnosis and effective management of STB. STB identification through chlorosis and its management will avoid or minimize huge damage to wheat crops from the attacking disease.

The necrotic stage (i.e. dying) occurs when the following generation of spores started spreading. Ideally, we need a technique that allows detection of the infection before the plant has reached this critical stage. It is possible to visualize the first steps of infection using conventional light, fluorescent and confocal microscopies, but none of these are suitable as they are destructive. The goal is thus to evaluate if OCT, which is adaptable for field measurement, can also be used for early detection of infection.

c) Resistance gene (*R* gene) in wheat plants

Most wheat varieties have only partial resistance to STB, which means they can still be infected but the disease develops more slowly [113, 164]. Some cultivars, like Cadenza, carry the Stb6 gene, which provides strong resistance against certain isolates of *Zymoseptoria tritici*, such as IPO323 [165]. Studies have shown that many European cultivated varieties remain partially susceptible to STB [166]. This allows for fast evolution and adaptation of the pathogen to new environmental and agricultural conditions, such as use of fungicides [167]. Therefore, within a short period, the pathogen would develop resistance to commonly used fungicides and develop high resistance to partial resistance that some wheat cultivars may possess.

d) Genetic drift in *Septoria tritici*

Many studies [168-170] have shown that *Z. tritici* expresses a high level of genetic variability. This variability has been partly attributed to genetic drift and frequent chromosomal rearrangements [171]. Genetic drift is defined as the random change in the frequency of alleles in a population over generations [172]. It thus occurs in small populations or when the effective population size has become small through sub-culturing. Further, chromosomal alterations like chromosomal translocations, duplication and deletions increase genetic diversity, hence fitness of the pathogen [173, 174].

In the laboratory, genetic drift could result in the loss of pathogenic traits. Genetic drift is one of the mechanisms of evolution involving random changes in the frequency of alleles in a

population [142]. These alleles would be lost by pure chance in successive generations if there was no selective pressure (cultured on artificial media) to retain pathogenicity factors, and storing inoculum in anoxic conditions [175]. too much subculturing generally results in loss of pathogenicity.

Therefore, every experiment must be initiated from fresh frozen stock derived from a bank of frozen isolates to the extent possible [176], in order to maintain the genetic integrity of the strain for its full pathogenic potential. This minimizes the effects resulting from genetic drift and chromosomal changes that may have occurred from repeated subculturing.

e) Morphology and Microscopic Review of *Septoria tritici*

Many literatures reviews [123, 177, 178] illustrated the appearance of *Septoria* in liquid culture media (Figure 9, A), and the *Septoria* pathogens symptoms in the wheat plant in the later stage of infection (Figure 9, B). Additionally, Microscopic images (Figure 10) illustrate the appearance of *Septoria* fungus within infected leaves.

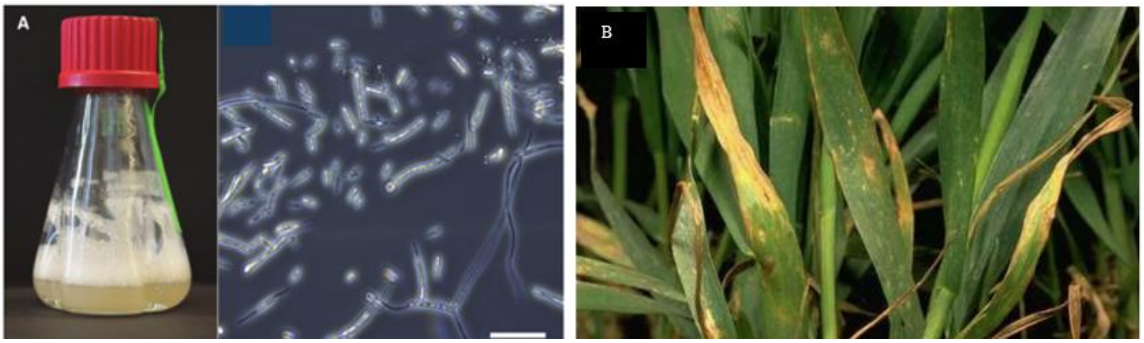


Figure 9: Shows (A) the appearance of *Septoria* in culture media. Figure adapted from [146]. (B) symptoms and signs of wheat leaves infected with *Septoria tritici* in early season infection. Figure adapted from [124].

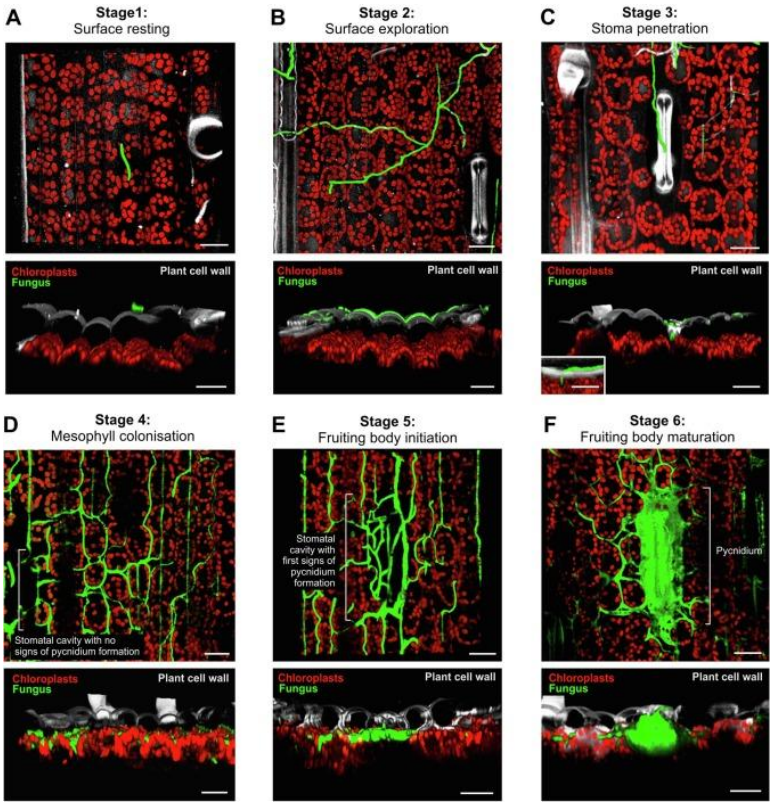


Figure 10: Confocal image stacks of infection process of *Septoria tritici* at different stages in wheat plants. The plants' epidermis (grey) and chloroplasts (red) are detected by their auto-fluorescence. The green fluorescence is an effect of cytoplasmic eGFP expression in the cells of the fungus. Scale bars: 20 µm. Figure adapted from [179]. (A) Stage 1, "Surface Resting": Spores settle on the surface of leaves. (B) Stage 2, "Surface Exploration": Spores form an infectious hypha to infect leaves through stomata. (C) Stage 3, "Stoma Penetration": Penetration of the host by the hyphae through the stomata apertures. (D) Stage 4, "Mesophyll Colonization": Colonization of mesophyll by fungus, but with no visible symptoms of infection. (E) Stage 5, "Fruiting Body Initiation": The hyphae grow and fills the inner space. This is a necrotrophic phase, where signs of infection on the leaf can be seen. (F) Stage 6, "Fruiting Body Maturation": The substomatal cavity fills with filaments, fruiting body, and pycnidium, to initiate spore production.

After colonizing the whole leaf, STB grows into fruiting bodies (pycnidia), through an asexual sporulation, to give fungal spores at the tip of hyphae (conidia) [152]. The symptoms, e.g. yellow spots that turn brown, usually appear on the leaves within two to three weeks only after infection [153, 154]. It is the subsequent necrosis of the leaves and of the plant that causes significant yield loss every year [155].

It is important to note that the defined stages coexist [179]. Since a single hyphae penetration (stage 3) suffice to initiate colonisation of the mesophyll (stage 4), it is expected that surface exploration (stage 2) of the majority of the hyphae, that have not yet "found" stomata to enter, progresses concomitantly with the first colonisation event.

The table below (Table 2) presents examples of methods with specified areas of application, outlining their advantages and disadvantages, and compares these techniques with the OCT imaging system in the field of plant research.

Table 2: Comparison of visualization methods for plant pathology with OCT.

| Method | Sample Preparation | Live Imaging | 3D | Specificity/ Sensitivity | Advantages | Disadvantages |
|---|---|---|---|---|---|---|
| Optical Coherence Tomography (OCT) | Minimal | Yes | Yes | Moderate | In vivo imaging, and non-invasive technique [23]. | Cost: Moderate to high. Limited contrast in some samples [180]. |
| Traditional Clearing and Staining | Extensive | No | No | Moderate | Simple and low-cost [181] | -Potential sample distortion due to hazardous chemicals and reagents.<br>-Lack of specificity in staining. |
| Antibodies with Confocal Microscopy | Extensive | Yes | Yes | High | High specificity and sensitivity [182] | -Cost: High.<br>-Photobleaching [183]. |
| Cell *Septoria* with Confocal Microscopy | Moderate | Yes | Yes | High | Detailed fungal morphology [184]. | Cost: High<br>Confocal microscopy often requires staining and clearing procedures, in addition to slow scanning process. |
| Freeze Fracture with SEM | Very Extensive | No | Maybe | High | Ultrastructural details [185]. | Cost: High<br>The process of freeze fracturing and SEM imaging requires skilled expertise. |
| Light Sheet Microscopy | Moderate | Yes | Yes | Moderate | Rapid volumetric imaging [186]. | -Cost: Moderate.<br>-The process of using light from both sides is tricky because the lights never fully match, and the image quality is not as good as when using light from just one side [187]. |
| Genetic Modification (GM) with Confocal Microscopy | Extensive (GM Development) | Yes | Yes | High | Increased crop yields.<br>Resistance to pathogens [188-190]. | -Cost: very high<br>-Cancer, allergy, and toxic for insects [191].<br>-Confocal has slow scanning process. |

Table 2 compares several visualization techniques used in plant pathology research, highlighting their specific applications, strengths, and limitations. OCT stands out for its ability to provide high-resolution, cross-sectional images of plant tissues in a non-invasive and label-free manner. Unlike traditional clearing and staining methods, OCT does not require sample destruction or time-consuming preparation. While confocal microscopy techniques (with or

without antibodies or genetic modification) offer excellent cellular and subcellular resolution, they typically require fluorescent labeling. Freeze fracture with scanning electron microscopy (SEM) delivers ultrastructural detail but involves complex and destructive sample processing. Light sheet microscopy provides fast imaging of large volumes but may still involve clearing and labeling steps. In contrast, OCT enables real-time imaging of intact tissues, making it especially advantageous for longitudinal studies. However, OCT's limitations include relatively lower resolution at the cellular level compared to confocal or electron microscopy. Despite these constraints, its speed, minimal invasiveness, and ability to monitor dynamic changes make OCT a powerful complementary tool in plant pathology research.

## 3. Conclusion

Wheat is one of the most vital staple crops worldwide, serving as an essential source of nutrition for billions of people and playing a critical role in global food security. However, its productivity is increasingly threatened by fungal diseases such as *Septoria tritici* blotch, which can cause substantial yield losses. As the global population continues to rise and climate change accelerates the spread and severity of plant diseases, the development of effective and sustainable methods for early detection and management of *Septoria* outbreaks becomes increasingly important.

To address this challenge, OCT is proposed as a novel imaging tool for non-invasive, in vivo, real-time monitoring of plant microstructures. This technique enables cross-sectional and three-dimensional visualization of internal plant tissues, with the potential to detect fungal spores before visible symptoms appear. By gaining insights into the early stages of infection, OCT may provide a valuable means of monitoring disease progression. Following proof-of-concept validation, the aim is to evaluate the technique's feasibility for field application, contributing to more effective disease management and enhanced crop sustainability.

## Chapter II: Material and methods

This section provides with technical characteristics of the various visualization methods employed in this study, as well as the methods of sample preparation.

1. Optical Coherence Tomography (OCT)

This section will discuss the use of OCT in plant research, with a specific focus on its application for the early detection of plant infections. The Lumedica OQ LabScope OCT imaging system (version 2.0) is utilized in this research and will be described in detail.

As mentioned, OCT is based on the principle of low-coherence interferometry, which utilizes light with a short coherence length to generate high-resolution cross-sectional images. Broadband light sources, such as superluminescent diodes (SLDs), are commonly used to achieve the low coherence length necessary for high axial resolution [192]. OCT systems often use near-infrared (NIR) light, typically within a wavelength range of 850–1050 nm [23].

OCT systems are used to generate either A-scan or B-scan. For A-scans, is single dimension. B-scans is two dimension and correspond to a XY-2D cross section of the sample, and all OCT systems can generate C-scan which it corresponds to a 3D volumetric representation of the sample [193].


Figure 11: Picture of the Lumedica OQ LabScope OCT imaging (version 2.0).

The OQ Labscope 2.0 from Lumedica is a low-cost, designed for research and industrial use. It is currently located in the university's central annexe, G 19 (adjacent to where the plant is grown). The Lumedica OQ Labscope version 2.0 is an FD-OCT system, as it offers much faster image acquisition than TD-OCT [194, 195], allowing it to capture 13,000 lines per second, which is critical for producing high-resolution, depth-resolved imaging scans with minimal

artefacts [196]. According to the company's user manual [197], OCT system generates 512 x 512 pixel images, with axial resolution of 5-7 µm and an imaging depth of 2-2.8 mm, and a lateral resolution of 15 µm. The light source is a superluminescent diode (SLD) with central wavelength 840 nm.

Volumetric images (7x5x5mm) are generated by default up to 512 B-scans, each separated by 9.78 µm. The scanner can either be handheld or mounted into a stand.

The OCT imaging system was modified to better accommodate live plant leaves. The resolution of the current Lumedica OCT system is suitable for investigating *Septoria* hyphae as they penetrate and extend within the mesophyll prior to necrosis and leaf decay. This setup included a scanner stand consisting of a base, a glass plate positioned on the base to support the leaf, and a vertical stage with adjustable travel to enable precise positioning. Additionally, a scanner holder was used instead of manual operation to minimize motion artifacts and ensure image stability (Figure 12).

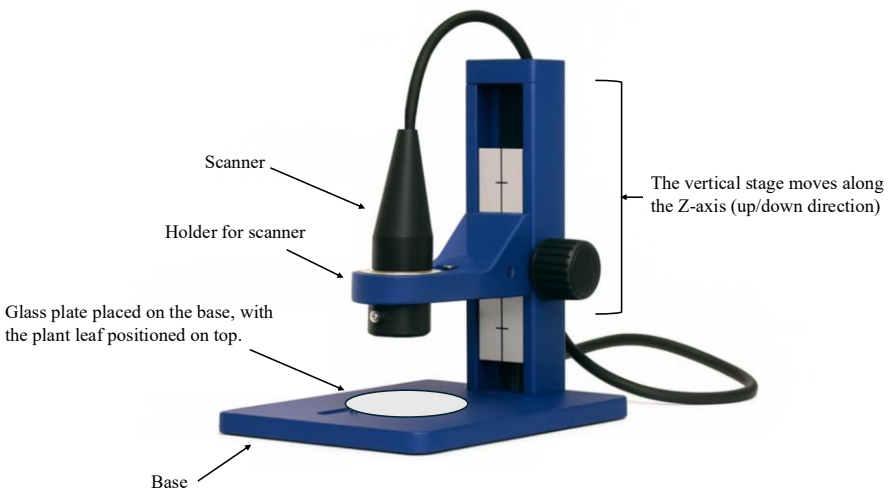


Figure 12: Lumedica OCT imaging setup.

The experiment began when the wheat plants were 21 days old. Scanning was conducted from Day 0, immediately before inoculation, until Day 14 after inoculation. Daily OCT scanning, along with morphological observations, was used to track the progression of infection in wheat leaves of the AxC 169 variety over a two-week period. The aim was to provide a clear view of the effects of *Septoria tritici* (the wild-type IPO 323) infection on leaf morphology and structure, while maintaining detailed records to ensure consistency and accuracy. One reading was taken from three different plants. Scanning was performed on the central area of the leaf,

specifically from the edge beside the main vein, to allow for clearer observation of physiological changes in the central region caused by biotic stress. The same approximate position was used for every examined leaf.

a) OCT image calibration using FIJI System software.

Although the Lumedica images have a resolution of 512 × 512 pixels, calibration of both axes is required. The two axes are independent of each other: the depth resolution depends on the wavelength used and the transversal range is given by the microscope objective used.

The aim is to calibrate the OCT images acquired using the Lumedica instrument and facilitate scientific image analysis such as estimation the length and thickness of the *Septoria* spores and hyphae. In this aim, the plan is to take OCT images of objects of knows thicknesses, such as a stack of microscope glass plate. The microscope slides from Thermo Scientific, 25x75x1.0mm. FIJI software will then be used to measure the thicknesses in pixel, set calibration, and add the scale bar on the image.

The slides have a length (longest edge=75mm), a width (25mm), and a thickness (shortest edge=1mm). These slides were placed on top of each other, slightly shifted from one another so that the edge looks like a staircase (Figure 13).

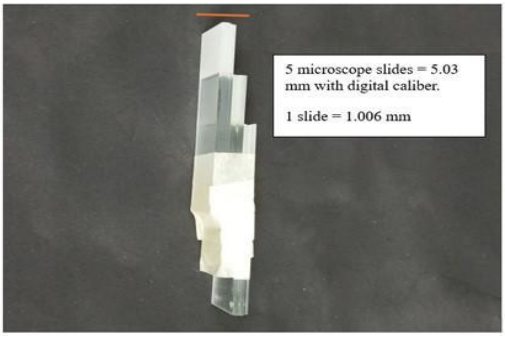


Figure 13: A known thicknesses and lengths of the glass plates (microscope slides) are placed on top of each other, slightly shifted from one another so that the edge looks like a stair.

Three glass plates are used to facilitate calibration of both axes, lateral and axial. The axial axis corresponds to the direction defined by two objects that is parallel to the light beam, and the lateral axis corresponds to the direction defined by two objects that is perpendicular to the light beam [198] (Figure 14).

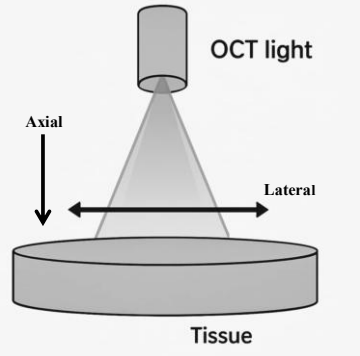


Figure 14: Shows the difference between the lateral and axial axis.

According to [23, 199, 200], the following section outlines the orientation of the glass plates used during the calibration process.

- Set Scale for Lateral (X/Y) Calibration

In the first step, the glass plates were located horizontally under the scanner stand as shown in Figure 15. The X/Y-axis in the OCT system represents the physical distance the beam travels across the sample surface during scanning.

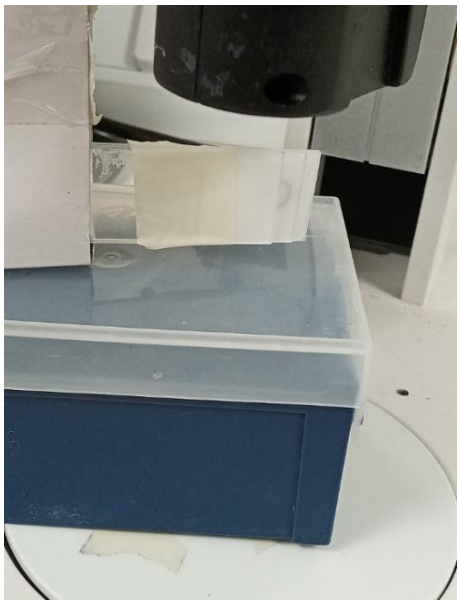

Figure 15: Setting the slides horizontally (laid flat) to calibrate the lateral axes (X and Y).

The software of Lumedica OCT system starts by clicking on the L icon on the screen and pressing the (start scan) button on the main tab. The images should look like this (Figure 16). The image should be dragged into the FIJI image and line tool were used to measure the length of known thickness of microscope slide. The result is the axial calibration of 1mm is equal to 100 pixels.

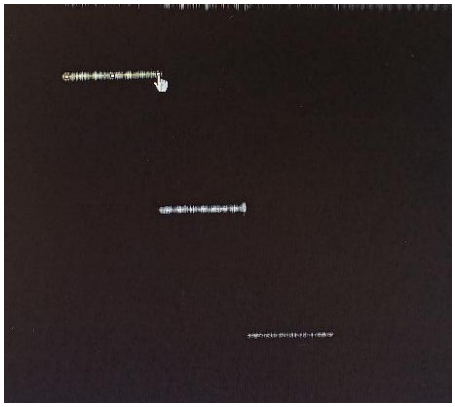

Figure 16: Using the line tool in FIJI image to know how many pixels correspond to 1mm. The result is 100 pixels /mm.

- Set Scale for Axial (Z) Calibration

In the second step, the glass plates must be placed vertically (Figure 17). The Z-axis in the OCT system represents the optical path length, which is influenced by the refractive index (n), as it is based on how light travels through the tissue [23].

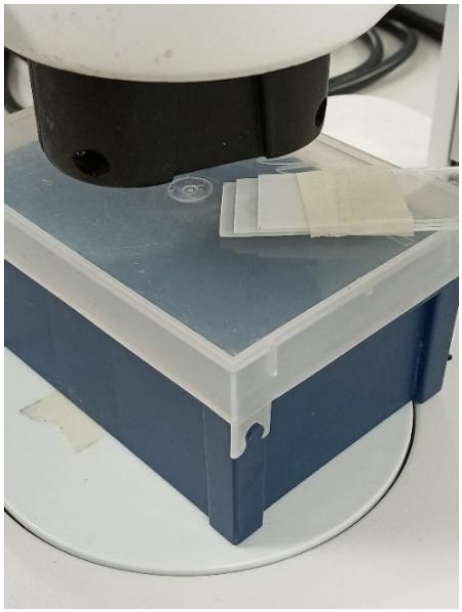

Figure 17: Setting the slides vertically (on edge or tilted) to calibrate the axial (Z) axis.

The image is imported into FIJI, as shown in Figure 18, and the line tool is utilized to measure the length of 1 mm thickness of the microscope slide. With a lateral calibration set at 1 mm equal to 100 pixels.

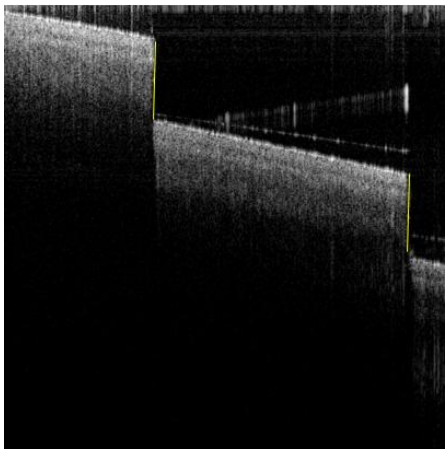

Figure 18: Using the line tool in FIJI image to know how many pixels per 1mm. The result is 100 pixels /mm.

The image scale was set in Fiji as follows, the pixel width and height correspond to 100 pixels/mm, with a pixel aspect ratio of 1.0 to reflect equal lateral resolution in both axes as shown in Figure 19.

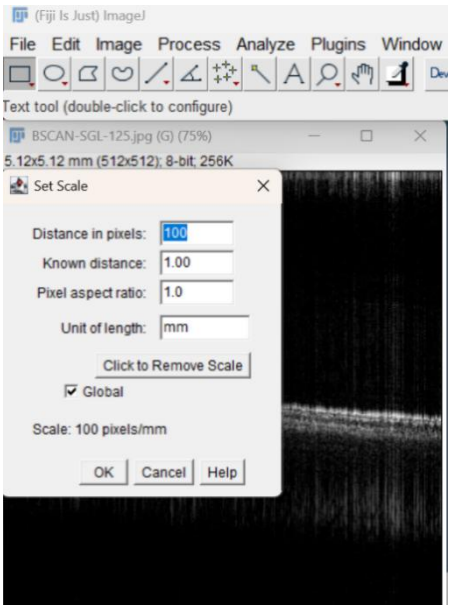


Figure 19: FIJI set scale option for 2D image.

Finally, the 'Scale Bar' option under 'Tools' in the 'Analyze' menu was used to set a scale on the unscaled image (Figure 20). The same data can then be applied to automatically generate scale bars on all unscaled Lumedica images, as shown in Figure 21.

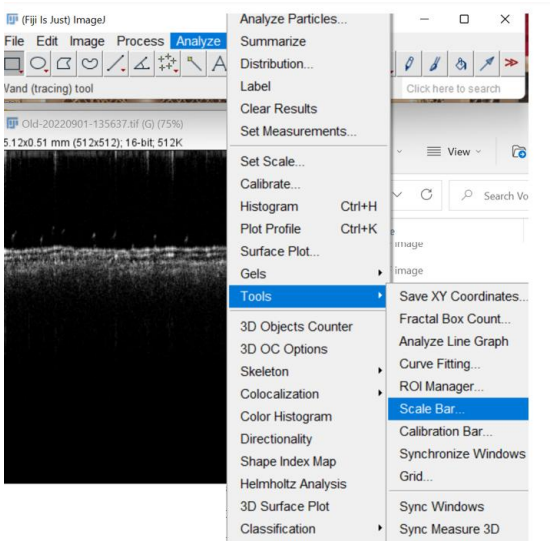


Figure 20: illustrates the process of navigating to 'Analyze' > 'Tools' and selecting 'Scale Bar".

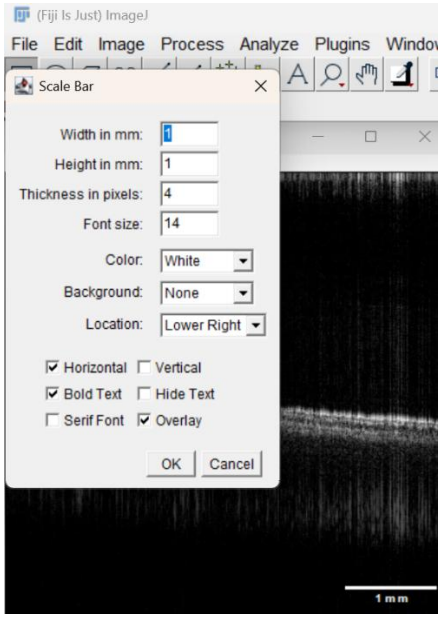


Figure 21: Shows the scale in the FIJI image which automatically generates the scale on all OCT images.

When imaging a leaf, the Lumedica OCT system provides 2D (B-scan) images, whether the cross-section is taken across the sample's width or along its length, the OCT system translate those B-scans, (width vs depth) into a volumetric image c-scan (width vs depth vs length) to form 3D images.

b) Detection of Small Particles Using the Lumedica OCT System

The aim is to evaluate whether OCT can directly resolve such small *Septoria* hyphae, which have a size of 2.5-4 x 9-16 µm [146]. To determine the resolution of the instrument, objects of various sizes were imaged. Surgical threads made of PROLENE Polypropylene (Ethicon, LLC) were first used to assess the minimum detectable particle size by the OCT system. This set

included threads with diameters of 0.35 mm, 0.2 mm, 0.15 mm, and 0.07 mm. In addition, spider silk with a diameter smaller than 0.07 mm [201] was used to further evaluate the system's sensitivity. All materials, including the spider silk, were successfully detected using OCT. A single strand of spider silk, which is smaller than 0.07 mm in diameter, was selected for this experiment and carefully placed on a slide using two needles under a light microscope. The prepared slide was then scanned using the OCT system, and the presence of the silk strand was clearly detected, as shown in Figure 22.

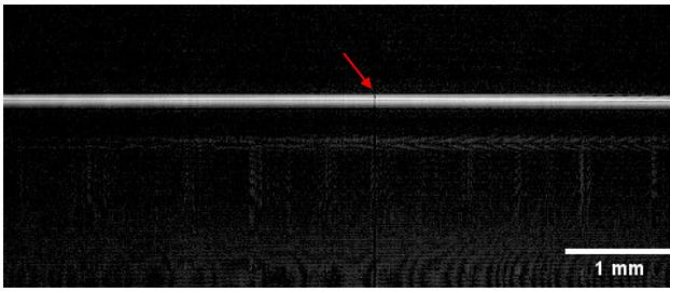


Figure 22: Diameter of the spider's single strand is 0.01 mm (10 µm) in the axial direction.

The thread width was then measured using FIJI image software and found to be 10 µm. Using the calibration described above, the width of the thread from the OCT image was determined to be approximately 0.01 mm.

My results demonstrate that the Lumedica OCT system resolves particles as small as 0.01 mm, or 10 µm. The lower limit of detection remains to be determined, but a resolution of approximately 0.01 mm is likely insufficient to directly visualize *Septoria* hyphae. This challenge is the main focus of this section. The next step will be to finally confirm OCT as a new imaging modality for in vivo, two- dimensional and three-dimensional monitoring of microstructures within plants.

2. Confocal microscopy

Confocal microscopy is a very potent imaging technique to visualize the fine structure of the hyphae and spores of the fungus *Septoria* within tissues of plants. It has several advantages in studying *Septoria* infections in wheat plants.

Confocal microscopy was developed to improve fluorescence microscopy. It provides 2D and 3D images of stained samples with calcofluor white stain (CWS) at wavelength 350- 488 nm. Epifluorescence microscopy makes use of high-intensity UV to continuously illuminate the sample. As a result, the high-intensity UV light causes photobleaching, and the image obtained becomes blurred because of out of plane signal. To counter such problems, confocal

microscopes use laser light (about 1 to 10 mW) instead of a mercury arc lamp (50 to 200 W). But most importantly, confocal microscopy uses a pinhole which allows the light of only one confocal plane to be focused on the digital camera. The fluorescent light that comes from above and below the focal plane and is blocked [202, 203]. Accordingly, the introduction of a pinhole enables greater spatial resolution in both the axial and vertical axis. Confocal microscopy thus allows the acquisition of 3D structures [204].

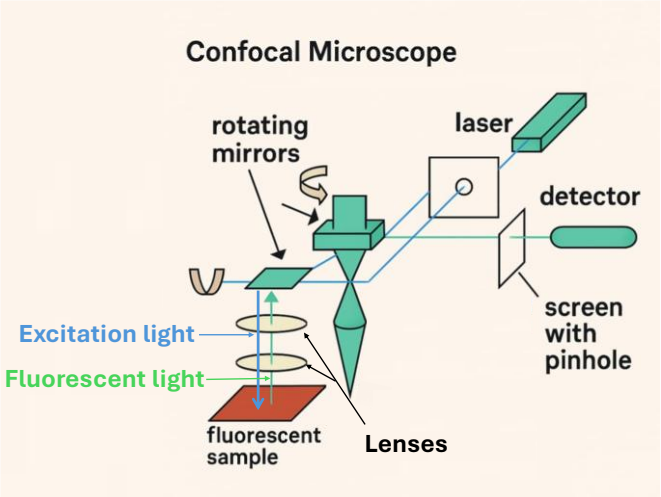


Figure 23: The principle of confocal microscopy. This version was enhanced based on the original image from [205].

As shown in Figure 23, confocal microscopy makes use of a laser, as a source of light, which is focused on a small region of the sample. The excited fluorescent dye or fluorophore can then emit light. The fluorescent light is finally captured by a digital camera. Two rotating mirrors allow you to scan in the x and y direction. The depth profile is acquired by repeating such a 2D scan at different sample heights. A software then generates 3D images by compiling stacks of 2D scans [203]. The maximum magnification of a confocal microscope is 1000x and it has a resolution around 180 nm. In this study, the Olympus confocal microscope located at the Wolfson Light Microscopy Facility (LMF), School of Biosciences, B51 Firth Court, University of Sheffield, was employed.

3. Epifluorescence microscopy

Epifluorescence microscope is a combination of the light microscope with fluorescence microscopy which it emits a range of electromagnetic waves. In epifluorescence microscopy, the excitation and emission light is propagating through the same sample to illuminated and

emitted the same objective lens [206], and the term “epi” is Greek original name means “same”[207].

It is possible to fluorescence microscope to magnify up to 1000x. Fluorescence microscopy is commonly used in biology to study cells in depth, absorbing higher intensity light sources to excite a fluorescent molecule called a fluorophore. The fluorophore absorbs photons (photons describe as a zero mass and able to produce a light or a photon when an electron transitions from a higher energy level to a lower energy level [208]. A digital camera used for epifluorescence microscopes can capture the images of the specimen with lateral resolution up to 20μm [209] which is the lateral resolution of the Leica used is ~ 400 μm [210]. In this study, we used the Olympus BX51 at APS Microscopy and Histology Unit (MHU), lab C41.

4. Scanning electron microscopy (SEM)

SEM is one of the common uses for imagining morphology of the surface of the sample due to its resolution of 10 nm, and a magnification range spanning from 10x to 500,000x. SEM is based on the interactions of electrons [211]. Enhanced by the inclusion of a digital camera within the system, SEM enables the capture of specimen images along with scale bars for accurate measurement. This study employed the Hitachi TM3030Plus benchtop SEM at the APS Microscopy and Histology Unit (MHU), lab C41, University of Sheffield.

The principle of SEM involves the utilization of an electron beam, rather than light [211], to generate images with nanometre-scale resolution (Figure 24). Electrons are emitted from the top of the microscope through an electron gun and subsequently accelerated by the positively charged anode. Guided by a series of lenses, the electron beam follows a vertical trajectory towards the sample surface [14]. In SEM, condenser lenses, also referred as magnetic lenses, are used to control the diameter and convergence of the electron beam, adjust beam current (affecting brightness and resolution), and focus and direct the electron beam onto the sample in combination with the objective lens. Both the condenser and objective lenses are electromagnetic lenses [212]. To facilitate uninterrupted electron travel within the instrument towards the detectors, the electron column must maintain a vacuum [15]. Additionally, scanning coils within the system are employed to traverse the electron beam across the sample surface [16].

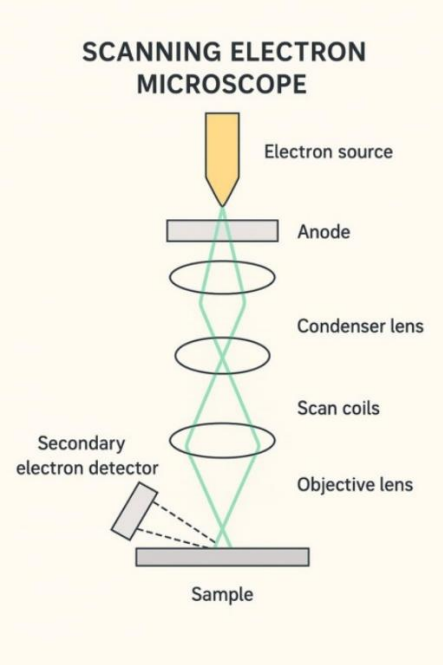


Figure 24: This diagram is a simplified schematic of SEM, showing key components and electron path. This version was enhanced based on the original image [16].

1. Freeze Fracture with SEM

As previously mentioned, SEM creates an image by scanning a focused electron beam over the surface of a specimen with high-resolution images. Freeze-fracture method includes quick freezing of the plant tissue followed by fracturing to reveal the inner structure. The sample is then coated with a thin layer of metal and viewed with a SEM [189]. For this experiment, the samples did not need to be frozen, as the aim was not to study membrane structures, but rather to compare trichome morphology before and after *Septoria tritici* infection and to visualize the emergence of *Septoria* from the stomata.

5. Traditional Clearing, and Staining

The purpose of staining is to directly visualize the various structures within wheat plant leaf before and after *Septoria* infection. The sample preparation is as follow:

a) Hand-cut sectioning

The procedure was determined according to the method described by [213], The thin sections of leaf are created by laying the leaf on the microscope slide position and chopping in an up-and-down motion at a perpendicular angle to the long axis of the leaf. Sections that are too thick and sections that are not oriented correctly should be removed using forceps. The remaining sections are then immersed in water and covered by a coverslip.

b) Removal of cuticles

The cuticle corresponds to the waxy upper surface of leaves. It is made of cutin, which is a wax-like material produced by a plant that is composed of hydroxy fatty acids. This covering plays an important role in helping the plant retain water, but it is also highly reflective and induces imaging artefacts while using OCT. It is possible to remove the cuticle by washing the leaves for 30 seconds to 1 min in organic solvents for microscopic studies [214]. There are other organic solvent can be use such as chloroform and ethanol removes surface waxes as reported in [215]. This method is useful for studying the outer surface of control leaves, including structures such as stomata (Figure *25*). However, it is not applied to infected leaves, as the organic solvents can wash away the hyphae, preventing observation of fungal morphology.

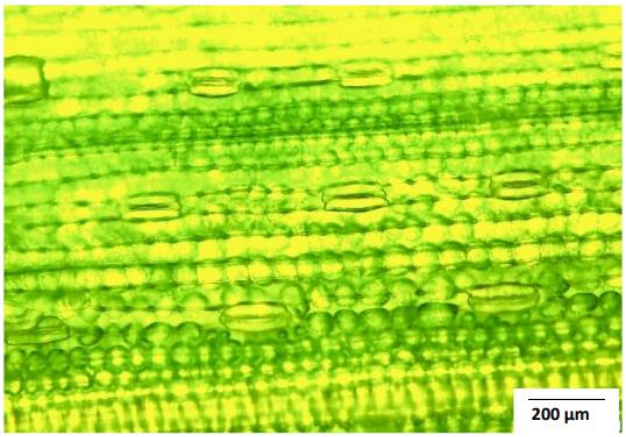


Figure 25: Shows stomata in a control wheat leaf (8-day-old). The image was taken under light microscope after removing the wax from the leaves to make a stomata imprint.

c) Staining and Confocal Microscopy

Calcofluor White Stain (CWS) was employed to directly visualise *Septoria* disease on wheat leaves. CWS is commonly used to detect fungal cell walls, providing a fluorescent signal under ultraviolet light. This technique was chosen for this study for its effectiveness in accurately identifying and characterizing *Septoria* disease progression on wheat leaves

CWS is a fluorescent blue dye, which binds to the cellulose and the chitin contained in the cell walls of fungi [216]. And has been used to stain *Septoria tritici* [217]. First, the specimen was carefully put on a clean glass slide. One drop of CWS was added to specimen, along with a drop of 10% w/v solution potassium hydroxide with the formula (KOH). The KOH solution was prepared, according to [218], by dissolving 10g of KOH crystals into 100 ml of distilled water. KOH solution is commonly used to prepare wet mounts in mycology laboratories. The

specimen is then covered with coverslip and left to absorb the stain for 1 minute. The excesses dye is removed using a piece of absorbent paper. The observation should be under an epifluorescence microscope at x100-x400 magnification.

Several fluorophores have been utilized for microscopic studies on *Septoria* and other plant pathogens. Such fluorophores are selected for specific binding to certain cellular components and become observable with fluorescence microscopy. The excitation wavelength approximately 340–380 nm (typically UV or near-UV light), and emission wavelength around 435–480 nm, resulting in a blue-white fluorescence when the samples stained with CWS.

If *Septoria* is genetically modified to produce GFP, its hyphae will glow under a fluorescence microscope, making them easy to see under the appropriate excitation and emission filters. Instead, CWS, which binds to cellulose and the chitin in fungal walls, is a more suitable for epifluorescence or confocal microscopy. The Olympus BX51 microscope, located at the APS Microscopy and Histology Unit (MHU), lab C41, University of Sheffield, was used in this study.

These imaging techniques, i.e. Light microscopy, epifluorescence microscopy, and confocal microscopy, and stained wheat leaves with CWS, enabled examination of the morphology of fungal pathogens and their development within plant tissues, laying the groundwork for OCT experiments. This will be detailed in next chapters.

6. Plant material

Seeds are key sources of carbohydrates in diets around the world [219]. Most wheat grains are between 5-9 mm in length and weigh between 25-50 mg[220, 221]. Wheat seeds is monocot or have only one cotyledon which it indicates the embryonic leaf or leaf part inside the seed [222].

The wheat for this proof-of-concept experiment belonged to the AxC 169 and AxC 157 varieties. The seeds are grown in M3 compost supplemented with 0.5 g osmocote. The Osmocote fertilizer, rich of organic and mineral components, was designed to support the optimal development of the plants. It included the following nutrients:15% Total nitrogen (N), 6.6% Nitrate nitrogen (NO3-N), 8.4% Ammoniacal nitrogen (NH4-N), 9% Phosphorus pentoxide (P2O5), soluble in neutral ammonium citrate and water (6.8% water-soluble), 12% Potassium oxide (K2O), soluble in water (12% water-soluble), 2% Magnesium oxide (MgO), with 1.3% being water-soluble. Trace elements such as 0.03% Boron (B), 0.050% Copper (Cu),

0.45% Iron (Fe), 0.08% of which is chelated by EDTA, 0.06% Manganese (Mn), 0.020% Molybdenum (Mo), and 0.015% Zinc (Zn).

7. Growth Chambers

In total, 6 plants were grown for the experimental run whose results are discussed in Chapter IV and V: 3 control plants and 3 plants destined to be infected. The plants were incubated at 20 °C, in a 14-h:10-h a light-dark cycle, at 61% of relative humidity and levels of carbon dioxide was kept at 455 ppm (i.e. 55 ppm above the usual ~400 ppm outdoors level to enhance plant growth [223]), these adjustments were made as part of the experimental conditions set for all growth chambers. The inoculation started when the plants were 21-day old.

8. Inoculation with *Septoria tritici*

Regarding the solid culture media preparation for fungus, *Zymoseptoria* tritici IPO323 [224], was incubated on Potato Dextrose Broth (PDB) media composed of 24 g/L of PDB and 15 g/L Agar mixed with 1000 ml of 18megogm water. It should be noted that incubating agar plates for extended periods may increase the risk of contamination, which could affect the purity of the spore suspension. Inoculation was performed via spray to mimic the natural spread of spores in high humidity atmosphere. The spray solution was prepared by adding 10 mL of 0.01% Tween 20 in water to a petri dish containing black heads (pycnidia spores). The spores are then gently scraped off using a sterile spatula and poured into a Falcon tube [124, 224]. 20 µL of the supernatant was placed onto a counting chamber, ensuring the liquid spread evenly between the chamber and the cover slip. Excess liquid was removed using tissue paper. Spores were observed at 20X magnification using a Leica microscope.

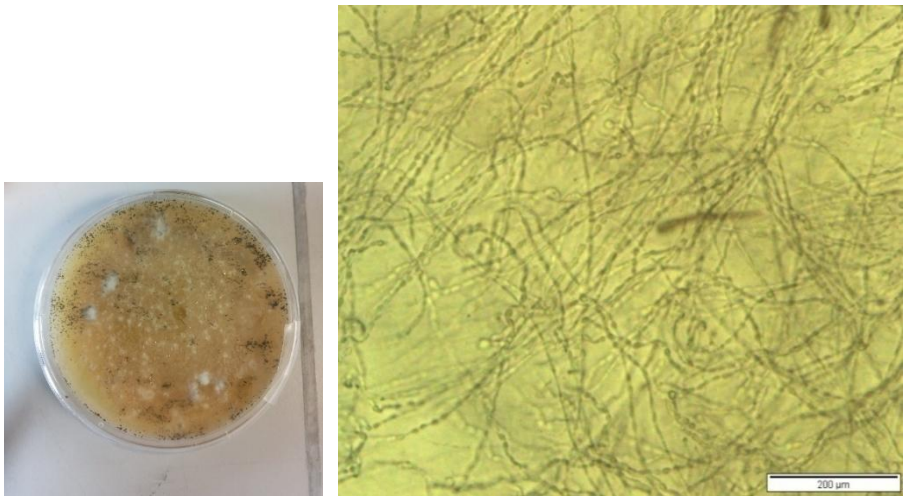


Figure 26: Pycnidia “black spores’ growth in petri dish observed after 2 months. Filaments were transferred from the Petri dish to a slide microscope. The image was taken under the light microscope (Olympus BX51) as a Leica

model is for direct observation without capturing images. Mean (length) is 1.878 µm and width is between 0.02-0.05 mm using FIJI measurement tool.

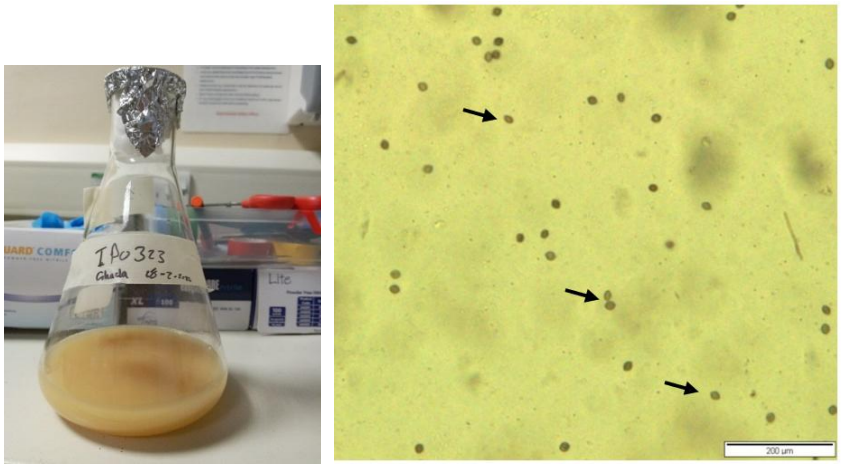


Figure 27: Shows *Septoria* suspension in the conical flask. A drop from it on a slide microscope for spore shape examination. The image was taken under the light microscope (Olympus BX51) as a Leica model is for direct observation without capturing images. Scale bar 200 µm. Width of the spores is between 0.02-0.05 µm using FIJI measurement tool. In contrast to the filamentous morphology observed in Figure 26, the spores in suspension appeared darker and more oval. However, these were derived from confirmed IPO323 cultures (arrowheads) and were considered representative of *Z. tritici* inoculum.

To calculate the inoculum concentration, Following the method described in [225], the counting chamber consists of sections as shown in Figure 28. The researcher can either count everything or only four sections and extrapolate the average to the remaining area. The latter method consists in summing up of the 4 sections and dividing by 4 to get an average. The average is then multiplied by 16 as there are 16 squares on the chamber.

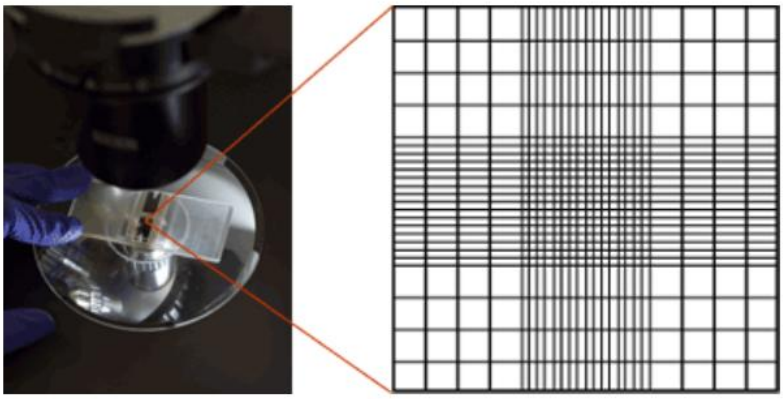

Figure 28: How the counting chamber looks under a microscope. The image adapted from [226].

After spores were counted, using the formula:

$$V1 = \frac{C2V2}{C1} \quad (1)$$

Where:

- C1= Counted spores
- V1= Volume of inoculum to use (required)
- C2= Desired concentration ($1 \times 10^6$/ml)
- V2 = Final volume required (20 ml)

The inoculum was adjusted accordingly, using sterile Tween20 water, to achieve a concentration of $1 \times 10^6$ spores/mL [227].

For inoculation, the plants were taken out of the growth chamber and placed inside a laminar airflow. The inoculum was sprayed by a mixture of the inoculum with water on the top sides of the second newest leaf (GS31, following Zadoks system [130]). After inoculation, plants were covered with propagator lids (to maintain high humidity). The plants were then watered and placed in a sealed propagator and placed back in the growth chamber for 24 hours recovery [228]. It I important to note that our controls were only water sprayed, in accordance with previously published works, also on wheat, and similarly infected by *Septoria* [229-232]. The spraying of purified water was automatically performed within the chamber to preserve a humidity level of 61%.

It is worth highlighting that both control and inoculated plants are regularly sprayed with purified water to maintain the high humidity level. Accordingly, the inoculant is prone to be washed away during the experimental run. Furthermore, the estimated concentration of Tween in the final spore-loaded solution is about 0.01%, which is significantly less compared to the 0.1 % and 1% used in the previous works on wheat infected by *Septoria* which also used water-sprayed controls. Therefore, it is unlikely that such a low concentration of Tween would trigger a systemic response; rather, we expect that colonization by *Septoria* is the factor responsible for such a response.

## 9. Alternative Systems for Producing *Zymoseptoria tritici* Inoculum

There are several alternative systems for producing *Zymoseptoria tritici* inoculum beyond the petri dish/pycnidia scraping method.

a) Isolation of spores from wheat leaf

Following the procedure described by [233], in order to isolate wild-type strain IPO323 from wheat (after 4 days of inoculation), infected leaves were cut and put on agar in Petri dishes at 20 °C. Three weeks later, one can observe a presence of pycnidia on the plates. The culture is revitalized by transferring it to a fresh PDB medium (potato dextrose agar, 39 g/L) and incubated at 18 °C with a photoperiod of 12 h over 10 days.

d) Liquid media preparation

Following the method described by [224] for growing *Zymoseptoria tritici* IPO323, 10 g of yeast extract and 10 g of sucrose are well mixed with 100 m L of dd$H_2O$ and autoclave for sterilization. To isolate *Septoria* spores from contaminated plates to new liquid media culture, the spores should be scraped off with 20 µl sterile distilled water and 20 µl Tween 20 by using a sterile spatula, and the suspension was then transferred to conical flask.

c) Revival of culture

In order to start a new culture, the frozen solution was left to thaw. In this manner, fine particles of fungus would be released in the new falcon tube. A pipette was used to transfer small quantities of liquid (1000µL) containing Septoria fungus to the center of a Petri dish. A sterilizer and a plate spreader were used to spread the dispensed liquid around the plate and leave it to be dried. A parafilm was used for sealing Petri dishes and incubating them upside-down at an appropriate temperature (20°C) and kept in the dark for 7-10 days. Spores' growth should be observed after 2 weeks. The growth of the spore is usually very slow and its growth in the media looks like a small button of white mass because that was the early stages of development.

## Chapter III: Comparative Study of OCT Imaging and SEM.

In this study, different tissue types (other than leaves) were selected to evaluate the strengths and limitations of using OCT for these tissues. This addresses the scientific question of whether OCT signals can penetrate thick internal tissue structures with sufficient resolution to detect changes caused by biotic and abiotic stress, potentially opening new avenues for OCT applications in plant research. In this chapter, the growth stages of wheat plants, as defined by the Zadoks system, will be discussed in detail using the OCT imaging technique. This section compares OCT images with those obtained using light microscopes and SEM of different parts of the plant. Such a correlation highlights the strengths and limitations of OCT.

1. Revealing of Wheat Plant Morphology using OCT

Morphologically [109, 234], Wheat is grass that has long thin, hollow stems and slender shaped leaves. Basically, according to Zadoks system, the mature wheat plant is made up of roots (GS00-09), shoot and tillering (stem and leaves) (GS20-29), as shown in Figure 29, A. The roots are for the uptake of minerals from the soil. On the other hand, the leaves are tall and thin, serving the purposes of photosynthesis. In Figure 29, B shows the cross- section of a control wheat plant leaf. The image was taken under a light microscope. This yellowish background generally characterizes older light sources using tungsten or halogen lamps [235]. Although this can typically be corrected using camera software, the original color was retained in this study to preserve the raw appearance of the image and avoid altering potential signal characteristics.

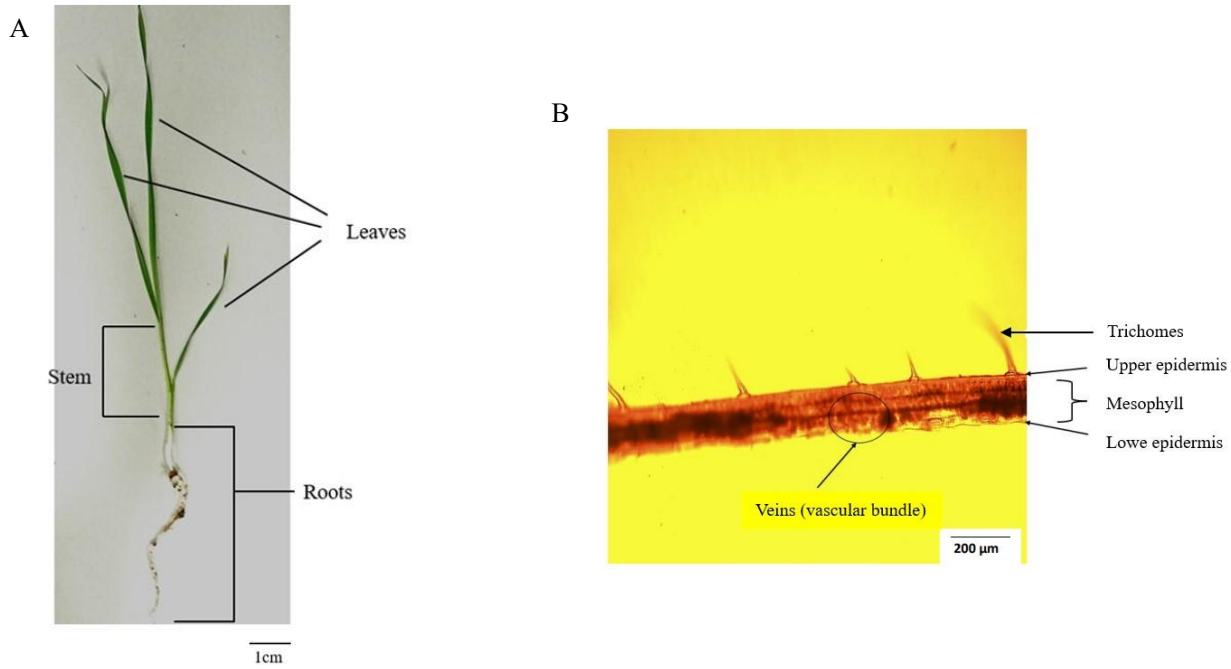


Figure 29: (A) Shows the external parts of the wheat plant. The age of the sample is 2 weeks. (B) shows cross-section of a control wheat leaf (8-day-old). In this image, each spike in the upper epidermis is a trichome, the vascular bundle is a longitudinal tube in the middle part of the leaf. The image was taken under a light microscope, scale bar 200 micron.

a) Leaf

The next figure (Figure 30) is a three-dimensional OCT image of a control wheat leaf (300 B-scan images). The distance between each OCT B-scan, in order to recreate the volumetric C-scan with proper axes, is 5 mm x 5 mm [197]. Therefore, the spacing is calculated as: 5 mm / (n-1), which equals 5 / 299 = 0.016 mm.

Scanning was performed midway along the leaf's length, beside the main vein. Incomplete scans (i.e. in which the edge of the leaf appear) are dismissed for the automated analysis (because the leaf's edge misleads the automated segmentation, as discussed afterwards). A typical volumetric (c-scan) is shown in Figure 30.

In this image, we observe trichomes, or hair-like structures, are visible on the external surface of the leaf. It is also worth noting that healthy leaves already have air gaps within their mesophyll to facilitate gas exchange [236].

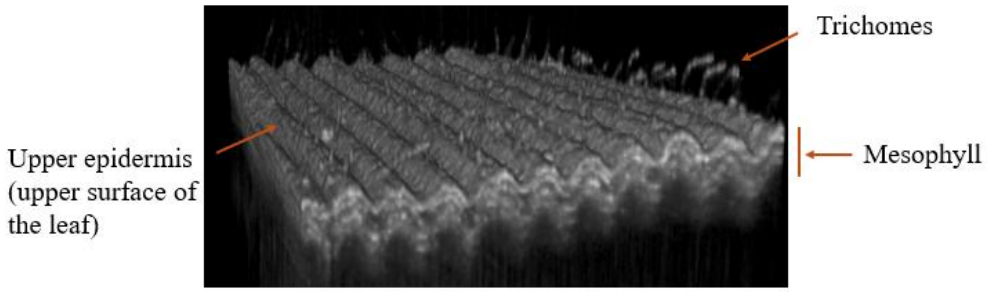


Figure 30: Three-dimensional OCT images (C-scan) of a cross-section of a control wheat leaf. In this image, each spike above the upper epidermis represents a trichome. The image has a range of 5mm x 5mm and is generated using 300 consecutive B-scans, each separated by 0.01 mm.

b. Spikelets

After six months of cultivation and regular watering twice a week, a thick leaf sheet (Figure 31) will wrap around the spikelet (GS 30-39), which contains the florets, with a single leaf at the tip of the stem. This tissue will eventually break open, revealing the spikelet containing the florets. After fertilization, these florets will develop into kernels, forming seeds at the end of the wheat life cycle.


Figure 31: The arrow indicates the area where spikelets are covered by leaf sheath.

Next figure (Figure 32), using the OCT imaging system to image the area where seeds will be produced in the future (the arrow). Through the OCT image, we can see the leaf sheath protecting the young spikelet, and the hollow centre. There is no image of spikelet within the leaf sheath, which may indicate that OCT has poor penetration depth.

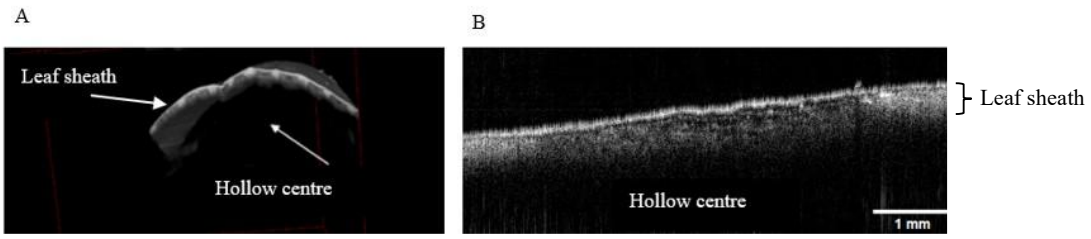


Figure 32: (A) Three- dimensional OCT image (C- scan) of a wheat leaf stem surrounded by a leaf sheath. C-Scan has a range of 5mm x 5mm and is generated using 512 consecutive B-scans. (B) Cross-section OCT image of a wheat leaf stem surrounded by a leaf sheath, which protects the young spikelets. However, the image does not capture the immature spikelet within the hollow stem.

After three months, the leaf sheath removed, and the first spikelet became visible (GS 50-59) (the arrow in Figure 33).

Figure 33: An image of wheat's spikelets, each spikelet contains a few florets, after 9 months of the plantation. Scale bar is 1cm.

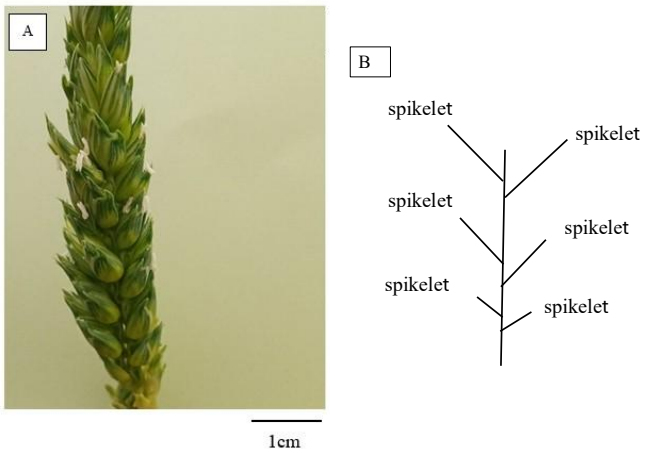


Figure 34: (A) A close-up image of wheat's spikelets contains florets (B) a diagram of the spikelet arrangement of the wheat plant.

After three weeks, the first signs of flowering were observed (GS 60–69). At this stage, the grass produces a small flower called a floret, which is composed of the anther, filaments, stigma, ovary, glume, and lemma. During this transition from the vegetative to the reproductive phase, the plant has a high demand for nitrogen, which is mobilized from the leaves to the grain for the synthesis of total soluble protein (TSP) [237].

c. Florets

According to Figure 35, an observation can be made that three florets compose one kernel. The ovary in the florets with the stigma is the female part, whereas the anther containing pollen is the male part. Filaments are the long, threadlike structures supporting an anther. Pollen is attached to the sticky, receptive surface of the stigma, which attaches the pollen, after which they move to the ovary, and the process of fertilization begins. Some specialized leaves are lemma and glume, which are associated with reproductive structures. The main difference between them is the position, as one is present at the base known as glumes, while each floret is covered by a lemma [238-240].

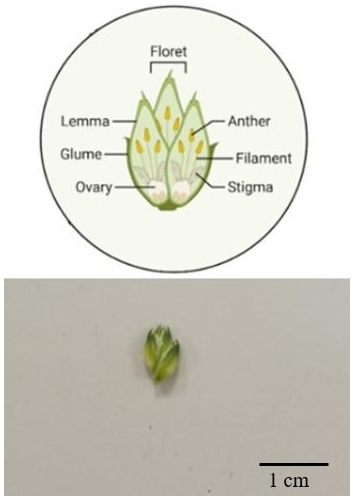


Figure 35: Anatomy of wheat plant floret. The figure adapted from [241].

The floret will be imaged using OCT system to examine the inner structures within the bracts. The next images, Figure 36, A and B, represent two-dimensional and three-dimensional OCT images of wheat bracts. According to [242], these bracts, in an immature floret of wheat, cover the reproductive organs of it. They are made up of three well-marked tissues: the outer circle of tissue called glume, the middle circle called lemma, and the inner circle called palea.

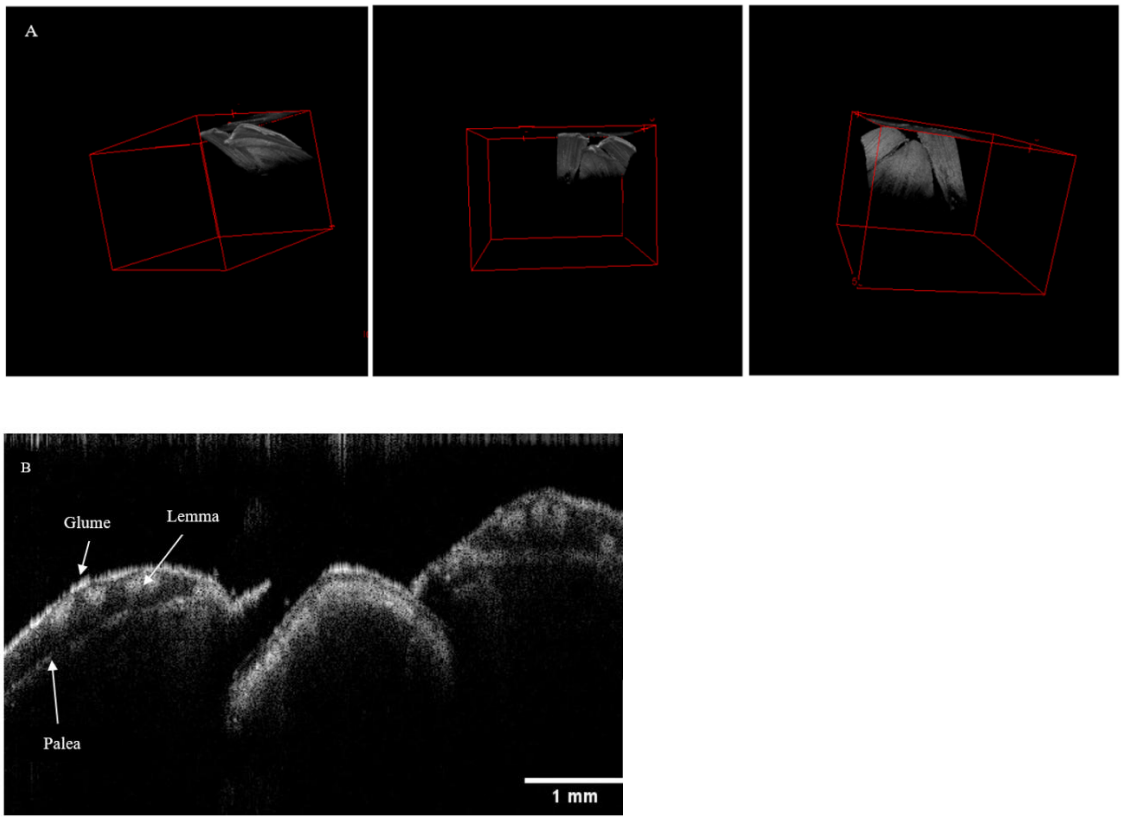


Figure 36: (A) The three-dimensional OCT (C- scan) illustrate the bracts enclosing the grass floret observed in image. C-Scan has a range of 5mm x 5mm and is generated using 512 consecutive B-scans. (B) The two-dimensional OCT image effectively illustrates the outer structure of the wheat sample, including the bracts (specifically the glume, lemma, and palea). However, this imaging proves limited in its utility, as it fails to reveal the inner structure of the sample.

The following section involves dissecting the floret to carefully extract both the ovary and anther (Figure 37 and Figure 38) using tweezers. These components will then be subjected to examination under SEM technique and OCT as well.

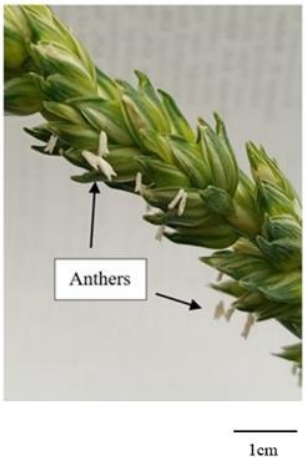


Figure 37: Shows the anthers pushed up the floret for pollination.

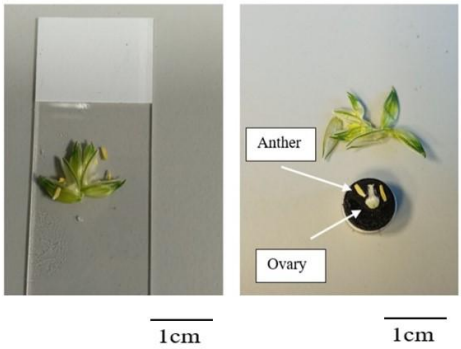


Figure 38: The samples had been prepared for SEM technique.

In the next figures (Figure 39, A and B) this study explores images of the ovary and anther using SEM and light microscopy. We will then compare the resolution of these images with those obtained using OCT imaging techniques.

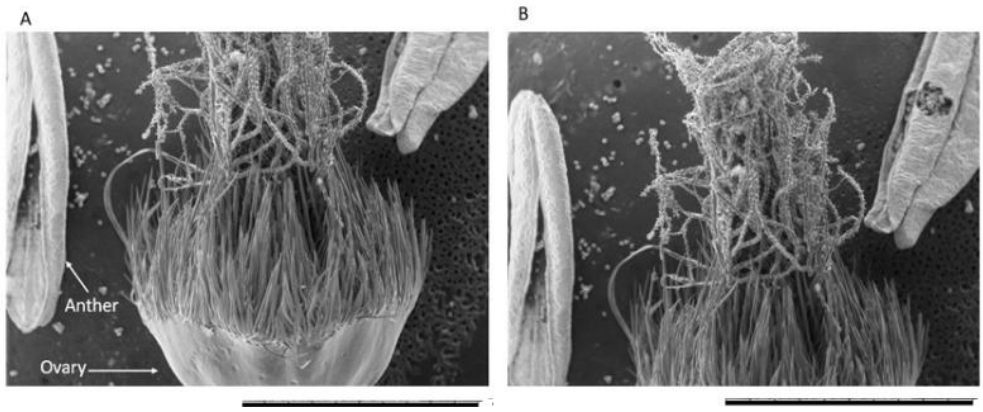


Figure 39: (A) Shows the ovary, a component of the female reproductive organ of the flower, alongside the anther, representing the male reproductive organ of the flower containing pollen. (B) Illustrates the movement of the slide upwards to reveal the upper portion of the sample. Scale bar 2mm.

According to [243], the anther normally contains two lobes, each lobe has two pollen sacs. In total, four chambers for a single anther. These are usually filled with pollen grains for pollination process.

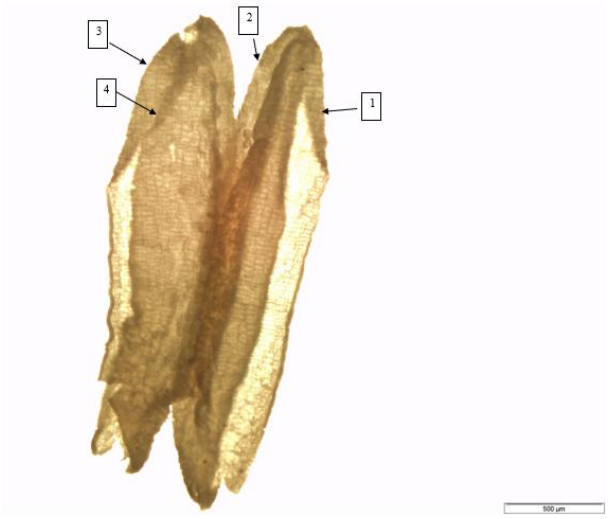


Figure 40: Anther under a light microscope shows the 4 chambers. The scale bar is 500µm.

The size of pollen, in general, ranges from 20 to 40µm (0.02-0.04 mm), that is very small to be visible with a naked eye. However, the anther length was approximately 2.5 to 4 mm long [244], and it width is around 0.5 to 1.4 mm [245].

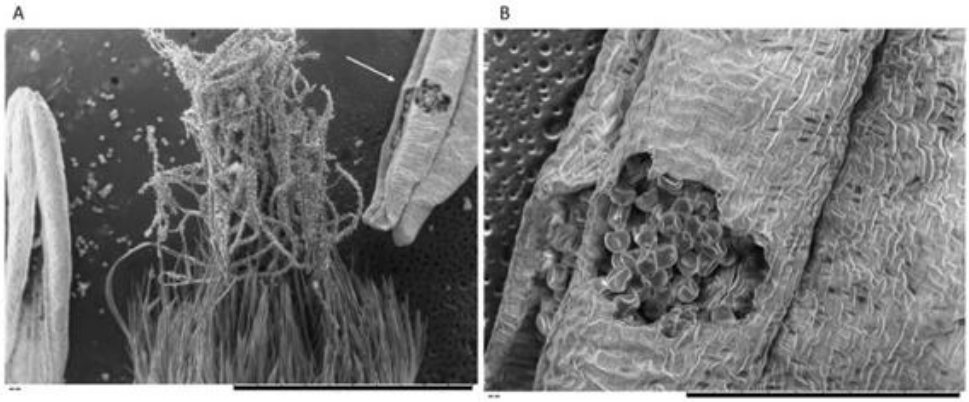


Figure 41: (A) The arrow indicates that the front view shows three chambers of the anther, with the fourth chamber located at the back. These chambers contain pollen. Scale bar 2 mm. (B) Pollen discharged from one of the chambers of anther in order to fertilize the female ovule. Scale bar 500 µm.

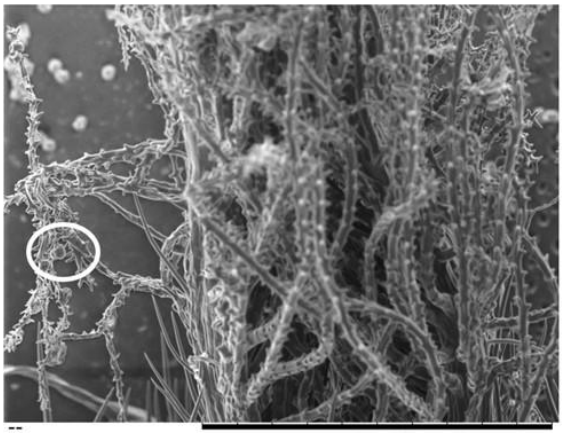

Figure 42: The pollen, represented by the circle, is on its way to the ovary, indicating that the fertilization process in plants is underway, ultimately leading to the formation of grains. Scale bar 1mm.

Previously, in Figure 38, A slide was prepared for SEM examination. In the next section, OCT scanning was performed on the same prepared sample to examine two parts of the florets: the ovary and the anther (Figure 43, Figure 44, and Figure 45).

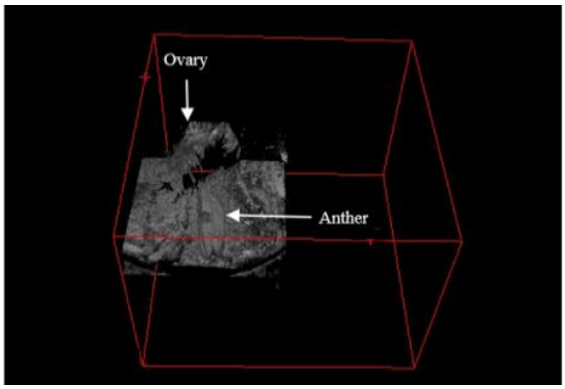


Figure 43: Three- dimensional OCT image (512 B- scan) shows an anther and a portion of an ovary. C-Scan range 5mm x 5mm.

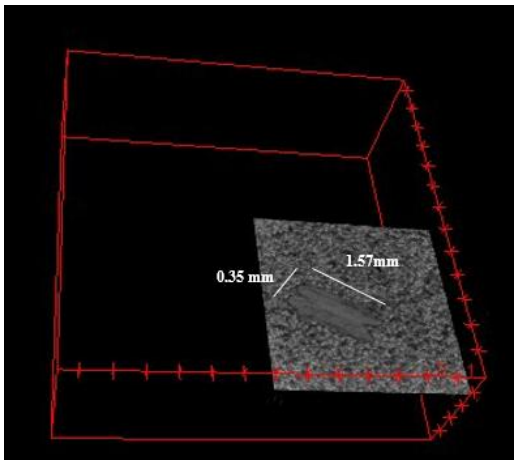


Figure 44: Three- dimensional OCT image (C- scan) of the anther, the length of the anther is proximately 1.57 mm, and its width is proximately 0.35mm by FIJI image measurements. C-Scan has a range of 5mm x 5mm and is generated using 512 consecutive B-scans.

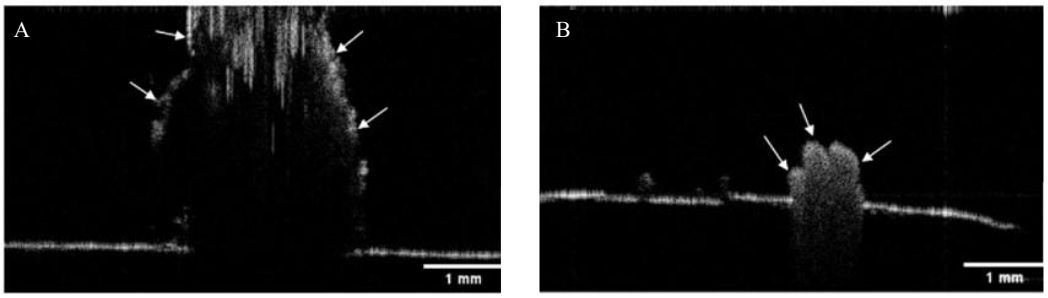


Figure 45: (A)Two-dimensional OCT image. Arrows indicate the outer layer of the ovary, without internal structures. (B) Two-dimensional OCT image. The three arrows indicate that the three chambers of the anther. A scale bar is 1 mm.

During examination under a light microscope, a tiny, elongated insect was observed crawling around the ovary. This insect is commonly known as a thrip. Thrips are known to contribute to pollination, with a single thrip capable of carrying anywhere from 10 to 50 pollen grains [246]. However, when their numbers increase, thrips can become detrimental and may even consume pollen [246] potentially leading to visible presence within the growth chamber. In such cases, biocontrol, involving the introduction of living organisms or natural substances, are recommended. The control of thrips and sciarid flies involves placing Petri dishes with biocontrol agents in the growing cabinets, which are natural insect predators. Because these pests can easily enter growing areas, especially through Levington M3 compost, technicians recommend using biocontrol regularly to help prevent outbreaks.

After nine-ten months of cultivation, the spikelet of wheat turns yellow as they prepare for kernels “seed formation” (flowering to maturity GS70-79).


Figure 46: Forming yellow spikelets of wheat after nine months of plantation.

d. Seeds

Grains (Hard dough stage GS 58) and then seeds (Harvest Ripeness GS 90-99) are the last growth stage of wheat plants. They are the result of florets developing into kernels after pollination and fertilization. The harvested seed was cut using razor blades for surface scanning. The seed can be divided into three main parts [247], as shown in SEM image (Figure 48) and OCT image (Figure 49), (1) the bran or outer layer, which is rich with fibers, vitamin B, and contains trace minerals such as Cu, Fe, Mn, and Zn [248] as well as phytochemicals such as phenolic acids and carotenoids [249]; (2) the endosperm or inner layer, which is the larger part of the seed containing carbohydrates and protein; and (3) the germ, which is a rich

source of vitamin B and E, and also contains trace minerals, phytochemicals and unsaturated lipids [247].


Figure 47: Some harvested wheat seeds. 5-9 mm in length and weight between 30-50 mg.

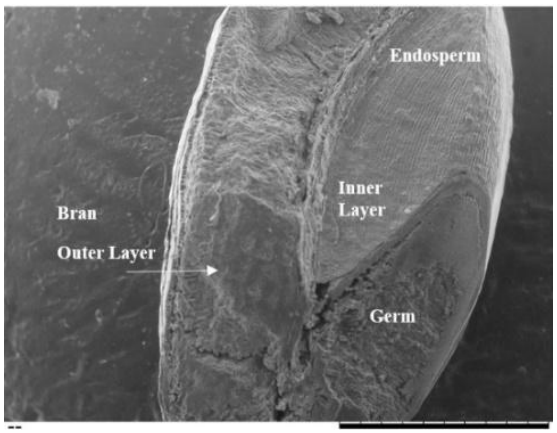


Figure 48: The structure of wheat grain is depicted in SEM image. The seed can be divided into three main parts, bran or outer layer, the endosperm or inner layer, and the germ. Scale bar 2mm.

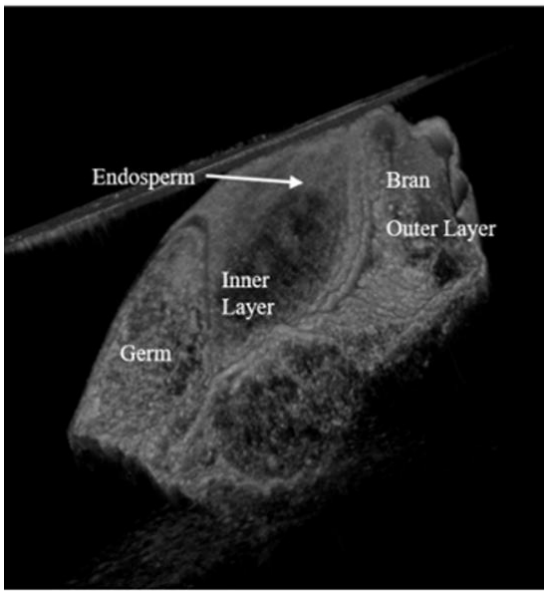


Figure 49: Three- dimensional OCT image (C- scan) of the wheat grain structure. The seed can be divided into three main parts, bran or outer layer, the endosperm or inner layer, and the germ. C-Scan has a range of 5mm x 5mm and is generated using 512 consecutive B-scans.

## 2. Conclusions

This chapter explored the morphology of the wheat plant throughout its developmental stages using OCT and SEM, with a focus on evaluating the imaging capacity of OCT in comparison to the well-established SEM method. The findings demonstrate both the potential and the limitations of OCT as a non-invasive tool in agricultural imaging, particularly in studying the external structures of wheat. OCT successfully captured detailed images of the outer surfaces of plant structures, such as trichomes on leaves, the arrangement of bracts, and external morphology of florets and spikelets. Its ability to generate both 2D and 3D reconstructions allowed for the visualization of surface texture and overall shape in real time, without the need for destructive sample preparation. This capability is especially valuable for longitudinal studies where repeated imaging of live tissues is needed. However, a key limitation identified was the restricted penetration depth of OCT light, particularly when imaging denser or deeper tissues such as the immature spikelets within the leaf sheath. Despite imaging the sheath and stem successfully, OCT could not visualize the enclosed spikelet, suggesting that tissue density and internal air–water interfaces hinder light transmission. This outcome aligns with known limitations of OCT in highly scattering media and highlights the need for cautious interpretation when internal features are not visible. Overall, the findings support the application of OCT as a valuable tool for non-destructive, real-time imaging of plant surface morphology, particularly for tissues with higher water content like leaves. These results lay the groundwork for further exploration of OCT in detecting biotic stresses, such as fungal infections, in early growth stages topics that will be addressed in the following chapter.

## Chapter IV: Evaluating the Suitability of OCT for Early Detection of Plant Infections.

### 1. Introduction

The scientific question driving this work is: can OCT detect early-stage *Septoria tritici* infections in wheat leaves before visible symptoms appear? Answering this question is important because early detection is critical for effective disease management. Traditional detection methods, including visual inspection, typically identify infections only after significant tissue damage has occurred. By that point, chemical treatments may be less effective, and crop yield is already compromised. An imaging tool like OCT, capable of identifying microstructural changes at the cellular level before necrosis develops, could transform plant pathology by enabling pre-symptomatic diagnosis. This would support more timely and targeted interventions, reducing fungicide use, limiting environmental impact, and ultimately improving crop health and food security.

The wheat leaf comprises three primary internal structures: the epidermis, the mesophyll, and the vascular tissue [250]. The epidermis consists of long cylindrical cells with wavy walls and is covered by a cuticle containing strongly developed epicuticular wax [251]. This wax serves as the first line of defense against biotic and abiotic stressors, reflecting potentially harmful ultraviolet light and contributing to the formation of an ultra-hydrophobic and self-cleaning surface. Additionally, it acts as an anti-climb surface [252-254]. The vascular tissue is small veins within parenchyma tissue consisting of phloem and xylem. They are conducting elements surrounded by parenchyma cells [255]. The mesophyll cells contain chloroplasts, and they contain photosynthetic machinery to convert solar radiation, water and $CO_2$ to sugar (carbohydrate) and $O_2$ [256]. Rubisco is a central protein in photosynthesis that represents 40-58% of the total soluble protein in wheat leaves [257]. Photosynthesis in flag leaf photosynthesis is a large contributor to grain production [258].

To maximize crop survival and reduce the use of chemical treatments, and their environmental impact, early detection of infections is essential. OCT is proposed as a novel imaging tool to provide cross-sectional and three-dimensional, non-invasive, real-time monitoring of plant microstructures in vivo. This technique aims to enable early detection of infection before crops show any visible signs of infection and to enhance understanding of the different infection stages. Once the technique passes the proof-of-concept stage, the goal is to evaluate its use in the field.

As discussed in chapter 1, to detect and quantify STB, among the various techniques available, hyperspectral imaging (HSI) is increasingly used, in field, because of its non-invasiveness, efficacy, and ability to assess whole crops [227, 259, 260]. However convenient and reliable, HSI only detects the spectral signature associated with the necrosis of wheat leaves. It thus assesses the extent of infection within an already damaged crop. Ideally, we would need a technique that can detect the presence of *Septoria* before necrosis of the leaves occurs.

This chapter will examine the strengths and limitations of using OCT in plant research to detect pathogens. Specifically, on wheat leaves, AxC 169 variety, infected with *Septoria tritici* (the wild-type IPO 323). In this experiment, we will explore OCT images to assess how effectively OCT detects *Septoria* and link the results with findings from other techniques, such as confocal microscopy and SEM.

## 2. Results

The first step in this proof of concept was to choose the seeds that is the most venerable to *Septoria tritici* fungus to ensure effective preparation of infected wheat specimen with clear symptoms. Using a more resistant variety would only delay this initial study. My result show both AxC169 and AxC157 wheat varieties are highly susceptible to *Septoria* (wild-type strain IPO323), with yellow spots appearing approximately 8–11 days and 12–13 days after inoculation, respectively. Therefore, AxC169 was selected as the primary focus for this research.

The following section presents the external morphology observed daily through OCT experiments during the period of 15 days. Only one leaf is shown per set of controlled (mock) and infected plants. Alongside with microscopic and SEM images showing both the presence and absence of *Septoria* infection. Imaging results are then compared with OCT technique.

### a) External morphology

The next figure (Figure 50) presents daily observations of both mock (control) and infected leaves with *Septoria tritici*. Symptoms, such as yellow spotting, began to appear on Day 7 and progressively increased in severity through Day 14.

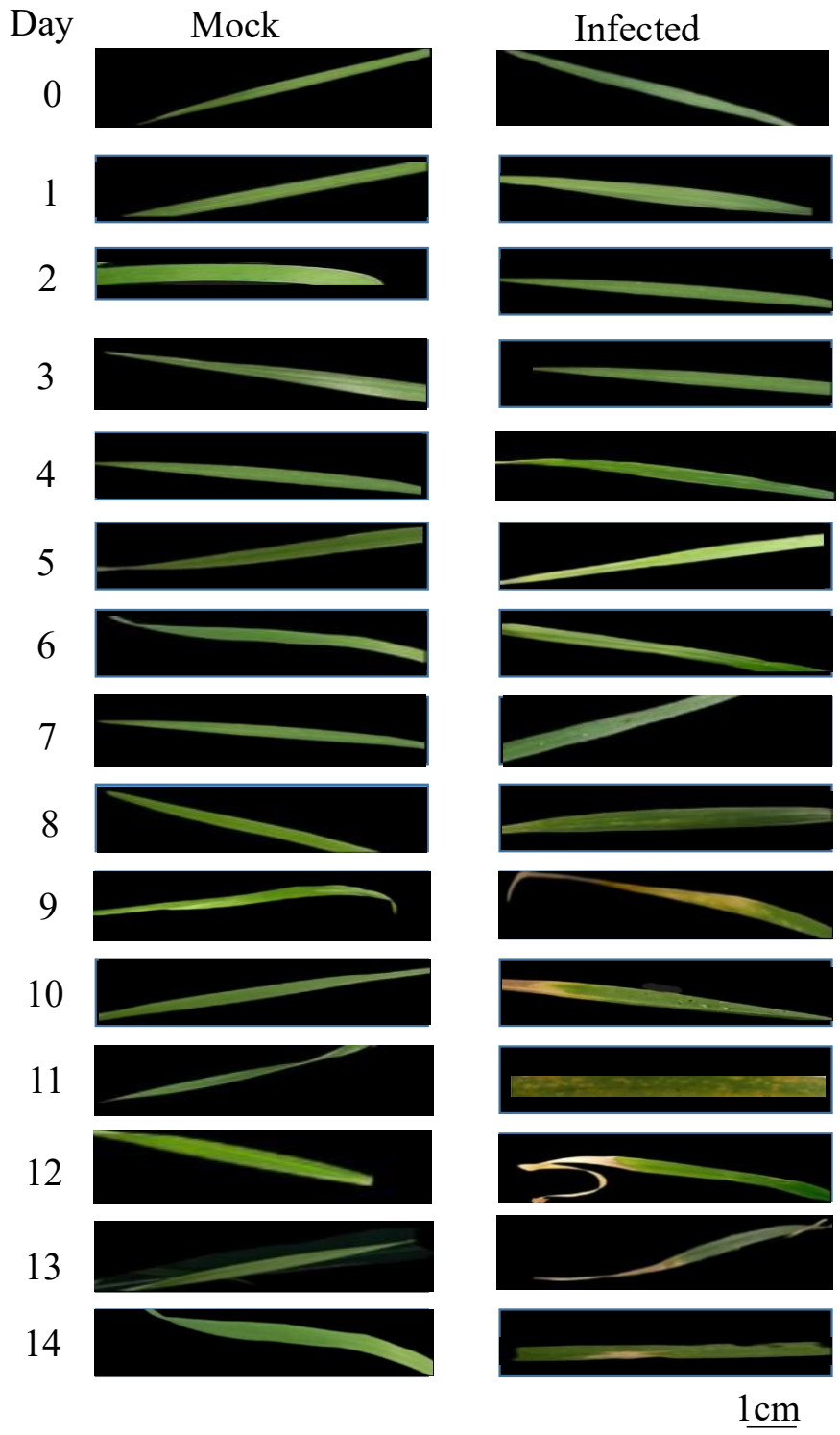


Figure 50: Imaging the same leaf everyday shows the various stages that wheat leaves, starting at 21-day-old, undergo when exposed to *Septoria* tritici. Visible yellow spots begin to form on day 7, rapidly increasing until they develop into damaged areas in the later stages of infection, from day 9 to day 14.

b) Epifluorescence microscopy

The aim of this experiment is to compare control, and infected wheat leaves with *Septoria tritici* six days after inoculation, using CWS under an epifluorescence microscope. The result is that fungal hyphae in the infected leaves in Figure 51 (B) will be stained, appearing as dark structures around the stomata due to the binding of CWS to the fungal cell walls. In contrast, the control leaves are expected to appear clear, with no staining observed as shown in Figure 51 (A).

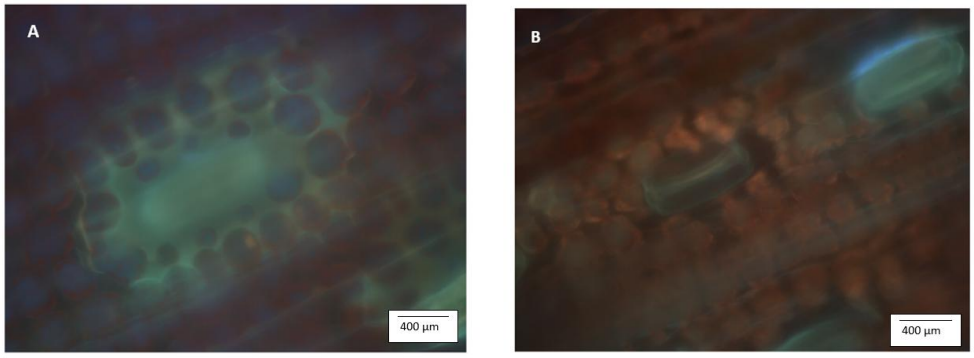


Figure 51:(A) Is a control leaf (27-day-old) stained with CWS, and (B) is the infected leaf with *Septoria tritici* (after 6 days of inoculation) stained with CWS. (A) appears there is no sign of the infections within mesophyll cells while (B) shows the fungus grows within mesophyll cells. The images were taken under an epifluorescence microscope (scale bar 400 µm), with an exciting wavelength between 460-490 nm.

c) Visualization of Trichomes with SEM

This study utilized SEM to observe the effects of fungal infection on trichomes. As shown in Figure 53, fungal stress clearly damages the trichomes when compared with the control (Figure 52). This damage makes it difficult to accurately evaluate trichome number or length using OCT images due to their blurriness. Given this limitation, the study instead prioritizes the analysis of the inner tissue structures of infected wheat plants.

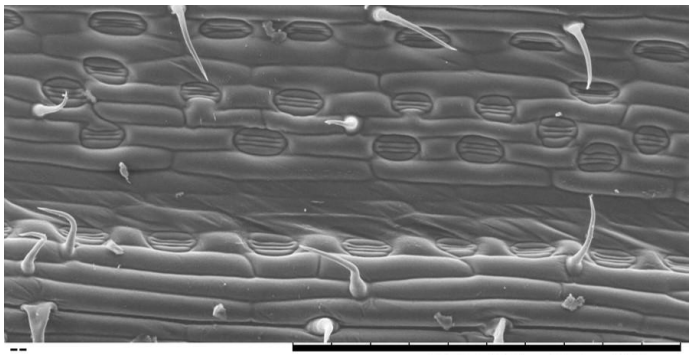

Figure 52: SEM images of a non-infected wheat leaf, illustrating trichomes with full length. Scale bar 500µm.

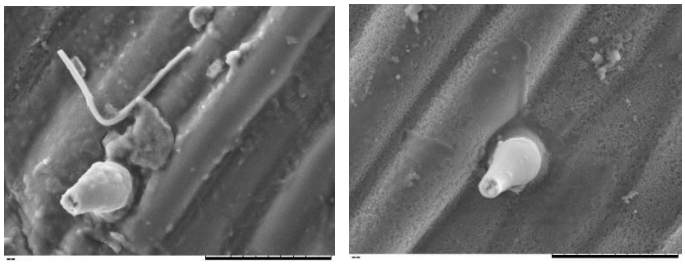

Figure 53: Presents SEM images of an infected wheat leaf, 31-day-old, taken after 10 days of inoculation. The SEM image reveal some broken trichomes, which correlates with the decrease observed in both the length and number of trichomes in OCT images. Scale bar 50µm.

d) Visualization of Septoria hyphae with SEM

Figure 54, illustrates cross- section cutting and SEM, used to visualize fungal infection within the mesophyll. The images reveal fungal hyphae between tissue layers in infected wheat leaves (B and C), compared to the non-infected leaf (A).

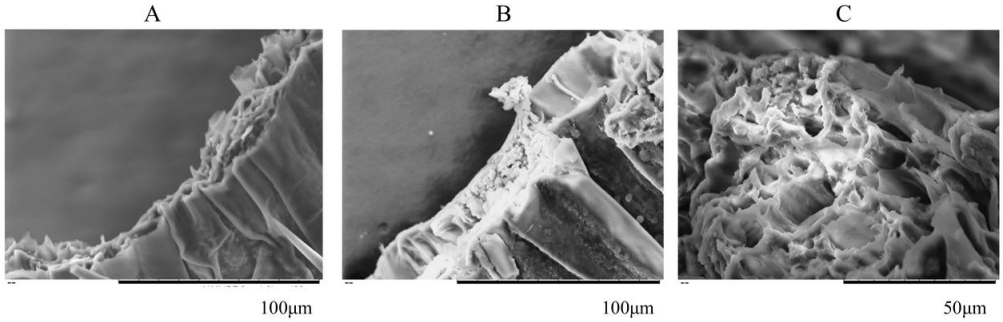


Figure 54: Cross- section cutting and SEM of wheat leaf, 31- day- old. (A) Control leaf. (B and C) infected leaves after 10 days of inoculation.

e) Confocal microscopy

Confocal microscopy provides 2D and 3D images for non- infected leaf and infected wheat leaves. Figure 55, Figure 56, Figure 57, and Figure 58 stained with CWS at excitation wavelength 350-488 nm to illuminate the sample. Grayscale was used to get good quality image to detect *Septoria* spores and hyphae through stomata.

Figure 56 (B) and (C) show spores within the stomata between 3 and 11 days after inoculation, compared to the control (Figure 56 A). After 2 weeks, hyphal structures have already formed (Figure 56 D), and by three weeks after inoculation, the fungal growth progresses to a critical stage, as shown in Figure 56 (E).

Measurements of both the length and width of the hyphae in Figure 56 (E) were conducted using FIJI image software. The average hyphae length was 142.84 µm, and the average filament thickness was 2.302 µm.

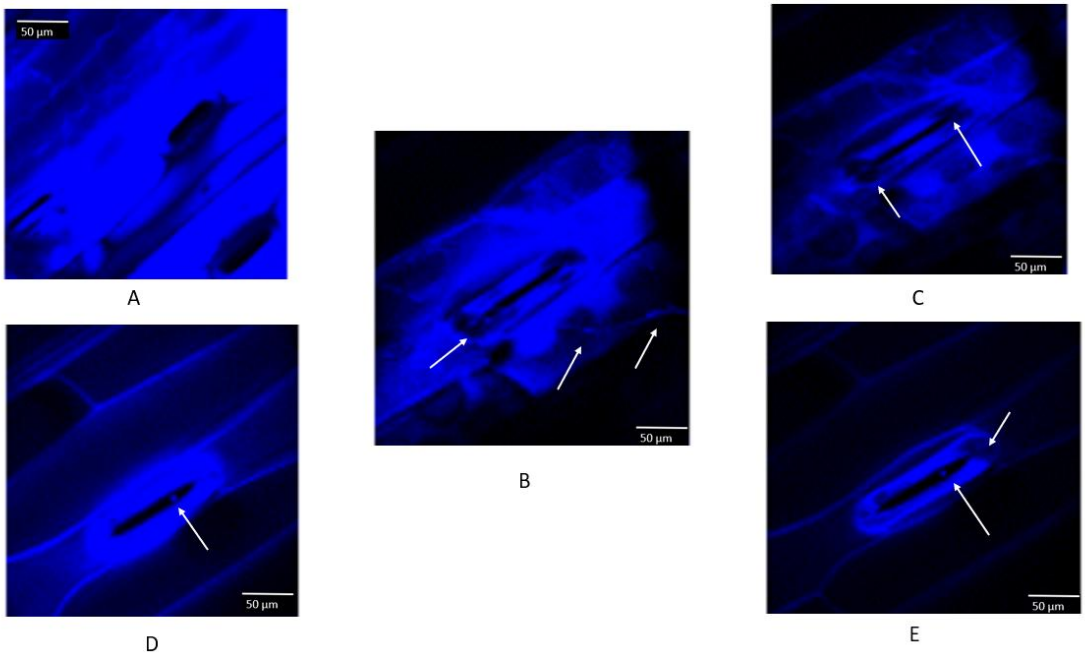


Figure 55: 2D images for wheat leaf , 28-day-old (A): A control wheat leaf with CWS under confocal microscopy (wavelength 350- 488 nm), ( B, C, D and D): four samples of wheat leaf infected with *Septoria tritici* after 7 days of inoculation and stained with calcofluor white stain. The images were taken under confocal microscopy (wavelength 350- 488 nm), scale bar 50µm.

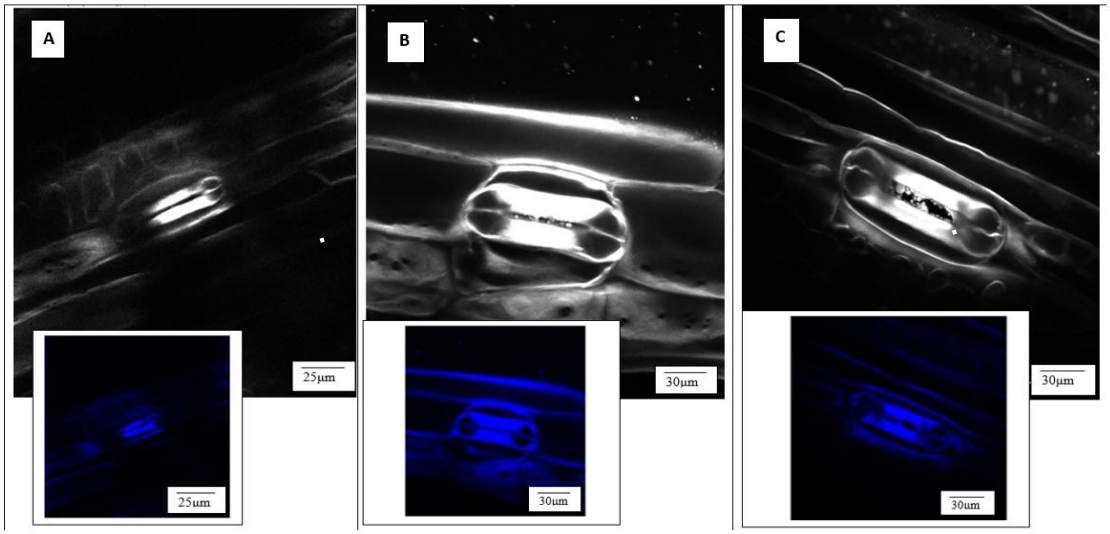

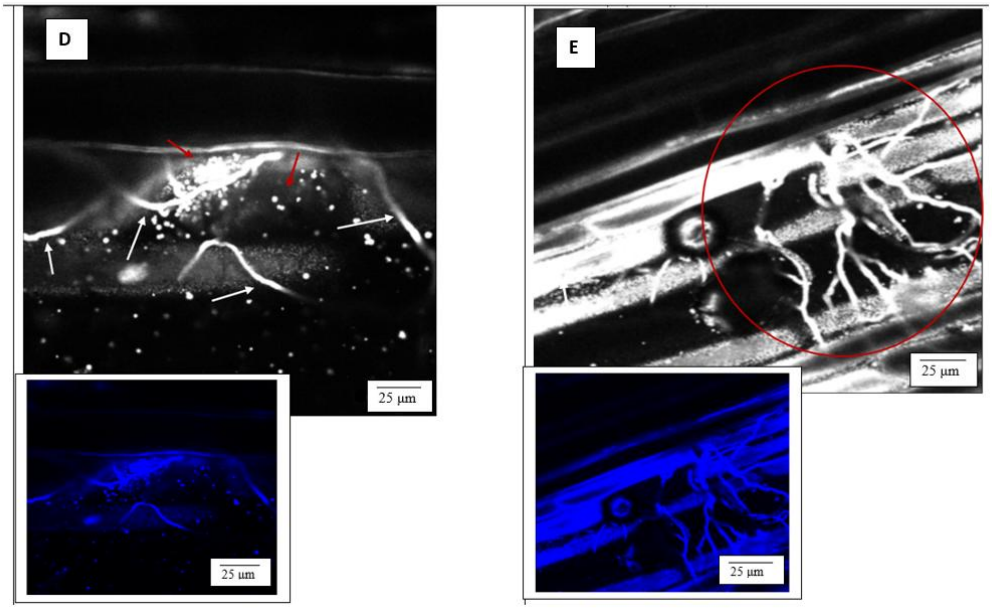


Figure 56: Shows the confocal microscope 2D images for wheat leaf , 32-day-old (A) a control (B) infected with *Septoria tritici* after 3 days of inoculation, (C) a wheat leaf (22-day-old) infected with *Septoria tritici* (After 11 days of inoculation), (D) a wheat leaf (35-day-old) infected with *Septoria tritici* (After 2 weeks of inoculation), (E) a wheat leaf (45-day-old) infected with *Septoria tritici* (After 3 weeks of inoculation). All images used CWS and using excitation wavelength between 350- 488 nm. (D) White arrows indicate *Septoria* hyphae come out from stomata and red arrows indicate spores around the stomata (E) the infection sign is clear, the developing of hyphae within the mesophyll and the plant has reached a critical stage in (E).

## f) 3D Confocal Microscopy Images

Three-dimensional images of stomata were obtained using confocal microscopy from both control (non-infected) and *Septoria tritici*-infected leaves at 15 days and 3 weeks after inoculation. The images were captured from both the upper and lower surfaces of the infected leaves. These 3D images reveal lesion formation resulting from fungal mycelium growth.

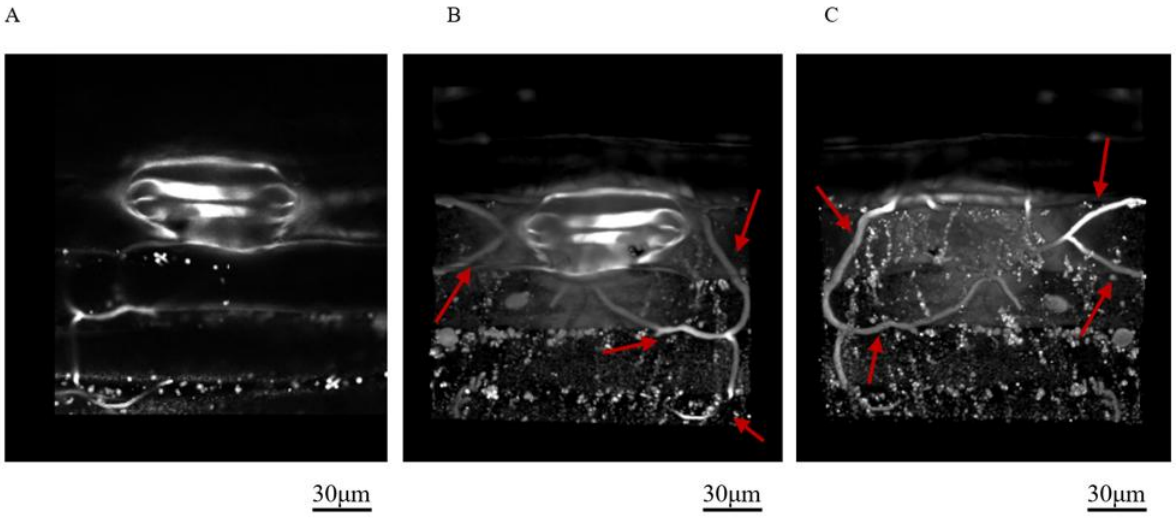

Figure 57: Confocal microscopy 3D images of 64 B scans of stomata:(A) control, non- infected leaf. (B) Infected leaf, after two weeks of inoculation. The image shows the mycelium in the top of the leaf (indicated by arrows). (C) shows the mycelium underneath the same leaf taken two weeks after inoculation (indicated by arrows).

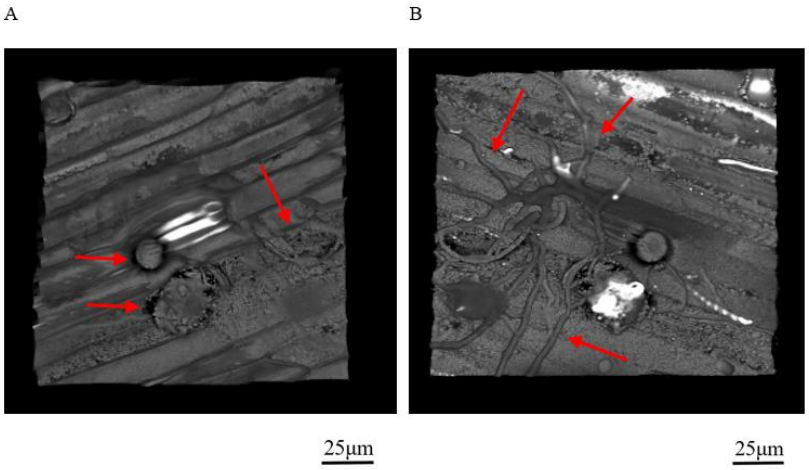


Figure 58: (A) Confocal microscopy 3D images of 108 B scans of a wheat leaf (45-day-old) taken after three weeks of inoculation, arrows show a lesion on the top of the leaf. (B) shows the mycelium underneath the same leaf.

## g) OCT imaging system

This section presents three-dimensional OCT images and compares images of non-infected and infected leaves to observe how *Septoria* infection appears using the OCT technique (Figure 59).

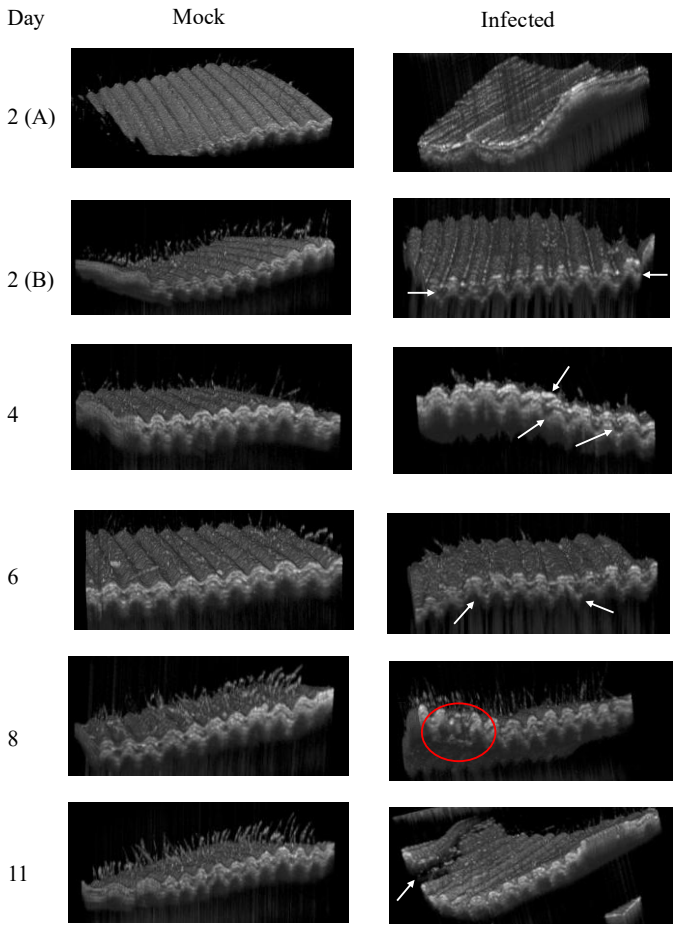


Figure 59: Representative 3D OCT images (C-scans, 5 mm × 5 mm) of wheat leaves from 21 to 32 days old, generated from 300 consecutive B-scans. Changes in leaf structure due to *Septoria tritici* infection are visualized across multiple time points. Infected leaves show progressive internal structural changes, including widening gaps, thinning trichomes, and tissue collapse, compared to control leaves. These alterations correlate with key stages of the *Septoria* life cycle, from early colonization to necrotrophic growth.

In Figure 59, Explore some three-dimensional OCT images (C-scans) for wheat plants, staring at 21-day-old, taken along the leaf's length. C-Scan has a range of 5mm x 5mm and is generated using 300 consecutive B-scans.

For this experiment, a control suspension was prepared by aiming to kill *Septoria* using UV radiation before spraying it onto the leaves. The live *Septoria* suspension was placed in a laminar flow cabinet within the laboratory equipped with a UV light emitting at a wavelength (λ) of 254 nm. The exposure routine consisted of two sessions, each lasting one hour of UV radiation per session.

OCT image on Day 2, (A) reveals the effects of exposing *Septoria*-suspension to UV radiation and then sprayed on wheat leaves (23-day-old). Notably, gaps start to emerge within the foliage, marked by either the absence of trichomes or the presence of notably tiny and thin trichomes.

Furthermore, the main vein of the leaves tends to orient upwards. Three replicates were performed, all showing the same results, which supports this effect. This phenomenon can be attributed to the properties of Tween 20 water, which contains fatty acid esters [261]. When subjected to UV radiation, the photons break bonds within the solution [262, 263]. Consequently, when this *Septoria* solution is exposed to UV radiation is sprayed onto the leaves, it accelerates the infection process, particularly evident one day after inoculation. The presence of acid and alcohol in the solution exerts harsh effects on the leaf tissue, causing damage and resulting in the removal of trichomes from the leaf surface. However, there are no data showing that all cells in a *Septoria* suspension are killed as the genome of *Z. tritici* contains many genes involved in repairing DNA damage from UV exposure [264]. Therefore, it is preferable to leave the control leaves sprayed with purified water, as discussed in Chapter II, in order to preserve their natural state.

On day 2, B, OCT image for non-infected leaves, 23-day-old, shows the upper surface of the wheat leaf, showing the trichomes appearing full length and thick and no wide gaps in the inner space. Unlike the infected leaves, their trichomes appear thin and short and the gaps are wider than the control one. According to *Septoria* life cycle, after 24-48 hours of pathogen attachment, the fungus grows in the spaces between the mesophyll cells, or “the inner space” as indicated by the arrows.

On day 4, there are primary signs of damage on the surface of the infected leaf, which are not visible to the naked eye, as shown in Figure 59. On Days 4, 6, and 8, the arrows in the OCT images of infected wheat leaves, aged 16, 18, and 20 days respectively, indicate an increase in gaps compared to the control. This is attributed to the growth of fungal hyphae within the mesophyll, as observed in comparison with the control leaves. According to the *Septoria* life cycle, 2–8 days after contact, the hyphae extend within the mesophyll, causing cells in the inner space to collapse and become destroyed, as indicated by the arrows.

On day 11, OCT for infected leaves with *Septoria*, 32-day-old, the yellow spots and necrotic areas on the leaves appear under OCT damage as indicated by the arrow due to the development of fungus in the later stages of infection. According to *Septoria* life cycle, 11-18 days after infection, this phase in the infection cycle is referred to as ‘necrotrophic growth’ which is the leaf increasingly becoming yellow and brown due to contents of dead or dying cells. These dead cells can still release elicitors, and the OCT images may indirectly capture the plant’s ongoing responses to these signals [265, 266].

In the next section, some two-dimensional OCT images are explored OCT images for both infected and non-infected leaf staring at age 21-day-old (Figure 60).

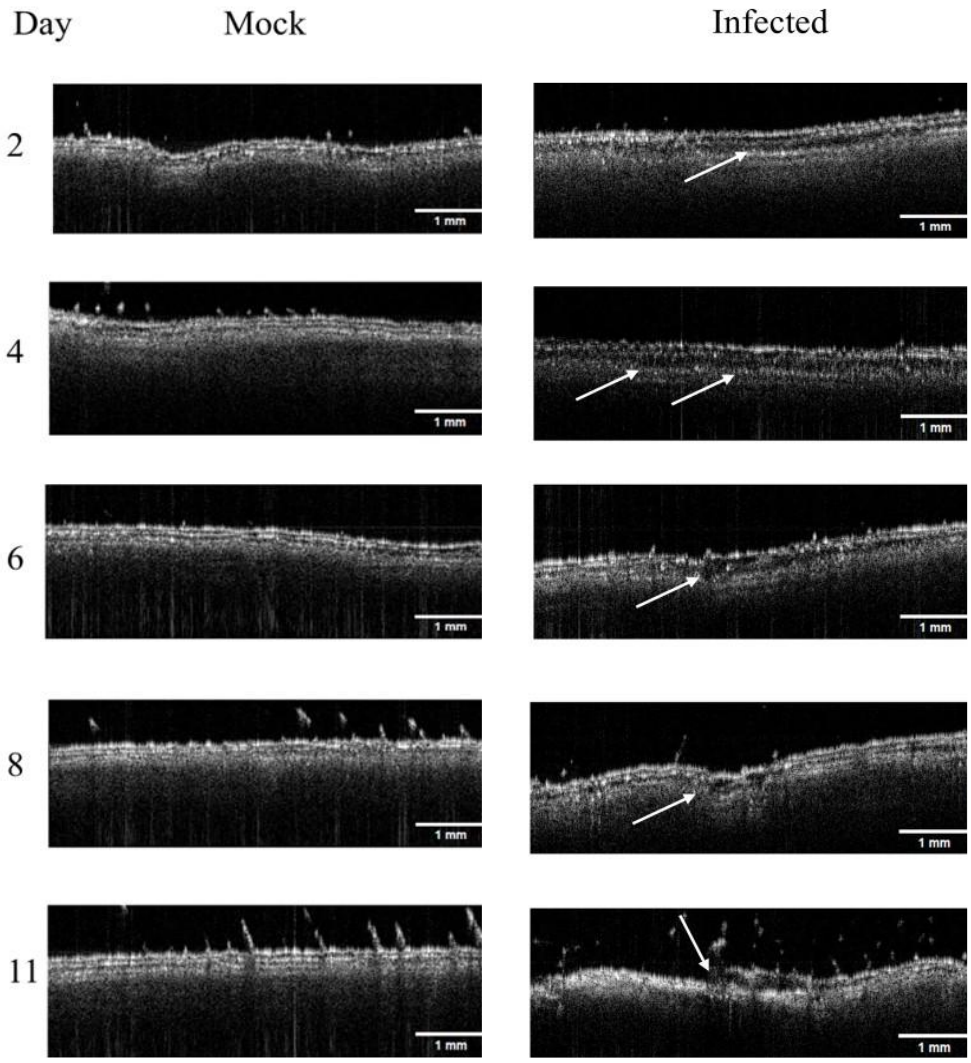


Figure 60: Explore some two-dimensional OCT images, time-lapse data for control and infected leaves with *Septoria*, for wheat plants, starting at 21-day-old, taken along the leaf's length. The scale bar is 1mm.

Figure 60 demonstrates OCT's adequacy by using a low-cost, compact commercial system to acquire cross-sectional images of leaves (~6 × 2 mm) with approximately 10 micrometre resolution. Although the system only resolves the first 3-5 cell layers, this resolution is sufficient to monitor internal structural differences between intact and infected leaves. The project thus consists of examining the internal structure of leaves through cross-sectional OCT images. The hypothesis is to indirectly monitor the growth of the fungus within the mesophyll, which is expected to push apart the different cell layers. And although the fungus' hyphae are

too small (~2µm in diameter [160]) to be seen via OCT, the spacing between these cell layer is readily monitored.

On day 2, OCT image for the infected leaves, the gaps the first 2-3 cell layers are wider than the control leaf. According to *Septoria* life cycle, after 24-48 hours of pathogen attachment, the fungus grows in the spaces between the mesophyll cells, or "the inner space" as indicated by the arrows.

On days 4, 6 and 8, the arrows in the wheat leaves, aged 16, 18, and 20 days respectively, indicate the collapse of the inner spaces due to the growth of fungal hyphae within the mesophyll, as observed in comparison with the control leaves. According to the *Septoria* life cycle, 2–8 days after contact, the hyphae extend within the mesophyll, causing cells in the inner space to collapse and become destroyed, as indicated by the arrows.

On day 11, OCT for infected leaves with *Septoria*, 23-day-old, the yellow spots and necrotic areas on the leaves appear under OCT damage as indicated by the arrow due to the development of fungus in the later stages of infection. According to *Septoria* life cycle, 11-18 days after infection, this phase in the infection cycle is referred to as 'necrotrophic growth' which is the leaf increasingly becoming yellow and brown due to contents of dead or dying cells.

## 3. Conclusion

*Septoria* hyphae can be directly identified using epifluorescence, confocal, and SEM due to the high resolution of these techniques. However, OCT detects the disease indirectly by revealing increased gaps in the mesophyll tissue, as expected in response to fungal infection. In the next chapter, a detailed analysis of these apparent gaps is presented through segmentation.

## Chapter V: Early detection of infection via OCT image segmentation

Early detection of crops infection by fungus is the very first step to deploying a timely and effective treatment. Early and reliable detection is thus key to improving yields, sustainability, and achieving food security. This study demonstrates the use of low-cost OCT to monitoring wheat (cultivar AxC 169) when infected by *Septoria tritici*. This study shows that OCT analysis can effectively detect signs of infection before any external symptoms appear. Although OCT cannot directly visualize fungal hyphae, OCT reveals that apparent "gaps" in OCT scans appear where the fungal hyphae are expected to develop. This study thus focuses on monitoring and correlating the mesophyll's structural organisation with the state of infection. Such an analysis shows distinct difference between intact and infected wheat plants starting two days only after infection. Finally, machine learning is applied for high throughput segmentation of OCT scans, providing a foundation for future automated fungus-detection analysis.

### 1. Introduction

The scientific question addressed here is: Can automated segmentation of OCT images reliably detect and differentiate infection-induced structural changes in wheat leaves? This question is important because while manual segmentation is accurate, it is time-consuming, subjective, and impractical for large-scale monitoring. Automating the segmentation process enables high-throughput, consistent analysis of leaf microstructures, making it feasible to detect early fungal infections across extensive crop populations. Developing robust image analysis algorithms for OCT data is therefore essential for scaling up this diagnostic technique and integrating it into precision agriculture systems.

Several software tools have been specifically developed for OCT image analysis and segmentation, primarily within the medical field most notably in ophthalmology and cardiology. Many of these tools incorporate machine learning (ML) algorithms to enhance segmentation accuracy and support automation, thereby minimizing the need for manual intervention. For example, Livelayer, is a semi-automatic software designed for segmenting retinal layers and detecting pathologies such as diabetic macular edema (DME) [267, 268]. Other tools have been developed specifically for retinal OCT image segmentation [269-271] cardiac OCT image segmentation [272-275], and for the analysis of various other pathological conditions [276, 277].

In comparison, there are currently no widely established OCT segmentation software tools developed specifically for plant research that match the sophistication of those in the medical domain. Researchers working with OCT in plant sciences typically adapt general-purpose image analysis platforms or develop custom algorithms and software to segment and analyze plant microstructures. Commonly used tools in this field include ImageJ/Fiji and MATLAB, which offer flexibility for custom segmentation workflows.

Given this context, this chapter will discuss the potential applications of ML techniques for the segmentation and analysis of OCT images in plant research, highlighting opportunities for improving the accuracy, efficiency, and scalability of plant tissue imaging studies.

This work aims to analyse differences in mesophyll structure between control and infected leaves to provide insights about the state of infection and tissue integrity. In healthy control leaves, thinner and more uniform cell layers typically indicate intact tissue structure. Conversely, in infected leaves, the monitored increase in layer thickness and irregularity of the cell layers may suggest structural degradation, possibly due to the accumulation of fungal material between the cells [169, 184].

## 2. Results

### a) SEM images

The effectiveness of the inoculation procedure is demonstrated in Figure 61, where hyphae can be seen emerging from the stomatal pores of infected leaves 12 days after inoculation. At this stage, visible symptoms “yellow spots” are already present on the wheat leaves. This test is essential to confirm that all OCT segmentation of infected plants at very early stages corresponds to fungal development, even when the plants still appear healthy and green.

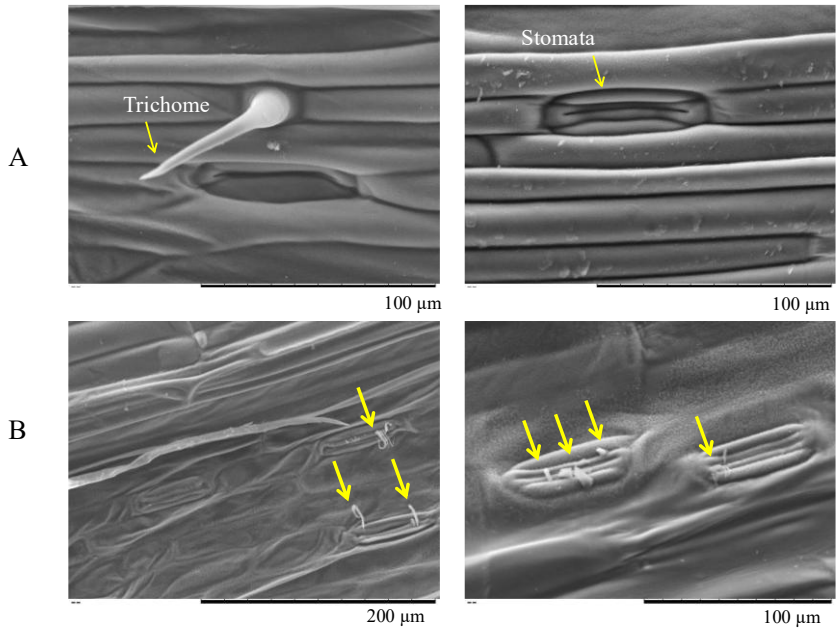


Figure 61: SEM images showing control wheat plant (A), and infected wheat plant 12 days after inoculation by Septoria (B). Arrows indicate hyphae located at stomatal pores. This corresponds to an advanced stage of colonisation (stage 4) with signs of necrosis (deflated cells, stage 5).

b) Manual segmentation of OCT image

It is also worth noting that healthy leaves already have air gaps within their mesophyll (as shown in Figure 62-A), which it uses to facilitate gas exchange [236]. But these interstitial spaces notably increase when the plant is infected, while the leaves are still green and seemingly healthy, as shown in Figure 62-B, D.

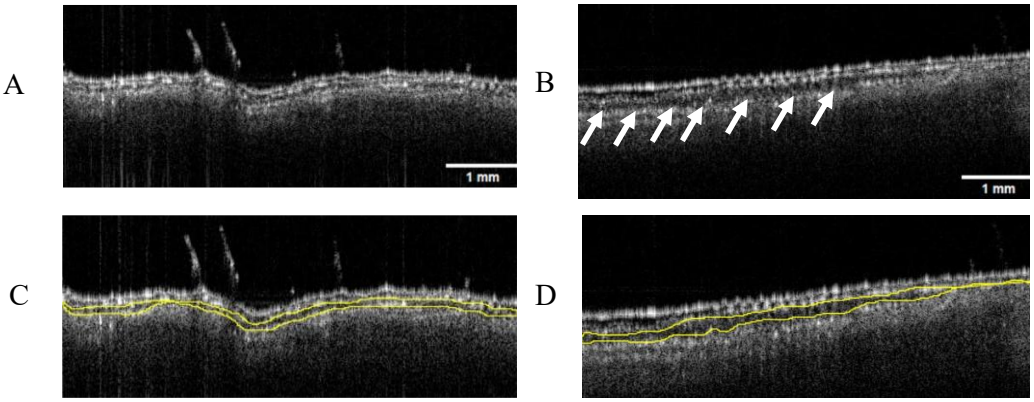


Figure 62: Individual B-scan of non-infected (control) wheat leaf (A) and infected wheat leaf taken 3 days after inoculation (B). The arrows indicate a larger gap between the second and third cell layers. Scale bars represent 1mm. (C and D) Example of manual segmentation in the first 2-3 cell layers using the freehand Tool within FIJI image for a control (C) and an infected (D) wheat leaf, 4 days after inoculation.

These interstitial spaces, or dark regions, are however highly heterogeneous and not easily distinguished (given the uneven leaf morphology). As such it was decided to restrict the analysis to the thickness (or height) of the apparent inter-cellular gap.

The following table (Table 3) shows the average thickness of the gaps present in a selection of 20 OCT scans out of each volumetric reading, for both control and infected leaves, ranging from day 0 (i.e. right before inoculation) to Day 1 (i.e. 24h after inoculation) and up to Day 7. Every day, one reading was performed per plant, on the three different controlled and 3 different infected plants.

Table 3 : Mean thickness of the apparent gap from Day 0 (right before inoculation) to Day 7 (after inoculation) of wheat leaves with *Septoria* (One reading per plant, on three different controlled and 3 different infected plants). Every mean value is an average of 250 individual thickness measurements taken manually from a selection of 20 OCT scans out of each volumetric reading. For each day, only a single image of the inoculated leaf is shown to appreciate its lack of external symptoms. The unit of the "mean ± standard deviation (SD)" is expressed in millimeters (mm).

| | Day 0 | | | | | | Day 1 | | | | | |
|---|---|---|---|---|---|---|---|---|---|---|---|---|
| | Control | | | Infected | | | Control | | | Infected | | |
| | R1 | R2 | R3 | R1 | R2 | R3 | R1 | R2 | R3 | R1 | R2 | R3 |
| Mean ± SD | 0.055±0.018 | 0.046±0.016 | 0.048±0.017 | 0.045±0.015 | 0.0463±0.015 | 0.049±0.017 | 0.044±0.015 | 0.038±0.015 | 0.0412±0.014 | 0.0496±0.014 | 0.0543±0.009 | 0.0499±0.015 |
| Image |  1cm | | |  1cm | | |  1cm | | | 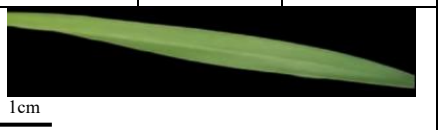 1cm | | |
| | Day 2 | | | | | | Day 3 | | | | | |
| | Control | | | Infected | | | Control | | | Infected | | |
| | R1 | R2 | R3 | R1 | R2 | R3 | R1 | R2 | R3 | R1 | R2 | R3 |
| Mean ± SD | 0.039±0.014 | 0.041±0.014 | 0.0431±0.016 | 0.051±0.019 | 0.068±0.026 | 0.067±0.024 | 0.039±0.014 | 0.039±0.013 | 0.042±0.014 | 0.067±0.024 | 0.075±0.027 | 0.082±0.028 |
| Image |  1cm | | |  1cm | | |  1cm | | |  1cm | | |
| | Day 4 | | | | | | Day 5 | | | | | |
| | Control | | | Infected | | | Control | | | Infected | | |
| | R1 | R2 | R3 | R1 | R2 | R3 | R1 | R2 | R3 | R1 | R2 | R3 |
| Mean ± SD | 0.042±0.015 | 0.049±0.015 | 0.046±0.013 | 0.076±0.024 | 0.082±0.03 | 0.073±0.024 | 0.049±0.02 | 0.049±0.02 | 0.054±0.02 | 0.068±0.03 | 0.069±0.03 | 0.083±0.03 |
| |  1cm | | |  1cm | | |  1cm | | |  1cm | | |
| | Day 6 | | | | | | Day 7 | | | | | |
| | Control | | | Infected | | | Control | | | Infected | | |
| | R1 | R2 | R3 | R1 | R2 | R3 | R1 | R2 | R3 | R1 | R2 | R3 |
| Mean ± SD | 0.05±0.017 | 0.047±0.018 | 0.053±0.02 | 0.082±0.04 | 0.063±0.024 | 0.067±0.02 | 0.044±0.02 | 0.04±0.017 | 0.046±0.02 | 0.073±0.024 | 0.083±0.03 | 0.07±0.024 |
| Image |  1cm | | |  1cm | | |  1cm | | |  1cm | | |

When analysing the individual measurements used to compute the averages shown in the above table, the measured gap thicknesses reveal distinct trend between control and infected leaves, as depicted in Figure 63. From day 1 after inoculation onward, infected leaves exhibit consistently larger gap thicknesses, exceeding 0.05 mm in average, while measurements on control leaves remains below or around that value. Furthermore, the width of the Gaussian-fit for the infected leaves group is typically broader (FWHM ~0.2 compared to that of the control group (FWHM ~0.15). Accordingly, the apparent gaps in infected leaves are more heterogenous than those in intact leaves. This increased in gap thickness and in heterogeneity of the gap size is expected to be a direct result of the mesophyll colonisation by the hyphae (stage 4). However, other fungal-associated factors may also contribute, such as the recognition of fungal PAMPs by plant immune receptors or changes in water potential arising from altered stomatal behaviour [278, 279]. As discussed earlier, colonisation of the mesophyll is initiated by the very first hyphae intrusion through a stoma (stage 3). The fact that we start monitoring an increase in gap thickness as early as 24h after inoculation (instead of day 3, as per Fantozzi, E., et al. [179]) can be a result of our choice of cultivar. Indeed, AxC 169 variety was chosen, which is considered one of the varieties susceptible to *Septoria*. It is also possible that inoculation via spray facilitates entry of the developing hyphae through the stomata. It has been shown that spore germination typically occurs within 12 hours after contact with a leaf when humidity levels are high [30]. And while the presence of water droplets is not expected to trigger any direct reaction from the stomata, the overall increased humidity due to the spray implies that most stomata will be open [280], thus facilitating entry of the hyphae within the first 24 hours. It is also possible that upon the first intrusion event, before full colonisation takes place, the whole plant reacts by modifying its mesophyll structure, which might give rise to the increased in apparent gap thickness. If such is the case, this study still demonstrates that OCT can effectively be used to detect early signs of infection by monitoring the increased intercellular spacing.

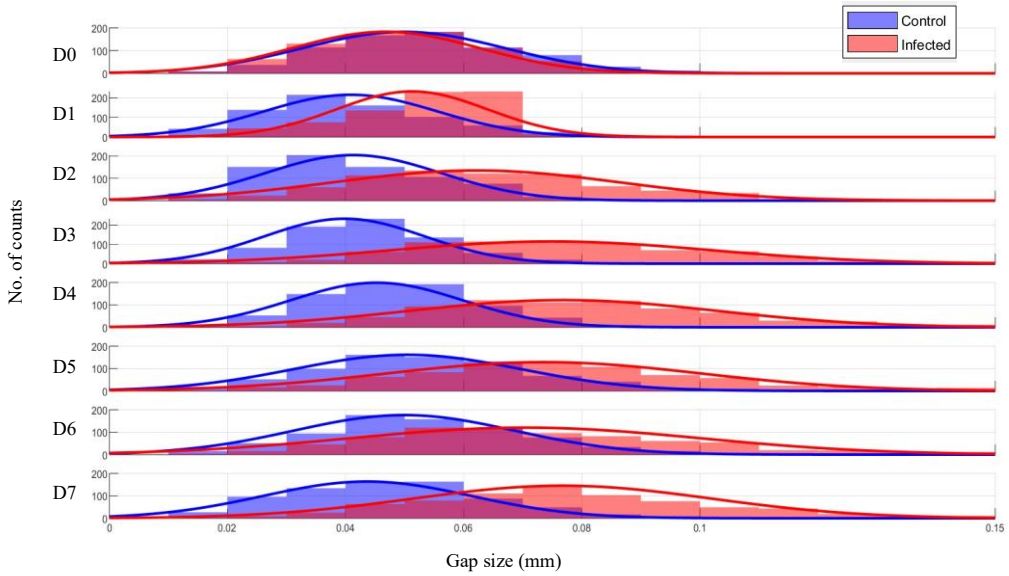


Figure 63: Void size distribution for manual thickness measurements from Day 0 to Day 7. Superimposed histograms of control (blue) and infected leaves (red) groups with their Gaussian fits. The histograms used a bin width of 0.01 mm.

It can be seen in Figure 63 that the superimposed histograms show the distributions of the two groups (control and infected) are clearly different. From the average gap values, we could theoretically set a threshold value for the average gap's thickness of 0.05 mm, above which the leaf can be classified as being infected. If such was the case, effective assessment of infection could already be made from day 1 and affirmed from day 2 after inoculation.

The following section introduces a custom software tool, developed specifically for this project, to perform automated segmentation, focusing on the potential rather than the actual detection of infection, to clarify that we are monitoring regions of varying optical density, not the fungus itself.

c) Automated segmentation of OCT image

Building upon the encouraging results from the manual analysis, a machine learning (ML) algorithm was developed in collaboration with Cyber Infrastructure Systems (CIS, http://www.cisin.com) to automatically segment these apparent gaps and classify the leaves. The Python code designed for OCT segmentation is a PyQt5-based GUI application that uses OpenCV, TensorFlow, NumPy, and Pandas for image processing and ML-based analysis. After training, the U-Net model (unet_masking3.keras) is used for generating segmentation masks via MaskThread class. The code is provided in appendices.

The automated procedure, like the manual one, focuses on analyzing the thickness of apparent gaps between the second and third upper layers of the mesophyll.

To further benefit from OCT's fast scanning rate and systematically processing large stacks of OCT images, a bespoke machine learning (ML)-based software for image segmentation was used instead of the manual labelling. The automated analysis is based on the same concept as the previous manual analysis: it aims to segment the apparent gap between the second and third cell layer within the defined region of interest (ROI) and compute its averaged thickness. Example of the automated segmentation is shown in Figure 64.

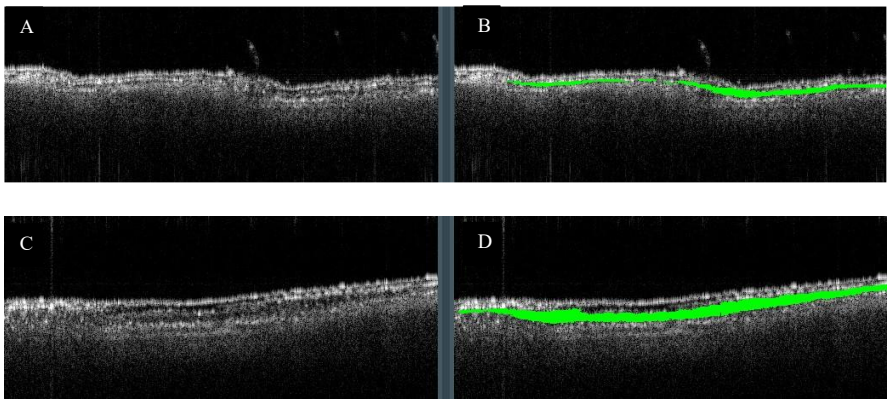


Figure 64: Examples of automated segmentation using OCT image analysis to classify the spacing between the second and third cell layers in a control wheat leaf (A) with ROI (B), and an infected leaf (C) with ROI (D), 2 days after inoculation.

In comparison to the previous analysis, for each day and for each of the three OCT volumetric readings on control and infected plants, 200 images are selected (instead of 20 for the manual analysis) and analysed using the ML-based software. The computed average thickness of the segmented gap from each image is used to build the histograms shown in Figure 65.

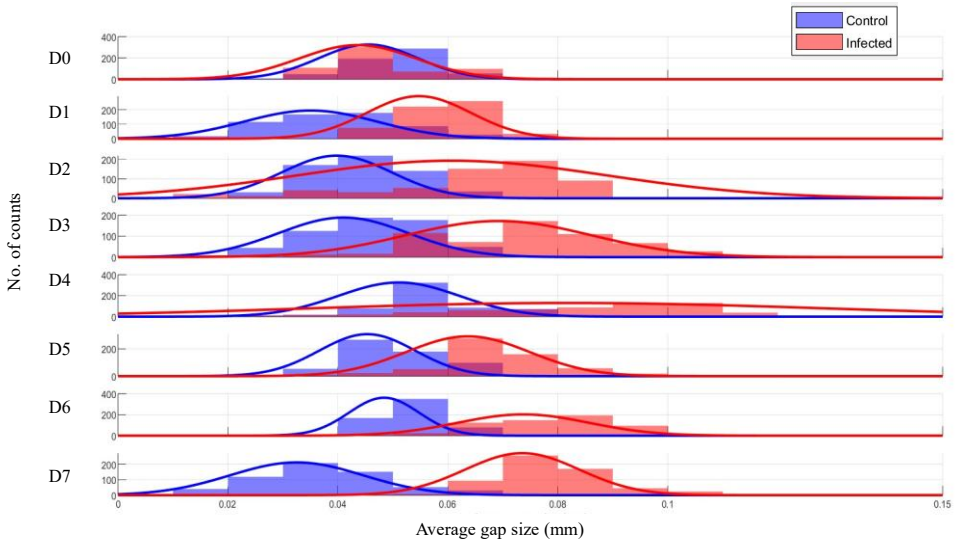


Figure 65: Average gap size distribution in control (blue) and infected (red) wheat leaves extracted from automated segmentation, from D0 to D7 after inoculation, with superimposed Gaussian fits. The histograms use a bin width of 0.01 mm.

The results from the ML-based image analysis appear more scattered compared to the previous manual analysis. This scattering might be a direct consequence in the apparent difficulty in adequately segmenting the OCT images, which is in part due to the uneven leaf structures. Although histograms resulting from the automated segmentation analysis are not as consistent compared to those generated from the manual analysis, a similar pattern nonetheless emerges. Starting from day 1 after inoculation, the apparent gaps in infected leaves are consistently larger compared to those in intact leaves. And similarly, the widths of the Gaussian fits in infected leaves are also larger compared to those in controlled leaves. Accordingly, these differences could be used as markers to automatically distinguish between controlled and infected leaves.

It is also important to note that the ML-based segmentation software was here trained using the AxC 169 variety. The same automated procedure was used on images taken from another variety (AxC 157) and yielded, to a lesser extent, similar results (i.e. broader Gaussian fit and shifted Gaussian centre toward larger gap size for infected leaves, this outcome is consistent with the expectation that the Cadenza background introduces some resistance. results shown in SI). One main difference between the two varieties is that intact leaves from cultivars AxC157 have already larger apparent gaps between the second and third cell layers (of ~ 0.06 mm). Therefore, the distinction between infected and intact cannot be based on a single threshold value across different cultivars.

Overall, the current ML-based analysis, with its unique distinguishing parameter, is shown to already be promising in differentiating between infected and intact plants, with the caveat that

a single threshold value might not be common to differing cultivars. To circumvent this limitation, it is planned to pursue such studies to include more parameters to take into account the 3-dimentional shape of the gaps since it is readily available from the OCT volumetric scans. Additionally, the training model will be improved by expanding the study to multiple wheat varieties.

## 3. Conclusions

In this proof-of-concept experiment, low-cost OCT was demonstrated to be a promising tool for effective detection of infections before any visible signs appear on the plant. Systematic analysis of several thousands of images acquired, over time and non-invasively, is made possible by using bespoke ML-based analysis. And although the analysis currently relies on a single parameter (apparent gap thickness), clear differences between controlled and infected leaves can be seen from day 1 after inoculation. Accordingly, OCT imaging holds the promise for quick and accurate identification of infection, even at an asymptomatic stage. The application of OCT coupled with ML analysis thus presents a valuable opportunity to assess crop's health more effectively and enables timely treatments. By harnessing and combining these cutting-edge technologies, this work paves the way to revolutionizing agricultural practices by helping farmers mitigate crop losses, enhance sustainability, and contribute to global food security.

# Chapter VI: Conclusion and Future Work

## 1. Conclusions

This thesis employed an interdisciplinary research approach to evaluate the suitability of OCT for the early detection of plant infections, particularly focusing on *Septoria tritici* in wheat leaves. A series of experiments and analyses were conducted to address the following key research questions:

1. Why were wheat plants chosen as the host, *Septoria* as the pathogen, and OCT as the imaging tool for this research?
2. Why was the AxC169 mapping population used instead of the parental lines Avalon and Cadenza?
3. Why should OCT be evaluated for plant research applications?
4. Which parts of the wheat plant yield meaningful OCT imaging data?
5. Can OCT detect *Septoria tritici* at early stages of infection?
6. What are the strengths and limitations of OCT as an imaging tool in plant research?
7. How can machine learning (ML) enhance OCT image segmentation and analysis for plant research?
8. What are the next steps for evaluating the application of OCT in agricultural settings?

To address these questions, wheat is a staple food crop and the main ingredient in many foods. It is rich in carbohydrates, proteins, minerals, and other essential nutrients, making it vital for global food security. Beyond its nutritional role, wheat also holds high commercial value, as many countries rely on it to support their national income, which makes this crop particularly interesting for plant research. *Septoria tritici* is a fungal pathogen that infects wheat and can cause yield losses of up to 40%. Reducing its impact and minimizing the need for chemical treatments were central aims of this study. OCT is a live imaging technique that operates in real time and in vivo. It provides non-invasive cross-sectional and three-dimensional images, making it well suited for plant research. This proof-of-concept study demonstrates its capability and highlights its potential for broader application in plant science.

AxC169 variety seeds from this mapping population are widely available in research seedbanks and have well-characterized resistance and susceptibility traits. The parental lines, Avalon and Cadenza, differ markedly in their response to *Septoria tritici* blotch (STB), with Avalon being

susceptible and Cadenza resistant. Using Cadenza to improve Avalon's resistance is a common and effective breeding approach. Crossing these lines introduces resistance alleles into Avalon's background, producing offspring that combine Avalon's desirable agronomic traits with Cadenza's resistance. This genetically defined and well-documented population is therefore ideal for testing OCT as a phenotyping tool.

A reliable *Septoria tritici* inoculation protocol was established, and plant growth was carefully managed under controlled conditions. A combination of microscopy techniques, including SEM, confocal, and epifluorescence, was used to validate infection progression and plant responses. These microscopic observations were essential for comparing direct visualization methods with OCT imaging.

Chapters IV and V demonstrate that OCT can detect early mesophyll disruptions in infected leaves, even when plants still appear visually healthy. The successful implementation of automated OCT image segmentation using ML significantly enhances processing efficiency. This opens promising pathways for high-throughput phenotyping and real-time plant disease monitoring. While automated OCT segmentation is well-established in medical imaging, especially in ophthalmology and cardiology, its application in plant sciences remains novel. This study confirms its feasibility and paves the way for broader adoption in agricultural diagnostics.

Although OCT provides high resolution, it cannot directly visualize fungal hyphae and instead detects them indirectly through changes in the internal leaf structure caused by pathogen development. Its penetration depth may also be insufficient for imaging thicker plant tissues. However, the penetration depth is adequate for studying leaves under biotic and abiotic stress, where OCT can provide detailed depth profiles. Furthermore, ML-based models require large, high-quality annotated datasets and rigorous validation to ensure robustness across different plant species and pathogens.

Despite these challenges, the findings of this research are promising and highlight the potential of OCT as a non-destructive, rapid imaging technique capable of detecting early structural changes associated with fungal infections. The integration of ML tools is amplified with this potential, suggesting that OCT could play a vital role in advancing precision agriculture and sustainable crop disease management in the future.

2. Future Work

Avalon and Cadenza are both UK winter and spring wheat cultivars that were originally grown as commercial varieties but later became especially valuable in research and mapping populations, such as the Avalon × Cadenza (AxC) population, which was developed to improve resistance to *Septoria tritici* blotch (STB). In this research, the AxC mapping population was used to build on previous genetic studies and to connect these findings with OCT imaging for morphological examination. For future work, it is highly recommended to apply OCT directly to the parental lines, Avalon and Cadenza, and perform gap thickness measurements to observe how *Septoria* develops in Avalon and why Cadenza exhibits resistance.

This research focuses on AxC169, but extending the analysis to other AxC lines, such as AxC157, could provide valuable baseline data on gap sizes and morphological differences across genotypes. Additionally, applying OCT to drought-stressed leaves or other abiotic stresses could reveal whether similar changes in mesophyll void spaces occur under environmental stress, thereby allowing differentiation between biotic and abiotic causes of tissue alterations.

The current software, which is based on Python code for OCT image segmentation, was trained specifically on a single wheat variety (AxC169). Future work should expand the dataset to include multiple wheat varieties and other plant species to improve the generalizability and robustness of the model. Furthermore, additional development is needed to incorporate classification capabilities, enabling the software not only to segment but also to determine whether a leaf is infected or healthy. Incorporating this functionality could significantly enhance its utility in precision agriculture, allowing for rapid screening and automated disease diagnosis across diverse crops.

In real field, it will also be critical to determine how farmers can reliably distinguish *Septoria* infection from other fungal pathogens or environmental stresses using OCT. For example, environmental stress typically affects all plants in a given area, whereas biotic stresses such as fungal infections usually impact only some plants. This distinction highlights the need to educate farmers on how to collect OCT images in the field, which can then be analyzed with OCT analyzer software to extract meaningful data.

The findings for AxC169 and some experiments on AxC157 lines, presented as Excel files in the SI, provide a foundation for such analyses and allow reviewers and researchers to perform

their own statistical tests or export the data for further analysis via Google drive. It would be valuable to perform more rigorous statistical analyses, in addition to gap thickness measurements, such as t-tests or calculation of p-values, to quantitatively assess differences between groups. When comparing two groups, it is important to determine whether the observed differences are real or could have occurred by chance. A t-test helps assess whether the means of two groups differ significantly, while the p-value provides the probability that the observed difference arose by chance. A low p-value (commonly $< 0.05$) indicates statistical significance. Such analyses move beyond visual comparisons (e.g., Gaussian histograms) and provide stronger, quantitative evidence of group differences.

Integrating OCT with additional biomarkers or sensors, such as measurements of leaf water potential, stomatal conductance, or chlorophyll fluorescence, could provide a more robust analysis of crop stress physiology, informing the most appropriate management responses for farmers.

Finally, for widespread adoption in agricultural settings, OCT systems should be designed to be cost-effective, user-friendly, and portable, ensuring practical utility for both researchers and farmers.

## References


1. Fercher, A. and E. Roth, *Ophthalmic Laser Interferometry*. 1986 International Symposium/Innsbruck. Vol. 0658. 1986: SPIE.
2. Wolfgang Drexler, M.L., Abhishek Kumar, Tschackad Kamali, Angelika Unterhuber, Rainer A Leitgeb, *Optical coherence tomography today: speed, contrast, and multimodality.* J Biomed Opt, 2014. **19**(7): p. 071412.
3. Fujimoto, J.G., S. De Silvestri, E.P. Ippen, C.A. Puliafito, R. Margolis, and A. Oseroff, *Femtosecond optical ranging in biological systems.* Optics Letters, 1986. **11**(3): p. 150-152.
4. Huang, D., E.A. Swanson, C.P. Lin, J.S. Schuman, W.G. Stinson, W. Chang, M.R. Hee, T. Flotte, K. Gregory, C.A. Puliafito, and J.G. Fujimoto, *Optical coherence tomography.* Science, 1991. **254**(5035): p. 1178-81.
5. Fujimoto, J., *Fujimoto, J.G. Optical coherence tomography for ultrahigh resolution in vivo imaging. Nat. Biotechnol. 21, 1361-1367.* Nature biotechnology, 2003. **21**: p. 1361-7.
6. Drexler, W., *Optical Coherence Tomography*, in *Encyclopedia of the Eye*, D.A. Dartt, Editor. 2010, Academic Press: Oxford. p. 194-204.
7. Sibylle Scholtz, a.L.M. *The 30-year history of optical coherence tomography of the human eye*. 2021 [cited 2021 Available from: https://europe.ophthalmologytimes.com/view/the-30-year-history-of-optical-coherence-tomography-of-the-human-eye.
8. Li, M., S. Landahl, A.R. East, P. Verboven, and L.A. Terry, *Optical coherence tomography—A review of the opportunities and challenges for postharvest quality evaluation.* Postharvest Biology and Technology, 2019. **150**: p. 9-18.
9. Sapozhnikova, V.V., V.A. Kamensky, R.V. Kuranov, I. Kutis, L.B. Snopova, and A.V. Myakov, *In vivo visualization of Tradescantia leaf tissue and monitoring the physiological and morphological states under different water supply conditions using optical coherence tomography.* Planta, 2004. **219**(4): p. 601-609.
10. Bouma, B.E., J.F. de Boer, D. Huang, I.K. Jang, T. Yonetsu, C.L. Leggett, R. Leitgeb, D.D. Sampson, M. Suter, B. Vakoc, M. Villiger, and M. Wojtkowski, *Optical coherence tomography.* Nat Rev Methods Primers, 2022. **2**.
11. Gabriele, M.L., G. Wollstein, H. Ishikawa, L. Kagemann, J. Xu, L.S. Folio, and J.S. Schuman, *Optical coherence tomography: history, current status, and laboratory work.* Invest Ophthalmol Vis Sci, 2011. **52**(5): p. 2425-36.
12. de Amorim Garcia Filho, C.A., Z. Yehoshua, G. Gregori, C.A. Puliafito, and P.J. Rosenfeld, *Chapter 3 - Optical Coherence Tomography*, in *Retina (Fifth Edition)*, S.J. Ryan, S.R. Sadda, D.R. Hinton, A.P. Schachat, S.R. Sadda, C.P. Wilkinson, P. Wiedemann, and A.P. Schachat, Editors. 2013, W.B. Saunders: London. p. 82-110.
13. Nanda, T., Michelle C. Liang, and Jay S. Duker. *Optical Coherence Tomography*. 2021 [cited 2023 Available from: https://retinahistory.asrs.org/milestones-developments/history-of-oct?utm_source=chatgpt.com.
14. Zeppieri, M., S. Marsili, E.S. Enaholo, A.O. Shuaibu, N. Uwagboe, C. Salati, L. Spadea, and M. Musa, *Optical Coherence Tomography (OCT): A Brief Look at the Uses and Technological Evolution of Ophthalmology.* Medicina (Kaunas), 2023. **59**(12).
15. Fujimoto, J. and E. Swanson, *The Development, Commercialization, and Impact of Optical Coherence Tomography.* Investigative Ophthalmology & Visual Science, 2016. **57**(9): p. OCT1-OCT13.
16. A F Fercher, W.D., C K Hitzenberger and T Lasser. *Optical coherence tomography - principles and applications*. 2003 2021]; Available from: https://iopscience.iop.org/article/10.1088/0034-4885/66/2/204.
17. GAO, W. and X. WU, *Differences between time domain and Fourier domain optical coherence tomography in imaging tissues.* Journal of Microscopy, 2017. **268**(2): p. 119-128.
18. Popescu, D.P., L.P. Choo-Smith, C. Flueraru, Y. Mao, S. Chang, J. Disano, S. Sherif, and M.G. Sowa, *Optical coherence tomography: fundamental principles, instrumental designs and biomedical applications.* Biophys Rev, 2011. **3**(3): p. 155.
19. Comsa, G. *The Coherence Length in Molecular and Electron Beam Diffraction*. in *Dynamics of Gas-Surface Interaction*. 1982. Berlin, Heidelberg: Springer Berlin Heidelberg.
20. Nassif, N., B. Park, M. Pierce, S. Yun, B. Bouma, G. Tearney, T. Chen, and J. Boer, *In vivo high-resolution video-rate spectral-domain optical coherence tomography of the human retina and optic nerve.* Optics Express, 2004. **12**: p. 367-376.
21. Leitgeb, R., C.K. Hitzenberger, and A.F. Fercher, *Performance of fourier domain vs. time domain optical coherence tomography.* Optics Express, 2003. **11**(8): p. 889-894.

22. de Boer, J.F., B. Cense, B.H. Park, M.C. Pierce, G.J. Tearney, and B.E. Bouma, *Improved signal-to-noise ratio in spectral-domain compared with time-domain optical coherence tomography.* Opt Lett, 2003. **28**(21): p. 2067-9.
23. Aumann, S., S. Donner, J. Fischer, and F. Müller, *Optical Coherence Tomography (OCT): Principle and Technical Realization*, in *High Resolution Imaging in Microscopy and Ophthalmology: New Frontiers in Biomedical Optics*, J.F. Bille, Editor. 2019, Springer International Publishing: Cham. p. 59-85.
24. Torre-Ibarra, M.H.D.l., P.D. Ruiz, and J.M. Huntley, *Double-shot depth-resolved displacement field measurement using phase-contrast spectral optical coherence tomography.* Optics Express, 2006. **14**(21): p. 9643-9656.
25. Teramura, Y., M. Suekuni, and F. Kannari, *Two-dimensional optical coherence tomography using spectral domain interferometry.* Journal of Optics A: Pure and Applied Optics, 2000. **2**(1): p. 21.
26. *Lumedica OQ Labscope 2.0*. Available from: https://www.lumedicasystems.com/oq-labscope/.
27. Sahyoun, Christine C., H. Molly Subhash, D. Peru, Roger P. Ellwood, and Mark C. Pierce, *An Experimental Review of Optical Coherence Tomography Systems for Noninvasive Assessment of Hard Dental Tissues.* Caries Research, 2019. **54**: p. 1-12.
28. Fercher, A., *Optical coherence tomography-development, principles, applications.* Zeitschrift für medizinische Physik, 2010. **20**: p. 251-76.
29. Fujimoto, J.G., *Optical Coherence Tomography: Principles and Applications.* The Review of Laser Engineering, 2003. **31**: p. 635-642.
30. Yang, S. and R.E. Rothman, *PCR-based diagnostics for infectious diseases: uses, limitations, and future applications in acute-care settings.* Lancet Infect Dis, 2004. **4**(6): p. 337-48.
31. Pinhero, A., A. M L, V. P, C.A. Visaggio, A. N, A. S, and A. S, *Malware detection employed by visualization and deep neural network.* Computers & Security, 2021. **105**: p. 102247.
32. Kior, A., L. Yudina, Y. Zolin, V. Sukhov, and E. Sukhova, *RGB Imaging as a Tool for Remote Sensing of Characteristics of Terrestrial Plants: A Review.* Plants, 2024. **13**(9): p. 1262.
33. Fayad, L.M. *CT Scan Versus MRI Versus X-Ray: What Type of Imaging Do I Need?* [cited 2023; Available from: https://www.hopkinsmedicine.org/health/treatment-tests-and-therapies/ct-vs-mri-vs-xray#:~:text=A%20CT%20scan%2C%20or%20computed,fast%20(about%20one%20minute).
34. Staedler, Y.M., D. Masson, and J. Schönenberger, *Plant tissues in 3D via X-ray tomography: simple contrasting methods allow high resolution imaging.* PLoS One, 2013. **8**(9): p. e75295.
35. Cnudde, V. and M.N. Boone, *High-resolution X-ray computed tomography in geosciences: A review of the current technology and applications.* Earth-Science Reviews, 2013. **123**: p. 1-17.
36. Zappala, S., J.R. Helliwell, S.R. Tracy, S. Mairhofer, C.J. Sturrock, T. Pridmore, M. Bennett, and S.J. Mooney, *Effects of X-Ray Dose On Rhizosphere Studies Using X-Ray Computed Tomography.* PLoS One, 2013. **8**(6): p. e67250.
37. Sasi, G.S., *Responses of some plants to treatment with industrial ceramic – waste water sludge*, in *Botany*. 2019, Ain Shams University: Egyptian Universities Libraries Consortium (EULC), Cairo, Egypt. p. 62-147.
38. Chaturvedi, A. and V. Jain, *Effect of Ionizing Radiation on Human Health.* International Journal of Plant and Environment, 2019. **5**.
39. Heath, M., D. St-Onge, and R. Hausler, *UV reflectance in crop remote sensing: Assessing the current state of knowledge and extending research with strawberry cultivars.* PLoS One, 2024. **19**(3): p. e0285912.
40. Liu, H., S.-H. Lee, and J. Chahl, *An evaluation of the contribution of ultraviolet in fused multispectral images for invertebrate detection on green leaves.* Precision Agriculture, 2016. **18**.
41. *Hyperspectral imaging in agriculture and vegetation*. [cited 2023; Available from: https://www.specim.com/hyperspectral-imaging-applications/agriculture-and-vegetation/#:~:text=Crop%20Health%20Assessment,nutrient%20deficiencies%2C%20or%20water%20scarcity.
42. Xinya Wang, Qian Hu, Yingsong Cheng, and J. Ma, *Hyperspectral Image Super-Resolution Meets Deep Learning: A Survey and Perspective.* IEEE/CAA Journal of Automatica Sinica, 2023. **10**: p. 1668-1691.
43. Rostron, P.G., Safa; Gaber; D, *Raman Spectroscopy, Review.* International Journal of Engineering and Technical Research (IJETR), 2016. **6**(1).
44. Kuhar, N.S., Sanchita; Verma, Taru; and Umapathy, Siva, *Challenges in application of Raman spectroscopy to biology and materials.* RSC Advances, 2018. **8**: p. 25888-25908.
45. Sil, S. and S. Umapathy, *Raman spectroscopy explores molecular structural signatures of hidden materials in depth: Universal Multiple Angle Raman Spectroscopy.* Scientific Reports, 2014. **4**(1): p. 5308.

46. Dong, D. and C. Zhao, *Limitations and challenges of using Raman spectroscopy to detect the abiotic plant stress response.* Proceedings of the National Academy of Sciences, 2017. **114**(28): p. E5486-E5487.
47. Saito, Y., R. Saito, T.D. Kawahara, A. Nomura, and S. Takeda, *Development and performance characteristics of laser-induced fluorescence imaging lidar for forestry applications.* Forest Ecology and Management, 2000. **128**(1): p. 129-137.
48. Wan, W. and J. Su, *Study of laser-induced plant fluorescence lifetime imaging technology for plant remote sensing monitor.* Measurement, 2018. **125**: p. 564-571.
49. Van As, H., T. Scheenen, and F.J. Vergeldt, *MRI of intact plants.* Photosynth Res, 2009. **102**(2-3): p. 213-22.
50. Peelle, J. *Introduction to MRI*. [cited 2025; Available from: http://jpeelle.net/mri/general/preliminaries.html.
51. Zhang, S., Martin Uecker, Dirk Voit, Klaus-Dietmar Merboldt, and J. Frahm, *Real-time cardiovascular magnetic resonance at high temporal resolution: radial FLASH with nonlinear inverse reconstruction.* J Cardiovasc Magn Reson, 2010. **12**(1): p. 39.
52. Toma, M., M. Vinatoru, L. Paniwnyk, and T.J. Mason, *Investigation of the effects of ultrasound on vegetal tissues during solvent extraction.* Ultrasonics Sonochemistry, 2001. **8**(2): p. 137-142.
53. Fujimoto, J.G., C. Pitris, S.A. Boppart, and M.E. Brezinski, *Optical coherence tomography: an emerging technology for biomedical imaging and optical biopsy.* Neoplasia, 2000. **2**(1-2): p. 9-25.
54. Laschke, M.W., C. Körbel, J. Rudzitis-Auth, I. Gashaw, M. Reinhardt, P. Hauff, T.M. Zollner, and M.D. Menger, *High-resolution ultrasound imaging: a novel technique for the noninvasive in vivo analysis of endometriotic lesion and cyst formation in small animal models.* Am J Pathol, 2010. **176**(2): p. 585-93.
55. El-Sattar, A.M.A. and E. Tawfik, *Effects of ultrasonic waves on seedling growth, biochemical constituents, genetic stability of fenugreek (Trigonella foenum-graecum) under salinity stress.* Vegetos, 2022.
56. Pircher, M., C.K. Hitzenberger, and U. Schmidt-Erfurth, *Polarization sensitive optical coherence tomography in the human eye.* Progress in Retinal and Eye Research, 2011. **30**(6): p. 431-451.
57. Cense, B., T.C. Chen, B.H. Park, M.C. Pierce, and J.F. de Boer, *In vivo depth-resolved birefringence measurements of the human retinal nerve fiber layer by polarization-sensitive optical coherence tomography.* Optics Letters, 2002. **27**(18): p. 1610-1612.
58. Aguirre, A.D., C. Zhou, H.-C. Lee, O.O. Ahsen, and J.G. Fujimoto, *Optical Coherence Microscopy*, in *Optical Coherence Tomography: Technology and Applications*, W. Drexler and J.G. Fujimoto, Editors. 2015, Springer International Publishing: Cham. p. 865-911.
59. Leitgeb, R.A., *En face optical coherence tomography: a technology review [Invited].* Biomed Opt Express, 2019. **10**(5): p. 2177-2201.
60. Dubois, A. and A.C. Boccara, *Full-Field Optical Coherence Tomography*, in *Optical Coherence Tomography: Technology and Applications*, W. Drexler and J.G. Fujimoto, Editors. 2008, Springer Berlin Heidelberg: Berlin, Heidelberg. p. 565-591.
61. Morgner, U., W. Drexler, F.X. Kärtner, X.D. Li, C. Pitris, E.P. Ippen, and J.G. Fujimoto, *Spectroscopic optical coherence tomography.* Optics Letters, 2000. **25**(2): p. 111-113.
62. Oldenburg, A.L., C. Xu, and S.A. Boppart, *Spectroscopic Optical Coherence Tomography and Microscopy.* IEEE Journal of Selected Topics in Quantum Electronics, 2007. **13**(6): p. 1629-1640.
63. Fujii, H., T. Asakura, K. Nohira, Y. Shintomi, and T. Ohura, *Blood flow observed by time-varying laser speckle.* Optics Letters, 1985. **10**(3): p. 104-106.
64. Azzollini, S., T. Monfort, O. Thouvenin, and K. Grieve, *Dynamic optical coherence tomography for cell analysis [Invited].* Biomedical Optics Express, 2023. **14**: p. 3362-3379.
65. Spaide, R.F., J.G. Fujimoto, N.K. Waheed, S.R. Sadda, and G. Staurenghi, *Optical coherence tomography angiography.* Prog Retin Eye Res, 2018. **64**: p. 1-55.
66. de Wit, J., S. Tonn, M.-R. Shao, G. Van den Ackerveken, and J. Kalkman, *Revealing real-time 3D in vivo pathogen dynamics in plants by label-free optical coherence tomography.* Nature Communications, 2024. **15**(1): p. 8353.
67. Hope, J., M. Goodwin, and F. Vanholsbeeck, *Inverse spectroscopic optical coherence tomography (IS-OCT) for characterization of particle size and concentration.* OSA Continuum, 2021. **4**(8): p. 2260-2274.
68. Gong, P., M. Almasian, G. van Soest, D. de Bruin, T. van Leeuwen, D. Sampson, and D. Faber, *Parametric imaging of attenuation by optical coherence tomography: review of models, methods, and clinical translation.* J Biomed Opt, 2020. **25**(4): p. 1-34.
69. Hettinger, J., M. Mattozzi, W. Myers, M. Williams, A. Reeves, R. Parsons, R. Haskell, D. Petersen, R. Wang, and J. Medford, *Optical Coherence Microscopy. A Technology for Rapid, in Vivo, Non-Destructive Visualization of Plants and Plant Cells.* Plant physiology, 2000. **123**: p. 3-16.

70. Magwaza, L., H. Ford, P. Cronje, U. Opara, S. Landahl, R. Tatam, and L. Terry, *Application of optical coherence tomography to non-destructively characterise rind breakdown disorder of 'Nules Clementine' mandarins.* Postharvest Biology and Technology, 2013. **84**: p. 16-21.
71. Loeb, G. and J. Barton, *Imaging botanical subjects with optical coherence tomography: A feasibility study.* Transactions of the American Society of Agricultural Engineers, 2003. **46**: p. 1751-1757.
72. Kutis, I., V. Sapozhnikova, R. Kuranov, and V.A. Kamenskii, *Study of the Morphological and Functional State of Higher Plant Tissues by Optical Coherence Microscopy and Optical Coherence Tomography.* Russian Journal of Plant Physiology, 2005. **52**: p. 559-564.
73. Clements, J.C., A.V. Zvyagin, K.K.M.B.D. Silva, T. Wanner, D.D. Sampson, and W.A. Cowling, *Optical coherence tomography as a novel tool for non-destructive measurement of the hull thickness of lupin seeds.* Plant Breeding, 2004. **123**(3): p. 266-270.
74. H. Ullah, F.H., E. Ahmad & M. Ikram *A rapid and non-invasive bio-photonic technique to monitor the quality of onions.* Optics and Spectroscopy, 2015. **119**: p. 295–299.
75. Wedding, B.B., C. Wright, S. Grauf, and R.D. White, *Wavelength variation of the depth of penetration of near infrared radiation in'Hass' avocado fruit.* Technology in Horticulture, 2024. **4**(1).
76. Veraverbeke, E.A., N. Van Bruaene, P. Van Oostveldt, and B.M. Nicolaï, *Non destructive analysis of the wax layer of apple (Malus domestica Borkh.) by means of confocal laser scanning microscopy.* Planta, 2001. **213**(4): p. 525-33.
77. Reeves, A., R.L. Parsons, J.W. Hettinger, and J.I. Medford, *In vivo three-dimensional imaging of plants with optical coherence microscopy.* J Microsc, 2002. **208**(Pt 3): p. 177-89.
78. Anna, T., S. Chakraborty, C.-Y. Cheng, V. Srivastava, A. Chiou, and W.-C. Kuo, *Elucidation of microstructural changes in leaves during senescence using spectral domain optical coherence tomography.* Scientific Reports, 2019. **9**: p. 1167.
79. Spicer, G.L.C., A. Eid, D. Wangpraseurt, T.D. Swain, J.A. Winkelmann, J. Yi, M. Kühl, L.A. Marcelino, and V. Backman, *Measuring light scattering and absorption in corals with Inverse Spectroscopic Optical Coherence Tomography (ISOCT): a new tool for non-invasive monitoring.* Sci Rep, 2019. **9**(1): p. 14148.
80. Wijesinghe, R.E., S.-Y. Lee, N.K. Ravichandran, M.F. Shirazi, B. Moon, H.-Y. Jung, M. Jeon, and J. Kim, *Bio-photonic detection method for morphological analysis of anthracnose disease and physiological disorders of Diospyros kaki.* Optical Review, 2017. **24**(2): p. 199-205.
81. *Anthracnose plant disease*. Science & Tech [cited 2022; Available from: https://www.britannica.com/science/anthracnose.
82. Wijesinghe, R., S.-Y. Lee, N.K. Ravichandran, M.F. Shirazi, P. Kim, H.-Y. Jung, M. Jeon, and A. Kim, *Optical screening of Venturianashicola caused Pyruspyrifolia (Asian pear) scab using optical coherence tomography.* International Journal of Applied Engineering Research, 2016. **11**: p. 7728-7731.
83. Wijesinghe, R.E., S.-Y. Lee, P. Kim, H.-Y. Jung, M. Jeon, and J. Kim, *Optical sensing method to analyze germination rate of Capsicum annum seeds treated with growth-promoting chemical compounds using optical coherence tomography.* Journal of Biomedical Optics, 2017. **22**(9): p. 091502.
84. Wijesinghe, R.E., S.Y. Lee, N.K. Ravichandran, M.F. Shirazi, P. Kim, H.Y. Jung, M. Jeon, and J. Kim, *Biophotonic approach for the characterization of initial bitter-rot progression on apple specimens using optical coherence tomography assessments.* Sci Rep, 2018. **8**(1): p. 15816.
85. Ravichandran, N.K., R. Wijesinghe, M.F. Shirazi, K. Park, S.-Y. Lee, H.-Y. Jung, M. Jeon, and J. Kim, *In Vivo Monitoring on Growth and Spread of Gray Leaf Spot Disease in Capsicum annuum Leaf Using Spectral Domain Optical Coherence Tomography.* Journal of Spectroscopy, 2016. **2016**: p. 1-6.
86. Lee, D.-H., C.-G. Back, N.K.K. Win, K.-H. Choi, K.-M. Kim, I.-K. Kang, C. Choi, T.-M. Yoon, J.Y. Uhm, and H.-Y. Jung, *Biological Characterization of Marssonina coronaria Associated with Apple Blotch Disease.* Mycobiology, 2011. **39**(3): p. 200-205.
87. Lee, S.-Y., C. Lee, J. Kim, and H.-Y. Jung, *Application of optical coherence tomography to detect Cucumber green mottle mosaic virus (CGMMV) infected cucumber seed.* Horticulture, Environment, and Biotechnology, 2012. **53**: p. 428-433.
88. Lee, C., S.Y. Lee, J.Y. Kim, H.Y. Jung, and J. Kim, *Optical sensing method for screening disease in melon seeds by using optical coherence tomography.* Sensors (Basel), 2011. **11**(10): p. 9467-77.
89. Ford, H., R. Tatam, S. Landahl, and L. Terry, *Investigation of disease in stored onions using optical coherence tomography.* ISHS Acta Horticulturae, 2011.
90. Bharti, Y.T., Lee Byeong Ha, *Identification of Fungus-infected Tomato Seeds Based on Full-Field Optical Coherence Tomography.* 2019. **3**(6): p. 571~576.
91. Tzu Hao, C., T. Khay-Ming Eddie, N. Beng-Koon, G. Razul Sirajudeen, T. Chia Meng, C. Tet Fatt, and P. Wee Tang, *Diagnosis of virus infection in orchid plants with high-resolution optical coherence tomography.* Journal of Biomedical Optics, 2009. **14**(1): p. 1-6.

92. Meglinski, I., C. Buranachai, and L. Terry, *Plant photonics: Application of optical coherence tomography to monitor defects and rots in onion.* Laser Physics Letters, 2010. **7**: p. 307-310.
93. Sapozhnikova, V., V. Kamensky, and R. Kuranov, *Optical coherence tomography for visualization of plant tissues*. International Conference on Lasers, Applications, and Technologies 2002. Vol. 5149. 2003, Moscow, Russian, 22–27 June 2002: SPIE.
94. Thanuja Srimal, L.K., M. R.U, and H. Kadono, *Optical Coherence Tomography biospeckle signal analysis to investigate response of plant leaves to ozone*. 2014.
95. Verboven, P., A. Nemeth, M.K. Abera, E. Bongaers, D. Daelemans, P. Estrade, E. Herremans, M. Hertog, W. Saeys, E. Vanstreels, B. Verlinden, M. Leitner, and B. Nicolaï, *Optical coherence tomography visualizes microstructure of apple peel.* Postharvest Biology and Technology, 2013. **78**: p. 123-132.
96. Mo, L., P. Verboven, A. Buchsbaum, D. Cantre, B. Nicolai, J. Heyes, A. Mowat, and A. East, *Characterising kiwifruit (Actinidia sp.) near skin cellular structures using optical coherence tomography.* Postharvest Biology and Technology, 2015. **110**: p. 247--256.
97. Wijesinghe, R., S.-Y. Lee, N.K. Ravichandran, S. Han, H. Jeong, Y. Han, H.-Y. Jung, P. Kim, and M. Jeon, *Optical coherence tomography-integrated, wearable (backpack-type), compact diagnostic imaging modality for in situ leaf quality assessment.* Applied Optics, 2017. **56**: p. D108.
98. Larimer, C.J., E.H. Denis, J.D. Suter, and J.J. Moran, *Optical coherence tomography imaging of plant root growth in soil.* Applied Optics, 2020. **59**(8): p. 2474-2481.
99. Thanuja Srimal, L.K., M. R.U, and H. Kadono, *Functional optical coherence tomography (fOCT) biospeckle imaging to investigate response of plant leaves to ultra-short term exposure of Ozone.* Journal of Physics: Conference Series, 2015. **605**.
100. L. K. T. Srimal, H.K., U. M. Rajagopalan, *Optical coherence tomography biospeckle imaging for fast monitoring varying surface responses of a plant leaf under ozone stress.* In Proceedings of the 2013 SPIE, SPIE SeTBio, Yokohama, Japan, 23–26 April 2013 2013. **8881**: p. 88810H.
101. Boccara, M., W. Schwartz, E. Guiot, G. Vidal, R.D. Paepe, A. Dubois, and A.-C. Boccara, *Early chloroplastic alterations analysed by optical coherence tomography during a harpin-induced hypersensitive response.* The Plant Journal, 2007. **50**(2): p. 338-346.
102. Williams, J., Wai Ching Lin, Wei Li, and S.J.M. Shuangyu Wang, Adrien A. P. Chauvet, *Translating Optical Coherence Tomography Technologies from Clinical Studies to Botany: Real Time Imaging of Long-Distance Signaling in Plants*. 2020, White Rose Research Online: Washington DC, USA.
103. Cheong, H., S. Krishna Devalla, T. Chuangsuwanich, T.A. Tun, X. Wang, T. Aung, L. Schmetterer, M.L. Buist, C. Boote, A.H. Thiéry, and M.J.A. Girard, *OCT-GAN: single step shadow and noise removal from optical coherence tomography images of the human optic nerve head.* Biomed Opt Express, 2021. **12**(3): p. 1482-1498.
104. Ramachandiran, R., G. KIshwariya, and R.G. A. *A Survey on Speckle Removal for Optical Coherence Tomography Images*. in *2019 IEEE International Conference on System, Computation, Automation and Networking (ICSCAN), Pondicherry, India*. 2019.
105. Rueckert, D. and J.A. Schnabel, *Registration and Segmentation in Medical Imaging*, in *Registration and Recognition in Images and Videos*, R. Cipolla, S. Battiato, and G.M. Farinella, Editors. 2014, Springer Berlin Heidelberg: Berlin, Heidelberg. p. 137-156.
106. Rufai, S.R., *Handheld optical coherence tomography removes barriers to imaging the eyes of young children.* Eye, 2022. **36**(5): p. 907-908.
107. *Handheld optical coherence tomography*. 2024 [cited 2024; Available from: https://cordis.europa.eu/project/id/871312.
108. Rastogi, K. *Which Countries Produce the Most Wheat?* 2022 [cited 2021; Available from: https://www.visualcapitalist.com/cp/visualizing-global-wheat-production-by-country/.
109. Jaenisch, B.R., L.B. Munaro, S.V.K. Jagadish, and R.P. Lollato, *Modulation of Wheat Yield Components in Response to Management Intensification to Reduce Yield Gaps.* Frontiers in Plant Science, 2022. **13**.
110. G, P. *Wheat: Origin, Distribution and Importance | Agronomy*. [cited 2023; Available from: https://www.agricultureinindia.net/agronomy/wheat-cultivation/wheat-origin-distribution-and-importance-agronomy/11973#:~:text=Wheat%20is%20cultivated%20in%20about,Federation%2C%20Canada%2C%20Australia%20etc.
111. Shewry, P.R., *Wheat.* Journal of Experimental Botany, 2009. **60**(6): p. 1537-1553.
112. *Wheat*. 2024 [cited 2024; Available from: https://www.agricentre.basf.co.uk/en/Crop-Solutions/Cereals/Wheat/.
113. *Imports & Exports: Wheat & Flour*. [cited 2022 Aug]; Available from: https://www.ukflourmillers.org/importsexports.

114. Arvanitoyannis, I.S. and P. Tserkezou, *10 - Cereal Waste Management: Treatment Methods and Potential Uses of Treated Waste*, in *Waste Management for the Food Industries*, I.S. Arvanitoyannis, Editor. 2008, Academic Press: Amsterdam. p. 629-702.
115. Hansen, M., B. Hidayat, K. Mogensen, M. Jeppesen, B. Jørgensen, K. Johansen, and L. Thygesen, *Enzyme affinity to cell types in wheat straw (Triticum aestivum L.) before and after hydrothermal pretreatment.* Biotechnology for biofuels, 2013. **6**: p. 54.
116. Bishaw, Z., Y. Yigezu, M. Keser, A. Niane, M. Engiz, S. Popay, and M. Küçükçongar, *Political Economy of the Wheat Sector in Turkey: Seed Systems, Varietal Adoption, and Impacts*. 2021.
117. Overend, A., *Shifting Food Facts: Dietary Discourse in a Post-Truth Culture*. 2020.
118. S.B.Goodwin, *Instant Insights. Septoria tritici blotch in cereals*. Disease affecting wheat:Septoria tritici blotch. 2019: Burleigh Dodds Science Publisheing Limited. 158.
119. Nizolli, V.O., V.E. Viana, C. Pegoraro, L.C.d. Maia, and A.C.d. Oliveira, *Wheat blast: The last enemy of hunger fighters.* Genetics and Molecular Biology, 2023. **46**.
120. Darino, M., M. Urban, N. Kaur, A. Machado Wood, M. Grimwade-Mann, D. Smith, A. Beacham, and K. Hammond-Kosack, *Identification and functional characterisation of a locus for target site integration in Fusarium graminearum.* Fungal Biology and Biotechnology, 2024. **11**(1): p. 2.
121. Figueroa, M., K.E. Hammond-Kosack, and P.S. Solomon, *A review of wheat diseases-a field perspective.* Mol Plant Pathol, 2018. **19**(6): p. 1523-1536.
122. Impey, L. *Guide to tackling septoria disease in wheat*. 2021 [cited 2022; Available from: https://www.fwi.co.uk/arable/crop-management/disease-management/a-guide-to-tackling-septoria-in-wheat.
123. *Septoria tritici in winter wheat*. 2024 [cited 2024; Available from: https://ahdb.org.uk/knowledge-library/septoria-tritici-in-winter-wheat.
124. *Septoria tritici in wheat*. [cited 2024; Available from: https://cropscience.bayer.co.uk/agronomy-id/diseases/wheat-diseases/septoria-tritici-in-wheat.
125. Zubrod, J.P., M. Bundschuh, G. Arts, C.A. Brühl, G. Imfeld, A. Knäbel, S. Payraudeau, J.J. Rasmussen, J. Rohr, A. Scharmüller, K. Smalling, S. Stehle, R. Schulz, and R.B. Schäfer, *Fungicides: An Overlooked Pesticide Class?* Environ Sci Technol, 2019. **53**(7): p. 3347-3365.
126. Sisson, A., *Fungicide Use in Field Crops Web Book*. The Crop Protection Network (CPN)
127. *Fungicide Efficacy for Control of Wheat Diseases*. 2024.
128. Cook, Hims, and Vaughan, *Effects of fungicide spray timing on winter wheat disease control.* Plant Pathology, 2002. **48**: p. 33-50.
129. Jacquet, F., M.-H. Jeuffroy, J. Jouan, E. Le Cadre, I. Litrico, T. Malausa, X. Reboud, and C. Huyghe, *Pesticide-free agriculture as a new paradigm for research.* Agronomy for Sustainable Development, 2022. **42**: p. 8.
130. *Growth stages*. [cited 2024; Available from: www.wheat-training.com.
131. *Measurement of stem extension and stem reserves in wheat*. 2024 [cited 2024; Available from: https://ahdb.org.uk/knowledge-library/measurement-of-stem-extension-and-stem-reserves-in-wheat#:~:text=Stem%20elongation%20and%20how%20to%20measure%20it,-Benchmark:%20Five%20internodes&text=Stem%20height%20is%20determined%20by,last%20five%20or%20six%20internodes.&text=Each%20internode%20starts%20to%20extend,=%2069%20cm%20(final%20height).
132. *STB warning*. 2019 [cited 2024; Available from: https://www.smallfarms.net/stb-warning/.
133. IANNOTTI, M. *What Are Cotyledons, Monocots, and Dicots?* 2022 2024 Mar]; Available from: https://www.thespruce.com/what-are-cotyledons-monocots-and-dicots-1403098#:~:text=Cotyledons%20are%20not%20considered%20true,leaves%20develop%20and%20begin%20photosynthesizing.
134. Borsuk, A.M., A.B. Roddy, G. Théroux-Rancourt, and C.R. Brodersen, *Structural organization of the spongy mesophyll.* New Phytologist, 2022. **234**(3): p. 946-960.
135. *Constraints to cereal-based rainfed cropping in Mediterranean environments and methods to measure and minimize their effects*. [cited 2025; Available from: https://www.fao.org/4/y5146e/y5146e04.htm.
136. Nielsen, V. *What Effect Does UV Light have on Plants?* 2023 [cited 2023; Available from: https://mammothlighting.com/pages/why-uv.
137. Marks, M., *Molecular Genetic Analysis of Trichome Development in Arabidopsis.* Annual review of plant physiology and plant molecular biology, 1997. **48**: p. 137-163.
138. Hülskamp, M., *Plant trichomes: a model for cell differentiation.* Nature Reviews Molecular Cell Biology, 2004. **5**(6): p. 471-480.
139. Pesch, M. and M. Hülskamp, *One, two, three...models for trichome patterning in Arabidopsis?* Current opinion in plant biology, 2009. **12**(5): p. 587-592.

140. Yang, C. and Z. Ye, *Trichomes as models for studying plant cell differentiation.* Cell Mol Life Sci, 2013. **70**(11): p. 1937-48.
141. Kjær, A., K. Grevsen, and M. Jensen, *Effect of external stress on density and size of glandular trichomes in full-grown Artemisia annua, the source of anti-malarial artemisinin.* AoB Plants, 2012. **2012**: p. pls018.
142. Arraiano, L.S. and J.K. Brown, *Sources of resistance and susceptibility to Septoria tritici blotch of wheat.* Mol Plant Pathol, 2017. **18**(2): p. 276-292.
143. O'Brien, L. and R. DePauw, *WHEAT | Breeding*, in *Encyclopedia of Grain Science*, C. Wrigley, Editor. 2004, Elsevier: Oxford. p. 330-336.
144. Ma, J., L.U. Wingen, S. Orford, P. Fenwick, J. Wang, and S. Griffiths, *Using the UK reference population Avalon × Cadenza as a platform to compare breeding strategies in elite Western European bread wheat.* Molecular breeding : new strategies in plant improvement, 2015. **35**(2): p. 70-70.
145. Fones, H. and S. Gurr, *The impact of Septoria tritici Blotch disease on wheat: An EU perspective.* Fungal Genetics and Biology, 2015. **79**: p. 3-7.
146. Ponomarenko A., S.B.G., and G.H.J. Kema., *Septoria tritici blotch (STB) of wheat.* ASP, 2011.
147. Wenham, H.T., *Studies on septaria leaf blotch disease of wheat (Triticum aestivum L.) caused by Septoria tritici Desm.* New Zealand Journal of Agricultural Research, 1959. **2**(2): p. 208-213.
148. Abhinandan, K., L. Skori, M. Stanic, N.M.N. Hickerson, M. Jamshed, and M.A. Samuel, *Abiotic Stress Signaling in Wheat – An Inclusive Overview of Hormonal Interactions During Abiotic Stress Responses in Wheat.* Frontiers in Plant Science, 2018. **9**.
149. Lahlali, R., M. Taoussi, S.-E. Laasli, G. Gachara, R. Ezzouggari, Z. Belabess, K. Aberkani, A. Assouguem, A. Meddich, M. El Jarroudi, and E.A. Barka, *Effects of climate change on plant pathogens and host-pathogen interactions.* Crop and Environment, 2024. **3**(3): p. 159-170.
150. Singh, B.K., M. Delgado-Baquerizo, E. Egidi, E. Guirado, J.E. Leach, H. Liu, and P. Trivedi, *Climate change impacts on plant pathogens, food security and paths forward.* Nature Reviews Microbiology, 2023. **21**(10): p. 640-656.
151. Verkley, G.J.M., W. Quaedvlieg, H.D. Shin, and P.W. Crous, *A new approach to species delimitation in Septoria.* Studies in mycology, 2013. **75**(1): p. 213-305.
152. Quaedvlieg, W., G.H.J. Kema, J.Z. Groenewald, G.J.M. Verkley, S. Seifbarghi, M. Razavi, A. Mirzadi Gohari, R. Mehrabi, and P.W. Crous, *Zymoseptoria gen. nov.: a new genus to accommodate Septoria-like species occurring on graminicolous hosts.* Persoonia, 2011. **26**: p. 57-69.
153. Toropova, E.Y., O.A. Kazakova, and V.V. Piskarev, *Septoria blotch epidemic process on spring wheat varieties.* Vavilovskii zhurnal genetiki i selektsii, 2020. **24**(2): p. 139-148.
154. Chaudhary, R. and M. Pujari, *MAJOR DISEASES OF WHEAT AND THEIR MANAGEMENT: A REVIEW.* PLANT ARCHIVES, 2021. **21**.
155. Mirzadi Gohari, A., S.B. Ware, A.H.J. Wittenberg, R. Mehrabi, S. Ben M'Barek, E.C.P. Verstappen, T.A.J. van der Lee, O. Robert, H.J. Schouten, P.P.J.G.M. de Wit, and G.H.J. Kema, *Effector discovery in the fungal wheat pathogen Zymoseptoria tritici.* Molecular plant pathology, 2015. **16**(9): p. 931-945.
156. Gohari, A., *Identification and functional characterization of putative (a)virulence factors in the fungal wheat pathogen Zymoseptoria tritici*. 2015.
157. Orton, E., S. Deller, and J. Brown, *Mycosphaerella graminicola: From genomics to disease control.* Molecular plant pathology, 2011. **12**: p. 413-24.
158. H. A. B. Wösten, P.K., M. Montalti, H. Läkk, *Growing Fungi Structures in Space* 2018: European Space Agency.
159. Das, S. and S. Pattanayak, *Over view of Septoria Diseases on Different Crops and its Management.* International Journal of Agriculture Environment and Biotechnology, 2020. **13**: p. 351-370.
160. Zitter, T.A. *Septoria Leaf Spot*. APS 1992 [cited 2024; Available from: https://www.apsnet.org/edcenter/apsnetfeatures/Pages/SeptoriaLeafSpot.aspx.
161. Welch, T., C. Bayon, J.J. Rudd, K. Kanyuka, and G.J. Kettles, *Induction of distinct plant cell death programs by secreted proteins from the wheat pathogen Zymoseptoria tritici.* Sci Rep, 2022. **12**(1): p. 17880.
162. *Septoria Life Cycle*. 2016 [cited 2022; Available from: https://www.youtube.com/watch?v=NrBHK4RJ3Eo&t=46s.
163. Yang, H. and P. Luo, *Changes in Photosynthesis Could Provide Important Insight into the Interaction between Wheat and Fungal Pathogens.* Int J Mol Sci, 2021. **22**(16).
164. Collin, F., P. Bancal, J. Spink, P.K. Appelgren, J. Smith, N.D. Paveley, M.O. Bancal, and M.J. Foulkes, *Wheat lines exhibiting variation in tolerance of Septoria tritici blotch differentiated by grain source limitation.* Field Crops Research, 2018. **217**: p. 1-10.
165. Stephens, C., F. Ölmez, H. Blyth, M. McDonald, A. Bansal, E. Turgay, F. Hahn, C. Saintenac, V. Nekrasov, P. Solomon, A. Milgate, B. Fraaije, J. Rudd, and K. Kanyuka, *Remarkable recent changes in*

*the genetic diversity of the avirulence gene AvrStb6 in global populations of the wheat pathogen Zymoseptoria tritici.* Molecular Plant Pathology, 2021. **22**.
166. Habig, M., C. Lorrain, A. Feurtey, J. Komluski, and E.H. Stukenbrock, *Epigenetic modifications affect the rate of spontaneous mutations in a pathogenic fungus.* Nat Commun, 2021. **12**(1): p. 5869.
167. Lavrukaitė, K., T.M. Heick, J. Ramanauskienė, R. Armonienė, and A. Ronis, *Fungicide sensitivity levels in the Lithuanian Zymoseptoria tritici population in 2021.* Front Plant Sci, 2022. **13**: p. 1075038.
168. Dalvand, M., D. Zafar, M. Pari, R. Roohparvar, and M. Ghafari, *Studying Genetic Diversity in Zymoseptoria tritici, Causal Agent of Septoria Tritici Blotch, by Using ISSR and SSR Markers.* 2018: p. 1307-1316.
169. Haueisen, J., M. Möller, C. Eschenbrenner, J. Grandaubert, H. Seybold, H. Adamiak, and E. Stukenbrock, *Highly flexible infection programs in a specialized wheat pathogen.* Ecology and Evolution, 2018. **9**.
170. Mekonnen, T., T. Haileselassie, S. Goodwin, and T. Kassahun, *Genetic diversity and population structure of Zymoseptoria tritici in Ethiopia as revealed by microsatellite markers.* Fungal Genetics and Biology, 2020. **141**: p. 103413.
171. McDonald, B.A., F. Suffert, A. Bernasconi, and A. Mikaberidze, *How large and diverse are field populations of fungal plant pathogens? The case of Zymoseptoria tritici.* Evol Appl, 2022. **15**(9): p. 1360-1373.
172. Honnay, O., *Genetic Drift*. 2013. p. 251-253.
173. Priest, S.J., V. Yadav, and J. Heitman, *Advances in understanding the evolution of fungal genome architecture.* F1000Res, 2020. **9**.
174. Chedli, R.B.H., L. Aouini, S.B. M'Barek, B.A. Bahri, E. Verstappen, H.J. Kema Gerrit, S. Rezgui, A. Yahyaoui, and H. Chaabane, *Genetic diversity and population structure of Zymoseptoria tritici on bread wheat in Tunisia using SSR markers.* European Journal of Plant Pathology, 2022. **163**(2): p. 429-440.
175. Suffert, F., I. Sache, and C. Lannou, *Early stages of septoria tritici blotch epidemics of winter wheat: build-up, overseasoning, and release of primary inoculum.* Plant Pathology, 2011. **60**(2): p. 166-177.
176. Fagundes, W.C., J. Haueisen, and E.H. Stukenbrock, *Dissecting the Biology of the Fungal Wheat Pathogen Zymoseptoria tritici: A Laboratory Workflow.* Current Protocols in Microbiology, 2020. **59**(1): p. e128.
177. Eyal, Z., A.L. Scharen, J.M. Prescott, and M. van Ginkel, *The Septoria Diseases of Wheat: Concepts and Methods of Disease Management*. 1987.
178. Goodwin, S., *Diseases affecting wheat: Septoria tritici blotch*. 2018. p. 47-68.
179. Fantozzi, E., S. Kilaru, S.J. Gurr, and G. Steinberg, *Asynchronous development of Zymoseptoria tritici infection in wheat.* Fungal Genetics and Biology, 2021. **146**: p. 103504.
180. Wang, A., W. Qi, T. Gao, and X. Tang, *Molecular Contrast Optical Coherence Tomography and Its Applications in Medicine.* Int J Mol Sci, 2022. **23**(6).
181. Siguenza, N., A. Jangid, E.B. Strong, J. Merriam, A.W. Martinez, and N.W. Martinez, *Micro-staining microbes: An alternative to traditional staining of microbiological specimens using microliter volumes of reagents.* Journal of Microbiological Methods, 2019. **164**: p. 105654.
182. Gao, F., Y. Zhang, J. Lv, S. Wang, X. He, P. Liu, and W. Cui, *How to improve the sensitivity and specificity of cell-based assays in detecting autoantibodies in neuroimmune diseases.* Ann Transl Med, 2023. **11**(7): p. 281.
183. *Fluorescent Dyes for Secondary Antibodies*. [cited 2024; Available from: https://www.dianova.com/en/faq/fluorescent-dyes-for-secondary-antibodies/.
184. Steinberg, G., *Cell biology of Zymoseptoria tritici: Pathogen cell organization and wheat infection.* Fungal Genetics and Biology, 2015. **79**.
185. Barnes, S.H., *Ultrastructural imaging of freeze-fractured plant cells in the scanning electron microscope.* Microscopy Research and Technique, 1992. **22**(2): p. 160-169.
186. Johnson, M. *Light Sheet Tutorial*. 2018 [cited 2024; Available from: https://www.youtube.com/watch?v=afIkWHx3duc.
187. Santi, P.A., *Light sheet fluorescence microscopy: a review.* J Histochem Cytochem, 2011. **59**(2): p. 129-38.
188. Phillips, T., *Genetically Modified Organisms (GMOs): Transgenic Crops and Recombinant DNA Technology.* 2008. **1**(1): p. 213.
189. Severs, N.J., *Freeze-fracture electron microscopy.* Nat Protoc, 2007. **2**(3): p. 547-76.
190. Dong, O.X. and P.C. Ronald, *Genetic Engineering for Disease Resistance in Plants: Recent Progress and Future Perspectives.* Plant Physiol, 2019. **180**(1): p. 26-38.
191. Karalis, D.T., T. Karalis, S. Karalis, and A.S. Kleisiari, *Genetically Modified Products, Perspectives and Challenges.* Cureus, 2020. **12**(3): p. e7306.

192. Shu, X., L. Beckmann, and H. Zhang, *Visible-light optical coherence tomography: a review.* J Biomed Opt, 2017. **22**(12): p. 1-14.
193. DAVID HUANG, M.D., PH.D, *OCT Terminology – Demystified.* Ophthalmology Management, 2009.
194. Kelly A. Townsend, G.W., and Joel S. Schuman. *Fourier-Domain Optical Coherence Tomography*. 2007 [cited 2024; Available from: https://glaucomatoday.com/articles/2007-nov-dec/GT1107_08-php#:~:text=Because%20each%20A%2Dscan%20is,movement%20of%20the%20reference%20mirror.
195. Tomlins, P. and R. Wang, *Theory, developments and applications of optical coherence tomography.* J. Phys. D: Appl. Phys, 2005. **38**: p. 2519-2535.
196. *Go faster with the OQ LabScope 2.0 /X*. [cited 2024; Available from: https://www.photonics.com/Products/Go_faster_with_the_OQ_LabScope_20_X/pr65565.
197. *Lumedica OQ LabScope 2.0 OCT Imaging System*. Edmund Optics. p. 23.
198. *OCT Tutorial*. [cited 2025; Available from: https://wasatchphotonics.com/oct-tutorial/?utm_source=chatgpt.com.
199. Brown, W., *Principles of OCT Whitepaper 2.2*. 2018: Lumedica and Edmund Optics
200. Jeeseong C. Hwang, Kimberly Briggman, Nikki Rentz, Hyun-Jin Kim, David W. Allen, Lee J. Richter, and J.L. Sowon Yoon, *Certification of Standard Reference Material® 2196 Axial Resolution Standard for Optical Medical Imaging.* Special Publication (NIST SP), National Institute of Standards and Technology, Gaithersburg, 2023. **2196**: p. 260-228.
201. Scheibel, T., *Spider silks: recombinant synthesis, assembly, spinning, and engineering of synthetic proteins.* Microb Cell Fact, 2004. **3**(1): p. 14.
202. Haeberlé, O. and B. Simon, *Improving the lateral resolution in confocal fluorescence microscopy using laterally interfering excitation beams.* Optics Communications, 2006. **259**: p. 400-408.
203. Elliott, A.D., *Confocal Microscopy: Principles and Modern Practices.* Current protocols in cytometry, 2020. **92**(1): p. e68-e68.
204. Everall, N., J. Lapham, F. Adar, A. Whitley, E. Lee, and S. Mamedov, *Optimizing Depth Resolution in Confocal Raman Microscopy: A Comparison of Metallurgical, Dry Corrected, and Oil Immersion Objectives.* Applied spectroscopy, 2007. **61**: p. 251-9.
205. Bulgarelli, N., *Emulsion Microstructure and Dynamics.* 2022.
206. Webb, D. and C. Brown, *Epi-Fluorescence Microscopy.* Methods in molecular biology (Clifton, N.J.), 2013. **931**: p. 29-59.
207. ThermoFisherScientific. *Epifluorescence Microscope Basics*. Available from: https://www.thermofisher.com/uk/en/home/life-science/cell-analysis/cell-analysis-learning-center/molecular-probes-school-of-fluorescence/imaging-basics/fundamentals-of-fluorescence-microscopy/epifluorescence-microscope-basics.html.
208. Young, H.D. and R.A. Freedman, *University Physics with modern physics*. 14th ed. 2016.
209. Huang, B., M. Bates, and X. Zhuang, *Super-resolution fluorescence microscopy.* Annual review of biochemistry, 2009. **78**: p. 993-1016.
210. Carsten Forthmann, J.J.S., Tamara Straube *Quantifying the Resolution of a Leica SR GSD 3D Localization Microscopy System with 2D and 3D Nanorulers*

*Measuring the nano world (updated version).* 2016; Available from: https://www.leica-microsystems.com/science-lab/quantifying-the-resolution-of-a-leica-sr-gsd-3d-localization-microscopy-system-with-2d-and-3d-nanorulers/.
211. *what is scanning electon microscopy?* Scanning Electon Microscopy [cited 2024; Available from: https://www.nanoscience.com/techniques/scanning-electron-microscopy/.
212. Ahmad, P. *Roles of Magnetic Lenses in Scanning Electron Microscopy (SEM)*. 2023 [cited 2025; Available from: https://www.youtube.com/watch?v=h1T_nmLZvZY.
213. Metusala, D., *An alternative simple method for preparing and preserving cross-section of leaves and roots in herbaceous plants: Case study in Orchidaceae.* AIP Conference Proceedings, 2017. **1862**(1): p. 030113.
214. Myung, K., A. Parobek, J. Godbey, A. Bowling, and H. Pence, *Interaction of Organic Solvents with the Epicuticular Wax Layer of Wheat Leaves.* Journal of agricultural and food chemistry, 2013. **61**.
215. Thomas, A.B., G.S. Donn, and Q. Robert, *Evaluation of Epicuticular Wax Removal from Whole Leaves with Chloroform.* Weed Technology, 1993. **7**(3): p. 706-716.
216. Gurung, S., P. Prakash, P. Bhutia, A. Gupta, I. Bairy, J. Pradhan, U. Pradhan, D. Sharma, and T. Peggy, *Onychomycosis in two geographically distinct regions in India.* Archives of Clinical Microbiology, 2012. **3**: p. 1-6.
217. Sardinha Francisco, C., X. Ma, M. Zwyssig, B. McDonald, and J. Palma-Guerrero, *Morphological changes in response to environmental stresses in the fungal plant pathogen Zymoseptoria tritici.* Scientific Reports, 2019. **9**.

218. Gautam, M. and S. Bhatia, *Mount the Menace! – Potassium hydroxide in superficial fungal infections.* Indian Journal of Paediatric Dermatology, 2020. **21**(4): p. 343-346.
219. Seal, C.J., C.M. Courtin, K. Venema, and J. de Vries, *Health benefits of whole grain: effects on dietary carbohydrate quality, the gut microbiome, and consequences of processing.* Comprehensive Reviews in Food Science and Food Safety, 2021. **20**(3): p. 2742-2768.
220. Huang, C., Z. Qin, X. Hua, Z. Zhang, W. Xiao, X. Liang, P. Song, and W. Yang, *An Intelligent Analysis Method for 3D Wheat Grain and Ventral Sulcus Traits Based on Structured Light Imaging.* Front Plant Sci, 2022. **13**: p. 840908.
221. *Wheat Kernel. What is the wheat kernel?* [cited 2025; Available from: https://bakerpedia.com/ingredients/wheat-kernel/?utm_source=chatgpt.com.
222. Sapkota, A. *Monocot vs Dicot Seed- Definition, Structure, 10 Differences, Examples*. 2021 [cited 2022; Available from: https://thebiologynotes.com/monocot-and-dicot-seed/.
223. Shriram, s., R. K, and R. Swaminathan, *Effect of occupant-induced indoor CO2 concentration and bioeffluents on human physiology using a spirometric test.* Building and Environment, 2018. **149**.
224. Zain, M., A. Razak, H. El-Sheikh, H. Soliman, and A. Khalil, *Influence of growth medium on diagnostic characters of Aspergillus and Penicillium species.* African journal of microbiology research, 2009. **3**: p. 280-286.
225. Alqaisi, M., *Hemocytometer Calculator*. 2018.
226. *Sources of Hemacytometer Counting Errors*. Available from: https://www.nexcelom.com/applications/cellometer/cell-counting/counting-errors/?gclid=CjwKCAjw14uVBhBEEiwAaufYxxteGmhW8iHHxiN1PoUohmchZr4_Tj_C-OEgSvByf7v6LrRCsMdBLxoCGRYQAvD_BwE.
227. Anderegg, J., A. Hund, P. Karisto, and A. Mikaberidze, *In-Field Detection and Quantification of Septoria Tritici Blotch in Diverse Wheat Germplasm Using Spectral-Temporal Features.* Front Plant Sci, 2019. **10**: p. 1355.
228. Gupta, S. and A. Saxena, *Experimental comparison: Methods for the preservation of fungal cultures.* Current Research in Environmental & Applied Mycology, 2019. **9**: p. 208-212.
229. Odilbekov, F., R. Armoniené, T. Henriksson, and A. Chawade, *Proximal Phenotyping and Machine Learning Methods to Identify Septoria Tritici Blotch Disease Symptoms in Wheat.* Frontiers in Plant Science, 2018. **Volume 9 - 2018**.
230. Yang, F., M.N. Melo-Braga, M.R. Larsen, H.J. Jørgensen, and G. Palmisano, *Battle through signaling between wheat and the fungal pathogen Septoria tritici revealed by proteomics and phosphoproteomics.* Mol Cell Proteomics, 2013. **12**(9): p. 2497-508.
231. Cerón-Bustamante, M., F. Tini, G. Beccari, P. Benincasa, and L. Covarelli, *Effect of Different Light Wavelengths on Zymoseptoria tritici Development and Leaf Colonization in Bread Wheat.* J Fungi (Basel), 2023. **9**(6).
232. Yang, F., W. Li, M. Derbyshire, M.R. Larsen, J.J. Rudd, and G. Palmisano, *Unraveling incompatibility between wheat and the fungal pathogen Zymoseptoria tritici through apoplastic proteomics.* BMC Genomics, 2015. **16**(1): p. 362.
233. Sørensen, C.K., T. Thach, and M.S. Hovmøller, *Evaluation of Spray and Point Inoculation Methods for the Phenotyping of Puccinia striiformis on Wheat.* Plant Dis, 2016. **100**(6): p. 1064-1070.
234. Khan, T. and U. Mubeen, *Wheat Straw: A Pragmatic Overview.* Current Research Journal of Biological Sciences, 2012. **4**.
235. Davidson, M.W. *Education in Microscopy and Digital Imaging*. [cited 2024; Available from: https://zeiss-campus.magnet.fsu.edu/articles/lightsources/tungstenhalogen.html.
236. Lundgren, M.R., A. Mathers, A.L. Baillie, J. Dunn, M.J. Wilson, L. Hunt, R. Pajor, M. Fradera-Soler, S. Rolfe, C.P. Osborne, C.J. Sturrock, J.E. Gray, S.J. Mooney, and A.J. Fleming, *Mesophyll porosity is modulated by the presence of functional stomata.* Nature Communications, 2019. **10**(1): p. 2825.
237. Sharma, S., T. Kumar, M.J. Foulkes, S. Orford, A.M. Singh, L.U. Wingen, V. Karnam, L.S. Nair, P.K. Mandal, S. Griffiths, M.J. Hawkesford, P.R. Shewry, A.R. Bentley, and R. Pandey, *Nitrogen uptake and remobilization from pre- and post-anthesis stages contribute towards grain yield and grain protein concentration in wheat grown in limited nitrogen conditions.* CABI Agriculture and Bioscience, 2023. **4**(1): p. 12.
238. Homer-Smith, B. *Grass Spikelets* [cited 2024; Available from: https://plantid.net/Classic/Glossary/Grass%20Flowers.htm?AspxAutoDetectCookieSupport=1.
239. *Stigma in a Flower | Definition, Function & Parts*. [cited 2024; Available from: https://study.com/academy/lesson/stigma-in-a-flower-function-parts-quiz.html.
240. Schader, M. *Definition of Flower Filament*. 2021 [cited 2024; Available from: https://sciencing.com/definition-of-flower-filament-13426316.html.

241. *Anatomy of Wheat Plant buds*. 2022 [cited 2024; Available from: https://www.biorender.com/template/anatomy-of-wheat-plant-and-spikelet.
242. Miller, S., D. Chabot, T. Ouellet, L. Harris, and G. Fedak, *Use of a Fusarium graminearum strain transformed with green fluorescent protein to study infection in wheat ( Triticum aestivum ).* Canadian Journal of Plant Pathology, 2004. **26**: p. 453-463.
243. Ruel. *Development of pollen grains and embryo sac*. 2021 [cited 2024; Available from: https://mrrueltuition.com/development-of-pollen-grains-and-embryo-sac/.
244. *Things to look at with microscopes: Pollen*. 2020 [cited 2024; Available from: https://www.quekett.org/wp-content/uploads/2020/06/pollen-leaflet-2020.pdf.
245. Shunmugam, A.S.K., V. Bollina, S. Dukowic-Schulze, P. Bhowmik, C. Ambrose, J. Higgins, C. Pozniak, A. Sharpe, K. Rozwadowski, and S. Kagale, *MeioCapture: an efficient method for staging and isolation of meiocytes in the prophase I sub-stages of meiosis in wheat.* BMC Plant Biology, 2018. **18**.
246. PIERCE, S. *Thrips And Pollination: Is Pollination By Thrips Possible*. 2021 [cited 2024; Available from: https://www.gardeningknowhow.com/garden-how-to/beneficial/thrips-and-pollination.htm.
247. Vithana Pathirannehelage, N. and I. Joye, *Dietary Fibre from Whole Grains and Their Benefits on Metabolic Health.* Nutrients, 2020. **12**.
248. Teklić, T., Z. Lončarić, V. Kovačević, and B.R. Singh, *Metallic trace elements in cereal grain – a review: how much metal do we eat?* Food and Energy Security, 2013. **2**(2): p. 81-95.
249. Luthria, D.L., Y. Lu, and K.M.M. John, *Bioactive phytochemicals in wheat: Extraction, analysis, processing, and functional properties.* Journal of Functional Foods, 2015. **18**: p. 910-925.
250. Lersten, N.R., *Morphology and Anatomy of the Wheat Plant*, in *Wheat and Wheat Improvement*. 1987. p. 33-75.
251. Bruggmann, R., O. Abderhalden, P. Reymond, and R. Dudler, *Analysis of epidermis- and mesophyll-specific transcript accumulation in powdery mildew-inoculated wheat leaves.* Plant Molecular Biology, 2005. **58**(2): p. 247-267.
252. Camarillo-Castillo, F., T.D. Huggins, S. Mondal, M.P. Reynolds, M. Tilley, and D.B. Hays, *High-resolution spectral information enables phenotyping of leaf epicuticular wax in wheat.* Plant Methods, 2021. **17**(1): p. 58.
253. Mohammed, A., A. Borhana, Z. Hasan, I. R.A, S. Sapuan, and C. Santulli, *Wheat Biocomposite Extraction, Structure, Properties and Characterization: A Review.* Polymers, 2021. **13**: p. 1-27.
254. Stosch, Solga, Steiner, Oerke, C. E, W. Barthlott, and Z. Cerman, *Efficiency of self-cleaning properties in wheat (Triticum aestivum L.).* Journal of Applied Botany and Food Quality, 2007. **81**: p. 49-55.
255. BLACKMAN, E., *The Morphology and Development of Cross Veins in the Leaves of Bread Wheat (Triticum aestivum L.).* Annals of Botany, 1971. **35**(3): p. 653-665.
256. Johnson, Matthew P., *Photosynthesis.* Essays In Biochemistry, 2016. **60**: p. 255-273.
257. Carmo-Silva, E., J.C. Scales, P.J. Madgwick, and M.A. Parry, *Optimizing Rubisco and its regulation for greater resource use efficiency.* Plant Cell Environ, 2015. **38**(9): p. 1817-32.
258. Perdomo, J.A., S. Capó-Bauçà, E. Carmo-Silva, and J. Galmés, *Rubisco and Rubisco Activase Play an Important Role in the Biochemical Limitations of Photosynthesis in Rice, Wheat, and Maize under High Temperature and Water Deficit.* Front Plant Sci, 2017. **8**: p. 490.
259. Mathieu, L., M. Reder, A. Siah, A. Ducasse, C. Langlands-Perry, T.C. Marcel, J.-B. Morel, C. Saintenac, and E. Ballini, *SeptoSympto: a precise image analysis of Septoria tritici blotch disease symptoms using deep learning methods on scanned images.* Plant Methods, 2024. **20**(1): p. 18.
260. Yu, K., J. Anderegg, A. Mikaberidze, P. Karisto, F. Mascher, B.A. McDonald, A. Walter, and A. Hund, *Hyperspectral Canopy Sensing of Wheat Septoria Tritici Blotch Disease.* Front Plant Sci, 2018. **9**: p. 1195.
261. Ferguson, P., R. Cross, and G. Schad, *Chapter 8 - Application of SFC for the characterization of formulated drug products*, in *Separation Science and Technology*, M. Hicks and P. Ferguson, Editors. 2022, Academic Press. p. 221-255.
262. Ophardt, C., Steven Farmer, Dietmar Kennepohl, Layne Morsch, and L. Morsch. *21.6: Chemistry of Esters*. [cited 2024; Available from: https://chem.libretexts.org/Bookshelves/Organic_Chemistry/Organic_Chemistry_(Morsch_et_al.)/21%3A_Carboxylic_Acid_Derivatives-_Nucleophilic_Acyl_Substitution_Reactions/21.06%3A_Chemistry_of_Esters.
263. Rockett, C. *UV Degradation Effects in Materials – An Elementary Overview*. 2019 [cited 2024; Available from: https://uvsolutionsmag.com/articles/2019/uv-degradation-effects-in-materials-an-elementary-overview/#:~:text=The%20basic%20premise%20is%20always,microstructural%20changes%20in%20the%20material.

264. McCorison, C.B., *Illuminating how light affects the wheat fungal pathogen Zymoseptoria tritici*, in *Purdue University Graduate School*. 2020.
265. Meena, M., G. Yadav, P. Sonigra, A. Nagda, T. Mehta, P. Swapnil, Harish, and A. Marwal, *Role of elicitors to initiate the induction of systemic resistance in plants to biotic stress.* Plant Stress, 2022. **5**: p. 100103.
266. Cordo, C.A., C.I. Monaco, C.I. Segarra, M.R. Simon, A.Y. Mansilla, A.E. Perelló, N.I. Kripelz, D. Bayo, and R.D. Conde, *Trichoderma spp. as elicitors of wheat plant defense responses against Septoria tritici.* Biocontrol Science and Technology, 2007. **17**(7): p. 687-698.
267. Montazerin, M., Z. Sajjadifar, E. Khalili Pour, H. Riazi-Esfahani, T. Mahmoudi, H. Rabbani, H. Movahedian, A. Dehghani, M. Akhlaghi, and R. Kafieh, *Livelayer: a semi-automatic software program for segmentation of layers and diabetic macular edema in optical coherence tomography images.* Scientific Reports, 2021. **11**(1): p. 13794.
268. Ye, X., S. He, X. Zhong, J. Yu, S. Yang, Y. Shen, Y. Chen, Y. Wang, X. Huang, and L. Shen, *OIMHS: An Optical Coherence Tomography Image Dataset Based on Macular Hole Manual Segmentation.* Scientific Data, 2023. **10**(1): p. 769.
269. Huihong, Z., B. Yang, L. Sanqian, X. Zhang, X. Li, T. Liu, R. Higashita, and J. Liu, *Retinal OCT image segmentation with deep learning: A review of advances, datasets, and evaluation metrics.* Computerized Medical Imaging and Graphics, 2025: p. 102539.
270. Sampath Kumar, A., T. Schlosser, H. Langner, M. Ritter, and D. Kowerko, *Improving OCT Image Segmentation of Retinal Layers by Utilizing a Machine Learning Based Multistage System of Stacked Multiscale Encoders and Decoders.* Bioengineering, 2023. **10**(10): p. 1177.
271. Li, Q., S. Li, Z. He, H. Guan, R. Chen, Y. Xu, T. Wang, S. Qi, J. Mei, and W. Wang, *DeepRetina: Layer Segmentation of Retina in OCT Images Using Deep Learning.* Translational Vision Science & Technology, 2020. **9**(2): p. 61-61.
272. Hamana, T., M. Nishimori, S. Shibata, H. Kawamori, T. Toba, T. Hiromasa, S. Kakizaki, S. Sasaki, H. Fujii, Y. Osumi, S. Iwane, T. Yamamoto, S. Naniwa, Y. Sakamoto, Y. Fukuishi, K. Matsuhama, H. Tsunamoto, H. Okamoto, K. Higuchi, T. Kitagawa, M. Shinohara, K. Kuroda, M. Iwasaki, A. Kozuki, J. Shite, T. Takaya, K.-i. Hirata, and H. Otake, *Deep-learning-driven optical coherence tomography analysis for cardiovascular outcome prediction in patients with acute coronary syndrome.* European Heart Journal - Digital Health, 2024. **5**(6): p. 692-701.
273. Ling, S., B.J. Blackburn, M.W. Jenkins, M. Watanabe, S.M. Ford, M. Lapierre-Landry, and A.M. Rollins, *Segmentation of beating embryonic heart structures from 4-D OCT images using deep learning.* Biomed Opt Express, 2023. **14**(5): p. 1945-1958.
274. Carpenter, H.J., M.H. Ghayesh, A.C. Zander, J. Li, G. Di Giovanni, and P.J. Psaltis, *Automated Coronary Optical Coherence Tomography Feature Extraction with Application to Three-Dimensional Reconstruction.* Tomography, 2022. **8**(3): p. 1307-1349.
275. Chen, C., C. Qin, H. Qiu, G. Tarroni, J. Duan, W. Bai, and D. Rueckert, *Deep Learning for Cardiac Image Segmentation: A Review.* Frontiers in Cardiovascular Medicine, 2020. **Volume 7 - 2020**.
276. Kulyabin, M., A. Zhdanov, A. Nikiforova, A. Stepichev, A. Kuznetsova, M. Ronkin, V. Borisov, A. Bogachev, S. Korotkich, P.A. Constable, and A. Maier, *OCTDL: Optical Coherence Tomography Dataset for Image-Based Deep Learning Methods.* Scientific Data, 2024. **11**(1): p. 365.
277. Nawaz, M., A. Uvaliyev, K. Bibi, H. Wei, S.M.D. Abaxi, A. Masood, P. Shi, H.-P. Ho, and W. Yuan, *Unraveling the complexity of Optical Coherence Tomography image segmentation using machine and deep learning techniques: A review.* Computerized Medical Imaging and Graphics, 2023. **108**: p. 102269.
278. Guo, J. and Y. Cheng, *Advances in Fungal Elicitor-Triggered Plant Immunity.* International Journal of Molecular Sciences, 2022. **23**(19): p. 12003.
279. Meddya, S., S. Meshram, D. Sarkar, R. S, R. Datta, S. Singh, G. Avinash, A. Kumar Kondeti, A.K. Savani, and T. Thulasinathan, *Plant Stomata: An Unrealized Possibility in Plant Defense against Invading Pathogens and Stress Tolerance.* Plants (Basel), 2023. **12**(19).
280. Pantin, F. and M.R. Blatt, *Stomatal Response to Humidity: Blurring the Boundary between Active and Passive Movement.* Plant Physiology, 2018. **176**(1): p. 485-488.

## Appendices for Chapter V

1. Collaboration with the CIS company

This collaboration involves the University of Sheffield, Department of Chemistry and Cyber Infrastructure (CIS, http://www.cisin.com). CIS offers comprehensive IT services such as custom software application development. CIS company established in 2003, - Cyber Infrastructure, "CIS" - Central India's Largest Technology Company | www.cisin.com | https://www.cisin.com/.

2. OCT Leaf Analyzer User Guide (provided by CIS company)

a) Application Overview

The interface is split into two main sections: the left panel displays the original OCT leaf image, and the right panel shows the processed image with highlighted segmentation. Controls for image operations, insights generation, and navigation are provided below these panels.

i. Loading an OCT Leaf Image

- Drag and Drop: Drag and drop a file or folder onto the left panel.
- Load OCT Image Button: Opens a dialog to manually select an image or folder.

ii. Applying Segmentation and Highlighting

After loading an image, click **Apply Masking** to initiate segmentation between the second and third layers, highlighting the inner space. The right panel will update with the processed image, and segmentation details will appear below.

iii. Generating Insights

For batch processing of images from a folder, click **Generate insights for all**. The application will analyse each image, providing a summary of the segmentation results, including the average dimensions of the inner spaces.

b) Navigation (for folders)

1. Use **Previous** and **Next** to navigate through images.
2. The index display shows the current and total number of images.

c) Image and Analysis Details

- Image Details: Shows current image information (name, size, shape, format).
- Analysis Results**:** Displays segmentation outcomes, measurements, and classifications related to the highlighted inner space.

d) Working of infected leaves detection and segmentation

We labelled the infected areas on images of leaves by marking regions that displayed the infected area. These annotated images were then utilized to train a U-Net model, which is particularly effective for image segmentation tasks. The trained U-Net model can automatically detect and outline the infected areas on new, unseen leaf images by generating masks that highlight these regions. This approach enables efficient and automated detection of leaf infections.

e) Python code structure and the main components

To develop the OCT Leaf Analyzer software, we used Python along with several libraries. Here's a brief overview of the code structure and the main components:

i. TensorFlow: Used for building and training the U-Net model to segment the inner spaces between the layers in the OCT leaf images and also used for building and training the prediction model that prediction image is infected or non-infected model.
ii. OpenCV: Employed for preprocessing the OCT images, such as resizing, converting to grayscale if necessary, and enhancing image features to improve model accuracy.
iii. PyQt5: Utilized to create the graphical user interface (GUI) of the desktop application. This includes setting up the panels for displaying original and processed images, as well asimplementing the drag-and-drop functionality and buttons for loading images, applying segmentation, and generating insights.

Confusion Matrix:

```
[[177   7]
 [2   158]]
```

- Python code

```
import cv2
import os
```

```
import sys

import numpy as np

import pandas as pd

import tensorflow as tf

from PIL import Image

import logging

from PyQt5.QtCore import Qt, QSize, QThread, pyqtSignal

from PyQt5.QtGui import QPixmap, QImage

from PyQt5.QtWidgets import QApplication, QMainWindow, QLabel, QPushButton, QVBoxLayout,
QHBoxLayout, QWidget, QFileDialog, QTextEdit, QProgressBar, QProgressDialog

# Configure logging

logging.basicConfig(filename='test.log', level=logging.INFO, format='%(asctime)s - %(levelname)s -
%(message)s')

class ProgressDialog(QProgressDialog):

    """

    Custom progress dialog that extends QProgressDialog for displaying operation progress.

    """

    def __init__(self, parent=None):

        super().__init__(parent)

        self.setWindowModality(Qt.WindowModal)

        self.setWindowTitle("Progress")

        self.setMinimum(0)

        self.setMaximum(100)

        self.setValue(0)

    def set_value(self, value):

        self.setValue(value)


class MaskThread(QThread):

    """

    Thread to handle image masking operations asynchronously to avoid UI freezing.

    """

    mask_generated = pyqtSignal(np.ndarray, dict)

    progress_updated = pyqtSignal(int)
```

```
    def __init__(self, image_app_instance, image, masking_model, predict_using_thickness_data_model):
        super().__init__()
        self.image_app_instance = image_app_instance
        self.image = image
        self.masking_model = masking_model
        self.predict_using_thickness_data_model = predict_using_thickness_data_model
        self.is_running = True
    def run(self):
        mask = self.image_app_instance.generate_mask(self.image)[135]
        image_with_boundary = self.image_app_instance.create_boundary(mask, self.image)
        filled_mask_area_image = self.image_app_instance.fill_mask(mask, self.image.copy())
        straighten_image = self.image_app_instance.straight_images([image_with_boundary])
        thickness_data = self.image_app_instance.calculate_thickness(straighten_image)
        df = pd.DataFrame(thickness_data)
        results = self.predict_using_thickness_data_model.predict(df)
        tag = "Non-Infected" if results[0] > 0.5 else "Infected"
        details = {"tag": tag, "max": round(df['max'][0],2), "min": round(df['min'][0],2), "avg":
round(df['avg'][0],2)}
        self.mask_generated.emit(np.array(filled_mask_area_image), details)
    def stop(self):
        self.is_running = False
class InsightsThread(QThread):
    """
    Thread for generating insights across multiple images. Handles bulk processing.
    """
    insights_generated = pyqtSignal(dict)
    progress_updated = pyqtSignal(int)
    def __init__(self, image_app_instance, file_paths, masking_model, predict_using_thickness_data_model):
        super().__init__()
        self.image_app_instance = image_app_instance
        self.file_paths = file_paths
        self.masking_model = masking_model
        self.predict_using_thickness_data_model = predict_using_thickness_data_model
```

```
        self.is_running = True
    def run(self):
        straighten_image = []
        total_files = len(self.file_paths)
        for idx, file_path in enumerate(self.file_paths):
            if not self.is_running:
                break
            img_for_calculation = cv2.imread(file_path, cv2.IMREAD_COLOR)
            if img_for_calculation is not None:
                mask = self.image_app_instance.generate_mask(img_for_calculation.copy())
                image_with_boundary = self.image_app_instance.create_boundary(mask, img_for_calculation)
                straighten_image.append(self.image_app_instance.straight_images([image_with_boundary])[0])
            self.progress_updated.emit(int((idx + 1) * 90 / total_files))
        if straighten_image:
            thickness_data = self.image_app_instance.calculate_thickness(straighten_image)
            self.progress_updated.emit(95)
            df = pd.DataFrame(thickness_data)
            results = self.predict_using_thickness_data_model.predict(df)
            mean_df = df.mean(axis=0)
            mean_df_for_pred = pd.DataFrame([{'min': mean_df['min'], 'max': mean_df['max'], 'avg':
mean_df['avg']}])
            mean_result = self.predict_using_thickness_data_model.predict(mean_df_for_pred)
            tag = "Non-Infected" if mean_result[0] > 0.5 else "Infected"
            details = {
                "tag": tag, "max": round(mean_df_for_pred['max'][0], 2),
                "min": round(mean_df_for_pred['min'][0], 2),
                "avg": round(mean_df_for_pred['avg'][0], 2),
                "total images": len(results),
                "detected non-infected images": list(results).count(1),
                "detected infected images": list(results).count(0)
            }
            self.insights_generated.emit(details)
            self.progress_updated.emit(98)
```

```
        self.progress_updated.emit(100)
        self.finished.emit()
    def stop(self):
        self.is_running = False
class Label(QLabel):
    """
    Custom QLabel with drag-and-drop support for images or image folders.
    """
    imageLoaded = pyqtSignal()
    def __init__(self, title, parent):
        super().__init__(title, parent)
        self.setAcceptDrops(True)
        self.file_paths = []

    def dragEnterEvent(self, e):
        if e.mimeData().hasUrls():
            e.accept()
        else:
            e.ignore()
    def dropEvent(self, e):
        m = e.mimeData()
        if m.hasUrls():
            for url in m.urls():
                if url.isLocalFile():
                    file_path = url.toLocalFile()
                    if os.path.isfile(file_path):
                        self.file_paths = []
                        self.window().load_image(file_path)
                        self.window().image_count_label.setText(f"Image 1 of 1")
                    elif os.path.isdir(file_path):
                        self.current_index = -1
```

```
                image_files = [f for f in os.listdir(file_path) if f.endswith(('.png', '.jpg', '.jpeg', '.bmp', '.tif', '.tiff'))]
                self.file_paths = [os.path.join(file_path, f) for f in sorted(image_files)]
                self.load_next_image()
    def load_next_image(self):
        if self.file_paths and self.current_index < len(self.file_paths) - 1:
            self.current_index += 1
            self.window().load_image(self.file_paths[self.current_index])
            self.imageLoaded.emit()
    def load_previous_image(self):
        if self.file_paths and self.current_index > 0:
            self.current_index -= 1
            self.window().load_image(self.file_paths[self.current_index])
            self.imageLoaded.emit()
class ImageApp(QMainWindow):
    """
    Main application window for the OCT Leaf Analyzer.
    """
    def __init__(self, masking_model, predict_using_thickness_data_model):
        super().__init__()
        self.masking_model = masking_model
        self.predict_using_thickness_data_model = predict_using_thickness_data_model
        self.setup_ui()
    def setup_ui(self):
        self.setWindowTitle("OCT Leaf Analyzer")
        self.setGeometry(100, 100, 1000, 600)
        central_widget = QWidget(self)
        self.setCentralWidget(central_widget)
        main_layout = QVBoxLayout(central_widget)
        image_container = QWidget()
        image_layout = QHBoxLayout(image_container)
        self.original_label = Label("Drag and Drop image or folder here", self)
        self.original_label.setAlignment(Qt.AlignCenter)
```

```
image_layout.addWidget(self.original_label)
self.masked_label = QLabel("", self)
self.masked_label.setAlignment(Qt.AlignCenter)
image_layout.addWidget(self.masked_label)
main_layout.addWidget(image_container)
button_layout = QHBoxLayout()
self.load_button = QPushButton("Load OCT Image", self)
self.load_button.clicked.connect(self.load_image)
button_layout.addWidget(self.load_button)
self.mask_button = QPushButton("Apply Masking", self)
self.mask_button.clicked.connect(self.apply_mask_async)
button_layout.addWidget(self.mask_button)
self.generate_insights_button = QPushButton("Generate Insights for All", self)
self.generate_insights_button.clicked.connect(self.generate_insights_for_all)
button_layout.addWidget(self.generate_insights_button)
self.details_textedit = QTextEdit(self)
self.details_textedit.setReadOnly(True)
main_layout.addLayout(button_layout)
main_layout.addWidget(self.details_textedit)
arrow_layout = QHBoxLayout()
self.prev_button = QPushButton("Previous", self)
self.prev_button.clicked.connect(self.original_label.load_previous_image)
arrow_layout.addWidget(self.prev_button)
self.image_count_label = QLabel("", self)
self.image_count_label.setAlignment(Qt.AlignCenter)
arrow_layout.addWidget(self.image_count_label)
self.next_button = QPushButton("Next", self)
self.next_button.clicked.connect(self.original_label.load_next_image)
arrow_layout.addWidget(self.next_button)
main_layout.addLayout(arrow_layout)
self.setStyleSheet("""
    QMainWindow {
```

```
        background-color: #37474F;
    }
    QPushButton {
        background-color: #FFC107;
        color: #37474F;
        border-radius: 15px;
        padding: 10px;
        margin: 6px;
        font-size: 14px;
    }
    QPushButton:hover {
        background-color: #FFD54F;
    }
    QLabel {
        color: #FFFFFF;
        background-color: #455A64;
        padding: 5px;
        border-radius: 5px;
        font-size: 16px;
        font-weight: semi-bold;
    }
    QTextEdit, QLineEdit {
        background-color: #CFD8DC;
        color: #37474F;
        font-size: 14px;
        border: none;
        padding: 5px;
        border-radius: 5px;
    }
""")
self.original_label.imageLoaded.connect(self.update_details)
```

```
    def load_image(self, file_path=None):
        """
        Load an image from the file dialog or from a dropped file.
        """
        if not file_path:
            options = QFileDialog.Options()
            file_path, _ = QFileDialog.getOpenFileName(self, "Select OCT Image", "", "Image Files (*.png *.jpg *.jpeg *.bmp *.tif *.tiff)", options=options)
        if file_path:
            self.image = cv2.imread(file_path, cv2.IMREAD_COLOR)
            self.image = cv2.resize(self.image, (512, 512), interpolation=cv2.INTER_AREA)
            if self.image is not None:
                self.display_image(self.image, self.original_label)
                self.update_details(file_path)
        self.masked_label.clear()
    def apply_mask_async(self):
        """
        Apply mask to the loaded image asynchronously.
        """
        if self.image is not None:
            self.progress_dialog = ProgressDialog(self)
            self.progress_dialog.show()
            self.progress_dialog.setLabelText("Applying Masking")
            self.mask_thread = MaskThread(self, self.image.copy(), self.masking_model, self.predict_using_thickness_data_model)BookGap thickness. AxC169. Manual.xls
            self.mask_thread.mask_generated.connect(self.show_mask_result)
            self.mask_thread.progress_updated.connect(self.update_progress_bar)
            self.mask_thread.finished.connect(self.progress_dialog.accept)
            self.progress_dialog.canceled.connect(self.stop_mask_thread)
            self.mask_thread.start()
    def stop_mask_thread(self):
        """
        Stop the mask thread if it is still running.
```

```
        """
        if self.mask_thread.isRunning():
            self.mask_thread.stop()
    def generate_insights_for_all(self):
        """
        Generate insights for all images loaded into the application.
        """
        if not self.original_label.file_paths:
            return  # No files loaded, exit the function

        self.progress_dialog = ProgressDialog(self)
        self.progress_dialog.show()
        self.progress_dialog.setLabelText("Generating Insights")
        self.insights_thread = InsightsThread(self, self.original_label.file_paths, self.masking_model,
self.predict_using_thickness_data_model)
        self.insights_thread.insights_generated.connect(self.show_insights)
        self.insights_thread.progress_updated.connect(self.update_progress_bar)
        self.insights_thread.finished.connect(self.progress_dialog.accept)
        self.progress_dialog.canceled.connect(self.stop_insights_thread)

        self.insights_thread.start()

    def stop_insights_thread(self):
        """
        Stop the insights generation thread if it is still running.
        """
        if self.insights_thread.isRunning():
            self.insights_thread.stop()
    def update_progress_bar(self, progress_percent):
        """
        Update the progress bar in the UI.
        """
        self.progress_dialog.set_value(progress_percent)
```

```
def show_mask_result(self, masked_image, details):
    """
    Display the masked image and details in the UI.
    """
    self.display_image(self.image, self.original_label)
    self.display_image(masked_image, self.masked_label)
    self.show_details(details)
def show_insights(self, detail):
    """
    Display the insights for all processed images in the UI.
    """
    details = (f"<b>Total images</b>: {detail['total images']}<br>"
               f"<b>Detected Non-Infected images</b>: {detail['detected non-infected images']}<br>"
               f"<b>Detected Infected images</b>: {detail['detected infected images']}<br><br>"
               f"<b>Mean insights for all images</b> :-<br><br>"
               f"<b>Tag</b>: {detail['tag']}<br>"
               f"<b>Maximum Thickness</b>: {detail['max']}mm<br>"
               f"<b>Minimum Thickness</b>: {detail['min']}mm<br>"
               f"<b>Average Thickness</b>: {detail['avg']}mm<br><br>"
               f"<b>Note</b>: 100px = 1mm")
    self.details_textedit.setHtml(details)
def display_image(self, image, label):
    """
    Utility function to display an image on a QLabel.
    """
    if image is not None:
        if len(image.shape) == 3:
            height, width, channel = image.shape
        else:
            height, width = image.shape
        image = cv2.cvtColor(image, cv2.COLOR_BGR2RGB)
```

```
            bytesPerLine = 3 * width
            qImg = QImage(image.data, width, height, bytesPerLine, QImage.Format_RGB888).rgbSwapped()
            pixmap = QPixmap.fromImage(qImg)
            pixmap = pixmap.scaled(QSize(512, 512), Qt.KeepAspectRatio)
            label.setPixmap(pixmap)


def load_model(path):
    """
    Load a TensorFlow model from a specified path.
    """
    try:
        if getattr(sys, 'frozen', False):
            # When running as a PyInstaller bundle
            base_path = sys._MEIPASS
        else:
            # When running as a script
            base_path = os.path.dirname(os.path.abspath(__file__))
        model_path = os.path.join(base_path, path)
        model = tf.keras.models.load_model(model_path)
        logging.info('Model loaded successfully from main')
        return model
    except FileNotFoundError:
        logging.error('Model file not found. Please verify the file path.')
    except Exception as e:
        logging.error(f'Failed to load model: {e}')
if __name__ == "__main__":
    tf.compat.v1.enable_eager_execution()
    predict_using_thickness_data_model = load_model("classification_model.keras")
    masking_model = load_model('unet_masking3.keras')
    app = QApplication(sys.argv)
    window = ImageApp(masking_model, predict_using_thickness_data_model)
    window.show()
```

```
sys.exit(app.exec_())
```

f) The software's operational steps

This section outlines the steps involved in operating the OCT image segmentation, using figures to provide visual guidance.


Figure 66: Shows the home page of the OCT Image Segmentation.

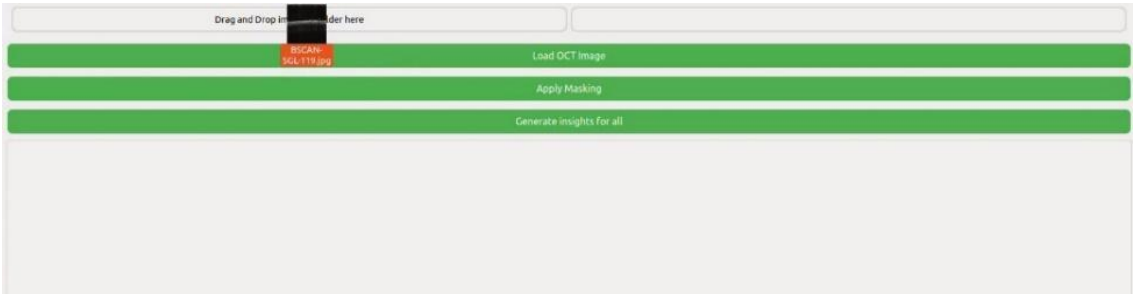


Figure 67: Drag OCT image or data set to the “Load OCT image” option.

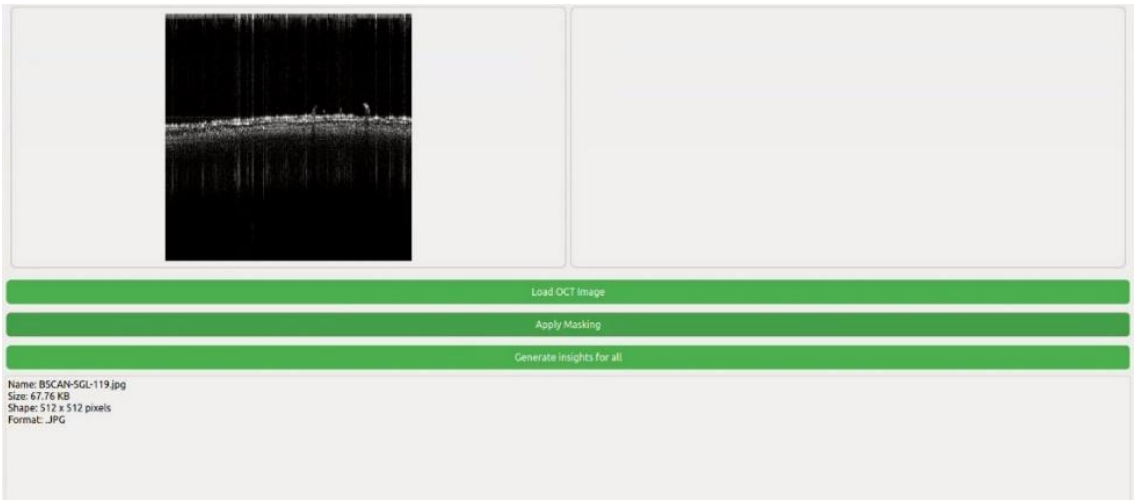


Figure 68: Then, click on “apply mask” option on OCT image/s.

The software can automatically analyse the thickness of inner spaces, providing key information such as maximum, minimum, and average gap thickness in no time.

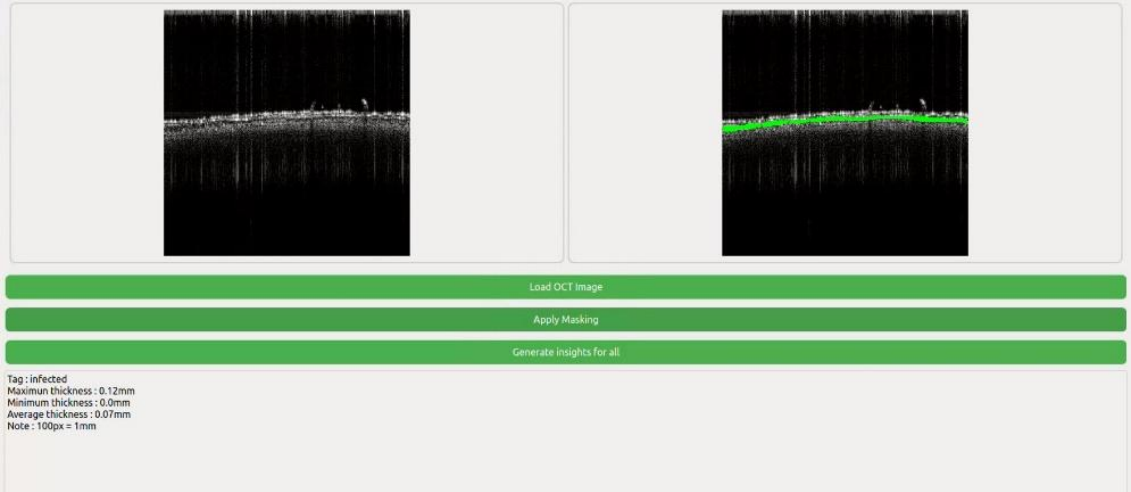


Figure 69: Demonstrates the key information, including the maximum and minimum thickness values along with their averages, as a result of masking the gap.

The OCT analyzer software is available for download at the following link

https://drive.google.com/file/d/1xDpiNgIyM85NAjBNc00EPw2RB7S2u9jU/view?usp=drive_link

3. Tables of manual gap thickness measurements for AxC169 variety

The following tables illustrate the total number of OCT images used for manual gap thickness measurements in the AxC169 variety. A total of 250 OCT images were analyzed, with segmentation of the first 2–3 cell layers performed using the Freehand Tool in FIJI. For both control and infected leaves, three readings were taken from Day 0 (D0) to Day 7 (D7).

| Day 0<br>Before inoculation | | | | | | | Day1 | | | | | |
|---|---|---|---|---|---|---|---|---|---|---|---|---|
| OCT image | Control | | | Before inoculation | | | Control | | | Infected | | |
| | 1 | 2 | 3 | 1 | 2 | 3 | 1 | 2 | 3 | 1 | 2 | 3 |
| 1 | 0.08 | 0.08 | 0.084 | 0.06 | 0.05 | 0.052 | 0.031 | 0.061 | 0.031 | 0.051 | 0.05 | 0.022 |
| 2 | 0.071 | 0.05 | 0.08 | 0.02 | 0.057 | 0.042 | 0.048 | 0.039 | 0.055 | 0.05 | 0.051 | 0.034 |
| 3 | 0.05 | 0.042 | 0.07 | 0.033 | 0.033 | 0.03 | 0.061 | 0.034 | 0.038 | 0.055 | 0.055 | 0.039 |
| 4 | 0.07 | 0.04 | 0.098 | 0.03 | 0.06 | 0.052 | 0.027 | 0.038 | 0.027 | 0.05 | 0.055 | 0.052 |
| 5 | 0.091 | 0.04 | 0.01 | 0.06 | 0.04 | 0.05 | 0.058 | 0.027 | 0.07 | 0.039 | 0.05 | 0.039 |
| 6 | 0.081 | 0.02 | 0.042 | 0.075 | 0.04 | 0.04 | 0.026 | 0.039 | 0.039 | 0.059 | 0.055 | 0.013 |
| 7 | 0.057 | 0.03 | 0.091 | 0.04 | 0.048 | 0.05 | 0.039 | 0.027 | 0.055 | 0.055 | 0.057 | 0.038 |
| 8 | 0.07 | 0.033 | 0.08 | 0.07 | 0.024 | 0.061 | 0.033 | 0.033 | 0.059 | 0.044 | 0.05 | 0.049 |
| 9 | 0.057 | 0.02 | 0.048 | 0.057 | 0.057 | 0.05 | 0.037 | 0.016 | 0.028 | 0.055 | 0.056 | 0.049 |
| 10 | 0.04 | 0.04 | 0.071 | 0.05 | 0.033 | 0.033 | 0.039 | 0.044 | 0.064 | 0.067 | 0.05 | 0.038 |
| 11 | 0.05 | 0.052 | 0.052 | 0.07 | 0.061 | 0.04 | 0.023 | 0.039 | 0.023 | 0.053 | 0.054 | 0.034 |
| 12 | 0.061 | 0.024 | 0.09 | 0.06 | 0.04 | 0.03 | 0.049 | 0.034 | 0.048 | 0.049 | 0.056 | 0.062 |
| 13 | 0.071 | 0.075 | 0.052 | 0.057 | 0.05 | 0.05 | 0.049 | 0.044 | 0.045 | 0.038 | 0.056 | 0.034 |
| 14 | 0.084 | 0.057 | 0.06 | 0.03 | 0.04 | 0.05 | 0.039 | 0.033 | 0.044 | 0.05 | 0.05 | 0.028 |
| 15 | 0.129 | 0.04 | 0.06 | 0.08 | 0.042 | 0.07 | 0.033 | 0.054 | 0.05 | 0.045 | 0.055 | 0.045 |
| 16 | 0.04 | 0.04 | 0.05 | 0.02 | 0.05 | 0.052 | 0.027 | 0.031 | 0.033 | 0.054 | 0.06 | 0.055 |
| 17 | 0.066 | 0.06 | 0.03 | 0.061 | 0.05 | 0.02 | 0.071 | 0.031 | 0.038 | 0.045 | 0.053 | 0.057 |
| 18 | 0.02 | 0.033 | 0.042 | 0.04 | 0.05 | 0.042 | 0.038 | 0.028 | 0.049 | 0.036 | 0.055 | 0.022 |
| 19 | 0.052 | 0.042 | 0.07 | 0.071 | 0.04 | 0.03 | 0.044 | 0.04 | 0.027 | 0.055 | 0.042 | 0.04 |
| 20 | 0.04 | 0.033 | 0.03 | 0.05 | 0.04 | 0.05 | 0.031 | 0.057 | 0.045 | 0.058 | 0.051 | 0.041 |
| 21 | 0.033 | 0.02 | 0.06 | 0.06 | 0.02 | 0.06 | 0.036 | 0.062 | 0.049 | 0.058 | 0.059 | 0.064 |
| 22 | 0.084 | 0.04 | 0.071 | 0.061 | 0.052 | 0.052 | 0.049 | 0.045 | 0.044 | 0.04 | 0.056 | 0.066 |
| 23 | 0.04 | 0.04 | 0.048 | 0.061 | 0.05 | 0.052 | 0.011 | 0.044 | 0.041 | 0.06 | 0.06 | 0.075 |
| 24 | 0.071 | 0.04 | 0.057 | 0.04 | 0.04 | 0.05 | 0.028 | 0.016 | 0.05 | 0.057 | 0.055 | 0.045 |
| 25 | 0.061 | 0.066 | 0.06 | 0.048 | 0.061 | 0.091 | 0.05 | 0.041 | 0.05 | 0.046 | 0.06 | 0.026 |

| | | | | | | | | | | | | |
|---|---|---|---|---|---|---|---|---|---|---|---|---|
| 26 | 0.033 | 0.06 | 0.05 | 0.066 | 0.02 | 0.052 | 0.044 | 0.084 | 0.022 | 0.044 | 0.043 | 0.071 |
| 27 | 0.033 | 0.03 | 0.05 | 0.033 | 0.07 | 0.061 | 0.07 | 0.034 | 0.027 | 0.044 | 0.061 | 0.027 |
| 28 | 0.061 | 0.03 | 0.05 | 0.03 | 0.04 | 0.066 | 0.034 | 0.057 | 0.027 | 0.045 | 0.061 | 0.033 |
| 29 | 0.057 | 0.03 | 0.04 | 0.052 | 0.061 | 0.05 | 0.062 | 0.035 | 0.018 | 0.04 | 0.06 | 0.044 |
| 30 | 0.042 | 0.061 | 0.04 | 0.07 | 0.05 | 0.066 | 0.045 | 0.028 | 0.054 | 0.028 | 0.054 | 0.049 |
| 31 | 0.024 | 0.071 | 0.05 | 0.03 | 0.03 | 0.06 | 0.055 | 0.041 | 0.057 | 0.049 | 0.04 | 0.023 |
| 32 | 0.03 | 0.05 | 0.042 | 0.024 | 0.04 | 0.07 | 0.038 | 0.033 | 0.033 | 0.046 | 0.061 | 0.049 |
| 33 | 0.052 | 0.05 | 0.048 | 0.06 | 0.02 | 0.05 | 0.041 | 0.016 | 0.049 | 0.027 | 0.064 | 0.027 |
| 34 | 0.05 | 0.033 | 0.061 | 0.03 | 0.042 | 0.06 | 0.031 | 0.028 | 0.049 | 0.063 | 0.065 | 0.061 |
| 35 | 0.061 | 0.03 | 0.042 | 0.05 | 0.05 | 0.048 | 0.072 | 0.022 | 0.055 | 0.06 | 0.06 | 0.041 |
| 36 | 0.052 | 0.04 | 0.04 | 0.06 | 0.03 | 0.033 | 0.038 | 0.034 | 0.028 | 0.055 | 0.061 | 0.04 |
| 37 | 0.091 | 0.071 | 0.07 | 0.03 | 0.033 | 0.052 | 0.049 | 0.05 | 0.057 | 0.06 | 0.06 | 0.049 |
| 38 | 0.02 | 0.042 | 0.052 | 0.057 | 0.03 | 0.03 | 0.06 | 0.049 | 0.034 | 0.062 | 0.052 | 0.055 |
| 39 | 0.03 | 0.042 | 0.057 | 0.06 | 0.04 | 0.048 | 0.044 | 0.034 | 0.027 | 0.068 | 0.061 | 0.049 |
| 40 | 0.04 | 0.075 | 0.05 | 0.024 | 0.04 | 0.03 | 0.05 | 0.027 | 0.027 | 0.05 | 0.054 | 0.035 |
| 41 | 0.04 | 0.05 | 0.05 | 0.03 | 0.03 | 0.042 | 0.06 | 0.034 | 0.023 | 0.066 | 0.051 | 0.072 |
| 42 | 0.06 | 0.052 | 0.033 | 0.07 | 0.02 | 0.033 | 0.078 | 0.016 | 0.034 | 0.055 | 0.061 | 0.062 |
| 43 | 0.061 | 0.052 | 0.05 | 0.04 | 0.066 | 0.04 | 0.049 | 0.038 | 0.049 | 0.063 | 0.065 | 0.088 |
| 44 | 0.061 | 0.03 | 0.06 | 0.04 | 0.03 | 0.05 | 0.027 | 0.034 | 0.045 | 0.06 | 0.065 | 0.023 |
| 45 | 0.07 | 0.042 | 0.07 | 0.042 | 0.042 | 0.05 | 0.033 | 0.034 | 0.034 | 0.028 | 0.06 | 0.045 |
| 46 | 0.03 | 0.033 | 0.07 | 0.033 | 0.033 | 0.048 | 0.022 | 0.039 | 0.027 | 0.054 | 0.063 | 0.067 |
| 47 | 0.071 | 0.03 | 0.071 | 0.01 | 0.02 | 0.071 | 0.044 | 0.049 | 0.022 | 0.045 | 0.056 | 0.05 |
| 48 | 0.05 | 0.024 | 0.03 | 0.033 | 0.042 | 0.08 | 0.039 | 0.044 | 0.027 | 0.033 | 0.056 | 0.053 |
| 49 | 0.04 | 0.042 | 0.04 | 0.06 | 0.02 | 0.04 | 0.055 | 0.054 | 0.023 | 0.031 | 0.05 | 0.039 |
| 50 | 0.024 | 0.06 | 0.052 | 0.02 | 0.03 | 0.02 | 0.045 | 0.027 | 0.075 | 0.024 | 0.057 | 0.048 |
| 51 | 0.052 | 0.01 | 0.04 | 0.052 | 0.06 | 0.052 | 0.018 | 0.027 | 0.05 | 0.018 | 0.056 | 0.018 |
| 52 | 0.07 | 0.052 | 0.04 | 0.06 | 0.061 | 0.06 | 0.049 | 0.038 | 0.038 | 0.011 | 0.06 | 0.022 |
| 53 | 0.06 | 0.05 | 0.052 | 0.042 | 0.05 | 0.05 | 0.044 | 0.048 | 0.05 | 0.049 | 0.065 | 0.028 |
| 54 | 0.061 | 0.04 | 0.081 | 0.02 | 0.04 | 0.081 | 0.041 | 0.07 | 0.034 | 0.05 | 0.05 | 0.034 |
| 55 | 0.05 | 0.042 | 0.04 | 0.052 | 0.033 | 0.04 | 0.011 | 0.04 | 0.011 | 0.056 | 0.054 | 0.044 |

| | | | | | | | | | | | | |
|---|---|---|---|---|---|---|---|---|---|---|---|---|
| 56 | 0.05 | 0.052 | 0.057 | 0.06 | 0.03 | 0.042 | 0.039 | 0.038 | 0.033 | 0.06 | 0.056 | 0.071 |
| 57 | 0.052 | 0.052 | 0.071 | 0.04 | 0.04 | 0.03 | 0.077 | 0.023 | 0.038 | 0.062 | 0.06 | 0.038 |
| 58 | 0.052 | 0.01 | 0.052 | 0.05 | 0.052 | 0.061 | 0.06 | 0.054 | 0.027 | 0.034 | 0.061 | 0.053 |
| 59 | 0.02 | 0.05 | 0.05 | 0.02 | 0.06 | 0.017 | 0.045 | 0.044 | 0.057 | 0.038 | 0.051 | 0.052 |
| 60 | 0.05 | 0.02 | 0.071 | 0.03 | 0.042 | 0.084 | 0.055 | 0.033 | 0.027 | 0.054 | 0.061 | 0.088 |
| 61 | 0.071 | 0.04 | 0.07 | 0.05 | 0.05 | 0.061 | 0.052 | 0.088 | 0.033 | 0.052 | 0.06 | 0.033 |
| 62 | 0.071 | 0.03 | 0.091 | 0.052 | 0.052 | 0.07 | 0.044 | 0.049 | 0.06 | 0.061 | 0.061 | 0.059 |
| 63 | 0.04 | 0.04 | 0.052 | 0.033 | 0.02 | 0.052 | 0.055 | 0.052 | 0.044 | 0.041 | 0.06 | 0.061 |
| 64 | 0.061 | 0.061 | 0.08 | 0.03 | 0.042 | 0.042 | 0.022 | 0.033 | 0.05 | 0.062 | 0.052 | 0.057 |
| 65 | 0.084 | 0.06 | 0.061 | 0.03 | 0.033 | 0.06 | 0.038 | 0.061 | 0.039 | 0.061 | 0.062 | 0.027 |
| 66 | 0.1 | 0.052 | 0.05 | 0.04 | 0.06 | 0.07 | 0.033 | 0.052 | 0.05 | 0.067 | 0.042 | 0.05 |
| 67 | 0.04 | 0.02 | 0.03 | 0.05 | 0.071 | 0.052 | 0.044 | 0.034 | 0.022 | 0.062 | 0.05 | 0.05 |
| 68 | 0.071 | 0.03 | 0.02 | 0.07 | 0.03 | 0.03 | 0.038 | 0.022 | 0.049 | 0.058 | 0.054 | 0.072 |
| 69 | 0.033 | 0.05 | 0.033 | 0.07 | 0.057 | 0.06 | 0.022 | 0.033 | 0.039 | 0.064 | 0.06 | 0.05 |
| 70 | 0.06 | 0.03 | 0.03 | 0.024 | 0.057 | 0.06 | 0.034 | 0.033 | 0.039 | 0.062 | 0.031 | 0.044 |
| 71 | 0.07 | 0.04 | 0.033 | 0.05 | 0.05 | 0.06 | 0.039 | 0.041 | 0.052 | 0.05 | 0.051 | 0.028 |
| 72 | 0.05 | 0.03 | 0.05 | 0.052 | 0.042 | 0.06 | 0.022 | 0.013 | 0.044 | 0.036 | 0.054 | 0.027 |
| 73 | 0.061 | 0.05 | 0.05 | 0.03 | 0.052 | 0.042 | 0.027 | 0.044 | 0.027 | 0.041 | 0.06 | 0.066 |
| 74 | 0.071 | 0.05 | 0.04 | 0.071 | 0.052 | 0.05 | 0.027 | 0.034 | 0.058 | 0.053 | 0.051 | 0.062 |
| 75 | 0.091 | 0.04 | 0.03 | 0.04 | 0.05 | 0.07 | 0.023 | 0.023 | 0.039 | 0.039 | 0.03 | 0.04 |
| 76 | 0.091 | 0.03 | 0.048 | 0.024 | 0.04 | 0.05 | 0.028 | 0.028 | 0.034 | 0.066 | 0.05 | 0.046 |
| 77 | 0.091 | 0.03 | 0.04 | 0.033 | 0.071 | 0.071 | 0.039 | 0.028 | 0.034 | 0.039 | 0.048 | 0.028 |
| 78 | 0.05 | 0.04 | 0.071 | 0.08 | 0.03 | 0.07 | 0.06 | 0.027 | 0.054 | 0.04 | 0.009 | 0.041 |
| 79 | 0.071 | 0.04 | 0.04 | 0.05 | 0.091 | 0.05 | 0.041 | 0.034 | 0.049 | 0.039 | 0.011 | 0.033 |
| 80 | 0.061 | 0.05 | 0.05 | 0.061 | 0.04 | 0.06 | 0.034 | 0.054 | 0.038 | 0.066 | 0.017 | 0.052 |
| 81 | 0.04 | 0.04 | 0.05 | 0.04 | 0.052 | 0.052 | 0.035 | 0.033 | 0.018 | 0.055 | 0.044 | 0.053 |
| 82 | 0.071 | 0.05 | 0.04 | 0.048 | 0.05 | 0.05 | 0.028 | 0.05 | 0.044 | 0.062 | 0.05 | 0.06 |
| 83 | 0.03 | 0.05 | 0.091 | 0.05 | 0.045 | 0.02 | 0.022 | 0.038 | 0.04 | 0.034 | 0.051 | 0.062 |
| 84 | 0.04 | 0.033 | 0.03 | 0.04 | 0.073 | 0.073 | 0.06 | 0.052 | 0.013 | 0.044 | 0.06 | 0.044 |
| 85 | 0.04 | 0.07 | 0.05 | 0.05 | 0.05 | 0.024 | 0.038 | 0.033 | 0.064 | 0.033 | 0.056 | 0.05 |

| | | | | | | | | | | | | |
|---|---|---|---|---|---|---|---|---|---|---|---|---|
| 86 | 0.05 | 0.03 | 0.01 | 0.05 | 0.042 | 0.042 | 0.053 | 0.022 | 0.013 | 0.028 | 0.057 | 0.049 |
| 87 | 0.1 | 0.04 | 0.057 | 0.06 | 0.03 | 0.084 | 0.034 | 0.023 | 0.062 | 0.011 | 0.065 | 0.044 |
| 88 | 0.04 | 0.061 | 0.045 | 0.052 | 0.042 | 0.042 | 0.039 | 0.022 | 0.044 | 0.057 | 0.06 | 0.065 |
| 89 | 0.05 | 0.06 | 0.03 | 0.033 | 0.06 | 0.03 | 0.022 | 0.033 | 0.028 | 0.062 | 0.061 | 0.061 |
| 90 | 0.05 | 0.03 | 0.03 | 0.03 | 0.02 | 0.07 | 0.038 | 0.045 | 0.066 | 0.057 | 0.064 | 0.05 |
| 91 | 0.03 | 0.042 | 0.05 | 0.05 | 0.05 | 0.033 | 0.044 | 0.035 | 0.033 | 0.049 | 0.051 | 0.057 |
| 92 | 0.066 | 0.05 | 0.066 | 0.04 | 0.03 | 0.03 | 0.034 | 0.06 | 0.038 | 0.064 | 0.064 | 0.053 |
| 93 | 0.066 | 0.042 | 0.061 | 0.03 | 0.06 | 0.05 | 0.033 | 0.028 | 0.049 | 0.046 | 0.063 | 0.052 |
| 94 | 0.052 | 0.033 | 0.07 | 0.02 | 0.03 | 0.05 | 0.06 | 0.054 | 0.06 | 0.08 | 0.065 | 0.028 |
| 95 | 0.04 | 0.03 | 0.03 | 0.08 | 0.04 | 0.03 | 0.045 | 0.085 | 0.075 | 0.016 | 0.065 | 0.044 |
| 96 | 0.04 | 0.03 | 0.02 | 0.04 | 0.033 | 0.017 | 0.059 | 0.023 | 0.027 | 0.038 | 0.057 | 0.033 |
| 97 | 0.042 | 0.04 | 0.05 | 0.03 | 0.03 | 0.04 | 0.049 | 0.055 | 0.045 | 0.045 | 0.06 | 0.055 |
| 98 | 0.061 | 0.024 | 0.03 | 0.05 | 0.06 | 0.071 | 0.062 | 0.023 | 0.045 | 0.044 | 0.065 | 0.057 |
| 99 | 0.042 | 0.05 | 0.04 | 0.028 | 0.05 | 0.04 | 0.049 | 0.011 | 0.041 | 0.049 | 0.03 | 0.059 |
| 100 | 0.042 | 0.033 | 0.061 | 0.04 | 0.07 | 0.07 | 0.05 | 0.038 | 0.039 | 0.06 | 0.04 | 0.044 |
| 101 | 0.05 | 0.05 | 0.04 | 0.05 | 0.075 | 0.017 | 0.066 | 0.033 | 0.044 | 0.045 | 0.041 | 0.055 |
| 102 | 0.02 | 0.03 | 0.05 | 0.04 | 0.042 | 0.05 | 0.041 | 0.044 | 0.027 | 0.066 | 0.04 | 0.06 |
| 103 | 0.06 | 0.07 | 0.042 | 0.057 | 0.05 | 0.042 | 0.059 | 0.049 | 0.045 | 0.052 | 0.057 | 0.055 |
| 104 | 0.04 | 0.042 | 0.048 | 0.04 | 0.02 | 0.02 | 0.083 | 0.028 | 0.027 | 0.066 | 0.055 | 0.065 |
| 105 | 0.04 | 0.05 | 0.04 | 0.033 | 0.052 | 0.052 | 0.071 | 0.039 | 0.052 | 0.022 | 0.06 | 0.06 |
| 106 | 0.052 | 0.02 | 0.05 | 0.061 | 0.03 | 0.042 | 0.033 | 0.066 | 0.045 | 0.027 | 0.053 | 0.033 |
| 107 | 0.04 | 0.02 | 0.03 | 0.03 | 0.04 | 0.02 | 0.073 | 0.039 | 0.061 | 0.04 | 0.06 | 0.078 |
| 108 | 0.04 | 0.03 | 0.066 | 0.05 | 0.052 | 0.052 | 0.066 | 0.068 | 0.044 | 0.06 | 0.05 | 0.033 |
| 109 | 0.04 | 0.04 | 0.05 | 0.052 | 0.061 | 0.05 | 0.035 | 0.055 | 0.055 | 0.044 | 0.055 | 0.067 |
| 110 | 0.075 | 0.066 | 0.024 | 0.04 | 0.05 | 0.048 | 0.041 | 0.044 | 0.071 | 0.053 | 0.065 | 0.044 |
| 111 | 0.075 | 0.052 | 0.02 | 0.04 | 0.042 | 0.09 | 0.038 | 0.034 | 0.039 | 0.041 | 0.057 | 0.049 |
| 112 | 0.075 | 0.071 | 0.05 | 0.03 | 0.04 | 0.061 | 0.06 | 0.038 | 0.05 | 0.022 | 0.04 | 0.044 |
| 113 | 0.052 | 0.09 | 0.066 | 0.05 | 0.06 | 0.05 | 0.05 | 0.039 | 0.066 | 0.04 | 0.06 | 0.067 |
| 114 | 0.061 | 0.061 | 0.052 | 0.03 | 0.03 | 0.084 | 0.055 | 0.044 | 0.033 | 0.039 | 0.052 | 0.028 |
| 115 | 0.05 | 0.07 | 0.061 | 0.061 | 0.042 | 0.081 | 0.096 | 0.049 | 0.027 | 0.065 | 0.04 | 0.073 |

| | | | | | | | | | | | | |
|---|---|---|---|---|---|---|---|---|---|---|---|---|
| 116 | 0.052 | 0.052 | 0.05 | 0.064 | 0.071 | 0.061 | 0.045 | 0.038 | 0.033 | 0.06 | 0.04 | 0.055 |
| 117 | 0.04 | 0.06 | 0.07 | 0.05 | 0.04 | 0.05 | 0.066 | 0.033 | 0.066 | 0.052 | 0.03 | 0.094 |
| 118 | 0.042 | 0.05 | 0.02 | 0.048 | 0.061 | 0.06 | 0.044 | 0.055 | 0.055 | 0.023 | 0.046 | 0.066 |
| 119 | 0.1 | 0.033 | 0.02 | 0.033 | 0.03 | 0.017 | 0.038 | 0.044 | 0.038 | 0.055 | 0.05 | 0.034 |
| 120 | 0.066 | 0.05 | 0.071 | 0.06 | 0.048 | 0.075 | 0.044 | 0.046 | 0.027 | 0.049 | 0.052 | 0.046 |
| 121 | 0.07 | 0.05 | 0.03 | 0.04 | 0.061 | 0.05 | 0.05 | 0.033 | 0.027 | 0.049 | 0.057 | 0.06 |
| 122 | 0.071 | 0.05 | 0.03 | 0.061 | 0.04 | 0.05 | 0.05 | 0.016 | 0.022 | 0.049 | 0.055 | 0.049 |
| 123 | 0.07 | 0.066 | 0.04 | 0.042 | 0.052 | 0.048 | 0.049 | 0.039 | 0.072 | 0.058 | 0.04 | 0.066 |
| 124 | 0.061 | 0.06 | 0.052 | 0.042 | 0.061 | 0.052 | 0.022 | 0.027 | 0.046 | 0.033 | 0.06 | 0.06 |
| 125 | 0.057 | 0.04 | 0.071 | 0.04 | 0.01 | 0.03 | 0.083 | 0.033 | 0.055 | 0.046 | 0.06 | 0.06 |
| 126 | 0.07 | 0.033 | 0.04 | 0.066 | 0.091 | 0.05 | 0.049 | 0.034 | 0.027 | 0.062 | 0.051 | 0.06 |
| 127 | 0.07 | 0.06 | 0.03 | 0.05 | 0.03 | 0.05 | 0.049 | 0.044 | 0.052 | 0.036 | 0.05 | 0.061 |
| 128 | 0.08 | 0.064 | 0.052 | 0.042 | 0.048 | 0.04 | 0.044 | 0.016 | 0.026 | 0.025 | 0.052 | 0.055 |
| 129 | 0.052 | 0.071 | 0.04 | 0.042 | 0.052 | 0.033 | 0.06 | 0.072 | 0.016 | 0.045 | 0.06 | 0.055 |
| 130 | 0.052 | 0.04 | 0.042 | 0.03 | 0.05 | 0.1 | 0.082 | 0.055 | 0.062 | 0.026 | 0.055 | 0.068 |
| 131 | 0.06 | 0.075 | 0.03 | 0.07 | 0.05 | 0.05 | 0.044 | 0.027 | 0.046 | 0.059 | 0.061 | 0.066 |
| 132 | 0.06 | 0.033 | 0.05 | 0.07 | 0.073 | 0.02 | 0.06 | 0.044 | 0.049 | 0.057 | 0.06 | 0.049 |
| 133 | 0.05 | 0.03 | 0.033 | 0.04 | 0.05 | 0.03 | 0.049 | 0.027 | 0.05 | 0.031 | 0.056 | 0.038 |
| 134 | 0.075 | 0.04 | 0.061 | 0.048 | 0.048 | 0.091 | 0.039 | 0.038 | 0.034 | 0.055 | 0.06 | 0.061 |
| 135 | 0.06 | 0.033 | 0.061 | 0.052 | 0.057 | 0.05 | 0.038 | 0.046 | 0.033 | 0.044 | 0.051 | 0.062 |
| 136 | 0.06 | 0.05 | 0.052 | 0.033 | 0.07 | 0.052 | 0.041 | 0.027 | 0.077 | 0.062 | 0.05 | 0.06 |
| 137 | 0.052 | 0.04 | 0.04 | 0.06 | 0.03 | 0.048 | 0.036 | 0.027 | 0.016 | 0.04 | 0.06 | 0.055 |
| 138 | 0.101 | 0.04 | 0.07 | 0.03 | 0.02 | 0.052 | 0.033 | 0.033 | 0.038 | 0.049 | 0.061 | 0.044 |
| 139 | 0.048 | 0.071 | 0.08 | 0.04 | 0.04 | 0.03 | 0.045 | 0.072 | 0.034 | 0.06 | 0.042 | 0.038 |
| 140 | 0.06 | 0.02 | 0.05 | 0.052 | 0.081 | 0.07 | 0.055 | 0.033 | 0.028 | 0.064 | 0.06 | 0.044 |
| 141 | 0.05 | 0.052 | 0.02 | 0.07 | 0.061 | 0.05 | 0.027 | 0.066 | 0.039 | 0.039 | 0.061 | 0.039 |
| 142 | 0.066 | 0.071 | 0.048 | 0.061 | 0.07 | 0.05 | 0.057 | 0.049 | 0.05 | 0.039 | 0.06 | 0.034 |
| 143 | 0.061 | 0.05 | 0.052 | 0.07 | 0.064 | 0.033 | 0.058 | 0.059 | 0.034 | 0.06 | 0.061 | 0.062 |
| 144 | 0.07 | 0.04 | 0.07 | 0.052 | 0.05 | 0.042 | 0.061 | 0.022 | 0.028 | 0.049 | 0.053 | 0.055 |
| 145 | 0.061 | 0.03 | 0.06 | 0.03 | 0.06 | 0.04 | 0.046 | 0.033 | 0.027 | 0.055 | 0.06 | 0.036 |

| | | | | | | | | | | | | |
|---|---|---|---|---|---|---|---|---|---|---|---|---|
| 146 | 0.03 | 0.04 | 0.02 | 0.06 | 0.052 | 0.033 | 0.041 | 0.044 | 0.033 | 0.055 | 0.06 | 0.057 |
| 147 | 0.04 | 0.03 | 0.03 | 0.06 | 0.042 | 0.03 | 0.027 | 0.022 | 0.027 | 0.06 | 0.064 | 0.065 |
| 148 | 0.072 | 0.042 | 0.03 | 0.042 | 0.081 | 0.02 | 0.034 | 0.028 | 0.061 | 0.049 | 0.063 | 0.039 |
| 149 | 0.071 | 0.03 | 0.05 | 0.05 | 0.04 | 0.05 | 0.01 | 0.033 | 0.034 | 0.054 | 0.06 | 0.038 |
| 150 | 0.075 | 0.03 | 0.04 | 0.04 | 0.048 | 0.052 | 0.037 | 0.038 | 0.027 | 0.062 | 0.05 | 0.057 |
| 151 | 0.052 | 0.042 | 0.05 | 0.081 | 0.096 | 0.033 | 0.037 | 0.058 | 0.049 | 0.028 | 0.065 | 0.072 |
| 152 | 0.052 | 0.02 | 0.04 | 0.05 | 0.052 | 0.071 | 0.037 | 0.022 | 0.033 | 0.054 | 0.06 | 0.082 |
| 153 | 0.03 | 0.03 | 0.052 | 0.024 | 0.04 | 0.052 | 0.037 | 0.031 | 0.046 | 0.034 | 0.065 | 0.053 |
| 154 | 0.04 | 0.03 | 0.042 | 0.024 | 0.042 | 0.04 | 0.037 | 0.049 | 0.031 | 0.041 | 0.061 | 0.053 |
| 155 | 0.048 | 0.04 | 0.042 | 0.03 | 0.06 | 0.042 | 0.044 | 0.033 | 0.036 | 0.046 | 0.062 | 0.052 |
| 156 | 0.04 | 0.07 | 0.04 | 0.02 | 0.03 | 0.05 | 0.044 | 0.028 | 0.016 | 0.036 | 0.063 | 0.061 |
| 157 | 0.061 | 0.02 | 0.06 | 0.02 | 0.04 | 0.066 | 0.052 | 0.05 | 0.062 | 0.049 | 0.058 | 0.066 |
| 158 | 0.052 | 0.061 | 0.03 | 0.03 | 0.02 | 0.06 | 0.059 | 0.028 | 0.027 | 0.061 | 0.062 | 0.065 |
| 159 | 0.052 | 0.04 | 0.06 | 0.04 | 0.052 | 0.04 | 0.059 | 0.027 | 0.049 | 0.064 | 0.065 | 0.033 |
| 160 | 0.057 | 0.05 | 0.06 | 0.061 | 0.04 | 0.02 | 0.066 | 0.018 | 0.049 | 0.061 | 0.05 | 0.027 |
| 161 | 0.042 | 0.061 | 0.04 | 0.04 | 0.052 | 0.024 | 0.066 | 0.022 | 0.04 | 0.033 | 0.051 | 0.061 |
| 162 | 0.075 | 0.04 | 0.052 | 0.066 | 0.05 | 0.052 | 0.066 | 0.057 | 0.051 | 0.052 | 0.033 | 0.05 |
| 163 | 0.05 | 0.081 | 0.01 | 0.052 | 0.05 | 0.04 | 0.067 | 0.033 | 0.027 | 0.055 | 0.04 | 0.051 |
| 164 | 0.042 | 0.033 | 0.03 | 0.05 | 0.04 | 0.04 | 0.067 | 0.016 | 0.028 | 0.055 | 0.066 | 0.052 |
| 165 | 0.06 | 0.05 | 0.061 | 0.033 | 0.052 | 0.033 | 0.07 | 0.039 | 0.061 | 0.055 | 0.06 | 0.054 |
| 166 | 0.101 | 0.04 | 0.03 | 0.06 | 0.081 | 0.08 | 0.027 | 0.046 | 0.052 | 0.044 | 0.065 | 0.045 |
| 167 | 0.071 | 0.052 | 0.03 | 0.052 | 0.028 | 0.04 | 0.044 | 0.045 | 0.062 | 0.05 | 0.066 | 0.052 |
| 168 | 0.06 | 0.03 | 0.03 | 0.04 | 0.024 | 0.07 | 0.038 | 0.044 | 0.045 | 0.044 | 0.059 | 0.06 |
| 169 | 0.04 | 0.061 | 0.02 | 0.06 | 0.042 | 0.066 | 0.066 | 0.034 | 0.033 | 0.062 | 0.053 | 0.044 |
| 170 | 0.04 | 0.08 | 0.06 | 0.04 | 0.06 | 0.04 | 0.054 | 0.034 | 0.044 | 0.066 | 0.06 | 0.038 |
| 171 | 0.06 | 0.033 | 0.042 | 0.05 | 0.06 | 0.03 | 0.027 | 0.045 | 0.022 | 0.048 | 0.04 | 0.022 |
| 172 | 0.081 | 0.05 | 0.03 | 0.08 | 0.05 | 0.04 | 0.057 | 0.022 | 0.027 | 0.035 | 0.04 | 0.022 |
| 173 | 0.081 | 0.052 | 0.03 | 0.1 | 0.033 | 0.02 | 0.049 | 0.038 | 0.038 | 0.016 | 0.055 | 0.033 |
| 174 | 0.061 | 0.048 | 0.03 | 0.042 | 0.042 | 0.033 | 0.045 | 0.036 | 0.044 | 0.055 | 0.061 | 0.044 |
| 175 | 0.04 | 0.071 | 0.03 | 0.03 | 0.02 | 0.07 | 0.045 | 0.054 | 0.022 | 0.033 | 0.06 | 0.066 |

| | | | | | | | | | | | | |
|---|---|---|---|---|---|---|---|---|---|---|---|---|
| 176 | 0.04 | 0.04 | 0.042 | 0.061 | 0.05 | 0.042 | 0.066 | 0.038 | 0.028 | 0.055 | 0.054 | 0.035 |
| 177 | 0.081 | 0.042 | 0.052 | 0.024 | 0.04 | 0.04 | 0.033 | 0.028 | 0.016 | 0.022 | 0.06 | 0.034 |
| 178 | 0.061 | 0.03 | 0.061 | 0.042 | 0.05 | 0.06 | 0.044 | 0.028 | 0.034 | 0.026 | 0.061 | 0.028 |
| 179 | 0.071 | 0.03 | 0.057 | 0.05 | 0.03 | 0.06 | 0.049 | 0.055 | 0.078 | 0.052 | 0.062 | 0.041 |
| 180 | 0.07 | 0.05 | 0.04 | 0.03 | 0.033 | 0.07 | 0.046 | 0.022 | 0.036 | 0.06 | 0.05 | 0.048 |
| 181 | 0.05 | 0.04 | 0.04 | 0.04 | 0.03 | 0.081 | 0.055 | 0.027 | 0.05 | 0.063 | 0.064 | 0.05 |
| 182 | 0.03 | 0.052 | 0.05 | 0.03 | 0.061 | 0.033 | 0.055 | 0.016 | 0.031 | 0.06 | 0.064 | 0.05 |
| 183 | 0.05 | 0.042 | 0.03 | 0.05 | 0.042 | 0.04 | 0.038 | 0.016 | 0.039 | 0.06 | 0.057 | 0.044 |
| 184 | 0.052 | 0.07 | 0.05 | 0.04 | 0.042 | 0.061 | 0.038 | 0.034 | 0.044 | 0.033 | 0.056 | 0.061 |
| 185 | 0.03 | 0.03 | 0.02 | 0.02 | 0.033 | 0.066 | 0.049 | 0.016 | 0.04 | 0.063 | 0.05 | 0.044 |
| 186 | 0.033 | 0.05 | 0.042 | 0.024 | 0.052 | 0.052 | 0.044 | 0.039 | 0.018 | 0.061 | 0.06 | 0.066 |
| 187 | 0.04 | 0.052 | 0.03 | 0.024 | 0.04 | 0.061 | 0.033 | 0.068 | 0.016 | 0.062 | 0.061 | 0.068 |
| 188 | 0.075 | 0.08 | 0.04 | 0.04 | 0.04 | 0.06 | 0.05 | 0.038 | 0.033 | 0.058 | 0.061 | 0.061 |
| 189 | 0.052 | 0.06 | 0.024 | 0.033 | 0.057 | 0.03 | 0.07 | 0.022 | 0.044 | 0.064 | 0.057 | 0.055 |
| 190 | 0.05 | 0.04 | 0.03 | 0.04 | 0.04 | 0.04 | 0.036 | 0.023 | 0.039 | 0.05 | 0.05 | 0.061 |
| 191 | 0.061 | 0.09 | 0.042 | 0.052 | 0.042 | 0.024 | 0.041 | 0.016 | 0.025 | 0.048 | 0.061 | 0.061 |
| 192 | 0.061 | 0.06 | 0.033 | 0.03 | 0.042 | 0.066 | 0.031 | 0.049 | 0.027 | 0.062 | 0.06 | 0.055 |
| 193 | 0.052 | 0.052 | 0.042 | 0.04 | 0.05 | 0.04 | 0.055 | 0.041 | 0.043 | 0.061 | 0.065 | 0.071 |
| 194 | 0.052 | 0.042 | 0.04 | 0.024 | 0.042 | 0.061 | 0.046 | 0.033 | 0.035 | 0.052 | 0.064 | 0.068 |
| 195 | 0.05 | 0.04 | 0.033 | 0.042 | 0.052 | 0.04 | 0.038 | 0.05 | 0.035 | 0.062 | 0.061 | 0.044 |
| 196 | 0.072 | 0.05 | 0.052 | 0.057 | 0.061 | 0.042 | 0.033 | 0.072 | 0.059 | 0.046 | 0.062 | 0.055 |
| 197 | 0.01 | 0.061 | 0.05 | 0.02 | 0.052 | 0.033 | 0.066 | 0.057 | 0.044 | 0.059 | 0.065 | 0.053 |
| 198 | 0.071 | 0.05 | 0.05 | 0.033 | 0.052 | 0.06 | 0.052 | 0.022 | 0.031 | 0.065 | 0.064 | 0.055 |
| 199 | 0.04 | 0.052 | 0.042 | 0.024 | 0.04 | 0.052 | 0.044 | 0.022 | 0.039 | 0.05 | 0.05 | 0.058 |
| 200 | 0.02 | 0.042 | 0.06 | 0.057 | 0.02 | 0.05 | 0.044 | 0.016 | 0.061 | 0.037 | 0.053 | 0.06 |
| 201 | 0.042 | 0.04 | 0.061 | 0.033 | 0.06 | 0.057 | 0.033 | 0.018 | 0.025 | 0.049 | 0.058 | 0.061 |
| 202 | 0.061 | 0.075 | 0.06 | 0.048 | 0.03 | 0.033 | 0.027 | 0.05 | 0.044 | 0.055 | 0.06 | 0.037 |
| 203 | 0.057 | 0.081 | 0.052 | 0.042 | 0.08 | 0.052 | 0.044 | 0.044 | 0.066 | 0.045 | 0.054 | 0.044 |
| 204 | 0.06 | 0.05 | 0.07 | 0.02 | 0.05 | 0.052 | 0.06 | 0.016 | 0.045 | 0.028 | 0.06 | 0.06 |
| 205 | 0.05 | 0.075 | 0.071 | 0.03 | 0.06 | 0.05 | 0.048 | 0.022 | 0.044 | 0.049 | 0.055 | 0.053 |

| | | | | | | | | | | | | |
|---|---|---|---|---|---|---|---|---|---|---|---|---|
| 206 | 0.02 | 0.033 | 0.052 | 0.02 | 0.04 | 0.05 | 0.038 | 0.057 | 0.044 | 0.038 | 0.06 | 0.049 |
| 207 | 0.05 | 0.042 | 0.04 | 0.02 | 0.042 | 0.061 | 0.038 | 0.038 | 0.044 | 0.049 | 0.061 | 0.052 |
| 208 | 0.052 | 0.06 | 0.061 | 0.02 | 0.02 | 0.052 | 0.058 | 0.038 | 0.022 | 0.061 | 0.066 | 0.022 |
| 209 | 0.06 | 0.07 | 0.05 | 0.05 | 0.048 | 0.05 | 0.033 | 0.016 | 0.027 | 0.065 | 0.057 | 0.034 |
| 210 | 0.084 | 0.052 | 0.033 | 0.03 | 0.06 | 0.05 | 0.023 | 0.027 | 0.028 | 0.061 | 0.058 | 0.038 |
| 211 | 0.03 | 0.052 | 0.048 | 0.052 | 0.024 | 0.072 | 0.033 | 0.007 | 0.034 | 0.062 | 0.051 | 0.031 |
| 212 | 0.052 | 0.03 | 0.08 | 0.033 | 0.057 | 0.03 | 0.071 | 0.013 | 0.044 | 0.038 | 0.06 | 0.04 |
| 213 | 0.057 | 0.033 | 0.072 | 0.03 | 0.048 | 0.033 | 0.049 | 0.075 | 0.036 | 0.028 | 0.051 | 0.062 |
| 214 | 0.05 | 0.04 | 0.06 | 0.05 | 0.057 | 0.06 | 0.044 | 0.039 | 0.033 | 0.044 | 0.052 | 0.057 |
| 215 | 0.048 | 0.033 | 0.03 | 0.04 | 0.071 | 0.033 | 0.031 | 0.022 | 0.05 | 0.028 | 0.057 | 0.062 |
| 216 | 0.03 | 0.06 | 0.061 | 0.04 | 0.06 | 0.05 | 0.038 | 0.011 | 0.05 | 0.055 | 0.051 | 0.061 |
| 217 | 0.06 | 0.061 | 0.03 | 0.057 | 0.06 | 0.096 | 0.023 | 0.022 | 0.05 | 0.059 | 0.05 | 0.049 |
| 218 | 0.024 | 0.06 | 0.04 | 0.042 | 0.075 | 0.064 | 0.033 | 0.033 | 0.077 | 0.044 | 0.041 | 0.06 |
| 219 | 0.05 | 0.05 | 0.05 | 0.066 | 0.04 | 0.02 | 0.045 | 0.011 | 0.062 | 0.023 | 0.045 | 0.061 |
| 220 | 0.066 | 0.066 | 0.06 | 0.05 | 0.094 | 0.04 | 0.044 | 0.06 | 0.022 | 0.036 | 0.043 | 0.06 |
| 221 | 0.052 | 0.042 | 0.064 | 0.033 | 0.04 | 0.04 | 0.045 | 0.06 | 0.072 | 0.022 | 0.049 | 0.062 |
| 222 | 0.05 | 0.04 | 0.04 | 0.048 | 0.03 | 0.052 | 0.033 | 0.044 | 0.062 | 0.01 | 0.052 | 0.062 |
| 223 | 0.08 | 0.071 | 0.03 | 0.042 | 0.07 | 0.04 | 0.066 | 0.038 | 0.035 | 0.063 | 0.06 | 0.06 |
| 224 | 0.07 | 0.05 | 0.02 | 0.02 | 0.04 | 0.05 | 0.033 | 0.027 | 0.054 | 0.055 | 0.061 | 0.055 |
| 225 | 0.052 | 0.05 | 0.06 | 0.04 | 0.04 | 0.06 | 0.026 | 0.016 | 0.033 | 0.058 | 0.06 | 0.055 |
| 226 | 0.05 | 0.05 | 0.042 | 0.067 | 0.033 | 0.04 | 0.027 | 0.055 | 0.055 | 0.061 | 0.05 | 0.061 |
| 227 | 0.07 | 0.04 | 0.06 | 0.04 | 0.033 | 0.08 | 0.038 | 0.016 | 0.071 | 0.06 | 0.051 | 0.071 |
| 228 | 0.03 | 0.061 | 0.057 | 0.03 | 0.042 | 0.052 | 0.033 | 0.028 | 0.035 | 0.049 | 0.054 | 0.07 |
| 229 | 0.042 | 0.081 | 0.042 | 0.071 | 0.04 | 0.071 | 0.033 | 0.027 | 0.039 | 0.066 | 0.053 | 0.048 |
| 230 | 0.033 | 0.08 | 0.05 | 0.04 | 0.07 | 0.057 | 0.038 | 0.033 | 0.055 | 0.055 | 0.06 | 0.022 |
| 231 | 0.05 | 0.033 | 0.061 | 0.05 | 0.042 | 0.061 | 0.066 | 0.028 | 0.061 | 0.055 | 0.053 | 0.055 |
| 232 | 0.01 | 0.048 | 0.02 | 0.07 | 0.071 | 0.06 | 0.023 | 0.055 | 0.033 | 0.062 | 0.055 | 0.027 |
| 233 | 0.052 | 0.071 | 0.04 | 0.024 | 0.033 | 0.07 | 0.028 | 0.049 | 0.044 | 0.067 | 0.054 | 0.011 |
| 234 | 0.06 | 0.04 | 0.04 | 0.06 | 0.057 | 0.057 | 0.033 | 0.045 | 0.031 | 0.062 | 0.052 | 0.027 |
| 235 | 0.03 | 0.02 | 0.057 | 0.033 | 0.05 | 0.06 | 0.045 | 0.027 | 0.041 | 0.056 | 0.051 | 0.057 |

| | | | | | | | | | | | | |
|---|---|---|---|---|---|---|---|---|---|---|---|---|
| 236 | 0.052 | 0.05 | 0.081 | 0.06 | 0.03 | 0.05 | 0.044 | 0.05 | 0.016 | 0.061 | 0.05 | 0.022 |
| 237 | 0.061 | 0.061 | 0.052 | 0.052 | 0.052 | 0.07 | 0.026 | 0.06 | 0.035 | 0.055 | 0.04 | 0.039 |
| 238 | 0.042 | 0.06 | 0.01 | 0.03 | 0.033 | 0.02 | 0.027 | 0.066 | 0.055 | 0.045 | 0.04 | 0.044 |
| 239 | 0.061 | 0.033 | 0.04 | 0.03 | 0.042 | 0.061 | 0.027 | 0.038 | 0.044 | 0.073 | 0.055 | 0.033 |
| 240 | 0.081 | 0.05 | 0.052 | 0.06 | 0.03 | 0.04 | 0.034 | 0.033 | 0.055 | 0.055 | 0.059 | 0.071 |
| 241 | 0.02 | 0.04 | 0.042 | 0.06 | 0.061 | 0.042 | 0.041 | 0.044 | 0.034 | 0.069 | 0.05 | 0.07 |
| 242 | 0.01 | 0.06 | 0.066 | 0.03 | 0.03 | 0.033 | 0.033 | 0.023 | 0.035 | 0.09 | 0.055 | 0.07 |
| 243 | 0.052 | 0.07 | 0.048 | 0.04 | 0.033 | 0.04 | 0.053 | 0.011 | 0.055 | 0.061 | 0.045 | 0.055 |
| 244 | 0.03 | 0.04 | 0.06 | 0.05 | 0.071 | 0.024 | 0.027 | 0.026 | 0.06 | 0.04 | 0.04 | 0.035 |
| 245 | 0.052 | 0.05 | 0.03 | 0.052 | 0.03 | 0.03 | 0.034 | 0.039 | 0.045 | 0.046 | 0.049 | 0.066 |
| 246 | 0.07 | 0.042 | 0.067 | 0.04 | 0.033 | 0.02 | 0.011 | 0.023 | 0.041 | 0.039 | 0.04 | 0.06 |
| 247 | 0.084 | 0.03 | 0.042 | 0.03 | 0.061 | 0.05 | 0.022 | 0.055 | 0.038 | 0.061 | 0.03 | 0.062 |
| 248 | 0.04 | 0.033 | 0.057 | 0.061 | 0.01 | 0.07 | 0.039 | 0.044 | 0.039 | 0.04 | 0.042 | 0.058 |
| 249 | 0.08 | 0.052 | 0.042 | 0.03 | 0.06 | 0.064 | 0.018 | 0.05 | 0.035 | 0.044 | 0.04 | 0.05 |
| 250 | 0.061 | 0.061 | 0.033 | 0.052 | 0.03 | 0.024 | 0.049 | 0.052 | 0.031 | 0.098 | 0.031 | 0.058 |
| Mean | 0.054944 | 0.046432 | 0.048164 | 0.044836 | 0.046288 | 0.049404 | 0.043752 | 0.037676 | 0.041152 | 0.04956 | 0.054264 | 0.049892 |
| SD | 0.018334 | 0.0155 | 0.016504 | 0.01544 | 0.015385 | 0.016533 | 0.01461 | 0.014888 | 0.014022 | 0.013575 | 0.009137 | 0.01457 |

| | Day 2 | | | | | | Day 3 | | | | | |
|---|---|---|---|---|---|---|---|---|---|---|---|---|
| OCT images | Control | | | Infected | | | Control | | | Infected | | |
| | 1 | 2 | 3 | 1 | 2 | 3 | 1 | 2 | 3 | 1 | 2 | 3 |
| 1 | 0.044 | 0.046 | 0.05 | 0.066 | 0.04 | 0.06 | 0.02 | 0.033 | 0.04 | 0.033 | 0.091 | 0.072 |
| 2 | 0.033 | 0.059 | 0.011 | 0.071 | 0.071 | 0.105 | 0.04 | 0.07 | 0.05 | 0.061 | 0.06 | 0.071 |
| 3 | 0.055 | 0.033 | 0.066 | 0.052 | 0.081 | 0.07 | 0.05 | 0.03 | 0.024 | 0.071 | 0.033 | 0.061 |
| 4 | 0.016 | 0.033 | 0.039 | 0.03 | 0.02 | 0.04 | 0.033 | 0.04 | 0.05 | 0.07 | 0.103 | 0.06 |
| 5 | 0.011 | 0.016 | 0.028 | 0.042 | 0.101 | 0.05 | 0.05 | 0.03 | 0.04 | 0.05 | 0.071 | 0.052 |
| 6 | 0.039 | 0.041 | 0.057 | 0.052 | 0.066 | 0.12 | 0.052 | 0.04 | 0.03 | 0.071 | 0.052 | 0.052 |
| 7 | 0.038 | 0.052 | 0.022 | 0.066 | 0.048 | 0.02 | 0.07 | 0.042 | 0.04 | 0.08 | 0.05 | 0.071 |
| 8 | 0.041 | 0.038 | 0.044 | 0.02 | 0.052 | 0.024 | 0.071 | 0.03 | 0.04 | 0.091 | 0.042 | 0.071 |

| | | | | | | | | | | | | |
|---|---|---|---|---|---|---|---|---|---|---|---|---|
| 9 | 0.045 | 0.049 | 0.031 | 0.06 | 0.042 | 0.061 | 0.061 | 0.01 | 0.04 | 0.1 | 0.06 | 0.07 |
| 10 | 0.038 | 0.023 | 0.039 | 0.03 | 0.04 | 0.05 | 0.04 | 0.01 | 0.05 | 0.09 | 0.071 | 0.1 |
| 11 | 0.034 | 0.055 | 0.022 | 0.081 | 0.042 | 0.033 | 0.06 | 0.024 | 0.061 | 0.05 | 0.08 | 0.113 |
| 12 | 0.044 | 0.027 | 0.044 | 0.03 | 0.03 | 0.101 | 0.061 | 0.045 | 0.07 | 0.06 | 0.06 | 0.042 |
| 13 | 0.045 | 0.022 | 0.036 | 0.01 | 0.061 | 0.061 | 0.05 | 0.03 | 0.01 | 0.04 | 0.081 | 0.131 |
| 14 | 0.045 | 0.041 | 0.055 | 0.017 | 0.03 | 0.071 | 0.061 | 0.04 | 0.042 | 0.04 | 0.12 | 0.081 |
| 15 | 0.038 | 0.027 | 0.044 | 0.03 | 0.04 | 0.06 | 0.052 | 0.02 | 0.03 | 0.04 | 0.111 | 0.081 |
| 16 | 0.028 | 0.028 | 0.023 | 0.042 | 0.042 | 0.05 | 0.04 | 0.03 | 0.04 | 0.04 | 0.05 | 0.113 |
| 17 | 0.038 | 0.036 | 0.038 | 0.03 | 0.06 | 0.042 | 0.042 | 0.033 | 0.064 | 0.061 | 0.042 | 0.08 |
| 18 | 0.027 | 0.045 | 0.034 | 0.052 | 0.04 | 0.071 | 0.04 | 0.02 | 0.057 | 0.05 | 0.05 | 0.094 |
| 19 | 0.028 | 0.044 | 0.016 | 0.04 | 0.03 | 0.05 | 0.024 | 0.024 | 0.04 | 0.02 | 0.057 | 0.06 |
| 20 | 0.049 | 0.033 | 0.027 | 0.07 | 0.013 | 0.071 | 0.04 | 0.042 | 0.042 | 0.05 | 0.081 | 0.071 |
| 21 | 0.071 | 0.044 | 0.034 | 0.04 | 0.033 | 0.06 | 0.04 | 0.02 | 0.042 | 0.057 | 0.07 | 0.057 |
| 22 | 0.044 | 0.062 | 0.072 | 0.072 | 0.071 | 0.06 | 0.03 | 0.02 | 0.05 | 0.06 | 0.042 | 0.05 |
| 23 | 0.049 | 0.046 | 0.033 | 0.07 | 0.02 | 0.07 | 0.061 | 0.04 | 0.033 | 0.09 | 0.12 | 0.071 |
| 24 | 0.033 | 0.055 | 0.038 | 0.108 | 0.04 | 0.05 | 0.042 | 0.03 | 0.05 | 0.101 | 0.136 | 0.052 |
| 25 | 0.039 | 0.055 | 0.068 | 0.073 | 0.066 | 0.06 | 0.05 | 0.04 | 0.04 | 0.07 | 0.126 | 0.06 |
| 26 | 0.025 | 0.022 | 0.016 | 0.07 | 0.052 | 0.07 | 0.052 | 0.03 | 0.057 | 0.052 | 0.06 | 0.111 |
| 27 | 0.062 | 0.06 | 0.054 | 0.07 | 0.04 | 0.048 | 0.066 | 0.02 | 0.033 | 0.04 | 0.09 | 0.042 |
| 28 | 0.066 | 0.049 | 0.023 | 0.04 | 0.071 | 0.05 | 0.052 | 0.03 | 0.04 | 0.066 | 0.071 | 0.07 |
| 29 | 0.044 | 0.04 | 0.033 | 0.04 | 0.07 | 0.05 | 0.02 | 0.033 | 0.048 | 0.052 | 0.081 | 0.05 |
| 30 | 0.06 | 0.028 | 0.045 | 0.017 | 0.06 | 0.071 | 0.01 | 0.048 | 0.024 | 0.05 | 0.094 | 0.091 |
| 31 | 0.016 | 0.064 | 0.022 | 0.08 | 0.091 | 0.081 | 0.061 | 0.04 | 0.04 | 0.06 | 0.111 | 0.09 |
| 32 | 0.055 | 0.038 | 0.049 | 0.033 | 0.091 | 0.08 | 0.05 | 0.042 | 0.03 | 0.08 | 0.05 | 0.091 |
| 33 | 0.038 | 0.022 | 0.061 | 0.052 | 0.07 | 0.06 | 0.071 | 0.03 | 0.048 | 0.042 | 0.06 | 0.05 |
| 34 | 0.033 | 0.022 | 0.028 | 0.07 | 0.071 | 0.03 | 0.05 | 0.033 | 0.052 | 0.024 | 0.091 | 0.09 |
| 35 | 0.027 | 0.023 | 0.039 | 0.101 | 0.081 | 0.06 | 0.02 | 0.033 | 0.03 | 0.04 | 0.06 | 0.08 |
| 36 | 0.04 | 0.05 | 0.039 | 0.04 | 0.052 | 0.05 | 0.04 | 0.05 | 0.033 | 0.033 | 0.081 | 0.052 |
| 37 | 0.055 | 0.026 | 0.064 | 0.05 | 0.07 | 0.05 | 0.04 | 0.042 | 0.02 | 0.05 | 0.071 | 0.05 |
| 38 | 0.055 | 0.027 | 0.055 | 0.07 | 0.05 | 0.08 | 0.042 | 0.04 | 0.08 | 0.01 | 0.061 | 0.081 |

| | | | | | | | | | | | | |
|---|---|---|---|---|---|---|---|---|---|---|---|---|
| 39 | 0.044 | 0.075 | 0.062 | 0.02 | 0.071 | 0.07 | 0.03 | 0.04 | 0.02 | 0.061 | 0.066 | 0.098 |
| 40 | 0.033 | 0.031 | 0.022 | 0.06 | 0.042 | 0.042 | 0.04 | 0.03 | 0.042 | 0.08 | 0.048 | 0.09 |
| 41 | 0.036 | 0.038 | 0.049 | 0.12 | 0.042 | 0.042 | 0.03 | 0.03 | 0.05 | 0.1 | 0.121 | 0.06 |
| 42 | 0.034 | 0.046 | 0.034 | 0.09 | 0.04 | 0.04 | 0.04 | 0.013 | 0.04 | 0.13 | 0.1 | 0.08 |
| 43 | 0.016 | 0.027 | 0.06 | 0.042 | 0.04 | 0.061 | 0.01 | 0.033 | 0.05 | 0.1 | 0.08 | 0.08 |
| 44 | 0.034 | 0.057 | 0.038 | 0.04 | 0.03 | 0.072 | 0.042 | 0.061 | 0.04 | 0.08 | 0.052 | 0.061 |
| 45 | 0.027 | 0.027 | 0.06 | 0.061 | 0.05 | 0.071 | 0.02 | 0.052 | 0.03 | 0.091 | 0.08 | 0.06 |
| 46 | 0.039 | 0.038 | 0.049 | 0.071 | 0.06 | 0.096 | 0.02 | 0.02 | 0.05 | 0.05 | 0.057 | 0.071 |
| 47 | 0.028 | 0.059 | 0.052 | 0.033 | 0.042 | 0.066 | 0.02 | 0.02 | 0.04 | 0.07 | 0.07 | 0.081 |
| 48 | 0.075 | 0.066 | 0.045 | 0.042 | 0.04 | 0.042 | 0.04 | 0.042 | 0.061 | 0.05 | 0.09 | 0.072 |
| 49 | 0.023 | 0.062 | 0.06 | 0.081 | 0.052 | 0.05 | 0.04 | 0.02 | 0.04 | 0.03 | 0.06 | 0.057 |
| 50 | 0.016 | 0.022 | 0.034 | 0.081 | 0.061 | 0.07 | 0.052 | 0.024 | 0.04 | 0.05 | 0.05 | 0.061 |
| 51 | 0.027 | 0.061 | 0.062 | 0.024 | 0.05 | 0.091 | 0.05 | 0.03 | 0.04 | 0.03 | 0.061 | 0.042 |
| 52 | 0.059 | 0.078 | 0.036 | 0.03 | 0.09 | 0.075 | 0.03 | 0.042 | 0.033 | 0.042 | 0.061 | 0.111 |
| 53 | 0.018 | 0.06 | 0.049 | 0.03 | 0.084 | 0.091 | 0.04 | 0.04 | 0.06 | 0.06 | 0.06 | 0.1 |
| 54 | 0.022 | 0.028 | 0.034 | 0.03 | 0.052 | 0.071 | 0.05 | 0.04 | 0.04 | 0.061 | 0.101 | 0.06 |
| 55 | 0.033 | 0.059 | 0.038 | 0.061 | 0.091 | 0.057 | 0.03 | 0.042 | 0.03 | 0.072 | 0.071 | 0.07 |
| 56 | 0.011 | 0.038 | 0.06 | 0.061 | 0.07 | 0.03 | 0.04 | 0.071 | 0.042 | 0.05 | 0.06 | 0.07 |
| 57 | 0.038 | 0.039 | 0.013 | 0.04 | 0.061 | 0.04 | 0.01 | 0.05 | 0.06 | 0.033 | 0.061 | 0.09 |
| 58 | 0.044 | 0.016 | 0.066 | 0.03 | 0.03 | 0.052 | 0.04 | 0.052 | 0.04 | 0.09 | 0.06 | 0.06 |
| 59 | 0.016 | 0.034 | 0.018 | 0.024 | 0.066 | 0.11 | 0.03 | 0.04 | 0 | 0.061 | 0.05 | 0.04 |
| 60 | 0.033 | 0.055 | 0.066 | 0.05 | 0.05 | 0.11 | 0.03 | 0.02 | 0.05 | 0.07 | 0.126 | 0.091 |
| 61 | 0.026 | 0.028 | 0.038 | 0.061 | 0.02 | 0.071 | 0.052 | 0.033 | 0.03 | 0.03 | 0.07 | 0.07 |
| 62 | 0.049 | 0.083 | 0.009 | 0.071 | 0.05 | 0.072 | 0.03 | 0.03 | 0.042 | 0.04 | 0.111 | 0.081 |
| 63 | 0.034 | 0.044 | 0.04 | 0.02 | 0.05 | 0.089 | 0.02 | 0.042 | 0.04 | 0.05 | 0.05 | 0.071 |
| 64 | 0.034 | 0.033 | 0.055 | 0.07 | 0.04 | 0.03 | 0.042 | 0.033 | 0.033 | 0.05 | 0.052 | 0.1 |
| 65 | 0.04 | 0.027 | 0.022 | 0.06 | 0.06 | 0.042 | 0.04 | 0.03 | 0.057 | 0.04 | 0.03 | 0.042 |
| 66 | 0.054 | 0.046 | 0.034 | 0.05 | 0.01 | 0.052 | 0.03 | 0.03 | 0.07 | 0.03 | 0.04 | 0.113 |
| 67 | 0.041 | 0.061 | 0.039 | 0.04 | 0.061 | 0.04 | 0.042 | 0.048 | 0.04 | 0.04 | 0.042 | 0.07 |
| 68 | 0.018 | 0.061 | 0.027 | 0.07 | 0.04 | 0.1 | 0.04 | 0.03 | 0.03 | 0.052 | 0.05 | 0.02 |

| | | | | | | | | | | | | |
|---|---|---|---|---|---|---|---|---|---|---|---|---|
| 69 | 0.005 | 0.049 | 0.026 | 0.042 | 0.052 | 0.06 | 0.03 | 0.04 | 0.048 | 0.06 | 0.04 | 0.133 |
| 70 | 0.045 | 0.049 | 0.06 | 0.06 | 0.075 | 0.09 | 0.03 | 0.04 | 0.057 | 0.052 | 0.06 | 0.091 |
| 71 | 0.028 | 0.018 | 0.041 | 0.04 | 0.103 | 0.04 | 0.03 | 0.05 | 0.057 | 0.073 | 0.07 | 0.09 |
| 72 | 0.022 | 0.038 | 0.027 | 0.04 | 0.07 | 0.07 | 0.01 | 0.03 | 0.052 | 0.07 | 0.094 | 0.103 |
| 73 | 0.016 | 0.023 | 0.023 | 0.04 | 0.07 | 0.08 | 0.042 | 0.02 | 0.033 | 0.08 | 0.09 | 0.084 |
| 74 | 0.033 | 0.039 | 0.052 | 0.04 | 0.091 | 0.061 | 0.03 | 0.05 | 0.033 | 0.06 | 0.09 | 0.084 |
| 75 | 0.044 | 0.044 | 0.033 | 0.052 | 0.091 | 0.09 | 0.03 | 0.04 | 0.05 | 0.05 | 0.052 | 0.094 |
| 76 | 0.038 | 0.033 | 0.027 | 0.04 | 0.094 | 0.09 | 0.02 | 0.03 | 0.02 | 0.052 | 0.061 | 0.096 |
| 77 | 0.027 | 0.066 | 0.022 | 0.061 | 0.071 | 0.07 | 0.042 | 0.03 | 0.05 | 0.071 | 0.09 | 0.048 |
| 78 | 0.038 | 0.033 | 0.073 | 0.061 | 0.06 | 0.131 | 0.06 | 0.02 | 0.033 | 0.048 | 0.113 | 0.09 |
| 79 | 0.027 | 0.07 | 0.022 | 0.042 | 0.071 | 0.151 | 0.03 | 0.052 | 0.061 | 0.042 | 0.06 | 0.111 |
| 80 | 0.049 | 0.05 | 0.027 | 0.033 | 0.066 | 0.101 | 0.02 | 0.04 | 0.03 | 0.03 | 0.04 | 0.07 |
| 81 | 0.022 | 0.016 | 0.039 | 0.052 | 0.07 | 0.071 | 0.03 | 0.094 | 0.05 | 0.042 | 0.081 | 0.052 |
| 82 | 0.045 | 0.041 | 0.027 | 0.052 | 0.1 | 0.061 | 0.048 | 0.06 | 0.01 | 0.05 | 0.081 | 0.06 |
| 83 | 0.028 | 0.022 | 0.034 | 0.04 | 0.04 | 0.06 | 0.04 | 0.04 | 0.024 | 0.081 | 0.052 | 0.061 |
| 84 | 0.027 | 0.062 | 0.038 | 0.07 | 0.05 | 0.061 | 0.03 | 0.04 | 0.04 | 0.081 | 0.061 | 0.06 |
| 85 | 0.022 | 0.022 | 0.055 | 0.052 | 0.07 | 0.052 | 0.052 | 0.07 | 0.01 | 0.061 | 0.094 | 0.03 |
| 86 | 0.027 | 0.039 | 0.038 | 0.061 | 0.07 | 0.081 | 0.03 | 0.04 | 0.05 | 0.066 | 0.03 | 0.05 |
| 87 | 0.05 | 0.033 | 0.038 | 0.08 | 0.08 | 0.06 | 0.061 | 0.042 | 0.05 | 0.05 | 0.111 | 0.103 |
| 88 | 0.038 | 0.031 | 0.038 | 0.07 | 0.111 | 0.048 | 0.04 | 0.04 | 0.052 | 0.06 | 0.08 | 0.024 |
| 89 | 0.045 | 0.033 | 0.027 | 0.06 | 0.091 | 0.126 | 0.061 | 0.04 | 0.033 | 0.042 | 0.07 | 0.081 |
| 90 | 0.027 | 0.033 | 0.027 | 0.057 | 0.101 | 0.04 | 0.03 | 0.05 | 0.042 | 0.08 | 0.081 | 0.11 |
| 91 | 0.022 | 0.028 | 0.033 | 0.09 | 0.101 | 0.06 | 0.03 | 0.05 | 0.052 | 0.06 | 0.143 | 0.075 |
| 92 | 0.033 | 0.022 | 0.039 | 0.06 | 0.06 | 0.075 | 0.04 | 0.02 | 0.042 | 0.06 | 0.19 | 0.103 |
| 93 | 0.023 | 0.06 | 0.045 | 0.05 | 0.04 | 0.091 | 0.03 | 0.02 | 0.03 | 0.057 | 0.06 | 0.103 |
| 94 | 0.06 | 0.023 | 0.049 | 0.05 | 0.081 | 0.081 | 0.02 | 0.03 | 0.033 | 0.071 | 0.057 | 0.04 |
| 95 | 0.052 | 0.046 | 0.06 | 0.061 | 0.08 | 0.052 | 0.033 | 0.05 | 0.042 | 0.03 | 0.03 | 0.061 |
| 96 | 0.022 | 0.028 | 0.055 | 0.061 | 0.07 | 0.101 | 0.04 | 0.033 | 0.052 | 0.072 | 0.101 | 0.09 |
| 97 | 0.055 | 0.045 | 0.044 | 0.05 | 0.061 | 0.09 | 0.03 | 0.03 | 0.052 | 0.08 | 0.08 | 0.081 |
| 98 | 0.055 | 0.026 | 0.044 | 0.057 | 0.057 | 0.06 | 0.042 | 0.04 | 0.07 | 0.05 | 0.05 | 0.05 |

| | | | | | | | | | | | | |
|---|---|---|---|---|---|---|---|---|---|---|---|---|
| 99 | 0.016 | 0.083 | 0.023 | 0.052 | 0.071 | 0.075 | 0.03 | 0.071 | 0.07 | 0.081 | 0.05 | 0.081 |
| 100 | 0.016 | 0.062 | 0.022 | 0.06 | 0.108 | 0.091 | 0.017 | 0.04 | 0.052 | 0.081 | 0.07 | 0.089 |
| 101 | 0.027 | 0.045 | 0.072 | 0.084 | 0.042 | 0.1 | 0.01 | 0.042 | 0.033 | 0.071 | 0.09 | 0.101 |
| 102 | 0.033 | 0.016 | 0.022 | 0.06 | 0.06 | 0.071 | 0.042 | 0.061 | 0.05 | 0.07 | 0.06 | 0.09 |
| 103 | 0.039 | 0.031 | 0.045 | 0.033 | 0.094 | 0.094 | 0.04 | 0.042 | 0.033 | 0.061 | 0.061 | 0.071 |
| 104 | 0.07 | 0.055 | 0.044 | 0.06 | 0.07 | 0.072 | 0.04 | 0.03 | 0.03 | 0.052 | 0.04 | 0.09 |
| 105 | 0.027 | 0.033 | 0.044 | 0.052 | 0.091 | 0.091 | 0.033 | 0.042 | 0.01 | 0.05 | 0.04 | 0.05 |
| 106 | 0.033 | 0.071 | 0.033 | 0.04 | 0.08 | 0.03 | 0.042 | 0.03 | 0.042 | 0.048 | 0.04 | 0.084 |
| 107 | 0.033 | 0.038 | 0.066 | 0.03 | 0.08 | 0.066 | 0.033 | 0.03 | 0.042 | 0.052 | 0.081 | 0.061 |
| 108 | 0.066 | 0.055 | 0.038 | 0.04 | 0.061 | 0.061 | 0.04 | 0.052 | 0.02 | 0.06 | 0.075 | 0.04 |
| 109 | 0.033 | 0.044 | 0.033 | 0.05 | 0.05 | 0.052 | 0.042 | 0.05 | 0.05 | 0.04 | 0.08 | 0.05 |
| 110 | 0.036 | 0.055 | 0.055 | 0.045 | 0.05 | 0.02 | 0.02 | 0.04 | 0.04 | 0.05 | 0.1 | 0.057 |
| 111 | 0.055 | 0.026 | 0.038 | 0.04 | 0.04 | 0.05 | 0.033 | 0.033 | 0.04 | 0.04 | 0.03 | 0.052 |
| 112 | 0.023 | 0.011 | 0.05 | 0.05 | 0.061 | 0.071 | 0.042 | 0.04 | 0.05 | 0.05 | 0.06 | 0.07 |
| 113 | 0.039 | 0.055 | 0.034 | 0.04 | 0.04 | 0.113 | 0.03 | 0.033 | 0.04 | 0.06 | 0.091 | 0.07 |
| 114 | 0.055 | 0.033 | 0.033 | 0.05 | 0.04 | 0.08 | 0.05 | 0.052 | 0.04 | 0.071 | 0.07 | 0.111 |
| 115 | 0.025 | 0.022 | 0.033 | 0.091 | 0.04 | 0.08 | 0.02 | 0.04 | 0.04 | 0.075 | 0.042 | 0.08 |
| 116 | 0.041 | 0.039 | 0.027 | 0.04 | 0.05 | 0.07 | 0.03 | 0.05 | 0.04 | 0.11 | 0.07 | 0.07 |
| 117 | 0.033 | 0.033 | 0.034 | 0.057 | 0.052 | 0.04 | 0.03 | 0.033 | 0.033 | 0.03 | 0.06 | 0.09 |
| 118 | 0.044 | 0.041 | 0.044 | 0.02 | 0.075 | 0.042 | 0.02 | 0.04 | 0.03 | 0.06 | 0.111 | 0.08 |
| 119 | 0.044 | 0.044 | 0.033 | 0.07 | 0.05 | 0.052 | 0.042 | 0.03 | 0.02 | 0.052 | 0.1 | 0.061 |
| 120 | 0.045 | 0.022 | 0.049 | 0.024 | 0.131 | 0.06 | 0.03 | 0.04 | 0.02 | 0.04 | 0.081 | 0.052 |
| 121 | 0.038 | 0.055 | 0.055 | 0.048 | 0.066 | 0.05 | 0.02 | 0.04 | 0.05 | 0.042 | 0.13 | 0.07 |
| 122 | 0.038 | 0.044 | 0.022 | 0.066 | 0.081 | 0.061 | 0.03 | 0.03 | 0.03 | 0.089 | 0.075 | 0.04 |
| 123 | 0.038 | 0.034 | 0.022 | 0.052 | 0.103 | 0.07 | 0.03 | 0.04 | 0.033 | 0.04 | 0.061 | 0.061 |
| 124 | 0.038 | 0.055 | 0.045 | 0.061 | 0.03 | 0.06 | 0.02 | 0.01 | 0.03 | 0.071 | 0.042 | 0.06 |
| 125 | 0.033 | 0.066 | 0.034 | 0.052 | 0.057 | 0.071 | 0.04 | 0.033 | 0.04 | 0.061 | 0.15 | 0.06 |
| 126 | 0.038 | 0.045 | 0.022 | 0.042 | 0.066 | 0.03 | 0.033 | 0.03 | 0.03 | 0.101 | 0.121 | 0.084 |
| 127 | 0.055 | 0.022 | 0.033 | 0.033 | 0.075 | 0.042 | 0.04 | 0.02 | 0.033 | 0.075 | 0.08 | 0.09 |
| 128 | 0.022 | 0.061 | 0.044 | 0.033 | 0.071 | 0.04 | 0.04 | 0.04 | 0.042 | 0.06 | 0.052 | 0.061 |

| | | | | | | | | | | | | |
|---|---|---|---|---|---|---|---|---|---|---|---|---|
| 129 | 0.033 | 0.028 | 0.022 | 0.052 | 0.09 | 0.084 | 0.05 | 0.02 | 0.04 | 0.06 | 0.12 | 0.1 |
| 130 | 0.052 | 0.028 | 0.061 | 0.033 | 0.03 | 0.05 | 0.042 | 0.042 | 0.033 | 0.071 | 0.064 | 0.09 |
| 131 | 0.033 | 0.046 | 0.027 | 0.04 | 0.024 | 0.05 | 0.03 | 0.04 | 0.042 | 0.061 | 0.057 | 0.081 |
| 132 | 0.022 | 0.06 | 0.027 | 0.057 | 0.042 | 0.09 | 0.05 | 0.052 | 0.042 | 0.1 | 0.08 | 0.143 |
| 133 | 0.044 | 0.049 | 0.044 | 0.052 | 0.1 | 0.06 | 0.052 | 0.042 | 0.03 | 0.02 | 0.061 | 0.07 |
| 134 | 0.05 | 0.044 | 0.028 | 0.075 | 0.03 | 0.07 | 0.05 | 0.03 | 0.06 | 0.07 | 0.064 | 0.071 |
| 135 | 0.038 | 0.059 | 0.016 | 0.04 | 0.05 | 0.091 | 0.03 | 0.06 | 0.04 | 0.12 | 0.066 | 0.05 |
| 136 | 0.068 | 0.031 | 0.033 | 0.052 | 0.061 | 0.07 | 0.02 | 0.042 | 0.061 | 0.091 | 0.057 | 0.08 |
| 137 | 0.031 | 0.038 | 0.039 | 0.042 | 0.094 | 0.04 | 0.03 | 0.052 | 0.033 | 0.08 | 0.04 | 0.07 |
| 138 | 0.038 | 0.044 | 0.027 | 0.05 | 0.04 | 0.03 | 0.06 | 0.03 | 0.03 | 0.024 | 0.052 | 0.061 |
| 139 | 0.046 | 0.049 | 0.061 | 0.05 | 0.057 | 0.04 | 0.052 | 0.033 | 0.02 | 0.05 | 0.09 | 0.071 |
| 140 | 0.027 | 0.034 | 0.046 | 0.03 | 0.06 | 0.024 | 0.052 | 0.033 | 0.04 | 0.05 | 0.061 | 0.07 |
| 141 | 0.031 | 0.044 | 0.055 | 0.06 | 0.04 | 0.071 | 0.052 | 0.02 | 0.05 | 0.08 | 0.07 | 0.07 |
| 142 | 0.027 | 0.039 | 0.049 | 0.05 | 0.04 | 0.07 | 0.03 | 0.033 | 0.03 | 0.081 | 0.101 | 0.07 |
| 143 | 0.023 | 0.023 | 0.022 | 0.052 | 0.06 | 0.141 | 0.03 | 0.03 | 0.05 | 0.052 | 0.13 | 0.111 |
| 144 | 0.044 | 0.055 | 0.055 | 0.033 | 0.05 | 0.101 | 0.05 | 0.02 | 0.05 | 0.06 | 0.09 | 0.101 |
| 145 | 0.061 | 0.038 | 0.034 | 0.033 | 0.091 | 0.052 | 0.033 | 0.05 | 0.081 | 0.071 | 0.05 | 0.09 |
| 146 | 0.039 | 0.055 | 0.046 | 0.05 | 0.108 | 0.061 | 0.04 | 0.02 | 0.04 | 0.05 | 0.061 | 0.03 |
| 147 | 0.044 | 0.062 | 0.038 | 0.072 | 0.07 | 0.057 | 0.03 | 0.033 | 0.04 | 0.06 | 0.1 | 0.06 |
| 148 | 0.031 | 0.045 | 0.027 | 0.057 | 0.094 | 0.05 | 0.03 | 0.017 | 0.03 | 0.06 | 0.07 | 0.05 |
| 149 | 0.062 | 0.045 | 0.06 | 0.057 | 0.071 | 0.1 | 0.03 | 0.033 | 0.05 | 0.05 | 0.05 | 0.042 |
| 150 | 0.033 | 0.034 | 0.049 | 0.071 | 0.06 | 0.081 | 0.033 | 0.052 | 0.07 | 0.061 | 0.057 | 0.05 |
| 151 | 0.031 | 0.034 | 0.049 | 0.06 | 0.05 | 0.101 | 0.052 | 0.042 | 0.061 | 0.06 | 0.07 | 0.08 |
| 152 | 0.045 | 0.052 | 0.028 | 0.04 | 0.075 | 0.081 | 0.01 | 0.03 | 0.06 | 0.09 | 0.091 | 0.08 |
| 153 | 0.062 | 0.044 | 0.05 | 0.06 | 0.098 | 0.101 | 0.017 | 0.02 | 0.04 | 0.103 | 0.04 | 0.071 |
| 154 | 0.038 | 0.034 | 0.034 | 0.06 | 0.113 | 0.08 | 0.052 | 0.03 | 0.03 | 0.101 | 0.052 | 0.081 |
| 155 | 0.011 | 0.046 | 0.028 | 0.06 | 0.042 | 0.08 | 0.05 | 0.033 | 0.02 | 0.061 | 0.117 | 0.06 |
| 156 | 0.023 | 0.039 | 0.039 | 0.05 | 0.052 | 0.061 | 0.03 | 0.03 | 0.03 | 0.07 | 0.1 | 0.09 |
| 157 | 0.033 | 0.044 | 0.068 | 0.05 | 0.075 | 0.052 | 0.033 | 0.04 | 0.042 | 0.06 | 0.09 | 0.07 |
| 158 | 0.033 | 0.028 | 0.044 | 0.06 | 0.057 | 0.094 | 0.01 | 0.04 | 0.052 | 0.06 | 0.06 | 0.06 |

| | | | | | | | | | | | | |
|---|---|---|---|---|---|---|---|---|---|---|---|---|
| 159 | 0.062 | 0.057 | 0.082 | 0.105 | 0.061 | 0.06 | 0.04 | 0.042 | 0.03 | 0.057 | 0.1 | 0.111 |
| 160 | 0.044 | 0.06 | 0.033 | 0.052 | 0.052 | 0.066 | 0.04 | 0.05 | 0.024 | 0.08 | 0.08 | 0.05 |
| 161 | 0.027 | 0.049 | 0.018 | 0.052 | 0.075 | 0.04 | 0.033 | 0.06 | 0.024 | 0.071 | 0.07 | 0.07 |
| 162 | 0.038 | 0.027 | 0.055 | 0.08 | 0.089 | 0.094 | 0.04 | 0.066 | 0.042 | 0.05 | 0.08 | 0.081 |
| 163 | 0.035 | 0.038 | 0.038 | 0.08 | 0.08 | 0.094 | 0.04 | 0.033 | 0.048 | 0.06 | 0.05 | 0.091 |
| 164 | 0.027 | 0.055 | 0.034 | 0.04 | 0.096 | 0.084 | 0.042 | 0.06 | 0.042 | 0.12 | 0.05 | 0.1 |
| 165 | 0.038 | 0.062 | 0.039 | 0.061 | 0.071 | 0.113 | 0.04 | 0.042 | 0.042 | 0.091 | 0.05 | 0.061 |
| 166 | 0.075 | 0.026 | 0.055 | 0.05 | 0.094 | 0.09 | 0.033 | 0.05 | 0.042 | 0.03 | 0.04 | 0.1 |
| 167 | 0.052 | 0.055 | 0.055 | 0.081 | 0.084 | 0.042 | 0.042 | 0.04 | 0.042 | 0.05 | 0.081 | 0.081 |
| 168 | 0.038 | 0.05 | 0.038 | 0.042 | 0.05 | 0.08 | 0.024 | 0.03 | 0.057 | 0.042 | 0.091 | 0.071 |
| 169 | 0.033 | 0.038 | 0.057 | 0.052 | 0.101 | 0.09 | 0.04 | 0.04 | 0.04 | 0.04 | 0.08 | 0.072 |
| 170 | 0.033 | 0.06 | 0.066 | 0.05 | 0.061 | 0.05 | 0.05 | 0.04 | 0.033 | 0.061 | 0.11 | 0.042 |
| 171 | 0.049 | 0.034 | 0.027 | 0.042 | 0.061 | 0.042 | 0.02 | 0.05 | 0.06 | 0.061 | 0.066 | 0.113 |
| 172 | 0.022 | 0.082 | 0.018 | 0.03 | 0.084 | 0.08 | 0.024 | 0.05 | 0.05 | 0.07 | 0.05 | 0.141 |
| 173 | 0.049 | 0.022 | 0.041 | 0.03 | 0.05 | 0.09 | 0.04 | 0.04 | 0.033 | 0.05 | 0.05 | 0.07 |
| 174 | 0.061 | 0.055 | 0.05 | 0.085 | 0.06 | 0.05 | 0.05 | 0.042 | 0.02 | 0.08 | 0.042 | 0.071 |
| 175 | 0.031 | 0.016 | 0.061 | 0.052 | 0.075 | 0.07 | 0.04 | 0.02 | 0.033 | 0.08 | 0.06 | 0.08 |
| 176 | 0.039 | 0.038 | 0.055 | 0.06 | 0.088 | 0.081 | 0.03 | 0.05 | 0.02 | 0.042 | 0.113 | 0.071 |
| 177 | 0.041 | 0.049 | 0.049 | 0.03 | 0.06 | 0.033 | 0.042 | 0.042 | 0.05 | 0.101 | 0.06 | 0.101 |
| 178 | 0.023 | 0.038 | 0.031 | 0.03 | 0.094 | 0.071 | 0.057 | 0.057 | 0.03 | 0.05 | 0.04 | 0.1 |
| 179 | 0.023 | 0.054 | 0.062 | 0.042 | 0.098 | 0.1 | 0.033 | 0.05 | 0.033 | 0.08 | 0.061 | 0.161 |
| 180 | 0.055 | 0.049 | 0.022 | 0.04 | 0.071 | 0.052 | 0.06 | 0.02 | 0.042 | 0.084 | 0.091 | 0.101 |
| 181 | 0.061 | 0.049 | 0.036 | 0.042 | 0.089 | 0.052 | 0.024 | 0.05 | 0.05 | 0.084 | 0.08 | 0.091 |
| 182 | 0.034 | 0.044 | 0.038 | 0.03 | 0.084 | 0.04 | 0.03 | 0.042 | 0.052 | 0.081 | 0.06 | 0.111 |
| 183 | 0.044 | 0.054 | 0.027 | 0.042 | 0.033 | 0.052 | 0.024 | 0.03 | 0.05 | 0.081 | 0.081 | 0.05 |
| 184 | 0.038 | 0.038 | 0.022 | 0.05 | 0.071 | 0.03 | 0.052 | 0.033 | 0.03 | 0.071 | 0.075 | 0.08 |
| 185 | 0.022 | 0.028 | 0.035 | 0.033 | 0.061 | 0.052 | 0.04 | 0.03 | 0.042 | 0.061 | 0.052 | 0.061 |
| 186 | 0.045 | 0.052 | 0.027 | 0.02 | 0.12 | 0.052 | 0.04 | 0.042 | 0.04 | 0.111 | 0.06 | 0.07 |
| 187 | 0.057 | 0.039 | 0.016 | 0.02 | 0.108 | 0.05 | 0.052 | 0.04 | 0.05 | 0.05 | 0.048 | 0.06 |
| 188 | 0.022 | 0.045 | 0.055 | 0.042 | 0.091 | 0.033 | 0.017 | 0.075 | 0.06 | 0.1 | 0.04 | 0.052 |

| | | | | | | | | | | | | |
|---|---|---|---|---|---|---|---|---|---|---|---|---|
| 189 | 0.05 | 0.044 | 0.06 | 0.03 | 0.061 | 0.05 | 0.033 | 0.052 | 0.04 | 0.071 | 0.057 | 0.08 |
| 190 | 0.028 | 0.05 | 0.055 | 0.02 | 0.121 | 0.061 | 0.05 | 0.02 | 0.03 | 0.101 | 0.04 | 0.084 |
| 191 | 0.033 | 0.018 | 0.055 | 0.061 | 0.06 | 0.05 | 0.03 | 0.04 | 0.06 | 0.075 | 0.052 | 0.113 |
| 192 | 0.06 | 0.049 | 0.034 | 0.03 | 0.061 | 0.1 | 0.024 | 0.02 | 0.042 | 0.07 | 0.1 | 0.11 |
| 193 | 0.033 | 0.072 | 0.055 | 0.04 | 0.108 | 0.133 | 0.02 | 0.042 | 0.048 | 0.066 | 0.113 | 0.123 |
| 194 | 0.034 | 0.046 | 0.039 | 0.03 | 0.088 | 0.111 | 0.04 | 0.02 | 0.05 | 0.098 | 0.09 | 0.117 |
| 195 | 0.038 | 0.044 | 0.027 | 0.04 | 0.08 | 0.033 | 0.05 | 0.03 | 0.05 | 0.04 | 0.061 | 0.104 |
| 196 | 0.016 | 0.044 | 0.044 | 0.07 | 0.05 | 0.04 | 0.03 | 0.033 | 0.06 | 0.071 | 0.105 | 0.081 |
| 197 | 0.061 | 0.052 | 0.039 | 0.05 | 0.075 | 0.042 | 0.06 | 0.03 | 0.06 | 0.081 | 0.05 | 0.081 |
| 198 | 0.027 | 0.041 | 0.038 | 0.02 | 0.071 | 0.061 | 0.03 | 0.042 | 0.04 | 0.111 | 0.108 | 0.101 |
| 199 | 0.07 | 0.04 | 0.048 | 0.07 | 0.06 | 0.05 | 0.05 | 0.024 | 0.04 | 0.111 | 0.144 | 0.136 |
| 200 | 0.066 | 0.038 | 0.066 | 0.07 | 0.07 | 0.06 | 0.03 | 0.05 | 0.06 | 0.117 | 0.064 | 0.094 |
| 201 | 0.044 | 0.023 | 0.034 | 0.075 | 0.05 | 0.02 | 0.052 | 0.04 | 0.05 | 0.1 | 0.048 | 0.066 |
| 202 | 0.052 | 0.033 | 0.039 | 0.104 | 0.071 | 0.075 | 0.03 | 0.03 | 0.061 | 0.081 | 0.14 | 0.075 |
| 203 | 0.039 | 0.027 | 0.044 | 0.048 | 0.081 | 0.05 | 0.04 | 0.04 | 0.081 | 0.057 | 0.13 | 0.071 |
| 204 | 0.052 | 0.045 | 0.044 | 0.057 | 0.052 | 0.06 | 0.052 | 0.052 | 0.05 | 0.09 | 0.071 | 0.11 |
| 205 | 0.052 | 0.044 | 0.027 | 0.071 | 0.071 | 0.03 | 0.071 | 0.042 | 0.04 | 0.05 | 0.113 | 0.155 |
| 206 | 0.044 | 0.05 | 0.057 | 0.072 | 0.075 | 0.042 | 0.08 | 0.04 | 0.04 | 0.094 | 0.033 | 0.1 |
| 207 | 0.066 | 0.038 | 0.044 | 0.066 | 0.075 | 0.071 | 0.052 | 0.033 | 0.03 | 0.05 | 0.081 | 0.133 |
| 208 | 0.059 | 0.038 | 0.055 | 0.04 | 0.06 | 0.04 | 0.052 | 0.033 | 0.04 | 0.081 | 0.075 | 0.081 |
| 209 | 0.052 | 0.033 | 0.06 | 0.06 | 0.05 | 0.05 | 0.033 | 0.042 | 0.07 | 0.06 | 0.12 | 0.07 |
| 210 | 0.084 | 0.028 | 0.049 | 0.061 | 0.042 | 0.08 | 0.033 | 0.04 | 0.05 | 0.06 | 0.07 | 0.08 |
| 211 | 0.044 | 0.033 | 0.06 | 0.02 | 0.057 | 0.073 | 0.061 | 0.05 | 0.03 | 0.081 | 0.081 | 0.05 |
| 212 | 0.034 | 0.033 | 0.05 | 0.05 | 0.042 | 0.033 | 0.07 | 0.07 | 0.024 | 0.143 | 0.033 | 0.081 |
| 213 | 0.049 | 0.027 | 0.027 | 0.04 | 0.071 | 0.071 | 0.042 | 0.061 | 0.05 | 0.113 | 0.111 | 0.108 |
| 214 | 0.027 | 0.022 | 0.038 | 0.04 | 0.057 | 0.06 | 0.06 | 0.052 | 0.03 | 0.071 | 0.108 | 0.09 |
| 215 | 0.058 | 0.028 | 0.044 | 0.05 | 0.108 | 0.048 | 0.05 | 0.05 | 0.028 | 0.061 | 0.09 | 0.08 |
| 216 | 0.06 | 0.026 | 0.044 | 0.08 | 0.052 | 0.061 | 0.024 | 0.03 | 0.071 | 0.123 | 0.09 | 0.1 |
| 217 | 0.055 | 0.05 | 0.071 | 0.03 | 0.081 | 0.071 | 0.05 | 0.03 | 0.052 | 0.126 | 0.084 | 0.084 |
| 218 | 0.023 | 0.045 | 0.088 | 0.033 | 0.066 | 0.052 | 0.033 | 0.04 | 0.06 | 0.121 | 0.131 | 0.1 |

| | | | | | | | | | | | | |
|---|---|---|---|---|---|---|---|---|---|---|---|---|
| 219 | 0.033 | 0.052 | 0.091 | 0.072 | 0.052 | 0.052 | 0.01 | 0.04 | 0.02 | 0.081 | 0.088 | 0.075 |
| 220 | 0.066 | 0.058 | 0.062 | 0.07 | 0.048 | 0.081 | 0.052 | 0.033 | 0.03 | 0.11 | 0.143 | 0.08 |
| 221 | 0.055 | 0.049 | 0.07 | 0.05 | 0.094 | 0.075 | 0.06 | 0.04 | 0.08 | 0.1 | 0.108 | 0.152 |
| 222 | 0.044 | 0.055 | 0.031 | 0.08 | 0.103 | 0.061 | 0.033 | 0.04 | 0.042 | 0.05 | 0.094 | 0.113 |
| 223 | 0.06 | 0.033 | 0.05 | 0.05 | 0.071 | 0.08 | 0.06 | 0.033 | 0.04 | 0.071 | 0.108 | 0.136 |
| 224 | 0.027 | 0.038 | 0.055 | 0.07 | 0.06 | 0.061 | 0.03 | 0.04 | 0.07 | 0.08 | 0.094 | 0.1 |
| 225 | 0.028 | 0.049 | 0.045 | 0.03 | 0.08 | 0.075 | 0.04 | 0.042 | 0.064 | 0.071 | 0.084 | 0.081 |
| 226 | 0.023 | 0.027 | 0.06 | 0.06 | 0.081 | 0.169 | 0.061 | 0.04 | 0.06 | 0.103 | 0.075 | 0.207 |
| 227 | 0.044 | 0.049 | 0.045 | 0.052 | 0.101 | 0.081 | 0.052 | 0.06 | 0.05 | 0.06 | 0.096 | 0.081 |
| 228 | 0.066 | 0.044 | 0.057 | 0.061 | 0.123 | 0.061 | 0.02 | 0.04 | 0.04 | 0.094 | 0.06 | 0.071 |
| 229 | 0.049 | 0.044 | 0.052 | 0.057 | 0.071 | 0.09 | 0.042 | 0.02 | 0.04 | 0.111 | 0.05 | 0.108 |
| 230 | 0.044 | 0.033 | 0.049 | 0.061 | 0.123 | 0.05 | 0.04 | 0.042 | 0.033 | 0.098 | 0.111 | 0.071 |
| 231 | 0.055 | 0.022 | 0.022 | 0.03 | 0.071 | 0.071 | 0.06 | 0.06 | 0.06 | 0.081 | 0.081 | 0.151 |
| 232 | 0.045 | 0.038 | 0.044 | 0.024 | 0.075 | 0.06 | 0.042 | 0.05 | 0.03 | 0.162 | 0.04 | 0.16 |
| 233 | 0.018 | 0.033 | 0.06 | 0.042 | 0.111 | 0.06 | 0.04 | 0.03 | 0.03 | 0.081 | 0.028 | 0.101 |
| 234 | 0.039 | 0.038 | 0.082 | 0.064 | 0.033 | 0.081 | 0.05 | 0.04 | 0.05 | 0.098 | 0.136 | 0.14 |
| 235 | 0.055 | 0.033 | 0.078 | 0.052 | 0.15 | 0.136 | 0.04 | 0.064 | 0.02 | 0.066 | 0.05 | 0.101 |
| 236 | 0.038 | 0.033 | 0.071 | 0.061 | 0.081 | 0.08 | 0.024 | 0.06 | 0.04 | 0.08 | 0.1 | 0.108 |
| 237 | 0.049 | 0.026 | 0.066 | 0.01 | 0.061 | 0.094 | 0.024 | 0.06 | 0.05 | 0.05 | 0.081 | 0.064 |
| 238 | 0.027 | 0.033 | 0.057 | 0.05 | 0.066 | 0.12 | 0.017 | 0.042 | 0.042 | 0.05 | 0.1 | 0.081 |
| 239 | 0.059 | 0.028 | 0.038 | 0.06 | 0.129 | 0.05 | 0.024 | 0.06 | 0.052 | 0.08 | 0.07 | 0.09 |
| 240 | 0.011 | 0.038 | 0.033 | 0.042 | 0.081 | 0.06 | 0.02 | 0.042 | 0.05 | 0.07 | 0.09 | 0.12 |
| 241 | 0.034 | 0.084 | 0.06 | 0.04 | 0.07 | 0.05 | 0.04 | 0.04 | 0.052 | 0.075 | 0.05 | 0.075 |
| 242 | 0.059 | 0.06 | 0.059 | 0.024 | 0.042 | 0.061 | 0.017 | 0.02 | 0.07 | 0.1 | 0.052 | 0.143 |
| 243 | 0.028 | 0.027 | 0.045 | 0.03 | 0.165 | 0.075 | 0.057 | 0.01 | 0.042 | 0.05 | 0.091 | 0.151 |
| 244 | 0.052 | 0.044 | 0.064 | 0.03 | 0.05 | 0.075 | 0.048 | 0.04 | 0.03 | 0.02 | 0.084 | 0.1 |
| 245 | 0.055 | 0.061 | 0.09 | 0.042 | 0.103 | 0.084 | 0.033 | 0.03 | 0.042 | 0.101 | 0.075 | 0.081 |
| 246 | 0.038 | 0.023 | 0.057 | 0.03 | 0.13 | 0.07 | 0.03 | 0.057 | 0.03 | 0.061 | 0.091 | 0.091 |
| 247 | 0.045 | 0.022 | 0.05 | 0.084 | 0.131 | 0.075 | 0.024 | 0.06 | 0.071 | 0.1 | 0.071 | 0.071 |
| 248 | 0.033 | 0.027 | 0.046 | 0.064 | 0.101 | 0.042 | 0.061 | 0.05 | 0.02 | 0.103 | 0.06 | 0.159 |

| | | | | | | | | | | | | |
|---|---|---|---|---|---|---|---|---|---|---|---|---|
| 249 | 0.064 | 0.022 | 0.049 | 0.081 | 0.084 | 0.07 | 0.02 | 0.03 | 0.042 | 0.09 | 0.07 | 0.131 |
| 250 | 0.034 | 0.023 | 0.062 | 0.089 | 0.14 | 0.101 | 0.052 | 0.033 | 0.03 | 0.042 | 0.04 | 0.108 |
| Mean | 0.039464 | 0.041356 | 0.04306 | 0.051408 | 0.068032 | 0.066956 | 0.038552 | 0.038552 | 0.042352 | 0.067364 | 0.075124 | 0.082024 |
| SD | 0.014338 | 0.014403 | 0.015639 | 0.01887 | 0.025509 | 0.024352 | 0.013775 | 0.012903 | 0.013805 | 0.024287 | 0.027394 | 0.027534 |

| | Day 4 | | | | | | Day 5 | | | | | |
|---|---|---|---|---|---|---|---|---|---|---|---|---|
| OCT images | Control | | | Infected | | | Control | | | Infected | | |
| | 1 | 2 | 3 | 1 | 2 | 3 | 1 | 2 | 3 | 1 | 2 | 3 |
| 1 | 0.08 | 0.052 | 0.052 | 0.081 | 0.111 | 0.052 | 0.033 | 0.017 | 0.052 | 0.052 | 0.08 | 0.066 |
| 2 | 0.07 | 0.033 | 0.057 | 0.06 | 0.09 | 0.05 | 0.061 | 0.04 | 0.04 | 0.091 | 0.08 | 0.131 |
| 3 | 0.02 | 0.033 | 0.04 | 0.06 | 0.08 | 0.09 | 0.045 | 0.04 | 0.061 | 0.08 | 0.071 | 0.101 |
| 4 | 0.042 | 0.042 | 0.03 | 0.071 | 0.05 | 0.05 | 0.048 | 0.07 | 0.061 | 0.071 | 0.06 | 0.1 |
| 5 | 0.01 | 0.042 | 0.06 | 0.04 | 0.07 | 0.06 | 0.04 | 0.03 | 0.05 | 0.07 | 0.09 | 0.05 |
| 6 | 0.057 | 0.033 | 0.061 | 0.12 | 0.136 | 0.052 | 0.042 | 0.04 | 0.04 | 0.042 | 0.081 | 0.081 |
| 7 | 0.04 | 0.06 | 0.01 | 0.09 | 0.121 | 0.042 | 0.024 | 0.042 | 0.052 | 0.05 | 0.05 | 0.05 |
| 8 | 0.024 | 0.05 | 0.04 | 0.05 | 0.08 | 0.052 | 0.052 | 0.06 | 0.05 | 0.072 | 0.07 | 0.08 |
| 9 | 0.03 | 0.04 | 0.03 | 0.052 | 0.09 | 0.066 | 0.04 | 0.091 | 0.06 | 0.057 | 0.03 | 0.08 |
| 10 | 0.05 | 0.03 | 0.033 | 0.07 | 0.123 | 0.05 | 0.073 | 0.028 | 0.04 | 0.081 | 0.091 | 0.05 |
| 11 | 0.03 | 0.033 | 0.04 | 0.06 | 0.071 | 0.061 | 0.066 | 0.04 | 0.061 | 0.066 | 0.061 | 0.042 |
| 12 | 0.05 | 0.017 | 0.02 | 0.07 | 0.04 | 0.042 | 0.06 | 0.05 | 0.06 | 0.081 | 0.06 | 0.071 |
| 13 | 0.03 | 0.02 | 0.05 | 0.06 | 0.08 | 0.06 | 0.042 | 0.05 | 0.02 | 0.091 | 0.101 | 0.113 |
| 14 | 0.03 | 0.071 | 0.042 | 0.075 | 0.061 | 0.094 | 0.03 | 0.042 | 0.02 | 0.042 | 0.06 | 0.08 |
| 15 | 0.05 | 0.033 | 0.033 | 0.08 | 0.052 | 0.061 | 0.033 | 0.066 | 0.033 | 0.04 | 0.09 | 0.081 |
| 16 | 0.02 | 0.052 | 0.061 | 0.081 | 0.02 | 0.07 | 0.03 | 0.066 | 0.042 | 0.05 | 0.1 | 0.04 |
| 17 | 0.04 | 0.04 | 0.02 | 0.103 | 0.071 | 0.05 | 0.03 | 0.04 | 0.04 | 0.04 | 0.09 | 0.07 |
| 18 | 0.075 | 0.03 | 0.017 | 0.094 | 0.08 | 0.061 | 0.052 | 0.052 | 0.03 | 0.06 | 0.06 | 0.091 |
| 19 | 0.052 | 0.024 | 0.03 | 0.084 | 0.126 | 0.05 | 0.03 | 0.05 | 0.06 | 0.091 | 0.089 | 0.084 |
| 20 | 0.04 | 0.033 | 0.02 | 0.09 | 0.13 | 0.061 | 0.03 | 0.052 | 0.04 | 0.094 | 0.04 | 0.048 |
| 21 | 0.057 | 0.033 | 0.04 | 0.141 | 0.091 | 0.07 | 0.024 | 0.04 | 0.05 | 0.108 | 0.024 | 0.15 |

| | | | | | | | | | | | | |
|---|---|---|---|---|---|---|---|---|---|---|---|---|
| 22 | 0.03 | 0.048 | 0.052 | 0.1 | 0.081 | 0.061 | 0.052 | 0.042 | 0.03 | 0.061 | 0.071 | 0.09 |
| 23 | 0.061 | 0.057 | 0.04 | 0.081 | 0.09 | 0.061 | 0.052 | 0.04 | 0.052 | 0.06 | 0.091 | 0.08 |
| 24 | 0.042 | 0.057 | 0.04 | 0.091 | 0.03 | 0.081 | 0.042 | 0.061 | 0.081 | 0.075 | 0.05 | 0.075 |
| 25 | 0.057 | 0.033 | 0.052 | 0.091 | 0.07 | 0.09 | 0.04 | 0.03 | 0.04 | 0.05 | 0.061 | 0.052 |
| 26 | 0.066 | 0.033 | 0.05 | 0.075 | 0.06 | 0.07 | 0.042 | 0.03 | 0.03 | 0.02 | 0.101 | 0.071 |
| 27 | 0.033 | 0.042 | 0.02 | 0.06 | 0.071 | 0.042 | 0.05 | 0.04 | 0.06 | 0.052 | 0.06 | 0.103 |
| 28 | 0.04 | 0.052 | 0.04 | 0.06 | 0.08 | 0.123 | 0.042 | 0.02 | 0.05 | 0.052 | 0.06 | 0.071 |
| 29 | 0.057 | 0.057 | 0.03 | 0.103 | 0.04 | 0.04 | 0.06 | 0.042 | 0.02 | 0.081 | 0.071 | 0.07 |
| 30 | 0.01 | 0.061 | 0.042 | 0.05 | 0.061 | 0.02 | 0.03 | 0.02 | 0.042 | 0.06 | 0.06 | 0.081 |
| 31 | 0.057 | 0.033 | 0.02 | 0.06 | 0.06 | 0.03 | 0.042 | 0.066 | 0.103 | 0.091 | 0.08 | 0.066 |
| 32 | 0.042 | 0.03 | 0.03 | 0.033 | 0.081 | 0.08 | 0.04 | 0.01 | 0.03 | 0.071 | 0.081 | 0.06 |
| 33 | 0.05 | 0.03 | 0.071 | 0.094 | 0.108 | 0.066 | 0.06 | 0.071 | 0.042 | 0.101 | 0.071 | 0.08 |
| 34 | 0.033 | 0.03 | 0.04 | 0.07 | 0.09 | 0.111 | 0.052 | 0.05 | 0.06 | 0.07 | 0.1 | 0.061 |
| 35 | 0.04 | 0.04 | 0.048 | 0.02 | 0.08 | 0.097 | 0.02 | 0.052 | 0.06 | 0.066 | 0.09 | 0.071 |
| 36 | 0.02 | 0.05 | 0.052 | 0.05 | 0.08 | 0.11 | 0.04 | 0.08 | 0.05 | 0.07 | 0.06 | 0.042 |
| 37 | 0.03 | 0.064 | 0.05 | 0.094 | 0.061 | 0.07 | 0.07 | 0.08 | 0.052 | 0.03 | 0.07 | 0.152 |
| 38 | 0.03 | 0.04 | 0.02 | 0.091 | 0.101 | 0.071 | 0.042 | 0.03 | 0.03 | 0.061 | 0.03 | 0.081 |
| 39 | 0.04 | 0.071 | 0.042 | 0.081 | 0.04 | 0.143 | 0.04 | 0.05 | 0.06 | 0.06 | 0.066 | 0.071 |
| 40 | 0.03 | 0.04 | 0.04 | 0.094 | 0.061 | 0.07 | 0.04 | 0.017 | 0.045 | 0.042 | 0.061 | 0.08 |
| 41 | 0.033 | 0.07 | 0.057 | 0.02 | 0.11 | 0.081 | 0.05 | 0.09 | 0.081 | 0.09 | 0.061 | 0.111 |
| 42 | 0.05 | 0.067 | 0.042 | 0.057 | 0.066 | 0.01 | 0.03 | 0.01 | 0.05 | 0.07 | 0.042 | 0.121 |
| 43 | 0.03 | 0.01 | 0.052 | 0.066 | 0.09 | 0.041 | 0.017 | 0.03 | 0.042 | 0.113 | 0.05 | 0.05 |
| 44 | 0.02 | 0.05 | 0.04 | 0.033 | 0.146 | 0.064 | 0.052 | 0.024 | 0.033 | 0.091 | 0.05 | 0.094 |
| 45 | 0.061 | 0.04 | 0.033 | 0.06 | 0.133 | 0.057 | 0.03 | 0.03 | 0.04 | 0.091 | 0.061 | 0.07 |
| 46 | 0.052 | 0.04 | 0.048 | 0.121 | 0.061 | 0.09 | 0.03 | 0.017 | 0.01 | 0.071 | 0.08 | 0.071 |
| 47 | 0.02 | 0.06 | 0.057 | 0.075 | 0.089 | 0.061 | 0.033 | 0.06 | 0.03 | 0.06 | 0.04 | 0.071 |
| 48 | 0.04 | 0.024 | 0.052 | 0.06 | 0.121 | 0.05 | 0.04 | 0.042 | 0.033 | 0.103 | 0.09 | 0.08 |
| 49 | 0.024 | 0.052 | 0.04 | 0.071 | 0.06 | 0.101 | 0.04 | 0.05 | 0.071 | 0.06 | 0.08 | 0.101 |
| 50 | 0.033 | 0.061 | 0.024 | 0.08 | 0.143 | 0.123 | 0.042 | 0.03 | 0.061 | 0.121 | 0.06 | 0.03 |
| 51 | 0.04 | 0.05 | 0.033 | 0.113 | 0.061 | 0.103 | 0.033 | 0.048 | 0.071 | 0.072 | 0.06 | 0.04 |

| | | | | | | | | | | | | |
|---|---|---|---|---|---|---|---|---|---|---|---|---|
| 52 | 0.04 | 0.03 | 0.042 | 0.06 | 0.071 | 0.121 | 0.042 | 0.05 | 0.052 | 0.057 | 0.07 | 0.08 |
| 53 | 0.04 | 0.066 | 0.042 | 0.1 | 0.071 | 0.071 | 0.05 | 0.02 | 0.101 | 0.103 | 0.06 | 0.071 |
| 54 | 0.03 | 0.04 | 0.05 | 0.05 | 0.103 | 0.12 | 0.04 | 0.01 | 0.052 | 0.042 | 0.04 | 0.094 |
| 55 | 0.03 | 0.042 | 0.05 | 0.052 | 0.075 | 0.081 | 0.052 | 0.04 | 0.03 | 0.101 | 0.061 | 0.071 |
| 56 | 0.03 | 0.04 | 0.024 | 0.042 | 0.05 | 0.081 | 0.06 | 0.07 | 0.01 | 0.09 | 0.066 | 0.08 |
| 57 | 0.024 | 0.04 | 0.05 | 0.04 | 0.071 | 0.091 | 0.05 | 0.04 | 0.024 | 0.07 | 0.06 | 0.121 |
| 58 | 0.024 | 0.05 | 0.042 | 0.06 | 0.091 | 0.111 | 0.06 | 0.052 | 0.042 | 0.071 | 0.07 | 0.11 |
| 59 | 0.03 | 0.042 | 0.04 | 0.04 | 0.075 | 0.05 | 0.04 | 0.061 | 0.03 | 0.094 | 0.04 | 0.101 |
| 60 | 0.02 | 0.06 | 0.033 | 0.042 | 0.071 | 0.07 | 0.052 | 0.02 | 0.048 | 0.042 | 0.06 | 0.09 |
| 61 | 0.033 | 0.02 | 0.06 | 0.061 | 0.052 | 0.05 | 0.05 | 0.024 | 0.091 | 0.07 | 0.03 | 0.071 |
| 62 | 0.02 | 0.04 | 0.05 | 0.071 | 0.052 | 0.052 | 0.024 | 0.033 | 0.07 | 0.061 | 0.052 | 0.091 |
| 63 | 0.033 | 0.06 | 0.03 | 0.071 | 0.052 | 0.066 | 0.052 | 0.052 | 0.07 | 0.07 | 0.084 | 0.081 |
| 64 | 0.01 | 0.03 | 0.06 | 0.04 | 0.052 | 0.091 | 0.07 | 0.04 | 0.06 | 0.061 | 0.04 | 0.123 |
| 65 | 0.03 | 0.03 | 0.04 | 0.05 | 0.096 | 0.117 | 0.05 | 0.04 | 0.033 | 0.033 | 0.08 | 0.02 |
| 66 | 0.04 | 0.04 | 0.042 | 0.05 | 0.07 | 0.061 | 0.042 | 0.042 | 0.081 | 0.091 | 0.06 | 0.103 |
| 67 | 0.05 | 0.061 | 0.04 | 0.081 | 0.03 | 0.081 | 0.03 | 0.042 | 0.066 | 0.094 | 0.04 | 0.089 |
| 68 | 0.03 | 0.048 | 0.05 | 0.071 | 0.121 | 0.094 | 0.05 | 0.057 | 0.04 | 0.09 | 0.02 | 0.11 |
| 69 | 0.042 | 0.061 | 0.04 | 0.061 | 0.05 | 0.07 | 0.033 | 0.05 | 0.04 | 0.04 | 0.09 | 0.061 |
| 70 | 0.052 | 0.042 | 0.04 | 0.06 | 0.071 | 0.1 | 0.02 | 0.08 | 0.09 | 0.084 | 0.1 | 0.061 |
| 71 | 0.052 | 0.042 | 0.04 | 0.052 | 0.052 | 0.131 | 0.091 | 0.06 | 0.075 | 0.04 | 0.1 | 0.042 |
| 72 | 0.02 | 0.06 | 0.042 | 0.072 | 0.052 | 0.08 | 0.061 | 0.061 | 0.042 | 0.05 | 0.101 | 0.05 |
| 73 | 0.06 | 0.06 | 0.05 | 0.081 | 0.033 | 0.126 | 0.06 | 0.05 | 0.05 | 0.066 | 0.081 | 0.061 |
| 74 | 0.033 | 0.04 | 0.05 | 0.108 | 0.06 | 0.033 | 0.05 | 0.05 | 0.094 | 0.052 | 0.084 | 0.165 |
| 75 | 0.052 | 0.06 | 0.033 | 0.081 | 0.071 | 0.05 | 0.052 | 0.04 | 0.071 | 0.01 | 0.057 | 0.1 |
| 76 | 0.033 | 0.042 | 0.072 | 0.071 | 0.09 | 0.066 | 0.081 | 0.05 | 0.052 | 0.071 | 0.048 | 0.113 |
| 77 | 0.042 | 0.061 | 0.057 | 0.094 | 0.07 | 0.05 | 0.075 | 0.052 | 0.057 | 0.08 | 0.08 | 0.06 |
| 78 | 0.057 | 0.07 | 0.04 | 0.057 | 0.052 | 0.06 | 0.04 | 0.024 | 0.09 | 0.06 | 0.04 | 0.101 |
| 79 | 0.01 | 0.05 | 0.033 | 0.071 | 0.07 | 0.08 | 0.052 | 0.081 | 0.08 | 0.03 | 0.04 | 0.071 |
| 80 | 0.024 | 0.083 | 0.048 | 0.075 | 0.057 | 0.071 | 0.075 | 0.06 | 0.03 | 0.06 | 0.066 | 0.081 |
| 81 | 0.033 | 0.08 | 0.052 | 0.07 | 0.061 | 0.09 | 0.06 | 0.06 | 0.06 | 0.084 | 0.05 | 0.09 |

| | | | | | | | | | | | | |
|---|---|---|---|---|---|---|---|---|---|---|---|---|
| 82 | 0.06 | 0.061 | 0.042 | 0.101 | 0.05 | 0.08 | 0.04 | 0.03 | 0.084 | 0.061 | 0.09 | 0.05 |
| 83 | 0.048 | 0.05 | 0.08 | 0.101 | 0.048 | 0.04 | 0.042 | 0.05 | 0.02 | 0.081 | 0.071 | 0.12 |
| 84 | 0.052 | 0.042 | 0.03 | 0.103 | 0.081 | 0.131 | 0.071 | 0.07 | 0.02 | 0.04 | 0.07 | 0.081 |
| 85 | 0.042 | 0.05 | 0.042 | 0.091 | 0.11 | 0.06 | 0.05 | 0.033 | 0.024 | 0.05 | 0.05 | 0.1 |
| 86 | 0.03 | 0.05 | 0.06 | 0.06 | 0.09 | 0.04 | 0.033 | 0.03 | 0.033 | 0.04 | 0.06 | 0.08 |
| 87 | 0.03 | 0.075 | 0.048 | 0.11 | 0.03 | 0.084 | 0.04 | 0.05 | 0.03 | 0.091 | 0.052 | 0.061 |
| 88 | 0.048 | 0.057 | 0.05 | 0.103 | 0.15 | 0.075 | 0.033 | 0.04 | 0.02 | 0.033 | 0.03 | 0.11 |
| 89 | 0.066 | 0.071 | 0.066 | 0.081 | 0.075 | 0.061 | 0.05 | 0.02 | 0.06 | 0.06 | 0.06 | 0.071 |
| 90 | 0.033 | 0.09 | 0.06 | 0.04 | 0.081 | 0.075 | 0.042 | 0.06 | 0.052 | 0.06 | 0.07 | 0.061 |
| 91 | 0.02 | 0.057 | 0.06 | 0.09 | 0.108 | 0.04 | 0.042 | 0.02 | 0.05 | 0.052 | 0.081 | 0.08 |
| 92 | 0.042 | 0.06 | 0.04 | 0.042 | 0.101 | 0.071 | 0.033 | 0.03 | 0.05 | 0.111 | 0.07 | 0.05 |
| 93 | 0.033 | 0.07 | 0.05 | 0.057 | 0.08 | 0.07 | 0.03 | 0.03 | 0.07 | 0.091 | 0.06 | 0.061 |
| 94 | 0.033 | 0.033 | 0.05 | 0.07 | 0.101 | 0.091 | 0.07 | 0.02 | 0.045 | 0.1 | 0.08 | 0.07 |
| 95 | 0.02 | 0.05 | 0.04 | 0.06 | 0.121 | 0.07 | 0.071 | 0.033 | 0.02 | 0.07 | 0.071 | 0.081 |
| 96 | 0.042 | 0.04 | 0.052 | 0.066 | 0.1 | 0.1 | 0.04 | 0.033 | 0.071 | 0.081 | 0.04 | 0.111 |
| 97 | 0.052 | 0.04 | 0.04 | 0.06 | 0.11 | 0.05 | 0.103 | 0.052 | 0.05 | 0.052 | 0.06 | 0.131 |
| 98 | 0.033 | 0.05 | 0.05 | 0.089 | 0.131 | 0.08 | 0.033 | 0.02 | 0.071 | 0.09 | 0.103 | 0.08 |
| 99 | 0.02 | 0.05 | 0.04 | 0.042 | 0.091 | 0.045 | 0.024 | 0.048 | 0.05 | 0.03 | 0.024 | 0.12 |
| 100 | 0.07 | 0.05 | 0.05 | 0.108 | 0.081 | 0.052 | 0.04 | 0.052 | 0.061 | 0.061 | 0.06 | 0.101 |
| 101 | 0.071 | 0.03 | 0.024 | 0.05 | 0.084 | 0.05 | 0.061 | 0.033 | 0.01 | 0.024 | 0.03 | 0.057 |
| 102 | 0.048 | 0.042 | 0.057 | 0.066 | 0.11 | 0.04 | 0.03 | 0.02 | 0.089 | 0.066 | 0.071 | 0.091 |
| 103 | 0.04 | 0.04 | 0.052 | 0.1 | 0.075 | 0.05 | 0.04 | 0.02 | 0.042 | 0.08 | 0.09 | 0.09 |
| 104 | 0.052 | 0.042 | 0.061 | 0.1 | 0.081 | 0.09 | 0.03 | 0.04 | 0.06 | 0.101 | 0.061 | 0.081 |
| 105 | 0.033 | 0.052 | 0.06 | 0.071 | 0.08 | 0.08 | 0.06 | 0.02 | 0.052 | 0.061 | 0.072 | 0.05 |
| 106 | 0.05 | 0.05 | 0.03 | 0.11 | 0.111 | 0.101 | 0.05 | 0.05 | 0.042 | 0.07 | 0.052 | 0.071 |
| 107 | 0.05 | 0.052 | 0.04 | 0.07 | 0.09 | 0.05 | 0.07 | 0.042 | 0.02 | 0.061 | 0.098 | 0.042 |
| 108 | 0.04 | 0.042 | 0.06 | 0.16 | 0.06 | 0.04 | 0.033 | 0.04 | 0.024 | 0.05 | 0.113 | 0.07 |
| 109 | 0.05 | 0.033 | 0.052 | 0.1 | 0.081 | 0.042 | 0.048 | 0.048 | 0.061 | 0.071 | 0.05 | 0.06 |
| 110 | 0.078 | 0.042 | 0.033 | 0.14 | 0.07 | 0.05 | 0.066 | 0.033 | 0.07 | 0.06 | 0.071 | 0.05 |
| 111 | 0.08 | 0.071 | 0.071 | 0.101 | 0.113 | 0.06 | 0.061 | 0.052 | 0.052 | 0.061 | 0.05 | 0.108 |

| | | | | | | | | | | | | |
|---|---|---|---|---|---|---|---|---|---|---|---|---|
| 112 | 0.06 | 0.033 | 0.052 | 0.08 | 0.121 | 0.091 | 0.033 | 0.06 | 0.052 | 0.03 | 0.04 | 0.17 |
| 113 | 0.071 | 0.061 | 0.052 | 0.066 | 0.11 | 0.06 | 0.061 | 0.061 | 0.042 | 0.1 | 0.05 | 0.06 |
| 114 | 0.033 | 0.08 | 0.052 | 0.07 | 0.1 | 0.04 | 0.06 | 0.02 | 0.081 | 0.052 | 0.07 | 0.108 |
| 115 | 0.024 | 0.061 | 0.048 | 0.061 | 0.08 | 0.03 | 0.04 | 0.02 | 0.04 | 0.123 | 0.057 | 0.052 |
| 116 | 0.061 | 0.061 | 0.042 | 0.08 | 0.1 | 0.052 | 0.084 | 0.04 | 0.03 | 0.042 | 0.06 | 0.071 |
| 117 | 0.057 | 0.07 | 0.071 | 0.08 | 0.071 | 0.06 | 0.04 | 0.082 | 0.05 | 0.066 | 0.06 | 0.08 |
| 118 | 0.07 | 0.06 | 0.05 | 0.1 | 0.101 | 0.081 | 0.033 | 0.033 | 0.061 | 0.061 | 0.06 | 0.05 |
| 119 | 0.07 | 0.042 | 0.04 | 0.03 | 0.141 | 0.091 | 0.052 | 0.03 | 0.05 | 0.057 | 0.06 | 0.13 |
| 120 | 0.04 | 0.033 | 0.048 | 0.075 | 0.103 | 0.11 | 0.052 | 0.061 | 0.06 | 0.075 | 0.07 | 0.05 |
| 121 | 0.03 | 0.07 | 0.05 | 0.061 | 0.081 | 0.081 | 0.06 | 0.07 | 0.05 | 0.1 | 0.042 | 0.07 |
| 122 | 0.042 | 0.072 | 0.071 | 0.06 | 0.08 | 0.084 | 0.07 | 0.071 | 0.06 | 0.091 | 0.061 | 0.06 |
| 123 | 0.052 | 0.05 | 0.02 | 0.09 | 0.103 | 0.06 | 0.07 | 0.057 | 0.042 | 0.091 | 0.081 | 0.06 |
| 124 | 0.033 | 0.048 | 0.048 | 0.121 | 0.081 | 0.061 | 0.061 | 0.02 | 0.052 | 0.081 | 0.061 | 0.061 |
| 125 | 0.033 | 0.06 | 0.04 | 0.075 | 0.14 | 0.033 | 0.05 | 0.057 | 0.04 | 0.05 | 0.113 | 0.07 |
| 126 | 0.04 | 0.03 | 0.057 | 0.075 | 0.1 | 0.061 | 0.06 | 0.01 | 0.033 | 0.141 | 0.05 | 0.081 |
| 127 | 0.061 | 0.02 | 0.04 | 0.08 | 0.091 | 0.091 | 0.033 | 0.03 | 0.033 | 0.081 | 0.052 | 0.101 |
| 128 | 0.05 | 0.042 | 0.024 | 0.07 | 0.06 | 0.075 | 0.08 | 0.075 | 0.06 | 0.06 | 0.05 | 0.07 |
| 129 | 0.033 | 0.052 | 0.052 | 0.08 | 0.143 | 0.084 | 0.01 | 0.081 | 0.057 | 0.057 | 0.071 | 0.08 |
| 130 | 0.04 | 0.03 | 0.05 | 0.081 | 0.1 | 0.123 | 0.04 | 0.05 | 0.066 | 0.061 | 0.033 | 0.08 |
| 131 | 0.06 | 0.071 | 0.052 | 0.13 | 0.08 | 0.1 | 0.04 | 0.03 | 0.02 | 0.05 | 0.05 | 0.075 |
| 132 | 0.024 | 0.052 | 0.052 | 0.09 | 0.1 | 0.08 | 0.042 | 0.057 | 0.071 | 0.04 | 0.061 | 0.061 |
| 133 | 0.04 | 0.066 | 0.061 | 0.066 | 0.05 | 0.081 | 0.075 | 0.061 | 0.075 | 0.1 | 0.04 | 0.081 |
| 134 | 0.04 | 0.04 | 0.05 | 0.061 | 0.12 | 0.066 | 0.04 | 0.04 | 0.04 | 0.06 | 0.01 | 0.103 |
| 135 | 0.03 | 0.05 | 0.052 | 0.07 | 0.03 | 0.103 | 0.03 | 0.067 | 0.061 | 0.033 | 0.042 | 0.057 |
| 136 | 0.052 | 0.03 | 0.04 | 0.042 | 0.05 | 0.057 | 0.052 | 0.04 | 0.06 | 0.061 | 0.071 | 0.1 |
| 137 | 0.033 | 0.061 | 0.042 | 0.04 | 0.08 | 0.06 | 0.04 | 0.04 | 0.04 | 0.071 | 0.024 | 0.064 |
| 138 | 0.03 | 0.06 | 0.033 | 0.091 | 0.094 | 0.101 | 0.04 | 0.04 | 0.061 | 0.052 | 0.024 | 0.1 |
| 139 | 0.04 | 0.061 | 0.04 | 0.052 | 0.084 | 0.04 | 0.033 | 0.04 | 0.061 | 0.06 | 0.05 | 0.072 |
| 140 | 0.04 | 0.033 | 0.04 | 0.061 | 0.061 | 0.09 | 0.02 | 0.061 | 0.042 | 0.07 | 0.052 | 0.07 |
| 141 | 0.05 | 0.061 | 0.05 | 0.061 | 0.172 | 0.071 | 0.052 | 0.052 | 0.066 | 0.05 | 0.028 | 0.09 |

| | | | | | | | | | | | | |
|---|---|---|---|---|---|---|---|---|---|---|---|---|
| 142 | 0.02 | 0.06 | 0.042 | 0.071 | 0.09 | 0.07 | 0.01 | 0.03 | 0.081 | 0.061 | 0.06 | 0.075 |
| 143 | 0.057 | 0.071 | 0.075 | 0.066 | 0.075 | 0.091 | 0.033 | 0.061 | 0.08 | 0.061 | 0.02 | 0.08 |
| 144 | 0.03 | 0.081 | 0.061 | 0.05 | 0.05 | 0.128 | 0.042 | 0.091 | 0.04 | 0.1 | 0.101 | 0.057 |
| 145 | 0.04 | 0.052 | 0.075 | 0.07 | 0.07 | 0.081 | 0.066 | 0.04 | 0.052 | 0.1 | 0.06 | 0.08 |
| 146 | 0.1 | 0.08 | 0.061 | 0.101 | 0.05 | 0.06 | 0.08 | 0.04 | 0.02 | 0.141 | 0.081 | 0.08 |
| 147 | 0.061 | 0.05 | 0.064 | 0.1 | 0.091 | 0.09 | 0.084 | 0.04 | 0.057 | 0.071 | 0.05 | 0.094 |
| 148 | 0.066 | 0.05 | 0.052 | 0.081 | 0.08 | 0.08 | 0.05 | 0.05 | 0.06 | 0.081 | 0.061 | 0.075 |
| 149 | 0.03 | 0.06 | 0.05 | 0.1 | 0.117 | 0.081 | 0.061 | 0.02 | 0.04 | 0.091 | 0.07 | 0.042 |
| 150 | 0.01 | 0.042 | 0.057 | 0.071 | 0.111 | 0.1 | 0.06 | 0.04 | 0.061 | 0.08 | 0.081 | 0.08 |
| 151 | 0.05 | 0.08 | 0.024 | 0.06 | 0.19 | 0.12 | 0.075 | 0.01 | 0.033 | 0.071 | 0.1 | 0.06 |
| 152 | 0.05 | 0.057 | 0.061 | 0.11 | 0.133 | 0.061 | 0.04 | 0.06 | 0.066 | 0.089 | 0.091 | 0.131 |
| 153 | 0.03 | 0.06 | 0.02 | 0.09 | 0.091 | 0.04 | 0.052 | 0.066 | 0.06 | 0.098 | 0.09 | 0.084 |
| 154 | 0.042 | 0.06 | 0.052 | 0.07 | 0.08 | 0.08 | 0.042 | 0.05 | 0.066 | 0.103 | 0.094 | 0.072 |
| 155 | 0.05 | 0.066 | 0.06 | 0.121 | 0.07 | 0.057 | 0.042 | 0.057 | 0.121 | 0.075 | 0.052 | 0.08 |
| 156 | 0.052 | 0.04 | 0.052 | 0.1 | 0.111 | 0.117 | 0.1 | 0.057 | 0.072 | 0.071 | 0.03 | 0.071 |
| 157 | 0.024 | 0.061 | 0.05 | 0.042 | 0.091 | 0.091 | 0.061 | 0.06 | 0.073 | 0.084 | 0.05 | 0.061 |
| 158 | 0.05 | 0.081 | 0.06 | 0.05 | 0.103 | 0.081 | 0.05 | 0.06 | 0.042 | 0.08 | 0.02 | 0.094 |
| 159 | 0.048 | 0.03 | 0.04 | 0.108 | 0.161 | 0.084 | 0.081 | 0.057 | 0.066 | 0.07 | 0.052 | 0.101 |
| 160 | 0.04 | 0.03 | 0.04 | 0.08 | 0.121 | 0.042 | 0.072 | 0.066 | 0.06 | 0.091 | 0.033 | 0.152 |
| 161 | 0.02 | 0.03 | 0.04 | 0.05 | 0.111 | 0.05 | 0.04 | 0.07 | 0.07 | 0.081 | 0.048 | 0.084 |
| 162 | 0.042 | 0.02 | 0.05 | 0.09 | 0.04 | 0.11 | 0.033 | 0.057 | 0.052 | 0.084 | 0.071 | 0.04 |
| 163 | 0.033 | 0.06 | 0.05 | 0.07 | 0.061 | 0.07 | 0.061 | 0.066 | 0.033 | 0.108 | 0.04 | 0.081 |
| 164 | 0.033 | 0.033 | 0.033 | 0.101 | 0.081 | 0.075 | 0.04 | 0.061 | 0.061 | 0.03 | 0.024 | 0.075 |
| 165 | 0.033 | 0.04 | 0.04 | 0.084 | 0.061 | 0.071 | 0.06 | 0.08 | 0.07 | 0.04 | 0.03 | 0.07 |
| 166 | 0.05 | 0.05 | 0.03 | 0.09 | 0.133 | 0.081 | 0.057 | 0.06 | 0.052 | 0.03 | 0.042 | 0.111 |
| 167 | 0.05 | 0.042 | 0.06 | 0.113 | 0.131 | 0.091 | 0.042 | 0.06 | 0.081 | 0.075 | 0.04 | 0.06 |
| 168 | 0.04 | 0.05 | 0.071 | 0.17 | 0.105 | 0.061 | 0.061 | 0.04 | 0.052 | 0.02 | 0.075 | 0.07 |
| 169 | 0.042 | 0.057 | 0.06 | 0.052 | 0.081 | 0.07 | 0.048 | 0.05 | 0.084 | 0.04 | 0.033 | 0.08 |
| 170 | 0.02 | 0.04 | 0.042 | 0.081 | 0.071 | 0.081 | 0.04 | 0.064 | 0.1 | 0.05 | 0.07 | 0.1 |
| 171 | 0.02 | 0.04 | 0.05 | 0.05 | 0.071 | 0.066 | 0.091 | 0.052 | 0.05 | 0.081 | 0.05 | 0.06 |

| | | | | | | | | | | | | |
|---|---|---|---|---|---|---|---|---|---|---|---|---|
| 172 | 0.05 | 0.071 | 0.042 | 0.081 | 0.071 | 0.04 | 0.033 | 0.042 | 0.04 | 0.024 | 0.06 | 0.081 |
| 173 | 0.04 | 0.061 | 0.057 | 0.141 | 0.091 | 0.061 | 0.08 | 0.067 | 0.057 | 0.04 | 0.06 | 0.061 |
| 174 | 0.033 | 0.04 | 0.052 | 0.09 | 0.07 | 0.06 | 0.06 | 0.048 | 0.07 | 0.081 | 0.052 | 0.05 |
| 175 | 0.033 | 0.061 | 0.06 | 0.081 | 0.04 | 0.066 | 0.07 | 0.04 | 0.07 | 0.071 | 0.057 | 0.07 |
| 176 | 0.042 | 0.06 | 0.03 | 0.098 | 0.094 | 0.117 | 0.05 | 0.048 | 0.06 | 0.04 | 0.04 | 0.042 |
| 177 | 0.048 | 0.042 | 0.04 | 0.08 | 0.061 | 0.08 | 0.05 | 0.033 | 0.042 | 0.07 | 0.05 | 0.061 |
| 178 | 0.033 | 0.071 | 0.04 | 0.113 | 0.06 | 0.07 | 0.066 | 0.081 | 0.042 | 0.07 | 0.071 | 0.071 |
| 179 | 0.042 | 0.05 | 0.04 | 0.084 | 0.121 | 0.061 | 0.06 | 0.075 | 0.05 | 0.06 | 0.07 | 0.08 |
| 180 | 0.05 | 0.033 | 0.04 | 0.09 | 0.071 | 0.11 | 0.064 | 0.052 | 0.075 | 0.066 | 0.06 | 0.052 |
| 181 | 0.03 | 0.05 | 0.052 | 0.03 | 0.133 | 0.05 | 0.02 | 0.071 | 0.057 | 0.042 | 0.066 | 0.084 |
| 182 | 0.05 | 0.05 | 0.052 | 0.061 | 0.108 | 0.08 | 0.033 | 0.05 | 0.04 | 0.07 | 0.042 | 0.09 |
| 183 | 0.05 | 0.052 | 0.05 | 0.105 | 0.052 | 0.05 | 0.05 | 0.075 | 0.066 | 0.1 | 0.05 | 0.03 |
| 184 | 0.052 | 0.05 | 0.05 | 0.071 | 0.075 | 0.05 | 0.024 | 0.04 | 0.064 | 0.052 | 0.042 | 0.04 |
| 185 | 0.042 | 0.057 | 0.04 | 0.1 | 0.07 | 0.091 | 0.07 | 0.101 | 0.071 | 0.061 | 0.113 | 0.06 |
| 186 | 0.061 | 0.064 | 0.04 | 0.121 | 0.091 | 0.08 | 0.066 | 0.06 | 0.089 | 0.091 | 0.094 | 0.111 |
| 187 | 0.048 | 0.048 | 0.03 | 0.09 | 0.111 | 0.057 | 0.081 | 0.091 | 0.081 | 0.066 | 0.075 | 0.042 |
| 188 | 0.04 | 0.04 | 0.061 | 0.052 | 0.048 | 0.1 | 0.03 | 0.042 | 0.071 | 0.071 | 0.101 | 0.131 |
| 189 | 0.04 | 0.066 | 0.04 | 0.04 | 0.081 | 0.042 | 0.03 | 0.07 | 0.04 | 0.052 | 0.084 | 0.11 |
| 190 | 0.042 | 0.06 | 0.052 | 0.091 | 0.071 | 0.091 | 0.024 | 0.033 | 0.06 | 0.096 | 0.033 | 0.071 |
| 191 | 0.033 | 0.05 | 0.052 | 0.08 | 0.07 | 0.152 | 0.05 | 0.02 | 0.08 | 0.112 | 0.09 | 0.081 |
| 192 | 0.042 | 0.03 | 0.05 | 0.024 | 0.061 | 0.03 | 0.024 | 0.066 | 0.071 | 0.05 | 0.108 | 0.07 |
| 193 | 0.03 | 0.052 | 0.075 | 0.05 | 0.03 | 0.101 | 0.05 | 0.075 | 0.052 | 0.033 | 0.09 | 0.071 |
| 194 | 0.033 | 0.03 | 0.04 | 0.071 | 0.07 | 0.081 | 0.033 | 0.05 | 0.03 | 0.075 | 0.101 | 0.101 |
| 195 | 0.03 | 0.09 | 0.052 | 0.06 | 0.13 | 0.084 | 0.06 | 0.052 | 0.05 | 0.033 | 0.081 | 0.103 |
| 196 | 0.042 | 0.06 | 0.06 | 0.066 | 0.151 | 0.061 | 0.09 | 0.03 | 0.061 | 0.075 | 0.06 | 0.133 |
| 197 | 0.042 | 0.05 | 0.03 | 0.084 | 0.094 | 0.057 | 0.03 | 0.01 | 0.05 | 0.048 | 0.04 | 0.071 |
| 198 | 0.03 | 0.042 | 0.033 | 0.07 | 0.094 | 0.075 | 0.06 | 0.084 | 0.01 | 0.072 | 0.081 | 0.07 |
| 199 | 0.033 | 0.052 | 0.066 | 0.06 | 0.098 | 0.066 | 0.03 | 0.08 | 0.06 | 0.072 | 0.146 | 0.094 |
| 200 | 0.042 | 0.052 | 0.03 | 0.06 | 0.06 | 0.081 | 0.042 | 0.081 | 0.057 | 0.084 | 0.091 | 0.081 |
| 201 | 0.033 | 0.04 | 0.071 | 0.061 | 0.06 | 0.061 | 0.05 | 0.08 | 0.073 | 0.07 | 0.071 | 0.084 |

| | | | | | | | | | | | | |
|---|---|---|---|---|---|---|---|---|---|---|---|---|
| 202 | 0.05 | 0.052 | 0.03 | 0.052 | 0.08 | 0.066 | 0.04 | 0.052 | 0.06 | 0.084 | 0.061 | 0.084 |
| 203 | 0.042 | 0.05 | 0.02 | 0.07 | 0.08 | 0.089 | 0.071 | 0.09 | 0.03 | 0.071 | 0.075 | 0.05 |
| 204 | 0.05 | 0.04 | 0.07 | 0.081 | 0.052 | 0.072 | 0.04 | 0.07 | 0.101 | 0.07 | 0.112 | 0.12 |
| 205 | 0.05 | 0.06 | 0.04 | 0.042 | 0.08 | 0.066 | 0.042 | 0.06 | 0.052 | 0.081 | 0.066 | 0.08 |
| 206 | 0.06 | 0.02 | 0.057 | 0.057 | 0.061 | 0.084 | 0.04 | 0.05 | 0.061 | 0.081 | 0.123 | 0.066 |
| 207 | 0.061 | 0.061 | 0.05 | 0.066 | 0.089 | 0.057 | 0.04 | 0.05 | 0.052 | 0.07 | 0.071 | 0.07 |
| 208 | 0.02 | 0.02 | 0.05 | 0.052 | 0.091 | 0.096 | 0.06 | 0.061 | 0.04 | 0.08 | 0.141 | 0.103 |
| 209 | 0.03 | 0.05 | 0.03 | 0.08 | 0.04 | 0.064 | 0.08 | 0.075 | 0.071 | 0.121 | 0.091 | 0.06 |
| 210 | 0.033 | 0.061 | 0.033 | 0.084 | 0.14 | 0.057 | 0.07 | 0.03 | 0.05 | 0.071 | 0.101 | 0.094 |
| 211 | 0.061 | 0.052 | 0.03 | 0.052 | 0.12 | 0.05 | 0.03 | 0.042 | 0.07 | 0.061 | 0.081 | 0.084 |
| 212 | 0.03 | 0.071 | 0.04 | 0.126 | 0.081 | 0.081 | 0.03 | 0.11 | 0.08 | 0.04 | 0.052 | 0.113 |
| 213 | 0.05 | 0.04 | 0.05 | 0.061 | 0.101 | 0.03 | 0.02 | 0.04 | 0.111 | 0.11 | 0.071 | 0.143 |
| 214 | 0.03 | 0.04 | 0.052 | 0.061 | 0.08 | 0.052 | 0.02 | 0.052 | 0.02 | 0.052 | 0.075 | 0.071 |
| 215 | 0.057 | 0.061 | 0.03 | 0.113 | 0.08 | 0.08 | 0.07 | 0.02 | 0.04 | 0.04 | 0.09 | 0.12 |
| 216 | 0.05 | 0.03 | 0.02 | 0.04 | 0.05 | 0.04 | 0.03 | 0.048 | 0.04 | 0.061 | 0.08 | 0.103 |
| 217 | 0.02 | 0.071 | 0.03 | 0.09 | 0.03 | 0.06 | 0.042 | 0.052 | 0.052 | 0.052 | 0.081 | 0.09 |
| 218 | 0.033 | 0.03 | 0.057 | 0.081 | 0.081 | 0.03 | 0.01 | 0.06 | 0.052 | 0.05 | 0.121 | 0.121 |
| 219 | 0.04 | 0.057 | 0.064 | 0.04 | 0.052 | 0.1 | 0.06 | 0.061 | 0.091 | 0.057 | 0.06 | 0.162 |
| 220 | 0.03 | 0.05 | 0.071 | 0.071 | 0.03 | 0.08 | 0.04 | 0.11 | 0.03 | 0.042 | 0.141 | 0.131 |
| 221 | 0.042 | 0.04 | 0.061 | 0.05 | 0.057 | 0.103 | 0.04 | 0.04 | 0.057 | 0.057 | 0.06 | 0.121 |
| 222 | 0.052 | 0.05 | 0.052 | 0.1 | 0.07 | 0.091 | 0.052 | 0.052 | 0.05 | 0.084 | 0.071 | 0.07 |
| 223 | 0.052 | 0.052 | 0.05 | 0.09 | 0.081 | 0.052 | 0.06 | 0.06 | 0.1 | 0.08 | 0.071 | 0.081 |
| 224 | 0.05 | 0.02 | 0.05 | 0.1 | 0.1 | 0.13 | 0.04 | 0.08 | 0.05 | 0.084 | 0.066 | 0.141 |
| 225 | 0.04 | 0.03 | 0.033 | 0.101 | 0.08 | 0.105 | 0.05 | 0.08 | 0.061 | 0.089 | 0.101 | 0.071 |
| 226 | 0.03 | 0.03 | 0.042 | 0.094 | 0.088 | 0.066 | 0.061 | 0.042 | 0.042 | 0.061 | 0.1 | 0.081 |
| 227 | 0.061 | 0.04 | 0.052 | 0.091 | 0.057 | 0.1 | 0.02 | 0.05 | 0.06 | 0.072 | 0.09 | 0.14 |
| 228 | 0.03 | 0.03 | 0.03 | 0.089 | 0.052 | 0.061 | 0.03 | 0.052 | 0.071 | 0.131 | 0.09 | 0.081 |
| 229 | 0.052 | 0.042 | 0.06 | 0.09 | 0.066 | 0.075 | 0.06 | 0.05 | 0.071 | 0.033 | 0.094 | 0.111 |
| 230 | 0.05 | 0.04 | 0.042 | 0.081 | 0.057 | 0.094 | 0.04 | 0.05 | 0.061 | 0.057 | 0.04 | 0.067 |
| 231 | 0.052 | 0.02 | 0.03 | 0.05 | 0.033 | 0.084 | 0.06 | 0.02 | 0.103 | 0.024 | 0.14 | 0.091 |

| | | | | | | | | | | | | |
|---|---|---|---|---|---|---|---|---|---|---|---|---|
| 232 | 0.03 | 0.052 | 0.03 | 0.061 | 0.075 | 0.08 | 0.052 | 0.01 | 0.033 | 0.05 | 0.121 | 0.14 |
| 233 | 0.052 | 0.02 | 0.06 | 0.101 | 0.096 | 0.06 | 0.07 | 0.05 | 0.04 | 0.024 | 0.121 | 0.09 |
| 234 | 0.033 | 0.075 | 0.042 | 0.081 | 0.091 | 0.08 | 0.052 | 0.071 | 0.03 | 0.07 | 0.048 | 0.091 |
| 235 | 0.03 | 0.042 | 0.03 | 0.071 | 0.06 | 0.06 | 0.03 | 0.061 | 0.08 | 0.05 | 0.113 | 0.101 |
| 236 | 0.052 | 0.06 | 0.05 | 0.052 | 0.07 | 0.071 | 0.052 | 0.045 | 0.052 | 0.07 | 0.11 | 0.162 |
| 237 | 0.07 | 0.052 | 0.04 | 0.09 | 0.06 | 0.101 | 0.033 | 0.042 | 0.04 | 0.131 | 0.071 | 0.07 |
| 238 | 0.04 | 0.04 | 0.024 | 0.052 | 0.091 | 0.06 | 0.057 | 0.04 | 0.024 | 0.06 | 0.08 | 0.143 |
| 239 | 0.057 | 0.05 | 0.066 | 0.071 | 0.12 | 0.06 | 0.061 | 0.1 | 0.061 | 0.09 | 0.061 | 0.08 |
| 240 | 0.071 | 0.04 | 0.01 | 0.066 | 0.101 | 0.052 | 0.02 | 0.017 | 0.048 | 0.071 | 0.07 | 0.151 |
| 241 | 0.066 | 0.03 | 0.042 | 0.061 | 0.052 | 0.071 | 0.05 | 0.075 | 0.064 | 0.101 | 0.091 | 0.071 |
| 242 | 0.033 | 0.05 | 0.04 | 0.066 | 0.101 | 0.05 | 0.03 | 0.05 | 0.07 | 0.081 | 0.081 | 0.111 |
| 243 | 0.042 | 0.03 | 0.042 | 0.091 | 0.066 | 0.07 | 0.042 | 0.06 | 0.06 | 0.111 | 0.101 | 0.094 |
| 244 | 0.033 | 0.04 | 0.02 | 0.06 | 0.09 | 0.07 | 0.071 | 0.052 | 0.04 | 0.042 | 0.08 | 0.15 |
| 245 | 0.03 | 0.03 | 0.03 | 0.072 | 0.04 | 0.075 | 0.052 | 0.066 | 0.03 | 0.06 | 0.169 | 0.06 |
| 246 | 0.04 | 0.042 | 0.05 | 0.071 | 0.083 | 0.08 | 0.09 | 0.042 | 0.06 | 0.048 | 0.101 | 0.042 |
| 247 | 0.042 | 0.052 | 0.06 | 0.071 | 0.071 | 0.07 | 0.081 | 0.033 | 0.07 | 0.04 | 0.17 | 0.091 |
| 248 | 0.04 | 0.05 | 0.05 | 0.061 | 0.04 | 0.071 | 0.052 | 0.04 | 0.033 | 0.05 | 0.098 | 0.09 |
| 249 | 0.048 | 0.061 | 0.072 | 0.06 | 0.05 | 0.078 | 0.08 | 0.048 | 0.048 | 0.061 | 0.1 | 0.05 |
| 250 | 0.048 | 0.071 | 0.072 | 0.11 | 0.06 | 0.09 | 0.06 | 0.03 | 0.05 | 0.061 | 0.12 | 0.07 |
| Mean | 0.041644 | 0.048516 | 0.045596 | 0.075524 | 0.08222 | 0.07284 | 0.048512 | 0.049028 | 0.053868 | 0.068308 | 0.069316 | 0.083024 |
| SD | 0.0145 | 0.015029 | 0.013368 | 0.024143 | 0.028821 | 0.023843 | 0.017391 | 0.019727 | 0.01986 | 0.023365 | 0.026394 | 0.027543 |

| | Day 6 | | | | | | Day 7 | | | | | |
|---|---|---|---|---|---|---|---|---|---|---|---|---|
| OCT images | Control | | | Infected | | | Control | | | Infected | | |
| | 1 | 2 | 3 | 1 | 2 | 3 | 1 | 2 | 3 | 1 | 2 | 3 |
| 1 | 0.071 | 0.042 | 0.042 | 0.07 | 0.052 | 0.03 | 0.048 | 0.033 | 0.06 | 0.055 | 0.06 | 0.066 |
| 2 | 0.042 | 0.033 | 0.04 | 0.08 | 0.09 | 0.03 | 0.01 | 0.03 | 0.06 | 0.071 | 0.108 | 0.071 |
| 3 | 0.06 | 0.05 | 0.05 | 0.05 | 0.042 | 0.091 | 0.05 | 0.02 | 0.052 | 0.06 | 0.071 | 0.073 |
| 4 | 0.04 | 0.02 | 0.03 | 0.07 | 0.052 | 0.07 | 0.07 | 0.052 | 0.04 | 0.044 | 0.09 | 0.061 |

| | | | | | | | | | | | | |
|---|---|---|---|---|---|---|---|---|---|---|---|---|
| 5 | 0.04 | 0.05 | 0.02 | 0.05 | 0.075 | 0.07 | 0.02 | 0.01 | 0.033 | 0.033 | 0.1 | 0.093 |
| 6 | 0.06 | 0.071 | 0.05 | 0.04 | 0.061 | 0.042 | 0.033 | 0.052 | 0.066 | 0.093 | 0.098 | 0.077 |
| 7 | 0.05 | 0.081 | 0.061 | 0.06 | 0.05 | 0.02 | 0.04 | 0.02 | 0.05 | 0.077 | 0.07 | 0.057 |
| 8 | 0.06 | 0.05 | 0.081 | 0.06 | 0.1 | 0.061 | 0.03 | 0.048 | 0.03 | 0.049 | 0.103 | 0.077 |
| 9 | 0.02 | 0.07 | 0.061 | 0.03 | 0.07 | 0.042 | 0.05 | 0.03 | 0.04 | 0.057 | 0.07 | 0.088 |
| 10 | 0.042 | 0.06 | 0.071 | 0.052 | 0.071 | 0.071 | 0.061 | 0.03 | 0.057 | 0.038 | 0.05 | 0.149 |
| 11 | 0.04 | 0.071 | 0.05 | 0.042 | 0.07 | 0.061 | 0.042 | 0.061 | 0.048 | 0.049 | 0.084 | 0.082 |
| 12 | 0.03 | 0.05 | 0.052 | 0.057 | 0.052 | 0.05 | 0.05 | 0.04 | 0.04 | 0.072 | 0.113 | 0.054 |
| 13 | 0.05 | 0.06 | 0.07 | 0.03 | 0.08 | 0.05 | 0.04 | 0.05 | 0.02 | 0.066 | 0.06 | 0.11 |
| 14 | 0.057 | 0.01 | 0.1 | 0.04 | 0.05 | 0.03 | 0.05 | 0.01 | 0.03 | 0.041 | 0.05 | 0.13 |
| 15 | 0.03 | 0.024 | 0.081 | 0.03 | 0.06 | 0.06 | 0.042 | 0.02 | 0.03 | 0.077 | 0.07 | 0.121 |
| 16 | 0.033 | 0.03 | 0.04 | 0.061 | 0.07 | 0.105 | 0.071 | 0.02 | 0.03 | 0.105 | 0.11 | 0.1 |
| 17 | 0.06 | 0.052 | 0.052 | 0.05 | 0.03 | 0.089 | 0.02 | 0.042 | 0.03 | 0.093 | 0.07 | 0.091 |
| 18 | 0.052 | 0.03 | 0.066 | 0.084 | 0.05 | 0.057 | 0.033 | 0.04 | 0.066 | 0.11 | 0.16 | 0.071 |
| 19 | 0.11 | 0.05 | 0.02 | 0.05 | 0.07 | 0.033 | 0.052 | 0.05 | 0.05 | 0.093 | 0.042 | 0.049 |
| 20 | 0.048 | 0.017 | 0.02 | 0.05 | 0.131 | 0.101 | 0.052 | 0.06 | 0.064 | 0.066 | 0.071 | 0.134 |
| 21 | 0.04 | 0.052 | 0.06 | 0.05 | 0.05 | 0.11 | 0.033 | 0.042 | 0.052 | 0.078 | 0.159 | 0.049 |
| 22 | 0.04 | 0.052 | 0.05 | 0.04 | 0.05 | 0.09 | 0.05 | 0.02 | 0.06 | 0.083 | 0.091 | 0.044 |
| 23 | 0.02 | 0.05 | 0.061 | 0.1 | 0.12 | 0.101 | 0.042 | 0.091 | 0.052 | 0.055 | 0.131 | 0.066 |
| 24 | 0.06 | 0.03 | 0.06 | 0.08 | 0.06 | 0.09 | 0.06 | 0.05 | 0.06 | 0.075 | 0.09 | 0.096 |
| 25 | 0.03 | 0.04 | 0.05 | 0.08 | 0.06 | 0.09 | 0.02 | 0.05 | 0.03 | 0.072 | 0.11 | 0.122 |
| 26 | 0.03 | 0.04 | 0.042 | 0.052 | 0.061 | 0.066 | 0.03 | 0.04 | 0.02 | 0.088 | 0.033 | 0.073 |
| 27 | 0.052 | 0.061 | 0.07 | 0.07 | 0.05 | 0.061 | 0.06 | 0.024 | 0.061 | 0.091 | 0.075 | 0.121 |
| 28 | 0.04 | 0.03 | 0.048 | 0.08 | 0.06 | 0.084 | 0.05 | 0.061 | 0.05 | 0.072 | 0.061 | 0.099 |
| 29 | 0.061 | 0.02 | 0.057 | 0.05 | 0.042 | 0.05 | 0.05 | 0.05 | 0.057 | 0.078 | 0.111 | 0.094 |
| 30 | 0.06 | 0.02 | 0.052 | 0.03 | 0.042 | 0.08 | 0.048 | 0.061 | 0.04 | 0.055 | 0.094 | 0.104 |
| 31 | 0.081 | 0.05 | 0.033 | 0.04 | 0.048 | 0.042 | 0.04 | 0.04 | 0.07 | 0.062 | 0.04 | 0.049 |
| 32 | 0.04 | 0.061 | 0.03 | 0.081 | 0.042 | 0.05 | 0.042 | 0.02 | 0.05 | 0.055 | 0.061 | 0.061 |
| 33 | 0.05 | 0.05 | 0.02 | 0.094 | 0.04 | 0.081 | 0.08 | 0.05 | 0.09 | 0.073 | 0.084 | 0.049 |
| 34 | 0.042 | 0.071 | 0.03 | 0.089 | 0.08 | 0.09 | 0.07 | 0.033 | 0.03 | 0.066 | 0.094 | 0.073 |

| | | | | | | | | | | | | |
|---|---|---|---|---|---|---|---|---|---|---|---|---|
| 35 | 0.02 | 0.05 | 0.03 | 0.084 | 0.06 | 0.121 | 0.061 | 0.042 | 0.03 | 0.061 | 0.06 | 0.11 |
| 36 | 0.061 | 0.05 | 0.05 | 0.052 | 0.08 | 0.103 | 0.052 | 0.061 | 0.03 | 0.104 | 0.07 | 0.122 |
| 37 | 0.061 | 0.052 | 0.048 | 0.111 | 0.01 | 0.06 | 0.02 | 0.02 | 0.05 | 0.075 | 0.08 | 0.055 |
| 38 | 0.071 | 0.02 | 0.04 | 0.066 | 0.061 | 0.05 | 0.05 | 0.02 | 0.01 | 0.089 | 0.052 | 0.027 |
| 39 | 0.042 | 0.08 | 0.05 | 0.081 | 0.081 | 0.042 | 0.02 | 0.033 | 0.01 | 0.082 | 0.071 | 0.099 |
| 40 | 0.052 | 0.061 | 0.05 | 0.042 | 0.094 | 0.02 | 0.06 | 0.06 | 0.02 | 0.111 | 0.098 | 0.038 |
| 41 | 0.052 | 0.04 | 0.07 | 0.02 | 0.07 | 0.05 | 0.07 | 0.033 | 0.033 | 0.084 | 0.057 | 0.071 |
| 42 | 0.06 | 0.042 | 0.03 | 0.03 | 0.05 | 0.13 | 0.052 | 0.05 | 0.024 | 0.11 | 0.091 | 0.077 |
| 43 | 0.07 | 0.05 | 0.061 | 0.12 | 0.03 | 0.09 | 0.04 | 0.042 | 0.07 | 0.088 | 0.071 | 0.061 |
| 44 | 0.04 | 0.05 | 0.04 | 0.03 | 0.03 | 0.101 | 0.03 | 0.04 | 0.02 | 0.115 | 0.071 | 0.08 |
| 45 | 0.072 | 0.052 | 0.03 | 0.06 | 0.061 | 0.06 | 0.02 | 0.04 | 0.07 | 0.082 | 0.06 | 0.061 |
| 46 | 0.04 | 0.05 | 0.02 | 0.108 | 0.133 | 0.071 | 0.02 | 0.03 | 0.07 | 0.066 | 0.081 | 0.033 |
| 47 | 0.071 | 0.061 | 0.061 | 0.101 | 0.091 | 0.098 | 0.017 | 0.04 | 0.04 | 0.044 | 0.081 | 0.094 |
| 48 | 0.05 | 0.071 | 0.04 | 0.094 | 0.091 | 0.081 | 0.052 | 0.04 | 0.07 | 0.083 | 0.071 | 0.104 |
| 49 | 0.071 | 0.05 | 0.03 | 0.14 | 0.06 | 0.071 | 0.04 | 0.061 | 0.071 | 0.11 | 0.1 | 0.052 |
| 50 | 0.042 | 0.061 | 0.02 | 0.04 | 0.06 | 0.033 | 0.081 | 0.01 | 0.04 | 0.066 | 0.08 | 0.028 |
| 51 | 0.05 | 0.06 | 0.02 | 0.081 | 0.04 | 0.061 | 0.04 | 0.03 | 0.05 | 0.11 | 0.091 | 0.06 |
| 52 | 0.02 | 0.061 | 0.061 | 0.1 | 0.05 | 0.06 | 0.02 | 0.042 | 0.04 | 0.06 | 0.081 | 0.049 |
| 53 | 0.071 | 0.05 | 0.04 | 0.101 | 0.033 | 0.07 | 0.03 | 0.03 | 0.05 | 0.05 | 0.07 | 0.049 |
| 54 | 0.03 | 0.04 | 0.04 | 0.131 | 0.07 | 0.07 | 0.05 | 0.04 | 0.052 | 0.055 | 0.05 | 0.038 |
| 55 | 0.01 | 0.057 | 0.05 | 0.1 | 0.057 | 0.05 | 0 | 0.02 | 0.052 | 0.044 | 0.075 | 0.127 |
| 56 | 0.081 | 0.03 | 0.05 | 0.131 | 0.07 | 0.05 | 0.091 | 0.01 | 0.07 | 0.057 | 0.081 | 0.121 |
| 57 | 0.07 | 0.06 | 0.05 | 0.141 | 0.05 | 0.04 | 0.033 | 0.03 | 0.052 | 0.085 | 0.098 | 0.049 |
| 58 | 0.042 | 0.01 | 0.052 | 0.09 | 0.07 | 0.1 | 0.024 | 0.052 | 0.03 | 0.073 | 0.101 | 0.112 |
| 59 | 0.042 | 0.024 | 0.05 | 0.141 | 0.06 | 0.06 | 0.03 | 0.02 | 0.04 | 0.027 | 0.151 | 0.08 |
| 60 | 0.061 | 0.084 | 0.03 | 0.07 | 0.071 | 0.08 | 0.05 | 0.03 | 0.042 | 0.072 | 0.061 | 0.066 |
| 61 | 0.048 | 0.066 | 0.02 | 0.084 | 0.05 | 0.05 | 0.04 | 0.02 | 0.04 | 0.027 | 0.08 | 0.077 |
| 62 | 0.052 | 0.04 | 0.07 | 0.071 | 0.121 | 0.08 | 0.075 | 0.04 | 0.05 | 0.055 | 0.075 | 0.073 |
| 63 | 0.03 | 0.05 | 0.04 | 0.06 | 0.08 | 0.06 | 0.042 | 0.033 | 0.05 | 0.062 | 0.101 | 0.05 |
| 64 | 0.03 | 0.06 | 0.091 | 0.01 | 0.05 | 0.02 | 0.03 | 0.03 | 0.05 | 0.095 | 0.052 | 0.044 |

| | | | | | | | | | | | | |
|---|---|---|---|---|---|---|---|---|---|---|---|---|
| 65 | 0.04 | 0.057 | 0.03 | 0.061 | 0.05 | 0.04 | 0.03 | 0.02 | 0.07 | 0.038 | 0.081 | 0.068 |
| 66 | 0.02 | 0.033 | 0.04 | 0.08 | 0.052 | 0.11 | 0.052 | 0.033 | 0.07 | 0.077 | 0.042 | 0.066 |
| 67 | 0.07 | 0.04 | 0.075 | 0.084 | 0.05 | 0.101 | 0.02 | 0.042 | 0.08 | 0.049 | 0.07 | 0.075 |
| 68 | 0.061 | 0.033 | 0.052 | 0.07 | 0.07 | 0.08 | 0.01 | 0.02 | 0.03 | 0.088 | 0.061 | 0.055 |
| 69 | 0.061 | 0.042 | 0.042 | 0.094 | 0.02 | 0.01 | 0.042 | 0.052 | 0.07 | 0.078 | 0.08 | 0.049 |
| 70 | 0.03 | 0.024 | 0.057 | 0.097 | 0.071 | 0.033 | 0.04 | 0.066 | 0.071 | 0.038 | 0.131 | 0.038 |
| 71 | 0.05 | 0.03 | 0.06 | 0.122 | 0.06 | 0.02 | 0.04 | 0.05 | 0.03 | 0.068 | 0.071 | 0.06 |
| 72 | 0.06 | 0.04 | 0.02 | 0.101 | 0.094 | 0.033 | 0.033 | 0.042 | 0.066 | 0.078 | 0.084 | 0.084 |
| 73 | 0.05 | 0.01 | 0.061 | 0.091 | 0.1 | 0.048 | 0.02 | 0.033 | 0.07 | 0.05 | 0.06 | 0.1 |
| 74 | 0.052 | 0.06 | 0.048 | 0.084 | 0.061 | 0.052 | 0.01 | 0.071 | 0.03 | 0.055 | 0.111 | 0.049 |
| 75 | 0.04 | 0.03 | 0.05 | 0.131 | 0.091 | 0.103 | 0.066 | 0.04 | 0.057 | 0.044 | 0.113 | 0.071 |
| 76 | 0.05 | 0.033 | 0.02 | 0.075 | 0.09 | 0.07 | 0.096 | 0.01 | 0.06 | 0.111 | 0.05 | 0.1 |
| 77 | 0.03 | 0.05 | 0.024 | 0.08 | 0.06 | 0.05 | 0.02 | 0.01 | 0.04 | 0.099 | 0.048 | 0.055 |
| 78 | 0.06 | 0.061 | 0.05 | 0.094 | 0.06 | 0.042 | 0.06 | 0.033 | 0.113 | 0.06 | 0.101 | 0.077 |
| 79 | 0.06 | 0.04 | 0.05 | 0.1 | 0.081 | 0.101 | 0.05 | 0.052 | 0.09 | 0.095 | 0.11 | 0.095 |
| 80 | 0.06 | 0.03 | 0.01 | 0.091 | 0.057 | 0.05 | 0.04 | 0.07 | 0.066 | 0.082 | 0.117 | 0.075 |
| 81 | 0.05 | 0.04 | 0.042 | 0.04 | 0.05 | 0.07 | 0.042 | 0.08 | 0.05 | 0.089 | 0.084 | 0.064 |
| 82 | 0.05 | 0.024 | 0.04 | 0.13 | 0.091 | 0.03 | 0.02 | 0.05 | 0.02 | 0.077 | 0.123 | 0.073 |
| 83 | 0.04 | 0.04 | 0.03 | 0.09 | 0.098 | 0.05 | 0.05 | 0.052 | 0.07 | 0.028 | 0.091 | 0.079 |
| 84 | 0.04 | 0.04 | 0.05 | 0.18 | 0.03 | 0.052 | 0.042 | 0.04 | 0.042 | 0.055 | 0.08 | 0.064 |
| 85 | 0.06 | 0.04 | 0.048 | 0.05 | 0.05 | 0.03 | 0.024 | 0.071 | 0.09 | 0.116 | 0.03 | 0.075 |
| 86 | 0.064 | 0.05 | 0 | 0.084 | 0.07 | 0.08 | 0.03 | 0.071 | 0.084 | 0.068 | 0.057 | 0.044 |
| 87 | 0.042 | 0.033 | 0.03 | 0.05 | 0.04 | 0.081 | 0.033 | 0.091 | 0.052 | 0.07 | 0.071 | 0.052 |
| 88 | 0.03 | 0.02 | 0.05 | 0.101 | 0.06 | 0.03 | 0.04 | 0.05 | 0.05 | 0.064 | 0.06 | 0.055 |
| 89 | 0.042 | 0.061 | 0.01 | 0.04 | 0.061 | 0.094 | 0.04 | 0.03 | 0.07 | 0.055 | 0.061 | 0.071 |
| 90 | 0.04 | 0.024 | 0.061 | 0.081 | 0.08 | 0.042 | 0.071 | 0.07 | 0.084 | 0.068 | 0.084 | 0.071 |
| 91 | 0.03 | 0.04 | 0.05 | 0.07 | 0.066 | 0.05 | 0.07 | 0.03 | 0.05 | 0.077 | 0.081 | 0.077 |
| 92 | 0.048 | 0.042 | 0.04 | 0.091 | 0.075 | 0.06 | 0.057 | 0.04 | 0.024 | 0.016 | 0.094 | 0.093 |
| 93 | 0.061 | 0.02 | 0.048 | 0.1 | 0.08 | 0.071 | 0.04 | 0.03 | 0.05 | 0.055 | 0.073 | 0.034 |
| 94 | 0.033 | 0.075 | 0.04 | 0.091 | 0.042 | 0.081 | 0.042 | 0.04 | 0.07 | 0.06 | 0.081 | 0.099 |

| | | | | | | | | | | | | |
|---|---|---|---|---|---|---|---|---|---|---|---|---|
| 95 | 0.01 | 0.03 | 0.04 | 0.103 | 0.06 | 0.064 | 0.03 | 0.042 | 0.03 | 0.071 | 0.081 | 0.093 |
| 96 | 0.057 | 0.03 | 0.052 | 0.07 | 0.042 | 0.091 | 0.02 | 0.03 | 0.02 | 0.073 | 0.081 | 0.103 |
| 97 | 0.05 | 0.05 | 0.04 | 0.11 | 0.06 | 0.05 | 0.04 | 0.05 | 0.033 | 0.073 | 0.088 | 0.077 |
| 98 | 0.024 | 0.02 | 0.06 | 0.024 | 0.081 | 0.081 | 0.06 | 0.05 | 0.03 | 0.1 | 0.075 | 0.066 |
| 99 | 0.08 | 0.03 | 0.04 | 0.01 | 0.07 | 0.071 | 0.066 | 0.05 | 0.06 | 0.119 | 0.03 | 0.066 |
| 100 | 0.04 | 0.03 | 0.04 | 0.05 | 0.06 | 0.075 | 0.04 | 0.07 | 0.05 | 0.093 | 0.08 | 0.071 |
| 101 | 0.04 | 0.02 | 0.048 | 0.07 | 0.033 | 0.066 | 0.066 | 0.06 | 0.02 | 0.11 | 0.081 | 0.038 |
| 102 | 0.033 | 0.05 | 0.04 | 0.08 | 0.05 | 0.057 | 0.01 | 0.05 | 0.05 | 0.089 | 0.14 | 0.055 |
| 103 | 0.02 | 0.042 | 0.052 | 0.04 | 0.03 | 0.064 | 0.03 | 0.033 | 0.02 | 0.116 | 0.057 | 0.06 |
| 104 | 0.045 | 0.042 | 0.05 | 0.06 | 0.024 | 0.091 | 0.052 | 0.052 | 0.04 | 0.055 | 0.07 | 0.049 |
| 105 | 0.05 | 0.03 | 0.071 | 0.101 | 0.042 | 0.052 | 0.05 | 0.05 | 0.04 | 0.104 | 0.146 | 0.044 |
| 106 | 0.06 | 0.066 | 0.03 | 0.072 | 0.05 | 0.1 | 0.06 | 0.02 | 0.052 | 0.045 | 0.113 | 0.045 |
| 107 | 0.05 | 0.052 | 0.07 | 0.057 | 0.06 | 0.1 | 0.061 | 0.052 | 0.071 | 0.064 | 0.08 | 0.083 |
| 108 | 0.084 | 0.06 | 0.094 | 0.071 | 0.06 | 0.057 | 0.07 | 0.041 | 0.02 | 0.13 | 0.105 | 0.049 |
| 109 | 0.057 | 0.052 | 0.048 | 0.12 | 0.042 | 0.061 | 0.05 | 0.024 | 0.05 | 0.064 | 0.15 | 0.077 |
| 110 | 0.024 | 0.06 | 0.061 | 0.091 | 0.066 | 0.06 | 0.061 | 0.04 | 0.057 | 0.071 | 0.071 | 0.057 |
| 111 | 0.04 | 0.05 | 0.1 | 0.052 | 0.09 | 0.075 | 0.052 | 0.048 | 0.042 | 0.052 | 0.081 | 0.077 |
| 112 | 0.01 | 0.05 | 0.061 | 0.04 | 0.05 | 0.042 | 0.071 | 0.042 | 0.033 | 0.077 | 0.04 | 0.06 |
| 113 | 0.057 | 0.04 | 0.042 | 0.08 | 0.075 | 0.066 | 0.05 | 0.071 | 0.033 | 0.072 | 0.103 | 0.064 |
| 114 | 0.042 | 0.057 | 0.07 | 0.066 | 0.052 | 0.04 | 0.052 | 0.042 | 0.033 | 0.044 | 0.052 | 0.077 |
| 115 | 0.03 | 0.02 | 0.04 | 0.11 | 0.05 | 0.06 | 0.05 | 0.05 | 0.05 | 0.062 | 0.071 | 0.033 |
| 116 | 0.045 | 0.061 | 0.07 | 0.11 | 0.06 | 0.066 | 0.05 | 0.03 | 0.03 | 0.001 | 0.04 | 0.071 |
| 117 | 0.04 | 0.048 | 0.08 | 0.091 | 0.101 | 0.084 | 0.02 | 0.02 | 0.03 | 0.055 | 0.103 | 0.071 |
| 118 | 0.03 | 0.071 | 0.042 | 0.071 | 0.1 | 0.07 | 0.052 | 0.06 | 0.02 | 0.05 | 0.06 | 0.088 |
| 119 | 0.052 | 0.05 | 0.03 | 0.061 | 0.084 | 0.09 | 0.04 | 0.03 | 0.06 | 0.084 | 0.05 | 0.082 |
| 120 | 0.061 | 0.05 | 0.02 | 0.052 | 0.121 | 0.101 | 0.089 | 0.02 | 0.05 | 0.106 | 0.052 | 0.061 |
| 121 | 0.03 | 0.061 | 0.1 | 0.05 | 0.042 | 0.04 | 0.052 | 0.04 | 0.07 | 0.055 | 0.075 | 0.06 |
| 122 | 0.02 | 0.081 | 0.03 | 0.057 | 0.042 | 0.081 | 0.033 | 0.03 | 0.061 | 0.049 | 0.081 | 0.05 |
| 123 | 0.05 | 0.04 | 0.05 | 0.064 | 0.024 | 0.08 | 0.081 | 0.04 | 0.052 | 0.033 | 0.04 | 0.039 |
| 124 | 0.06 | 0.04 | 0.07 | 0.05 | 0.042 | 0.061 | 0.04 | 0.02 | 0.04 | 0.05 | 0.08 | 0.066 |

| | | | | | | | | | | | | |
|---|---|---|---|---|---|---|---|---|---|---|---|---|
| 125 | 0.033 | 0.04 | 0.042 | 0.1 | 0.052 | 0.08 | 0.06 | 0.052 | 0.045 | 0.094 | 0.071 | 0.095 |
| 126 | 0.04 | 0.042 | 0.04 | 0.03 | 0.048 | 0.06 | 0.05 | 0.033 | 0.057 | 0.075 | 0.07 | 0.156 |
| 127 | 0.06 | 0.061 | 0.06 | 0.052 | 0.02 | 0.061 | 0.052 | 0.08 | 0.057 | 0.102 | 0.1 | 0.147 |
| 128 | 0.052 | 0.04 | 0.04 | 0.071 | 0.101 | 0.052 | 0.05 | 0.033 | 0.05 | 0.111 | 0.052 | 0.103 |
| 129 | 0.06 | 0.05 | 0.024 | 0.06 | 0.061 | 0.1 | 0.06 | 0.06 | 0.064 | 0.05 | 0.08 | 0.084 |
| 130 | 0.042 | 0.033 | 0.066 | 0.143 | 0.05 | 0.033 | 0.052 | 0.04 | 0.048 | 0.088 | 0.08 | 0.06 |
| 131 | 0.05 | 0.01 | 0.08 | 0.111 | 0.06 | 0.06 | 0.04 | 0.03 | 0.08 | 0.072 | 0.081 | 0.121 |
| 132 | 0.061 | 0.071 | 0.06 | 0.05 | 0.09 | 0.06 | 0.04 | 0.024 | 0.057 | 0.088 | 0.08 | 0.088 |
| 133 | 0.03 | 0.042 | 0.06 | 0.07 | 0.121 | 0.06 | 0.04 | 0.04 | 0.064 | 0.093 | 0.07 | 0.06 |
| 134 | 0.07 | 0.111 | 0.07 | 0.02 | 0.061 | 0.07 | 0.06 | 0.03 | 0.064 | 0.066 | 0.091 | 0.077 |
| 135 | 0.066 | 0.07 | 0.081 | 0.03 | 0.03 | 0.061 | 0.04 | 0.02 | 0.052 | 0.093 | 0.1 | 0.099 |
| 136 | 0.07 | 0.052 | 0.101 | 0.123 | 0.05 | 0.05 | 0.072 | 0 | 0.033 | 0.093 | 0.05 | 0.094 |
| 137 | 0.05 | 0.08 | 0.05 | 0.066 | 0.048 | 0.042 | 0.05 | 0.02 | 0.094 | 0.088 | 0.06 | 0.094 |
| 138 | 0.01 | 0.09 | 0.04 | 0.08 | 0.03 | 0.05 | 0.06 | 0.04 | 0.013 | 0.104 | 0.091 | 0.088 |
| 139 | 0.06 | 0.071 | 0.071 | 0.07 | 0.024 | 0.052 | 0.03 | 0.03 | 0.057 | 0.093 | 0.042 | 0.049 |
| 140 | 0.02 | 0.04 | 0.042 | 0.123 | 0.042 | 0.042 | 0.01 | 0.017 | 0.042 | 0.094 | 0.06 | 0.083 |
| 141 | 0.061 | 0.08 | 0.07 | 0.04 | 0.07 | 0.042 | 0.05 | 0.02 | 0.071 | 0.059 | 0.061 | 0.077 |
| 142 | 0.05 | 0.04 | 0.052 | 0.05 | 0.04 | 0.06 | 0.03 | 0.02 | 0.04 | 0.099 | 0.06 | 0.064 |
| 143 | 0.05 | 0.024 | 0.061 | 0.081 | 0.075 | 0.07 | 0.05 | 0.05 | 0.06 | 0.099 | 0.061 | 0.072 |
| 144 | 0.04 | 0.04 | 0.042 | 0.121 | 0.066 | 0.06 | 0.05 | 0.03 | 0.04 | 0.066 | 0.103 | 0.08 |
| 145 | 0.04 | 0.075 | 0.061 | 0.03 | 0.042 | 0.05 | 0.061 | 0.071 | 0.03 | 0.06 | 0.101 | 0.077 |
| 146 | 0.048 | 0.091 | 0.07 | 0.06 | 0.04 | 0.071 | 0.02 | 0.04 | 0.04 | 0.121 | 0.066 | 0.111 |
| 147 | 0.066 | 0.075 | 0.042 | 0.042 | 0.05 | 0.06 | 0.03 | 0.04 | 0.03 | 0.072 | 0.111 | 0.082 |
| 148 | 0.04 | 0.071 | 0.033 | 0.084 | 0.08 | 0.052 | 0.052 | 0.02 | 0.02 | 0.077 | 0.113 | 0.066 |
| 149 | 0.05 | 0.033 | 0.03 | 0.136 | 0.12 | 0.09 | 0.06 | 0.024 | 0.02 | 0.122 | 0.06 | 0.072 |
| 150 | 0.033 | 0.04 | 0.071 | 0.08 | 0.121 | 0.08 | 0.04 | 0.02 | 0.033 | 0.073 | 0.05 | 0.066 |
| 151 | 0.05 | 0.03 | 0.04 | 0.084 | 0.06 | 0.09 | 0.052 | 0.03 | 0.06 | 0.044 | 0.07 | 0.131 |
| 152 | 0.042 | 0.04 | 0.09 | 0.113 | 0.061 | 0.07 | 0.084 | 0.04 | 0.02 | 0.116 | 0.066 | 0.052 |
| 153 | 0.061 | 0.03 | 0.04 | 0.07 | 0.05 | 0.06 | 0.07 | 0.033 | 0.052 | 0.148 | 0.075 | 0.082 |
| 154 | 0.07 | 0.103 | 0.081 | 0.081 | 0.06 | 0.05 | 0.094 | 0.017 | 0.071 | 0.088 | 0.081 | 0.077 |

| | | | | | | | | | | | | |
|---|---|---|---|---|---|---|---|---|---|---|---|---|
| 155 | 0.052 | 0.03 | 0.07 | 0.103 | 0.06 | 0.05 | 0.04 | 0.057 | 0.033 | 0.057 | 0.066 | 0.08 |
| 156 | 0.04 | 0.01 | 0.061 | 0.061 | 0.052 | 0.03 | 0.061 | 0.033 | 0.05 | 0.022 | 0.073 | 0.09 |
| 157 | 0.04 | 0.04 | 0.06 | 0.09 | 0.07 | 0.071 | 0.061 | 0.048 | 0.057 | 0.11 | 0.088 | 0.109 |
| 158 | 0.02 | 0.04 | 0.052 | 0.057 | 0.09 | 0.05 | 0.048 | 0.05 | 0.064 | 0.072 | 0.105 | 0.111 |
| 159 | 0.06 | 0.01 | 0.02 | 0.179 | 0.07 | 0.061 | 0.04 | 0.02 | 0.03 | 0.077 | 0.071 | 0.055 |
| 160 | 0.05 | 0.091 | 0.04 | 0.121 | 0.08 | 0.08 | 0.066 | 0.05 | 0.05 | 0.044 | 0.05 | 0.038 |
| 161 | 0.033 | 0.071 | 0.061 | 0.1 | 0.052 | 0.111 | 0.04 | 0.03 | 0 | 0.077 | 0.05 | 0.101 |
| 162 | 0.042 | 0.03 | 0.048 | 0.09 | 0.06 | 0.14 | 0.05 | 0.06 | 0.04 | 0.071 | 0.033 | 0.064 |
| 163 | 0.07 | 0.05 | 0.066 | 0.113 | 0.05 | 0.057 | 0.02 | 0.052 | 0.024 | 0.077 | 0.04 | 0.077 |
| 164 | 0.071 | 0.042 | 0.08 | 0.113 | 0.101 | 0.04 | 0.024 | 0.04 | 0.057 | 0.066 | 0.066 | 0.055 |
| 165 | 0.042 | 0.071 | 0.104 | 0.071 | 0.066 | 0.075 | 0.06 | 0.03 | 0.052 | 0.066 | 0.126 | 0.077 |
| 166 | 0.05 | 0.033 | 0.072 | 0.071 | 0.141 | 0.052 | 0.04 | 0.04 | 0.061 | 0.094 | 0.165 | 0.071 |
| 167 | 0.033 | 0.042 | 0.064 | 0.05 | 0.03 | 0.042 | 0.07 | 0.052 | 0.03 | 0.066 | 0.066 | 0.08 |
| 168 | 0.05 | 0.052 | 0.064 | 0.061 | 0.06 | 0.03 | 0.05 | 0.01 | 0.042 | 0.121 | 0.089 | 0.115 |
| 169 | 0.042 | 0.04 | 0.096 | 0.1 | 0.05 | 0.05 | 0.05 | 0.03 | 0.04 | 0.049 | 0.113 | 0.077 |
| 170 | 0.03 | 0.042 | 0.08 | 0.03 | 0.081 | 0.07 | 0.042 | 0.04 | 0.042 | 0.088 | 0.108 | 0.055 |
| 171 | 0.066 | 0.02 | 0.072 | 0.08 | 0.061 | 0.1 | 0.04 | 0.03 | 0.01 | 0.055 | 0.098 | 0.114 |
| 172 | 0.06 | 0.04 | 0.052 | 0.07 | 0.075 | 0.098 | 0.07 | 0.02 | 0.03 | 0.121 | 0.084 | 0.044 |
| 173 | 0.06 | 0.042 | 0.04 | 0.141 | 0.066 | 0.08 | 0.03 | 0.03 | 0.03 | 0.055 | 0.075 | 0.049 |
| 174 | 0.07 | 0.033 | 0.08 | 0.141 | 0.091 | 0.08 | 0.04 | 0.024 | 0.04 | 0.083 | 0.066 | 0.038 |
| 175 | 0.05 | 0.05 | 0.048 | 0.13 | 0.1 | 0.061 | 0.061 | 0.04 | 0.024 | 0.143 | 0.07 | 0.116 |
| 176 | 0.05 | 0.033 | 0.094 | 0.131 | 0.07 | 0.03 | 0.04 | 0.024 | 0.01 | 0.082 | 0.094 | 0.055 |
| 177 | 0.08 | 0.08 | 0.08 | 0.143 | 0.07 | 0.081 | 0.04 | 0.042 | 0.05 | 0.045 | 0.081 | 0.055 |
| 178 | 0.071 | 0.04 | 0.06 | 0.141 | 0.02 | 0.052 | 0.052 | 0.02 | 0.05 | 0.077 | 0.091 | 0.066 |
| 179 | 0.042 | 0.05 | 0.061 | 0.11 | 0.06 | 0.06 | 0.03 | 0.04 | 0.042 | 0.045 | 0.081 | 0.096 |
| 180 | 0.04 | 0.02 | 0.04 | 0.094 | 0.061 | 0.05 | 0.03 | 0.04 | 0.04 | 0.061 | 0.05 | 0.094 |
| 181 | 0.06 | 0.061 | 0.03 | 0.081 | 0.061 | 0.11 | 0.03 | 0.04 | 0.033 | 0.06 | 0.094 | 0.071 |
| 182 | 0.06 | 0.05 | 0.033 | 0.057 | 0.06 | 0.071 | 0.03 | 0.071 | 0.057 | 0.05 | 0.084 | 0.066 |
| 183 | 0.06 | 0.03 | 0.088 | 0.052 | 0.03 | 0.103 | 0.08 | 0.052 | 0.033 | 0.071 | 0.097 | 0.088 |
| 184 | 0.05 | 0.05 | 0.06 | 0.05 | 0.071 | 0.09 | 0.04 | 0.061 | 0.048 | 0.049 | 0.071 | 0.068 |

| | | | | | | | | | | | | |
|---|---|---|---|---|---|---|---|---|---|---|---|---|
| 185 | 0.06 | 0.042 | 0.04 | 0.06 | 0.061 | 0.06 | 0.05 | 0.05 | 0.052 | 0.09 | 0.133 | 0.044 |
| 186 | 0.042 | 0.057 | 0.03 | 0.101 | 0.05 | 0.091 | 0.042 | 0.08 | 0.03 | 0.107 | 0.1 | 0.066 |
| 187 | 0.05 | 0.04 | 0.05 | 0.1 | 0.08 | 0.081 | 0.02 | 0.05 | 0.04 | 0.066 | 0.091 | 0.077 |
| 188 | 0.075 | 0.042 | 0.052 | 0.2 | 0.091 | 0.071 | 0.033 | 0.08 | 0.017 | 0.082 | 0.081 | 0.049 |
| 189 | 0.081 | 0.061 | 0.04 | 0.04 | 0.133 | 0.081 | 0.033 | 0.02 | 0.06 | 0.072 | 0.071 | 0.088 |
| 190 | 0.075 | 0.052 | 0.091 | 0.103 | 0.048 | 0.06 | 0.061 | 0.01 | 0.052 | 0.084 | 0.1 | 0.094 |
| 191 | 0.042 | 0.06 | 0.09 | 0.091 | 0.111 | 0.042 | 0.05 | 0.052 | 0.06 | 0.104 | 0.081 | 0.066 |
| 192 | 0.03 | 0.024 | 0.033 | 0.121 | 0.061 | 0.081 | 0.06 | 0.04 | 0.1 | 0.044 | 0.07 | 0.049 |
| 193 | 0.08 | 0.03 | 0.04 | 0.09 | 0.07 | 0.05 | 0.061 | 0.052 | 0.05 | 0.055 | 0.07 | 0.062 |
| 194 | 0.04 | 0.042 | 0.06 | 0.09 | 0.1 | 0.04 | 0.042 | 0.03 | 0.06 | 0.055 | 0.084 | 0.061 |
| 195 | 0.033 | 0.017 | 0.081 | 0.113 | 0.06 | 0.07 | 0.03 | 0.02 | 0.071 | 0.049 | 0.081 | 0.066 |
| 196 | 0.042 | 0.05 | 0.071 | 0.08 | 0.091 | 0.06 | 0.02 | 0.04 | 0.04 | 0.027 | 0.07 | 0.071 |
| 197 | 0.05 | 0.075 | 0.06 | 0.08 | 0.04 | 0.071 | 0.05 | 0.042 | 0.05 | 0.045 | 0.072 | 0.082 |
| 198 | 0.04 | 0.057 | 0.071 | 0.081 | 0.042 | 0.098 | 0.06 | 0.04 | 0.03 | 0.033 | 0.07 | 0.033 |
| 199 | 0.04 | 0.071 | 0.052 | 0.06 | 0.081 | 0.111 | 0.02 | 0.061 | 0.061 | 0.055 | 0.05 | 0.088 |
| 200 | 0.05 | 0.02 | 0.111 | 0.04 | 0.042 | 0.123 | 0.03 | 0.061 | 0.05 | 0.055 | 0.133 | 0.044 |
| 201 | 0.07 | 0.042 | 0.06 | 0.07 | 0.05 | 0.103 | 0.02 | 0.06 | 0.04 | 0.038 | 0.121 | 0.061 |
| 202 | 0.05 | 0.042 | 0.05 | 0.081 | 0.061 | 0.06 | 0.02 | 0.05 | 0.05 | 0.072 | 0.075 | 0.077 |
| 203 | 0.042 | 0.03 | 0.05 | 0.17 | 0.08 | 0.071 | 0.03 | 0.05 | 0.03 | 0.083 | 0.094 | 0.066 |
| 204 | 0.033 | 0.042 | 0.042 | 0.111 | 0.042 | 0.075 | 0.02 | 0.02 | 0.024 | 0.066 | 0.126 | 0.055 |
| 205 | 0.07 | 0.05 | 0.04 | 0.057 | 0.04 | 0.048 | 0.06 | 0.042 | 0.05 | 0.082 | 0.09 | 0.082 |
| 206 | 0.02 | 0.052 | 0.052 | 0.061 | 0.081 | 0.052 | 0.042 | 0.066 | 0.01 | 0.104 | 0.08 | 0.049 |
| 207 | 0.04 | 0.08 | 0.05 | 0.071 | 0.057 | 0.081 | 0.06 | 0.024 | 0.052 | 0.088 | 0.094 | 0.055 |
| 208 | 0.03 | 0.06 | 0.061 | 0.042 | 0.057 | 0.05 | 0.05 | 0.05 | 0.042 | 0.066 | 0.066 | 0.082 |
| 209 | 0.07 | 0.06 | 0.08 | 0.09 | 0.075 | 0.071 | 0.061 | 0.042 | 0.071 | 0.107 | 0.117 | 0.071 |
| 210 | 0.066 | 0.06 | 0.094 | 0.121 | 0.075 | 0.06 | 0.04 | 0.071 | 0.04 | 0.088 | 0.088 | 0.073 |
| 211 | 0.07 | 0.05 | 0.05 | 0.101 | 0.045 | 0.042 | 0.03 | 0.024 | 0.02 | 0.055 | 0.081 | 0.077 |
| 212 | 0.05 | 0.02 | 0.09 | 0.101 | 0.057 | 0.052 | 0.061 | 0.04 | 0.02 | 0.094 | 0.09 | 0.039 |
| 213 | 0.04 | 0.01 | 0.091 | 0.207 | 0.057 | 0.094 | 0.024 | 0.052 | 0.024 | 0.099 | 0.111 | 0.093 |
| 214 | 0.057 | 0.03 | 0.08 | 0.131 | 0.052 | 0.094 | 0.033 | 0.033 | 0.02 | 0.08 | 0.12 | 0.11 |

| | | | | | | | | | | | | |
|---|---|---|---|---|---|---|---|---|---|---|---|---|
| 215 | 0.071 | 0.03 | 0.101 | 0.161 | 0.048 | 0.061 | 0.07 | 0.06 | 0.05 | 0.071 | 0.111 | 0.071 |
| 216 | 0.061 | 0.013 | 0.07 | 0.081 | 0.033 | 0.071 | 0.066 | 0.042 | 0.03 | 0.049 | 0.11 | 0.084 |
| 217 | 0.052 | 0.075 | 0.04 | 0.06 | 0.08 | 0.108 | 0.04 | 0.04 | 0.052 | 0.055 | 0.06 | 0.044 |
| 218 | 0.057 | 0.048 | 0.03 | 0.07 | 0.064 | 0.08 | 0.03 | 0.02 | 0.03 | 0.06 | 0.101 | 0.062 |
| 219 | 0.04 | 0.042 | 0.05 | 0.16 | 0.052 | 0.071 | 0.02 | 0.04 | 0.042 | 0.088 | 0.141 | 0.079 |
| 220 | 0.03 | 0.02 | 0.03 | 0.18 | 0.104 | 0.103 | 0.04 | 0.07 | 0.05 | 0.046 | 0.103 | 0.061 |
| 221 | 0.02 | 0.052 | 0.05 | 0.091 | 0.103 | 0.08 | 0.017 | 0.05 | 0.02 | 0.062 | 0.09 | 0.05 |
| 222 | 0.033 | 0.033 | 0.07 | 0.05 | 0.072 | 0.113 | 0.061 | 0.03 | 0.03 | 0.06 | 0.052 | 0.1 |
| 223 | 0.071 | 0.042 | 0.042 | 0.061 | 0.066 | 0.075 | 0.04 | 0.061 | 0.06 | 0.028 | 0.06 | 0.084 |
| 224 | 0.081 | 0.042 | 0.052 | 0.06 | 0.1 | 0.088 | 0.04 | 0.03 | 0.03 | 0.071 | 0.061 | 0.101 |
| 225 | 0.07 | 0.042 | 0.03 | 0.1 | 0.048 | 0.081 | 0.04 | 0.061 | 0.052 | 0.1 | 0.09 | 0.033 |
| 226 | 0.061 | 0.06 | 0.06 | 0.071 | 0.048 | 0.075 | 0.05 | 0.04 | 0.033 | 0.044 | 0.113 | 0.068 |
| 227 | 0.075 | 0.066 | 0.071 | 0.192 | 0.07 | 0.12 | 0.06 | 0.02 | 0.02 | 0.049 | 0.141 | 0.044 |
| 228 | 0.081 | 0.03 | 0.02 | 0.192 | 0.08 | 0.042 | 0.02 | 0.052 | 0.042 | 0.077 | 0.136 | 0.128 |
| 229 | 0.097 | 0.03 | 0.09 | 0.1 | 0.071 | 0.052 | 0.061 | 0.06 | 0.04 | 0.073 | 0.133 | 0.027 |
| 230 | 0.061 | 0.04 | 0.071 | 0.14 | 0.03 | 0.07 | 0.04 | 0.04 | 0.017 | 0.049 | 0.09 | 0.046 |
| 231 | 0.05 | 0.052 | 0.04 | 0.131 | 0.075 | 0.111 | 0.05 | 0.05 | 0.04 | 0.078 | 0.103 | 0.064 |
| 232 | 0.04 | 0.033 | 0.03 | 0.131 | 0.162 | 0.052 | 0.06 | 0.07 | 0.06 | 0.088 | 0.09 | 0.055 |
| 233 | 0.052 | 0.024 | 0.061 | 0.1 | 0.02 | 0.042 | 0.03 | 0.081 | 0.03 | 0.055 | 0.143 | 0.083 |
| 234 | 0.061 | 0.052 | 0.1 | 0.1 | 0.05 | 0.11 | 0.03 | 0.052 | 0.071 | 0.066 | 0.12 | 0.116 |
| 235 | 0.04 | 0.07 | 0.06 | 0.091 | 0.052 | 0.042 | 0.033 | 0.06 | 0.04 | 0.05 | 0.061 | 0.066 |
| 236 | 0.091 | 0.05 | 0.052 | 0.03 | 0.081 | 0.07 | 0.02 | 0.052 | 0.03 | 0.066 | 0.09 | 0.127 |
| 237 | 0.042 | 0.04 | 0.04 | 0.04 | 0.05 | 0.04 | 0.06 | 0.01 | 0.05 | 0.072 | 0.094 | 0.104 |
| 238 | 0.066 | 0.05 | 0.042 | 0.06 | 0.03 | 0.071 | 0.04 | 0.052 | 0.05 | 0.058 | 0.104 | 0.077 |
| 239 | 0.084 | 0.04 | 0.05 | 0.06 | 0 | 0.042 | 0.04 | 0.042 | 0.04 | 0.072 | 0.07 | 0.044 |
| 240 | 0.05 | 0.071 | 0.06 | 0.081 | 0.03 | 0.04 | 0.02 | 0.061 | 0.07 | 0.071 | 0.101 | 0.062 |
| 241 | 0.033 | 0.05 | 0.04 | 0.094 | 0.03 | 0.048 | 0.033 | 0.05 | 0.03 | 0.077 | 0.07 | 0.073 |
| 242 | 0.052 | 0.052 | 0.075 | 0.05 | 0.03 | 0.033 | 0.05 | 0.05 | 0.052 | 0.093 | 0.07 | 0.107 |
| 243 | 0.083 | 0.057 | 0.05 | 0.033 | 0.033 | 0.02 | 0.05 | 0.02 | 0.033 | 0.11 | 0.081 | 0.093 |
| 244 | 0.04 | 0.06 | 0.075 | 0.094 | 0.042 | 0.042 | 0.033 | 0.04 | 0.052 | 0.099 | 0.11 | 0.098 |

| | | | | | | | | | | | | |
|---|---|---|---|---|---|---|---|---|---|---|---|---|
| 245 | 0.06 | 0.04 | 0.061 | 0.057 | 0.06 | 0.024 | 0.04 | 0.057 | 0.033 | 0.039 | 0.061 | 0.09 |
| 246 | 0.04 | 0.052 | 0.033 | 0.061 | 0.06 | 0.05 | 0.042 | 0.03 | 0.03 | 0.088 | 0.101 | 0.06 |
| 247 | 0.08 | 0.071 | 0.02 | 0.07 | 0.07 | 0.091 | 0.02 | 0.033 | 0.03 | 0.062 | 0.075 | 0.07 |
| 248 | 0.052 | 0.06 | 0.05 | 0.033 | 0.052 | 0.061 | 0.042 | 0.04 | 0.024 | 0.072 | 0.042 | 0.05 |
| 249 | 0.042 | 0.07 | 0.03 | 0.091 | 0.07 | 0.071 | 0.08 | 0.081 | 0.042 | 0.059 | 0.084 | 0.099 |
| 250 | 0.03 | 0.071 | 0.06 | 0.096 | 0.071 | 0.06 | 0.033 | 0.03 | 0.017 | 0.066 | 0.131 | 0.071 |
| Mean | 0.049896 | 0.046764 | 0.053108 | 0.081824 | 0.062988 | 0.066424 | 0.04442 | 0.041016 | 0.045524 | 0.072556 | 0.0833 | 0.074256 |
| SD | 0.016858 | 0.018157 | 0.020395 | 0.035977 | 0.024304 | 0.023748 | 0.017363 | 0.016998 | 0.018366 | 0.023735 | 0.025888 | 0.024478 |

4. Tables of automated gap thickness measurements for AxC169 variety

The following tables show the total number of OCT images used for manual gap thickness measurements in the AxC169 variety. A total of 200 OCT images were analyzed, with segmentation of the first 2–3 cell layers performed using the OCT Analyzer software. For both control and infected leaves, three measurements were taken daily from Day 0 (D0) to Day 7 (D7). The software provided values for the maximum (Max), minimum (Min), and average gap thickness. The average value being the most relevant for our study.

| | Control (mm) | | | | | | | | | Infected (mm) | | | | | | | | |
|---|---|---|---|---|---|---|---|---|---|---|---|---|---|---|---|---|---|---|
| Day 0 | R1 | | | R2 | | | R3 | | | R1 | | | R2 | | | R3 | | |
| | Max | Min | Average | Max | Min | Average | Max | Min | Average | Max | Min | Average | Max | Min | Average | Max | Min | Average |
| 1 | 0.04 | 0 | 0.02 | 0.09 | 0 | 0.03 | 0.08 | 0 | 0.03 | 0.07 | 0 | 0.03 | 0.08 | 0 | 0.03 | 0.07 | 0 | 0.03 |
| 2 | 0.05 | 0 | 0.03 | 0.06 | 0 | 0.04 | 0.06 | 0 | 0.04 | 0.07 | 0 | 0.04 | 0.1 | 0 | 0.04 | 0.07 | 0 | 0.03 |
| 3 | 0.05 | 0 | 0.02 | 0.07 | 0 | 0.03 | 0.08 | 0 | 0.04 | 0.07 | 0 | 0.04 | 0.09 | 0 | 0.04 | 0.09 | 0 | 0.04 |
| 4 | 0.05 | 0 | 0.01 | 0.08 | 0 | 0.04 | 0.07 | 0 | 0.04 | 0.07 | 0 | 0.04 | 0.09 | 0 | 0.04 | 0.08 | 0 | 0.03 |
| 5 | 0.04 | 0 | 0.02 | 0.08 | 0 | 0.04 | 0.08 | 0 | 0.04 | 0.08 | 0 | 0.04 | 0.08 | 0 | 0.04 | 0.07 | 0 | 0.03 |
| 6 | 0.04 | 0 | 0.01 | 0.08 | 0 | 0.04 | 0.07 | 0 | 0.04 | 0.07 | 0 | 0.03 | 0.07 | 0 | 0.04 | 0.08 | 0 | 0.03 |
| 7 | 0.02 | 0 | 0.01 | 0.07 | 0 | 0.04 | 0.09 | 0 | 0.04 | 0.08 | 0 | 0.04 | 0.07 | 0 | 0.04 | 0.08 | 0 | 0.03 |
| 8 | 0.02 | 0 | 0.01 | 0.07 | 0 | 0.04 | 0.07 | 0 | 0.04 | 0.07 | 0 | 0.04 | 0.08 | 0 | 0.04 | 0.08 | 0 | 0.04 |
| 9 | 0.02 | 0 | 0.01 | 0.08 | 0 | 0.04 | 0.08 | 0 | 0.04 | 0.07 | 0 | 0.04 | 0.07 | 0 | 0.03 | 0.08 | 0 | 0.03 |
| 10 | 0.04 | 0 | 0.02 | 0.09 | 0 | 0.04 | 0.08 | 0 | 0.04 | 0.08 | 0 | 0.04 | 0.07 | 0 | 0.04 | 0.08 | 0 | 0.04 |
| 11 | 0.05 | 0 | 0.03 | 0.08 | 0 | 0.04 | 0.07 | 0 | 0.04 | 0.09 | 0 | 0.04 | 0.08 | 0 | 0.04 | 0.08 | 0 | 0.04 |
| 12 | 0.06 | 0 | 0.04 | 0.1 | 0 | 0.05 | 0.08 | 0 | 0.04 | 0.09 | 0.01 | 0.04 | 0.08 | 0 | 0.04 | 0.08 | 0 | 0.04 |
| 13 | 0.06 | 0 | 0.04 | 0.09 | 0 | 0.04 | 0.08 | 0 | 0.05 | 0.08 | 0 | 0.04 | 0.08 | 0 | 0.04 | 0.08 | 0 | 0.03 |
| 14 | 0.06 | 0.01 | 0.04 | 0.09 | 0 | 0.04 | 0.08 | 0 | 0.04 | 0.07 | 0 | 0.04 | 0.08 | 0 | 0.03 | 0.08 | 0 | 0.03 |
| 15 | 0.06 | 0 | 0.04 | 0.1 | 0 | 0.04 | 0.07 | 0 | 0.04 | 0.07 | 0 | 0.04 | 0.08 | 0 | 0.04 | 0.09 | 0 | 0.04 |
| 16 | 0.07 | 0 | 0.05 | 0.09 | 0 | 0.04 | 0.08 | 0 | 0.04 | 0.06 | 0 | 0.04 | 0.08 | 0 | 0.04 | 0.09 | 0 | 0.04 |
| 17 | 0.06 | 0.03 | 0.05 | 0.08 | 0 | 0.04 | 0.08 | 0 | 0.04 | 0.08 | 0 | 0.04 | 0.08 | 0 | 0.04 | 0.08 | 0 | 0.04 |
| 18 | 0.07 | 0 | 0.05 | 0.09 | 0 | 0.05 | 0.07 | 0 | 0.04 | 0.07 | 0.01 | 0.04 | 0.08 | 0 | 0.04 | 0.09 | 0 | 0.04 |
| 19 | 0.07 | 0 | 0.04 | 0.09 | 0.01 | 0.05 | 0.08 | 0 | 0.05 | 0.09 | 0 | 0.04 | 0.08 | 0 | 0.04 | 0.08 | 0 | 0.04 |
| 20 | 0.07 | 0 | 0.05 | 0.09 | 0 | 0.05 | 0.08 | 0 | 0.04 | 0.09 | 0 | 0.04 | 0.07 | 0 | 0.04 | 0.08 | 0 | 0.04 |
| 21 | 0.07 | 0.03 | 0.06 | 0.08 | 0 | 0.05 | 0.1 | 0 | 0.05 | 0.08 | 0 | 0.04 | 0.07 | 0 | 0.05 | 0.09 | 0 | 0.03 |
| 22 | 0.08 | 0 | 0.05 | 0.08 | 0 | 0.04 | 0.09 | 0 | 0.05 | 0.09 | 0 | 0.04 | 0.08 | 0 | 0.05 | 0.1 | 0 | 0.03 |
| 23 | 0.08 | 0 | 0.05 | 0.08 | 0.02 | 0.06 | 0.08 | 0 | 0.05 | 0.09 | 0 | 0.04 | 0.08 | 0 | 0.05 | 0.08 | 0 | 0.03 |
| 24 | 0.08 | 0.04 | 0.06 | 0.07 | 0 | 0.06 | 0.08 | 0 | 0.05 | 0.09 | 0 | 0.04 | 0.09 | 0 | 0.04 | 0.08 | 0 | 0.03 |
| 25 | 0.08 | 0.04 | 0.06 | 0.08 | 0 | 0.06 | 0.08 | 0 | 0.04 | 0.07 | 0 | 0.04 | 0.09 | 0 | 0.04 | 0.08 | 0 | 0.04 |
| 26 | 0.07 | 0 | 0.05 | 0.08 | 0 | 0.04 | 0.08 | 0 | 0.05 | 0.1 | 0 | 0.04 | 0.09 | 0 | 0.04 | 0.08 | 0 | 0.03 |
| 27 | 0.07 | 0 | 0.04 | 0.08 | 0 | 0.04 | 0.09 | 0 | 0.05 | 0.07 | 0 | 0.04 | 0.08 | 0 | 0.04 | 0.08 | 0 | 0.04 |
| 28 | 0.06 | 0 | 0.03 | 0.07 | 0 | 0.04 | 0.09 | 0 | 0.05 | 0.08 | 0 | 0.05 | 0.1 | 0 | 0.04 | 0.08 | 0 | 0.03 |
| 29 | 0.05 | 0 | 0.03 | 0.07 | 0 | 0.04 | 0.09 | 0 | 0.05 | 0.09 | 0 | 0.04 | 0.09 | 0 | 0.03 | 0.09 | 0 | 0.03 |
| 30 | 0.05 | 0 | 0.03 | 0.09 | 0 | 0.04 | 0.11 | 0 | 0.06 | 0.08 | 0 | 0.05 | 0.09 | 0 | 0.03 | 0.08 | 0 | 0.03 |
| 31 | 0.05 | 0 | 0.03 | 0.07 | 0 | 0.04 | 0.09 | 0.03 | 0.06 | 0.07 | 0 | 0.04 | 0.08 | 0 | 0.03 | 0.09 | 0 | 0.03 |
| 32 | 0.05 | 0 | 0.03 | 0.07 | 0 | 0.04 | 0.08 | 0 | 0.04 | 0.07 | 0 | 0.04 | 0.1 | 0 | 0.04 | 0.09 | 0 | 0.03 |
| 33 | 0.04 | 0 | 0.03 | 0.08 | 0 | 0.04 | 0.08 | 0 | 0.04 | 0.07 | 0 | 0.04 | 0.09 | 0 | 0.04 | 0.09 | 0 | 0.04 |
| 34 | 0.04 | 0 | 0.03 | 0.08 | 0 | 0.04 | 0.1 | 0 | 0.05 | 0.08 | 0 | 0.04 | 0.1 | 0 | 0.05 | 0.08 | 0 | 0.04 |

| | | | | | | | | | | | | | | | | | |
|---|---|---|---|---|---|---|---|---|---|---|---|---|---|---|---|---|---|
| 35 | 0.05 | 0 | 0.03 | 0.07 | 0 | 0.04 | 0.08 | 0 | 0.05 | 0.06 | 0 | 0.04 | 0.11 | 0 | 0.05 | 0.09 | 0 | 0.04 |
| 36 | 0.04 | 0 | 0.03 | 0.1 | 0 | 0.04 | 0.08 | 0.08 | 0.06 | 0.07 | 0 | 0.04 | 0.09 | 0 | 0.05 | 0.08 | 0 | 0.03 |
| 37 | 0.04 | 0 | 0.03 | 0.09 | 0 | 0.05 | 0.08 | 0 | 0.05 | 0.07 | 0 | 0.04 | 0.09 | 0 | 0.05 | 0.07 | 0 | 0.03 |
| 38 | 0.05 | 0 | 0.03 | 0.08 | 0 | 0.04 | 0.08 | 0 | 0.05 | 0.08 | 0 | 0.04 | 0.08 | 0 | 0.03 | 0.06 | 0 | 0.03 |
| 39 | 0.06 | 0 | 0.04 | 0.08 | 0 | 0.05 | 0.09 | 0 | 0.05 | 0.07 | 0 | 0.04 | 0.09 | 0 | 0.04 | 0.08 | 0 | 0.03 |
| 40 | 0.06 | 0 | 0.04 | 0.08 | 0 | 0.05 | 0.09 | 0.03 | 0.05 | 0.09 | 0 | 0.04 | 0.09 | 0 | 0.03 | 0.08 | 0 | 0.03 |
| 41 | 0.06 | 0 | 0.04 | 0.09 | 0 | 0.05 | 0.08 | 0 | 0.05 | 0.08 | 0 | 0.04 | 0.08 | 0 | 0.03 | 0.08 | 0 | 0.03 |
| 42 | 0.07 | 0 | 0.04 | 0.07 | 0 | 0.05 | 0.1 | 0 | 0.05 | 0.07 | 0 | 0.04 | 0.09 | 0 | 0.03 | 0.08 | 0 | 0.03 |
| 43 | 0.08 | 0 | 0.04 | 0.08 | 0 | 0.05 | 0.09 | 0.02 | 0.05 | 0.08 | 0 | 0.04 | 0.08 | 0 | 0.03 | 0.08 | 0 | 0.03 |
| 44 | 0.07 | 0 | 0.04 | 0.1 | 0 | 0.04 | 0.06 | 0 | 0.04 | 0.07 | 0 | 0.04 | 0.1 | 0 | 0.05 | 0.08 | 0 | 0.03 |
| 45 | 0.08 | 0 | 0.05 | 0.09 | 0 | 0.05 | 0.08 | 0 | 0.04 | 0.09 | 0 | 0.04 | 0.08 | 0 | 0.06 | 0.08 | 0 | 0.03 |
| 46 | 0.08 | 0 | 0.05 | 0.09 | 0 | 0.05 | 0.12 | 0 | 0.04 | 0.1 | 0 | 0.04 | 0.1 | 0 | 0.06 | 0.1 | 0 | 0.03 |
| 47 | 0.06 | 0 | 0.04 | 0.09 | 0.02 | 0.05 | 0.1 | 0 | 0.04 | 0.09 | 0 | 0.04 | 0.09 | 0 | 0.06 | 0.08 | 0 | 0.03 |
| 48 | 0.08 | 0.02 | 0.05 | 0.09 | 0.01 | 0.05 | 0.08 | 0 | 0.04 | 0.1 | 0 | 0.04 | 0.09 | 0 | 0.06 | 0.08 | 0 | 0.04 |
| 49 | 0.07 | 0 | 0.04 | 0.1 | 0.03 | 0.05 | 0.11 | 0 | 0.04 | 0.08 | 0 | 0.04 | 0.11 | 0 | 0.06 | 0.09 | 0 | 0.02 |
| 50 | 0.06 | 0 | 0.04 | 0.1 | 0 | 0.05 | 0.09 | 0.02 | 0.05 | 0.09 | 0 | 0.04 | 0.09 | 0 | 0.06 | 0.09 | 0 | 0.03 |
| 51 | 0.06 | 0 | 0.04 | 0.1 | 0 | 0.06 | 0.08 | 0.02 | 0.05 | 0.1 | 0 | 0.04 | 0.09 | 0 | 0.06 | 0.09 | 0 | 0.03 |
| 52 | 0.07 | 0 | 0.04 | 0.1 | 0.03 | 0.06 | 0.08 | 0 | 0.04 | 0.07 | 0 | 0.04 | 0.09 | 0 | 0.06 | 0.07 | 0 | 0.03 |
| 53 | 0.05 | 0 | 0.03 | 0.08 | 0 | 0.06 | 0.1 | 0.03 | 0.05 | 0.1 | 0 | 0.04 | 0.11 | 0 | 0.06 | 0.08 | 0 | 0.03 |
| 54 | 0.04 | 0 | 0.03 | 0.1 | 0 | 0.06 | 0.11 | 0 | 0.06 | 0.1 | 0 | 0.04 | 0.11 | 0 | 0.06 | 0.08 | 0 | 0.03 |
| 55 | 0.04 | 0 | 0.03 | 0.09 | 0.02 | 0.06 | 0.13 | 0.03 | 0.06 | 0.09 | 0 | 0.05 | 0.09 | 0 | 0.06 | 0.09 | 0 | 0.03 |
| 56 | 0.05 | 0 | 0.03 | 0.07 | 0.02 | 0.06 | 0.09 | 0 | 0.05 | 0.08 | 0 | 0.04 | 0.1 | 0 | 0.06 | 0.08 | 0 | 0.03 |
| 57 | 0.06 | 0 | 0.04 | 0.08 | 0.01 | 0.06 | 0.09 | 0 | 0.04 | 0.09 | 0 | 0.05 | 0.09 | 0 | 0.06 | 0.08 | 0 | 0.03 |
| 58 | 0.06 | 0 | 0.04 | 0.07 | 0.01 | 0.06 | 0.09 | 0.01 | 0.05 | 0.09 | 0 | 0.06 | 0.1 | 0 | 0.07 | 0.09 | 0 | 0.03 |
| 59 | 0.06 | 0 | 0.04 | 0.1 | 0 | 0.06 | 0.09 | 0 | 0.05 | 0.08 | 0 | 0.06 | 0.09 | 0 | 0.07 | 0.07 | 0 | 0.03 |
| 60 | 0.07 | 0 | 0.04 | 0.11 | 0.02 | 0.06 | 0.09 | 0 | 0.05 | 0.09 | 0 | 0.06 | 0.09 | 0 | 0.06 | 0.09 | 0 | 0.03 |
| 61 | 0.08 | 0 | 0.04 | 0.08 | 0 | 0.06 | 0.1 | 0 | 0.05 | 0.09 | 0 | 0.06 | 0.11 | 0 | 0.06 | 0.08 | 0 | 0.03 |
| 62 | 0.07 | 0 | 0.04 | 0.09 | 0 | 0.06 | 0.07 | 0 | 0.05 | 0.07 | 0 | 0.06 | 0.1 | 0 | 0.06 | 0.08 | 0 | 0.04 |
| 63 | 0.08 | 0 | 0.05 | 0.07 | 0 | 0.06 | 0.07 | 0 | 0.05 | 0.09 | 0 | 0.06 | 0.1 | 0 | 0.06 | 0.08 | 0 | 0.03 |
| 64 | 0.08 | 0 | 0.05 | 0.08 | 0 | 0.06 | 0.09 | 0.01 | 0.05 | 0.09 | 0 | 0.06 | 0.1 | 0 | 0.06 | 0.08 | 0 | 0.05 |
| 65 | 0.06 | 0 | 0.04 | 0.09 | 0 | 0.04 | 0.1 | 0 | 0.05 | 0.08 | 0 | 0.06 | 0.09 | 0 | 0.06 | 0.08 | 0 | 0.05 |
| 66 | 0.08 | 0.02 | 0.05 | 0.1 | 0 | 0.05 | 0.12 | 0 | 0.04 | 0.08 | 0 | 0.07 | 0.08 | 0 | 0.06 | 0.09 | 0 | 0.06 |
| 67 | 0.07 | 0 | 0.04 | 0.09 | 0 | 0.05 | 0.12 | 0 | 0.05 | 0.09 | 0 | 0.07 | 0.09 | 0 | 0.05 | 0.08 | 0 | 0.06 |
| 68 | 0.06 | 0 | 0.04 | 0.11 | 0 | 0.05 | 0.11 | 0 | 0.05 | 0.08 | 0 | 0.07 | 0.12 | 0 | 0.05 | 0.09 | 0 | 0.06 |
| 69 | 0.06 | 0 | 0.04 | 0.11 | 0 | 0.05 | 0.12 | 0 | 0.05 | 0.08 | 0 | 0.07 | 0.11 | 0 | 0.05 | 0.08 | 0 | 0.06 |
| 70 | 0.07 | 0 | 0.04 | 0.09 | 0 | 0.05 | 0.11 | 0 | 0.04 | 0.09 | 0 | 0.06 | 0.12 | 0 | 0.05 | 0.1 | 0 | 0.06 |
| 71 | 0.08 | 0 | 0.04 | 0.11 | 0 | 0.05 | 0.1 | 0 | 0.04 | 0.11 | 0 | 0.06 | 0.12 | 0 | 0.04 | 0.09 | 0 | 0.04 |
| 72 | 0.07 | 0 | 0.04 | 0.11 | 0 | 0.06 | 0.1 | 0 | 0.04 | 0.09 | 0 | 0.06 | 0.11 | 0 | 0.04 | 0.09 | 0 | 0.04 |
| 73 | 0.06 | 0 | 0.03 | 0.13 | 0 | 0.06 | 0.1 | 0 | 0.05 | 0.07 | 0 | 0.06 | 0.1 | 0 | 0.04 | 0.08 | 0 | 0.03 |

| | | | | | | | | | | | | | | | | | |
|---|---|---|---|---|---|---|---|---|---|---|---|---|---|---|---|---|---|
| 74 | 0.06 | 0 | 0.03 | 0.12 | 0 | 0.06 | 0.08 | 0 | 0.04 | 0.09 | 0 | 0.06 | 0.1 | 0 | 0.04 | 0.08 | 0 | 0.03 |
| 75 | 0.07 | 0 | 0.03 | 0.12 | 0.02 | 0.05 | 0.09 | 0 | 0.04 | 0.07 | 0 | 0.06 | 0.11 | 0 | 0.06 | 0.09 | 0 | 0.03 |
| 76 | 0.09 | 0 | 0.03 | 0.16 | 0.03 | 0.05 | 0.09 | 0 | 0.04 | 0.08 | 0 | 0.06 | 0.09 | 0 | 0.07 | 0.08 | 0 | 0.03 |
| 77 | 0.08 | 0 | 0.04 | 0.11 | 0 | 0.05 | 0.1 | 0 | 0.05 | 0.09 | 0 | 0.06 | 0.08 | 0 | 0.07 | 0.09 | 0 | 0.03 |
| 78 | 0.08 | 0.02 | 0.05 | 0.11 | 0 | 0.05 | 0.13 | 0 | 0.06 | 0.08 | 0 | 0.06 | 0.09 | 0 | 0.08 | 0.09 | 0 | 0.04 |
| 79 | 0.07 | 0 | 0.04 | 0.09 | 0.03 | 0.06 | 0.12 | 0 | 0.07 | 0.07 | 0 | 0.07 | 0.09 | 0 | 0.08 | 0.09 | 0 | 0.04 |
| 80 | 0.06 | 0 | 0.04 | 0.09 | 0 | 0.05 | 0.11 | 0 | 0.07 | 0.1 | 0 | 0.07 | 0.09 | 0 | 0.08 | 0.08 | 0 | 0.03 |
| 81 | 0.07 | 0.01 | 0.05 | 0.09 | 0 | 0.05 | 0.17 | 0 | 0.05 | 0.09 | 0 | 0.06 | 0.11 | 0 | 0.07 | 0.1 | 0 | 0.04 |
| 82 | 0.07 | 0 | 0.05 | 0.1 | 0 | 0.05 | 0.13 | 0 | 0.05 | 0.09 | 0 | 0.06 | 0.1 | 0 | 0.04 | 0.1 | 0 | 0.04 |
| 83 | 0.08 | 0 | 0.05 | 0.1 | 0 | 0.06 | 0.13 | 0 | 0.05 | 0.09 | 0 | 0.06 | 0.11 | 0 | 0.04 | 0.1 | 0 | 0.04 |
| 84 | 0.08 | 0 | 0.05 | 0.1 | 0 | 0.05 | 0.13 | 0 | 0.05 | 0.09 | 0 | 0.06 | 0.11 | 0 | 0.04 | 0.11 | 0 | 0.05 |
| 85 | 0.08 | 0 | 0.04 | 0.12 | 0 | 0.05 | 0.13 | 0 | 0.05 | 0.08 | 0 | 0.06 | 0.11 | 0 | 0.05 | 0.1 | 0 | 0.04 |
| 86 | 0.08 | 0 | 0.04 | 0.11 | 0 | 0.05 | 0.09 | 0 | 0.05 | 0.08 | 0 | 0.06 | 0.1 | 0 | 0.04 | 0.09 | 0 | 0.04 |
| 87 | 0.06 | 0 | 0.04 | 0.1 | 0.01 | 0.05 | 0.08 | 0 | 0.04 | 0.09 | 0 | 0.06 | 0.09 | 0 | 0.04 | 0.1 | 0 | 0.04 |
| 88 | 0.06 | 0 | 0.03 | 0.09 | 0 | 0.04 | 0.1 | 0 | 0.05 | 0.08 | 0 | 0.06 | 0.1 | 0 | 0.04 | 0.09 | 0 | 0.04 |
| 89 | 0.06 | 0 | 0.03 | 0.1 | 0 | 0.04 | 0.1 | 0 | 0.05 | 0.08 | 0 | 0.06 | 0.09 | 0 | 0.04 | 0.1 | 0 | 0.04 |
| 90 | 0.06 | 0 | 0.04 | 0.12 | 0 | 0.04 | 0.1 | 0 | 0.04 | 0.09 | 0 | 0.06 | 0.09 | 0 | 0.05 | 0.11 | 0 | 0.04 |
| 91 | 0.06 | 0 | 0.03 | 0.12 | 0.02 | 0.04 | 0.1 | 0 | 0.05 | 0.08 | 0 | 0.06 | 0.09 | 0 | 0.04 | 0.11 | 0 | 0.05 |
| 92 | 0.06 | 0 | 0.04 | 0.13 | 0 | 0.05 | 0.09 | 0 | 0.05 | 0.08 | 0 | 0.06 | 0.09 | 0 | 0.04 | 0.11 | 0 | 0.05 |
| 93 | 0.06 | 0 | 0.04 | 0.12 | 0.01 | 0.05 | 0.08 | 0 | 0.05 | 0.08 | 0 | 0.06 | 0.08 | 0 | 0.04 | 0.11 | 0 | 0.06 |
| 94 | 0.06 | 0 | 0.04 | 0.11 | 0 | 0.05 | 0.08 | 0 | 0.05 | 0.09 | 0 | 0.06 | 0.09 | 0 | 0.04 | 0.09 | 0 | 0.06 |
| 95 | 0.06 | 0 | 0.04 | 0.1 | 0 | 0.05 | 0.14 | 0 | 0.06 | 0.09 | 0 | 0.06 | 0.09 | 0 | 0.04 | 0.1 | 0 | 0.06 |
| 96 | 0.06 | 0.02 | 0.04 | 0.11 | 0.01 | 0.05 | 0.13 | 0 | 0.05 | 0.1 | 0 | 0.06 | 0.08 | 0 | 0.04 | 0.1 | 0 | 0.04 |
| 97 | 0.06 | 0 | 0.04 | 0.11 | 0 | 0.05 | 0.12 | 0 | 0.05 | 0.08 | 0 | 0.07 | 0.09 | 0 | 0.05 | 0.09 | 0 | 0.04 |
| 98 | 0.07 | 0 | 0.04 | 0.14 | 0 | 0.05 | 0.14 | 0 | 0.05 | 0.09 | 0 | 0.07 | 0.1 | 0 | 0.05 | 0.1 | 0 | 0.04 |
| 99 | 0.09 | 0 | 0.04 | 0.15 | 0 | 0.05 | 0.13 | 0 | 0.05 | 0.09 | 0 | 0.07 | 0.09 | 0 | 0.04 | 0.1 | 0 | 0.04 |
| 100 | 0.11 | 0 | 0.05 | 0.13 | 0.01 | 0.06 | 0.12 | 0 | 0.05 | 0.09 | 0 | 0.07 | 0.08 | 0 | 0.04 | 0.1 | 0 | 0.03 |
| 101 | 0.11 | 0 | 0.05 | 0.12 | 0.02 | 0.06 | 0.12 | 0 | 0.05 | 0.11 | 0 | 0.06 | 0.1 | 0 | 0.04 | 0.1 | 0 | 0.04 |
| 102 | 0.08 | 0 | 0.04 | 0.12 | 0 | 0.05 | 0.1 | 0 | 0.05 | 0.1 | 0 | 0.06 | 0.09 | 0 | 0.05 | 0.1 | 0 | 0.04 |
| 103 | 0.07 | 0 | 0.04 | 0.14 | 0 | 0.05 | 0.1 | 0 | 0.05 | 0.09 | 0 | 0.06 | 0.09 | 0 | 0.04 | 0.11 | 0 | 0.04 |
| 104 | 0.08 | 0 | 0.04 | 0.14 | 0 | 0.06 | 0.09 | 0 | 0.04 | 0.08 | 0 | 0.06 | 0.09 | 0 | 0.04 | 0.09 | 0 | 0.03 |
| 105 | 0.09 | 0 | 0.04 | 0.13 | 0 | 0.06 | 0.08 | 0 | 0.05 | 0.09 | 0 | 0.06 | 0.08 | 0 | 0.04 | 0.1 | 0 | 0.04 |
| 106 | 0.09 | 0 | 0.04 | 0.12 | 0.02 | 0.05 | 0.08 | 0 | 0.05 | 0.09 | 0 | 0.06 | 0.12 | 0 | 0.06 | 0.11 | 0 | 0.04 |
| 107 | 0.1 | 0 | 0.05 | 0.1 | 0 | 0.05 | 0.1 | 0 | 0.05 | 0.08 | 0 | 0.06 | 0.1 | 0 | 0.04 | 0.1 | 0 | 0.05 |
| 108 | 0.08 | 0.02 | 0.05 | 0.12 | 0.02 | 0.05 | 0.13 | 0 | 0.06 | 0.08 | 0.01 | 0.06 | 0.09 | 0 | 0.04 | 0.09 | 0 | 0.04 |
| 109 | 0.09 | 0 | 0.05 | 0.1 | 0 | 0.05 | 0.12 | 0 | 0.05 | 0.09 | 0 | 0.06 | 0.08 | 0 | 0.04 | 0.1 | 0 | 0.04 |
| 110 | 0.07 | 0 | 0.05 | 0.12 | 0 | 0.05 | 0.12 | 0 | 0.05 | 0.07 | 0 | 0.06 | 0.09 | 0 | 0.04 | 0.11 | 0 | 0.04 |
| 111 | 0.07 | 0.03 | 0.05 | 0.13 | 0 | 0.05 | 0.12 | 0 | 0.05 | 0.08 | 0 | 0.06 | 0.09 | 0 | 0.04 | 0.09 | 0 | 0.03 |
| 112 | 0.08 | 0.02 | 0.05 | 0.14 | 0 | 0.05 | 0.11 | 0 | 0.05 | 0.1 | 0 | 0.06 | 0.08 | 0 | 0.03 | 0.09 | 0 | 0.04 |

| | | | | | | | | | | | | | | | | | |
|---|---|---|---|---|---|---|---|---|---|---|---|---|---|---|---|---|---|
| 113 | 0.08 | 0 | 0.05 | 0.14 | 0 | 0.04 | 0.11 | 0 | 0.05 | 0.1 | 0 | 0.06 | 0.11 | 0 | 0.04 | 0.1 | 0 | 0.03 |
| 114 | 0.06 | 0.01 | 0.04 | 0.13 | 0 | 0.04 | 0.09 | 0 | 0.06 | 0.1 | 0 | 0.06 | 0.09 | 0 | 0.04 | 0.11 | 0 | 0.04 |
| 115 | 0.07 | 0 | 0.04 | 0.13 | 0 | 0.05 | 0.09 | 0 | 0.05 | 0.07 | 0 | 0.04 | 0.08 | 0 | 0.04 | 0.09 | 0 | 0.04 |
| 116 | 0.06 | 0.01 | 0.04 | 0.11 | 0 | 0.04 | 0.09 | 0 | 0.05 | 0.09 | 0 | 0.06 | 0.1 | 0 | 0.04 | 0.1 | 0 | 0.03 |
| 117 | 0.07 | 0.02 | 0.04 | 0.12 | 0 | 0.05 | 0.12 | 0 | 0.05 | 0.09 | 0 | 0.06 | 0.1 | 0 | 0.04 | 0.1 | 0 | 0.03 |
| 118 | 0.07 | 0 | 0.03 | 0.12 | 0 | 0.04 | 0.11 | 0 | 0.05 | 0.09 | 0 | 0.05 | 0.09 | 0 | 0.04 | 0.09 | 0 | 0.04 |
| 119 | 0.06 | 0 | 0.04 | 0.14 | 0 | 0.05 | 0.11 | 0 | 0.05 | 0.09 | 0 | 0.05 | 0.09 | 0 | 0.04 | 0.1 | 0 | 0.04 |
| 120 | 0.07 | 0 | 0.04 | 0.12 | 0 | 0.05 | 0.12 | 0 | 0.05 | 0.12 | 0 | 0.05 | 0.1 | 0 | 0.04 | 0.08 | 0 | 0.03 |
| 121 | 0.07 | 0 | 0.03 | 0.13 | 0 | 0.05 | 0.1 | 0 | 0.05 | 0.1 | 0 | 0.05 | 0.09 | 0 | 0.03 | 0.09 | 0 | 0.03 |
| 122 | 0.06 | 0 | 0.03 | 0.12 | 0 | 0.05 | 0.09 | 0 | 0.04 | 0.1 | 0 | 0.05 | 0.1 | 0 | 0.04 | 0.1 | 0 | 0.03 |
| 123 | 0.06 | 0 | 0.04 | 0.08 | 0 | 0.05 | 0.1 | 0 | 0.04 | 0.09 | 0 | 0.05 | 0.1 | 0 | 0.04 | 0.11 | 0 | 0.04 |
| 124 | 0.05 | 0 | 0.03 | 0.13 | 0 | 0.05 | 0.08 | 0 | 0.04 | 0.09 | 0 | 0.05 | 0.09 | 0 | 0.04 | 0.09 | 0 | 0.04 |
| 125 | 0.05 | 0 | 0.02 | 0.12 | 0 | 0.05 | 0.08 | 0 | 0.04 | 0.1 | 0 | 0.05 | 0.09 | 0 | 0.04 | 0.12 | 0 | 0.03 |
| 126 | 0.04 | 0 | 0.02 | 0.1 | 0 | 0.05 | 0.08 | 0 | 0.04 | 0.09 | 0 | 0.05 | 0.08 | 0 | 0.03 | 0.11 | 0 | 0.04 |
| 127 | 0.04 | 0 | 0.02 | 0.09 | 0 | 0.05 | 0.08 | 0 | 0.05 | 0.11 | 0 | 0.05 | 0.09 | 0 | 0.03 | 0.09 | 0 | 0.04 |
| 128 | 0.04 | 0 | 0.02 | 0.12 | 0.02 | 0.05 | 0.08 | 0 | 0.05 | 0.09 | 0 | 0.05 | 0.08 | 0 | 0.04 | 0.1 | 0 | 0.04 |
| 129 | 0.06 | 0 | 0.03 | 0.11 | 0.02 | 0.05 | 0.11 | 0 | 0.05 | 0.1 | 0 | 0.05 | 0.08 | 0 | 0.03 | 0.08 | 0 | 0.04 |
| 130 | 0.06 | 0 | 0.04 | 0.13 | 0 | 0.05 | 0.08 | 0 | 0.05 | 0.1 | 0 | 0.06 | 0.09 | 0 | 0.04 | 0.1 | 0 | 0.04 |
| 131 | 0.06 | 0 | 0.04 | 0.13 | 0 | 0.05 | 0.09 | 0 | 0.06 | 0.11 | 0 | 0.06 | 0.07 | 0 | 0.03 | 0.11 | 0 | 0.05 |
| 132 | 0.06 | 0 | 0.04 | 0.14 | 0 | 0.05 | 0.11 | 0 | 0.05 | 0.1 | 0 | 0.06 | 0.08 | 0 | 0.04 | 0.09 | 0 | 0.04 |
| 133 | 0.07 | 0 | 0.04 | 0.1 | 0 | 0.05 | 0.11 | 0 | 0.05 | 0.09 | 0 | 0.06 | 0.09 | 0 | 0.03 | 0.09 | 0 | 0.05 |
| 134 | 0.1 | 0 | 0.04 | 0.13 | 0 | 0.05 | 0.1 | 0 | 0.05 | 0.12 | 0 | 0.06 | 0.09 | 0 | 0.04 | 0.1 | 0 | 0.04 |
| 135 | 0.1 | 0 | 0.06 | 0.13 | 0 | 0.05 | 0.12 | 0 | 0.05 | 0.08 | 0 | 0.06 | 0.09 | 0 | 0.03 | 0.11 | 0 | 0.04 |
| 136 | 0.09 | 0 | 0.05 | 0.12 | 0 | 0.05 | 0.09 | 0 | 0.05 | 0.1 | 0 | 0.06 | 0.08 | 0 | 0.03 | 0.09 | 0 | 0.04 |
| 137 | 0.11 | 0 | 0.05 | 0.13 | 0 | 0.05 | 0.1 | 0 | 0.05 | 0.1 | 0 | 0.05 | 0.08 | 0 | 0.03 | 0.09 | 0 | 0.04 |
| 138 | 0.12 | 0 | 0.05 | 0.13 | 0 | 0.05 | 0.09 | 0 | 0.05 | 0.1 | 0 | 0.05 | 0.07 | 0 | 0.03 | 0.1 | 0 | 0.04 |
| 139 | 0.1 | 0 | 0.04 | 0.14 | 0 | 0.05 | 0.1 | 0 | 0.05 | 0.09 | 0 | 0.05 | 0.06 | 0 | 0.03 | 0.08 | 0 | 0.04 |
| 140 | 0.09 | 0 | 0.04 | 0.14 | 0 | 0.05 | 0.09 | 0 | 0.05 | 0.11 | 0 | 0.05 | 0.07 | 0 | 0.03 | 0.11 | 0 | 0.04 |
| 141 | 0.08 | 0 | 0.05 | 0.13 | 0 | 0.04 | 0.12 | 0 | 0.05 | 0.09 | 0 | 0.05 | 0.07 | 0 | 0.04 | 0.09 | 0 | 0.04 |
| 142 | 0.09 | 0 | 0.05 | 0.15 | 0 | 0.05 | 0.1 | 0 | 0.05 | 0.09 | 0 | 0.05 | 0.07 | 0 | 0.03 | 0.1 | 0 | 0.04 |
| 143 | 0.08 | 0.02 | 0.05 | 0.11 | 0 | 0.05 | 0.11 | 0 | 0.05 | 0.09 | 0 | 0.05 | 0.08 | 0 | 0.03 | 0.09 | 0 | 0.04 |
| 144 | 0.09 | 0 | 0.05 | 0.13 | 0.01 | 0.06 | 0.12 | 0 | 0.05 | 0.1 | 0 | 0.06 | 0.08 | 0 | 0.04 | 0.1 | 0 | 0.04 |
| 145 | 0.09 | 0 | 0.05 | 0.12 | 0 | 0.05 | 0.09 | 0 | 0.05 | 0.11 | 0 | 0.06 | 0.09 | 0 | 0.03 | 0.09 | 0 | 0.04 |
| 146 | 0.11 | 0 | 0.05 | 0.13 | 0 | 0.05 | 0.09 | 0.03 | 0.05 | 0.24 | 0 | 0.06 | 0.06 | 0 | 0.05 | 0.11 | 0 | 0.04 |
| 147 | 0.09 | 0 | 0.05 | 0.1 | 0 | 0.05 | 0.09 | 0 | 0.05 | 0.18 | 0 | 0.06 | 0.08 | 0 | 0.04 | 0.09 | 0 | 0.04 |
| 148 | 0.1 | 0 | 0.05 | 0.09 | 0 | 0.05 | 0.1 | 0 | 0.05 | 0.1 | 0 | 0.06 | 0.08 | 0 | 0.04 | 0.08 | 0 | 0.04 |
| 149 | 0.09 | 0.03 | 0.05 | 0.08 | 0 | 0.05 | 0.1 | 0 | 0.05 | 0.09 | 0 | 0.06 | 0.09 | 0 | 0.04 | 0.09 | 0 | 0.04 |
| 150 | 0.08 | 0 | 0.05 | 0.1 | 0 | 0.05 | 0.11 | 0 | 0.04 | 0.08 | 0 | 0.06 | 0.1 | 0 | 0.04 | 0.09 | 0 | 0.04 |
| 151 | 0.08 | 0 | 0.04 | 0.12 | 0 | 0.05 | 0.11 | 0 | 0.03 | 0.08 | 0 | 0.06 | 0.09 | 0 | 0.03 | 0.1 | 0 | 0.04 |

| | | | | | | | | | | | | | | | | | |
|---|---|---|---|---|---|---|---|---|---|---|---|---|---|---|---|---|---|
| 152 | 0.07 | 0 | 0.04 | 0.11 | 0 | 0.05 | 0.1 | 0 | 0.03 | 0.07 | 0 | 0.06 | 0.1 | 0 | 0.04 | 0.1 | 0 | 0.05 |
| 153 | 0.11 | 0 | 0.05 | 0.11 | 0.03 | 0.06 | 0.11 | 0 | 0.04 | 0.09 | 0 | 0.05 | 9 | 0 | 0.04 | 0.07 | 0 | 0.04 |
| 154 | 0.08 | 0 | 0.04 | 0.11 | 0 | 0.05 | 0.11 | 0 | 0.04 | 0.08 | 0 | 0.04 | 0.09 | 0 | 0.04 | 0.1 | 0 | 0.04 |
| 155 | 0.07 | 0 | 0.03 | 0.11 | 0 | 0.05 | 0.11 | 0 | 0.04 | 0.08 | 0 | 0.04 | 0.09 | 0 | 0.04 | 0.1 | 0 | 0.04 |
| 156 | 0.07 | 0 | 0.03 | 0.09 | 0 | 0.05 | 0.06 | 0 | 0.04 | 0.08 | 0 | 0.04 | 0.08 | 0 | 0.03 | 0.09 | 0 | 0.04 |
| 157 | 0.06 | 0 | 0.04 | 0.1 | 0 | 0.05 | 0.07 | 0 | 0.04 | 0.08 | 0 | 0.05 | 0.09 | 0 | 0.04 | 0.1 | 0 | 0.05 |
| 158 | 0.06 | 0 | 0.04 | 0.09 | 0 | 0.05 | 0.06 | 0 | 0.04 | 0.09 | 0 | 0.05 | 0.09 | 0 | 0.04 | 0.1 | 0 | 0.05 |
| 159 | 0.06 | 0 | 0.03 | 0.09 | 0 | 0.05 | 0.11 | 0 | 0.05 | 0.08 | 0 | 0.04 | 0.08 | 0 | 0.03 | 0.1 | 0 | 0.04 |
| 160 | 0.07 | 0 | 0.04 | 0.09 | 0 | 0.05 | 0.11 | 0 | 0.06 | 0.09 | 0 | 0.04 | 0.11 | 0 | 0.04 | 0.09 | 0 | 0.04 |
| 161 | 0.08 | 0 | 0.03 | 0.09 | 0 | 0.05 | 0.08 | 0 | 0.06 | 0.09 | 0 | 0.03 | 0.09 | 0 | 0.04 | 0.08 | 0 | 0.05 |
| 162 | 0.1 | 0 | 0.04 | 0.1 | 0 | 0.04 | 0.08 | 0 | 0.07 | 0.08 | 0 | 0.04 | 0.08 | 0 | 0.04 | 0.09 | 0 | 0.05 |
| 163 | 0.09 | 0 | 0.04 | 0.09 | 0 | 0.04 | 0.12 | 0 | 0.06 | 0.1 | 0 | 0.04 | 0.1 | 0 | 0.04 | 0.11 | 0 | 0.05 |
| 164 | 0.1 | 0 | 0.05 | 0.1 | 0 | 0.04 | 0.12 | 0 | 0.05 | 0.08 | 0 | 0.05 | 0.1 | 0 | 0.04 | 0.09 | 0 | 0.04 |
| 165 | 0.11 | 0 | 0.05 | 0.09 | 0 | 0.04 | 0.11 | 0 | 0.05 | 0.07 | 0 | 0.04 | 0.09 | 0 | 0.04 | 0.09 | 0 | 0.04 |
| 166 | 0.11 | 0 | 0.05 | 0.09 | 0 | 0.04 | 0.1 | 0 | 0.05 | 0.09 | 0 | 0.04 | 0.09 | 0 | 0.04 | 0.08 | 0 | 0.04 |
| 167 | 0.09 | 0 | 0.05 | 0.08 | 0 | 0.03 | 0.1 | 0 | 0.05 | 0.1 | 0 | 0.04 | 0.09 | 0 | 0.04 | 0.09 | 0 | 0.05 |
| 168 | 0.11 | 0 | 0.05 | 0.11 | 0 | 0.04 | 0.1 | 0 | 0.04 | 0.1 | 0 | 0.04 | 0.09 | 0 | 0.05 | 0.08 | 0 | 0.04 |
| 169 | 0.09 | 0 | 0.05 | 0.1 | 0 | 0.04 | 0.1 | 0 | 0.05 | 0.09 | 0 | 0.04 | 0.09 | 0 | 0.04 | 0.09 | 0 | 0.04 |
| 170 | 0.09 | 0 | 0.06 | 0.12 | 0 | 0.04 | 0.1 | 0 | 0.04 | 0.1 | 0 | 0.05 | 0.09 | 0 | 0.05 | 0.1 | 0 | 0.04 |
| 171 | 0.09 | 0 | 0.05 | 0.13 | 0 | 0.05 | 0.06 | 0 | 0.03 | 0.09 | 0 | 0.04 | 0.09 | 0 | 0.04 | 0.09 | 0 | 0.04 |
| 172 | 0.1 | 0 | 0.05 | 0.1 | 0 | 0.05 | 0.09 | 0 | 0.04 | 0.09 | 0.01 | 0.06 | 0.08 | 0 | 0.04 | 0.1 | 0 | 0.05 |
| 173 | 0.08 | 0 | 0.05 | 0.09 | 0.1 | 0.05 | 0.11 | 0 | 0.05 | 0.09 | 0 | 0.06 | 0.08 | 0 | 0.04 | 0.09 | 0 | 0.04 |
| 174 | 0.09 | 0.02 | 0.05 | 0.09 | 0 | 0.05 | 0.11 | 0 | 0.05 | 0.1 | 0 | 0.06 | 0.07 | 0 | 0.04 | 0.09 | 0 | 0.04 |
| 175 | 0.09 | 0 | 0.06 | 0.11 | 0 | 0.05 | 0.09 | 0 | 0.04 | 0.08 | 0 | 0.04 | 0.11 | 0 | 0.04 | 0.09 | 0 | 0.03 |
| 176 | 0.1 | 0 | 0.05 | 0.11 | 0 | 0.04 | 0.08 | 0 | 0.03 | 0.09 | 0 | 0.04 | 0.09 | 0 | 0.05 | 0.09 | 0 | 0.03 |
| 177 | 0.07 | 0 | 0.05 | 0.1 | 0 | 0.05 | 0.14 | 0 | 0.05 | 0.08 | 0 | 0.04 | 0.1 | 0 | 0.04 | 0.09 | 0 | 0.04 |
| 178 | 0.08 | 0 | 0.04 | 0.09 | 0 | 0.05 | 0.08 | 0.03 | 0.05 | 0.11 | 0 | 0.04 | 0.1 | 0 | 0.04 | 0.09 | 0 | 0.04 |
| 179 | 0.07 | 0 | 0.04 | 0.08 | 0 | 0.05 | 0.08 | 0 | 0.05 | 0.08 | 0 | 0.04 | 0.1 | 0 | 0.04 | 0.11 | 0 | 0.04 |
| 180 | 0.07 | 0 | 0.04 | 0.09 | 0 | 0.05 | 0.09 | 0.02 | 0.06 | 0.1 | 0 | 0.04 | 0.09 | 0 | 0.04 | 0.09 | 0 | 0.04 |
| 181 | 0.07 | 0 | 0.04 | 0.08 | 0 | 0.05 | 0.1 | 0.01 | 0.05 | 0.08 | 0 | 0.03 | 0.09 | 0 | 0.05 | 0.08 | 0 | 0.04 |
| 182 | 0.07 | 0 | 0.03 | 0.09 | 0 | 0.05 | 0.12 | 0.02 | 0.05 | 0.09 | 0 | 0.04 | 0.09 | 0 | 0.04 | 0.08 | 0 | 0.03 |
| 183 | 0.07 | 0 | 0.04 | 0.07 | 0 | 0.04 | 0.12 | 0.02 | 0.05 | 0.1 | 0 | 0.04 | 0.1 | 0 | 0.04 | 0.08 | 0 | 0.04 |
| 184 | 0.06 | 0 | 0.04 | 0.08 | 0 | 0.04 | 0.1 | 0 | 0.05 | 0.11 | 0 | 0.04 | 0.09 | 0 | 0.05 | 0.09 | 0 | 0.04 |
| 185 | 0.06 | 0 | 0.04 | 0.08 | 0 | 0.05 | 0.12 | 0.01 | 0.05 | 0.1 | 0 | 0.04 | 0.09 | 0 | 0.04 | 0.1 | 0 | 0.04 |
| 186 | 0.07 | 0 | 0.04 | 0.08 | 0 | 0.05 | 0.11 | 0 | 0.05 | 0.09 | 0 | 0.04 | 0.1 | 0 | 0.04 | 0.1 | 0 | 0.04 |
| 187 | 0.06 | 0 | 0.04 | 0.09 | 0 | 0.05 | 0.09 | 0.02 | 0.05 | 0.1 | 0 | 0.05 | 0.12 | 0 | 0.05 | 0.08 | 0 | 0.04 |
| 188 | 0.06 | 0 | 0.03 | 0.09 | 0 | 0.05 | 0.08 | 0 | 0.05 | 0.11 | 0 | 0.04 | 0.12 | 0 | 0.04 | 0.1 | 0 | 0.04 |
| 189 | 0.07 | 0.02 | 0.04 | 0.1 | 0 | 0.04 | 0.11 | 0 | 0.06 | 0.12 | 0 | 0.05 | 0.11 | 0 | 0.04 | 0.08 | 0 | 0.04 |
| 190 | 0.06 | 0 | 0.04 | 0.09 | 0 | 0.04 | 0.12 | 0 | 0.07 | 0.08 | 0 | 0.04 | 0.1 | 0 | 0.04 | 0.08 | 0 | 0.04 |

| | | | | | | | | | | | | | | | | | |
|---|---|---|---|---|---|---|---|---|---|---|---|---|---|---|---|---|---|
| 191 | 0.08 | 0 | 0.05 | 0.1 | 0 | 0.04 | 0.1 | 0 | 0.06 | 0.09 | 0 | 0.04 | 0.11 | 0 | 0.04 | 0.09 | 0 | 0.04 |
| 192 | 0.11 | 0 | 0.06 | 0.1 | 0 | 0.05 | 0.1 | 0 | 0.05 | 0.1 | 0 | 0.04 | 0.12 | 0 | 0.05 | 0.07 | 0 | 0.03 |
| 193 | 0.11 | 0 | 0.06 | 0.13 | 0 | 0.05 | 0.1 | 0.1 | 0.05 | 0.09 | 0 | 0.04 | 0.11 | 0 | 0.04 | 0.09 | 0 | 0.04 |
| 194 | 0.09 | 0 | 0.05 | 0.13 | 0 | 0.05 | 0.08 | 0 | 0.03 | 0.1 | 0 | 0.04 | 0.09 | 0 | 0.03 | 0.08 | 0 | 0.03 |
| 195 | 0.11 | 0 | 0.06 | 0.12 | 0 | 0.05 | 0.08 | 0 | 0.03 | 0.1 | 0 | 0.04 | 0.09 | 0 | 0.03 | 0.08 | 0 | 0.03 |
| 196 | 0.08 | 0 | 0.05 | 0.13 | 0 | 0.05 | 0.1 | 0 | 0.04 | 0.11 | 0 | 0.04 | 0.1 | 0 | 0.03 | 0.08 | 0 | 0.03 |
| 197 | 0.09 | 0 | 0.05 | 0.09 | 0 | 0.05 | 0.09 | 0 | 0.04 | 0.09 | 0 | 0.04 | 0.1 | 0 | 0.03 | 0.11 | 0 | 0.04 |
| 198 | 0.1 | 0 | 0.06 | 0.09 | 0 | 0.05 | 0.09 | 0 | 0.03 | 0.1 | 0 | 0.04 | 0.09 | 0 | 0.04 | 0.07 | 0 | 0.03 |
| 199 | 0.11 | 0 | 0.05 | 0.1 | 0 | 0.05 | 0.08 | 0 | 0.03 | 0.12 | 0 | 0.04 | 0.1 | 0 | 0.04 | 0.08 | 0 | 0.03 |
| 200 | 0.1 | 0.03 | 0.06 | 0.1 | 0 | 0.04 | 0.08 | 0 | 0.03 | 0.08 | 0 | 0.04 | 0.1 | 0 | 0.05 | 0.08 | 0 | 0.03 |

| | | | | | | | | | | | | | | | | | | |
|---|---|---|---|---|---|---|---|---|---|---|---|---|---|---|---|---|---|---|
| | | | | | Control (mm) | | | | | | | | Infected (mm) | | | | | |
| Day 1 | | R1 | | | R2 | | | R3 | | | R1 | | | R2 | | | R3 | |
| | | Max | Min | Average | Max | Min | Average | Max | Min | Average | Max | Min | Average | Max | Min | Average | Max | Min | Average |
| | 1 | 0.04 | 0 | 0.02 | 0.06 | 0 | 0.03 | 0.05 | 0 | 0.03 | 0.13 | 0.02 | 0.07 | 0.15 | 0 | 0.06 | 0.09 | 0 | 0.05 |
| | 2 | 0.04 | 0 | 0.01 | 0.06 | 0 | 0.03 | 0.05 | 0 | 0.03 | 0.12 | 0 | 0.06 | 0.15 | 0 | 0.06 | 0.11 | 0 | 0.05 |
| | 3 | 0.06 | 0 | 0.02 | 0.06 | 0 | 0.02 | 0.05 | 0 | 0.02 | 0.14 | 0 | 0.07 | 0.14 | 0 | 0.06 | 0.09 | 0 | 0.05 |
| | 4 | 0.05 | 0 | 0.03 | 0.06 | 0 | 0.03 | 0.06 | 0 | 0.03 | 0.13 | 0 | 0.06 | 0.13 | 0 | 0.06 | 0.11 | 0 | 0.05 |
| | 5 | 0.05 | 0 | 0.03 | 0.06 | 0 | 0.02 | 0.05 | 0 | 0.01 | 0.14 | 0 | 0.06 | 0.12 | 0 | 0.06 | 0.11 | 0 | 0.05 |
| | 6 | 0.05 | 0 | 0.02 | 0.07 | 0 | 0.02 | 0.07 | 0 | 0.02 | 0.12 | 0 | 0.06 | 0.12 | 0 | 0.06 | 0.11 | 0 | 0.05 |
| | 7 | 0.04 | 0 | 0.02 | 0.07 | 0 | 0.03 | 0.07 | 0 | 0.02 | 0.11 | 0 | 0.06 | 0.12 | 0 | 0.06 | 0.1 | 0 | 0.05 |
| | 8 | 0.04 | 0 | 0.02 | 0.07 | 0 | 0.02 | 0.07 | 0 | 0.02 | 0.11 | 0 | 0.06 | 0.13 | 0 | 0.06 | 0.12 | 0 | 0.05 |
| | 9 | 0.06 | 0 | 0.03 | 0.06 | 0 | 0.02 | 0.05 | 0 | 0.02 | 0.12 | 0 | 0.06 | 0.12 | 0 | 0.07 | 0.12 | 0 | 0.05 |
| | 10 | 0.05 | 0 | 0.02 | 0.05 | 0 | 0.03 | 0.04 | 0 | 0.02 | 0.12 | 0 | 0.06 | 0.13 | 0 | 0.06 | 0.11 | 0 | 0.06 |
| | 11 | 0.07 | 0 | 0.02 | 0.06 | 0 | 0.03 | 0.04 | 0 | 0.02 | 0.12 | 0 | 0.06 | 0.11 | 0 | 0.06 | 0.12 | 0 | 0.05 |
| | 12 | 0.05 | 0 | 0.03 | 0.06 | 0 | 0.02 | 0.07 | 0 | 0.02 | 0.11 | 0 | 0.06 | 0.11 | 0 | 0.06 | 0.12 | 0 | 0.05 |
| | 13 | 0.06 | 0 | 0.02 | 0.05 | 0 | 0.02 | 0.04 | 0 | 0.02 | 0.13 | 0 | 0.06 | 0.1 | 0 | 0.06 | 0.12 | 0 | 0.06 |
| | 14 | 0.05 | 0 | 0.02 | 0.05 | 0 | 0.02 | 0.04 | 0 | 0.01 | 0.12 | 0 | 0.05 | 0.13 | 0 | 0.07 | 0.13 | 0 | 0.06 |
| | 15 | 0.07 | 0 | 0.03 | 0.04 | 0 | 0.02 | 0.05 | 0 | 0.03 | 0.11 | 0 | 0.06 | 0.1 | 0 | 0.06 | 0.14 | 0 | 0.06 |
| | 16 | 0.05 | 0 | 0.03 | 0.05 | 0 | 0.02 | 0.07 | 0 | 0.03 | 0.12 | 0 | 0.05 | 0.11 | 0 | 0.06 | 0.11 | 0 | 0.06 |
| | 17 | 0.09 | 0 | 0.02 | 0.06 | 0 | 0.02 | 0.09 | 0 | 0.03 | 0.11 | 0 | 0.05 | 0.11 | 0 | 0.06 | 0.12 | 0 | 0.06 |
| | 18 | 0.01 | 0 | 0.03 | 0.06 | 0 | 0.02 | 0.07 | 0 | 0.03 | 0.11 | 0 | 0.05 | 0.1 | 0 | 0.05 | 0.12 | 0 | 0.06 |
| | 19 | 0.07 | 0 | 0.03 | 0.05 | 0 | 0.02 | 0.15 | 0 | 0.03 | 0.13 | 0 | 0.05 | 0.12 | 0 | 0.07 | 0.13 | 0 | 0.06 |
| | 20 | 0.04 | 0 | 0.02 | 0.05 | 0 | 0.02 | 0.05 | 0 | 0.03 | 0.11 | 0 | 0.05 | 0.11 | 0 | 0.06 | 0.2 | 0 | 0.06 |
| | 21 | 0.05 | 0 | 0.02 | 0.04 | 0 | 0.03 | 0.02 | 0 | 0.04 | 0.12 | 0 | 0.05 | 0.1 | 0 | 0.06 | 0.12 | 0 | 0.05 |

| | | | | | | | | | | | | | | | | | |
|---|---|---|---|---|---|---|---|---|---|---|---|---|---|---|---|---|---|
| 22 | 0.05 | 0 | 0.02 | 0.07 | 0 | 0.03 | 0.19 | 0 | 0.03 | 0.11 | 0 | 0.05 | 0.13 | 0 | 0.06 | 0.12 | 0 | 0.05 |
| 23 | 0.05 | 0 | 0.02 | 0.08 | 0 | 0.03 | 0.04 | 0 | 0.02 | 0.13 | 0 | 0.06 | 0.1 | 0 | 0.06 | 0.12 | 0 | 0.05 |
| 24 | 0.06 | 0 | 0.02 | 0.06 | 0 | 0.02 | 0.11 | 0 | 0.02 | 0.13 | 0 | 0.06 | 0.12 | 0 | 0.05 | 0.1 | 0 | 0.05 |
| 25 | 0.05 | 0 | 0.02 | 0.06 | 0 | 0.02 | 0.13 | 0 | 0.02 | 0.13 | 0 | 0.06 | 0.11 | 0 | 0.06 | 0.12 | 0 | 0.06 |
| 26 | 0.05 | 0 | 0.03 | 0.06 | 0 | 0.02 | 0.15 | 0 | 0.03 | 0.16 | 0 | 0.06 | 0.23 | 0 | 0.07 | 0.11 | 0 | 0.05 |
| 27 | 0.05 | 0 | 0.03 | 0.07 | 0 | 0.03 | 0.09 | 0 | 0.03 | 0.16 | 0 | 0.06 | 0.1 | 0 | 0.06 | 0.19 | 0 | 0.05 |
| 28 | 0.05 | 0 | 0.03 | 0.06 | 0 | 0.02 | 0.17 | 0 | 0.03 | 0.16 | 0 | 0.07 | 0.13 | 0 | 0.05 | 0.22 | 0 | 0.06 |
| 29 | 0.07 | 0 | 0.03 | 0.08 | 0 | 0.02 | 0.05 | 0 | 0.02 | 0.15 | 0 | 0.06 | 0.16 | 0 | 0.06 | 0.13 | 0 | 0.04 |
| 30 | 0.07 | 0 | 0.03 | 0.05 | 0 | 0.03 | 0.04 | 0 | 0.02 | 0.17 | 0 | 0.06 | 0.09 | 0 | 0.05 | 0.1 | 0 | 0.04 |
| 31 | 0.06 | 0 | 0.02 | 0.05 | 0 | 0.02 | 0.05 | 0 | 0.03 | 0.14 | 0 | 0.06 | 0.13 | 0 | 0.06 | 0.13 | 0 | 0.05 |
| 32 | 0.07 | 0 | 0.02 | 0.05 | 0 | 0.03 | 0.06 | 0 | 0.02 | 0.13 | 0 | 0.06 | 0.14 | 0 | 0.06 | 0.1 | 0 | 0.05 |
| 33 | 0.04 | 0 | 0.02 | 0.06 | 0 | 0.03 | 0.06 | 0 | 0.03 | 0.16 | 0 | 0.05 | 0.13 | 0 | 0.06 | 0.1 | 0 | 0.04 |
| 34 | 0.05 | 0 | 0.02 | 0.06 | 0 | 0.04 | 0.07 | 0 | 0.03 | 0.14 | 0 | 0.05 | 0.13 | 0 | 0.06 | 0.13 | 0 | 0.06 |
| 35 | 0.05 | 0 | 0.02 | 0.05 | 0 | 0.03 | 0.07 | 0 | 0.03 | 0.13 | 0 | 0.05 | 0.12 | 0 | 0.06 | 0.22 | 0 | 0.06 |
| 36 | 0.06 | 0 | 0.03 | 0.05 | 0 | 0.03 | 0.08 | 0 | 0.03 | 0.15 | 0 | 0.05 | 0.11 | 0 | 0.05 | 0.11 | 0 | 0.06 |
| 37 | 0.05 | 0 | 0.03 | 0.08 | 0 | 0.02 | 0.08 | 0 | 0.03 | 0.15 | 0 | 0.06 | 0.12 | 0 | 0.06 | 0.14 | 0 | 0.06 |
| 38 | 0.05 | 0 | 0.03 | 0.08 | 0 | 0.03 | 0.06 | 0 | 0.03 | 0.13 | 0 | 0.05 | 0.12 | 0 | 0.05 | 0.13 | 0 | 0.06 |
| 39 | 0.06 | 0 | 0.03 | 0.08 | 0 | 0.03 | 0.07 | 0 | 0.03 | 0.16 | 0 | 0.06 | 0.11 | 0 | 0.05 | 0.12 | 0 | 0.06 |
| 40 | 0.05 | 0 | 0.02 | 0.07 | 0 | 0.03 | 0.06 | 0 | 0.03 | 0.14 | 0 | 0.05 | 0.12 | 0 | 0.05 | 0.12 | 0 | 0.07 |
| 41 | 0.06 | 0 | 0.03 | 0.08 | 0 | 0.02 | 0.04 | 0 | 0.02 | 0.15 | 0 | 0.05 | 0.11 | 0 | 0.07 | 0.12 | 0 | 0.07 |
| 42 | 0.07 | 0 | 0.03 | 0.07 | 0 | 0.03 | 0.09 | 0 | 0.02 | 0.12 | 0 | 0.06 | 0.12 | 0 | 0.06 | 0.14 | 0 | 0.06 |
| 43 | 0.08 | 0 | 0.03 | 0.08 | 0 | 0.04 | 0.05 | 0 | 0.02 | 0.12 | 0 | 0.06 | 0.12 | 0 | 0.06 | 0.14 | 0 | 0.06 |
| 44 | 0.06 | 0 | 0.03 | 0.08 | 0 | 0.04 | 0.05 | 0 | 0.02 | 0.13 | 0 | 0.06 | 0.14 | 0 | 0.07 | 0.12 | 0 | 0.06 |
| 45 | 0.06 | 0 | 0.03 | 0.07 | 0 | 0.03 | 0.03 | 0 | 0.01 | 0.27 | 0 | 0.08 | 0.12 | 0 | 0.06 | 0.11 | 0 | 0.06 |
| 46 | 0.06 | 0 | 0.03 | 0.09 | 0 | 0.03 | 0.04 | 0 | 0.03 | 0.11 | 0 | 0.06 | 0.17 | 0 | 0.06 | 0.11 | 0 | 0.06 |
| 47 | 0.06 | 0 | 0.03 | 0.09 | 0 | 0.04 | 0.05 | 0 | 0.02 | 0.11 | 0 | 0.06 | 0.12 | 0 | 0.06 | 0.14 | 0 | 0.06 |
| 48 | 0.06 | 0 | 0.03 | 0.09 | 0 | 0.03 | 0.05 | 0 | 0.02 | 0.13 | 0 | 0.06 | 0.15 | 0 | 0.06 | 0.15 | 0 | 0.06 |
| 49 | 0.05 | 0 | 0.03 | 0.08 | 0 | 0.03 | 0.05 | 0 | 0.02 | 0.12 | 0 | 0.07 | 0.11 | 0 | 0.06 | 0.14 | 0 | 0.05 |
| 50 | 0.06 | 0 | 0.03 | 0.06 | 0 | 0.03 | 0.04 | 0 | 0.02 | 0.13 | 0 | 0.07 | 0.15 | 0 | 0.05 | 0.13 | 0 | 0.05 |
| 51 | 0.06 | 0 | 0.03 | 0.06 | 0 | 0.03 | 0.03 | 0 | 0.01 | 0.14 | 0 | 0.06 | 0.12 | 0 | 0.05 | 0.13 | 0 | 0.06 |
| 52 | 0.07 | 0 | 0.03 | 0.05 | 0 | 0.02 | 0.03 | 0 | 0.01 | 0.14 | 0 | 0.06 | 0.11 | 0 | 0.06 | 0.11 | 0 | 0.06 |
| 53 | 0.06 | 0 | 0.03 | 0.06 | 0 | 0.03 | 0.04 | 0 | 0.02 | 0.12 | 0 | 0.06 | 0.1 | 0 | 0.06 | 0.14 | 0 | 0.06 |
| 54 | 0.05 | 0 | 0.03 | 0.06 | 0 | 0.03 | 0.03 | 0 | 0.01 | 0.11 | 0 | 0.06 | 0.15 | 0 | 0.06 | 0.22 | 0 | 0.06 |
| 55 | 0.07 | 0 | 0.02 | 0.06 | 0 | 0.03 | 0.04 | 0 | 0.02 | 0.12 | 0 | 0.06 | 0.16 | 0 | 0.07 | 0.14 | 0 | 0.06 |
| 56 | 0.08 | 0 | 0.02 | 0.06 | 0 | 0.02 | 0.03 | 0 | 0.02 | 0.12 | 0 | 0.06 | 0.14 | 0 | 0.07 | 0.15 | 0 | 0.06 |
| 57 | 0.06 | 0 | 0.03 | 0.07 | 0 | 0.03 | 0.05 | 0 | 0.02 | 0.13 | 0 | 0.06 | 0.23 | 0 | 0.06 | 0.13 | 0 | 0.06 |
| 58 | 0.08 | 0 | 0.03 | 0.05 | 0 | 0.02 | 0.08 | 0 | 0.04 | 0.11 | 0 | 0.06 | 0.14 | 0 | 0.07 | 0.18 | 0 | 0.05 |
| 59 | 0.07 | 0 | 0.02 | 0.06 | 0 | 0.02 | 0.09 | 0 | 0.05 | 0.12 | 0 | 0.06 | 0.17 | 0 | 0.07 | 0.15 | 0 | 0.07 |
| 60 | 0.08 | 0 | 0.03 | 0.05 | 0 | 0.02 | 0.09 | 0 | 0.05 | 0.12 | 0 | 0.06 | 0.15 | 0 | 0.06 | 0.15 | 0 | 0.06 |

| | | | | | | | | | | | | | | | | | |
|---|---|---|---|---|---|---|---|---|---|---|---|---|---|---|---|---|---|
| 61 | 0.06 | 0 | 0.03 | 0.06 | 0 | 0.03 | 0.08 | 0 | 0.04 | 0.12 | 0 | 0.06 | 0.13 | 0 | 0.06 | 0.13 | 0 | 0.07 |
| 62 | 0.08 | 0 | 0.03 | 0.07 | 0 | 0.03 | 0.08 | 0 | 0.04 | 0.12 | 0 | 0.06 | 0.12 | 0 | 0.05 | 0.13 | 0 | 0.06 |
| 63 | 0.07 | 0 | 0.03 | 0.08 | 0 | 0.03 | 0.08 | 0 | 0.04 | 0.13 | 0 | 0.06 | 0.11 | 0 | 0.06 | 0.15 | 0 | 0.07 |
| 64 | 0.08 | 0 | 0.03 | 0.07 | 0 | 0.03 | 0.07 | 0 | 0.04 | 0.11 | 0 | 0.06 | 0.14 | 0 | 0.05 | 0.12 | 0 | 0.07 |
| 65 | 0.08 | 0 | 0.04 | 0.07 | 0 | 0.02 | 0.07 | 0 | 0.04 | 0.1 | 0 | 0.06 | 0.14 | 0 | 0.06 | 0.15 | 0 | 0.07 |
| 66 | 0.08 | 0 | 0.03 | 0.07 | 0 | 0.02 | 0.06 | 0 | 0.04 | 0.12 | 0 | 0.06 | 0.14 | 0 | 0.06 | 0.16 | 0 | 0.07 |
| 67 | 0.11 | 0 | 0.03 | 0.07 | 0 | 0.03 | 0.07 | 0 | 0.04 | 0.13 | 0 | 0.06 | 0.21 | 0 | 0.06 | 0.27 | 0 | 0.07 |
| 68 | 0.11 | 0 | 0.04 | 0.06 | 0 | 0.03 | 0.07 | 0.02 | 0.03 | 0.13 | 0 | 0.06 | 0.13 | 0 | 0.05 | 0.16 | 0 | 0.07 |
| 69 | 0.1 | 0 | 0.03 | 0.07 | 0 | 0.03 | 0.06 | 0 | 0.03 | 0.14 | 0 | 0.06 | 0.13 | 0 | 0.05 | 0.14 | 0.02 | 0.07 |
| 70 | 0.11 | 0 | 0.04 | 0.06 | 0 | 0.02 | 0.06 | 0 | 0.03 | 0.14 | 0 | 0.05 | 0.14 | 0 | 0.06 | 0.12 | 0 | 0.06 |
| 71 | 0.09 | 0 | 0.04 | 0.05 | 0 | 0.02 | 0.05 | 0 | 0.03 | 0.1 | 0 | 0.05 | 0.13 | 0 | 0.06 | 0.12 | 0 | 0.06 |
| 72 | 0.09 | 0 | 0.04 | 0.08 | 0 | 0.02 | 0.04 | 0 | 0.02 | 0.13 | 0 | 0.05 | 0.12 | 0 | 0.06 | 0.14 | 0 | 0.06 |
| 73 | 0.1 | 0 | 0.03 | 0.07 | 0 | 0.03 | 0.04 | 0 | 0.02 | 0.12 | 0 | 0.06 | 0.11 | 0 | 0.06 | 0.12 | 0 | 0.06 |
| 74 | 0.09 | 0 | 0.03 | 0.06 | 0 | 0.03 | 0.04 | 0 | 0.01 | 0.12 | 0 | 0.06 | 0.13 | 0 | 0.06 | 0.12 | 0 | 0.06 |
| 75 | 0.09 | 0 | 0.04 | 0.08 | 0 | 0.03 | 0.04 | 0 | 0.02 | 0.11 | 0 | 0.06 | 0.12 | 0 | 0.06 | 0.13 | 0 | 0.06 |
| 76 | 0.1 | 0 | 0.04 | 0.08 | 0 | 0.03 | 0.04 | 0 | 0.02 | 0.15 | 0 | 0.06 | 0.11 | 0 | 0.05 | 0.11 | 0.02 | 0.06 |
| 77 | 0.09 | 0 | 0.03 | 0.07 | 0 | 0.03 | 0.04 | 0 | 0.02 | 0.15 | 0 | 0.06 | 0.12 | 0 | 0.05 | 0.1 | 0 | 0.06 |
| 78 | 0.11 | 0 | 0.04 | 0.08 | 0 | 0.03 | 0.04 | 0 | 0.01 | 0.12 | 0 | 0.06 | 0.12 | 0 | 0.05 | 0.1 | 0 | 0.06 |
| 79 | 0.11 | 0 | 0.04 | 0.07 | 0 | 0.03 | 0.06 | 0 | 0.02 | 0.13 | 0 | 0.06 | 0.15 | 0 | 0.06 | 0.13 | 0 | 0.05 |
| 80 | 0.09 | 0 | 0.04 | 0.09 | 0 | 0.03 | 0.09 | 0 | 0.04 | 0.11 | 0 | 0.06 | 0.15 | 0 | 0.06 | 0.11 | 0 | 0.05 |
| 81 | 0.08 | 0 | 0.03 | 0.08 | 0 | 0.03 | 0.08 | 0 | 0.05 | 0.11 | 0 | 0.05 | 0.76 | 0 | 0.13 | 0.1 | 0 | 0.06 |
| 82 | 0.08 | 0 | 0.03 | 0.09 | 0 | 0.03 | 0.09 | 0 | 0.04 | 0.13 | 0 | 0.06 | 0.13 | 0 | 0.06 | 0.11 | 0 | 0.06 |
| 83 | 0.09 | 0 | 0.03 | 0.1 | 0 | 0.03 | 0.07 | 0 | 0.03 | 0.15 | 0 | 0.07 | 0.11 | 0 | 0.06 | 0.1 | 0 | 0.06 |
| 84 | 0.11 | 0 | 0.04 | 0.09 | 0 | 0.03 | 0.08 | 0 | 0.03 | 0.13 | 0 | 0.06 | 0.12 | 0 | 0.05 | 0.2 | 0 | 0.07 |
| 85 | 0.1 | 0 | 0.04 | 0.07 | 0 | 0.03 | 0.09 | 0 | 0.03 | 0.12 | 0 | 0.06 | 0.11 | 0 | 0.06 | 0.12 | 0.01 | 0.06 |
| 86 | 0.08 | 0 | 0.03 | 0.07 | 0 | 0.03 | 0.08 | 0 | 0.03 | 0.11 | 0 | 0.06 | 0.12 | 0 | 0.06 | 0.11 | 0.03 | 0.06 |
| 87 | 0.09 | 0 | 0.03 | 0.06 | 0 | 0.03 | 0.08 | 0 | 0.04 | 0.11 | 0 | 0.06 | 0.13 | 0 | 0.06 | 0.11 | 0 | 0.06 |
| 88 | 0.09 | 0 | 0.03 | 0.07 | 0 | 0.03 | 0.13 | 0 | 0.04 | 0.12 | 0 | 0.06 | 0.12 | 0 | 0.06 | 0.12 | 0 | 0.06 |
| 89 | 0.09 | 0 | 0.04 | 0.07 | 0 | 0.03 | 0.09 | 0 | 0.03 | 0.13 | 0 | 0.06 | 0.13 | 0 | 0.06 | 0.13 | 0 | 0.05 |
| 90 | 0.09 | 0 | 0.04 | 0.08 | 0 | 0.03 | 0.06 | 0 | 0.01 | 0.12 | 0 | 0.06 | 0.11 | 0 | 0.06 | 0.11 | 0 | 0.06 |
| 91 | 0.13 | 0 | 0.04 | 0.07 | 0 | 0.04 | 0.03 | 0 | 0.01 | 0.15 | 0 | 0.06 | 0.11 | 0 | 0.06 | 0.12 | 0 | 0.06 |
| 92 | 0.13 | 0 | 0.04 | 0.08 | 0 | 0.04 | 0.04 | 0 | 0.02 | 0.15 | 0 | 0.06 | 0.13 | 0 | 0.06 | 0.12 | 0 | 0.06 |
| 93 | 0.14 | 0 | 0.05 | 0.07 | 0 | 0.03 | 0.04 | 0 | 0.02 | 0.14 | 0 | 0.06 | 0.13 | 0 | 0.06 | 0.13 | 0 | 0.06 |
| 94 | 0.14 | 0 | 0.05 | 0.06 | 0 | 0.03 | 0.04 | 0 | 0.02 | 0.14 | 0 | 0.05 | 0.11 | 0 | 0.06 | 0.11 | 0 | 0.06 |
| 95 | 0.14 | 0 | 0.03 | 0.08 | 0 | 0.04 | 0.03 | 0 | 0.01 | 0.15 | 0 | 0.06 | 0.1 | 0 | 0.06 | 0.26 | 0 | 0.07 |
| 96 | 0.12 | 0 | 0.04 | 0.07 | 0 | 0.04 | 0.04 | 0 | 0.02 | 0.12 | 0 | 0.06 | 0.09 | 0 | 0.06 | 0.13 | 0 | 0.07 |
| 97 | 0.11 | 0 | 0.04 | 0.11 | 0 | 0.06 | 0.04 | 0 | 0.01 | 0.1 | 0 | 0.06 | 0.1 | 0 | 0.06 | 0.12 | 0 | 0.06 |
| 98 | 0.1 | 0 | 0.04 | 0.15 | 0 | 0.06 | 0.03 | 0 | 0.02 | 0.14 | 0 | 0.05 | 0.09 | 0 | 0.05 | 0.14 | 0 | 0.06 |
| 99 | 0.09 | 0 | 0.04 | 0.08 | 0 | 0.04 | 0.05 | 0 | 0.03 | 0.11 | 0 | 0.06 | 0.09 | 0 | 0.05 | 0.13 | 0 | 0.05 |

| | | | | | | | | | | | | | | | | | |
|---|---|---|---|---|---|---|---|---|---|---|---|---|---|---|---|---|---|
| 100 | 0.12 | 0 | 0.04 | 0.08 | 0 | 0.03 | 0.05 | 0 | 0.03 | 0.1 | 0 | 0.05 | 0.25 | 0 | 0.06 | 0.13 | 0 | 0.05 |
| 101 | 0.11 | 0 | 0.04 | 0.07 | 0 | 0.04 | 0.06 | 0 | 0.03 | 0.12 | 0 | 0.06 | 0.11 | 0 | 0.05 | 0.11 | 0 | 0.06 |
| 102 | 0.12 | 0 | 0.04 | 0.07 | 0 | 0.04 | 0.06 | 0 | 0.03 | 0.11 | 0 | 0.05 | 0.28 | 0 | 0.07 | 0.15 | 0 | 0.06 |
| 103 | 0.11 | 0 | 0.04 | 0.08 | 0 | 0.04 | 0.07 | 0 | 0.04 | 0.1 | 0 | 0.06 | 0.12 | 0 | 0.06 | 0.11 | 0 | 0.05 |
| 104 | 0.11 | 0 | 0.04 | 0.07 | 0 | 0.04 | 0.07 | 0 | 0.05 | 0.12 | 0 | 0.06 | 0.09 | 0 | 0.05 | 0.11 | 0 | 0.05 |
| 105 | 0.11 | 0 | 0.05 | 0.07 | 0 | 0.04 | 0.09 | 0.02 | 0.04 | 0.12 | 0 | 0.06 | 0.14 | 0 | 0.06 | 0.12 | 0 | 0.05 |
| 106 | 0.09 | 0 | 0.04 | 0.08 | 0 | 0.04 | 0.06 | 0.01 | 0.04 | 0.14 | 0 | 0.06 | 0.13 | 0 | 0.05 | 0.12 | 0 | 0.05 |
| 107 | 0.1 | 0 | 0.04 | 0.09 | 0 | 0.04 | 0.06 | 0 | 0.03 | 0.12 | 0 | 0.06 | 0.12 | 0 | 0.05 | 0.13 | 0 | 0.06 |
| 108 | 0.09 | 0 | 0.04 | 0.09 | 0 | 0.04 | 0.07 | 0.01 | 0.04 | 0.11 | 0 | 0.06 | 0.12 | 0 | 0.05 | 0.13 | 0 | 0.06 |
| 109 | 0.08 | 0 | 0.04 | 0.08 | 0 | 0.04 | 0.05 | 0 | 0.04 | 0.13 | 0 | 0.06 | 0.11 | 0 | 0.05 | 0.11 | 0 | 0.06 |
| 110 | 0.08 | 0 | 0.04 | 0.09 | 0 | 0.04 | 0.08 | 0 | 0.04 | 0.12 | 0 | 0.06 | 0.14 | 0 | 0.05 | 0.14 | 0 | 0.06 |
| 111 | 0.09 | 0 | 0.04 | 0.09 | 0 | 0.04 | 0.1 | 0 | 0.04 | 0.12 | 0 | 0.05 | 0.13 | 0 | 0.05 | 0.11 | 0 | 0.07 |
| 112 | 0.09 | 0 | 0.04 | 0.09 | 0 | 0.04 | 0.1 | 0 | 0.04 | 0.1 | 0 | 0.05 | 0.13 | 0 | 0.05 | 0.12 | 0 | 0.05 |
| 113 | 0.09 | 0 | 0.04 | 0.09 | 0 | 0.04 | 0.7 | 0.01 | 0.04 | 0.13 | 0 | 0.06 | 0.16 | 0 | 0.06 | 0.12 | 0 | 0.06 |
| 114 | 0.11 | 0 | 0.04 | 0.09 | 0 | 0.04 | 0.05 | 0 | 0.03 | 0.12 | 0 | 0.05 | 0.12 | 0 | 0.06 | 0.11 | 0 | 0.05 |
| 115 | 0.11 | 0 | 0.04 | 0.11 | 0 | 0.04 | 0.06 | 0 | 0.02 | 0.09 | 0 | 0.05 | 0.13 | 0 | 0.05 | 0.11 | 0 | 0.05 |
| 116 | 0.1 | 0 | 0.04 | 0.08 | 0 | 0.04 | 0.07 | 0 | 0.03 | 0.11 | 0 | 0.05 | 0.14 | 0 | 0.05 | 0.1 | 0 | 0.04 |
| 117 | 0.09 | 0 | 0.04 | 0.09 | 0 | 0.04 | 0.07 | 0 | 0.03 | 0.12 | 0 | 0.04 | 0.11 | 0 | 0.06 | 0.11 | 0 | 0.05 |
| 118 | 0.09 | 0 | 0.04 | 0.1 | 0 | 0.04 | 0.05 | 0 | 0.02 | 0.12 | 0 | 0.04 | 0.11 | 0 | 0.06 | 0.1 | 0 | 0.05 |
| 119 | 0.09 | 0 | 0.05 | 0.1 | 0 | 0.05 | 0.05 | 0 | 0.01 | 0.11 | 0 | 0.05 | 0.22 | 0 | 0.06 | 0.1 | 0 | 0.05 |
| 120 | 0.08 | 0 | 0.04 | 0.09 | 0 | 0.04 | 0.05 | 0 | 0.02 | 0.11 | 0 | 0.05 | 0.1 | 0 | 0.05 | 0.6 | 0 | 0.1 |
| 121 | 0.09 | 0 | 0.04 | 0.08 | 0 | 0.04 | 0.06 | 0 | 0.03 | 0.11 | 0 | 0.05 | 0.11 | 0 | 0.06 | 0.13 | 0 | 0.06 |
| 122 | 0.1 | 0 | 0.05 | 0.09 | 0 | 0.04 | 0.06 | 0 | 0.03 | 0.14 | 0 | 0.05 | 0.12 | 0 | 0.05 | 0.09 | 0 | 0.05 |
| 123 | 0.14 | 0 | 0.05 | 0.09 | 0 | 0.04 | 0.09 | 0 | 0.04 | 0.13 | 0 | 0.05 | 0.11 | 0 | 0.05 | 0.12 | 0 | 0.06 |
| 124 | 0.13 | 0 | 0.05 | 0.09 | 0 | 0.04 | 0.12 | 0 | 0.05 | 0.13 | 0 | 0.05 | 0.15 | 0.01 | 0.06 | 0.11 | 0 | 0.06 |
| 125 | 0.13 | 0 | 0.04 | 0.1 | 0 | 0.04 | 0.12 | 0 | 0.05 | 0.12 | 0 | 0.05 | 0.12 | 0 | 0.06 | 0.1 | 0 | 0.06 |
| 126 | 0.13 | 0 | 0.05 | 0.1 | 0 | 0.05 | 0.11 | 0 | 0.04 | 0.11 | 0 | 0.05 | 0.14 | 0 | 0.05 | 0.11 | 0 | 0.06 |
| 127 | 0.12 | 0 | 0.05 | 0.07 | 0 | 0.04 | 0.07 | 0 | 0.03 | 0.12 | 0 | 0.05 | 0.09 | 0 | 0.05 | 0.11 | 0 | 0.06 |
| 128 | 0.11 | 0 | 0.05 | 0.09 | 0 | 0.04 | 0.08 | 0 | 0.03 | 0.13 | 0 | 0.05 | 0.09 | 0 | 0.05 | 0.09 | 0 | 0.06 |
| 129 | 0.12 | 0 | 0.05 | 0.09 | 0 | 0.04 | 0.07 | 0 | 0.04 | 0.1 | 0 | 0.05 | 0.1 | 0 | 0.05 | 0.11 | 0 | 0.05 |
| 130 | 0.12 | 0 | 0.05 | 0.09 | 0 | 0.04 | 0.07 | 0 | 0.04 | 0.12 | 0 | 0.05 | 0.11 | 0 | 0.06 | 0.11 | 0 | 0.06 |
| 131 | 0.1 | 0 | 0.05 | 0.09 | 0 | 0.04 | 0.07 | 0 | 0.04 | 0.1 | 0 | 0.04 | 0.09 | 0 | 0.06 | 0.74 | 0 | 0.08 |
| 132 | 0.12 | 0 | 0.05 | 0.08 | 0 | 0.03 | 0.04 | 0 | 0.03 | 0.1 | 0 | 0.04 | 0.11 | 0 | 0.06 | 0.1 | 0 | 0.06 |
| 133 | 0.1 | 0 | 0.05 | 0.1 | 0 | 0.04 | 0.05 | 0 | 0.02 | 0.08 | 0 | 0.04 | 0.1 | 0 | 0.06 | 0.1 | 0 | 0.06 |
| 134 | 0.11 | 0 | 0.05 | 0.09 | 0 | 0.04 | 0.05 | 0 | 0.03 | 0.12 | 0 | 0.05 | 0.1 | 0 | 0.06 | 0.13 | 0 | 0.06 |
| 135 | 0.13 | 0 | 0.05 | 0.09 | 0 | 0.04 | 0.05 | 0 | 0.04 | 0.1 | 0 | 0.05 | 0.13 | 0 | 0.06 | 0.1 | 0 | 0.05 |
| 136 | 0.12 | 0 | 0.05 | 0.09 | 0 | 0.04 | 0.05 | 0 | 0.03 | 0.22 | 0 | 0.05 | 0.1 | 0 | 0.06 | 0.26 | 0 | 0.07 |
| 137 | 0.11 | 0 | 0.05 | 0.11 | 0 | 0.04 | 0.05 | 0 | 0.03 | 0.12 | 0 | 0.05 | 0.1 | 0 | 0.05 | 0.11 | 0 | 0.06 |
| 138 | 0.11 | 0 | 0.05 | 0.1 | 0 | 0.04 | 0.04 | 0 | 0.02 | 0.12 | 0 | 0.05 | 0.13 | 0 | 0.06 | 0.11 | 0 | 0.05 |

| | | | | | | | | | | | | | | | | | |
|---|---|---|---|---|---|---|---|---|---|---|---|---|---|---|---|---|---|
| 139 | 0.1 | 0 | 0.04 | 0.12 | 0 | 0.04 | 0.04 | 0 | 0.02 | 0.28 | 0 | 0.08 | 0.12 | 0 | 0.05 | 0.1 | 0 | 0.05 |
| 140 | 0.12 | 0 | 0.05 | 0.11 | 0 | 0.04 | 0.04 | 0 | 0.03 | 0.25 | 0 | 0.06 | 0.11 | 0 | 0.05 | 0.11 | 0 | 0.05 |
| 141 | 0.12 | 0 | 0.05 | 0.12 | 0 | 0.05 | 0.04 | 0 | 0.02 | 0.09 | 0 | 0.04 | 0.12 | 0 | 0.05 | 0.09 | 0 | 0.05 |
| 142 | 0.11 | 0 | 0.05 | 0.11 | 0 | 0.05 | 0.03 | 0 | 0.01 | 0.09 | 0 | 0.05 | 0.11 | 0 | 0.05 | 0.1 | 0 | 0.05 |
| 143 | 0.12 | 0 | 0.05 | 0.1 | 0 | 0.04 | 0.04 | 0 | 0.02 | 0.08 | 0 | 0.04 | 0.11 | 0 | 0.05 | 0.1 | 0 | 0.05 |
| 144 | 0.11 | 0 | 0.05 | 0.1 | 0 | 0.05 | 0.04 | 0 | 0.02 | 0.09 | 0 | 0.05 | 0.09 | 0 | 0.05 | 0.11 | 0 | 0.05 |
| 145 | 0.12 | 0 | 0.06 | 0.1 | 0 | 0.06 | 0.04 | 0 | 0.02 | 0.11 | 0 | 0.05 | 0.11 | 0 | 0.04 | 0.1 | 0 | 0.04 |
| 146 | 0.12 | 0 | 0.05 | 0.15 | 0 | 0.06 | 0.04 | 0 | 0.02 | 0.08 | 0 | 0.04 | 0.12 | 0 | 0.04 | 0.1 | 0 | 0.05 |
| 147 | 0.13 | 0 | 0.05 | 0.11 | 0 | 0.05 | 0.06 | 0 | 0.03 | 0.09 | 0 | 0.05 | 0.13 | 0 | 0.05 | 0.1 | 0 | 0.06 |
| 148 | 0.11 | 0 | 0.05 | 0.09 | 0 | 0.04 | 0.05 | 0 | 0.03 | 0.08 | 0 | 0.04 | 0.21 | 0 | 0.06 | 0.09 | 0 | 0.05 |
| 149 | 0.11 | 0 | 0.05 | 0.11 | 0 | 0.04 | 0.06 | 0 | 0.02 | 0.08 | 0 | 0.03 | 0.09 | 0 | 0.04 | 0.1 | 0 | 0.05 |
| 150 | 0.12 | 0 | 0.05 | 0.1 | 0 | 0.04 | 0.07 | 0 | 0.02 | 0.08 | 0 | 0.04 | 0.09 | 0 | 0.05 | 0.81 | 0 | 0.06 |
| 151 | 0.12 | 0 | 0.05 | 0.1 | 0 | 0.06 | 0.12 | 0 | 0.06 | 0.09 | 0 | 0.04 | 0.11 | 0 | 0.05 | 0.13 | 0 | 0.06 |
| 152 | 0.11 | 0 | 0.05 | 0.1 | 0 | 0.06 | 0.13 | 0 | 0.07 | 0.18 | 0 | 0.04 | 0.12 | 0 | 0.04 | 0.09 | 0 | 0.05 |
| 153 | 0.12 | 0.02 | 0.06 | 0.09 | 0 | 0.04 | 0.14 | 0 | 0.07 | 0.11 | 0 | 0.04 | 0.12 | 0 | 0.05 | 0.08 | 0 | 0.05 |
| 154 | 0.11 | 0 | 0.05 | 0.09 | 0 | 0.04 | 0.12 | 0 | 0.06 | 0.09 | 0 | 0.04 | 0.08 | 0 | 0.04 | 0.14 | 0 | 0.05 |
| 155 | 0.11 | 0 | 0.05 | 0.09 | 0 | 0.04 | 0.11 | 0 | 0.06 | 0.1 | 0 | 0.05 | 0.08 | 0 | 0.04 | 0.1 | 0 | 0.05 |
| 156 | 0.1 | 0 | 0.05 | 0.18 | 0 | 0.04 | 0.09 | 0 | 0.06 | 0.1 | 0 | 0.05 | 0.09 | 0 | 0.04 | 0.18 | 0 | 0.05 |
| 157 | 0.11 | 0 | 0.05 | 0.09 | 0 | 0.04 | 0.1 | 0 | 0.06 | 0.1 | 0 | 0.05 | 0.1 | 0 | 0.04 | 0.15 | 0 | 0.05 |
| 158 | 0.11 | 0 | 0.05 | 0.1 | 0 | 0.04 | 0.08 | 0 | 0.06 | 0.11 | 0 | 0.05 | 0.09 | 0 | 0.05 | 0.11 | 0 | 0.05 |
| 159 | 0.11 | 0 | 0.05 | 0.1 | 0 | 0.04 | 0.07 | 0 | 0.04 | 0.11 | 0 | 0.05 | 0.13 | 0 | 0.04 | 0.14 | 0 | 0.05 |
| 160 | 0.11 | 0 | 0.05 | 0.11 | 0 | 0.04 | 0.07 | 0.03 | 0.04 | 0.11 | 0 | 0.05 | 0.1 | 0 | 0.05 | 0.1 | 0 | 0.05 |
| 161 | 0.12 | 0 | 0.04 | 0.1 | 0 | 0.04 | 0.08 | 0 | 0.04 | 0.1 | 0 | 0.04 | 0.11 | 0 | 0.04 | 0.15 | 0 | 0.06 |
| 162 | 0.1 | 0 | 0.05 | 0.1 | 0 | 0.04 | 0.07 | 0 | 0.03 | 0.12 | 0 | 0.05 | 0.1 | 0 | 0.04 | 0.12 | 0 | 0.06 |
| 163 | 0.12 | 0 | 0.04 | 0.1 | 0 | 0.04 | 0.06 | 0 | 0.03 | 0.1 | 0 | 0.04 | 0.12 | 0 | 0.05 | 0.11 | 0 | 0.06 |
| 164 | 0.12 | 0 | 0.05 | 0.11 | 0 | 0.04 | 0.06 | 0 | 0.02 | 0.1 | 0 | 0.05 | 0.11 | 0 | 0.04 | 0.1 | 0 | 0.05 |
| 165 | 0.12 | 0 | 0.05 | 0.09 | 0 | 0.04 | 0.06 | 0 | 0.02 | 0.11 | 0 | 0.05 | 0.12 | 0 | 0.05 | 0.1 | 0 | 0.05 |
| 166 | 0.12 | 0 | 0.05 | 0.1 | 0 | 0.04 | 0.06 | 0 | 0.03 | 0.09 | 0 | 0.04 | 0.14 | 0 | 0.05 | 0.1 | 0 | 0.05 |
| 167 | 0.12 | 0 | 0.05 | 0.09 | 0 | 0.04 | 0.04 | 0 | 0.02 | 0.9 | 0 | 0.13 | 0.1 | 0 | 0.05 | 0.1 | 0 | 0.05 |
| 168 | 0.1 | 0 | 0.05 | 0.1 | 0 | 0.04 | 0.04 | 0 | 0.02 | 0.85 | 0 | 0.09 | 0.1 | 0 | 0.05 | 0.11 | 0 | 0.05 |
| 169 | 0.11 | 0 | 0.05 | 0.1 | 0 | 0.04 | 0.05 | 0 | 0.03 | 0.17 | 0 | 0.05 | 0.1 | 0 | 0.04 | 0.1 | 0 | 0.05 |
| 170 | 0.1 | 0 | 0.05 | 0.11 | 0 | 0.05 | 0.04 | 0 | 0.02 | 0.17 | 0 | 0.06 | 0.12 | 0 | 0.05 | 0.09 | 0 | 0.05 |
| 171 | 0.11 | 0 | 0.05 | 0.12 | 0 | 0.05 | 0.06 | 0 | 0.03 | 0.24 | 0 | 0.07 | 0.1 | 0 | 0.04 | 0.1 | 0 | 0.05 |
| 172 | 0.12 | 0 | 0.05 | 0.12 | 0 | 0.06 | 0.09 | 0 | 0.04 | 0.17 | 0 | 0.05 | 0.11 | 0 | 0.04 | 0.1 | 0 | 0.04 |
| 173 | 0.11 | 0 | 0.05 | 0.13 | 0 | 0.06 | 0.1 | 0 | 0.07 | 0.17 | 0 | 0.05 | 0.1 | 0 | 0.04 | 0.09 | 0 | 0.04 |
| 174 | 0.1 | 0 | 0.05 | 0.12 | 0 | 0.06 | 0.1 | 0 | 0.07 | 0.11 | 0 | 0.05 | 0.11 | 0 | 0.04 | 0.1 | 0 | 0.04 |
| 175 | 0.1 | 0 | 0.05 | 0.11 | 0 | 0.06 | 0.11 | 0 | 0.05 | 0.13 | 0 | 0.05 | 0.09 | 0 | 0.04 | 0.09 | 0 | 0.04 |
| 176 | 0.09 | 0 | 0.04 | 0.1 | 0 | 0.06 | 0.11 | 0 | 0.05 | 0.11 | 0 | 0.05 | 0.1 | 0 | 0.04 | 0.1 | 0 | 0.05 |
| 177 | 0.1 | 0 | 0.04 | 0.15 | 0 | 0.06 | 0.08 | 0 | 0.04 | 0.09 | 0 | 0.04 | 0.08 | 0 | 0.04 | 0.09 | 0 | 0.04 |

| | | | | | | | | | | | | | | | | | |
|---|---|---|---|---|---|---|---|---|---|---|---|---|---|---|---|---|---|
| 178 | 0.1 | 0 | 0.05 | 0.09 | 0 | 0.04 | 0.07 | 0 | 0.04 | 0.11 | 0 | 0.04 | 0.09 | 0 | 0.04 | 0.22 | 0 | 0.04 |
| 179 | 0.1 | 0 | 0.05 | 0.1 | 0 | 0.04 | 0.07 | 0 | 0.04 | 0.1 | 0 | 0.05 | 0.11 | 0 | 0.04 | 0.24 | 0 | 0.06 |
| 180 | 0.11 | 0 | 0.05 | 0.11 | 0 | 0.05 | 0.07 | 0.02 | 0.05 | 0.09 | 0 | 0.05 | 0.11 | 0 | 0.04 | 0.08 | 0 | 0.04 |
| 181 | 0.09 | 0 | 0.05 | 0.11 | 0 | 0.04 | 0.07 | 0.01 | 0.04 | 0.09 | 0 | 0.05 | 0.09 | 0 | 0.03 | 0.1 | 0 | 0.04 |
| 182 | 0.09 | 0 | 0.04 | 0.1 | 0 | 0.05 | 0.07 | 0 | 0.04 | 0.09 | 0 | 0.04 | 0.11 | 0 | 0.04 | 0.09 | 0 | 0.04 |
| 183 | 0.1 | 0 | 0.05 | 0.09 | 0 | 0.05 | 0.07 | 0 | 0.04 | 0.08 | 0 | 0.05 | 0.13 | 0 | 0.04 | 0.1 | 0 | 0.04 |
| 184 | 0.1 | 0 | 0.04 | 0.09 | 0 | 0.04 | 0.06 | 0 | 0.03 | 0.11 | 0 | 0.04 | 0.12 | 0 | 0.05 | 0.09 | 0 | 0.05 |
| 185 | 0.12 | 0 | 0.06 | 0.12 | 0 | 0.04 | 0.05 | 0 | 0.02 | 0.12 | 0 | 0.05 | 0.1 | 0 | 0.05 | 0.09 | 0 | 0.05 |
| 186 | 0.11 | 0 | 0.06 | 0.09 | 0 | 0.04 | 0.04 | 0 | 0.02 | 0.1 | 0 | 0.05 | 0.09 | 0 | 0.04 | 0.1 | 0 | 0.04 |
| 187 | 0.1 | 0 | 0.05 | 0.12 | 0 | 0.04 | 0.04 | 0 | 0.02 | 0.11 | 0 | 0.05 | 0.12 | 0 | 0.05 | 0.1 | 0 | 0.04 |
| 188 | 0.1 | 0 | 0.04 | 0.11 | 0 | 0.04 | 0.04 | 0 | 0.01 | 0.13 | 0 | 0.06 | 0.11 | 0 | 0.05 | 0.12 | 0 | 0.04 |
| 189 | 0.04 | 0 | 0.04 | 0.12 | 0 | 0.04 | 0.03 | 0 | 0.01 | 0.13 | 0 | 0.05 | 0.1 | 0 | 0.05 | 0.13 | 0 | 0.05 |
| 190 | 0.1 | 0 | 0.05 | 0.11 | 0 | 0.04 | 0.03 | 0 | 0.01 | 0.1 | 0 | 0.05 | 0.12 | 0 | 0.06 | 0.13 | 0 | 0.04 |
| 191 | 0.09 | 0 | 0.05 | 0.1 | 0 | 0.05 | 0.06 | 0 | 0.03 | 0.12 | 0 | 0.05 | 0.11 | 0 | 0.06 | 0.13 | 0 | 0.04 |
| 192 | 0.1 | 0 | 0.04 | 0.11 | 0 | 0.04 | 0.08 | 0 | 0.03 | 0.12 | 0 | 0.05 | 0.12 | 0 | 0.04 | 0.14 | 0 | 0.05 |
| 193 | 0.1 | 0 | 0.04 | 0.12 | 0 | 0.05 | 0.03 | 0 | 0.04 | 0.1 | 0 | 0.05 | 0.14 | 0 | 0.05 | 0.14 | 0 | 0.04 |
| 194 | 0.09 | 0 | 0.04 | 0.11 | 0 | 0.05 | 0.07 | 0 | 0.04 | 0.1 | 0 | 0.05 | 0.13 | 0 | 0.05 | 0.12 | 0 | 0.04 |
| 195 | 0.09 | 0 | 0.05 | 0.12 | 0 | 0.04 | 0.08 | 0 | 0.05 | 0.09 | 0 | 0.05 | 0.12 | 0 | 0.05 | 0.16 | 0 | 0.04 |
| 196 | 0.1 | 0 | 0.04 | 0.12 | 0 | 0.05 | 0.09 | 0 | 0.06 | 0.1 | 0 | 0.05 | 0.14 | 0 | 0.05 | 0.15 | 0 | 0.04 |
| 197 | 0.1 | 0 | 0.05 | 0.1 | 0 | 0.06 | 0.1 | 0.02 | 0.06 | 0.12 | 0 | 0.06 | 0.14 | 0 | 0.05 | 0.15 | 0 | 0.04 |
| 198 | 0.1 | 0 | 0.04 | 0.15 | 0 | 0.06 | 0.01 | 0 | 0.04 | 0.12 | 0 | 0.06 | 0.18 | 0 | 0.06 | 0.12 | 0 | 0.04 |
| 199 | 0.1 | 0 | 0.04 | 0.12 | 0 | 0.06 | 0.09 | 0 | 0.04 | 0.1 | 0 | 0.05 | 0.13 | 0 | 0.06 | 0.09 | 0 | 0.04 |
| 200 | 0.09 | 0 | 0.04 | 0.11 | 0 | 0.06 | 0.08 | 0.02 | 0.04 | 0.09 | 0 | 0.05 | 0.13 | 0 | 0.05 | 0.14 | 0 | 0.05 |

| | | | | | | | | | | | | | | | | | |
|---|---|---|---|---|---|---|---|---|---|---|---|---|---|---|---|---|---|
| | Control (mm) | | | | | | | | | Infected (mm) | | | | | | | |
| Day 2 | R1 | | | R2 | | | R3 | | | R1 | | | R2 | | | R3 | |
| | Max | Min | Average | Max | Min | Average | Max | Min | Average | Max | Min | Average | Max | Min | Average | Max | Min | Average |
| 1 | 0.06 | 0 | 0.03 | 0.06 | 0 | 0.02 | 0.06 | 0 | 0.02 | 0.04 | 0 | 0.03 | 0.12 | 0 | 0.06 | 0.11 | 0 | 0.08 |
| 2 | 0.06 | 0 | 0.03 | 0.06 | 0 | 0.02 | 0.04 | 0 | 0.03 | 0.06 | 0 | 0.03 | 0.15 | 0 | 0.06 | 0.12 | 0 | 0.07 |
| 3 | 0.07 | 0 | 0.03 | 0.05 | 0 | 0.02 | 0.06 | 0 | 0.04 | 0.04 | 0 | 0.02 | 0.14 | 0 | 0.06 | 0.1 | 0 | 0.07 |
| 4 | 0.06 | 0 | 0.03 | 0.04 | 0 | 0.02 | 0.05 | 0 | 0.03 | 0.03 | 0 | 0.01 | 0.14 | 0 | 0.06 | 0.1 | 0 | 0.07 |
| 5 | 0.06 | 0 | 0.03 | 0.07 | 0 | 0.03 | 0.04 | 0 | 0.02 | 0.1 | 0 | 0.03 | 0.12 | 0 | 0.06 | 0.11 | 0 | 0.07 |
| 6 | 0.06 | 0 | 0.03 | 0.06 | 0 | 0.03 | 0.04 | 0 | 0.02 | 0.03 | 0 | 0.01 | 0.12 | 0 | 0.06 | 0.12 | 0 | 0.07 |
| 7 | 0.08 | 0 | 0.03 | 0.06 | 0 | 0.03 | 0.06 | 0 | 0.03 | 0.03 | 0 | 0.01 | 0.14 | 0 | 0.06 | 0.12 | 0 | 0.07 |
| 8 | 0.08 | 0 | 0.04 | 0.06 | 0 | 0.03 | 0.05 | 0 | 0.02 | 0.03 | 0 | 0.01 | 0.15 | 0 | 0.06 | 0.11 | 0 | 0.05 |
| 9 | 0.07 | 0 | 0.04 | 0.06 | 0 | 0.03 | 0.07 | 0 | 0.03 | 0.03 | 0 | 0.01 | 0.14 | 0 | 0.05 | 0.12 | 0 | 0.05 |

| | | | | | | | | | | | | | | | | | |
|---|---|---|---|---|---|---|---|---|---|---|---|---|---|---|---|---|---|
| 10 | 0.07 | 0 | 0.03 | 0.05 | 0 | 0.03 | 0.08 | 0 | 0.03 | 0.02 | 0 | 0.04 | 0.13 | 0 | 0.06 | 0.12 | 0 | 0.05 |
| 11 | 0.07 | 0 | 0.03 | 0.05 | 0 | 0.03 | 0.08 | 0 | 0.04 | 0.02 | 0 | 0.01 | 0.16 | 0 | 0.06 | 0.1 | 0 | 0.05 |
| 12 | 0.08 | 0 | 0.04 | 0.06 | 0 | 0.03 | 0.08 | 0 | 0.04 | 0.02 | 0 | 0.05 | 0.11 | 0 | 0.05 | 0.1 | 0 | 0.05 |
| 13 | 0.06 | 0 | 0.03 | 0.07 | 0 | 0.02 | 0.07 | 0 | 0.03 | 0.02 | 0 | 0.06 | 0.11 | 0 | 0.05 | 0.11 | 0 | 0.07 |
| 14 | 0.07 | 0 | 0.04 | 0.08 | 0 | 0.03 | 0.07 | 0 | 0.03 | 0.01 | 0 | 0.06 | 0.12 | 0 | 0.05 | 0.1 | 0 | 0.07 |
| 15 | 0.08 | 0 | 0.04 | 0.06 | 0 | 0.03 | 0.08 | 0 | 0.03 | 0.02 | 0 | 0.06 | 0.12 | 0 | 0.05 | 0.1 | 0 | 0.07 |
| 16 | 0.01 | 0 | 0.04 | 0.06 | 0 | 0.03 | 0.08 | 0 | 0.04 | 0.02 | 0 | 0.06 | 0.11 | 0 | 0.05 | 0.1 | 0 | 0.07 |
| 17 | 0.07 | 0 | 0.04 | 0.07 | 0 | 0.02 | 0.09 | 0 | 0.03 | 0.03 | 0 | 0.06 | 0.11 | 0 | 0.05 | 0.11 | 0 | 0.07 |
| 18 | 0.07 | 0 | 0.03 | 0.08 | 0 | 0.03 | 0.08 | 0 | 0.03 | 0.05 | 0 | 0.06 | 0.12 | 0 | 0.06 | 0.09 | 0 | 0.06 |
| 19 | 0.07 | 0 | 0.04 | 0.08 | 0 | 0.03 | 0.08 | 0 | 0.03 | 0.06 | 0 | 0.06 | 0.11 | 0 | 0.05 | 0.1 | 0 | 0.06 |
| 20 | 0.07 | 0 | 0.04 | 0.07 | 0 | 0.03 | 0.06 | 0 | 0.03 | 0.06 | 0 | 0.06 | 0.12 | 0 | 0.05 | 0.11 | 0 | 0.06 |
| 21 | 0.07 | 0 | 0.03 | 0.07 | 0 | 0.03 | 0.07 | 0 | 0.04 | 0.07 | 0 | 0.06 | 0.11 | 0 | 0.05 | 0.1 | 0 | 0.06 |
| 22 | 0.07 | 0 | 0.03 | 0.06 | 0 | 0.03 | 0.06 | 0 | 0.03 | 0.08 | 0 | 0.06 | 0.12 | 0 | 0.07 | 0.1 | 0 | 0.06 |
| 23 | 0.06 | 0 | 0.03 | 0.06 | 0 | 0.03 | 0.06 | 0 | 0.02 | 0.08 | 0 | 0.06 | 0.12 | 0 | 0.07 | 0.1 | 0 | 0.06 |
| 24 | 0.06 | 0 | 0.03 | 0.07 | 0 | 0.03 | 0.06 | 0 | 0.03 | 0.07 | 0 | 0.03 | 0.11 | 0 | 0.07 | 0.09 | 0 | 0.06 |
| 25 | 0.07 | 0 | 0.03 | 0.08 | 0 | 0.04 | 0.04 | 0 | 0.02 | 0.08 | 0 | 0.03 | 0.12 | 0 | 0.06 | 0.11 | 0 | 0.06 |
| 26 | 0.07 | 0 | 0.03 | 0.08 | 0 | 0.04 | 0.06 | 0 | 0.03 | 0.07 | 0 | 0.02 | 0.1 | 0 | 0.06 | 0.12 | 0 | 0.06 |
| 27 | 0.06 | 0 | 0.04 | 0.07 | 0 | 0.04 | 0.07 | 0 | 0.03 | 0.08 | 0 | 0.03 | 0.12 | 0 | 0.06 | 0.12 | 0 | 0.06 |
| 28 | 0.09 | 0 | 0.04 | 0.07 | 0 | 0.03 | 0.06 | 0 | 0.03 | 0.08 | 0 | 0.02 | 0.12 | 0 | 0.06 | 0.11 | 0 | 0.06 |
| 29 | 0.08 | 0 | 0.04 | 0.07 | 0 | 0.04 | 0.07 | 0 | 0.03 | 0.07 | 0 | 0.03 | 0.13 | 0 | 0.06 | 0.11 | 0 | 0.06 |
| 30 | 0.08 | 0 | 0.04 | 0.08 | 0 | 0.04 | 0.06 | 0 | 0.03 | 0.08 | 0 | 0.06 | 0.1 | 0 | 0.06 | 0.13 | 0 | 0.06 |
| 31 | 0.07 | 0 | 0.04 | 0.07 | 0 | 0.04 | 0.06 | 0 | 0.03 | 0.08 | 0 | 0.06 | 0.1 | 0 | 0.06 | 0.13 | 0 | 0.07 |
| 32 | 0.07 | 0 | 0.04 | 0.07 | 0 | 0.04 | 0.07 | 0 | 0.03 | 0.07 | 0 | 0.03 | 0.09 | 0 | 0.05 | 0.13 | 0 | 0.07 |
| 33 | 0.07 | 0 | 0.03 | 0.07 | 0 | 0.04 | 0.06 | 0 | 0.03 | 0.07 | 0 | 0.04 | 0.09 | 0 | 0.05 | 0.14 | 0 | 0.07 |
| 34 | 0.08 | 0 | 0.04 | 0.07 | 0 | 0.04 | 0.04 | 0 | 0.02 | 0.08 | 0 | 0.04 | 0.1 | 0 | 0.06 | 0.13 | 0 | 0.08 |
| 35 | 0.06 | 0 | 0.04 | 0.07 | 0 | 0.03 | 0.05 | 0 | 0.02 | 0.09 | 0 | 0.03 | 0.11 | 0 | 0.06 | 0.12 | 0.02 | 0.07 |
| 36 | 0.08 | 0 | 0.04 | 0.07 | 0 | 0.03 | 0.04 | 0 | 0.02 | 0.1 | 0 | 0.06 | 0.1 | 0 | 0.05 | 0.12 | 0.02 | 0.07 |
| 37 | 0.07 | 0 | 0.04 | 0.07 | 0 | 0.03 | 0.05 | 0 | 0.02 | 0.09 | 0.01 | 0.06 | 0.11 | 0 | 0.05 | 0.12 | 0 | 0.07 |
| 38 | 0.08 | 0 | 0.03 | 0.06 | 0 | 0.03 | 0.05 | 0 | 0.02 | 0.08 | 0 | 0.06 | 0.11 | 0 | 0.05 | 0.11 | 0.01 | 0.07 |
| 39 | 0.06 | 0 | 0.03 | 0.06 | 0 | 0.03 | 0.06 | 0 | 0.02 | 0.12 | 0 | 0.06 | 0.1 | 0 | 0.05 | 0.12 | 0 | 0.07 |
| 40 | 0.05 | 0 | 0.03 | 0.06 | 0 | 0.03 | 0.05 | 0 | 0.03 | 0.1 | 0 | 0.06 | 0.1 | 0 | 0.05 | 0.12 | 0 | 0.07 |
| 41 | 0.08 | 0 | 0.04 | 0.07 | 0 | 0.03 | 0.05 | 0 | 0.03 | 0.09 | 0 | 0.04 | 0.11 | 0 | 0.05 | 0.1 | 0.02 | 0.07 |
| 42 | 0.06 | 0 | 0.03 | 0.07 | 0 | 0.04 | 0.04 | 0 | 0.03 | 0.11 | 0 | 0.06 | 0.1 | 0 | 0.06 | 0.12 | 0 | 0.07 |
| 43 | 0.07 | 0 | 0.04 | 0.06 | 0 | 0.03 | 0.05 | 0 | 0.02 | 0.12 | 0 | 0.06 | 0.11 | 0 | 0.06 | 0.11 | 0.01 | 0.07 |
| 44 | 0.07 | 0 | 0.04 | 0.07 | 0 | 0.03 | 0.06 | 0 | 0.03 | 0.09 | 0 | 0.06 | 0.1 | 0 | 0.05 | 0.12 | 0.03 | 0.07 |
| 45 | 0.07 | 0 | 0.03 | 0.08 | 0 | 0.04 | 0.06 | 0 | 0.03 | 0.12 | 0 | 0.05 | 0.09 | 0 | 0.05 | 0.12 | 0 | 0.07 |
| 46 | 0.08 | 0 | 0.04 | 0.07 | 0 | 0.03 | 0.06 | 0 | 0.03 | 0.07 | 0 | 0.03 | 0.1 | 0 | 0.06 | 0.11 | 0 | 0.07 |
| 47 | 0.07 | 0 | 0.04 | 0.08 | 0 | 0.03 | 0.06 | 0 | 0.03 | 0.06 | 0 | 0.03 | 0.1 | 0 | 0.06 | 0.11 | 0 | 0.07 |
| 48 | 0.07 | 0 | 0.04 | 0.07 | 0 | 0.03 | 0.07 | 0 | 0.03 | 0.05 | 0 | 0.02 | 0.1 | 0 | 0.07 | 0.1 | 0 | 0.06 |

| | | | | | | | | | | | | | | | | | |
|---|---|---|---|---|---|---|---|---|---|---|---|---|---|---|---|---|---|
| 49 | 0.08 | 0 | 0.03 | 0.05 | 0 | 0.02 | 0.06 | 0 | 0.03 | 0.06 | 0 | 0.03 | 0.12 | 0 | 0.07 | 0.11 | 0 | 0.06 |
| 50 | 0.08 | 0 | 0.03 | 0.05 | 0 | 0.02 | 0.06 | 0 | 0.03 | 0.08 | 0 | 0.02 | 0.11 | 0 | 0.07 | 0.12 | 0.02 | 0.07 |
| 51 | 0.08 | 0 | 0.03 | 0.06 | 0 | 0.02 | 0.07 | 0 | 0.03 | 0.09 | 0 | 0.03 | 0.12 | 0 | 0.07 | 0.11 | 0 | 0.06 |
| 52 | 0.07 | 0 | 0.03 | 0.06 | 0 | 0.02 | 0.05 | 0 | 0.03 | 0.08 | 0 | 0.03 | 0.12 | 0 | 0.07 | 0.11 | 0 | 0.07 |
| 53 | 0.08 | 0 | 0.03 | 0.05 | 0 | 0.03 | 0.07 | 0 | 0.03 | 0.08 | 0 | 0.04 | 0.11 | 0 | 0.06 | 0.11 | 0 | 0.07 |
| 54 | 0.08 | 0 | 0.03 | 0.04 | 0 | 0.02 | 0.07 | 0 | 0.03 | 0.08 | 0 | 0.04 | 0.11 | 0 | 0.07 | 0.11 | 0 | 0.06 |
| 55 | 0.07 | 0 | 0.03 | 0.19 | 0 | 0.03 | 0.06 | 0 | 0.03 | 0.08 | 0 | 0.03 | 0.12 | 0 | 0.07 | 0.11 | 0 | 0.07 |
| 56 | 0.09 | 0 | 0.04 | 0.2 | 0 | 0.03 | 0.06 | 0 | 0.03 | 0.1 | 0 | 0.04 | 0.13 | 0 | 0.07 | 0.11 | 0 | 0.07 |
| 57 | 0.08 | 0 | 0.04 | 0.06 | 0 | 0.03 | 0.06 | 0 | 0.02 | 0.1 | 0 | 0.04 | 0.11 | 0 | 0.06 | 0.14 | 0 | 0.07 |
| 58 | 0.09 | 0 | 0.04 | 0.06 | 0 | 0.03 | 0.05 | 0 | 0.02 | 0.09 | 0 | 0.04 | 0.12 | 0 | 0.07 | 0.12 | 0 | 0.06 |
| 59 | 0.09 | 0 | 0.04 | 0.05 | 0 | 0.03 | 0.05 | 0 | 0.02 | 0.1 | 0 | 0.04 | 0.1 | 0 | 0.07 | 0.11 | 0 | 0.07 |
| 60 | 0.09 | 0 | 0.03 | 0.05 | 0 | 0.03 | 0.08 | 0 | 0.03 | 0.09 | 0 | 0.06 | 0.12 | 0 | 0.07 | 0.11 | 0 | 0.07 |
| 61 | 0.09 | 0 | 0.04 | 0.06 | 0 | 0.03 | 0.06 | 0 | 0.02 | 0.09 | 0 | 0.04 | 0.11 | 0 | 0.07 | 0.12 | 0 | 0.07 |
| 62 | 0.08 | 0 | 0.03 | 0.08 | 0 | 0.03 | 0.07 | 0 | 0.03 | 0.1 | 0 | 0.03 | 0.12 | 0 | 0.07 | 0.11 | 0 | 0.07 |
| 63 | 0.08 | 0 | 0.03 | 0.07 | 0 | 0.03 | 0.08 | 0 | 0.03 | 0.1 | 0 | 0.03 | 0.11 | 0 | 0.07 | 0.13 | 0 | 0.07 |
| 64 | 0.08 | 0 | 0.03 | 0.08 | 0 | 0.04 | 0.09 | 0 | 0.03 | 0.08 | 0 | 0.03 | 0.11 | 0 | 0.06 | 0.11 | 0 | 0.07 |
| 65 | 0.07 | 0 | 0.03 | 0.07 | 0 | 0.03 | 0.1 | 0 | 0.03 | 0.09 | 0 | 0.03 | 0.11 | 0 | 0.06 | 0.12 | 0 | 0.07 |
| 66 | 0.06 | 0 | 0.03 | 0.07 | 0 | 0.03 | 0.09 | 0 | 0.04 | 0.09 | 0 | 0.04 | 0.11 | 0 | 0.06 | 0.12 | 0 | 0.07 |
| 67 | 0.07 | 0 | 0.04 | 0.08 | 0 | 0.03 | 0.08 | 0 | 0.04 | 0.08 | 0 | 0.04 | 0.11 | 0 | 0.06 | 0.12 | 0 | 0.07 |
| 68 | 0.07 | 0 | 0.03 | 0.07 | 0 | 0.03 | 0.09 | 0 | 0.03 | 0.08 | 0 | 0.04 | 0.1 | 0 | 0.05 | 0.12 | 0 | 0.07 |
| 69 | 0.08 | 0 | 0.04 | 0.08 | 0 | 0.04 | 0.07 | 0 | 0.03 | 0.08 | 0 | 0.03 | 0.1 | 0 | 0.05 | 0.12 | 0 | 0.07 |
| 70 | 0.09 | 0 | 0.04 | 0.09 | 0 | 0.04 | 0.07 | 0 | 0.03 | 0.09 | 0 | 0.05 | 0.1 | 0 | 0.05 | 0.12 | 0 | 0.08 |
| 71 | 0.08 | 0 | 0.04 | 0.08 | 0 | 0.03 | 0.07 | 0 | 0.03 | 0.07 | 0 | 0.03 | 0.12 | 0 | 0.05 | 0.12 | 0 | 0.07 |
| 72 | 0.06 | 0 | 0.03 | 0.08 | 0 | 0.03 | 0.06 | 0 | 0.03 | 0.08 | 0 | 0.03 | 0.12 | 0 | 0.06 | 0.12 | 0 | 0.07 |
| 73 | 0.07 | 0 | 0.03 | 0.09 | 0 | 0.03 | 0.06 | 0 | 0.03 | 0.15 | 0 | 0.06 | 0.12 | 0 | 0.06 | 0.14 | 0 | 0.07 |
| 74 | 0.06 | 0 | 0.03 | 0.09 | 0 | 0.03 | 0.06 | 0 | 0.03 | 0.06 | 0 | 0.06 | 0.11 | 0 | 0.06 | 0.15 | 0 | 0.07 |
| 75 | 0.07 | 0 | 0.03 | 0.08 | 0 | 0.03 | 0.07 | 0 | 0.03 | 0.04 | 0 | 0.06 | 0.11 | 0 | 0.06 | 0.15 | 0 | 0.07 |
| 76 | 0.06 | 0 | 0.02 | 0.08 | 0 | 0.03 | 0.07 | 0 | 0.03 | 0.05 | 0 | 0.06 | 0.12 | 0.01 | 0.06 | 0.13 | 0 | 0.07 |
| 77 | 0.07 | 0 | 0.03 | 0.09 | 0 | 0.04 | 0.07 | 0 | 0.04 | 0.06 | 0 | 0.06 | 0.12 | 0 | 0.06 | 0.15 | 0 | 0.07 |
| 78 | 0.08 | 0 | 0.04 | 0.09 | 0 | 0.03 | 0.06 | 0 | 0.04 | 0.09 | 0 | 0.06 | 0.12 | 0 | 0.06 | 0.15 | 0 | 0.07 |
| 79 | 0.08 | 0 | 0.04 | 0.09 | 0 | 0.04 | 0.09 | 0 | 0.03 | 0.08 | 0 | 0.06 | 0.11 | 0 | 0.06 | 0.13 | 0 | 0.07 |
| 80 | 0.07 | 0 | 0.03 | 0.08 | 0 | 0.04 | 0.07 | 0 | 0.03 | 0.08 | 0 | 0.06 | 0.12 | 0 | 0.07 | 0.15 | 0.02 | 0.07 |
| 81 | 0.07 | 0 | 0.04 | 0.09 | 0 | 0.05 | 0.06 | 0 | 0.03 | 0.09 | 0 | 0.06 | 0.11 | 0 | 0.07 | 0.12 | 0 | 0.07 |
| 82 | 0.08 | 0 | 0.04 | 0.08 | 0 | 0.04 | 0.05 | 0 | 0.03 | 0.1 | 0 | 0.06 | 0.13 | 0 | 0.07 | 0.11 | 0 | 0.07 |
| 83 | 0.07 | 0 | 0.04 | 0.08 | 0 | 0.04 | 0.05 | 0 | 0.03 | 0.1 | 0 | 0.06 | 0.12 | 0 | 0.07 | 0.13 | 0 | 0.07 |
| 84 | 0.07 | 0 | 0.04 | 0.07 | 0 | 0.04 | 0.06 | 0 | 0.02 | 0.11 | 0 | 0.04 | 0.12 | 0 | 0.08 | 0.12 | 0.01 | 0.07 |
| 85 | 0.07 | 0 | 0.04 | 0.09 | 0 | 0.04 | 0.05 | 0 | 0.02 | 0.09 | 0 | 0.04 | 0.12 | 0 | 0.08 | 0.14 | 0 | 0.07 |
| 86 | 0.08 | 0.01 | 0.06 | 0.07 | 0 | 0.04 | 0.07 | 0 | 0.03 | 0.11 | 0 | 0.05 | 0.11 | 0 | 0.07 | 0.11 | 0 | 0.05 |
| 87 | 0.08 | 0 | 0.04 | 0.07 | 0 | 0.04 | 0.08 | 0 | 0.03 | 0.09 | 0 | 0.04 | 0.13 | 0 | 0.08 | 0.09 | 0 | 0.04 |

| | | | | | | | | | | | | | | | | | |
|---|---|---|---|---|---|---|---|---|---|---|---|---|---|---|---|---|---|
| 88 | 0.09 | 0 | 0.04 | 0.07 | 0 | 0.04 | 0.07 | 0 | 0.04 | 0.08 | 0 | 0.04 | 0.14 | 0 | 0.07 | 0.08 | 0 | 0.04 |
| 89 | 0.08 | 0 | 0.04 | 0.07 | 0 | 0.04 | 0.08 | 0 | 0.03 | 0.08 | 0 | 0.03 | 0.14 | 0 | 0.07 | 0.14 | 0 | 0.07 |
| 90 | 0.09 | 0 | 0.04 | 0.08 | 0 | 0.04 | 0.09 | 0 | 0.04 | 0.12 | 0 | 0.04 | 0.13 | 0 | 0.07 | 0.14 | 0 | 0.07 |
| 91 | 0.07 | 0 | 0.04 | 0.07 | 0 | 0.04 | 0.1 | 0 | 0.04 | 0.08 | 0 | 0.04 | 0.13 | 0 | 0.07 | 0.15 | 0 | 0.07 |
| 92 | 0.07 | 0 | 0.04 | 0.07 | 0 | 0.04 | 0.09 | 0 | 0.04 | 0.07 | 0 | 0.03 | 0.12 | 0 | 0.07 | 0.15 | 0.01 | 0.08 |
| 93 | 0.09 | 0 | 0.04 | 0.08 | 0 | 0.04 | 0.08 | 0 | 0.04 | 0.08 | 0 | 0.04 | 0.12 | 0 | 0.07 | 0.13 | 0 | 0.07 |
| 94 | 0.08 | 0 | 0.04 | 0.07 | 0 | 0.04 | 0.09 | 0 | 0.04 | 0.07 | 0 | 0.06 | 0.13 | 0.03 | 0.08 | 0.13 | 0 | 0.07 |
| 95 | 0.09 | 0 | 0.04 | 0.07 | 0 | 0.03 | 0.07 | 0 | 0.03 | 0.08 | 0 | 0.04 | 0.13 | 0 | 0.07 | 0.14 | 0 | 0.07 |
| 96 | 0.08 | 0 | 0.04 | 0.08 | 0 | 0.03 | 0.09 | 0.01 | 0.04 | 0.07 | 0 | 0.03 | 0.14 | 0 | 0.07 | 0.14 | 0 | 0.06 |
| 97 | 0.08 | 0 | 0.04 | 0.08 | 0 | 0.03 | 0.08 | 0 | 0.04 | 0.06 | 0 | 0.03 | 0.14 | 0 | 0.07 | 0.12 | 0.03 | 0.07 |
| 98 | 0.09 | 0 | 0.04 | 0.08 | 0 | 0.04 | 0.08 | 0 | 0.04 | 0.07 | 0 | 0.03 | 0.13 | 0 | 0.07 | 0.15 | 0 | 0.07 |
| 99 | 0.08 | 0 | 0.04 | 0.07 | 0 | 0.03 | 0.08 | 0 | 0.04 | 0.07 | 0 | 0.03 | 0.13 | 0 | 0.06 | 0.13 | 0 | 0.08 |
| 100 | 0.07 | 0 | 0.04 | 0.08 | 0 | 0.04 | 0.07 | 0 | 0.04 | 0.09 | 0 | 0.03 | 0.11 | 0.03 | 0.05 | 0.14 | 0 | 0.07 |
| 101 | 0.09 | 0 | 0.05 | 0.08 | 0 | 0.04 | 0.06 | 0 | 0.04 | 0.08 | 0 | 0.03 | 0.12 | 0.04 | 0.05 | 0.13 | 0 | 0.07 |
| 102 | 0.09 | 0 | 0.04 | 0.08 | 0 | 0.04 | 0.08 | 0 | 0.04 | 0.08 | 0 | 0.03 | 0.14 | 0 | 0.05 | 0.14 | 0 | 0.08 |
| 103 | 0.08 | 0 | 0.04 | 0.07 | 0 | 0.04 | 0.07 | 0 | 0.03 | 0.07 | 0 | 0.03 | 0.15 | 0 | 0.05 | 0.12 | 0 | 0.07 |
| 104 | 0.07 | 0 | 0.04 | 0.08 | 0 | 0.05 | 0.06 | 0 | 0.03 | 0.07 | 0 | 0.02 | 0.12 | 0 | 0.06 | 0.12 | 0 | 0.08 |
| 105 | 0.09 | 0 | 0.04 | 0.08 | 0 | 0.04 | 0.08 | 0 | 0.03 | 0.07 | 0 | 0.04 | 0.11 | 0 | 0.07 | 0.12 | 0.03 | 0.08 |
| 106 | 0.09 | 0 | 0.04 | 0.08 | 0 | 0.05 | 0.08 | 0 | 0.03 | 0.06 | 0 | 0.03 | 0.12 | 0 | 0.07 | 0.12 | 0 | 0.07 |
| 107 | 0.07 | 0 | 0.04 | 0.08 | 0 | 0.05 | 0.08 | 0 | 0.04 | 0.08 | 0 | 0.03 | 0.13 | 0 | 0.08 | 0.13 | 0.04 | 0.08 |
| 108 | 0.07 | 0 | 0.04 | 0.09 | 0 | 0.05 | 0.08 | 0 | 0.04 | 0.08 | 0 | 0.03 | 0.13 | 0 | 0.08 | 0.13 | 0.04 | 0.08 |
| 109 | 0.06 | 0 | 0.04 | 0.07 | 0 | 0.04 | 0.08 | 0 | 0.04 | 0.07 | 0 | 0.03 | 0.14 | 0 | 0.07 | 0.12 | 0.04 | 0.08 |
| 110 | 0.07 | 0 | 0.04 | 0.09 | 0 | 0.05 | 0.08 | 0 | 0.03 | 0.08 | 0 | 0.04 | 0.13 | 0 | 0.07 | 0.12 | 0 | 0.08 |
| 111 | 0.07 | 0 | 0.04 | 0.09 | 0.01 | 0.05 | 0.06 | 0 | 0.03 | 0.07 | 0 | 0.03 | 0.13 | 0 | 0.07 | 0.12 | 0.03 | 0.08 |
| 112 | 0.07 | 0 | 0.04 | 0.08 | 0 | 0.05 | 0.07 | 0 | 0.03 | 0.08 | 0 | 0.02 | 0.08 | 0 | 0.05 | 0.12 | 0 | 0.08 |
| 113 | 0.07 | 0 | 0.04 | 0.08 | 0 | 0.05 | 0.08 | 0 | 0.04 | 0.1 | 0 | 0.03 | 0.08 | 0 | 0.05 | 0.12 | 0.02 | 0.08 |
| 114 | 0.07 | 0 | 0.04 | 0.08 | 0.01 | 0.05 | 0.09 | 0 | 0.04 | 0.11 | 0 | 0.04 | 0.14 | 0.03 | 0.06 | 0.12 | 0.03 | 0.06 |
| 115 | 0.08 | 0 | 0.04 | 0.09 | 0 | 0.05 | 0.09 | 0 | 0.05 | 0.08 | 0 | 0.03 | 0.12 | 0 | 0.07 | 0.12 | 0.03 | 0.07 |
| 116 | 0.08 | 0 | 0.04 | 0.07 | 0 | 0.04 | 0.07 | 0 | 0.03 | 0.07 | 0 | 0.04 | 0.12 | 0 | 0.07 | 0.13 | 0.02 | 0.07 |
| 117 | 0.07 | 0 | 0.03 | 0.07 | 0 | 0.04 | 0.09 | 0 | 0.04 | 0.1 | 0 | 0.04 | 0.14 | 0.02 | 0.08 | 0.12 | 0 | 0.07 |
| 118 | 0.08 | 0 | 0.04 | 0.07 | 0.01 | 0.04 | 0.09 | 0 | 0.05 | 0.12 | 0 | 0.05 | 0.13 | 0 | 0.07 | 0.14 | 0 | 0.08 |
| 119 | 0.07 | 0 | 0.04 | 0.07 | 0 | 0.04 | 0.09 | 0 | 0.04 | 0.15 | 0 | 0.04 | 0.12 | 0 | 0.07 | 0.14 | 0 | 0.08 |
| 120 | 0.07 | 0.01 | 0.04 | 0.07 | 0 | 0.04 | 0.07 | 0 | 0.04 | 0.09 | 0 | 0.03 | 0.12 | 0 | 0.07 | 0.13 | 0 | 0.08 |
| 121 | 0.07 | 0 | 0.04 | 0.09 | 0.02 | 0.05 | 0.07 | 0 | 0.04 | 0.09 | 0 | 0.03 | 0.12 | 0 | 0.07 | 0.14 | 0 | 0.08 |
| 122 | 0.07 | 0 | 0.04 | 0.08 | 0 | 0.04 | 0.08 | 0 | 0.05 | 0.11 | 0 | 0.04 | 0.12 | 0 | 0.07 | 0.14 | 0 | 0.08 |
| 123 | 0.09 | 0 | 0.05 | 0.07 | 0.01 | 0.04 | 0.08 | 0 | 0.04 | 0.09 | 0 | 0.05 | 0.11 | 0 | 0.07 | 0.14 | 0 | 0.08 |
| 124 | 0.1 | 0 | 0.05 | 0.06 | 0 | 0.04 | 0.09 | 0 | 0.05 | 0.09 | 0 | 0.05 | 0.12 | 0 | 0.07 | 0.14 | 0.03 | 0.08 |
| 125 | 0.08 | 0 | 0.05 | 0.07 | 0 | 0.04 | 0.07 | 0 | 0.05 | 0.09 | 0 | 0.06 | 0.12 | 0 | 0.07 | 0.14 | 0 | 0.08 |
| 126 | 0.08 | 0 | 0.05 | 0.09 | 0 | 0.04 | 0.08 | 0.01 | 0.05 | 0.08 | 0 | 0.06 | 0.14 | 0 | 0.07 | 0.15 | 0 | 0.08 |

| | | | | | | | | | | | | | | | | | |
|---|---|---|---|---|---|---|---|---|---|---|---|---|---|---|---|---|---|
| 127 | 0.08 | 0 | 0.05 | 0.09 | 0 | 0.04 | 0.07 | 0 | 0.04 | 0.09 | 0 | 0.06 | 0.13 | 0 | 0.07 | 0.13 | 0.04 | 0.08 |
| 128 | 0.09 | 0 | 0.05 | 0.08 | 0 | 0.04 | 0.07 | 0 | 0.04 | 0.07 | 0 | 0.06 | 0.12 | 0 | 0.07 | 0.13 | 0.03 | 0.08 |
| 129 | 0.08 | 0 | 0.05 | 0.07 | 0 | 0.04 | 0.06 | 0 | 0.04 | 0.09 | 0 | 0.06 | 0.14 | 0 | 0.07 | 0.13 | 0 | 0.08 |
| 130 | 0.1 | 0 | 0.05 | 0.08 | 0 | 0.04 | 0.06 | 0 | 0.03 | 0.07 | 0 | 0.06 | 0.15 | 0.02 | 0.07 | 0.15 | 0 | 0.08 |
| 131 | 0.11 | 0 | 0.05 | 0.07 | 0 | 0.04 | 0.06 | 0.01 | 0.04 | 0.07 | 0 | 0.06 | 0.15 | 0 | 0.07 | 0.14 | 0 | 0.08 |
| 132 | 0.09 | 0 | 0.05 | 0.07 | 0 | 0.04 | 0.07 | 0 | 0.04 | 0.07 | 0 | 0.06 | 0.14 | 0 | 0.08 | 0.14 | 0 | 0.08 |
| 133 | 0.09 | 0 | 0.05 | 0.08 | 0 | 0.04 | 0.07 | 0 | 0.04 | 0.05 | 0 | 0.06 | 0.13 | 0 | 0.08 | 0.14 | 0 | 0.08 |
| 134 | 0.08 | 0 | 0.04 | 0.08 | 0 | 0.04 | 0.07 | 0 | 0.04 | 0.05 | 0 | 0.06 | 0.14 | 0 | 0.08 | 0.04 | 0 | 0.05 |
| 135 | 0.08 | 0 | 0.04 | 0.08 | 0 | 0.04 | 0.1 | 0 | 0.05 | 0.04 | 0 | 0.06 | 0.12 | 0 | 0.08 | 0.03 | 0 | 0.05 |
| 136 | 0.07 | 0 | 0.05 | 0.07 | 0 | 0.04 | 0.07 | 0 | 0.04 | 0.03 | 0 | 0.01 | 0.14 | 0.03 | 0.09 | 0.14 | 0 | 0.07 |
| 137 | 0.08 | 0 | 0.06 | 0.07 | 0 | 0.04 | 0.08 | 0 | 0.04 | 0.03 | 0 | 0.01 | 0.14 | 0 | 0.08 | 0.14 | 0 | 0.08 |
| 138 | 0.08 | 0 | 0.05 | 0.09 | 0 | 0.05 | 0.08 | 0 | 0.05 | 0.03 | 0 | 0.01 | 0.13 | 0 | 0.08 | 0.14 | 0 | 0.09 |
| 139 | 0.07 | 0 | 0.05 | 0.08 | 0 | 0.05 | 0.09 | 0 | 0.05 | 0.03 | 0 | 0.01 | 0.13 | 0 | 0.08 | 0.13 | 0 | 0.07 |
| 140 | 0.08 | 0 | 0.05 | 0.1 | 0 | 0.05 | 0.1 | 0 | 0.05 | 0.02 | 0 | 0.01 | 0.12 | 0 | 0.08 | 0.13 | 0 | 0.07 |
| 141 | 0.08 | 0 | 0.05 | 0.1 | 0 | 0.05 | 0.1 | 0 | 0.06 | 0.04 | 0 | 0.01 | 0.13 | 0 | 0.08 | 0.14 | 0 | 0.08 |
| 142 | 0.08 | 0 | 0.05 | 0.1 | 0.01 | 0.05 | 0.09 | 0 | 0.05 | 0.04 | 0 | 0.01 | 0.12 | 0 | 0.09 | 0.13 | 0 | 0.07 |
| 143 | 0.08 | 0.01 | 0.05 | 0.09 | 0 | 0.05 | 0.09 | 0.02 | 0.06 | 0.02 | 0 | 0.01 | 0.12 | 0 | 0.08 | 0.14 | 0 | 0.07 |
| 144 | 0.08 | 0 | 0.05 | 0.11 | 0 | 0.05 | 0.09 | 0.01 | 0.06 | 0.03 | 0 | 0.01 | 0.12 | 0 | 0.08 | 0.18 | 0 | 0.06 |
| 145 | 0.07 | 0.01 | 0.04 | 0.09 | 0 | 0.05 | 0.09 | 0 | 0.05 | 0.04 | 0 | 0.02 | 0.12 | 0 | 0.08 | 0.14 | 0.02 | 0.07 |
| 146 | 0.08 | 0 | 0.03 | 0.09 | 0 | 0.05 | 0.09 | 0 | 0.05 | 0.06 | 0 | 0.05 | 0.12 | 0 | 0.07 | 0.15 | 0 | 0.07 |
| 147 | 0.09 | 0 | 0.04 | 0.08 | 0 | 0.04 | 0.09 | 0 | 0.05 | 0.12 | 0 | 0.06 | 0.12 | 0 | 0.08 | 0.14 | 0 | 0.07 |
| 148 | 0.06 | 0 | 0.04 | 0.09 | 0 | 0.04 | 0.08 | 0.03 | 0.06 | 0.11 | 0 | 0.06 | 0.12 | 0 | 0.08 | 0.15 | 0 | 0.07 |
| 149 | 0.07 | 0 | 0.04 | 0.06 | 0 | 0.04 | 0.08 | 0 | 0.05 | 0.11 | 0 | 0.06 | 0.12 | 0 | 0.08 | 0.15 | 0 | 0.07 |
| 150 | 0.08 | 0 | 0.04 | 0.08 | 0 | 0.04 | 0.09 | 0 | 0.05 | 0.02 | 0 | 0.06 | 0.12 | 0 | 0.08 | 0.14 | 0 | 0.08 |
| 151 | 0.08 | 0 | 0.04 | 0.07 | 0 | 0.04 | 0.09 | 0 | 0.05 | 0.02 | 0 | 0.06 | 0.12 | 0 | 0.08 | 0.16 | 0 | 0.07 |
| 152 | 0.1 | 0 | 0.05 | 0.07 | 0 | 0.04 | 0.08 | 0 | 0.05 | 0.01 | 0 | 0.6 | 0.12 | 0 | 0.07 | 0.14 | 0 | 0.07 |
| 153 | 0.1 | 0.01 | 0.05 | 0.08 | 0 | 0.04 | 0.1 | 0 | 0.05 | 0.01 | 0.01 | 0.06 | 0.13 | 0 | 0.08 | 0.16 | 0 | 0.08 |
| 154 | 0.1 | 0 | 0.05 | 0.08 | 0 | 0.04 | 0.08 | 0 | 0.05 | 0.12 | 0 | 0.06 | 0.09 | 0 | 0.05 | 0.16 | 0.05 | 0.07 |
| 155 | 0.09 | 0 | 0.04 | 0.12 | 0 | 0.05 | 0.09 | 0.03 | 0.05 | 0.02 | 0 | 0.06 | 0.09 | 0 | 0.05 | 0.12 | 0 | 0.08 |
| 156 | 0.1 | 0 | 0.05 | 0.09 | 0 | 0.05 | 0.09 | 0 | 0.05 | 0.02 | 0 | 0.06 | 0.12 | 0 | 0.07 | 0.14 | 0 | 0.08 |
| 157 | 0.09 | 0 | 0.04 | 0.08 | 0 | 0.05 | 0.06 | 0 | 0.04 | 0.04 | 0 | 0.06 | 0.13 | 0 | 0.07 | 0.14 | 0 | 0.05 |
| 158 | 0.09 | 0.01 | 0.04 | 0.09 | 0 | 0.04 | 0.07 | 0 | 0.04 | 0.03 | 0 | 0.06 | 0.13 | 0 | 0.07 | 0.16 | 0 | 0.05 |
| 159 | 0.09 | 0 | 0.06 | 0.11 | 0 | 0.05 | 0.08 | 0 | 0.04 | 0.01 | 0 | 0.06 | 0.12 | 0 | 0.07 | 0.14 | 0 | 0.05 |
| 160 | 0.09 | 0.01 | 0.06 | 0.09 | 0 | 0.05 | 0.06 | 0 | 0.04 | 0.1 | 0 | 0.06 | 0.13 | 0 | 0.07 | 0.14 | 0.04 | 0.08 |
| 161 | 0.12 | 0 | 0.06 | 0.1 | 0 | 0.05 | 0.07 | 0 | 0.04 | 0.02 | 0 | 0.06 | 0.12 | 0 | 0.07 | 0.15 | 0 | 0.08 |
| 162 | 0.11 | 0 | 0.05 | 0.1 | 0 | 0.04 | 0.08 | 0 | 0.04 | 0.01 | 0 | 0.06 | 0.13 | 0 | 0.07 | 0.15 | 0 | 0.08 |
| 163 | 0.1 | 0.01 | 0.05 | 0.11 | 0 | 0.05 | 0.07 | 0 | 0.04 | 0.09 | 0 | 0.06 | 0.13 | 0 | 0.07 | 0.14 | 0.03 | 0.08 |
| 164 | 0.1 | 0 | 0.05 | 0.1 | 0 | 0.06 | 0.08 | 0 | 0.04 | 0.01 | 0 | 0.06 | 0.14 | 0 | 0.07 | 0.12 | 0 | 0.08 |
| 165 | 0.11 | 0 | 0.05 | 0.09 | 0 | 0.06 | 0.11 | 0 | 0.05 | 0.01 | 0 | 0.06 | 0.12 | 0 | 0.07 | 0.13 | 0.02 | 0.08 |

| | | | | | | | | | | | | | | | | | |
|---|---|---|---|---|---|---|---|---|---|---|---|---|---|---|---|---|---|
| 166 | 0.09 | 0 | 0.05 | 0.1 | 0 | 0.04 | 0.08 | 0 | 0.05 | 0.009 | 0 | 0.06 | 0.12 | 0 | 0.07 | 0.14 | 0 | 0.08 |
| 167 | 0.1 | 0 | 0.05 | 0.09 | 0 | 0.04 | 0.1 | 0 | 0.05 | 0.04 | 0 | 0.02 | 0.12 | 0 | 0.07 | 0.14 | 0.02 | 0.08 |
| 168 | 0.1 | 0 | 0.05 | 0.09 | 0 | 0.04 | 0.09 | 0 | 0.05 | 0.06 | 0 | 0.02 | 0.13 | 0 | 0.07 | 0.13 | 0 | 0.08 |
| 169 | 0.11 | 0.02 | 0.05 | 0.1 | 0 | 0.05 | 0.12 | 0 | 0.05 | 0.04 | 0 | 0.02 | 0.12 | 0 | 0.07 | 0.13 | 0 | 0.07 |
| 170 | 0.1 | 0.01 | 0.05 | 0.11 | 0 | 0.05 | 0.11 | 0 | 0.05 | 0.06 | 0 | 0.06 | 0.13 | 0 | 0.07 | 0.15 | 0 | 0.08 |
| 171 | 0.11 | 0 | 0.05 | 0.09 | 0 | 0.05 | 0.12 | 0 | 0.05 | 0.01 | 0 | 0.06 | 0.13 | 0 | 0.07 | 0.15 | 0.01 | 0.07 |
| 172 | 0.11 | 0 | 0.04 | 0.1 | 0 | 0.05 | 0.11 | 0 | 0.05 | 0.02 | 0 | 0.01 | 0.13 | 0 | 0.07 | 0.15 | 0 | 0.08 |
| 173 | 0.12 | 0 | 0.05 | 0.1 | 0 | 0.05 | 0.11 | 0 | 0.06 | 0.04 | 0.01 | 0.02 | 0.13 | 0 | 0.08 | 0.14 | 0.02 | 0.08 |
| 174 | 0.1 | 0 | 0.04 | 0.11 | 0 | 0.06 | 0.1 | 0 | 0.05 | 0.01 | 0 | 0.06 | 0.12 | 0 | 0.07 | 0.14 | 0.02 | 0.08 |
| 175 | 0.09 | 0 | 0.04 | 0.1 | 0 | 0.05 | 0.09 | 0.02 | 0.06 | 0.04 | 0 | 0.01 | 0.12 | 0 | 0.07 | 0.14 | 0 | 0.08 |
| 176 | 0.1 | 0 | 0.04 | 0.09 | 0.01 | 0.05 | 0.1 | 0.01 | 0.05 | 0.02 | 0 | 0.01 | 0.12 | 0 | 0.08 | 0.15 | 0 | 0.07 |
| 177 | 0.1 | 0 | 0.05 | 0.08 | 0.01 | 0.05 | 0.09 | 0.02 | 0.06 | 0.02 | 0 | 0.01 | 0.11 | 0 | 0.07 | 0.15 | 0 | 0.07 |
| 178 | 0.09 | 0 | 0.04 | 0.09 | 0 | 0.04 | 0.12 | 0.03 | 0.06 | 0.01 | 0 | 0.06 | 0.12 | 0.01 | 0.07 | 0.15 | 0 | 0.07 |
| 179 | 0.09 | 0 | 0.04 | 0.1 | 0 | 0.06 | 0.09 | 0.02 | 0.05 | 0.02 | 0 | 0.06 | 0.11 | 0 | 0.07 | 0.16 | 0 | 0.07 |
| 180 | 0.09 | 0 | 0.04 | 0.11 | 0 | 0.05 | 0.1 | 0 | 0.06 | 0.03 | 0 | 0.06 | 0.13 | 0 | 0.07 | 0.15 | 0 | 0.08 |
| 181 | 0.08 | 0 | 0.05 | 0.1 | 0 | 0.05 | 0.09 | 0.03 | 0.05 | 0.02 | 0 | 0.06 | 0.13 | 0 | 0.07 | 0.14 | 0 | 0.07 |
| 182 | 0.09 | 0 | 0.05 | 0.11 | 0 | 0.05 | 0.1 | 0 | 0.05 | 0.02 | 0 | 0.06 | 0.14 | 0 | 0.07 | 0.14 | 0 | 0.08 |
| 183 | 0.09 | 0 | 0.06 | 0.1 | 0 | 0.05 | 0.09 | 0.01 | 0.05 | 0.02 | 0 | 0.06 | 0.13 | 0 | 0.07 | 0.15 | 0 | 0.09 |
| 184 | 0.09 | 0 | 0.06 | 0.11 | 0 | 0.05 | 0.09 | 0 | 0.05 | 0.02 | 0 | 0.06 | 0.13 | 0 | 0.06 | 0.15 | 0 | 0.08 |
| 185 | 0.09 | 0 | 0.05 | 0.11 | 0 | 0.05 | 0.1 | 0 | 0.05 | 0.03 | 0 | 0.01 | 0.13 | 0 | 0.07 | 0.15 | 0 | 0.08 |
| 186 | 0.09 | 0 | 0.05 | 0.11 | 0 | 0.05 | 0.09 | 0.02 | 0.05 | 0.02 | 0 | 0.01 | 0.13 | 0 | 0.08 | 0.15 | 0 | 0.08 |
| 187 | 0.1 | 0 | 0.05 | 0.08 | 0 | 0.05 | 0.1 | 0 | 0.04 | 0.04 | 0 | 0.01 | 0.14 | 0 | 0.07 | 0.14 | 0 | 0.08 |
| 188 | 0.11 | 0.02 | 0.05 | 0.08 | 0 | 0.05 | 0.1 | 0 | 0.04 | 0.01 | 0 | 0.06 | 0.12 | 0.01 | 0.07 | 0.14 | 0.02 | 0.08 |
| 189 | 0.1 | 0 | 0.05 | 0.1 | 0 | 0.05 | 0.09 | 0 | 0.04 | 0.01 | 0 | 0.06 | 0.12 | 0 | 0.06 | 0.14 | 0 | 0.08 |
| 190 | 0.09 | 0 | 0.05 | 0.1 | 0.02 | 0.06 | 0.09 | 0 | 0.04 | 0.02 | 0 | 0.06 | 0.12 | 0 | 0.07 | 0.14 | 0.02 | 0.08 |
| 191 | 0.09 | 0 | 0.05 | 0.1 | 0 | 0.06 | 0.08 | 0 | 0.04 | 0.01 | 0 | 0.06 | 0.12 | 0 | 0.07 | 0.15 | 0 | 0.07 |
| 192 | 0.1 | 0 | 0.05 | 0.1 | 0 | 0.06 | 0.09 | 0.01 | 0.05 | 0.01 | 0 | 0.06 | 0.11 | 0 | 0.07 | 0.15 | 0 | 0.08 |
| 193 | 0.1 | 0 | 0.05 | 0.1 | 0 | 0.06 | 0.09 | 0 | 0.05 | 0.02 | 0 | 0.06 | 0.12 | 0 | 0.07 | 0.15 | 0 | 0.08 |
| 194 | 0.1 | 0 | 0.05 | 0.09 | 0 | 0.06 | 0.09 | 0.02 | 0.06 | 0.02 | 0 | 0.06 | 0.11 | 0 | 0.07 | 0.15 | 0 | 0.08 |
| 195 | 0.12 | 0 | 0.05 | 0.1 | 0 | 0.07 | 0.09 | 0.02 | 0.06 | 0.01 | 0 | 0.06 | 0.12 | 0 | 0.07 | 0.15 | 0.03 | 0.07 |
| 196 | 0.09 | 0 | 0.06 | 0.1 | 0 | 0.07 | 0.09 | 0 | 0.05 | 0.01 | 0 | 0.06 | 0.12 | 0 | 0.07 | 0.14 | 0.01 | 0.07 |
| 197 | 0.09 | 0 | 0.06 | 0.1 | 0 | 0.07 | 0.09 | 0 | 0.05 | 0.03 | 0 | 0.06 | 0.11 | 0 | 0.07 | 0.14 | 0 | 0.07 |
| 198 | 0.09 | 0 | 0.06 | 0.11 | 0 | 0.06 | 0.09 | 0 | 0.05 | 0.02 | 0 | 0.06 | 0.12 | 0 | 0.07 | 0.14 | 0 | 0.07 |
| 199 | 0.08 | 0 | 0.06 | 0.13 | 0 | 0.06 | 0.11 | 0 | 0.05 | 0.01 | 0 | 0.06 | 0.08 | 0 | 0.05 | 0.15 | 0.02 | 0.07 |
| 200 | 0.1 | 0 | 0.06 | 0.12 | 0 | 0.06 | 0.1 | 0 | 0.05 | 0.02 | 0 | 0.06 | 0.09 | 0 | 0.05 | 0.14 | 0.03 | 0.06 |

| | | | | | | | | | | | | | | | | | |
|---|---|---|---|---|---|---|---|---|---|---|---|---|---|---|---|---|---|
| | Control (mm) | | | | | | | | | Infected (mm) | | | | | | | |
| Day 3 | R1 | | | R2 | | | R3 | | | R1 | | | R2 | | | R3 | |
| | Max | Min | Average | Max | Min | Average | Max | Min | Average | Max | Min | Average | Max | Min | Average | Max | Min | Average |

| | | | | | | | | | | | | | | | | | |
|---|---|---|---|---|---|---|---|---|---|---|---|---|---|---|---|---|---|
| 1 | 0.06 | 0 | 0.04 | 0.05 | 0 | 0.02 | 0.09 | 0 | 0.04 | 0.11 | 0 | 0.05 | 0.12 | 0 | 0.05 | 0.11 | 0.03 | 0.07 |
| 2 | 0.06 | 0 | 0.04 | 0.06 | 0 | 0.03 | 0.07 | 0 | 0.04 | 0.11 | 0 | 0.05 | 0.13 | 0 | 0.05 | 0.1 | 0.04 | 0.07 |
| 3 | 0.06 | 0 | 0.03 | 0.06 | 0 | 0.03 | 0.07 | 0 | 0.03 | 0.1 | 0 | 0.05 | 0.12 | 0 | 0.05 | 0.1 | 0 | 0.07 |
| 4 | 0.06 | 0 | 0.03 | 0.05 | 0 | 0.02 | 0.07 | 0 | 0.04 | 0.1 | 0.2 | 0.06 | 0.12 | 0 | 0.05 | 0.1 | 0 | 0.08 |
| 5 | 0.05 | 0 | 0.03 | 0.05 | 0 | 0.03 | 0.08 | 0 | 0.04 | 0.12 | 0.02 | 0.06 | 0.11 | 0 | 0.05 | 0.1 | 0 | 0.08 |
| 6 | 0.06 | 0 | 0.04 | 0.05 | 0 | 0.03 | 0.08 | 0 | 0.04 | 0.12 | 0 | 0.05 | 0.11 | 0 | 0.05 | 0.1 | 0.04 | 0.08 |
| 7 | 0.06 | 0 | 0.03 | 0.06 | 0 | 0.04 | 0.08 | 0 | 0.04 | 0.09 | 0 | 0.05 | 0.11 | 0 | 0.05 | 0.11 | 0.02 | 0.07 |
| 8 | 0.06 | 0 | 0.03 | 0.06 | 0 | 0.04 | 0.08 | 0 | 0.04 | 0.09 | 0.03 | 0.05 | 0.1 | 0 | 0.05 | 0.09 | 0.03 | 0.06 |
| 9 | 0.06 | 0 | 0.03 | 0.05 | 0 | 0.03 | 0.08 | 0 | 0.04 | 0.12 | 0 | 0.05 | 0.11 | 0.01 | 0.06 | 0.09 | 0 | 0.05 |
| 10 | 0.05 | 0 | 0.03 | 0.06 | 0 | 0.04 | 0.09 | 0 | 0.04 | 0.16 | 0.03 | 0.05 | 0.12 | 0 | 0.05 | 0.09 | 0.02 | 0.05 |
| 11 | 0.05 | 0 | 0.03 | 0.06 | 0 | 0.03 | 0.09 | 0 | 0.04 | 0.21 | 0 | 0.05 | 0.13 | 0 | 0.05 | 0.09 | 0 | 0.05 |
| 12 | 0.06 | 0 | 0.03 | 0.05 | 0.02 | 0.04 | 0.09 | 0 | 0.04 | 0.2 | 0.03 | 0.05 | 0.11 | 0 | 0.05 | 0.09 | 0.03 | 0.05 |
| 13 | 0.05 | 0 | 0.03 | 0.05 | 0 | 0.04 | 0.09 | 0 | 0.04 | 0.19 | 0 | 0.05 | 0.12 | 0 | 0.05 | 0.09 | 0 | 0.06 |
| 14 | 0.05 | 0 | 0.03 | 0.05 | 0 | 0.04 | 0.09 | 0 | 0.04 | 0.16 | 0 | 0.05 | 0.12 | 0 | 0.05 | 0.09 | 0 | 0.07 |
| 15 | 0.04 | 0 | 0.02 | 0.04 | 0 | 0.03 | 0.08 | 0 | 0.04 | 0.18 | 0 | 0.06 | 0.11 | 0 | 0.05 | 0.09 | 0.04 | 0.07 |
| 16 | 0.04 | 0 | 0.02 | 0.05 | 0 | 0.03 | 0.07 | 0 | 0.03 | 0.2 | 0 | 0.06 | 0.12 | 0 | 0.05 | 0.1 | 0 | 0.07 |
| 17 | 0.04 | 0 | 0.03 | 0.05 | 0 | 0.03 | 0.09 | 0 | 0.03 | 0.11 | 0 | 0.05 | 0.12 | 0 | 0.05 | 0.1 | 0.05 | 0.08 |
| 18 | 0.04 | 0 | 0.02 | 0.05 | 0 | 0.03 | 0.06 | 0 | 0.03 | 0.12 | 0 | 0.05 | 0.11 | 0 | 0.05 | 0.12 | 0.05 | 0.08 |
| 19 | 0.05 | 0 | 0.02 | 0.05 | 0 | 0.03 | 0.07 | 0 | 0.03 | 0.11 | 0 | 0.05 | 0.11 | 0 | 0.05 | 0.1 | 0 | 0.08 |
| 20 | 0.04 | 0 | 0.01 | 0.05 | 0 | 0.02 | 0.09 | 0 | 0.03 | 0.11 | 0 | 0.05 | 0.11 | 0 | 0.05 | 0.1 | 0.05 | 0.08 |
| 21 | 0.08 | 0 | 0.03 | 0.05 | 0 | 0.02 | 0.09 | 0 | 0.03 | 0.11 | 0 | 0.05 | 0.12 | 0 | 0.05 | 0.1 | 0 | 0.07 |
| 22 | 0.08 | 0 | 0.03 | 0.05 | 0 | 0.02 | 0.08 | 0 | 0.03 | 0.12 | 0 | 0.05 | 0.21 | 0 | 0.07 | 0.09 | 0.02 | 0.07 |
| 23 | 0.08 | 0 | 0.03 | 0.04 | 0 | 0.01 | 0.09 | 0 | 0.03 | 0.11 | 0 | 0.05 | 0.12 | 0 | 0.08 | 0.11 | 0 | 0.07 |
| 24 | 0.08 | 0 | 0.04 | 0.07 | 0 | 0.02 | 0.07 | 0 | 0.03 | 0.12 | 0 | 0.08 | 0.11 | 0 | 0.07 | 0.1 | 0.05 | 0.08 |
| 25 | 0.08 | 0 | 0.04 | 0.05 | 0 | 0.02 | 0.08 | 0 | 0.03 | 0.12 | 0 | 0.07 | 0.11 | 0 | 0.07 | 0.12 | 0 | 0.08 |
| 26 | 0.08 | 0 | 0.04 | 0.06 | 0 | 0.03 | 0.08 | 0 | 0.03 | 0.12 | 0.01 | 0.08 | 0.12 | 0 | 0.07 | 0.12 | 0 | 0.09 |
| 27 | 0.09 | 0 | 0.04 | 0.08 | 0 | 0.04 | 0.1 | 0 | 0.04 | 0.11 | 0 | 0.08 | 0.13 | 0.02 | 0.08 | 0.11 | 0.05 | 0.09 |
| 28 | 0.08 | 0 | 0.04 | 0.08 | 0 | 0.05 | 0.1 | 0 | 0.04 | 0.15 | 0 | 0.08 | 0.13 | 0 | 0.07 | 0.12 | 0 | 0.09 |
| 29 | 0.08 | 0 | 0.05 | 0.07 | 0 | 0.04 | 0.1 | 0 | 0.03 | 0.11 | 0 | 0.08 | 0.11 | 0.02 | 0.07 | 0.12 | 0 | 0.09 |
| 30 | 0.08 | 0 | 0.05 | 0.07 | 0 | 0.04 | 0.08 | 0 | 0.04 | 0.1 | 0 | 0.08 | 0.1 | 0.03 | 0.07 | 0.12 | 0 | 0.08 |
| 31 | 0.07 | 0 | 0.04 | 0.08 | 0 | 0.05 | 0.08 | 0 | 0.04 | 0.11 | 0.06 | 0.08 | 0.11 | 0 | 0.07 | 0.12 | 0 | 0.05 |
| 32 | 0.07 | 0 | 0.04 | 0.08 | 0 | 0.05 | 0.09 | 0 | 0.04 | 0.11 | 0 | 0.08 | 0.11 | 0 | 0.07 | 0.11 | 0.04 | 0.07 |
| 33 | 0.07 | 0 | 0.03 | 0.06 | 0 | 0.04 | 0.09 | 0 | 0.04 | 0.12 | 0 | 0.08 | 0.11 | 0 | 0.06 | 0.11 | 0.01 | 0.06 |
| 34 | 0.07 | 0 | 0.03 | 0.06 | 0 | 0.04 | 0.08 | 0 | 0.04 | 0.12 | 0 | 0.07 | 0.11 | 0 | 0.07 | 0.11 | 0 | 0.05 |
| 35 | 0.06 | 0.01 | 0.04 | 0.07 | 0 | 0.04 | 0.09 | 0 | 0.04 | 0.12 | 0.03 | 0.07 | 0.14 | 0 | 0.08 | 0.1 | 0 | 0.05 |
| 36 | 0.06 | 0 | 0.04 | 0.06 | 0.02 | 0.04 | 0.08 | 0 | 0.05 | 0.12 | 0 | 0.05 | 0.12 | 0 | 0.06 | 0.1 | 0 | 0.04 |
| 37 | 0.06 | 0.01 | 0.03 | 0.07 | 0 | 0.04 | 0.08 | 0 | 0.04 | 0.12 | 0 | 0.05 | 0.11 | 0 | 0.07 | 0.06 | 0 | 0.03 |
| 38 | 0.05 | 0 | 0.03 | 0.07 | 0.01 | 0.03 | 0.09 | 0 | 0.04 | 0.12 | 0 | 0.05 | 0.11 | 0 | 0.06 | 0.08 | 0 | 0.03 |
| 39 | 0.05 | 0 | 0.03 | 0.07 | 0 | 0.03 | 0.07 | 0 | 0.04 | 0.11 | 0 | 0.07 | 0.12 | 0 | 0.07 | 0.08 | 0 | 0.03 |

| | | | | | | | | | | | | | | | | | |
|---|---|---|---|---|---|---|---|---|---|---|---|---|---|---|---|---|---|
| 40 | 0.06 | 0 | 0.03 | 0.06 | 0 | 0.03 | 0.08 | 0 | 0.05 | 0.1 | 0 | 0.05 | 0.11 | 0 | 0.06 | 0.06 | 0 | 0.03 |
| 41 | 0.06 | 0 | 0.03 | 0.05 | 0 | 0.03 | 0.08 | 0 | 0.04 | 0.09 | 0 | 0.05 | 0.12 | 0 | 0.06 | 0.07 | 0 | 0.04 |
| 42 | 0.07 | 0 | 0.03 | 0.06 | 0 | 0.04 | 0.08 | 0 | 0.04 | 0.09 | 0 | 0.05 | 0.11 | 0 | 0.07 | 0.08 | 0 | 0.04 |
| 43 | 0.07 | 0 | 0.03 | 0.06 | 0 | 0.04 | 0.07 | 0 | 0.04 | 0.1 | 0 | 0.05 | 0.11 | 0 | 0.06 | 0.08 | 0 | 0.05 |
| 44 | 0.05 | 0 | 0.03 | 0.06 | 0 | 0.03 | 0.08 | 0 | 0.04 | 0.09 | 0 | 0.04 | 0.11 | 0 | 0.06 | 0.08 | 0 | 0.05 |
| 45 | 0.06 | 0 | 0.03 | 0.05 | 0 | 0.03 | 0.08 | 0 | 0.04 | 0.09 | 0 | 0.04 | 0.11 | 0 | 0.06 | 0.09 | 0 | 0.05 |
| 46 | 0.06 | 0 | 0.03 | 0.05 | 0 | 0.03 | 0.07 | 0 | 0.04 | 0.09 | 0 | 0.04 | 0.11 | 0 | 0.06 | 0.11 | 0.03 | 0.07 |
| 47 | 0.06 | 0 | 0.03 | 0.06 | 0 | 0.03 | 0.08 | 0 | 0.03 | 0.09 | 0 | 0.04 | 0.11 | 0 | 0.06 | 0.12 | 0 | 0.07 |
| 48 | 0.08 | 0 | 0.04 | 0.06 | 0 | 0.03 | 0.06 | 0 | 0.04 | 0.07 | 0 | 0.03 | 0.11 | 0 | 0.07 | 0.12 | 0 | 0.08 |
| 49 | 0.08 | 0 | 0.05 | 0.04 | 0 | 0.02 | 0.08 | 0 | 0.04 | 0.07 | 0 | 0.02 | 0.11 | 0 | 0.07 | 0.12 | 0 | 0.08 |
| 50 | 0.09 | 0 | 0.04 | 0.04 | 0 | 0.02 | 0.09 | 0 | 0.04 | 0.09 | 0 | 0.04 | 0.12 | 0 | 0.07 | 0.12 | 0 | 0.09 |
| 51 | 0.08 | 0 | 0.03 | 0.04 | 0 | 0.02 | 0.08 | 0 | 0.04 | 0.1 | 0 | 0.04 | 0.12 | 0 | 0.07 | 0.12 | 0 | 0.09 |
| 52 | 0.08 | 0 | 0.03 | 0.05 | 0 | 0.02 | 0.08 | 0 | 0.04 | 0.1 | 0 | 0.04 | 0.1 | 0 | 0.07 | 0.13 | 0 | 0.1 |
| 53 | 0.08 | 0 | 0.04 | 0.07 | 0 | 0.04 | 0.08 | 0 | 0.04 | 0.11 | 0 | 0.05 | 0.13 | 0 | 0.06 | 0.12 | 0 | 0.09 |
| 54 | 0.07 | 0 | 0.04 | 0.08 | 0 | 0.04 | 0.08 | 0 | 0.04 | 0.1 | 0 | 0.05 | 0.11 | 0 | 0.07 | 0.13 | 0 | 0.09 |
| 55 | 0.1 | 0 | 0.05 | 0.08 | 0 | 0.05 | 0.1 | 0 | 0.04 | 0.12 | 0 | 0.05 | 0.11 | 0 | 0.07 | 0.13 | 0 | 0.09 |
| 56 | 0.08 | 0 | 0.04 | 0.08 | 0 | 0.05 | 0.1 | 0 | 0.05 | 0.11 | 0 | 0.07 | 0.11 | 0 | 0.06 | 0.13 | 0 | 0.08 |
| 57 | 0.09 | 0 | 0.04 | 0.06 | 0 | 0.04 | 0.09 | 0 | 0.04 | 0.1 | 0 | 0.07 | 0.1 | 0 | 0.07 | 0.13 | 0 | 0.08 |
| 58 | 0.08 | 0.01 | 0.04 | 0.08 | 0 | 0.04 | 0.09 | 0 | 0.05 | 0.11 | 0 | 0.08 | 0.11 | 0 | 0.07 | 0.12 | 0 | 0.08 |
| 59 | 0.08 | 0 | 0.04 | 0.07 | 0 | 0.04 | 0.08 | 0 | 0.04 | 0.11 | 0.01 | 0.07 | 0.12 | 0 | 0.07 | 0.12 | 0 | 0.09 |
| 60 | 0.08 | 0 | 0.04 | 0.07 | 0 | 0.04 | 0.09 | 0 | 0.04 | 0.11 | 0 | 0.07 | 0.13 | 0 | 0.07 | 0.12 | 0 | 0.09 |
| 61 | 0.07 | 0 | 0.04 | 0.07 | 0 | 0.04 | 0.09 | 0 | 0.04 | 0.11 | 0 | 0.07 | 0.11 | 0 | 0.07 | 0.12 | 0 | 0.09 |
| 62 | 0.06 | 0 | 0.03 | 0.06 | 0 | 0.04 | 0.08 | 0 | 0.04 | 0.12 | 0 | 0.07 | 0.12 | 0 | 0.07 | 0.12 | 0.02 | 0.09 |
| 63 | 0.08 | 0 | 0.03 | 0.07 | 0.01 | 0.04 | 0.06 | 0 | 0.04 | 0.11 | 0 | 0.07 | 0.11 | 0 | 0.07 | 0.14 | 0 | 0.1 |
| 64 | 0.06 | 0 | 0.03 | 0.07 | 0 | 0.03 | 0.08 | 0 | 0.05 | 0.11 | 0.04 | 0.07 | 0.13 | 0 | 0.07 | 0.13 | 0 | 0.1 |
| 65 | 0.06 | 0 | 0.03 | 0.07 | 0 | 0.03 | 0.1 | 0 | 0.05 | 0.12 | 0 | 0.08 | 0.12 | 0 | 0.05 | 0.13 | 0 | 0.1 |
| 66 | 0.08 | 0 | 0.03 | 0.05 | 0 | 0.03 | 0.1 | 0 | 0.05 | 0.11 | 0 | 0.07 | 0.1 | 0 | 0.05 | 0.14 | 0 | 0.1 |
| 67 | 0.05 | 0 | 0.03 | 0.06 | 0 | 0.03 | 0.08 | 0 | 0.05 | 0.11 | 0.05 | 0.08 | 0.12 | 0 | 0.05 | 0.14 | 0 | 0.09 |
| 68 | 0.07 | 0 | 0.03 | 0.05 | 0 | 0.02 | 0.08 | 0 | 0.05 | 0.11 | 0 | 0.08 | 0.1 | 0 | 0.05 | 0.13 | 0.06 | 0.09 |
| 69 | 0.07 | 0 | 0.01 | 0.06 | 0 | 0.01 | 0.11 | 0 | 0.05 | 0.1 | 0 | 0.07 | 0.1 | 0 | 0.05 | 0.12 | 0 | 0.08 |
| 70 | 0.04 | 0 | 0.02 | 0.05 | 0 | 0.02 | 0.1 | 0 | 0.05 | 0.1 | 0.04 | 0.07 | 0.09 | 0 | 0.05 | 0.12 | 0 | 0.07 |
| 71 | 0.05 | 0 | 0.02 | 0.05 | 0 | 0.02 | 0.1 | 0 | 0.05 | 0.1 | 0 | 0.06 | 0.12 | 0 | 0.07 | 0.13 | 0.06 | 0.07 |
| 72 | 0.05 | 0 | 0.02 | 0.05 | 0 | 0.02 | 0.09 | 0.01 | 0.05 | 0.09 | 0 | 0.06 | 0.1 | 0 | 0.07 | 0.12 | 0 | 0.07 |
| 73 | 0.05 | 0 | 0.02 | 0.05 | 0 | 0.02 | 0.11 | 0 | 0.04 | 0.1 | 0 | 0.06 | 0.12 | 0 | 0.07 | 0.1 | 0 | 0.05 |
| 74 | 0.03 | 0 | 0.01 | 0.05 | 0 | 0.02 | 0.1 | 0 | 0.05 | 0.1 | 0 | 0.06 | 0.11 | 0 | 0.07 | 0.08 | 0 | 0.06 |
| 75 | 0.04 | 0 | 0.01 | 0.04 | 0 | 0.02 | 0.08 | 0.02 | 0.05 | 0.11 | 0 | 0.06 | 0.11 | 0 | 0.07 | 0.09 | 0.04 | 0.07 |
| 76 | 0.05 | 0 | 0.01 | 0.05 | 0 | 0.03 | 0.08 | 0 | 0.05 | 0.1 | 0.04 | 0.06 | 0.12 | 0 | 0.07 | 0.09 | 0 | 0.06 |
| 77 | 0.09 | 0 | 0.03 | 0.04 | 0 | 0.02 | 0.09 | 0.03 | 0.05 | 0.1 | 0.02 | 0.06 | 0.12 | 0 | 0.08 | 0.1 | 0 | 0.07 |
| 78 | 0.12 | 0 | 0.06 | 0.04 | 0 | 0.02 | 0.07 | 0.02 | 0.05 | 0.1 | 0.03 | 0.06 | 0.15 | 0 | 0.07 | 0.11 | 0.03 | 0.08 |

| | | | | | | | | | | | | | | | | | |
|---|---|---|---|---|---|---|---|---|---|---|---|---|---|---|---|---|---|
| 79 | 0.12 | 0 | 0.08 | 0.04 | 0 | 0.01 | 0.13 | 0 | 0.05 | 0.09 | 0.03 | 0.06 | 0.14 | 0 | 0.07 | 0.11 | 0 | 0.07 |
| 80 | 0.1 | 0 | 0.07 | 0.03 | 0 | 0.01 | 0.11 | 0.01 | 0.05 | 0.09 | 0.01 | 0.06 | 0.12 | 0 | 0.07 | 0.11 | 0 | 0.09 |
| 81 | 0.09 | 0 | 0.05 | 0.06 | 0 | 0.02 | 0.12 | 0 | 0.05 | 0.11 | 0 | 0.05 | 0.12 | 0 | 0.07 | 0.11 | 0.04 | 0.09 |
| 82 | 0.1 | 0 | 0.04 | 0.09 | 0 | 0.04 | 0.1 | 0 | 0.06 | 0.12 | 0.03 | 0.05 | 0.13 | 0 | 0.07 | 0.11 | 0.06 | 0.09 |
| 83 | 0.11 | 0.01 | 0.05 | 0.11 | 0 | 0.07 | 0.1 | 0 | 0.06 | 0.11 | 0.03 | 0.07 | 0.13 | 0 | 0.07 | 0.11 | 0 | 0.08 |
| 84 | 0.09 | 0 | 0.05 | 0.1 | 0 | 0.07 | 0.11 | 0 | 0.05 | 0.12 | 0.03 | 0.07 | 0.11 | 0 | 0.07 | 0.11 | 0 | 0.09 |
| 85 | 0.08 | 0 | 0.04 | 0.1 | 0 | 0.07 | 0.12 | 0 | 0.05 | 0.11 | 0.03 | 0.07 | 0.12 | 0 | 0.07 | 0.33 | 0.05 | 0.11 |
| 86 | 0.1 | 0 | 0.04 | 0.08 | 0 | 0.05 | 0.11 | 0 | 0.05 | 0.12 | 0 | 0.07 | 0.13 | 0 | 0.07 | 0.12 | 0.04 | 0.09 |
| 87 | 0.09 | 0 | 0.04 | 0.1 | 0 | 0.05 | 0.09 | 0 | 0.05 | 0.12 | 0.03 | 0.07 | 0.13 | 0 | 0.07 | 0.11 | 0 | 0.09 |
| 88 | 0.09 | 0 | 0.04 | 0.09 | 0 | 0.05 | 0.11 | 0 | 0.05 | 0.11 | 0.03 | 0.07 | 0.12 | 0 | 0.07 | 0.12 | 0.04 | 0.09 |
| 89 | 0.08 | 0 | 0.04 | 0.1 | 0 | 0.05 | 0.11 | 0 | 0.05 | 0.12 | 0.01 | 0.07 | 0.13 | 0 | 0.07 | 0.12 | 0 | 0.1 |
| 90 | 0.08 | 0.02 | 0.05 | 0.09 | 0 | 0.05 | 0.1 | 0 | 0.05 | 0.15 | 0.02 | 0.08 | 0.12 | 0 | 0.07 | 0.12 | 0 | 0.1 |
| 91 | 0.09 | 0 | 0.04 | 0.1 | 0 | 0.04 | 0.11 | 0 | 0.06 | 0.13 | 0 | 0.08 | 0.13 | 0 | 0.07 | 0.12 | 0.07 | 0.1 |
| 92 | 0.08 | 0 | 0.04 | 0.1 | 0 | 0.04 | 0.12 | 0 | 0.05 | 0.12 | 0 | 0.08 | 0.13 | 0 | 0.07 | 0.12 | 0 | 0.1 |
| 93 | 0.08 | 0 | 0.03 | 0.08 | 0 | 0.04 | 0.1 | 0 | 0.05 | 0.11 | 0 | 0.07 | 0.13 | 0 | 0.08 | 0.13 | 0 | 0.09 |
| 94 | 0.07 | 0 | 0.03 | 0.09 | 0.01 | 0.04 | 0.1 | 0 | 0.06 | 0.11 | 0 | 0.08 | 0.15 | 0 | 0.07 | 0.15 | 0 | 0.09 |
| 95 | 0.07 | 0 | 0.03 | 0.07 | 0 | 0.04 | 0.12 | 0 | 0.06 | 0.1 | 0 | 0.08 | 0.12 | 0 | 0.07 | 0.12 | 0 | 0.08 |
| 96 | 0.09 | 0 | 0.03 | 0.09 | 0 | 0.04 | 0.1 | 0.02 | 0.06 | 0.12 | 0 | 0.08 | 0.18 | 0 | 0.07 | 0.14 | 0 | 0.05 |
| 97 | 0.07 | 0 | 0.03 | 0.08 | 0.01 | 0.04 | 0.1 | 0.04 | 0.06 | 0.13 | 0 | 0.08 | 0.11 | 0 | 0.07 | 0.11 | 0 | 0.05 |
| 98 | 0.05 | 0 | 0.03 | 0.06 | 0 | 0.03 | 0.1 | 0.04 | 0.06 | 0.12 | 0 | 0.07 | 0.12 | 0 | 0.07 | 0.12 | 0 | 0.05 |
| 99 | 0.08 | 0 | 0.04 | 0.06 | 0 | 0.03 | 0.1 | 0 | 0.05 | 0.11 | 0 | 0.06 | 0.12 | 0 | 0.06 | 0.12 | 0 | 0.04 |
| 100 | 0.09 | 0 | 0.03 | 0.07 | 0 | 0.03 | 0.12 | 0 | 0.05 | 0.11 | 0 | 0.05 | 0.11 | 0 | 0.06 | 0.11 | 0 | 0.03 |
| 101 | 0.1 | 0 | 0.03 | 0.05 | 0 | 0.02 | 0.12 | 0 | 0.05 | 0.1 | 0 | 0.06 | 0.11 | 0 | 0.07 | 0.09 | 0 | 0.05 |
| 102 | 0.07 | 0 | 0.02 | 0.06 | 0 | 0.02 | 0.12 | 0.02 | 0.05 | 0.09 | 0 | 0.05 | 0.14 | 0 | 0.07 | 0.09 | 0 | 0.03 |
| 103 | 0.1 | 0 | 0.04 | 0.05 | 0 | 0.02 | 0.11 | 0 | 0.05 | 0.12 | 0 | 0.05 | 0.13 | 0 | 0.07 | 0.26 | 0 | 0.06 |
| 104 | 0.12 | 0 | 0.05 | 0.05 | 0 | 0.03 | 0.11 | 0 | 0.04 | 0.11 | 0 | 0.06 | 0.12 | 0 | 0.06 | 0.07 | 0 | 0.04 |
| 105 | 0.1 | 0 | 0.05 | 0.05 | 0 | 0.03 | 0.11 | 0 | 0.04 | 0.28 | 0 | 0.05 | 0.12 | 0 | 0.06 | 0.11 | 0 | 0.05 |
| 106 | 0.08 | 0 | 0.04 | 0.07 | 0 | 0.03 | 0.11 | 0 | 0.04 | 0.3 | 0 | 0.05 | 0.12 | 0 | 0.06 | 0.09 | 0 | 0.05 |
| 107 | 0.08 | 0 | 0.03 | 0.08 | 0 | 0.03 | 0.11 | 0 | 0.04 | 0.09 | 0 | 0.04 | 0.11 | 0 | 0.06 | 0.64 | 0 | 0.07 |
| 108 | 0.08 | 0 | 0.04 | 0.1 | 0 | 0.05 | 0.1 | 0 | 0.04 | 0.08 | 0 | 0.04 | 0.12 | 0 | 0.07 | 0.1 | 0 | 0.05 |
| 109 | 0.08 | 0 | 0.04 | 0.11 | 0 | 0.06 | 0.09 | 0.01 | 0.04 | 0.09 | 0 | 0.05 | 0.12 | 0 | 0.07 | 0.1 | 0 | 0.07 |
| 110 | 0.08 | 0 | 0.04 | 0.11 | 0 | 0.06 | 0.09 | 0 | 0.04 | 0.11 | 0 | 0.05 | 0.12 | 0 | 0.06 | 0.12 | 0 | 0.07 |
| 111 | 0.07 | 0 | 0.04 | 0.1 | 0 | 0.05 | 0.09 | 0 | 0.04 | 0.11 | 0 | 0.06 | 0.14 | 0 | 0.08 | 0.11 | 0 | 0.08 |
| 112 | 0.08 | 0 | 0.04 | 0.09 | 0 | 0.04 | 0.09 | 0.02 | 0.05 | 0.12 | 0 | 0.06 | 0.11 | 0 | 0.07 | 0.12 | 0 | 0.08 |
| 113 | 0.07 | 0 | 0.04 | 0.07 | 0 | 0.04 | 0.09 | 0.02 | 0.05 | 0.11 | 0 | 0.07 | 0.11 | 0 | 0.07 | 0.13 | 0 | 0.09 |
| 114 | 0.06 | 0 | 0.04 | 0.07 | 0 | 0.04 | 0.08 | 0 | 0.04 | 0.11 | 0.01 | 0.07 | 0.11 | 0 | 0.07 | 0.12 | 0 | 0.09 |
| 115 | 0.07 | 0 | 0.05 | 0.07 | 0 | 0.03 | 0.14 | 0 | 0.05 | 0.13 | 0 | 0.08 | 0.11 | 0 | 0.08 | 0.12 | 0 | 0.09 |
| 116 | 0.07 | 0 | 0.04 | 0.07 | 0 | 0.04 | 0.13 | 0 | 0.05 | 0.12 | 0.01 | 0.08 | 0.11 | 0 | 0.07 | 0.12 | 0 | 0.09 |
| 117 | 0.08 | 0 | 0.04 | 0.06 | 0.01 | 0.04 | 0.1 | 0 | 0.04 | 0.12 | 0 | 0.08 | 0.13 | 0 | 0.08 | 0.11 | 0 | 0.09 |

| | | | | | | | | | | | | | | | | | |
|---|---|---|---|---|---|---|---|---|---|---|---|---|---|---|---|---|---|
| 118 | 0.08 | 0 | 0.04 | 0.07 | 0 | 0.04 | 0.11 | 0 | 0.04 | 0.12 | 0 | 0.08 | 0.11 | 0 | 0.07 | 0.12 | 0.04 | 0.09 |
| 119 | 0.08 | 0 | 0.03 | 0.07 | 0 | 0.03 | 0.11 | 0 | 0.05 | 0.12 | 0 | 0.08 | 0.11 | 0 | 0.07 | 0.12 | 0 | 0.09 |
| 120 | 0.06 | 0 | 0.04 | 0.08 | 0 | 0.03 | 0.11 | 0 | 0.06 | 0.11 | 0 | 0.08 | 0.14 | 0 | 0.08 | 0.12 | 0 | 0.09 |
| 121 | 0.07 | 0 | 0.03 | 0.06 | 0 | 0.02 | 0.11 | 0 | 0.05 | 0.11 | 0 | 0.08 | 0.15 | 0 | 0.08 | 0.13 | 0.04 | 0.09 |
| 122 | 0.06 | 0 | 0.03 | 0.06 | 0 | 0.03 | 0.12 | 0.02 | 0.05 | 0.11 | 0.04 | 0.08 | 0.13 | 0 | 0.08 | 0.13 | 0 | 0.1 |
| 123 | 0.06 | 0 | 0.02 | 0.06 | 0 | 0.03 | 0.14 | 0 | 0.05 | 0.11 | 0 | 0.08 | 0.13 | 0 | 0.08 | 0.15 | 0.08 | 0.11 |
| 124 | 0.08 | 0 | 0.03 | 0.06 | 0 | 0.03 | 0.16 | 0 | 0.05 | 0.11 | 0 | 0.08 | 0.12 | 0 | 0.08 | 0.15 | 0 | 0.09 |
| 125 | 0.07 | 0 | 0.02 | 0.05 | 0 | 0.02 | 0.14 | 0 | 0.05 | 0.12 | 0 | 0.08 | 0.13 | 0 | 0.08 | 0.13 | 0.03 | 0.09 |
| 126 | 0.06 | 0 | 0.03 | 0.06 | 0 | 0.03 | 0.14 | 0 | 0.06 | 0.12 | 0 | 0.08 | 0.13 | 0 | 0.08 | 0.12 | 0 | 0.08 |
| 127 | 0.06 | 0 | 0.03 | 0.08 | 0 | 0.03 | 0.13 | 0 | 0.06 | 0.12 | 0 | 0.08 | 0.29 | 0 | 0.09 | 0.14 | 0 | 0.09 |
| 128 | 0.09 | 0 | 0.05 | 0.06 | 0 | 0.03 | 0.14 | 0 | 0.06 | 0.13 | 0 | 0.08 | 0.14 | 0 | 0.08 | 0.15 | 0 | 0.08 |
| 129 | 0.1 | 0 | 0.06 | 0.05 | 0 | 0.02 | 0.12 | 0 | 0.05 | 0.1 | 0 | 0.07 | 0.13 | 0 | 0.07 | 0.14 | 0 | 0.08 |
| 130 | 0.12 | 0 | 0.05 | 0.05 | 0 | 0.02 | 0.13 | 0.01 | 0.05 | 0.1 | 0 | 0.07 | 0.11 | 0 | 0.07 | 0.13 | 0.03 | 0.07 |
| 131 | 0.11 | 0 | 0.05 | 0.04 | 0 | 0.02 | 0.12 | 0 | 0.05 | 0.1 | 0 | 0.06 | 0.13 | 0 | 0.07 | 0.13 | 0 | 0.06 |
| 132 | 0.09 | 0 | 0.05 | 0.06 | 0 | 0.03 | 0.11 | 0 | 0.05 | 0.1 | 0.02 | 0.06 | 0.12 | 0 | 0.07 | 0.14 | 0 | 0.06 |
| 133 | 0.07 | 0 | 0.04 | 0.1 | 0 | 0.05 | 0.12 | 0 | 0.05 | 0.1 | 0 | 0.06 | 0.12 | 0 | 0.07 | 0.76 | 0 | 0.07 |
| 134 | 0.08 | 0 | 0.05 | 0.1 | 0 | 0.05 | 0.11 | 0.01 | 0.05 | 0.1 | 0 | 0.05 | 0.11 | 0 | 0.07 | 0.74 | 0 | 0.07 |
| 135 | 0.1 | 0 | 0.04 | 0.11 | 0 | 0.05 | 0.11 | 0 | 0.05 | 0.13 | 0 | 0.05 | 0.12 | 0 | 0.07 | 0.12 | 0 | 0.05 |
| 136 | 0.08 | 0 | 0.05 | 0.11 | 0 | 0.05 | 0.19 | 0 | 0.05 | 0.1 | 0 | 0.06 | 0.12 | 0 | 0.07 | 0.11 | 0 | 0.06 |
| 137 | 0.08 | 0 | 0.05 | 0.09 | 0 | 0.05 | 0.11 | 0 | 0.06 | 0.1 | 0.02 | 0.07 | 0.14 | 0.03 | 0.08 | 0.13 | 0.03 | 0.06 |
| 138 | 0.09 | 0 | 0.05 | 0.08 | 0 | 0.04 | 0.1 | 0.02 | 0.06 | 0.14 | 0.03 | 0.07 | 0.12 | 0 | 0.07 | 0.67 | 0 | 0.14 |
| 139 | 0.1 | 0 | 0.05 | 0.08 | 0 | 0.05 | 0.1 | 0 | 0.05 | 0.12 | 0 | 0.08 | 0.13 | 0 | 0.08 | 0.3 | 0.05 | 0.09 |
| 140 | 0.07 | 0 | 0.05 | 0.09 | 0 | 0.05 | 0.11 | 0 | 0.05 | 0.11 | 0 | 0.08 | 0.12 | 0 | 0.08 | 0.11 | 0 | 0.09 |
| 141 | 0.06 | 0.02 | 0.04 | 0.08 | 0 | 0.05 | 0.11 | 0 | 0.05 | 0.11 | 0.03 | 0.08 | 0.12 | 0 | 0.08 | 0.12 | 0 | 0.09 |
| 142 | 0.06 | 0 | 0.04 | 0.07 | 0 | 0.04 | 0.1 | 0.01 | 0.05 | 0.12 | 0.04 | 0.08 | 0.12 | 0 | 0.08 | 0.59 | 0.05 | 0.13 |
| 143 | 0.07 | 0 | 0.04 | 0.07 | 0 | 0.05 | 0.12 | 0.02 | 0.06 | 0.12 | 0.04 | 0.08 | 0.14 | 0 | 0.08 | 0.12 | 0 | 0.09 |
| 144 | 0.07 | 0 | 0.04 | 0.07 | 0 | 0.04 | 0.09 | 0 | 0.05 | 0.11 | 0.04 | 0.09 | 0.14 | 0 | 0.08 | 0.13 | 0 | 0.09 |
| 145 | 0.07 | 0 | 0.04 | 0.07 | 0 | 0.04 | 0.09 | 0 | 0.05 | 0.13 | 0.04 | 0.09 | 0.16 | 0 | 0.08 | 0.12 | 0 | 0.09 |
| 146 | 0.06 | 0 | 0.04 | 0.07 | 0 | 0.04 | 0.11 | 0 | 0.06 | 0.12 | 0.05 | 0.09 | 0.13 | 0.02 | 0.08 | 0.12 | 0 | 0.09 |
| 147 | 0.08 | 0 | 0.04 | 0.07 | 0 | 0.04 | 0.1 | 0 | 0.05 | 0.13 | 0.05 | 0.09 | 0.12 | 0 | 0.08 | 0.12 | 0 | 0.09 |
| 148 | 0.09 | 0.02 | 0.04 | 0.07 | 0 | 0.05 | 0.14 | 0 | 0.06 | 0.12 | 0.03 | 0.09 | 0.15 | 0 | 0.08 | 0.16 | 0.05 | 0.1 |
| 149 | 0.08 | 0 | 0.04 | 0.07 | 0.02 | 0.05 | 0.1 | 0 | 0.05 | 0.12 | 0.04 | 0.09 | 0.15 | 0 | 0.08 | 0.14 | 0 | 0.1 |
| 150 | 0.06 | 0 | 0.03 | 0.09 | 0 | 0.04 | 0.11 | 0 | 0.05 | 0.12 | 0.07 | 0.09 | 0.12 | 0 | 0.07 | 0.13 | 0.07 | 0.1 |
| 151 | 0.09 | 0 | 0.04 | 0.07 | 0.02 | 0.04 | 0.1 | 0 | 0.05 | 0.12 | 0.07 | 0.09 | 0.13 | 0 | 0.08 | 0.15 | 0 | 0.1 |
| 152 | 0.1 | 0 | 0.05 | 0.07 | 0 | 0.03 | 0.11 | 0 | 0.05 | 0.12 | 0 | 0.08 | 0.13 | 0 | 0.07 | 0.13 | 0.08 | 0.11 |
| 153 | 0.13 | 0 | 0.05 | 0.07 | 0 | 0.03 | 0.1 | 0 | 0.05 | 0.11 | 0 | 0.08 | 0.14 | 0 | 0.07 | 0.16 | 0 | 0.1 |
| 154 | 0.12 | 0 | 0.06 | 0.07 | 0 | 0.03 | 0.1 | 0 | 0.06 | 0.12 | 0.03 | 0.07 | 0.14 | 0 | 0.07 | 0.15 | 0.06 | 0.1 |
| 155 | 0.12 | 0 | 0.06 | 0.08 | 0 | 0.04 | 0.1 | 0 | 0.05 | 0.11 | 0.04 | 0.07 | 0.13 | 0 | 0.06 | 0.16 | 0.05 | 0.09 |
| 156 | 0.12 | 0 | 0.06 | 0.09 | 0 | 0.05 | 0.1 | 0 | 0.05 | 0.13 | 0 | 0.07 | 0.14 | 0 | 0.06 | 0.14 | 0 | 0.09 |

| | | | | | | | | | | | | | | | | | |
|---|---|---|---|---|---|---|---|---|---|---|---|---|---|---|---|---|---|
| 157 | 0.1 | 0.03 | 0.05 | 0.09 | 0 | 0.06 | 0.12 | 0.01 | 0.05 | 0.11 | 0 | 0.06 | 0.14 | 0 | 0.07 | 0.14 | 0 | 0.07 |
| 158 | 0.09 | 0 | 0.06 | 0.12 | 0 | 0.06 | 0.11 | 0 | 0.05 | 0.13 | 0.01 | 0.06 | 0.14 | 0 | 0.07 | 0.16 | 0 | 0.07 |
| 159 | 0.1 | 0 | 0.05 | 0.12 | 0 | 0.06 | 0.1 | 0 | 0.05 | 0.11 | 0 | 0.06 | 0.13 | 0 | 0.07 | 0.18 | 0.04 | 0.08 |
| 160 | 0.1 | 0.02 | 0.05 | 0.12 | 0 | 0.05 | 0.11 | 0 | 0.05 | 0.1 | 0 | 0.05 | 0.12 | 0 | 0.05 | 0.14 | 0 | 0.07 |
| 161 | 0.1 | 0 | 0.05 | 0.11 | 0 | 0.04 | 0.11 | 0 | 0.05 | 0.1 | 0 | 0.05 | 0.14 | 0 | 0.07 | 0.14 | 0 | 0.07 |
| 162 | 0.08 | 0 | 0.05 | 0.12 | 0 | 0.05 | 0.1 | 0 | 0.05 | 0.09 | 0 | 0.04 | 0.14 | 0 | 0.07 | 0.13 | 0 | 0.07 |
| 163 | 0.06 | 0 | 0.04 | 0.12 | 0.01 | 0.05 | 0.1 | 0 | 0.05 | 0.09 | 0 | 0.03 | 0.13 | 0 | 0.07 | 0.12 | 0 | 0.06 |
| 164 | 0.08 | 0.03 | 0.05 | 0.11 | 0 | 0.04 | 0.08 | 0.02 | 0.05 | 0.1 | 0 | 0.03 | 0.14 | 0 | 0.07 | 0.12 | 0.03 | 0.06 |
| 165 | 0.07 | 0 | 0.04 | 0.1 | 0 | 0.04 | 0.07 | 0 | 0.05 | 0.07 | 0 | 0.03 | 0.12 | 0 | 0.05 | 0.12 | 0 | 0.06 |
| 166 | 0.07 | 0 | 0.04 | 0.1 | 0 | 0.05 | 0.08 | 0 | 0.05 | 0.05 | 0 | 0.03 | 0.13 | 0 | 0.05 | 0.11 | 0 | 0.06 |
| 167 | 0.08 | 0 | 0.04 | 0.08 | 0 | 0.05 | 0.1 | 0 | 0.05 | 0.06 | 0 | 0.03 | 0.12 | 0 | 0.05 | 0.11 | 0 | 0.06 |
| 168 | 0.08 | 0 | 0.04 | 0.09 | 0 | 0.04 | 0.1 | 0 | 0.05 | 0.09 | 0 | 0.03 | 0.13 | 0 | 0.05 | 0.1 | 0.05 | 0.07 |
| 169 | 0.06 | 0 | 0.03 | 0.07 | 0 | 0.04 | 0.1 | 0.01 | 0.05 | 0.1 | 0 | 0.04 | 0.13 | 0 | 0.05 | 0.1 | 0.04 | 0.08 |
| 170 | 0.09 | 0 | 0.04 | 0.06 | 0 | 0.04 | 0.09 | 0 | 0.06 | 0.1 | 0 | 0.06 | 0.13 | 0 | 0.05 | 0.11 | 0 | 0.08 |
| 171 | 0.05 | 0 | 0.03 | 0.06 | 0 | 0.04 | 0.12 | 0 | 0.06 | 0.12 | 0 | 0.07 | 0.13 | 0 | 0.05 | 0.14 | 0 | 0.09 |
| 172 | 0.07 | 0 | 0.03 | 0.06 | 0 | 0.05 | 0.09 | 0.02 | 0.05 | 0.11 | 0 | 0.06 | 0.12 | 0 | 0.05 | 0.13 | 0 | 0.09 |
| 173 | 0.07 | 0 | 0.03 | 0.07 | 0 | 0.05 | 0.09 | 0 | 0.05 | 0.11 | 0 | 0.07 | 0.12 | 0 | 0.05 | 0.13 | 0 | 0.09 |
| 174 | 0.06 | 0 | 0.03 | 0.06 | 0 | 0.04 | 0.09 | 0 | 0.06 | 0.11 | 0 | 0.07 | 0.12 | 0 | 0.05 | 0.12 | 0 | 0.1 |
| 175 | 0.05 | 0 | 0.02 | 0.06 | 0 | 0.03 | 0.09 | 0 | 0.05 | 0.11 | 0 | 0.07 | 0.13 | 0 | 0.05 | 0.13 | 0.05 | 0.1 |
| 176 | 0.06 | 0 | 0.03 | 0.05 | 0 | 0.03 | 0.09 | 0.03 | 0.06 | 0.12 | 0 | 0.08 | 0.15 | 0 | 0.05 | 0.12 | 0 | 0.1 |
| 177 | 0.07 | 0.01 | 0.04 | 0.05 | 0 | 0.03 | 0.09 | 0 | 0.05 | 0.11 | 0 | 0.08 | 0.09 | 0 | 0.05 | 0.12 | 0 | 0.1 |
| 178 | 0.08 | 0 | 0.04 | 0.05 | 0 | 0.03 | 0.09 | 0 | 0.06 | 0.12 | 0.01 | 0.08 | 0.08 | 0 | 0.05 | 0.13 | 0 | 0.1 |
| 179 | 0.08 | 0 | 0.05 | 0.06 | 0 | 0.02 | 0.09 | 0 | 0.06 | 0.11 | 0 | 0.08 | 0.09 | 0 | 0.05 | 0.14 | 0 | 0.1 |
| 180 | 0.09 | 0 | 0.04 | 0.05 | 0 | 0.02 | 0.09 | 0 | 0.06 | 0.13 | 0.01 | 0.08 | 0.08 | 0.03 | 0.05 | 0.14 | 0.04 | 0.1 |
| 181 | 0.06 | 0 | 0.05 | 0.06 | 0 | 0.02 | 0.09 | 0 | 0.05 | 0.12 | 0 | 0.09 | 0.08 | 0.02 | 0.05 | 0.13 | 0 | 0.1 |
| 182 | 0.11 | 0 | 0.06 | 0.06 | 0 | 0.03 | 0.08 | 0 | 0.05 | 0.12 | 0 | 0.09 | 0.15 | 0 | 0.05 | 0.13 | 0 | 0.09 |
| 183 | 0.13 | 0 | 0.07 | 0.08 | 0 | 0.04 | 0.09 | 0 | 0.05 | 0.12 | 0 | 0.09 | 0.13 | 0 | 0.05 | 0.13 | 0 | 0.1 |
| 184 | 0.13 | 0 | 0.06 | 0.08 | 0 | 0.04 | 0.08 | 0.03 | 0.05 | 0.12 | 0.01 | 0.09 | 0.16 | 0 | 0.05 | 0.14 | 0.05 | 0.1 |
| 185 | 0.11 | 0 | 0.06 | 0.08 | 0 | 0.04 | 0.08 | 0.02 | 0.05 | 0.12 | 0 | 0.08 | 0.15 | 0 | 0.05 | 0.13 | 0 | 0.09 |
| 186 | 0.11 | 0 | 0.06 | 0.11 | 0 | 0.05 | 0.09 | 0 | 0.04 | 0.12 | 0 | 0.08 | 0.15 | 0 | 0.05 | 0.13 | 0 | 0.08 |
| 187 | 0.11 | 0 | 0.05 | 0.11 | 0 | 0.06 | 0.09 | 0 | 0.04 | 0.13 | 0 | 0.08 | 0.14 | 0 | 0.08 | 0.13 | 0 | 0.07 |
| 188 | 0.1 | 0 | 0.05 | 0.13 | 0 | 0.07 | 0.09 | 0 | 0.05 | 0.12 | 0 | 0.08 | 0.17 | 0 | 0.07 | 0.15 | 0.03 | 0.08 |
| 189 | 0.1 | 0 | 0.05 | 0.14 | 0 | 0.08 | 0.11 | 0 | 0.05 | 0.12 | 0 | 0.07 | 0.18 | 0 | 0.07 | 0.14 | 0.04 | 0.07 |
| 190 | 0.09 | 0 | 0.04 | 0.13 | 0 | 0.06 | 0.09 | 0.02 | 0.05 | 0.11 | 0 | 0.06 | 0.18 | 0 | 0.07 | 0.13 | 0 | 0.07 |
| 191 | 0.12 | 0 | 0.05 | 0.11 | 0 | 0.06 | 0.08 | 0 | 0.05 | 0.15 | 0 | 0.06 | 0.16 | 0 | 0.07 | 0.14 | 0 | 0.07 |
| 192 | 0.12 | 0 | 0.05 | 0.09 | 0 | 0.06 | 0.09 | 0 | 0.05 | 0.11 | 0 | 0.06 | 0.15 | 0 | 0.07 | 0.14 | 0.03 | 0.07 |
| 193 | 0.11 | 0 | 0.05 | 0.11 | 0 | 0.05 | 0.09 | 0 | 0.05 | 0.13 | 0.03 | 0.06 | 0.15 | 0 | 0.07 | 0.13 | 0.02 | 0.07 |
| 194 | 0.09 | 0 | 0.05 | 0.1 | 0 | 0.06 | 0.08 | 0 | 0.05 | 0.12 | 0 | 0.06 | 0.16 | 0 | 0.07 | 0.13 | 0 | 0.08 |
| 195 | 0.08 | 0.03 | 0.05 | 0.1 | 0 | 0.06 | 0.11 | 0.02 | 0.06 | 0.1 | 0 | 0.06 | 0.14 | 0 | 0.07 | 0.12 | 0.03 | 0.09 |

| | | | | | | | | | | | | | | | | | | |
|---|---|---|---|---|---|---|---|---|---|---|---|---|---|---|---|---|---|---|
| | 196 | 0.07 | 0.02 | 0.05 | 0.09 | 0 | 0.05 | 0.1 | 0 | 0.05 | 0.13 | 0 | 0.07 | 0.14 | 0 | 0.07 | 0.92 | 0 | 0.13 |
| | 197 | 0.08 | 0 | 0.04 | 0.09 | 0 | 0.05 | 0.09 | 0.02 | 0.05 | 0.11 | 0 | 0.05 | 0.18 | 0 | 0.07 | 0.15 | 0 | 0.09 |
| | 198 | 0.07 | 0 | 0.04 | 0.09 | 0 | 0.05 | 0.11 | 0.02 | 0.06 | 0.12 | 0 | 0.05 | 0.12 | 0 | 0.05 | 0.12 | 0 | 0.09 |
| | 199 | 0.09 | 0 | 0.05 | 0.11 | 0 | 0.05 | 0.11 | 0 | 0.06 | 0.12 | 0 | 0.06 | 0.15 | 0 | 0.05 | 0.13 | 0.07 | 0.1 |
| | 200 | 0.08 | 0.01 | 0.04 | 0.09 | 0 | 0.04 | 0.1 | 0 | 0.05 | 0.11 | 0 | 0.07 | 0.13 | 0 | 0.05 | 0.13 | 0 | 0.1 |

| | | | | | | | | | | | | | | | | | | |
|---|---|---|---|---|---|---|---|---|---|---|---|---|---|---|---|---|---|---|
| | | | | | Control (mm) | | | | | | | | | Infected (mm) | | | | |
| Day 4 | | R1 | | | R2 | | | R3 | | | R1 | | | R2 | | | R3 | |
| | | Max | Min | Average | Max | Min | Average | Max | Min | Average | Max | Min | Average | Max | Min | Average | Max | Min | Average |
| | 1 | 0.09 | 0 | 0.05 | 0.1 | 0 | 0.05 | 0.07 | 0 | 0.03 | 0.1 | 0.04 | 0.06 | 0.09 | 0.01 | 0.05 | 0.14 | 0 | 0.08 |
| | 2 | 0.1 | 0 | 0.05 | 0.11 | 0 | 0.05 | 0.09 | 0 | 0.03 | 0.09 | 0 | 0.05 | 0.1 | 0.01 | 0.06 | 0.14 | 0 | 0.08 |
| | 3 | 0.1 | 0 | 0.05 | 0.1 | 0 | 0.05 | 0.09 | 0 | 0.04 | 0.1 | 0 | 0.05 | 0.1 | 0 | 0.07 | 0.14 | 0 | 0.08 |
| | 4 | 0.1 | 0 | 0.05 | 0.1 | 0 | 0.05 | 0.09 | 0 | 0.03 | 0.1 | 0 | 0.05 | 0.1 | 0 | 0.07 | 0.14 | 0 | 0.08 |
| | 5 | 0.1 | 0 | 0.05 | 0.11 | 0 | 0.05 | 0.09 | 0 | 0.04 | 0.1 | 0 | 0.06 | 0.1 | 0.03 | 0.07 | 0.13 | 0 | 0.08 |
| | 6 | 0.09 | 0 | 0.05 | 0.11 | 0 | 0.05 | 0.1 | 0 | 0.04 | 0.1 | 0.01 | 0.07 | 0.1 | 0 | 0.07 | 0.13 | 0 | 0.09 |
| | 7 | 0.09 | 0 | 0.04 | 0.11 | 0 | 0.05 | 0.08 | 0 | 0.04 | 0.11 | 0 | 0.07 | 0.1 | 0 | 0.06 | 0.13 | 0 | 0.09 |
| | 8 | 0.1 | 0 | 0.05 | 0.11 | 0 | 0.05 | 0.08 | 0 | 0.02 | 0.11 | 0.01 | 0.08 | 0.09 | 0.03 | 0.06 | 0.15 | 0 | 0.09 |
| | 9 | 0.1 | 0 | 0.05 | 0.1 | 0 | 0.05 | 0.04 | 0 | 0.02 | 0.11 | 0 | 0.08 | 0.09 | 0 | 0.05 | 0.18 | 0.02 | 0.1 |
| | 10 | 0.09 | 0 | 0.04 | 0.11 | 0 | 0.05 | 0.05 | 0 | 0.02 | 0.11 | 0 | 0.08 | 0.09 | 0 | 0.04 | 0.19 | 0.05 | 0.1 |
| | 11 | 0.08 | 0 | 0.05 | 0.11 | 0 | 0.05 | 0.05 | 0 | 0.01 | 0.12 | 0.05 | 0.08 | 0.08 | 0 | 0.04 | 0.17 | 0.06 | 0.1 |
| | 12 | 0.09 | 0 | 0.05 | 0.09 | 0 | 0.04 | 0.02 | 0 | 0.01 | 0.12 | 0.05 | 0.08 | 0.1 | 0 | 0.04 | 0.14 | 0.04 | 0.1 |
| | 13 | 0.08 | 0 | 0.05 | 0.09 | 0 | 0.05 | 0.02 | 0 | 0.01 | 0.11 | 0.04 | 0.08 | 0.1 | 0 | 0.06 | 0.13 | 0 | 0.09 |
| | 14 | 0.09 | 0.01 | 0.05 | 0.11 | 0 | 0.05 | 0.04 | 0 | 0.02 | 0.11 | 0 | 0.08 | 0.1 | 0 | 0.06 | 0.14 | 0 | 0.1 |
| | 15 | 0.08 | 0 | 0.05 | 0.1 | 0 | 0.05 | 0.05 | 0 | 0.04 | 0.11 | 0.04 | 0.08 | 0.1 | 0 | 0.07 | 0.13 | 0.05 | 0.1 |
| | 16 | 0.09 | 0.01 | 0.05 | 0.08 | 0 | 0.05 | 0.04 | 0 | 0.01 | 0.1 | 0.05 | 0.08 | 0.1 | 0 | 0.06 | 0.13 | 0.06 | 0.1 |
| | 17 | 0.09 | 0 | 0.04 | 0.12 | 0 | 0.05 | 0.11 | 0 | 0.05 | 0.12 | 0.05 | 0.08 | 0.1 | 0 | 0.06 | 0.12 | 0 | 0.09 |
| | 18 | 0.09 | 0 | 0.05 | 0.11 | 0 | 0.04 | 0.11 | 0 | 0.05 | 0.11 | 0.04 | 0.08 | 0.11 | 0 | 0.07 | 0.13 | 0 | 0.09 |
| | 19 | 0.09 | 0.01 | 0.05 | 0.12 | 0 | 0.05 | 0.11 | 0 | 0.05 | 0.12 | 0.04 | 0.09 | 0.11 | 0 | 0.08 | 0.13 | 0 | 0.09 |
| | 20 | 0.09 | 0 | 0.05 | 0.06 | 0 | 0.03 | 0.12 | 0 | 0.05 | 0.12 | 0.05 | 0.1 | 0.11 | 0 | 0.07 | 0.13 | 0 | 0.08 |
| | 21 | 0.09 | 0 | 0.05 | 0.06 | 0 | 0.02 | 0.12 | 0 | 0.05 | 0.13 | 0.06 | 0.1 | 0.12 | 0 | 0.08 | 0.12 | 0 | 0.07 |
| | 22 | 0.09 | 0.02 | 0.05 | 0.08 | 0 | 0.04 | 0.11 | 0 | 0.05 | 0.12 | 0 | 0.09 | 0.1 | 0 | 0.07 | 0.12 | 0.05 | 0.08 |
| | 23 | 0.1 | 0 | 0.05 | 0.07 | 0 | 0.04 | 0.11 | 0 | 0.05 | 0.12 | 0.04 | 0.08 | 0.11 | 0.06 | 0.08 | 0.14 | 0.05 | 0.08 |
| | 24 | 0.09 | 0.02 | 0.05 | 0.08 | 0 | 0.04 | 0.1 | 0 | 0.05 | 0.11 | 0.03 | 0.07 | 0.12 | 0 | 0.09 | 0.15 | 0.04 | 0.08 |
| | 25 | 0.1 | 0 | 0.05 | 0.05 | 0 | 0.03 | 0.11 | 0 | 0.05 | 0.1 | 0 | 0.06 | 0.14 | 0 | 0.09 | 0.2 | 0 | 0.08 |
| | 26 | 0.1 | 0 | 0.05 | 0.08 | 0 | 0.04 | 0.09 | 0 | 0.05 | 0.19 | 0.01 | 0.05 | 0.12 | 0.06 | 0.09 | 0.18 | 0.04 | 0.09 |
| | 27 | 0.1 | 0 | 0.05 | 0.1 | 0 | 0.05 | 0.1 | 0 | 0.05 | 0.08 | 0 | 0.05 | 0.12 | 0 | 0.09 | 0.21 | 0.04 | 0.09 |
| | 28 | 0.09 | 0 | 0.05 | 0.1 | 0 | 0.06 | 0.09 | 0 | 0.05 | 0.17 | 0 | 0.04 | 0.12 | 0 | 0.09 | 0.18 | 0.04 | 0.09 |
| | 29 | 0.12 | 0 | 0.05 | 0.11 | 0 | 0.06 | 0.11 | 0 | 0.05 | 0.07 | 0 | 0.03 | 0.11 | 0.05 | 0.09 | 0.16 | 0 | 0.08 |
| | 30 | 0.11 | 0 | 0.05 | 0.1 | 0 | 0.06 | 0.1 | 0 | 0.05 | 0.06 | 0 | 0.03 | 0.12 | 0 | 0.08 | 0.19 | 0.05 | 0.08 |

| | | | | | | | | | | | | | | | | | |
|---|---|---|---|---|---|---|---|---|---|---|---|---|---|---|---|---|---|
| 31 | 0.11 | 0 | 0.05 | 0.1 | 0 | 0.06 | 0.1 | 0 | 0.05 | 0.07 | 0 | 0.03 | 0.11 | 0 | 0.07 | 0.14 | 0 | 0.08 |
| 32 | 0.1 | 0 | 0.05 | 0.11 | 0 | 0.06 | 0.1 | 0 | 0.05 | 0.06 | 0 | 0.03 | 0.1 | 0.04 | 0.07 | 0.16 | 0 | 0.08 |
| 33 | 0.11 | 0 | 0.05 | 0.11 | 0 | 0.06 | 0.1 | 0 | 0.05 | 0.05 | 0 | 0.03 | 0.12 | 0.03 | 0.06 | 0.16 | 0 | 0.08 |
| 34 | 0.11 | 0 | 0.05 | 0.11 | 0 | 0.06 | 0.09 | 0 | 0.05 | 0.06 | 0 | 0.03 | 0.12 | 0 | 0.05 | 0.15 | 0.05 | 0.09 |
| 35 | 0.1 | 0 | 0.05 | 0.09 | 0 | 0.06 | 0.1 | 0 | 0.05 | 0.08 | 0 | 0.04 | 0.09 | 0.01 | 0.05 | 0.16 | 0 | 0.09 |
| 36 | 0.1 | 0 | 0.05 | 0.1 | 0 | 0.06 | 0.1 | 0 | 0.05 | 0.08 | 0.02 | 0.05 | 0.09 | 0.01 | 0.04 | 0.24 | 0 | 0.09 |
| 37 | 0.1 | 0 | 0.05 | 0.07 | 0 | 0.03 | 0.09 | 0 | 0.04 | 0.08 | 0 | 0.05 | 0.08 | 0 | 0.04 | 0.23 | 0 | 0.09 |
| 38 | 0.1 | 0 | 0.05 | 0.06 | 0 | 0.04 | 0.1 | 0 | 0.05 | 0.08 | 0 | 0.06 | 0.05 | 0 | 0.02 | 0.25 | 0 | 0.09 |
| 39 | 0.1 | 0 | 0.05 | 0.07 | 0 | 0.04 | 0.09 | 0 | 0.05 | 0.1 | 0 | 0.07 | 0.05 | 0 | 0.02 | 0.24 | 0 | 0.09 |
| 40 | 0.09 | 0 | 0.05 | 0.19 | 0 | 0.04 | 0.09 | 0 | 0.05 | 0.12 | 0.05 | 0.09 | 0.04 | 0 | 0.02 | 0.28 | 0 | 0.1 |
| 41 | 0.1 | 0 | 0.05 | 0.09 | 0 | 0.05 | 0.11 | 0 | 0.05 | 0.12 | 0 | 0.09 | 0.04 | 0 | 0.02 | 0.29 | 0 | 0.1 |
| 42 | 0.08 | 0 | 0.05 | 0.08 | 0 | 0.05 | 0.1 | 0 | 0.05 | 0.12 | 0.07 | 0.1 | 0.19 | 0 | 0.03 | 0.25 | 0 | 0.1 |
| 43 | 0.09 | 0 | 0.05 | 0.09 | 0 | 0.05 | 0.11 | 0 | 0.05 | 0.12 | 0 | 0.1 | 0.07 | 0.01 | 0.04 | 0.13 | 0 | 0.09 |
| 44 | 0.09 | 0.01 | 0.05 | 0.08 | 0 | 0.05 | 0.11 | 0 | 0.05 | 0.12 | 0 | 0.1 | 0.08 | 0 | 0.05 | 0.13 | 0 | 0.1 |
| 45 | 0.09 | 0 | 0.05 | 0.07 | 0 | 0.05 | 0.11 | 0 | 0.05 | 0.14 | 0 | 0.09 | 0.09 | 0 | 0.06 | 0.14 | 0.08 | 0.1 |
| 46 | 0.09 | 0.03 | 0.05 | 0.07 | 0 | 0.05 | 0.11 | 0 | 0.05 | 0.11 | 0 | 0.09 | 0.09 | 0 | 0.06 | 0.13 | 0 | 0.09 |
| 47 | 0.09 | 0 | 0.05 | 0.08 | 0 | 0.05 | 0.11 | 0 | 0.05 | 0.11 | 0.06 | 0.09 | 0.01 | 0 | 0.06 | 0.12 | 0 | 0.1 |
| 48 | 0.09 | 0 | 0.05 | 0.08 | 0 | 0.05 | 0.11 | 0 | 0.05 | 0.12 | 0.06 | 0.09 | 0.11 | 0 | 0.07 | 0.12 | 0 | 0.09 |
| 49 | 0.1 | 0 | 0.05 | 0.07 | 0.01 | 0.04 | 0.11 | 0 | 0.05 | 0.14 | 0.01 | 0.08 | 0.12 | 0 | 0.09 | 0.13 | 0 | 0.08 |
| 50 | 0.1 | 0 | 0.05 | 0.07 | 0.02 | 0.04 | 0.11 | 0 | 0.05 | 0.12 | 0 | 0.08 | 0.12 | 0.05 | 0.09 | 0.14 | 0 | 0.08 |
| 51 | 0.1 | 0 | 0.05 | 0.06 | 0 | 0.04 | 0.12 | 0 | 0.05 | 0.12 | 0 | 0.09 | 0.12 | 0 | 0.08 | 0.12 | 0 | 0.07 |
| 52 | 0.09 | 0 | 0.05 | 0.08 | 0 | 0.05 | 0.12 | 0 | 0.05 | 0.12 | 0.06 | 0.09 | 0.12 | 0 | 0.1 | 0.13 | 0.02 | 0.07 |
| 53 | 0.09 | 0 | 0.05 | 0.07 | 0 | 0.04 | 0.11 | 0 | 0.05 | 0.12 | 0.02 | 0.1 | 0.14 | 0 | 0.1 | 0.13 | 0 | 0.06 |
| 54 | 0.09 | 0 | 0.05 | 0.04 | 0 | 0.02 | 0.1 | 0 | 0.05 | 0.12 | 0.03 | 0.1 | 0.15 | 0.05 | 0.1 | 0.13 | 0 | 0.05 |
| 55 | 0.09 | 0 | 0.05 | 0.06 | 0 | 0.03 | 0.13 | 0 | 0.06 | 0.13 | 0.03 | 0.1 | 0.12 | 0 | 0.09 | 0.13 | 0 | 0.04 |
| 56 | 0.1 | 0 | 0.05 | 0.04 | 0 | 0.01 | 0.12 | 0 | 0.07 | 0.12 | 0.01 | 0.1 | 0.12 | 0 | 0.08 | 0.12 | 0 | 0.06 |
| 57 | 0.11 | 0 | 0.05 | 0.11 | 0 | 0.06 | 0.14 | 0 | 0.07 | 0.13 | 0 | 0.1 | 0.12 | 0 | 0.08 | 0.13 | 0 | 0.05 |
| 58 | 0.12 | 0 | 0.05 | 0.1 | 0 | 0.06 | 0.12 | 0 | 0.06 | 0.12 | 0.06 | 0.09 | 0.12 | 0 | 0.08 | 0.1 | 0 | 0.04 |
| 59 | 0.1 | 0 | 0.05 | 0.11 | 0 | 0.06 | 0.12 | 0 | 0.06 | 0.12 | 0 | 0.08 | 0.12 | 0.05 | 0.08 | 0.08 | 0 | 0.03 |
| 60 | 0.1 | 0 | 0.05 | 0.11 | 0 | 0.07 | 0.11 | 0 | 0.05 | 0.12 | 0.05 | 0.08 | 0.12 | 0 | 0.08 | 0.08 | 0 | 0.03 |
| 61 | 0.1 | 0 | 0.06 | 0.1 | 0 | 0.06 | 0.12 | 0 | 0.05 | 0.12 | 0 | 0.07 | 0.12 | 0 | 0.09 | 0.1 | 0 | 0.03 |
| 62 | 0.11 | 0 | 0.05 | 0.1 | 0 | 0.06 | 0.09 | 0 | 0.05 | 0.11 | 0 | 0.07 | 0.12 | 0 | 0.09 | 0.07 | 0 | 0.04 |
| 63 | 0.1 | 0 | 0.05 | 0.11 | 0 | 0.06 | 0.11 | 0 | 0.05 | 0.13 | 0 | 0.07 | 0.13 | 0.08 | 0.1 | 0.09 | 0 | 0.05 |
| 64 | 0.09 | 0 | 0.05 | 0.1 | 0 | 0.06 | 0.12 | 0 | 0.05 | 0.1 | 0.04 | 0.07 | 0.14 | 0.04 | 0.11 | 0.1 | 0 | 0.06 |
| 65 | 0.11 | 0 | 0.05 | 0.12 | 0 | 0.06 | 0.12 | 0 | 0.05 | 0.09 | 0.04 | 0.06 | 0.14 | 0.08 | 0.11 | 0.1 | 0 | 0.07 |
| 66 | 0.09 | 0 | 0.06 | 0.11 | 0 | 0.06 | 0.11 | 0 | 0.05 | 0.08 | 0.04 | 0.06 | 0.14 | 0 | 0.1 | 0.12 | 0 | 0.08 |
| 67 | 0.1 | 0 | 0.05 | 0.12 | 0 | 0.05 | 0.1 | 0 | 0.05 | 0.09 | 0.03 | 0.06 | 0.14 | 0.08 | 0.11 | 0.12 | 0.02 | 0.08 |
| 68 | 0.1 | 0.02 | 0.05 | 0.11 | 0 | 0.05 | 0.12 | 0 | 0.06 | 0.09 | 0 | 0.06 | 0.13 | 0 | 0.1 | 0.13 | 0 | 0.08 |
| 69 | 0.1 | 0.02 | 0.05 | 0.1 | 0 | 0.05 | 0.13 | 0.02 | 0.07 | 0.09 | 0 | 0.07 | 0.13 | 0 | 0.08 | 0.15 | 0 | 0.09 |

| | | | | | | | | | | | | | | | | | |
|---|---|---|---|---|---|---|---|---|---|---|---|---|---|---|---|---|---|
| 70 | 0.09 | 0 | 0.05 | 0.11 | 0 | 0.05 | 0.08 | 0 | 0.03 | 0.11 | 0 | 0.07 | 0.11 | 0 | 0.08 | 0.14 | 0 | 0.09 |
| 71 | 0.09 | 0 | 0.06 | 0.05 | 0 | 0.02 | 0.11 | 0 | 0.05 | 0.11 | 0 | 0.08 | 0.11 | 0 | 0.07 | 0.12 | 0.03 | 0.09 |
| 72 | 0.1 | 0.02 | 0.06 | 0.11 | 0 | 0.05 | 0.1 | 0 | 0.05 | 0.12 | 0 | 0.08 | 0.12 | 0.04 | 0.06 | 0.13 | 0 | 0.09 |
| 73 | 0.09 | 0 | 0.05 | 0.1 | 0 | 0.05 | 0.1 | 0 | 0.05 | 0.12 | 0.05 | 0.09 | 0.12 | 0 | 0.06 | 0.14 | 0 | 0.09 |
| 74 | 0.09 | 0.01 | 0.05 | 0.11 | 0 | 0.05 | 0.1 | 0 | 0.05 | 0.12 | 0 | 0.09 | 0.11 | 0.05 | 0.07 | 0.12 | 0.05 | 0.09 |
| 75 | 0.1 | 0 | 0.05 | 0.12 | 0 | 0.05 | 0.1 | 0 | 0.05 | 0.13 | 0.05 | 0.1 | 0.09 | 0 | 0.06 | 0.12 | 0 | 0.09 |
| 76 | 0.09 | 0 | 0.05 | 0.12 | 0 | 0.05 | 0.11 | 0 | 0.05 | 0.12 | 0.06 | 0.09 | 0.08 | 0 | 0.06 | 0.12 | 0.06 | 0.09 |
| 77 | 0.1 | 0 | 0.05 | 0.11 | 0 | 0.05 | 0.1 | 0 | 0.05 | 0.12 | 0 | 0.09 | 0.08 | 0.03 | 0.06 | 0.12 | 0 | 0.08 |
| 78 | 0.1 | 0 | 0.05 | 0.12 | 0 | 0.05 | 0.1 | 0 | 0.05 | 0.13 | 0.07 | 0.1 | 0.09 | 0.03 | 0.06 | 0.13 | 0 | 0.08 |
| 79 | 0.1 | 0 | 0.05 | 0.11 | 0 | 0.07 | 0.1 | 0 | 0.05 | 0.13 | 0.03 | 0.09 | 0.11 | 0 | 0.06 | 0.14 | 0 | 0.1 |
| 80 | 0.11 | 0 | 0.05 | 0.1 | 0.01 | 0.07 | 0.1 | 0 | 0.05 | 0.14 | 0.04 | 0.1 | 0.1 | 0 | 0.07 | 0.14 | 0 | 0.08 |
| 81 | 0.11 | 0 | 0.05 | 0.09 | 0 | 0.06 | 0.1 | 0 | 0.05 | 0.14 | 0.06 | 0.1 | 0.1 | 0 | 0.08 | 0.13 | 0.07 | 0.1 |
| 82 | 0.1 | 0 | 0.05 | 0.11 | 0 | 0.06 | 0.09 | 0 | 0.04 | 0.13 | 0.05 | 0.1 | 0.11 | 0 | 0.08 | 0.15 | 0 | 0.09 |
| 83 | 0.09 | 0 | 0.05 | 0.1 | 0 | 0.06 | 0.09 | 0 | 0.05 | 0.16 | 0.04 | 0.1 | 0.12 | 0 | 0.09 | 0.14 | 0.07 | 0.11 |
| 84 | 0.12 | 0 | 0.05 | 0.1 | 0.03 | 0.06 | 0.09 | 0 | 0.05 | 0.12 | 0.06 | 0.09 | 0.12 | 0.07 | 0.09 | 0.12 | 0 | 0.09 |
| 85 | 0.19 | 0 | 0.05 | 0.11 | 0 | 0.06 | 0.09 | 0 | 0.05 | 0.12 | 0.07 | 0.1 | 0.12 | 0 | 0.09 | 0.13 | 0 | 0.09 |
| 86 | 0.1 | 0.01 | 0.05 | 0.11 | 0 | 0.06 | 0.09 | 0 | 0.05 | 0.12 | 0 | 0.09 | 0.12 | 0 | 0.09 | 0.12 | 0 | 0.09 |
| 87 | 0.1 | 0 | 0.05 | 0.1 | 0.01 | 0.06 | 0.13 | 0 | 0.05 | 0.12 | 0 | 0.09 | 0.12 | 0 | 0.1 | 0.12 | 0 | 0.08 |
| 88 | 0.1 | 0 | 0.05 | 0.12 | 0 | 0.05 | 0.14 | 0 | 0.07 | 0.12 | 0.07 | 0.1 | 0.12 | 0 | 0.1 | 0.13 | 0 | 0.07 |
| 89 | 0.1 | 0 | 0.05 | 0.11 | 0 | 0.05 | 0.13 | 0 | 0.07 | 0.12 | 0.05 | 0.09 | 0.12 | 0.07 | 0.1 | 0.14 | 0 | 0.06 |
| 90 | 0.1 | 0 | 0.06 | 0.1 | 0 | 0.05 | 0.13 | 0 | 0.07 | 0.11 | 0.04 | 0.08 | 0.15 | 0.06 | 0.1 | 0.13 | 0 | 0.06 |
| 91 | 0.1 | 0 | 0.06 | 0.12 | 0 | 0.05 | 0.15 | 0 | 0.08 | 0.11 | 0 | 0.07 | 0.12 | 0 | 0.1 | 0.13 | 0 | 0.06 |
| 92 | 0.11 | 0.02 | 0.06 | 0.11 | 0 | 0.05 | 0.15 | 0.03 | 0.07 | 0.12 | 0 | 0.06 | 0.13 | 0.06 | 0.1 | 0.1 | 0.04 | 0.07 |
| 93 | 0.1 | 0 | 0.05 | 0.11 | 0 | 0.05 | 0.15 | 0 | 0.07 | 0.11 | 0 | 0.05 | 0.13 | 0.04 | 0.1 | 0.14 | 0 | 0.07 |
| 94 | 0.1 | 0 | 0.06 | 0.11 | 0 | 0.05 | 0.14 | 0 | 0.07 | 0.11 | 0 | 0.05 | 0.12 | 0 | 0.09 | 0.12 | 0 | 0.07 |
| 95 | 0.11 | 0 | 0.06 | 0.12 | 0 | 0.05 | 0.16 | 0 | 0.07 | 0.1 | 0 | 0.04 | 0.13 | 0 | 0.1 | 0.13 | 0 | 0.07 |
| 96 | 0.11 | 0 | 0.06 | 0.12 | 0 | 0.05 | 0.14 | 0 | 0.07 | 0.07 | 0 | 0.03 | 0.12 | 0.07 | 0.1 | 0.12 | 0 | 0.08 |
| 97 | 0.11 | 0 | 0.06 | 0.11 | 0 | 0.04 | 0.13 | 0 | 0.07 | 0.07 | 0 | 0.03 | 0.11 | 0 | 0.09 | 0.12 | 0 | 0.07 |
| 98 | 0.11 | 0 | 0.06 | 0.12 | 0 | 0.05 | 0.12 | 0 | 0.07 | 0.06 | 0 | 0.02 | 0.12 | 0 | 0.09 | 0.13 | 0 | 0.08 |
| 99 | 0.11 | 0 | 0.06 | 0.11 | 0 | 0.05 | 0.15 | 0 | 0.07 | 0.06 | 0 | 0.02 | 0.12 | 0.05 | 0.08 | 0.13 | 0 | 0.08 |
| 100 | 0.1 | 0 | 0.06 | 0.1 | 0 | 0.05 | 0.14 | 0.02 | 0.07 | 0.05 | 0 | 0.03 | 0.12 | 0.03 | 0.07 | 0.13 | 0 | 0.09 |
| 101 | 0.13 | 0 | 0.06 | 0.11 | 0 | 0.05 | 0.14 | 0.02 | 0.08 | 0.07 | 0 | 0.04 | 0.12 | 0.03 | 0.06 | 0.14 | 0.04 | 0.09 |
| 102 | 0.12 | 0 | 0.06 | 0.11 | 0 | 0.05 | 0.14 | 0 | 0.07 | 0.07 | 0 | 0.04 | 0.11 | 0 | 0.05 | 0.14 | 0 | 0.09 |
| 103 | 0.11 | 0 | 0.06 | 0.1 | 0 | 0.05 | 0.13 | 0 | 0.07 | 0.08 | 0 | 0.05 | 0.1 | 0 | 0.04 | 0.13 | 0 | 0.1 |
| 104 | 0.12 | 0 | 0.06 | 0.1 | 0 | 0.05 | 0.13 | 0 | 0.05 | 0.08 | 0 | 0.05 | 0.06 | 0 | 0.02 | 0.14 | 0 | 0.1 |
| 105 | 0.1 | 0 | 0.05 | 0.12 | 0 | 0.05 | 0.09 | 0 | 0.05 | 0.08 | 0.02 | 0.05 | 0.07 | 0 | 0.02 | 0.15 | 0.04 | 0.1 |
| 106 | 0.11 | 0.01 | 0.06 | 0.11 | 0 | 0.05 | 0.09 | 0 | 0.04 | 0.09 | 0.03 | 0.06 | 0.04 | 0 | 0.02 | 0.15 | 0.06 | 0.1 |
| 107 | 0.11 | 0.01 | 0.06 | 0.11 | 0 | 0.05 | 0.1 | 0 | 0.04 | 0.12 | 0.03 | 0.08 | 0.04 | 0 | 0.01 | 0.14 | 0.05 | 0.1 |
| 108 | 0.1 | 0 | 0.05 | 0.12 | 0 | 0.05 | 0.1 | 0 | 0.04 | 0.12 | 0 | 0.07 | 0.04 | 0 | 0.02 | 0.15 | 0.03 | 0.1 |

| | | | | | | | | | | | | | | | | | |
|---|---|---|---|---|---|---|---|---|---|---|---|---|---|---|---|---|---|
| 109 | 0.11 | 0 | 0.05 | 0.11 | 0 | 0.05 | 0.1 | 0 | 0.05 | 0.12 | 0 | 0.08 | 0.06 | 0 | 0.03 | 0.14 | 0 | 0.1 |
| 110 | 0.09 | 0 | 0.05 | 0.11 | 0 | 0.05 | 0.09 | 0 | 0.04 | 0.12 | 0 | 0.09 | 0.07 | 0 | 0.04 | 0.13 | 0 | 0.8 |
| 111 | 0.1 | 0 | 0.05 | 0.1 | 0 | 0.05 | 0.08 | 0 | 0.04 | 0.12 | 0 | 0.09 | 0.07 | 0 | 0.04 | 0.14 | 0.08 | 0.11 |
| 112 | 0.11 | 0 | 0.06 | 0.12 | 0 | 0.05 | 0.08 | 0 | 0.04 | 0.12 | 0.05 | 0.1 | 0.09 | 0 | 0.05 | 0.14 | 0.08 | 0.11 |
| 113 | 0.12 | 0 | 0.06 | 0.1 | 0 | 0.05 | 0.1 | 0 | 0.04 | 0.12 | 0.06 | 0.1 | 0.07 | 0 | 0.05 | 0.13 | 0 | 0.1 |
| 114 | 0.12 | 0.01 | 0.05 | 0.1 | 0 | 0.05 | 0.07 | 0 | 0.04 | 0.12 | 0.02 | 0.09 | 0.09 | 0 | 0.06 | 0.14 | 0 | 0.08 |
| 115 | 0.1 | 0 | 0.06 | 0.09 | 0 | 0.05 | 0.08 | 0 | 0.04 | 0.12 | 0.03 | 0.1 | 0.09 | 0 | 0.07 | 0.13 | 0 | 0.07 |
| 116 | 0.1 | 0 | 0.05 | 0.09 | 0 | 0.05 | 0.11 | 0 | 0.04 | 0.12 | 0.03 | 0.1 | 0.1 | 0.03 | 0.07 | 0.13 | 0 | 0.08 |
| 117 | 0.1 | 0 | 0.05 | 0.11 | 0 | 0.05 | 0.09 | 0 | 0.04 | 0.12 | 0.01 | 0.1 | 0.12 | 0 | 0.08 | 0.12 | 0.05 | 0.08 |
| 118 | 0.12 | 0 | 0.05 | 0.11 | 0 | 0.05 | 0.09 | 0 | 0.05 | 0.12 | 0.03 | 0.09 | 0.12 | 0.06 | 0.09 | 0.14 | 0 | 0.07 |
| 119 | 0.12 | 0 | 0.05 | 0.1 | 0 | 0.05 | 0.1 | 0 | 0.04 | 0.13 | 0.03 | 0.1 | 0.13 | 0 | 0.1 | 0.13 | 0 | 0.06 |
| 120 | 0.11 | 0 | 0.05 | 0.1 | 0 | 0.05 | 0.09 | 0 | 0.05 | 0.13 | 0.06 | 0.1 | 0.14 | 0.05 | 0.1 | 0.14 | 0 | 0.06 |
| 121 | 0.1 | 0 | 0.05 | 0.11 | 0 | 0.04 | 0.09 | 0 | 0.04 | 0.13 | 0 | 0.1 | 0.13 | 0 | 0.1 | 0.14 | 0 | 0.07 |
| 122 | 0.11 | 0 | 0.06 | 0.09 | 0 | 0.05 | 0.1 | 0 | 0.05 | 0.12 | 0.08 | 0.1 | 0.13 | 0 | 0.1 | 0.13 | 0 | 0.06 |
| 123 | 0.11 | 0 | 0.05 | 0.1 | 0 | 0.05 | 0.09 | 0 | 0.04 | 0.13 | 0 | 0.09 | 0.13 | 0.06 | 0.1 | 0.12 | 0.03 | 0.06 |
| 124 | 0.12 | 0 | 0.06 | 0.11 | 0 | 0.04 | 0.09 | 0 | 0.05 | 0.14 | 0 | 0.08 | 0.12 | 0.06 | 0.1 | 0.11 | 0 | 0.06 |
| 125 | 0.11 | 0 | 0.06 | 0.09 | 0 | 0.04 | 0.08 | 0 | 0.05 | 0.13 | 0.05 | 0.08 | 0.12 | 0.05 | 0.09 | 0.1 | 0 | 0.07 |
| 126 | 0.1 | 0 | 0.06 | 0.11 | 0 | 0.05 | 0.1 | 0 | 0.04 | 0.13 | 0 | 0.8 | 0.12 | 0 | 0.09 | 0.11 | 0 | 0.07 |
| 127 | 0.12 | 0 | 0.06 | 0.1 | 0 | 0.05 | 0.11 | 0 | 0.05 | 0.12 | 0 | 0.07 | 0.12 | 0.06 | 0.1 | 0.12 | 0 | 0.07 |
| 128 | 0.12 | 0 | 0.06 | 0.11 | 0 | 0.05 | 0.09 | 0 | 0.05 | 0.11 | 0 | 0.07 | 0.12 | 0 | 0.1 | 0.14 | 0 | 0.09 |
| 129 | 0.11 | 0 | 0.06 | 0.1 | 0 | 0.05 | 0.09 | 0 | 0.05 | 0.12 | 0 | 0.06 | 0.13 | 0 | 0.1 | 0.14 | 0 | 0.09 |
| 130 | 0.12 | 0 | 0.06 | 0.09 | 0 | 0.04 | 0.1 | 0 | 0.05 | 0.09 | 0 | 0.05 | 0.15 | 0.08 | 0.11 | 0.13 | 0 | 0.09 |
| 131 | 0.11 | 0 | 0.06 | 0.1 | 0 | 0.05 | 0.12 | 0.02 | 0.07 | 0.09 | 0 | 0.06 | 0.13 | 0 | 0.09 | 0.14 | 0 | 0.09 |
| 132 | 0.12 | 0 | 0.05 | 0.12 | 0.01 | 0.07 | 0.13 | 0 | 0.07 | 0.08 | 0 | 0.05 | 0.14 | 0.06 | 0.1 | 0.16 | 0 | 0.1 |
| 133 | 0.11 | 0 | 0.06 | 0.13 | 0 | 0.06 | 0.13 | 0 | 0.07 | 0.08 | 0 | 0.05 | 0.14 | 0 | 0.09 | 0.14 | 0.03 | 0.1 |
| 134 | 0.12 | 0 | 0.06 | 0.15 | 0 | 0.07 | 0.12 | 0.02 | 0.07 | 0.08 | 0 | 0.05 | 0.14 | 0 | 0.08 | 0.13 | 0 | 0.08 |
| 135 | 0.12 | 0 | 0.06 | 0.15 | 0 | 0.07 | 0.13 | 0 | 0.07 | 0.09 | 0 | 0.06 | 0.12 | 0 | 0.08 | 0.14 | 0.04 | 0.1 |
| 136 | 0.12 | 0 | 0.06 | 0.15 | 0.01 | 0.07 | 0.12 | 0 | 0.07 | 0.1 | 0 | 0.07 | 0.11 | 0 | 0.07 | 0.13 | 0 | 0.1 |
| 137 | 0.12 | 0 | 0.05 | 0.16 | 0 | 0.06 | 0.14 | 0.02 | 0.07 | 0.12 | 0 | 0.08 | 0.1 | 0 | 0.07 | 0.14 | 0.07 | 0.1 |
| 138 | 0.12 | 0 | 0.06 | 0.18 | 0 | 0.07 | 0.13 | 0.03 | 0.07 | 0.12 | 0 | 0.09 | 0.11 | 0 | 0.07 | 0.14 | 0 | 0.09 |
| 139 | 0.12 | 0 | 0.06 | 0.16 | 0 | 0.06 | 0.13 | 0 | 0.07 | 0.12 | 0 | 0.09 | 0.11 | 0.03 | 0.06 | 0.14 | 0 | 0.11 |
| 140 | 0.12 | 0 | 0.06 | 0.1 | 0 | 0.04 | 0.17 | 0.02 | 0.07 | 0.13 | 0.06 | 0.1 | 0.08 | 0 | 0.06 | 0.14 | 0 | 0.1 |
| 141 | 0.11 | 0 | 0.05 | 0.1 | 0 | 0.04 | 0.13 | 0.01 | 0.07 | 0.13 | 0.05 | 0.1 | 0.08 | 0 | 0.06 | 0.14 | 0 | 0.11 |
| 142 | 0.12 | 0 | 0.06 | 0.1 | 0 | 0.04 | 0.14 | 0 | 0.07 | 0.12 | 0 | 0.1 | 0.08 | 0 | 0.06 | 0.15 | 0 | 0.11 |
| 143 | 0.11 | 0 | 0.06 | 0.09 | 0 | 0.05 | 0.12 | 0 | 0.05 | 0.18 | 0.07 | 0.1 | 0.08 | 0 | 0.05 | 0.13 | 0 | 0.09 |
| 144 | 0.12 | 0 | 0.05 | 0.1 | 0 | 0.05 | 0.12 | 0 | 0.05 | 0.13 | 0 | 0.1 | 0.08 | 0.03 | 0.06 | 0.15 | 0.07 | 0.11 |
| 145 | 0.12 | 0 | 0.05 | 0.1 | 0 | 0.05 | 0.11 | 0 | 0.05 | 0.13 | 0 | 0.1 | 0.11 | 0.02 | 0.07 | 0.14 | 0 | 0.1 |
| 146 | 0.11 | 0 | 0.05 | 0.1 | 0 | 0.05 | 0.1 | 0 | 0.05 | 0.13 | 0.04 | 0.1 | 0.12 | 0 | 0.07 | 0.13 | 0 | 0.09 |
| 147 | 0.1 | 0 | 0.05 | 0.09 | 0 | 0.05 | 0.12 | 0 | 0.05 | 0.16 | 0.07 | 0.11 | 0.11 | 0 | 0.08 | 0.13 | 0.04 | 0.09 |

| | | | | | | | | | | | | | | | | | | |
|---|---|---|---|---|---|---|---|---|---|---|---|---|---|---|---|---|---|---|
| 148 | 0.12 | 0 | 0.05 | 0.09 | 0 | 0.04 | 0.13 | 0 | 0.07 | 0.16 | 0.06 | 0.11 | 0.12 | 0 | 0.09 | 0.14 | 0.06 | 0.09 |
| 149 | 0.11 | 0 | 0.06 | 0.09 | 0 | 0.05 | 0.15 | 0 | 0.07 | 0.16 | 0.07 | 0.12 | 0.13 | 0.06 | 0.1 | 0.13 | 0 | 0.09 |
| 150 | 0.11 | 0 | 0.05 | 0.08 | 0 | 0.04 | 0.13 | 0 | 0.07 | 0.18 | 0 | 0.11 | 0.13 | 0.06 | 0.1 | 0.13 | 0 | 0.09 |
| 151 | 0.12 | 0 | 0.06 | 0.08 | 0 | 0.05 | 0.13 | 0 | 0.07 | 0.16 | 0.06 | 0.11 | 0.13 | 0 | 0.11 | 0.16 | 0 | 0.09 |
| 152 | 0.12 | 0 | 0.06 | 0.09 | 0 | 0.04 | 0.14 | 0 | 0.07 | 0.15 | 0.05 | 0.1 | 0.14 | 0 | 0.1 | 0.14 | 0 | 0.09 |
| 153 | 0.12 | 0 | 0.06 | 0.08 | 0 | 0.04 | 0.12 | 0 | 0.05 | 0.13 | 0 | 0.09 | 0.13 | 0 | 0.1 | 0.13 | 0 | 0.08 |
| 154 | 0.11 | 0 | 0.06 | 0.08 | 0 | 0.04 | 0.12 | 0 | 0.05 | 0.13 | 0 | 0.08 | 0.17 | 0.07 | 0.1 | 0.14 | 0.04 | 0.09 |
| 155 | 0.11 | 0 | 0.05 | 0.08 | 0 | 0.04 | 0.11 | 0 | 0.05 | 0.12 | 0.06 | 0.09 | 0.13 | 0 | 0.09 | 0.14 | 0 | 0.09 |
| 156 | 0.12 | 0 | 0.05 | 0.08 | 0 | 0.04 | 0.1 | 0 | 0.05 | 0.13 | 0.05 | 0.08 | 0.13 | 0 | 0.09 | 0.16 | 0.04 | 0.09 |
| 157 | 0.11 | 0 | 0.05 | 0.08 | 0 | 0.04 | 0.12 | 0 | 0.05 | 0.12 | 0.04 | 0.07 | 0.13 | 0.08 | 0.1 | 0.15 | 0 | 0.1 |
| 158 | 0.11 | 0 | 0.05 | 0.09 | 0 | 0.04 | 0.07 | 0 | 0.04 | 0.11 | 0 | 0.07 | 0.14 | 0 | 0.1 | 0.15 | 0 | 0.1 |
| 159 | 0.12 | 0 | 0.06 | 0.08 | 0 | 0.04 | 0.19 | 0 | 0.04 | 0.11 | 0.03 | 0.06 | 0.14 | 0.05 | 0.11 | 0.16 | 0.03 | 0.1 |
| 160 | 0.11 | 0 | 0.05 | 0.09 | 0 | 0.04 | 0.13 | 0 | 0.06 | 0.1 | 0.03 | 0.06 | 0.14 | 0 | 0.11 | 0.15 | 0 | 0.1 |
| 161 | 0.12 | 0 | 0.05 | 0.08 | 0 | 0.05 | 0.13 | 0 | 0.07 | 0.11 | 0.05 | 0.06 | 0.14 | 0 | 0.09 | 0.15 | 0 | 0.1 |
| 162 | 0.12 | 0 | 0.05 | 0.13 | 0 | 0.05 | 0.12 | 0 | 0.07 | 0.08 | 0 | 0.05 | 0.14 | 0.07 | 0.011 | 0.14 | 0 | 0.1 |
| 163 | 0.12 | 0 | 0.05 | 0.08 | 0 | 0.04 | 0.12 | 0 | 0.07 | 0.07 | 0.03 | 0.05 | 0.16 | 0.07 | 0.1 | 0.15 | 0.06 | 0.11 |
| 164 | 0.12 | 0 | 0.04 | 0.09 | 0 | 0.03 | 0.12 | 0 | 0.07 | 0.07 | 0.02 | 0.05 | 0.13 | 0.06 | 0.09 | 0.15 | 0.07 | 0.11 |
| 165 | 0.12 | 0 | 0.05 | 0.09 | 0 | 0.04 | 0.13 | 0 | 0.07 | 0.07 | 0 | 0.05 | 0.12 | 0.04 | 0.08 | 0.16 | 0.05 | 0.12 |
| 166 | 0.11 | 0 | 0.05 | 0.08 | 0 | 0.04 | 0.13 | 0 | 0.07 | 0.1 | 0 | 0.06 | 0.12 | 0.05 | 0.08 | 0.16 | 0.07 | 0.12 |
| 167 | 0.11 | 0 | 0.05 | 0.08 | 0 | 0.03 | 0.13 | 0 | 0.07 | 0.12 | 0.02 | 0.07 | 0.12 | 0 | 0.06 | 0.16 | 0.05 | 0.11 |
| 168 | 0.1 | 0 | 0.05 | 0.09 | 0 | 0.04 | 0.12 | 0 | 0.07 | 0.12 | 0 | 0.08 | 0.09 | 0 | 0.06 | 0.15 | 0.03 | 0.1 |
| 169 | 0.11 | 0 | 0.05 | 0.09 | 0 | 0.04 | 0.14 | 0 | 0.07 | 0.12 | 0 | 0.08 | 0.22 | 0.03 | 0.07 | 0.14 | 0 | 0.1 |
| 170 | 0.11 | 0 | 0.05 | 0.09 | 0 | 0.04 | 0.14 | 0 | 0.07 | 0.14 | 0 | 0.09 | 0.08 | 0 | 0.05 | 0.14 | 0.05 | 0.1 |
| 171 | 0.1 | 0 | 0.05 | 0.08 | 0 | 0.03 | 0.13 | 0 | 0.07 | 0.13 | 0.04 | 0.1 | 0.08 | 0 | 0.06 | 0.13 | 0.06 | 0.09 |
| 172 | 0.1 | 0 | 0.05 | 0.09 | 0 | 0.04 | 0.12 | 0 | 0.07 | 0.13 | 0 | 0.1 | 0.09 | 0 | 0.06 | 0.15 | 0 | 0.09 |
| 173 | 0.12 | 0 | 0.05 | 0.09 | 0 | 0.05 | 0.12 | 0 | 0.07 | 0.14 | 0.04 | 0.11 | 0.08 | 0 | 0.05 | 0.15 | 0 | 0.07 |
| 174 | 0.11 | 0 | 0.05 | 0.08 | 0 | 0.04 | 0.13 | 0 | 0.07 | 0.16 | 0.03 | 0.11 | 0.08 | 0 | 0.05 | 0.13 | 0 | 0.04 |
| 175 | 0.11 | 0 | 0.04 | 0.08 | 0 | 0.03 | 0.12 | 0 | 0.07 | 0.16 | 0.07 | 0.11 | 0.07 | 0.04 | 0.05 | 0.12 | 0 | 0.05 |
| 176 | 0.12 | 0 | 0.05 | 0.09 | 0 | 0.04 | 0.12 | 0 | 0.07 | 0.14 | 0.02 | 0.11 | 0.1 | 0.02 | 0.06 | 0.14 | 0 | 0.05 |
| 177 | 0.11 | 0 | 0.05 | 0.09 | 0 | 0.04 | 0.12 | 0 | 0.07 | 0.15 | 0.07 | 0.11 | 0.12 | 0.01 | 0.07 | 0.12 | 0 | 0.04 |
| 178 | 0.11 | 0 | 0.05 | 0.08 | 0 | 0.04 | 0.12 | 0 | 0.07 | 0.15 | 0.04 | 0.1 | 0.12 | 0 | 0.08 | 0.14 | 0 | 0.05 |
| 179 | 0.1 | 0 | 0.05 | 0.08 | 0 | 0.04 | 0.13 | 0 | 0.07 | 0.15 | 0.03 | 0.1 | 0.11 | 0 | 0.08 | 0.13 | 0 | 0.05 |
| 180 | 0.12 | 0 | 0.05 | 0.08 | 0 | 0.04 | 0.12 | 0 | 0.07 | 0.15 | 0 | 0.1 | 0.14 | 0 | 0.09 | 0.09 | 0 | 0.05 |
| 181 | 0.1 | 0 | 0.05 | 0.06 | 0 | 0.03 | 0.12 | 0 | 0.07 | 0.14 | 0.06 | 0.1 | 0.14 | 0.06 | 0.11 | 0.08 | 0 | 0.04 |
| 182 | 0.1 | 0 | 0.05 | 0.07 | 0 | 0.04 | 0.12 | 0 | 0.07 | 0.12 | 0.05 | 0.09 | 0.13 | 0 | 0.1 | 0.11 | 0 | 0.06 |
| 183 | 0.09 | 0 | 0.05 | 0.06 | 0 | 0.03 | 0.14 | 0 | 0.07 | 0.14 | 0.05 | 0.09 | 0.14 | 0.07 | 0.11 | 0.1 | 0 | 0.05 |
| 184 | 0.09 | 0 | 0.05 | 0.08 | 0 | 0.03 | 0.14 | 0 | 0.07 | 0.12 | 0.04 | 0.09 | 0.13 | 0 | 0.11 | 0.09 | 0 | 0.06 |
| 185 | 0.09 | 0 | 0.05 | 0.06 | 0 | 0.02 | 0.14 | 0 | 0.07 | 0.12 | 0.02 | 0.09 | 0.13 | 0 | 0.1 | 0.11 | 0 | 0.07 |
| 186 | 0.11 | 0 | 0.05 | 0.06 | 0 | 0.02 | 0.15 | 0 | 0.07 | 0.14 | 0.05 | 0.08 | 0.13 | 0.08 | 0.11 | 0.14 | 0.01 | 0.08 |

| | | | | | | | | | | | | | | | | | |
|---|---|---|---|---|---|---|---|---|---|---|---|---|---|---|---|---|---|
| 187 | 0.11 | 0 | 0.05 | 0.07 | 0 | 0.03 | 0.14 | 0 | 0.07 | 0.12 | 0 | 0.07 | 0.13 | 0.05 | 0.1 | 0.13 | 0 | 0.08 |
| 188 | 0.1 | 0 | 0.05 | 0.07 | 0 | 0.02 | 0.15 | 0 | 0.07 | 0.12 | 0 | 0.07 | 0.13 | 0.06 | 0.1 | 0.15 | 0.01 | 0.09 |
| 189 | 0.1 | 0 | 0.05 | 0.04 | 0 | 0.02 | 0.13 | 0 | 0.07 | 0.12 | 0.03 | 0.07 | 0.13 | 0.07 | 0.1 | 0.13 | 0 | 0.1 |
| 190 | 0.1 | 0 | 0.04 | 0.06 | 0.01 | 0.03 | 0.12 | 0 | 0.06 | 0.1 | 0.03 | 0.07 | 0.15 | 0 | 0.1 | 0.14 | 0.02 | 0.1 |
| 191 | 0.09 | 0 | 0.05 | 0.09 | 0 | 0.03 | 0.11 | 0 | 0.06 | 0.1 | 0 | 0.06 | 0.13 | 0.06 | 0.1 | 0.17 | 0 | 0.11 |
| 192 | 0.1 | 0 | 0.05 | 0.07 | 0 | 0.03 | 0.12 | 0 | 0.06 | 0.11 | 0.05 | 0.07 | 0.12 | 0.08 | 0.1 | 0.15 | 0 | 0.1 |
| 193 | 0.11 | 0 | 0.04 | 0.04 | 0 | 0.02 | 0.12 | 0 | 0.06 | 0.11 | 0 | 0.07 | 0.12 | 0.04 | 0.1 | 0.16 | 0.03 | 0.1 |
| 194 | 0.09 | 0 | 0.04 | 0.12 | 0 | 0.05 | 0.12 | 0 | 0.06 | 0.12 | 0.05 | 0.08 | 0.13 | 0.06 | 0.09 | 0.18 | 0 | 0.11 |
| 195 | 0.11 | 0 | 0.05 | 0.12 | 0 | 0.05 | 0.12 | 0 | 0.05 | 0.12 | 0 | 0.08 | 0.12 | 0 | 0.09 | 0.18 | 0.05 | 0.11 |
| 196 | 0.1 | 0 | 0.05 | 0.11 | 0 | 0.05 | 0.12 | 0 | 0.05 | 0.12 | 0 | 0.1 | 0.11 | 0.05 | 0.09 | 0.16 | 0 | 0.1 |
| 197 | 0.11 | 0 | 0.05 | 0.1 | 0 | 0.05 | 0.11 | 0 | 0.05 | 0.14 | 0 | 0.1 | 0.01 | 0.04 | 0.07 | 0.16 | 0 | 0.11 |
| 198 | 0.1 | 0 | 0.05 | 0.12 | 0 | 0.06 | 0.1 | 0 | 0.05 | 0.15 | 0 | 0.1 | 0.11 | 0 | 0.07 | 0.14 | 0.06 | 0.11 |
| 199 | 0.09 | 0 | 0.04 | 0.13 | 0 | 0.07 | 0.12 | 0 | 0.05 | 0.15 | 0 | 0.11 | 0.11 | 0 | 0.07 | 0.15 | 0.07 | 0.11 |
| 200 | 0.1 | 0 | 0.05 | 0.13 | 0.01 | 0.07 | 0.12 | 0 | 0.05 | 0.15 | 0.01 | 0.11 | 0.1 | 0 | 0.06 | 0.14 | 0 | 0.09 |

| | Control (mm) | | | | | | | | | Infected (mm) | | | | | | | |
|---|---|---|---|---|---|---|---|---|---|---|---|---|---|---|---|---|---|
| Day 5 | R1 | | | R2 | | | R3 | | | R1 | | | R2 | | | R3 | |
| | Max | Min | Average | Max | Min | Average | Max | Min | Average | Max | Min | Average | Max | Min | Average | Max | Min | Average |
| 1 | 0.08 | 0 | 0.04 | 0.07 | 0 | 0.03 | 0.09 | 0 | 0.03 | 0.1 | 0 | 0.06 | 0.11 | 0 | 0.05 | 0.11 | 0 | 0.06 |
| 2 | 0.09 | 0 | 0.04 | 0.07 | 0.01 | 0.04 | 0.09 | 0 | 0.03 | 0.1 | 0 | 0.06 | 0.12 | 0 | 0.06 | 0.12 | 0 | 0.07 |
| 3 | 0.08 | 0 | 0.04 | 0.07 | 0 | 0.03 | 0.09 | 0 | 0.03 | 0.1 | 0 | 0.06 | 0.12 | 0 | 0.06 | 0.1 | 0 | 0.06 |
| 4 | 0.09 | 0 | 0.04 | 0.09 | 0 | 0.04 | 0.1 | 0 | 0.03 | 0.12 | 0.02 | 0.06 | 0.11 | 0 | 0.06 | 0.11 | 0 | 0.07 |
| 5 | 0.09 | 0 | 0.04 | 0.01 | 0 | 0.04 | 0.08 | 0 | 0.03 | 0.11 | 0 | 0.06 | 0.1 | 0 | 0.06 | 0.12 | 0.02 | 0.07 |
| 6 | 0.09 | 0 | 0.04 | 0.09 | 0 | 0.04 | 0.08 | 0 | 0.03 | 0.13 | 0 | 0.07 | 0.13 | 0 | 0.06 | 0.11 | 0 | 0.06 |
| 7 | 0.07 | 0 | 0.03 | 0.06 | 0 | 0.03 | 0.06 | 0 | 0.03 | 0.15 | 0 | 0.07 | 0.12 | 0 | 0.06 | 0.1 | 0.02 | 0.06 |
| 8 | 0.09 | 0 | 0.03 | 0.08 | 0 | 0.04 | 0.07 | 0 | 0.02 | 0.1 | 0.01 | 0.06 | 0.1 | 0 | 0.06 | 0.09 | 0 | 0.06 |
| 9 | 0.09 | 0 | 0.04 | 0.08 | 0 | 0.04 | 0.06 | 0 | 0.03 | 0.09 | 0.02 | 0.06 | 0.11 | 0 | 0.06 | 0.09 | 0.01 | 0.06 |
| 10 | 0.1 | 0 | 0.04 | 0.07 | 0 | 0.03 | 0.09 | 0 | 0.04 | 0.11 | 0.01 | 0.05 | 0.1 | 0 | 0.06 | 0.1 | 0 | 0.06 |
| 11 | 0.09 | 0 | 0.04 | 0.1 | 0 | 0.04 | 0.07 | 0 | 0.03 | 0.1 | 0 | 0.06 | 0.1 | 0 | 0.06 | 0.1 | 0 | 0.06 |
| 12 | 0.08 | 0 | 0.03 | 0.07 | 0 | 0.03 | 0.09 | 0 | 0.04 | 0.12 | 0 | 0.06 | 0.18 | 0 | 0.06 | 0.1 | 0 | 0.06 |
| 13 | 0.09 | 0 | 0.03 | 0.08 | 0 | 0.03 | 0.09 | 0 | 0.04 | 0.1 | 0 | 0.05 | 0.1 | 0 | 0.06 | 0.1 | 0 | 0.06 |
| 14 | 0.1 | 0 | 0.04 | 0.09 | 0 | 0.04 | 0.07 | 0 | 0.03 | 0.1 | 0 | 0.05 | 0.1 | 0 | 0.06 | 0.12 | 0 | 0.06 |
| 15 | 0.08 | 0 | 0.04 | 0.08 | 0 | 0.03 | 0.09 | 0 | 0.04 | 0.12 | 0 | 0.05 | 0.1 | 0 | 0.06 | 0.11 | 0 | 0.06 |
| 16 | 0.09 | 0 | 0.04 | 0.1 | 0 | 0.04 | 0.09 | 0 | 0.04 | 0.09 | 0 | 0.05 | 0.11 | 0 | 0.07 | 0.11 | 0 | 0.06 |
| 17 | 0.09 | 0 | 0.04 | 0.11 | 0 | 0.04 | 0.1 | 0 | 0.04 | 0.09 | 0 | 0.05 | 0.22 | 0 | 0.08 | 0.12 | 0 | 0.06 |
| 18 | 0.1 | 0 | 0.04 | 0.09 | 0 | 0.04 | 0.09 | 0 | 0.04 | 0.11 | 0 | 0.05 | 0.13 | 0 | 0.07 | 0.1 | 0 | 0.06 |
| 19 | 0.08 | 0 | 0.04 | 0.1 | 0 | 0.04 | 0.08 | 0 | 0.04 | 0.11 | 0.02 | 0.06 | 0.18 | 0.04 | 0.07 | 0.11 | 0 | 0.06 |
| 20 | 0.1 | 0 | 0.04 | 0.08 | 0 | 0.04 | 0.09 | 0 | 0.04 | 0.1 | 0 | 0.06 | 0.14 | 0 | 0.07 | 0.12 | 0 | 0.06 |
| 21 | 0.11 | 0 | 0.04 | 0.08 | 0 | 0.04 | 0.08 | 0 | 0.04 | 0.18 | 0 | 0.06 | 0.1 | 0 | 0.06 | 0.11 | 0 | 0.06 |

| | | | | | | | | | | | | | | | | | |
|---|---|---|---|---|---|---|---|---|---|---|---|---|---|---|---|---|---|
| 22 | 0.1 | 0 | 0.04 | 0.08 | 0.01 | 0.06 | 0.09 | 0 | 0.03 | 0.11 | 0 | 0.06 | 0.21 | 0 | 0.08 | 0.11 | 0 | 0.06 |
| 23 | 0.08 | 0 | 0.04 | 0.09 | 0 | 0.03 | 0.08 | 0 | 0.04 | 0.11 | 0 | 0.06 | 0.1 | 0 | 0.06 | 0.11 | 0 | 0.06 |
| 24 | 0.09 | 0 | 0.04 | 0.1 | 0 | 0.04 | 0.08 | 0 | 0.04 | 0.11 | 0 | 0.06 | 0.1 | 0 | 0.06 | 0.11 | 0 | 0.06 |
| 25 | 0.09 | 0 | 0.04 | 0.1 | 0 | 0.04 | 0.09 | 0 | 0.03 | 0.12 | 0 | 0.07 | 0.12 | 0 | 0.07 | 0.12 | 0 | 0.07 |
| 26 | 0.08 | 0 | 0.04 | 0.08 | 0 | 0.04 | 0.1 | 0 | 0.04 | 0.09 | 0 | 0.07 | 0.11 | 0 | 0.06 | 0.12 | 0 | 0.07 |
| 27 | 0.08 | 0 | 0.04 | 0.08 | 0 | 0.04 | 0.1 | 0 | 0.03 | 0.11 | 0 | 0.07 | 0.1 | 0 | 0.06 | 0.12 | 0 | 0.07 |
| 28 | 0.11 | 0 | 0.04 | 0.08 | 0 | 0.04 | 0.08 | 0 | 0.03 | 0.1 | 0.02 | 0.06 | 0.16 | 0 | 0.07 | 0.11 | 0 | 0.07 |
| 29 | 0.08 | 0 | 0.04 | 0.08 | 0 | 0.04 | 0.1 | 0 | 0.04 | 0.11 | 0 | 0.06 | 0.12 | 0 | 0.07 | 0.11 | 0 | 0.07 |
| 30 | 0.08 | 0 | 0.04 | 0.08 | 0 | 0.04 | 0.1 | 0 | 0.04 | 0.12 | 0 | 0.06 | 0.13 | 0.03 | 0.07 | 0.12 | 0 | 0.07 |
| 31 | 0.08 | 0.01 | 0.06 | 0.09 | 0 | 0.04 | 0.08 | 0 | 0.03 | 0.13 | 0 | 0.07 | 0.13 | 0.01 | 0.08 | 0.1 | 0 | 0.07 |
| 32 | 0.1 | 0 | 0.06 | 0.09 | 0 | 0.03 | 0.07 | 0 | 0.03 | 0.11 | 0.02 | 0.07 | 0.11 | 0 | 0.06 | 0.11 | 0.02 | 0.07 |
| 33 | 0.08 | 0 | 0.06 | 0.1 | 0 | 0.04 | 0.08 | 0 | 0.03 | 0.12 | 0 | 0.07 | 0.12 | 0.01 | 0.06 | 0.12 | 0 | 0.06 |
| 34 | 0.08 | 0 | 0.06 | 0.09 | 0 | 0.04 | 0.08 | 0 | 0.03 | 0.12 | 0 | 0.06 | 0.1 | 0 | 0.06 | 0.11 | 0.02 | 0.07 |
| 35 | 0.08 | 0 | 0.06 | 0.1 | 0 | 0.04 | 0.08 | 0 | 0.03 | 0.11 | 0 | 0.06 | 0.11 | 0 | 0.06 | 0.12 | 0.02 | 0.07 |
| 36 | 0.09 | 0 | 0.06 | 0.09 | 0 | 0.04 | 0.09 | 0 | 0.03 | 0.11 | 0 | 0.06 | 0.13 | 0 | 0.06 | 0.16 | 0.01 | 0.08 |
| 37 | 0.09 | 0 | 0.06 | 0.09 | 0 | 0.04 | 0.1 | 0 | 0.04 | 0.11 | 0 | 0.05 | 0.11 | 0 | 0.06 | 0.11 | 0 | 0.07 |
| 38 | 0.1 | 0 | 0.06 | 0.09 | 0 | 0.04 | 0.08 | 0 | 0.03 | 0.09 | 0 | 0.05 | 0.1 | 0 | 0.06 | 0.12 | 0.01 | 0.08 |
| 39 | 0.1 | 0 | 0.06 | 0.1 | 0 | 0.04 | 0.08 | 0 | 0.03 | 0.09 | 0 | 0.05 | 0.1 | 0 | 0.06 | 0.12 | 0 | 0.08 |
| 40 | 0.08 | 0 | 0.06 | 0.1 | 0 | 0.04 | 0.07 | 0 | 0.03 | 0.08 | 0 | 0.05 | 0.1 | 0 | 0.06 | 0.12 | 0.01 | 0.08 |
| 41 | 0.11 | 0 | 0.06 | 0.1 | 0 | 0.04 | 0.1 | 0 | 0.04 | 0.09 | 0 | 0.04 | 0.08 | 0 | 0.06 | 0.12 | 0 | 0.08 |
| 42 | 0.1 | 0 | 0.06 | 0.11 | 0 | 0.03 | 0.1 | 0 | 0.04 | 0.08 | 0 | 0.05 | 0.09 | 0 | 0.06 | 0.12 | 0 | 0.08 |
| 43 | 0.08 | 0 | 0.06 | 0.07 | 0 | 0.04 | 0.1 | 0 | 0.04 | 0.09 | 0 | 0.04 | 0.08 | 0 | 0.06 | 0.12 | 0.03 | 0.07 |
| 44 | 0.08 | 0 | 0.06 | 0.1 | 0 | 0.04 | 0.1 | 0 | 0.04 | 0.08 | 0 | 0.04 | 0.08 | 0 | 0.06 | 0.12 | 0.03 | 0.07 |
| 45 | 0.1 | 0 | 0.06 | 0.1 | 0 | 0.04 | 0.09 | 0 | 0.04 | 0.09 | 0 | 0.05 | 0.08 | 0 | 0.06 | 0.11 | 0 | 0.07 |
| 46 | 0.1 | 0 | 0.04 | 0.1 | 0 | 0.04 | 0.1 | 0 | 0.04 | 0.09 | 0 | 0.04 | 0.09 | 0 | 0.06 | 0.11 | 0 | 0.07 |
| 47 | 0.1 | 0 | 0.03 | 0.09 | 0 | 0.04 | 0.08 | 0 | 0.04 | 0.08 | 0 | 0.04 | 0.09 | 0 | 0.06 | 0.12 | 0.05 | 0.07 |
| 48 | 0.1 | 0 | 0.03 | 0.09 | 0 | 0.05 | 0.09 | 0 | 0.04 | 0.14 | 0 | 0.04 | 0.1 | 0.01 | 0.06 | 0.11 | 0 | 0.08 |
| 49 | 0.11 | 0 | 0.03 | 0.1 | 0 | 0.05 | 0.08 | 0 | 0.04 | 0.09 | 0 | 0.05 | 0.11 | 0 | 0.06 | 0.12 | 0 | 0.07 |
| 50 | 0.08 | 0 | 0.03 | 0.1 | 0.01 | 0.05 | 0.08 | 0 | 0.04 | 0.21 | 0 | 0.06 | 0.09 | 0 | 0.06 | 0.14 | 0.04 | 0.07 |
| 51 | 0.08 | 0 | 0.03 | 0.09 | 0.01 | 0.06 | 0.08 | 0 | 0.04 | 0.08 | 0 | 0.04 | 0.24 | 0 | 0.07 | 0.12 | 0.03 | 0.07 |
| 52 | 0.08 | 0 | 0.04 | 0.09 | 0 | 0.06 | 0.08 | 0 | 0.04 | 0.09 | 0 | 0.05 | 0.11 | 0 | 0.06 | 0.11 | 0 | 0.07 |
| 53 | 0.1 | 0 | 0.04 | 0.09 | 0 | 0.06 | 0.08 | 0 | 0.04 | 0.09 | 0 | 0.06 | 0.1 | 0 | 0.06 | 0.1 | 0.05 | 0.08 |
| 54 | 0.1 | 0 | 0.05 | 0.1 | 0 | 0.06 | 0.11 | 0 | 0.04 | 0.24 | 0 | 0.05 | 0.1 | 0 | 0.06 | 0.12 | 0 | 0.08 |
| 55 | 0.09 | 0 | 0.04 | 0.1 | 0 | 0.06 | 0.07 | 0 | 0.04 | 0.11 | 0 | 0.06 | 0.1 | 0.01 | 0.07 | 0.12 | 0 | 0.08 |
| 56 | 0.09 | 0 | 0.04 | 0.11 | 0 | 0.05 | 0.08 | 0 | 0.04 | 0.27 | 0 | 0.07 | 0.1 | 0.01 | 0.07 | 0.12 | 0 | 0.08 |
| 57 | 0.1 | 0 | 0.05 | 0.09 | 0 | 0.03 | 0.09 | 0 | 0.04 | 0.11 | 0 | 0.07 | 0.11 | 0 | 0.07 | 0.15 | 0 | 0.07 |
| 58 | 0.1 | 0 | 0.04 | 0.08 | 0 | 0.04 | 0.08 | 0 | 0.04 | 0.1 | 0 | 0.07 | 0.11 | 0 | 0.06 | 0.15 | 0 | 0.07 |
| 59 | 0.08 | 0 | 0.05 | 0.09 | 0 | 0.04 | 0.07 | 0 | 0.04 | 0.09 | 0 | 0.06 | 0.11 | 0 | 0.07 | 0.14 | 0 | 0.07 |
| 60 | 0.1 | 0 | 0.05 | 0.08 | 0 | 0.04 | 0.09 | 0 | 0.04 | 0.1 | 0 | 0.06 | 0.11 | 0 | 0.07 | 0.12 | 0 | 0.08 |

| | | | | | | | | | | | | | | | | | |
|---|---|---|---|---|---|---|---|---|---|---|---|---|---|---|---|---|---|
| 61 | 0.09 | 0 | 0.04 | 0.08 | 0 | 0.04 | 0.08 | 0 | 0.04 | 0.11 | 0 | 0.06 | 0.13 | 0 | 0.06 | 0.11 | 0 | 0.07 |
| 62 | 0.09 | 0 | 0.04 | 0.09 | 0 | 0.03 | 0.08 | 0 | 0.04 | 0.11 | 0 | 0.07 | 0.09 | 0 | 0.06 | 0.11 | 0.04 | 0.08 |
| 63 | 0.09 | 0 | 0.05 | 0.09 | 0 | 0.04 | 0.07 | 0 | 0.03 | 0.11 | 0 | 0.07 | 0.11 | 0 | 0.07 | 0.12 | 0 | 0.08 |
| 64 | 0.09 | 0 | 0.05 | 0.08 | 0 | 0.04 | 0.12 | 0 | 0.04 | 0.11 | 0 | 0.07 | 0.1 | 0 | 0.06 | 0.14 | 0 | 0.08 |
| 65 | 0.1 | 0 | 0.05 | 0.09 | 0 | 0.03 | 0.08 | 0 | 0.04 | 0.1 | 0.02 | 0.06 | 0.09 | 0 | 0.06 | 0.12 | 0 | 0.08 |
| 66 | 0.09 | 0 | 0.05 | 0.1 | 0 | 0.04 | 0.09 | 0 | 0.03 | 0.11 | 0 | 0.06 | 0.11 | 0.03 | 0.07 | 0.12 | 0 | 0.08 |
| 67 | 0.1 | 0 | 0.05 | 0.09 | 0 | 0.04 | 0.1 | 0 | 0.04 | 0.1 | 0 | 0.06 | 0.1 | 0 | 0.06 | 0.13 | 0 | 0.09 |
| 68 | 0.11 | 0 | 0.05 | 0.1 | 0 | 0.04 | 0.1 | 0 | 0.04 | 0.11 | 0.03 | 0.06 | 0.09 | 0 | 0.06 | 0.12 | 0 | 0.08 |
| 69 | 0.12 | 0 | 0.05 | 0.1 | 0 | 0.03 | 0.09 | 0 | 0.04 | 0.09 | 0 | 0.06 | 0.11 | 0.03 | 0.06 | 0.12 | 0 | 0.07 |
| 70 | 0.09 | 0 | 0.04 | 0.09 | 0 | 0.04 | 0.09 | 0 | 0.04 | 0.08 | 0 | 0.05 | 0.12 | 0 | 0.06 | 0.11 | 0 | 0.07 |
| 71 | 0.08 | 0 | 0.04 | 0.1 | 0 | 0.04 | 0.1 | 0 | 0.04 | 0.09 | 0 | 0.05 | 0.11 | 0 | 0.07 | 0.11 | 0 | 0.07 |
| 72 | 0.07 | 0 | 0.04 | 0.09 | 0 | 0.04 | 0.1 | 0 | 0.04 | 0.08 | 0 | 0.05 | 0.1 | 0 | 0.06 | 0.13 | 0 | 0.06 |
| 73 | 0.08 | 0 | 0.04 | 0.08 | 0 | 0.04 | 0.09 | 0 | 0.04 | 0.1 | 0 | 0.05 | 0.1 | 0.02 | 0.07 | 0.11 | 0 | 0.07 |
| 74 | 0.08 | 0 | 0.04 | 0.08 | 0 | 0.04 | 0.09 | 0 | 0.04 | 0.1 | 0.02 | 0.05 | 0.1 | 0.03 | 0.07 | 0.11 | 0 | 0.06 |
| 75 | 0.09 | 0 | 0.04 | 0.09 | 0 | 0.04 | 0.08 | 0 | 0.04 | 0.09 | 0 | 0.05 | 0.11 | 0.03 | 0.07 | 0.12 | 0 | 0.06 |
| 76 | 0.08 | 0 | 0.04 | 0.1 | 0 | 0.05 | 0.08 | 0 | 0.04 | 0.1 | 0 | 0.05 | 0.09 | 0 | 0.06 | 0.11 | 0 | 0.06 |
| 77 | 0.07 | 0 | 0.03 | 0.1 | 0 | 0.05 | 0.08 | 0 | 0.04 | 0.23 | 0 | 0.05 | 0.11 | 0 | 0.06 | 0.3 | 0 | 0.06 |
| 78 | 0.06 | 0 | 0.03 | 0.1 | 0 | 0.05 | 0.08 | 0 | 0.04 | 0.08 | 0 | 0.05 | 0.1 | 0 | 0.06 | 0.12 | 0 | 0.07 |
| 79 | 0.08 | 0 | 0.04 | 0.1 | 0 | 0.05 | 0.09 | 0 | 0.04 | 0.08 | 0.02 | 0.06 | 0.09 | 0 | 0.06 | 0.1 | 0 | 0.06 |
| 80 | 0.09 | 0 | 0.04 | 0.1 | 0 | 0.05 | 0.08 | 0 | 0.04 | 0.11 | 0.01 | 0.06 | 0.09 | 0 | 0.06 | 0.11 | 0 | 0.06 |
| 81 | 0.08 | 0.01 | 0.04 | 0.1 | 0 | 0.05 | 0.09 | 0 | 0.04 | 0.1 | 0 | 0.05 | 0.09 | 0 | 0.06 | 0.09 | 0 | 0.06 |
| 82 | 0.09 | 0 | 0.04 | 0.1 | 0 | 0.05 | 0.08 | 0 | 0.05 | 0.09 | 0 | 0.06 | 0.11 | 0 | 0.06 | 0.1 | 0 | 0.06 |
| 83 | 0.08 | 0 | 0.04 | 0.1 | 0 | 0.05 | 0.1 | 0 | 0.05 | 0.1 | 0 | 0.05 | 0.12 | 0 | 0.06 | 0.1 | 0 | 0.05 |
| 84 | 0.09 | 0 | 0.05 | 0.1 | 0 | 0.05 | 0.1 | 0 | 0.05 | 0.1 | 0 | 0.06 | 0.17 | 0 | 0.07 | 0.11 | 0 | 0.06 |
| 85 | 0.09 | 0 | 0.04 | 0.09 | 0 | 0.05 | 0.1 | 0 | 0.05 | 0.09 | 0 | 0.05 | 0.13 | 0 | 0.07 | 0.12 | 0 | 0.06 |
| 86 | 0.09 | 0 | 0.04 | 0.09 | 0 | 0.05 | 0.09 | 0 | 0.06 | 0.14 | 0 | 0.06 | 0.1 | 0 | 0.06 | 0.11 | 0 | 0.07 |
| 87 | 0.08 | 0 | 0.04 | 0.1 | 0 | 0.05 | 0.1 | 0 | 0.06 | 0.1 | 0 | 0.06 | 0.11 | 0 | 0.06 | 0.12 | 0 | 0.07 |
| 88 | 0.08 | 0 | 0.04 | 0.09 | 0 | 0.05 | 0.11 | 0 | 0.06 | 0.1 | 0 | 0.05 | 0.08 | 0 | 0.06 | 0.12 | 0 | 0.07 |
| 89 | 0.09 | 0 | 0.04 | 0.23 | 0 | 0.06 | 0.12 | 0 | 0.06 | 0.1 | 0 | 0.06 | 0.1 | 0 | 0.06 | 0.11 | 0 | 0.07 |
| 90 | 0.09 | 0 | 0.05 | 0.09 | 0 | 0.06 | 0.11 | 0 | 0.06 | 0.1 | 0 | 0.06 | 0.18 | 0 | 0.06 | 0.12 | 0 | 0.08 |
| 91 | 0.09 | 0 | 0.05 | 0.09 | 0 | 0.06 | 0.11 | 0 | 0.06 | 0.11 | 0.01 | 0.06 | 0.1 | 0.01 | 0.06 | 0.11 | 0 | 0.08 |
| 92 | 0.09 | 0 | 0.05 | 0.09 | 0 | 0.06 | 0.11 | 0 | 0.06 | 0.1 | 0 | 0.06 | 0.19 | 0 | 0.06 | 0.11 | 0 | 0.07 |
| 93 | 0.09 | 0 | 0.05 | 0.09 | 0 | 0.06 | 0.11 | 0 | 0.06 | 0.11 | 0 | 0.06 | 0.15 | 0 | 0.06 | 0.11 | 0 | 0.08 |
| 94 | 0.1 | 0.02 | 0.05 | 0.1 | 0 | 0.04 | 0.11 | 0 | 0.06 | 0.14 | 0 | 0.06 | 0.19 | 0 | 0.06 | 0.12 | 0 | 0.08 |
| 95 | 0.1 | 0 | 0.05 | 0.09 | 0 | 0.04 | 0.1 | 0 | 0.06 | 0.07 | 0 | 0.04 | 0.24 | 0 | 0.06 | 0.11 | 0 | 0.08 |
| 96 | 0.09 | 0 | 0.05 | 0.08 | 0 | 0.04 | 0.11 | 0 | 0.06 | 0.07 | 0 | 0.04 | 0.09 | 0 | 0.06 | 0.13 | 0 | 0.08 |
| 97 | 0.09 | 0 | 0.05 | 0.08 | 0 | 0.04 | 0.1 | 0 | 0.06 | 0.09 | 0 | 0.05 | 0.13 | 0 | 0.06 | 0.12 | 0 | 0.07 |
| 98 | 0.09 | 0 | 0.04 | 0.09 | 0 | 0.04 | 0.1 | 0 | 0.06 | 0.1 | 0 | 0.04 | 0.08 | 0 | 0.06 | 0.12 | 0 | 0.08 |
| 99 | 0.09 | 0 | 0.04 | 0.09 | 0 | 0.04 | 0.11 | 0 | 0.06 | 0.09 | 0 | 0.04 | 0.1 | 0 | 0.06 | 0.12 | 0 | 0.07 |

| | | | | | | | | | | | | | | | | | |
|---|---|---|---|---|---|---|---|---|---|---|---|---|---|---|---|---|---|
| 100 | 0.09 | 0 | 0.04 | 0.08 | 0 | 0.04 | 0.1 | 0 | 0.06 | 0.08 | 0 | 0.06 | 0.1 | 0 | 0.06 | 0.11 | 0 | 0.07 |
| 101 | 0.08 | 0 | 0.04 | 0.07 | 0 | 0.04 | 0.1 | 0 | 0.06 | 0.09 | 0 | 0.06 | 0.13 | 0 | 0.06 | 0.12 | 0.03 | 0.07 |
| 102 | 0.11 | 0 | 0.04 | 0.08 | 0 | 0.03 | 0.1 | 0 | 0.06 | 0.27 | 0 | 0.06 | 0.1 | 0 | 0.06 | 0.11 | 0.03 | 0.07 |
| 103 | 0.09 | 0 | 0.05 | 0.08 | 0 | 0.03 | 0.09 | 0 | 0.06 | 0.1 | 0 | 0.06 | 0.12 | 0 | 0.07 | 0.11 | 0 | 0.07 |
| 104 | 0.1 | 0 | 0.04 | 0.08 | 0 | 0.04 | 0.1 | 0 | 0.06 | 0.08 | 0.01 | 0.06 | 0.11 | 0 | 0.07 | 0.13 | 0 | 0.06 |
| 105 | 0.09 | 0 | 0.04 | 0.09 | 0 | 0.04 | 0.09 | 0 | 0.06 | 0.09 | 0 | 0.06 | 0.11 | 0 | 0.06 | 0.11 | 0.02 | 0.07 |
| 106 | 0.09 | 0 | 0.05 | 0.07 | 0 | 0.04 | 0.09 | 0 | 0.06 | 0.09 | 0 | 0.06 | 0.17 | 0 | 0.07 | 0.11 | 0 | 0.06 |
| 107 | 0.09 | 0 | 0.05 | 0.09 | 0 | 0.04 | 0.08 | 0 | 0.06 | 0.09 | 0 | 0.06 | 0.1 | 0 | 0.07 | 0.11 | 0 | 0.06 |
| 108 | 0.09 | 0 | 0.04 | 0.07 | 0 | 0.04 | 0.08 | 0 | 0.05 | 0.11 | 0.01 | 0.06 | 0.1 | 0 | 0.07 | 0.11 | 0 | 0.07 |
| 109 | 0.09 | 0 | 0.03 | 0.09 | 0 | 0.04 | 0.08 | 0 | 0.04 | 0.1 | 0 | 0.06 | 0.09 | 0 | 0.07 | 0.11 | 0 | 0.07 |
| 110 | 0.1 | 0 | 0.04 | 0.08 | 0 | 0.04 | 0.09 | 0.01 | 0.06 | 0.09 | 0 | 0.06 | 0.1 | 0 | 0.06 | 0.11 | 0 | 0.07 |
| 111 | 0.11 | 0 | 0.04 | 0.08 | 0 | 0.04 | 0.08 | 0 | 0.05 | 0.09 | 0 | 0.06 | 0.12 | 0 | 0.07 | 0.12 | 0 | 0.08 |
| 112 | 0.11 | 0 | 0.04 | 0.08 | 0 | 0.04 | 0.09 | 0.01 | 0.06 | 0.09 | 0 | 0.06 | 0.12 | 0 | 0.07 | 0.14 | 0 | 0.07 |
| 113 | 0.1 | 0 | 0.04 | 0.08 | 0 | 0.04 | 0.1 | 0.01 | 0.06 | 0.09 | 0 | 0.06 | 0.1 | 0.02 | 0.07 | 0.11 | 0 | 0.08 |
| 114 | 0.1 | 0 | 0.04 | 0.07 | 0 | 0.04 | 0.09 | 0 | 0.06 | 0.09 | 0 | 0.06 | 0.11 | 0 | 0.07 | 0.12 | 0.03 | 0.08 |
| 115 | 0.1 | 0 | 0.04 | 0.07 | 0 | 0.04 | 0.09 | 0 | 0.06 | 0.11 | 0 | 0.07 | 0.11 | 0 | 0.07 | 0.12 | 0.02 | 0.08 |
| 116 | 0.09 | 0 | 0.04 | 0.08 | 0 | 0.04 | 0.08 | 0 | 0.06 | 0.09 | 0 | 0.07 | 0.11 | 0 | 0.07 | 0.18 | 0 | 0.08 |
| 117 | 0.09 | 0 | 0.04 | 0.1 | 0 | 0.05 | 0.08 | 0 | 0.05 | 0.11 | 0 | 0.06 | 0.11 | 0 | 0.07 | 0.16 | 0 | 0.07 |
| 118 | 0.08 | 0 | 0.04 | 0.1 | 0 | 0.05 | 0.09 | 0 | 0.05 | 0.11 | 0 | 0.06 | 0.09 | 0.02 | 0.06 | 0.11 | 0 | 0.07 |
| 119 | 0.1 | 0 | 0.05 | 0.09 | 0 | 0.06 | 0.09 | 0 | 0.04 | 0.11 | 0 | 0.07 | 0.09 | 0.02 | 0.06 | 0.18 | 0 | 0.09 |
| 120 | 0.08 | 0 | 0.04 | 0.09 | 0 | 0.06 | 0.08 | 0 | 0.04 | 0.15 | 0 | 0.06 | 0.09 | 0 | 0.06 | 0.16 | 0 | 0.09 |
| 121 | 0.09 | 0 | 0.05 | 0.08 | 0 | 0.06 | 0.09 | 0 | 0.04 | 0.12 | 0.01 | 0.06 | 0.09 | 0.02 | 0.05 | 0.15 | 0 | 0.1 |
| 122 | 0.08 | 0 | 0.05 | 0.08 | 0 | 0.04 | 0.08 | 0 | 0.04 | 0.13 | 0 | 0.06 | 0.09 | 0.03 | 0.06 | 0.16 | 0.03 | 0.09 |
| 123 | 0.09 | 0 | 0.05 | 0.09 | 0 | 0.04 | 0.09 | 0 | 0.04 | 0.12 | 0 | 0.06 | 0.09 | 0 | 0.06 | 0.13 | 0 | 0.08 |
| 124 | 0.09 | 0.01 | 0.06 | 0.09 | 0 | 0.04 | 0.09 | 0 | 0.04 | 0.11 | 0 | 0.06 | 0.1 | 0 | 0.06 | 0.15 | 0 | 0.08 |
| 125 | 0.09 | 0 | 0.06 | 0.09 | 0 | 0.04 | 0.08 | 0 | 0.04 | 0.09 | 0.04 | 0.06 | 0.1 | 0 | 0.07 | 0.15 | 0 | 0.08 |
| 126 | 0.1 | 0 | 0.05 | 0.09 | 0 | 0.04 | 0.09 | 0 | 0.04 | 0.08 | 0.02 | 0.06 | 0.11 | 0 | 0.07 | 0.12 | 0 | 0.06 |
| 127 | 0.09 | 0 | 0.05 | 0.11 | 0 | 0.04 | 0.1 | 0 | 0.04 | 0.08 | 0 | 0.06 | 0.09 | 0.03 | 0.07 | 0.12 | 0 | 0.06 |
| 128 | 0.09 | 0 | 0.05 | 0.09 | 0 | 0.04 | 0 | 0 | 0.04 | 0.09 | 0.03 | 0.06 | 0.1 | 0 | 0.07 | 0.14 | 0 | 0.06 |
| 129 | 0.09 | 0 | 0.05 | 0.08 | 0 | 0.04 | 0.07 | 0 | 0.04 | 0.09 | 0 | 0.06 | 0.1 | 0 | 0.07 | 0.1 | 0 | 0.06 |
| 130 | 0.09 | 0 | 0.05 | 0.09 | 0 | 0.05 | 0.09 | 0 | 0.04 | 0.09 | 0 | 0.06 | 0.1 | 0 | 0.07 | 0.12 | 0 | 0.07 |
| 131 | 0.09 | 0 | 0.04 | 0.08 | 0 | 0.04 | 0.09 | 0 | 0.04 | 0.09 | 0 | 0.06 | 0.1 | 0.02 | 0.07 | 0.12 | 0 | 0.06 |
| 132 | 0.08 | 0 | 0.05 | 0.08 | 0 | 0.04 | 0.08 | 0 | 0.04 | 0.09 | 0 | 0.06 | 0.11 | 0.02 | 0.07 | 0.12 | 0 | 0.07 |
| 133 | 0.08 | 0 | 0.05 | 0.07 | 0 | 0.05 | 0.09 | 0 | 0.04 | 0.1 | 0 | 0.07 | 0.1 | 0 | 0.07 | 0.1 | 0 | 0.06 |
| 134 | 0.08 | 0 | 0.05 | 0.08 | 0 | 0.06 | 0.08 | 0 | 0.04 | 0.1 | 0 | 0.06 | 0.12 | 0 | 0.07 | 0.1 | 0.03 | 0.06 |
| 135 | 0.08 | 0 | 0.05 | 0.07 | 0 | 0.06 | 0.09 | 0 | 0.04 | 0.09 | 0 | 0.07 | 0.13 | 0 | 0.07 | 0.11 | 0 | 0.06 |
| 136 | 0.08 | 0 | 0.05 | 0.09 | 0 | 0.04 | 0.09 | 0 | 0.04 | 0.1 | 0 | 0.07 | 0.12 | 0.02 | 0.08 | 0.11 | 0.02 | 0.06 |
| 137 | 0.08 | 0 | 0.04 | 0.08 | 0 | 0.04 | 0.09 | 0 | 0.04 | 0.12 | 0 | 0.07 | 0.12 | 0.03 | 0.07 | 0.13 | 0 | 0.07 |
| 138 | 0.09 | 0 | 0.04 | 0.09 | 0 | 0.05 | 0.09 | 0 | 0.05 | 0.12 | 0.02 | 0.07 | 0.13 | 0.04 | 0.08 | 0.11 | 0 | 0.06 |

| | | | | | | | | | | | | | | | | | |
|---|---|---|---|---|---|---|---|---|---|---|---|---|---|---|---|---|---|
| 139 | 0.08 | 0.01 | 0.04 | 0.09 | 0 | 0.05 | 0.09 | 0.01 | 0.06 | 0.11 | 0.01 | 0.07 | 0.12 | 0.04 | 0.08 | 0.11 | 0 | 0.07 |
| 140 | 0.09 | 0 | 0.05 | 0.09 | 0 | 0.05 | 0.1 | 0 | 0.06 | 0.11 | 0.01 | 0.08 | 0.12 | 0 | 0.07 | 0.12 | 0 | 0.07 |
| 141 | 0.09 | 0 | 0.05 | 0.09 | 0 | 0.05 | 0.08 | 0 | 0.06 | 0.13 | 0 | 0.08 | 0.11 | 0 | 0.07 | 0.12 | 0 | 0.07 |
| 142 | 0.09 | 0 | 0.05 | 0.09 | 0 | 0.05 | 0.09 | 0 | 0.06 | 0.11 | 0 | 0.07 | 0.1 | 0 | 0.06 | 0.11 | 0 | 0.07 |
| 143 | 0.08 | 0 | 0.05 | 0.09 | 0 | 0.05 | 0.09 | 0 | 0.06 | 0.12 | 0 | 0.06 | 0.1 | 0.03 | 0.06 | 0.13 | 0 | 0.08 |
| 144 | 0.08 | 0 | 0.05 | 0.09 | 0 | 0.05 | 0.08 | 0 | 0.06 | 0.11 | 0 | 0.06 | 0.1 | 0.02 | 0.06 | 0.13 | 0 | 0.07 |
| 145 | 0.09 | 0 | 0.05 | 0.1 | 0 | 0.05 | 0.08 | 0 | 0.06 | 0.11 | 0 | 0.05 | 0.11 | 0 | 0.05 | 0.13 | 0 | 0.07 |
| 146 | 0.09 | 0 | 0.05 | 0.09 | 0 | 0.05 | 0.08 | 0 | 0.06 | 0.09 | 0.01 | 0.05 | 0.11 | 0 | 0.05 | 0.12 | 0 | 0.07 |
| 147 | 0.08 | 0 | 0.05 | 0.1 | 0 | 0.05 | 0.08 | 0 | 0.06 | 0.09 | 0 | 0.04 | 0.12 | 0 | 0.05 | 0.12 | 0 | 0.08 |
| 148 | 0.09 | 0 | 0.05 | 0.11 | 0 | 0.05 | 0.08 | 0 | 0.06 | 0.08 | 0 | 0.04 | 0.1 | 0 | 0.05 | 0.11 | 0 | 0.08 |
| 149 | 0.09 | 0 | 0.06 | 0.09 | 0 | 0.05 | 0.08 | 0 | 0.06 | 0.08 | 0 | 0.03 | 0.1 | 0 | 0.06 | 0.17 | 0 | 0.08 |
| 150 | 0.11 | 0.01 | 0.06 | 0.09 | 0 | 0.05 | 0.07 | 0 | 0.04 | 0.09 | 0 | 0.04 | 0.1 | 0 | 0.06 | 0.13 | 0 | 0.09 |
| 151 | 0.12 | 0.03 | 0.06 | 0.09 | 0 | 0.04 | 0.08 | 0 | 0.04 | 0.07 | 0 | 0.03 | 0.1 | 0 | 0.04 | 0.13 | 0 | 0.08 |
| 152 | 0.09 | 0 | 0.06 | 0.09 | 0 | 0.05 | 0.08 | 0 | 0.04 | 0.08 | 0 | 0.03 | 0.09 | 0 | 0.03 | 0.12 | 0 | 0.08 |
| 153 | 0.1 | 0 | 0.06 | 0.09 | 0 | 0.04 | 0.08 | 0 | 0.04 | 0.12 | 0 | 0.03 | 0.12 | 0 | 0.04 | 0.13 | 0.03 | 0.09 |
| 154 | 0.12 | 0 | 0.05 | 0.09 | 0 | 0.04 | 0.08 | 0 | 0.04 | 0.18 | 0 | 0.04 | 0.08 | 0 | 0.04 | 0.12 | 0.06 | 0.09 |
| 155 | 0.11 | 0 | 0.05 | 0.11 | 0 | 0.04 | 0.08 | 0 | 0.04 | 0.15 | 0 | 0.04 | 0.08 | 0 | 0.03 | 0.12 | 0 | 0.08 |
| 156 | 0.1 | 0 | 0.05 | 0.09 | 0 | 0.04 | 0.08 | 0 | 0.04 | 0.11 | 0 | 0.02 | 0.08 | 0 | 0.04 | 0.13 | 0 | 0.07 |
| 157 | 0.09 | 0 | 0.06 | 0.09 | 0 | 0.04 | 0.08 | 0 | 0.04 | 0.19 | 0 | 0.03 | 0.08 | 0 | 0.04 | 0.13 | 0 | 0.08 |
| 158 | 0.09 | 0 | 0.05 | 0.09 | 0 | 0.04 | 0.09 | 0 | 0.05 | 0.06 | 0 | 0.03 | 0.08 | 0 | 0.04 | 0.12 | 0 | 0.07 |
| 159 | 0.1 | 0 | 0.05 | 0.09 | 0 | 0.05 | 0.08 | 0.01 | 0.06 | 0.08 | 0 | 0.04 | 0.1 | 0 | 0.05 | 0.13 | 0 | 0.06 |
| 160 | 0.11 | 0 | 0.05 | 0.09 | 0 | 0.05 | 0.09 | 0 | 0.06 | 0.1 | 0 | 0.05 | 0.11 | 0 | 0.05 | 0.11 | 0 | 0.05 |
| 161 | 0.11 | 0 | 0.05 | 0.08 | 0 | 0.05 | 0.08 | 0 | 0.04 | 0.11 | 0 | 0.07 | 0.12 | 0 | 0.06 | 0.11 | 0.03 | 0.06 |
| 162 | 0.12 | 0 | 0.05 | 0.09 | 0 | 0.05 | 0.09 | 0 | 0.05 | 0.11 | 0 | 0.07 | 0.11 | 0 | 0.06 | 0.12 | 0.03 | 0.07 |
| 163 | 0.12 | 0 | 0.05 | 0.09 | 0 | 0.05 | 0.11 | 0 | 0.06 | 0.11 | 0 | 0.07 | 0.1 | 0 | 0.07 | 0.12 | 0 | 0.08 |
| 164 | 0.11 | 0 | 0.05 | 0.09 | 0.01 | 0.06 | 0.09 | 0 | 0.05 | 0.12 | 0 | 0.07 | 0.13 | 0 | 0.07 | 0.12 | 0 | 0.08 |
| 165 | 0.1 | 0.01 | 0.05 | 0.1 | 0.01 | 0.06 | 0.1 | 0 | 0.05 | 0.1 | 0 | 0.07 | 0.13 | 0 | 0.06 | 0.13 | 0.04 | 0.08 |
| 166 | 0.09 | 0 | 0.05 | 0.09 | 0.01 | 0.05 | 0.1 | 0 | 0.05 | 0.11 | 0 | 0.07 | 0.11 | 0 | 0.08 | 0.12 | 0.03 | 0.08 |
| 167 | 0.08 | 0 | 0.04 | 0.1 | 0 | 0.05 | 0.1 | 0 | 0.05 | 0.11 | 0 | 0.07 | 0.12 | 0.01 | 0.08 | 0.12 | 0 | 0.09 |
| 168 | 0.09 | 0 | 0.04 | 0.09 | 0 | 0.05 | 0.13 | 0 | 0.06 | 0.12 | 0 | 0.07 | 0.14 | 0 | 0.09 | 0.12 | 0.04 | 0.09 |
| 169 | 0.1 | 0 | 0.03 | 0.11 | 0 | 0.06 | 0.1 | 0 | 0.06 | 0.11 | 0.01 | 0.07 | 0.13 | 0 | 0.07 | 0.13 | 0.04 | 0.09 |
| 170 | 0.1 | 0 | 0.04 | 0.1 | 0 | 0.05 | 0.1 | 0 | 0.06 | 0.12 | 0 | 0.06 | 0.13 | 0 | 0.08 | 0.13 | 0.04 | 0.09 |
| 171 | 0.11 | 0 | 0.04 | 0.1 | 0 | 0.05 | 0.11 | 0.01 | 0.06 | 0.13 | 0.02 | 0.07 | 0.11 | 0 | 0.07 | 0.14 | 0.04 | 0.09 |
| 172 | 0.11 | 0 | 0.04 | 0.11 | 0.02 | 0.05 | 0.09 | 0 | 0.06 | 0.12 | 0 | 0.07 | 0.11 | 0 | 0.07 | 0.13 | 0 | 0.09 |
| 173 | 0.09 | 0 | 0.04 | 0.1 | 0.02 | 0.05 | 0.09 | 0 | 0.06 | 0.12 | 0.01 | 0.07 | 0.11 | 0 | 0.06 | 0.14 | 0.03 | 0.1 |
| 174 | 0.1 | 0 | 0.04 | 0.09 | 0 | 0.05 | 0.1 | 0 | 0.06 | 0.11 | 0 | 0.06 | 0.1 | 0.01 | 0.06 | 0.14 | 0 | 0.1 |
| 175 | 0.09 | 0 | 0.04 | 0.1 | 0 | 0.05 | 0.12 | 0 | 0.06 | 0.11 | 0 | 0.06 | 0.1 | 0 | 0.06 | 0.23 | 0 | 0.09 |
| 176 | 0.1 | 0 | 0.04 | 0.11 | 0 | 0.05 | 0.11 | 0 | 0.06 | 0.1 | 0 | 0.06 | 0.09 | 0 | 0.05 | 0.14 | 0 | 0.09 |
| 177 | 0.1 | 0 | 0.04 | 0.11 | 0 | 0.05 | 0.12 | 0 | 0.06 | 0.1 | 0 | 0.07 | 0.11 | 0 | 0.06 | 0.13 | 0 | 0.09 |

| | | | | | | | | | | | | | | | | | |
|---|---|---|---|---|---|---|---|---|---|---|---|---|---|---|---|---|---|
| 178 | 0.11 | 0 | 0.05 | 0.1 | 0 | 0.05 | 0.1 | 0 | 0.06 | 0.11 | 0 | 0.07 | 0.11 | 0 | 0.06 | 0.15 | 0 | 0.09 |
| 179 | 0.11 | 0.01 | 0.05 | 0.1 | 0 | 0.05 | 0.1 | 0 | 0.05 | 0.09 | 0 | 0.06 | 0.13 | 0 | 0.06 | 0.13 | 0 | 0.08 |
| 180 | 0.09 | 0 | 0.05 | 0.09 | 0 | 0.05 | 0.11 | 0 | 0.05 | 0.12 | 0 | 0.07 | 0.11 | 0 | 0.06 | 0.12 | 0 | 0.07 |
| 181 | 0.09 | 0 | 0.05 | 0.1 | 0 | 0.05 | 0.11 | 0 | 0.05 | 0.09 | 0 | 0.06 | 0.12 | 0 | 0.06 | 0.11 | 0.04 | 0.07 |
| 182 | 0.09 | 0 | 0.04 | 0.09 | 0 | 0.05 | 0.11 | 0 | 0.05 | 0.08 | 0 | 0.06 | 0.09 | 0 | 0.06 | 0.11 | 0 | 0.06 |
| 183 | 0.09 | 0 | 0.05 | 0.1 | 0 | 0.05 | 0.12 | 0 | 0.05 | 0.07 | 0 | 0.06 | 0.09 | 0 | 0.06 | 0.12 | 0 | 0.06 |
| 184 | 0.09 | 0 | 0.05 | 0.1 | 0 | 0.05 | 0.12 | 0 | 0.05 | 0.07 | 0 | 0.06 | 0.11 | 0 | 0.06 | 0.12 | 0 | 0.06 |
| 185 | 0.12 | 0 | 0.05 | 0.12 | 0 | 0.05 | 0.1 | 0 | 0.05 | 0.06 | 0 | 0.06 | 0.1 | 0 | 0.06 | 0.1 | 0 | 0.05 |
| 186 | 0.12 | 0 | 0.05 | 0.11 | 0 | 0.05 | 0.1 | 0 | 0.05 | 0.07 | 0 | 0.06 | 0.11 | 0 | 0.06 | 0.12 | 0 | 0.05 |
| 187 | 0.09 | 0 | 0.05 | 0.11 | 0 | 0.05 | 0.1 | 0 | 0.04 | 0.09 | 0 | 0.06 | 0.1 | 0 | 0.06 | 0.12 | 0 | 0.06 |
| 188 | 0.1 | 0 | 0.05 | 0.1 | 0 | 0.05 | 0.1 | 0 | 0.04 | 0.1 | 0 | 0.06 | 0.1 | 0 | 0.06 | 0.12 | 0 | 0.06 |
| 189 | 0.09 | 0 | 0.05 | 0.09 | 0 | 0.04 | 0.11 | 0 | 0.05 | 0.1 | 0 | 0.06 | 0.09 | 0 | 0.06 | 0.11 | 0 | 0.06 |
| 190 | 0.09 | 0 | 0.05 | 0.11 | 0 | 0.05 | 0.12 | 0 | 0.05 | 0.09 | 0 | 0.06 | 0.13 | 0 | 0.06 | 0.12 | 0 | 0.06 |
| 191 | 0.09 | 0 | 0.05 | 0.09 | 0 | 0.04 | 0.11 | 0 | 0.05 | 0.09 | 0.01 | 0.06 | 0.13 | 0 | 0.07 | 0.13 | 0 | 0.06 |
| 192 | 0.1 | 0 | 0.05 | 0.08 | 0 | 0.04 | 0.11 | 0 | 0.05 | 0.1 | 0 | 0.06 | 0.16 | 0 | 0.08 | 0.19 | 0 | 0.06 |
| 193 | 0.09 | 0 | 0.05 | 0.09 | 0 | 0.04 | 0.11 | 0 | 0.05 | 0.09 | 0 | 0.06 | 0.13 | 0 | 0.07 | 0.15 | 0 | 0.06 |
| 194 | 0.09 | 0 | 0.05 | 0.1 | 0 | 0.05 | 0.11 | 0 | 0.05 | 0.1 | 0 | 0.06 | 0.11 | 0 | 0.06 | 0.12 | 0 | 0.06 |
| 195 | 0.1 | 0 | 0.06 | 0.08 | 0 | 0.04 | 0.12 | 0 | 0.05 | 0.13 | 0 | 0.06 | 0.11 | 0 | 0.06 | 0.19 | 0 | 0.06 |
| 196 | 0.12 | 0 | 0.06 | 0.1 | 0 | 0.05 | 0.1 | 0 | 0.05 | 0.12 | 0 | 0.06 | 0.12 | 0 | 0.05 | 0.19 | 0 | 0.06 |
| 197 | 0.11 | 0 | 0.06 | 0.1 | 0 | 0.05 | 0.12 | 0 | 0.05 | 0.09 | 0 | 0.05 | 0.11 | 0 | 0.06 | 0.19 | 0 | 0.06 |
| 198 | 0.1 | 0 | 0.05 | 0.11 | 0 | 0.05 | 0.09 | 0 | 0.05 | 0.09 | 0 | 0.06 | 0.09 | 0 | 0.05 | 0.1 | 0 | 0.06 |
| 199 | 0.1 | 0 | 0.05 | 0.09 | 0 | 0.05 | 0.1 | 0 | 0.05 | 0.09 | 0 | 0.06 | 0.08 | 0 | 0.05 | 0.11 | 0 | 0.06 |
| 200 | 0.12 | 0 | 0.05 | 0.01 | 0 | 0.05 | 0.1 | 0 | 0.04 | 0.07 | 0 | 0.06 | 0.09 | 0 | 0.05 | 0.1 | 0 | 0.07 |

| | | | | | | | | | | | | | | | | | |
|---|---|---|---|---|---|---|---|---|---|---|---|---|---|---|---|---|---|
| | Control (mm) | | | | | | | | | Infected (mm) | | | | | | | |
| Day 6 | R1 | | | R2 | | | R3 | | | R1 | | | R2 | | | R3 | |
| | Max | Min | Average | Max | Min | Average | Max | Min | Average | Max | Min | Average | Max | Min | Average | Max | Min | Average |
| 1 | 0.07 | 0 | 0.04 | 0.07 | 0.01 | 0.04 | 0.07 | 0 | 0.04 | 0.13 | 0 | 0.06 | 0.1 | 0 | 0.05 | 0.08 | 0 | 0.06 |
| 2 | 0.06 | 0 | 0.04 | 0.08 | 0 | 0.04 | 0.07 | 0 | 0.04 | 0.12 | 0 | 0.06 | 0.14 | 0 | 0.06 | 0.09 | 0 | 0.06 |
| 3 | 0.08 | 0 | 0.04 | 0.08 | 0 | 0.04 | 0.07 | 0 | 0.04 | 0.12 | 0 | 0.06 | 0.12 | 0 | 0.06 | 0.1 | 0 | 0.06 |
| 4 | 0.06 | 0 | 0.04 | 0.08 | 0 | 0.04 | 0.07 | 0 | 0.04 | 0.11 | 0 | 0.06 | 0.12 | 0 | 0.06 | 0.09 | 0 | 0.06 |
| 5 | 0.06 | 0.01 | 0.04 | 0.07 | 0 | 0.04 | 0.07 | 0 | 0.04 | 0.1 | 0 | 0.06 | 0.12 | 0 | 0.06 | 0.09 | 0 | 0.06 |
| 6 | 0.07 | 0 | 0.05 | 0.07 | 0 | 0.04 | 0.07 | 0 | 0.04 | 0.11 | 0 | 0.06 | 0.13 | 0 | 0.06 | 0.09 | 0.02 | 0.06 |
| 7 | 0.07 | 0 | 0.04 | 0.07 | 0 | 0.04 | 0.07 | 0 | 0.04 | 0.13 | 0 | 0.06 | 0.12 | 0 | 0.06 | 0.09 | 0 | 0.06 |
| 8 | 0.07 | 0 | 0.04 | 0.07 | 0 | 0.04 | 0.08 | 0 | 0.04 | 0.13 | 0 | 0.06 | 0.12 | 0 | 0.05 | 0.09 | 0 | 0.06 |
| 9 | 0.08 | 0 | 0.05 | 0.06 | 0 | 0.04 | 0.08 | 0 | 0.05 | 0.11 | 0 | 0.06 | 0.12 | 0 | 0.06 | 0.09 | 0 | 0.06 |
| 10 | 0.08 | 0 | 0.04 | 0.08 | 0 | 0.04 | 0.09 | 0 | 0.04 | 0.12 | 0 | 0.06 | 0.12 | 0 | 0.06 | 0.08 | 0 | 0.06 |

| | | | | | | | | | | | | | | | | | |
|---|---|---|---|---|---|---|---|---|---|---|---|---|---|---|---|---|---|
| 11 | 0.08 | 0 | 0.05 | 0.08 | 0 | 0.03 | 0.08 | 0 | 0.04 | 0.12 | 0 | 0.07 | 0.12 | 0 | 0.06 | 0.09 | 0 | 0.06 |
| 12 | 0.08 | 0 | 0.05 | 0.08 | 0 | 0.04 | 0.09 | 0 | 0.04 | 0.14 | 0 | 0.07 | 0.12 | 0 | 0.07 | 0.11 | 0 | 0.06 |
| 13 | 0.09 | 0 | 0.05 | 0.07 | 0 | 0.04 | 0.09 | 0 | 0.04 | 0.11 | 0 | 0.06 | 0.11 | 0 | 0.06 | 0.1 | 0 | 0.06 |
| 14 | 0.09 | 0 | 0.05 | 0.08 | 0.01 | 0.04 | 0.08 | 0 | 0.04 | 0.11 | 0 | 0.06 | 0.13 | 0 | 0.07 | 0.12 | 0 | 0.07 |
| 15 | 0.09 | 0 | 0.05 | 0.09 | 0 | 0.04 | 0.08 | 0 | 0.04 | 0.11 | 0 | 0.06 | 0.13 | 0 | 0.08 | 0.12 | 0 | 0.07 |
| 16 | 0.09 | 0 | 0.05 | 0.11 | 0 | 0.04 | 0.08 | 0 | 0.05 | 0.11 | 0 | 0.06 | 0.14 | 0.01 | 0.08 | 0.12 | 0 | 0.07 |
| 17 | 0.08 | 0 | 0.05 | 0.11 | 0 | 0.04 | 0.09 | 0 | 0.05 | 0.11 | 0 | 0.06 | 0.13 | 0.01 | 0.09 | 0.1 | 0 | 0.07 |
| 18 | 0.08 | 0 | 0.05 | 0.11 | 0 | 0.04 | 0.08 | 0 | 0.04 | 0.11 | 0 | 0.06 | 0.12 | 0 | 0.09 | 0.11 | 0 | 0.07 |
| 19 | 0.08 | 0 | 0.05 | 0.07 | 0 | 0.04 | 0.09 | 0 | 0.04 | 0.11 | 0 | 0.06 | 0.13 | 0 | 0.08 | 0.1 | 0 | 0.07 |
| 20 | 0.08 | 0 | 0.05 | 0.07 | 0 | 0.04 | 0.08 | 0 | 0.05 | 0.11 | 0 | 0.06 | 0.12 | 0.04 | 0.08 | 0.11 | 0.01 | 0.07 |
| 21 | 0.08 | 0 | 0.05 | 0.08 | 0 | 0.05 | 0.08 | 0 | 0.05 | 0.11 | 0 | 0.06 | 0.12 | 0.05 | 0.08 | 0.1 | 0.03 | 0.07 |
| 22 | 0.09 | 0 | 0.04 | 0.07 | 0 | 0.05 | 0.09 | 0 | 0.05 | 0.11 | 0 | 0.06 | 0.17 | 0 | 0.07 | 0.11 | 0.04 | 0.07 |
| 23 | 0.07 | 0 | 0.04 | 0.08 | 0.02 | 0.05 | 0.08 | 0.03 | 0.05 | 0.1 | 0 | 0.05 | 0.13 | 0 | 0.07 | 0.12 | 0.03 | 0.07 |
| 24 | 0.09 | 0 | 0.05 | 0.09 | 0 | 0.05 | 0.09 | 0 | 0.05 | 0.12 | 0 | 0.05 | 0.14 | 0.04 | 0.08 | 0.11 | 0 | 0.06 |
| 25 | 0.08 | 0 | 0.05 | 0.08 | 0 | 0.05 | 0.09 | 0 | 0.05 | 0.11 | 0 | 0.07 | 0.12 | 0.04 | 0.07 | 0.11 | 0 | 0.06 |
| 26 | 0.08 | 0 | 0.05 | 0.09 | 0.01 | 0.05 | 0.1 | 0 | 0.05 | 0.11 | 0 | 0.06 | 0.12 | 0 | 0.07 | 0.1 | 0 | 0.06 |
| 27 | 0.08 | 0 | 0.05 | 0.08 | 0 | 0.04 | 0.09 | 0 | 0.05 | 0.12 | 0 | 0.06 | 0.12 | 0 | 0.06 | 0.11 | 0 | 0.06 |
| 28 | 0.09 | 0 | 0.05 | 0.08 | 0 | 0.05 | 0.09 | 0 | 0.06 | 0.13 | 0 | 0.06 | 0.11 | 0 | 0.07 | 0.12 | 0 | 0.06 |
| 29 | 0.09 | 0 | 0.05 | 0.09 | 0 | 0.05 | 0.09 | 0.01 | 0.05 | 0.12 | 0 | 0.06 | 0.11 | 0 | 0.06 | 0.1 | 0 | 0.06 |
| 30 | 0.11 | 0 | 0.05 | 0.08 | 0 | 0.05 | 0.09 | 0 | 0.05 | 0.11 | 0 | 0.07 | 0.12 | 0 | 0.06 | 0.1 | 0 | 0.04 |
| 31 | 0.09 | 0 | 0.05 | 0.08 | 0 | 0.05 | 0.08 | 0.03 | 0.05 | 0.11 | 0 | 0.06 | 0.12 | 0 | 0.08 | 0.09 | 0 | 0.05 |
| 32 | 0.09 | 0.01 | 0.05 | 0.1 | 0 | 0.05 | 0.08 | 0 | 0.05 | 0.12 | 0 | 0.06 | 0.13 | 0 | 0.08 | 0.11 | 0 | 0.04 |
| 33 | 0.09 | 0 | 0.06 | 0.08 | 0.02 | 0.05 | 0.09 | 0 | 0.05 | 0.11 | 0 | 0.07 | 0.12 | 0 | 0.08 | 0.11 | 0 | 0.04 |
| 34 | 0.09 | 0 | 0.05 | 0.08 | 0.02 | 0.05 | 0.08 | 0 | 0.05 | 0.12 | 0.01 | 0.07 | 0.13 | 0 | 0.08 | 0.09 | 0 | 0.05 |
| 35 | 0.1 | 0 | 0.05 | 0.08 | 0 | 0.05 | 0.08 | 0 | 0.05 | 0.12 | 0 | 0.07 | 0.12 | 0 | 0.07 | 0.08 | 0.01 | 0.05 |
| 36 | 0.08 | 0 | 0.04 | 0.09 | 0.01 | 0.05 | 0.08 | 0 | 0.05 | 0.11 | 0 | 0.07 | 0.12 | 0 | 0.08 | 0.12 | 0 | 0.05 |
| 37 | 0.08 | 0 | 0.04 | 0.09 | 0 | 0.05 | 0.08 | 0 | 0.05 | 0.11 | 0.04 | 0.07 | 0.11 | 0.05 | 0.08 | 0.12 | 0 | 0.05 |
| 38 | 0.08 | 0 | 0.04 | 0.09 | 0.02 | 0.05 | 0.09 | 0 | 0.05 | 0.12 | 0.03 | 0.07 | 0.13 | 0.05 | 0.08 | 0.14 | 0 | 0.06 |
| 39 | 0.08 | 0.02 | 0.05 | 0.09 | 0 | 0.05 | 0.09 | 0 | 0.05 | 0.12 | 0.03 | 0.07 | 0.12 | 0.04 | 0.08 | 0.12 | 0 | 0.06 |
| 40 | 0.09 | 0 | 0.05 | 0.08 | 0.01 | 0.04 | 0.09 | 0 | 0.05 | 0.11 | 0 | 0.07 | 0.13 | 0 | 0.08 | 0.12 | 0 | 0.06 |
| 41 | 0.09 | 0 | 0.05 | 0.08 | 0.01 | 0.05 | 0.08 | 0 | 0.05 | 0.12 | 0.03 | 0.07 | 0.12 | 0.05 | 0.09 | 0.13 | 0 | 0.07 |
| 42 | 0.08 | 0 | 0.04 | 0.09 | 0.01 | 0.04 | 0.08 | 0.01 | 0.05 | 0.12 | 0.03 | 0.07 | 0.12 | 0.05 | 0.08 | 0.12 | 0 | 0.07 |
| 43 | 0.09 | 0.02 | 0.05 | 0.08 | 0 | 0.04 | 0.07 | 0.02 | 0.05 | 0.12 | 0.03 | 0.07 | 0.12 | 0.04 | 0.08 | 0.13 | 0 | 0.07 |
| 44 | 0.09 | 0 | 0.05 | 0.08 | 0 | 0.05 | 0.08 | 0 | 0.04 | 0.11 | 0.02 | 0.07 | 0.12 | 0.04 | 0.08 | 0.16 | 0 | 0.07 |
| 45 | 0.09 | 0 | 0.04 | 0.08 | 0 | 0.05 | 0.08 | 0 | 0.04 | 0.14 | 0.02 | 0.08 | 0.12 | 0.04 | 0.08 | 0.14 | 0.01 | 0.07 |
| 46 | 0.07 | 0 | 0.05 | 0.08 | 0.02 | 0.05 | 0.09 | 0 | 0.04 | 0.11 | 0.03 | 0.07 | 0.12 | 0 | 0.08 | 0.12 | 0 | 0.07 |
| 47 | 0.08 | 0.03 | 0.05 | 0.08 | 0.03 | 0.05 | 0.09 | 0 | 0.05 | 0.12 | 0.03 | 0.07 | 0.12 | 0 | 0.08 | 0.12 | 0.02 | 0.07 |
| 48 | 0.07 | 0 | 0.04 | 0.08 | 0.03 | 0.05 | 0.09 | 0 | 0.05 | 0.11 | 0.03 | 0.07 | 0.13 | 0 | 0.08 | 0.12 | 0.05 | 0.08 |
| 49 | 0.07 | 0 | 0.04 | 0.09 | 0.03 | 0.06 | 0.09 | 0.02 | 0.05 | 0.11 | 0 | 0.07 | 0.11 | 0.02 | 0.07 | 0.12 | 0 | 0.08 |

| | | | | | | | | | | | | | | | | | |
|---|---|---|---|---|---|---|---|---|---|---|---|---|---|---|---|---|---|
| 50 | 0.07 | 0 | 0.04 | 0.08 | 0.03 | 0.05 | 0.09 | 0.02 | 0.05 | 0.12 | 0 | 0.06 | 0.11 | 0 | 0.07 | 0.12 | 0.03 | 0.08 |
| 51 | 0.07 | 0 | 0.05 | 0.09 | 0 | 0.05 | 0.09 | 0 | 0.05 | 0.1 | 0 | 0.06 | 0.12 | 0.01 | 0.07 | 0.13 | 0 | 0.09 |
| 52 | 0.08 | 0 | 0.05 | 0.09 | 0 | 0.05 | 0.11 | 0 | 0.06 | 0.1 | 0 | 0.06 | 0.1 | 0 | 0.06 | 0.12 | 0 | 0.09 |
| 53 | 0.07 | 0 | 0.05 | 0.08 | 0 | 0.05 | 0.09 | 0.03 | 0.05 | 0.1 | 0 | 0.07 | 0.11 | 0 | 0.06 | 0.13 | 0 | 0.09 |
| 54 | 0.07 | 0.02 | 0.05 | 0.08 | 0 | 0.05 | 0.08 | 0 | 0.05 | 0.1 | 0 | 0.06 | 0.11 | 0 | 0.06 | 0.12 | 0 | 0.09 |
| 55 | 0.08 | 0.02 | 0.04 | 0.08 | 0 | 0.05 | 0.08 | 0 | 0.05 | 0.11 | 0 | 0.06 | 0.12 | 0 | 0.06 | 0.12 | 0 | 0.08 |
| 56 | 0.08 | 0 | 0.05 | 0.09 | 0.02 | 0.05 | 0.09 | 0.02 | 0.05 | 0.11 | 0 | 0.06 | 0.13 | 0 | 0.07 | 0.14 | 0 | 0.09 |
| 57 | 0.09 | 0.02 | 0.05 | 0.08 | 0 | 0.05 | 0.08 | 0 | 0.05 | 0.11 | 0 | 0.06 | 0.11 | 0 | 0.06 | 0.12 | 0.05 | 0.08 |
| 58 | 0.1 | 0 | 0.05 | 0.08 | 0.02 | 0.05 | 0.08 | 0 | 0.04 | 0.09 | 0 | 0.05 | 0.11 | 0 | 0.06 | 0.12 | 0.05 | 0.08 |
| 59 | 0.09 | 0 | 0.05 | 0.08 | 0 | 0.05 | 0.08 | 0 | 0.05 | 0.1 | 0 | 0.05 | 0.12 | 0 | 0.06 | 0.12 | 0.04 | 0.08 |
| 60 | 0.09 | 0 | 0.05 | 0.09 | 0 | 0.04 | 0.09 | 0.02 | 0.05 | 0.1 | 0 | 0.05 | 0.13 | 0 | 0.06 | 0.12 | 0.03 | 0.08 |
| 61 | 0.08 | 0 | 0.05 | 0.17 | 0.02 | 0.05 | 0.08 | 0 | 0.05 | 0.09 | 0 | 0.05 | 0.12 | 0 | 0.06 | 0.13 | 0 | 0.08 |
| 62 | 0.09 | 0 | 0.05 | 0.09 | 0.03 | 0.05 | 0.08 | 0 | 0.05 | 0.1 | 0 | 0.05 | 0.11 | 0 | 0.06 | 0.12 | 0 | 0.08 |
| 63 | 0.09 | 0 | 0.06 | 0.09 | 0 | 0.05 | 0.08 | 0.03 | 0.05 | 0.11 | 0 | 0.06 | 0.13 | 0 | 0.06 | 0.12 | 0 | 0.07 |
| 64 | 0.09 | 0 | 0.06 | 0.09 | 0.01 | 0.05 | 0.09 | 0 | 0.06 | 0.11 | 0 | 0.06 | 0.1 | 0 | 0.05 | 0.12 | 0 | 0.07 |
| 65 | 0.09 | 0 | 0.05 | 0.09 | 0 | 0.04 | 0.01 | 0 | 0.05 | 0.11 | 0 | 0.06 | 0.12 | 0 | 0.06 | 0.11 | 0.05 | 0.07 |
| 66 | 0.08 | 0 | 0.05 | 0.09 | 0 | 0.05 | 0.1 | 0 | 0.05 | 0.11 | 0 | 0.06 | 0.11 | 0 | 0.06 | 0.12 | 0 | 0.07 |
| 67 | 0.09 | 0 | 0.05 | 0.08 | 0 | 0.04 | 0.12 | 0.01 | 0.06 | 0.12 | 0 | 0.06 | 0.12 | 0 | 0.06 | 0.12 | 0 | 0.07 |
| 68 | 0.1 | 0 | 0.05 | 0.09 | 0 | 0.04 | 0.09 | 0 | 0.05 | 0.12 | 0 | 0.07 | 0.12 | 0 | 0.06 | 0.11 | 0 | 0.07 |
| 69 | 0.08 | 0 | 0.05 | 0.08 | 0 | 0.04 | 0.09 | 0 | 0.06 | 0.11 | 0 | 0.06 | 0.11 | 0 | 0.06 | 0.1 | 0 | 0.06 |
| 70 | 0.08 | 0 | 0.05 | 0.1 | 0 | 0.04 | 0.08 | 0 | 0.05 | 0.11 | 0 | 0.06 | 0.12 | 0 | 0.07 | 0.12 | 0 | 0.06 |
| 71 | 0.08 | 0 | 0.04 | 0.09 | 0 | 0.04 | 0.08 | 0 | 0.05 | 0.12 | 0.01 | 0.07 | 0.12 | 0 | 0.07 | 0.11 | 0 | 0.07 |
| 72 | 0.09 | 0 | 0.05 | 0.07 | 0 | 0.04 | 0.08 | 0 | 0.05 | 0.12 | 0 | 0.07 | 0.12 | 0 | 0.07 | 0.13 | 0 | 0.08 |
| 73 | 0.08 | 0 | 0.04 | 0.09 | 0 | 0.04 | 0.08 | 0 | 0.05 | 0.12 | 0 | 0.07 | 0.11 | 0 | 0.06 | 0.13 | 0.02 | 0.07 |
| 74 | 0.08 | 0 | 0.04 | 0.08 | 0 | 0.04 | 0.09 | 0 | 0.05 | 0.12 | 0 | 0.07 | 0.11 | 0 | 0.07 | 0.12 | 0.04 | 0.08 |
| 75 | 0.09 | 0 | 0.04 | 0.09 | 0 | 0.04 | 0.1 | 0 | 0.05 | 0.12 | 0 | 0.07 | 0.12 | 0 | 0.08 | 0.13 | 0 | 0.08 |
| 76 | 0.08 | 0 | 0.04 | 0.08 | 0 | 0.04 | 0.08 | 0 | 0.04 | 0.12 | 0 | 0.07 | 0.12 | 0 | 0.08 | 0.13 | 0.04 | 0.08 |
| 77 | 0.06 | 0 | 0.04 | 0.09 | 0 | 0.04 | 0.09 | 0 | 0.04 | 0.13 | 0 | 0.07 | 0.13 | 0 | 0.08 | 0.12 | 0 | 0.08 |
| 78 | 0.06 | 0 | 0.04 | 0.08 | 0 | 0.04 | 0.09 | 0 | 0.05 | 0.12 | 0 | 0.08 | 0.12 | 0 | 0.08 | 0.13 | 0 | 0.08 |
| 79 | 0.07 | 0 | 0.04 | 0.08 | 0 | 0.04 | 0.07 | 0 | 0.04 | 0.12 | 0 | 0.08 | 0.13 | 0.03 | 0.08 | 0.12 | 0 | 0.09 |
| 80 | 0.11 | 0 | 0.04 | 0.08 | 0.01 | 0.04 | 0.07 | 0 | 0.03 | 0.12 | 0 | 0.08 | 0.12 | 0 | 0.08 | 0.12 | 0 | 0.08 |
| 81 | 0.1 | 0 | 0.05 | 0.08 | 0 | 0.04 | 0.07 | 0 | 0.04 | 0.12 | 0 | 0.07 | 0.13 | 0.02 | 0.08 | 0.13 | 0 | 0.08 |
| 82 | 0.09 | 0 | 0.05 | 0.08 | 0 | 0.04 | 0.08 | 0 | 0.04 | 0.11 | 0 | 0.07 | 0.12 | 0 | 0.08 | 0.13 | 0 | 0.09 |
| 83 | 0.08 | 0.02 | 0.05 | 0.09 | 0 | 0.05 | 0.11 | 0 | 0.04 | 0.11 | 0 | 0.06 | 0.12 | 0.04 | 0.08 | 0.12 | 0.07 | 0.09 |
| 84 | 0.09 | 0.01 | 0.05 | 0.09 | 0 | 0.05 | 0.1 | 0 | 0.05 | 0.11 | 0 | 0.06 | 0.12 | 0.02 | 0.08 | 0.11 | 0 | 0.09 |
| 85 | 0.1 | 0.02 | 0.05 | 0.08 | 0 | 0.05 | 0.1 | 0 | 0.05 | 0.11 | 0 | 0.06 | 0.12 | 0.03 | 0.08 | 0.11 | 0 | 0.08 |
| 86 | 0.09 | 0.01 | 0.04 | 0.1 | 0 | 0.05 | 0.09 | 0 | 0.04 | 0.11 | 0 | 0.06 | 0.14 | 0.03 | 0.08 | 0.11 | 0.06 | 0.08 |
| 87 | 0.09 | 0 | 0.05 | 0.1 | 0 | 0.06 | 0.09 | 0 | 0.05 | 0.11 | 0.02 | 0.07 | 0.14 | 0.04 | 0.08 | 0.13 | 0 | 0.08 |
| 88 | 0.08 | 0 | 0.04 | 0.09 | 0 | 0.05 | 0.09 | 0 | 0.04 | 0.11 | 0 | 0.07 | 0.12 | 0.04 | 0.08 | 0.14 | 0 | 0.07 |

| | | | | | | | | | | | | | | | | | |
|---|---|---|---|---|---|---|---|---|---|---|---|---|---|---|---|---|---|
| 89 | 0.09 | 0 | 0.04 | 0.09 | 0 | 0.05 | 0.09 | 0 | 0.05 | 0.11 | 0 | 0.06 | 0.13 | 0.03 | 0.08 | 0.11 | 0 | 0.06 |
| 90 | 0.07 | 0 | 0.05 | 0.08 | 0 | 0.04 | 0.09 | 0 | 0.04 | 0.11 | 0.03 | 0.07 | 0.13 | 0.05 | 0.08 | 0.11 | 0 | 0.06 |
| 91 | 0.08 | 0 | 0.05 | 0.08 | 0 | 0.04 | 0.11 | 0 | 0.05 | 0.11 | 0.03 | 0.07 | 0.12 | 0.04 | 0.07 | 0.12 | 0 | 0.06 |
| 92 | 0.08 | 0 | 0.05 | 0.08 | 0 | 0.05 | 0.11 | 0 | 0.05 | 0.12 | 0.03 | 0.07 | 0.12 | 0.03 | 0.07 | 0.11 | 0 | 0.06 |
| 93 | 0.07 | 0.01 | 0.04 | 0.09 | 0 | 0.04 | 0.1 | 0 | 0.05 | 0.13 | 0 | 0.07 | 0.12 | 0 | 0.07 | 0.11 | 0 | 0.06 |
| 94 | 0.06 | 0.02 | 0.04 | 0.09 | 0 | 0.04 | 0.1 | 0 | 0.05 | 0.12 | 0.4 | 0.08 | 0.12 | 0 | 0.07 | 0.12 | 0 | 0.05 |
| 95 | 0.08 | 0 | 0.04 | 0.1 | 0 | 0.04 | 0.1 | 0 | 0.04 | 0.12 | 0.04 | 0.08 | 0.13 | 0 | 0.07 | 0.13 | 0 | 0.05 |
| 96 | 0.08 | 0 | 0.04 | 0.08 | 0.01 | 0.04 | 0.09 | 0 | 0.04 | 0.13 | 0 | 0.08 | 0.12 | 0 | 0.07 | 0.11 | 0 | 0.04 |
| 97 | 0.08 | 0 | 0.04 | 0.09 | 0 | 0.04 | 0.1 | 0 | 0.04 | 0.12 | 0 | 0.08 | 0.11 | 0 | 0.06 | 0.11 | 0 | 0.04 |
| 98 | 0.08 | 0 | 0.05 | 0.08 | 0 | 0.04 | 0.09 | 0 | 0.04 | 0.12 | 0 | 0.09 | 0.12 | 0 | 0.07 | 0.11 | 0 | 0.05 |
| 99 | 0.08 | 0.01 | 0.05 | 0.08 | 0 | 0.04 | 0.09 | 0 | 0.04 | 0.12 | 0 | 0.08 | 0.14 | 0 | 0.07 | 0.1 | 0 | 0.04 |
| 100 | 0.08 | 0 | 0.05 | 0.08 | 0 | 0.04 | 0.1 | 0 | 0.04 | 0.12 | 0.04 | 0.08 | 0.12 | 0 | 0.08 | 0.09 | 0 | 0.05 |
| 101 | 0.08 | 0.01 | 0.05 | 0.08 | 0 | 0.04 | 0.11 | 0 | 0.04 | 0.12 | 0.03 | 0.08 | 0.12 | 0 | 0.08 | 0.09 | 0 | 0.06 |
| 102 | 0.1 | 0 | 0.05 | 0.09 | 0 | 0.04 | 0.1 | 0 | 0.04 | 0.12 | 0.04 | 0.08 | 0.12 | 0 | 0.07 | 0.12 | 0.02 | 0.06 |
| 103 | 0.09 | 0 | 0.05 | 0.09 | 0.01 | 0.04 | 0.1 | 0 | 0.04 | 0.12 | 0.03 | 0.08 | 0.11 | 0 | 0.07 | 0.12 | 0 | 0.07 |
| 104 | 0.11 | 0 | 0.05 | 0.09 | 0 | 0.04 | 0.08 | 0 | 0.04 | 0.14 | 0 | 0.08 | 0.12 | 0 | 0.07 | 0.12 | 0 | 0.07 |
| 105 | 0.08 | 0.02 | 0.04 | 0.08 | 0 | 0.04 | 0.09 | 0 | 0.04 | 0.14 | 0.04 | 0.09 | 0.12 | 0 | 0.08 | 0.12 | 0 | 0.08 |
| 106 | 0.07 | 0 | 0.04 | 0.09 | 0 | 0.04 | 0.08 | 0.01 | 0.04 | 0.15 | 0.04 | 0.08 | 0.13 | 0.04 | 0.09 | 0.12 | 0 | 0.08 |
| 107 | 0.09 | 0 | 0.05 | 0.09 | 0 | 0.05 | 0.08 | 0 | 0.04 | 0.14 | 0.04 | 0.08 | 0.15 | 0 | 0.09 | 0.12 | 0 | 0.07 |
| 108 | 0.1 | 0.03 | 0.05 | 0.1 | 0 | 0.05 | 0.09 | 0 | 0.04 | 0.15 | 0 | 0.08 | 0.14 | 0 | 0.09 | 0.13 | 0 | 0.08 |
| 109 | 0.08 | 0 | 0.04 | 0.09 | 0 | 0.05 | 0.09 | 0 | 0.04 | 0.14 | 0.03 | 0.08 | 0.15 | 0.03 | 0.09 | 0.13 | 0 | 0.08 |
| 110 | 0.07 | 0 | 0.04 | 0.09 | 0 | 0.04 | 0.09 | 0 | 0.04 | 0.13 | 0 | 0.08 | 0.14 | 0 | 0.09 | 0.13 | 0.02 | 0.08 |
| 111 | 0.07 | 0 | 0.04 | 0.08 | 0 | 0.04 | 0.1 | 0 | 0.05 | 0.12 | 0.02 | 0.08 | 0.14 | 0 | 0.09 | 0.12 | 0 | 0.08 |
| 112 | 0.07 | 0 | 0.05 | 0.08 | 0 | 0.04 | 0.1 | 0 | 0.05 | 0.13 | 0.03 | 0.08 | 0.16 | 0 | 0.09 | 0.12 | 0 | 0.09 |
| 113 | 0.07 | 0.02 | 0.05 | 0.07 | 0.01 | 0.04 | 0.09 | 0 | 0.05 | 0.12 | 0 | 0.07 | 0.14 | 0.04 | 0.09 | 0.13 | 0 | 0.09 |
| 114 | 0.08 | 0.02 | 0.04 | 0.08 | 0 | 0.05 | 0.09 | 0 | 0.05 | 0.13 | 0 | 0.07 | 0.14 | 0.04 | 0.09 | 0.14 | 0 | 0.09 |
| 115 | 0.07 | 0 | 0.04 | 0.08 | 0 | 0.05 | 0.1 | 0 | 0.05 | 0.11 | 0 | 0.07 | 0.14 | 0.05 | 0.09 | 0.16 | 0.06 | 0.1 |
| 116 | 0.07 | 0.03 | 0.05 | 0.09 | 0 | 0.05 | 0.09 | 0 | 0.04 | 0.11 | 0 | 0.07 | 0.15 | 0.04 | 0.09 | 0.12 | 0.07 | 0.1 |
| 117 | 0.08 | 0 | 0.05 | 0.08 | 0 | 0.05 | 0.09 | 0.01 | 0.05 | 0.11 | 0.03 | 0.07 | 0.14 | 0.04 | 0.08 | 0.12 | 0 | 0.09 |
| 118 | 0.08 | 0 | 0.05 | 0.09 | 0 | 0.05 | 0.08 | 0 | 0.05 | 0.11 | 0.01 | 0.07 | 0.14 | 0 | 0.08 | 0.12 | 0 | 0.08 |
| 119 | 0.07 | 0 | 0.05 | 0.09 | 0 | 0.05 | 0.08 | 0.01 | 0.05 | 0.11 | 0.03 | 0.07 | 0.12 | 0.04 | 0.08 | 0.13 | 0.04 | 0.09 |
| 120 | 0.07 | 0 | 0.05 | 0.08 | 0 | 0.05 | 0.08 | 0 | 0.05 | 0.1 | 0.03 | 0.07 | 0.12 | 0.03 | 0.07 | 0.12 | 0 | 0.08 |
| 121 | 0.08 | 0 | 0.05 | 0.08 | 0 | 0.05 | 0.08 | 0 | 0.05 | 0.1 | 0 | 0.06 | 0.15 | 0.03 | 0.08 | 0.12 | 0 | 0.07 |
| 122 | 0.08 | 0 | 0.05 | 0.08 | 0 | 0.05 | 0.08 | 0 | 0.05 | 0.11 | 0 | 0.06 | 0.14 | 0 | 0.07 | 0.13 | 0.04 | 0.08 |
| 123 | 0.07 | 0 | 0.04 | 0.1 | 0 | 0.05 | 0.09 | 0.02 | 0.05 | 0.12 | 0 | 0.07 | 0.13 | 0.04 | 0.07 | 0.12 | 0.04 | 0.07 |
| 124 | 0.07 | 0.01 | 0.05 | 0.08 | 0 | 0.05 | 0.08 | 0.03 | 0.03 | 0.12 | 0.03 | 0.07 | 0.13 | 0.03 | 0.07 | 0.11 | 0 | 0.07 |
| 125 | 0.07 | 0 | 0.05 | 0.11 | 0.01 | 0.05 | 0.09 | 0 | 0.06 | 0.14 | 0.03 | 0.07 | 0.15 | 0.03 | 0.08 | 0.12 | 0 | 0.07 |
| 126 | 0.08 | 0 | 0.05 | 0.1 | 0 | 0.05 | 0.09 | 0 | 0.06 | 0.14 | 0.02 | 0.08 | 0.16 | 0 | 0.08 | 0.14 | 0.05 | 0.07 |
| 127 | 0.08 | 0 | 0.05 | 0.1 | 0 | 0.05 | 0.09 | 0 | 0.06 | 0.13 | 0 | 0.08 | 0.15 | 0 | 0.08 | 0.14 | 0.05 | 0.08 |

| | | | | | | | | | | | | | | | | | |
|---|---|---|---|---|---|---|---|---|---|---|---|---|---|---|---|---|---|
| 128 | 0.08 | 0 | 0.05 | 0.12 | 0 | 0.05 | 0.09 | 0.01 | 0.06 | 0.13 | 0 | 0.08 | 0.17 | 0 | 0.08 | 0.14 | 0.05 | 0.08 |
| 129 | 0.08 | 0 | 0.05 | 0.11 | 0.02 | 0.05 | 0.09 | 0.01 | 0.06 | 0.12 | 0.01 | 0.08 | 0.13 | 0 | 0.08 | 0.14 | 0 | 0.07 |
| 130 | 0.08 | 0 | 0.05 | 0.08 | 0 | 0.04 | 0.09 | 0 | 0.06 | 0.13 | 0.03 | 0.08 | 0.13 | 0 | 0.08 | 0.13 | 0 | 0.07 |
| 131 | 0.09 | 0 | 0.05 | 0.11 | 0 | 0.05 | 0.09 | 0.01 | 0.06 | 0.13 | 0.02 | 0.08 | 0.13 | 0.04 | 0.09 | 0.12 | 0 | 0.07 |
| 132 | 0.09 | 0 | 0.05 | 0.08 | 0 | 0.05 | 0.08 | 0 | 0.05 | 0.13 | 0.02 | 0.07 | 0.12 | 0 | 0.08 | 0.11 | 0.04 | 0.08 |
| 133 | 0.09 | 0 | 0.05 | 0.08 | 0 | 0.04 | 0.09 | 0 | 0.05 | 0.14 | 0 | 0.08 | 0.13 | 0 | 0.08 | 0.15 | 0 | 0.08 |
| 134 | 0.08 | 0 | 0.05 | 0.08 | 0 | 0.05 | 0.1 | 0.01 | 0.05 | 0.13 | 0.01 | 0.08 | 0.12 | 0 | 0.08 | 0.12 | 0 | 0.08 |
| 135 | 0.09 | 0 | 0.06 | 0.08 | 0 | 0.05 | 0.09 | 0.02 | 0.05 | 0.12 | 0 | 0.08 | 0.12 | 0.02 | 0.08 | 0.14 | 0 | 0.08 |
| 136 | 0.08 | 0 | 0.05 | 0.09 | 0.03 | 0.05 | 0.09 | 0 | 0.05 | 0.12 | 0 | 0.08 | 0.12 | 0.01 | 0.08 | 0.13 | 0 | 0.09 |
| 137 | 0.09 | 0 | 0.05 | 0.11 | 0 | 0.05 | 0.1 | 0 | 0.05 | 0.12 | 0 | 0.08 | 0.12 | 0 | 0.09 | 0.13 | 0 | 0.08 |
| 138 | 0.08 | 0 | 0.06 | 0.08 | 0 | 0.05 | 0.09 | 0.03 | 0.06 | 0.12 | 0 | 0.08 | 0.13 | 0 | 0.09 | 0.17 | 0.03 | 0.09 |
| 139 | 0.08 | 0 | 0.05 | 0.09 | 0.03 | 0.06 | 0.08 | 0 | 0.05 | 0.12 | 0 | 0.09 | 0.14 | 0 | 0.08 | 0.13 | 0 | 0.08 |
| 140 | 0.09 | 0 | 0.05 | 0.08 | 0 | 0.05 | 0.09 | 0.03 | 0.06 | 0.12 | 0 | 0.09 | 0.12 | 0 | 0.09 | 0.12 | 0.05 | 0.08 |
| 141 | 0.09 | 0 | 0.05 | 0.09 | 0.02 | 0.06 | 0.09 | 0 | 0.04 | 0.12 | 0 | 0.08 | 0.12 | 0 | 0.09 | 0.14 | 0 | 0.08 |
| 142 | 0.09 | 0 | 0.05 | 0.08 | 0 | 0.06 | 0.11 | 0 | 0.06 | 0.12 | 0 | 0.08 | 0.14 | 0.06 | 0.09 | 0.13 | 0.01 | 0.09 |
| 143 | 0.09 | 0.02 | 0.05 | 0.08 | 0 | 0.05 | 0.1 | 0 | 0.06 | 0.12 | 0.04 | 0.08 | 0.12 | 0.06 | 0.09 | 0.12 | 0 | 0.09 |
| 144 | 0.09 | 0 | 0.05 | 0.09 | 0 | 0.05 | 0.1 | 0 | 0.06 | 0.11 | 0.05 | 0.08 | 0.12 | 0.05 | 0.09 | 0.13 | 0 | 0.1 |
| 145 | 0.08 | 0 | 0.05 | 0.09 | 0 | 0.06 | 0.09 | 0 | 0.06 | 0.12 | 0 | 0.08 | 0.13 | 0.06 | 0.08 | 0.12 | 0 | 0.09 |
| 146 | 0.09 | 0 | 0.05 | 0.11 | 0 | 0.06 | 0.1 | 0 | 0.06 | 0.12 | 0 | 0.08 | 0.12 | 0.02 | 0.08 | 0.13 | 0 | 0.09 |
| 147 | 0.09 | 0 | 0.06 | 0.08 | 0 | 0.06 | 0.1 | 0.02 | 0.06 | 0.12 | 0 | 0.07 | 0.12 | 0 | 0.08 | 0.14 | 0 | 0.09 |
| 148 | 0.09 | 0 | 0.05 | 0.11 | 0 | 0.06 | 0.1 | 0 | 0.06 | 0.12 | 0.05 | 0.09 | 0.12 | 0.04 | 0.08 | 0.13 | 0 | 0.08 |
| 149 | 0.08 | 0.02 | 0.05 | 0.1 | 0 | 0.06 | 0.11 | 0 | 0.06 | 0.14 | 0.04 | 0.08 | 0.11 | 0 | 0.08 | 0.13 | 0 | 0.08 |
| 150 | 0.09 | 0.02 | 0.05 | 0.09 | 0 | 0.06 | 0.09 | 0 | 0.06 | 0.13 | 0.04 | 0.08 | 0.13 | 0.05 | 0.08 | 0.15 | 0 | 0.08 |
| 151 | 0.09 | 0 | 0.05 | 0.1 | 0.03 | 0.06 | 0.11 | 0 | 0.06 | 0.12 | 0 | 0.08 | 0.13 | 0 | 0.07 | 0.13 | 0 | 0.08 |
| 152 | 0.09 | 0 | 0.05 | 0.09 | 0.03 | 0.06 | 0.11 | 0 | 0.06 | 0.13 | 0.04 | 0.09 | 0.13 | 0 | 0.08 | 0.16 | 0 | 0.08 |
| 153 | 0.09 | 0.03 | 0.06 | 0.09 | 0 | 0.05 | 0.09 | 0 | 0.06 | 0.13 | 0.04 | 0.09 | 0.13 | 0 | 0.08 | 0.15 | 0.04 | 0.08 |
| 154 | 0.09 | 0 | 0.05 | 0.09 | 0 | 0.06 | 0.1 | 0.02 | 0.06 | 0.12 | 0.04 | 0.09 | 0.14 | 0 | 0.09 | 0.16 | 0.03 | 0.08 |
| 155 | 0.08 | 0.02 | 0.05 | 0.11 | 0 | 0.06 | 0.09 | 0 | 0.05 | 0.13 | 0.01 | 0.09 | 0.13 | 0.04 | 0.09 | 0.15 | 0 | 0.07 |
| 156 | 0.08 | 0 | 0.05 | 0.09 | 0.02 | 0.06 | 0.1 | 0 | 0.05 | 0.14 | 0.03 | 0.09 | 0.13 | 0 | 0.09 | 0.15 | 0 | 0.07 |
| 157 | 0.09 | 0.01 | 0.05 | 0.1 | 0 | 0.06 | 0.1 | 0 | 0.05 | 0.14 | 0.03 | 0.09 | 0.13 | 0 | 0.09 | 0.13 | 0.03 | 0.07 |
| 158 | 0.09 | 0 | 0.05 | 0.11 | 0 | 0.05 | 0.09 | 0.03 | 0.06 | 0.14 | 0.05 | 0.09 | 0.13 | 0 | 0.1 | 0.13 | 0 | 0.07 |
| 159 | 0.09 | 0.02 | 0.05 | 0.1 | 0 | 0.05 | 0.08 | 0.03 | 0.05 | 0.13 | 0 | 0.08 | 0.13 | 0.04 | 0.09 | 0.12 | 0 | 0.07 |
| 160 | 0.1 | 0 | 0.06 | 0.1 | 0.02 | 0.05 | 0.1 | 0.01 | 0.06 | 0.13 | 0.05 | 0.09 | 0.13 | 0 | 0.09 | 0.11 | 0 | 0.07 |
| 161 | 0.1 | 0 | 0.05 | 0.1 | 0 | 0.05 | 0.09 | 0 | 0.04 | 0.13 | 0.01 | 0.09 | 0.12 | 0 | 0.09 | 0.12 | 0.04 | 0.07 |
| 162 | 0.1 | 0 | 0.06 | 0.1 | 0.02 | 0.05 | 0.1 | 0 | 0.04 | 0.14 | 0.04 | 0.09 | 0.13 | 0.03 | 0.1 | 0.14 | 0 | 0.08 |
| 163 | 0.1 | 0 | 0.05 | 0.09 | 0.03 | 0.05 | 0.1 | 0.01 | 0.05 | 0.13 | 0 | 0.09 | 0.15 | 0 | 0.1 | 0.12 | 0 | 0.08 |
| 164 | 0.09 | 0 | 0.05 | 0.09 | 0 | 0.05 | 0.09 | 0 | 0.04 | 0.14 | 0 | 0.09 | 0.13 | 0 | 0.09 | 0.12 | 0 | 0.08 |
| 165 | 0.1 | 0 | 0.05 | 0.11 | 0 | 0.05 | 0.08 | 0 | 0.04 | 0.13 | 0 | 0.08 | 0.14 | 0 | 0.09 | 0.14 | 0 | 0.08 |
| 166 | 0.09 | 0.03 | 0.05 | 0.11 | 0 | 0.05 | 0.08 | 0.02 | 0.05 | 0.13 | 0 | 0.08 | 0.14 | 0 | 0.09 | 0.12 | 0 | 0.08 |

| | | | | | | | | | | | | | | | | | | |
|---|---|---|---|---|---|---|---|---|---|---|---|---|---|---|---|---|---|---|
| 167 | 0.09 | 0 | 0.05 | 0.11 | 0.02 | 0.05 | 0.08 | 0.01 | 0.05 | 0.13 | 0 | 0.07 | 0.14 | 0.02 | 0.08 | 0.11 | 0 | 0.07 |
| 168 | 0.09 | 0.02 | 0.05 | 0.11 | 0 | 0.05 | 0.1 | 0 | 0.05 | 0.13 | 0 | 0.08 | 0.15 | 0 | 0.08 | 0.15 | 0 | 0.09 |
| 169 | 0.09 | 0.03 | 0.05 | 0.08 | 0 | 0.05 | 0.08 | 0 | 0.05 | 0.12 | 0.03 | 0.07 | 0.13 | 0 | 0.08 | 0.13 | 0.03 | 0.09 |
| 170 | 0.09 | 0 | 0.05 | 0.09 | 0 | 0.05 | 0.08 | 0 | 0.05 | 0.12 | 0 | 0.07 | 0.13 | 0 | 0.08 | 0.13 | 0 | 0.09 |
| 171 | 0.1 | 0 | 0.06 | 0.08 | 0.03 | 0.06 | 0.09 | 0 | 0.05 | 0.13 | 0 | 0.07 | 0.13 | 0 | 0.07 | 0.13 | 0 | 0.09 |
| 172 | 0.1 | 0 | 0.06 | 0.09 | 0 | 0.05 | 0.09 | 0 | 0.06 | 0.13 | 0 | 0.07 | 0.14 | 0 | 0.08 | 0.14 | 0 | 0.09 |
| 173 | 0.11 | 0.02 | 0.06 | 0.1 | 0.03 | 0.06 | 0.09 | 0.03 | 0.05 | 0.13 | 0 | 0.07 | 0.13 | 0 | 0.07 | 0.14 | 0 | 0.09 |
| 174 | 0.1 | 0 | 0.06 | 0.08 | 0 | 0.06 | 0.09 | 0.02 | 0.06 | 0.13 | 0 | 0.07 | 0.12 | 0 | 0.07 | 0.12 | 0 | 0.1 |
| 175 | 0.09 | 0.02 | 0.06 | 0.09 | 0 | 0.06 | 0.09 | 0 | 0.05 | 0.12 | 0 | 0.07 | 0.14 | 0 | 0.08 | 0.12 | 0 | 0.1 |
| 176 | 0.07 | 0 | 0.05 | 0.09 | 0 | 0.06 | 0.09 | 0 | 0.06 | 0.12 | 0 | 0.06 | 0.13 | 0 | 0.08 | 0.14 | 0.04 | 0.1 |
| 177 | 0.08 | 0 | 0.05 | 0.1 | 0 | 0.05 | 0.09 | 0.02 | 0.06 | 0.11 | 0 | 0.06 | 0.13 | 0.02 | 0.08 | 0.12 | 0 | 0.09 |
| 178 | 0.08 | 0.01 | 0.05 | 0.11 | 0 | 0.05 | 0.1 | 0.02 | 0.05 | 0.11 | 0 | 0.05 | 0.12 | 0 | 0.06 | 0.12 | 0 | 0.09 |
| 179 | 0.08 | 0 | 0.06 | 0.09 | 0 | 0.05 | 0.11 | 0 | 0.06 | 0.12 | 0 | 0.05 | 0.12 | 0 | 0.06 | 0.14 | 0.05 | 0.09 |
| 180 | 0.08 | 0.01 | 0.05 | 0.1 | 0 | 0.06 | 0.1 | 0 | 0.06 | 0.13 | 0 | 0.05 | 0.15 | 0 | 0.06 | 0.12 | 0 | 0.08 |
| 181 | 0.1 | 0.02 | 0.05 | 0.1 | 0 | 0.05 | 0.11 | 0.02 | 0.06 | 0.15 | 0 | 0.06 | 0.15 | 0 | 0.07 | 0.13 | 0 | 0.08 |
| 182 | 0.08 | 0.01 | 0.05 | 0.1 | 0 | 0.05 | 0.1 | 0 | 0.06 | 0.14 | 0 | 0.06 | 0.13 | 0 | 0.07 | 0.16 | 0 | 0.09 |
| 183 | 0.08 | 0 | 0.05 | 0.1 | 0 | 0.05 | 0.12 | 0 | 0.06 | 0.16 | 0 | 0.06 | 0.13 | 0 | 0.07 | 0.15 | 0.05 | 0.09 |
| 184 | 0.09 | 0 | 0.05 | 0.1 | 0 | 0.05 | 0.12 | 0 | 0.06 | 0.14 | 0 | 0.06 | 0.11 | 0 | 0.05 | 0.13 | 0 | 0.08 |
| 185 | 0.09 | 0 | 0.05 | 0.09 | 0 | 0.05 | 0.13 | 0 | 0.06 | 0.15 | 0 | 0.06 | 0.11 | 0 | 0.05 | 0.12 | 0 | 0.08 |
| 186 | 0.1 | 0 | 0.04 | 0.12 | 0 | 0.05 | 0.11 | 0 | 0.05 | 0.16 | 0 | 0.07 | 0.12 | 0 | 0.06 | 0.12 | 0 | 0.08 |
| 187 | 0.09 | 0 | 0.04 | 0.1 | 0 | 0.05 | 0.1 | 0 | 0.05 | 0.13 | 0 | 0.07 | 0.13 | 0 | 0.06 | 0.14 | 0 | 0.09 |
| 188 | 0.09 | 0 | 0.04 | 0.1 | 0 | 0.05 | 0.12 | 0 | 0.05 | 0.15 | 0 | 0.08 | 0.12 | 0 | 0.07 | 0.14 | 0 | 0.08 |
| 189 | 0.09 | 0 | 0.04 | 0.1 | 0 | 0.05 | 0.1 | 0 | 0.05 | 0.14 | 0 | 0.06 | 0.12 | 0 | 0.06 | 0.13 | 0 | 0.08 |
| 190 | 0.09 | 0 | 0.05 | 0.1 | 0 | 0.05 | 0.12 | 0 | 0.05 | 0.12 | 0 | 0.08 | 0.11 | 0 | 0.06 | 0.14 | 0 | 0.09 |
| 191 | 0.08 | 0 | 0.05 | 0.11 | 0 | 0.05 | 0.12 | 0 | 0.05 | 0.12 | 0 | 0.08 | 0.11 | 0 | 0.07 | 0.12 | 0 | 0.09 |
| 192 | 0.08 | 0 | 0.04 | 0.11 | 0 | 0.05 | 0.11 | 0 | 0.04 | 0.12 | 0 | 0.07 | 0.12 | 0.01 | 0.07 | 0.13 | 0 | 0.08 |
| 193 | 0.07 | 0 | 0.05 | 0.1 | 0 | 0.05 | 0.1 | 0 | 0.05 | 0.13 | 0 | 0.08 | 0.15 | 0 | 0.07 | 0.13 | 0 | 0.08 |
| 194 | 0.08 | 0 | 0.04 | 0.1 | 0 | 0.05 | 0.1 | 0 | 0.04 | 0.13 | 0 | 0.09 | 0.13 | 0 | 0.09 | 0.14 | 0 | 0.09 |
| 195 | 0.08 | 0 | 0.04 | 0.1 | 0.01 | 0.05 | 0.11 | 0 | 0.05 | 0.12 | 0 | 0.08 | 0.13 | 0 | 0.08 | 0.15 | 0 | 0.09 |
| 196 | 0.1 | 0 | 0.05 | 0.11 | 0 | 0.05 | 0.1 | 0 | 0.05 | 0.12 | 0 | 0.08 | 0.13 | 0.02 | 0.09 | 0.17 | 0 | 0.09 |
| 197 | 0.08 | 0 | 0.04 | 0.1 | 0 | 0.05 | 0.12 | 0 | 0.05 | 0.12 | 0 | 0.09 | 0.15 | 0 | 0.09 | 0.16 | 0 | 0.1 |
| 198 | 0.08 | 0 | 0.05 | 0.13 | 0 | 0.05 | 0.1 | 0 | 0.05 | 0.12 | 0 | 0.08 | 0.13 | 0 | 0.09 | 0.13 | 0 | 0.08 |
| 199 | 0.08 | 0.02 | 0.05 | 0.12 | 0 | 0.05 | 0.09 | 0.02 | 0.05 | 0.12 | 0.01 | 0.08 | 0.14 | 0 | 0.08 | 0.13 | 0 | 0.09 |
| 200 | 0.07 | 0 | 0.04 | 0.12 | 0 | 0.05 | 0.1 | 0 | 0.05 | 0.13 | 0 | 0.08 | 0.12 | 0 | 0.08 | 0.14 | 0 | 0.09 |

| | | | | | | | | | | | | | | | | | | |
|---|---|---|---|---|---|---|---|---|---|---|---|---|---|---|---|---|---|---|
| | | | | Control (mm) | | | | | | | | | Infected (mm) | | | | | |
| Day 7 | R1 | | | R2 | | | R3 | | | R1 | | | R2 | | | R3 | | |
| | Max | Min | Average | Max | Min | Average | Max | Min | Average | Max | Min | Average | Max | Min | Average | Max | Min | Average |
| 1 | 0.07 | 0 | 0.03 | 0.02 | 0 | 0.01 | 0.05 | 0 | 0.02 | 0.13 | 0 | 0.06 | 0.12 | 0 | 0.07 | 0.23 | 0 | 0.08 |

| | | | | | | | | | | | | | | | | | |
|---|---|---|---|---|---|---|---|---|---|---|---|---|---|---|---|---|---|
| 2 | 0.06 | 0 | 0.03 | 0.02 | 0 | 0.01 | 0.04 | 0 | 0.02 | 0.13 | 0 | 0.07 | 0.12 | 0 | 0.07 | 0.11 | 0 | 0.07 |
| 3 | 0.06 | 0 | 0.03 | 0.03 | 0 | 0.02 | 0.04 | 0 | 0.02 | 0.13 | 0.01 | 0.07 | 0.13 | 0 | 0.07 | 0.39 | 0 | 0.07 |
| 4 | 0.06 | 0 | 0.03 | 0.02 | 0.01 | 0.01 | 0.05 | 0 | 0.02 | 0.12 | 0 | 0.07 | 0.12 | 0 | 0.06 | 0.12 | 0 | 0.07 |
| 5 | 0.06 | 0 | 0.03 | 0.02 | 0 | 0.01 | 0.04 | 0 | 0.02 | 0.12 | 0 | 0.07 | 0.15 | 0 | 0.07 | 0.14 | 0 | 0.07 |
| 6 | 0.05 | 0 | 0.02 | 0.02 | 0 | 0.01 | 0.05 | 0 | 0.02 | 0.14 | 0.01 | 0.07 | 0.16 | 0 | 0.05 | 0.12 | 0 | 0.07 |
| 7 | 0.05 | 0 | 0.02 | 0.02 | 0 | 0.01 | 0.03 | 0 | 0.01 | 0.11 | 0 | 0.07 | 0.14 | 0 | 0.07 | 0.11 | 0 | 0.07 |
| 8 | 0.04 | 0 | 0.01 | 0.02 | 0 | 0.02 | 0.03 | 0 | 0.01 | 0.12 | 0 | 0.07 | 0.13 | 0 | 0.06 | 0.33 | 0 | 0.1 |
| 9 | 0.04 | 0 | 0.01 | 0.02 | 0 | 0.01 | 0.04 | 0 | 0.02 | 0.12 | 0 | 0.08 | 0.11 | 0 | 0.04 | 0.11 | 0 | 0.07 |
| 10 | 0.04 | 0 | 0.02 | 0.03 | 0 | 0.02 | 0.05 | 0 | 0.02 | 0.11 | 0 | 0.07 | 0.1 | 0 | 0.05 | 0.11 | 0 | 0.07 |
| 11 | 0.05 | 0 | 0.03 | 0.04 | 0 | 0.02 | 0.04 | 0 | 0.02 | 0.11 | 0 | 0.08 | 0.11 | 0 | 0.06 | 0.12 | 0 | 0.07 |
| 12 | 0.06 | 0 | 0.02 | 0.04 | 0 | 0.02 | 0.04 | 0 | 0.02 | 0.12 | 0 | 0.08 | 0.1 | 0 | 0.05 | 0.12 | 0.01 | 0.07 |
| 13 | 0.04 | 0 | 0.03 | 0.03 | 0 | 0.01 | 0.15 | 0 | 0.02 | 0.11 | 0 | 0.07 | 0.1 | 0 | 0.04 | 0.12 | 0 | 0.07 |
| 14 | 0.06 | 0 | 0.03 | 0.03 | 0 | 0.01 | 0.03 | 0 | 0.02 | 0.12 | 0 | 0.07 | 0.12 | 0 | 0.06 | 0.11 | 0.03 | 0.07 |
| 15 | 0.06 | 0 | 0.03 | 0.04 | 0 | 0.02 | 0.02 | 0 | 0.01 | 0.1 | 0 | 0.07 | 0.11 | 0 | 0.06 | 0.11 | 0 | 0.07 |
| 16 | 0.06 | 0 | 0.03 | 0.05 | 0 | 0.03 | 0.15 | 0 | 0.03 | 0.11 | 0 | 0.06 | 0.12 | 0 | 0.07 | 0.11 | 0 | 0.07 |
| 17 | 0.06 | 0 | 0.03 | 0.04 | 0 | 0.02 | 0.03 | 0 | 0.01 | 0.1 | 0 | 0.06 | 0.11 | 0 | 0.06 | 0.11 | 0 | 0.07 |
| 18 | 0.06 | 0 | 0.03 | 0.03 | 0 | 0.01 | 0.04 | 0 | 0.02 | 0.11 | 0.01 | 0.06 | 0.12 | 0 | 0.07 | 0.11 | 0.01 | 0.06 |
| 19 | 0.06 | 0 | 0.03 | 0.04 | 0 | 0.02 | 0.05 | 0 | 0.02 | 0.11 | 0 | 0.07 | 0.14 | 0 | 0.08 | 0.11 | 0 | 0.06 |
| 20 | 0.02 | 0 | 0.04 | 0.03 | 0 | 0.02 | 0.04 | 0 | 0.02 | 0.11 | 0 | 0.07 | 0.13 | 0 | 0.08 | 0.1 | 0 | 0.06 |
| 21 | 0.06 | 0 | 0.03 | 0.04 | 0 | 0.02 | 0.05 | 0 | 0.02 | 0.12 | 0 | 0.06 | 0.12 | 0 | 0.08 | 0.11 | 0 | 0.06 |
| 22 | 0.06 | 0 | 0.03 | 0.04 | 0 | 0.02 | 0.04 | 0 | 0.02 | 0.11 | 0 | 0.05 | 0.13 | 0 | 0.08 | 0.1 | 0 | 0.06 |
| 23 | 0.08 | 0 | 0.03 | 0.04 | 0 | 0.02 | 0.04 | 0 | 0.02 | 0.12 | 0 | 0.06 | 0.13 | 0 | 0.08 | 0.12 | 0 | 0.06 |
| 24 | 0.07 | 0 | 0.05 | 0.04 | 0 | 0.02 | 0.04 | 0 | 0.01 | 0.11 | 0 | 0.06 | 0.19 | 0 | 0.08 | 0.11 | 0 | 0.06 |
| 25 | 0.07 | 0 | 0.05 | 0.05 | 0 | 0.03 | 0.04 | 0 | 0.02 | 0.2 | 0 | 0.07 | 0.15 | 0 | 0.08 | 0.11 | 0 | 0.06 |
| 26 | 0.07 | 0 | 0.06 | 0.05 | 0 | 0.03 | 0.02 | 0 | 0.01 | 0.18 | 0 | 0.06 | 0.15 | 0 | 0.09 | 0.11 | 0 | 0.06 |
| 27 | 0.08 | 0 | 0.06 | 0.04 | 0 | 0.02 | 0.05 | 0 | 0.02 | 0.12 | 0 | 0.06 | 0.14 | 0.02 | 0.09 | 0.11 | 0 | 0.06 |
| 28 | 0.07 | 0.01 | 0.06 | 0.05 | 0 | 0.02 | 0.06 | 0 | 0.03 | 0.14 | 0 | 0.06 | 0.15 | 0 | 0.09 | 0.12 | 0 | 0.06 |
| 29 | 0.07 | 0 | 0.06 | 0.03 | 0 | 0.02 | 0.07 | 0 | 0.05 | 0.12 | 0 | 0.06 | 0.15 | 0.01 | 0.09 | 0.16 | 0 | 0.06 |
| 30 | 0.06 | 0 | 0.06 | 0.03 | 0 | 0.01 | 0.06 | 0 | 0.04 | 0.14 | 0 | 0.06 | 0.18 | 0 | 0.1 | 0.13 | 0 | 0.06 |
| 31 | 0.06 | 0 | 0.06 | 0.04 | 0 | 0.01 | 0.07 | 0 | 0.04 | 0.14 | 0 | 0.06 | 0.17 | 0 | 0.1 | 0.19 | 0 | 0.07 |
| 32 | 0.06 | 0 | 0.02 | 0.04 | 0 | 0.02 | 0.06 | 0 | 0.03 | 0.14 | 0 | 0.07 | 0.15 | 0 | 0.1 | 0.13 | 0 | 0.07 |
| 33 | 0.06 | 0 | 0.03 | 0.06 | 0 | 0.02 | 0 | 0 | 0.03 | 0.12 | 0 | 0.06 | 0.17 | 0.05 | 0.1 | 0.21 | 0 | 0.07 |
| 34 | 0.06 | 0 | 0.03 | 0.04 | 0 | 0.02 | 0.05 | 0 | 0.03 | 0.13 | 0 | 0.06 | 0.16 | 0.05 | 0.09 | 0.27 | 0 | 0.08 |
| 35 | 0.06 | 0 | 0.03 | 0.05 | 0 | 0.02 | 0.06 | 0.01 | 0.03 | 0.12 | 0 | 0.06 | 0.15 | 0.04 | 0.09 | 0.14 | 0 | 0.07 |
| 36 | 0.07 | 0 | 0.04 | 0.06 | 0 | 0.03 | 0.07 | 0 | 0.03 | 0.12 | 0 | 0.06 | 0.16 | 0 | 0.09 | 0.13 | 0 | 0.07 |
| 37 | 0.06 | 0 | 0.03 | 0.06 | 0 | 0.03 | 0.07 | 0 | 0.04 | 0.12 | 0 | 0.07 | 0.18 | 0.05 | 0.09 | 0.12 | 0 | 0.07 |
| 38 | 0.08 | 0 | 0.03 | 0.06 | 0 | 0.02 | 0.07 | 0 | 0.03 | 0.11 | 0 | 0.07 | 0.14 | 0.04 | 0.08 | 0.16 | 0 | 0.07 |
| 39 | 0.1 | 0 | 0.04 | 0.07 | 0 | 0.03 | 0.05 | 0 | 0.03 | 0.13 | 0 | 0.07 | 0.17 | 0 | 0.08 | 0.12 | 0 | 0.07 |
| 40 | 0.1 | 0 | 0.03 | 0.07 | 0 | 0.03 | 0.05 | 0 | 0.02 | 0.13 | 0 | 0.07 | 0.15 | 0 | 0.07 | 0.13 | 0 | 0.07 |

| | | | | | | | | | | | | | | | | | |
|---|---|---|---|---|---|---|---|---|---|---|---|---|---|---|---|---|---|
| 41 | 0.08 | 0 | 0.03 | 0.07 | 0 | 0.03 | 0.04 | 0 | 0.02 | 0.12 | 0 | 0.08 | 0.13 | 0.04 | 0.07 | 0.13 | 0 | 0.07 |
| 42 | 0.04 | 0 | 0.03 | 0.07 | 0 | 0.03 | 0.04 | 0 | 0.02 | 0.12 | 0 | 0.08 | 0.13 | 0 | 0.06 | 0.12 | 0 | 0.07 |
| 43 | 0.05 | 0 | 0.03 | 0.06 | 0 | 0.03 | 0.06 | 0 | 0.04 | 0.12 | 0 | 0.08 | 0.13 | 0 | 0.07 | 0.12 | 0 | 0.07 |
| 44 | 0.04 | 0 | 0.02 | 0.07 | 0 | 0.04 | 0.07 | 0 | 0.03 | 0.12 | 0 | 0.07 | 0.16 | 0 | 0.06 | 0.12 | 0 | 0.07 |
| 45 | 0.04 | 0 | 0.02 | 0.07 | 0 | 0.04 | 0.06 | 0 | 0.03 | 0.11 | 0 | 0.07 | 0.13 | 0.01 | 0.06 | 0.11 | 0 | 0.07 |
| 46 | 0.04 | 0 | 0.01 | 0.07 | 0.02 | 0.04 | 0.06 | 0 | 0.03 | 0.11 | 0 | 0.07 | 0.12 | 0.01 | 0.06 | 0.11 | 0 | 0.07 |
| 47 | 0.05 | 0 | 0.02 | 0.06 | 0 | 0.04 | 0.05 | 0 | 0.03 | 0.12 | 0 | 0.07 | 0.1 | 0 | 0.06 | 0.11 | 0.02 | 0.07 |
| 48 | 0.05 | 0 | 0.02 | 0.06 | 0 | 0.03 | 0.05 | 0 | 0.02 | 0.12 | 0 | 0.07 | 0.09 | 0 | 0.06 | 0.12 | 0 | 0.06 |
| 49 | 0.05 | 0 | 0.02 | 0.05 | 0.02 | 0.04 | 0.05 | 0 | 0.02 | 0.11 | 0 | 0.07 | 0.12 | 0 | 0.06 | 0.13 | 0 | 0.06 |
| 50 | 0.06 | 0 | 0.04 | 0.05 | 0 | 0.03 | 0.03 | 0 | 0.01 | 0.11 | 0 | 0.07 | 0.11 | 0 | 0.06 | 0.12 | 0 | 0.07 |
| 51 | 0.08 | 0 | 0.04 | 0.06 | 0 | 0.03 | 0.03 | 0 | 0.02 | 0.11 | 0 | 0.07 | 0.14 | 0 | 0.07 | 0.11 | 0 | 0.06 |
| 52 | 0.09 | 0 | 0.03 | 0.05 | 0 | 0.02 | 0.04 | 0 | 0.02 | 0.12 | 0 | 0.06 | 0.13 | 0 | 0.06 | 0.12 | 0 | 0.07 |
| 53 | 0.08 | 0 | 0.03 | 0.06 | 0 | 0.02 | 0.04 | 0 | 0.02 | 0.11 | 0 | 0.06 | 0.12 | 0 | 0.07 | 0.12 | 0 | 0.07 |
| 54 | 0.07 | 0 | 0.03 | 0.06 | 0 | 0.02 | 0.04 | 0 | 0.02 | 0.11 | 0 | 0.07 | 0.12 | 0 | 0.07 | 0.11 | 0 | 0.06 |
| 55 | 0.06 | 0 | 0.03 | 0.06 | 0 | 0.02 | 0.04 | 0 | 0.02 | 0.12 | 0 | 0.07 | 0.13 | 0 | 0.07 | 0.12 | 0 | 0.07 |
| 56 | 0.06 | 0 | 0.03 | 0.06 | 0 | 0.03 | 0.04 | 0 | 0.02 | 0.12 | 0 | 0.07 | 0.12 | 0 | 0.08 | 0.12 | 0 | 0.07 |
| 57 | 0.08 | 0 | 0.03 | 0.05 | 0 | 0.02 | 0.04 | 0 | 0.01 | 0.12 | 0 | 0.08 | 0.13 | 0.03 | 0.08 | 0.11 | 0 | 0.07 |
| 58 | 0.06 | 0 | 0.03 | 0.05 | 0 | 0.03 | 0.03 | 0 | 0.01 | 0.12 | 0 | 0.07 | 0.12 | 0 | 0.08 | 0.12 | 0 | 0.06 |
| 59 | 0.08 | 0 | 0.04 | 0.06 | 0 | 0.03 | 0.04 | 0 | 0.02 | 0.11 | 0 | 0.07 | 0.14 | 0 | 0.09 | 0.14 | 0 | 0.07 |
| 60 | 0.06 | 0 | 0.04 | 0.06 | 0 | 0.04 | 0.05 | 0 | 0.02 | 0.12 | 0 | 0.06 | 0.14 | 0 | 0.08 | 0.12 | 0 | 0.07 |
| 61 | 0.07 | 0 | 0.03 | 0.06 | 0 | 0.04 | 0.07 | 0 | 0.04 | 0.12 | 0 | 0.07 | 0.13 | 0.05 | 0.09 | 0.13 | 0 | 0.07 |
| 62 | 0.08 | 0 | 0.04 | 0.05 | 0 | 0.03 | 0.07 | 0 | 0.04 | 0.12 | 0 | 0.07 | 0.12 | 0 | 0.08 | 0.13 | 0 | 0.07 |
| 63 | 0.06 | 0 | 0.04 | 0.05 | 0 | 0.03 | 0.08 | 0.01 | 0.05 | 0.12 | 0 | 0.07 | 0.13 | 0 | 0.08 | 0.12 | 0 | 0.07 |
| 64 | 0.07 | 0 | 0.04 | 0.05 | 0 | 0.02 | 0.07 | 0 | 0.04 | 0.12 | 0 | 0.07 | 0.12 | 0 | 0.09 | 0.12 | 0 | 0.07 |
| 65 | 0.05 | 0 | 0.03 | 0.05 | 0 | 0.02 | 0.07 | 0.02 | 0.04 | 0.11 | 0 | 0.07 | 0.12 | 0.04 | 0.09 | 0.12 | 0.02 | 0.07 |
| 66 | 0.05 | 0 | 0.03 | 0.06 | 0 | 0.04 | 0.07 | 0 | 0.04 | 0.12 | 0 | 0.07 | 0.12 | 0.05 | 0.09 | 0.12 | 0 | 0.07 |
| 67 | 0.06 | 0 | 0.03 | 0.07 | 0 | 0.03 | 0.06 | 0 | 0.03 | 0.12 | 0 | 0.07 | 0.14 | 0 | 0.08 | 0.12 | 0 | 0.07 |
| 68 | 0.06 | 0 | 0.03 | 0.07 | 0 | 0.03 | 0.07 | 0 | 0.03 | 0.12 | 0 | 0.07 | 0.13 | 0.04 | 0.09 | 0.13 | 0 | 0.07 |
| 69 | 0.06 | 0 | 0.03 | 0.07 | 0 | 0.03 | 0.05 | 0 | 0.03 | 0.13 | 0 | 0.08 | 0.13 | 0 | 0.09 | 0.12 | 0 | 0.07 |
| 70 | 0.05 | 0 | 0.02 | 0.08 | 0 | 0.03 | 0.07 | 0 | 0.03 | 0.11 | 0 | 0.08 | 0.14 | 0.03 | 0.09 | 0.12 | 0 | 0.08 |
| 71 | 0.07 | 0 | 0.03 | 0.08 | 0 | 0.03 | 0.06 | 0 | 0.03 | 0.11 | 0 | 0.07 | 0.16 | 0.04 | 0.08 | 0.12 | 0 | 0.07 |
| 72 | 0.06 | 0 | 0.03 | 0.07 | 0 | 0.04 | 0.05 | 0 | 0.03 | 0.11 | 0 | 0.07 | 0.14 | 0 | 0.08 | 0.13 | 0 | 0.07 |
| 73 | 0.06 | 0 | 0.03 | 0.06 | 0 | 0.03 | 0.05 | 0 | 0.02 | 0.12 | 0 | 0.07 | 0.13 | 0 | 0.07 | 0.11 | 0 | 0.07 |
| 74 | 0.05 | 0 | 0.02 | 0.06 | 0 | 0.03 | 0.05 | 0 | 0.02 | 0.13 | 0 | 0.08 | 0.12 | 0 | 0.08 | 0.14 | 0 | 0.07 |
| 75 | 0.08 | 0 | 0.03 | 0.05 | 0 | 0.03 | 0.06 | 0 | 0.02 | 0.12 | 0 | 0.07 | 0.12 | 0 | 0.07 | 0.12 | 0 | 0.07 |
| 76 | 0.07 | 0 | 0.03 | 0.06 | 0 | 0.03 | 0.05 | 0 | 0.02 | 0.12 | 0 | 0.07 | 0.14 | 0 | 0.07 | 0.14 | 0.01 | 0.07 |
| 77 | 0.07 | 0 | 0.03 | 0.07 | 0 | 0.04 | 0.04 | 0 | 0.02 | 0.12 | 0 | 0.07 | 0.11 | 0 | 0.06 | 0.14 | 0 | 0.07 |
| 78 | 0.06 | 0 | 0.03 | 0.07 | 0 | 0.03 | 0.04 | 0 | 0.02 | 0.13 | 0 | 0.07 | 0.12 | 0 | 0.05 | 0.13 | 0 | 0.07 |
| 79 | 0.07 | 0 | 0.02 | 0.06 | 0 | 0.03 | 0.04 | 0 | 0.02 | 0.12 | 0 | 0.07 | 0.11 | 0 | 0.06 | 0.12 | 0 | 0.07 |

| | | | | | | | | | | | | | | | | | |
|---|---|---|---|---|---|---|---|---|---|---|---|---|---|---|---|---|---|
| 80 | 0.07 | 0 | 0.03 | 0.07 | 0 | 0.04 | 0.03 | 0 | 0.01 | 0.12 | 0 | 0.07 | 0.12 | 0 | 0.06 | 0.12 | 0 | 0.07 |
| 81 | 0.06 | 0 | 0.03 | 0.06 | 0 | 0.03 | 0.02 | 0 | 0.01 | 0.12 | 0 | 0.07 | 0.08 | 0 | 0.06 | 0.12 | 0 | 0.07 |
| 82 | 0.06 | 0 | 0.03 | 0.06 | 0 | 0.03 | 0.02 | 0 | 0.01 | 0.14 | 0 | 0.07 | 0.1 | 0 | 0.06 | 0.13 | 0 | 0.07 |
| 83 | 0.07 | 0 | 0.04 | 0.05 | 0 | 0.02 | 0.01 | 0.01 | 0.01 | 0.12 | 0 | 0.07 | 0.13 | 0 | 0.06 | 0.12 | 0 | 0.07 |
| 84 | 0.07 | 0 | 0.03 | 0.04 | 0 | 0.02 | 0.04 | 0 | 0.02 | 0.12 | 0 | 0.07 | 0.11 | 0.02 | 0.06 | 0.13 | 0 | 0.07 |
| 85 | 0.06 | 0 | 0.03 | 0.04 | 0 | 0.03 | 0.02 | 0 | 0.01 | 0.12 | 0 | 0.06 | 0.1 | 0 | 0.06 | 0.14 | 0 | 0.07 |
| 86 | 0.05 | 0 | 0.03 | 0.04 | 0 | 0.02 | 0.04 | 0 | 0.02 | 0.12 | 0.03 | 0.07 | 0.11 | 0 | 0.07 | 0.14 | 0 | 0.07 |
| 87 | 0.06 | 0 | 0.03 | 0.04 | 0 | 0.02 | 0.04 | 0 | 0.02 | 0.14 | 0 | 0.07 | 0.11 | 0 | 0.07 | 0.12 | 0 | 0.07 |
| 88 | 0.06 | 0 | 0.03 | 0.03 | 0 | 0.02 | 0.05 | 0 | 0.03 | 0.13 | 0 | 0.06 | 0.12 | 0 | 0.07 | 0.13 | 0 | 0.07 |
| 89 | 0.07 | 0 | 0.03 | 0.03 | 0 | 0.01 | 0.05 | 0 | 0.03 | 0.12 | 0 | 0.06 | 0.12 | 0 | 0.07 | 0.12 | 0 | 0.07 |
| 90 | 0.06 | 0 | 0.03 | 0.03 | 0 | 0.01 | 0.05 | 0 | 0.02 | 0.12 | 0 | 0.06 | 0.12 | 0 | 0.07 | 0.13 | 0 | 0.07 |
| 91 | 0.05 | 0 | 0.03 | 0.04 | 0 | 0.02 | 0.05 | 0 | 0.02 | 0.14 | 0 | 0.07 | 0.12 | 0 | 0.07 | 0.12 | 0 | 0.07 |
| 92 | 0.06 | 0 | 0.03 | 0.04 | 0 | 0.02 | 0.03 | 0 | 0.01 | 0.13 | 0 | 0.07 | 0.12 | 0 | 0.08 | 0.2 | 0.03 | 0.08 |
| 93 | 0.07 | 0 | 0.03 | 0.04 | 0 | 0.02 | 0.05 | 0 | 0.02 | 0.12 | 0 | 0.07 | 0.12 | 0 | 0.08 | 0.19 | 0 | 0.07 |
| 94 | 0.07 | 0 | 0.03 | 0.05 | 0 | 0.02 | 0.06 | 0 | 0.03 | 0.12 | 0 | 0.07 | 0.13 | 0.04 | 0.08 | 0.12 | 0 | 0.07 |
| 95 | 0.06 | 0 | 0.03 | 0.05 | 0 | 0.02 | 0.06 | 0 | 0.03 | 0.12 | 0 | 0.07 | 0.13 | 0 | 0.09 | 0.12 | 0 | 0.07 |
| 96 | 0.05 | 0 | 0.02 | 0.05 | 0 | 0.02 | 0.06 | 0 | 0.04 | 0.12 | 0.03 | 0.07 | 0.13 | 0 | 0.09 | 0.12 | 0 | 0.06 |
| 97 | 0.05 | 0 | 0.03 | 0.08 | 0 | 0.03 | 0.05 | 0 | 0.03 | 0.12 | 0.04 | 0.08 | 0.14 | 0 | 0.09 | 0.12 | 0 | 0.07 |
| 98 | 0.06 | 0 | 0.03 | 0.06 | 0 | 0.04 | 0.06 | 0 | 0.03 | 0.12 | 0 | 0.07 | 0.13 | 0.04 | 0.09 | 0.11 | 0.01 | 0.07 |
| 99 | 0.07 | 0 | 0.03 | 0.07 | 0 | 0.03 | 0.05 | 0 | 0.02 | 0.11 | 0 | 0.07 | 0.13 | 0 | 0.09 | 0.12 | 0 | 0.08 |
| 100 | 0.06 | 0 | 0.03 | 0.06 | 0 | 0.03 | 0.05 | 0 | 0.02 | 0.12 | 0 | 0.08 | 0.14 | 0 | 0.09 | 0.12 | 0 | 0.07 |
| 101 | 0.08 | 0 | 0.03 | 0.07 | 0 | 0.02 | 0.06 | 0 | 0.03 | 0.12 | 0 | 0.07 | 0.13 | 0.04 | 0.09 | 0.12 | 0 | 0.07 |
| 102 | 0.09 | 0 | 0.04 | 0.08 | 0 | 0.03 | 0.07 | 0 | 0.04 | 0.12 | 0.03 | 0.07 | 0.12 | 0 | 0.09 | 0.12 | 0 | 0.08 |
| 103 | 0.08 | 0 | 0.04 | 0.07 | 0 | 0.03 | 0.07 | 0 | 0.04 | 0.2 | 0 | 0.08 | 0.13 | 0.06 | 0.09 | 0.12 | 0 | 0.07 |
| 104 | 0.07 | 0 | 0.04 | 0.08 | 0 | 0.03 | 0.06 | 0 | 0.03 | 0.14 | 0.04 | 0.08 | 0.12 | 0.05 | 0.08 | 0.11 | 0 | 0.08 |
| 105 | 0.07 | 0 | 0.04 | 0.06 | 0 | 0.03 | 0.06 | 0 | 0.03 | 0.24 | 0 | 0.09 | 0.12 | 0 | 0.09 | 0.12 | 0.03 | 0.08 |
| 106 | 0.07 | 0 | 0.04 | 0.05 | 0 | 0.03 | 0.06 | 0 | 0.03 | 0.23 | 0 | 0.08 | 0.13 | 0.04 | 0.08 | 0.12 | 0 | 0.07 |
| 107 | 0.07 | 0 | 0.04 | 0.06 | 0 | 0.04 | 0.06 | 0 | 0.03 | 0.26 | 0 | 0.08 | 0.12 | 0 | 0.08 | 0.11 | 0 | 0.08 |
| 108 | 0.08 | 0 | 0.05 | 0.06 | 0 | 0.04 | 0.05 | 0 | 0.03 | 0.11 | 0 | 0.07 | 0.12 | 0.01 | 0.08 | 0.2 | 0 | 0.08 |
| 109 | 0.08 | 0 | 0.05 | 0.06 | 0 | 0.03 | 0.06 | 0 | 0.03 | 0.12 | 0 | 0.07 | 0.13 | 0 | 0.07 | 0.16 | 0 | 0.08 |
| 110 | 0.09 | 0.02 | 0.05 | 0.06 | 0 | 0.03 | 0.04 | 0 | 0.02 | 0.13 | 0 | 0.08 | 0.12 | 0 | 0.07 | 0.21 | 0 | 0.08 |
| 111 | 0.09 | 0 | 0.05 | 0.06 | 0 | 0.03 | 0.06 | 0 | 0.02 | 0.11 | 0 | 0.07 | 0.12 | 0 | 0.06 | 0.21 | 0 | 0.08 |
| 112 | 0.09 | 0 | 0.05 | 0.06 | 0 | 0.04 | 0.06 | 0 | 0.03 | 0.12 | 0 | 0.07 | 0.12 | 0.03 | 0.06 | 0.22 | 0 | 0.08 |
| 113 | 0.09 | 0 | 0.05 | 0.06 | 0 | 0.04 | 0.05 | 0 | 0.02 | 0.11 | 0 | 0.06 | 0.13 | 0 | 0.06 | 0.16 | 0 | 0.08 |
| 114 | 0.08 | 0 | 0.05 | 0.06 | 0 | 0.04 | 0.04 | 0 | 0.02 | 0.12 | 0 | 0.06 | 0.12 | 0 | 0.06 | 0.11 | 0 | 0.06 |
| 115 | 0.1 | 0 | 0.05 | 0.05 | 0 | 0.03 | 0.04 | 0 | 0.01 | 0.12 | 0 | 0.07 | 0.12 | 0 | 0.06 | 0.11 | 0 | 0.07 |
| 116 | 0.08 | 0 | 0.05 | 0.06 | 0 | 0.03 | 0.05 | 0 | 0.03 | 0.12 | 0 | 0.07 | 0.1 | 0 | 0.06 | 0.12 | 0 | 0.07 |
| 117 | 0.07 | 0 | 0.06 | 0.05 | 0 | 0.03 | 0.06 | 0 | 0.04 | 0.11 | 0 | 0.07 | 0.12 | 0 | 0.06 | 0.12 | 0 | 0.07 |
| 118 | 0.08 | 0 | 0.06 | 0.04 | 0 | 0.02 | 0.06 | 0 | 0.03 | 0.12 | 0 | 0.08 | 0.1 | 0 | 0.07 | 0.12 | 0 | 0.08 |

| | | | | | | | | | | | | | | | | | |
|---|---|---|---|---|---|---|---|---|---|---|---|---|---|---|---|---|---|
| 119 | 0.08 | 0 | 0.06 | 0.06 | 0 | 0.01 | 0.06 | 0 | 0.03 | 0.11 | 0 | 0.07 | 0.15 | 0 | 0.07 | 0.12 | 0 | 0.08 |
| 120 | 0.08 | 0.01 | 0.06 | 0.05 | 0 | 0.03 | 0.06 | 0 | 0.03 | 0.11 | 0.04 | 0.07 | 0.15 | 0 | 0.08 | 0.12 | 0 | 0.08 |
| 121 | 0.07 | 0.01 | 0.06 | 0.05 | 0 | 0.03 | 0.06 | 0 | 0.03 | 0.12 | 0 | 0.07 | 0.14 | 0 | 0.08 | 0.13 | 0 | 0.08 |
| 122 | 0.09 | 0 | 0.06 | 0.05 | 0 | 0.03 | 0.06 | 0 | 0.04 | 0.12 | 0 | 0.08 | 0.14 | 0 | 0.09 | 0.12 | 0 | 0.08 |
| 123 | 0.08 | 0 | 0.06 | 0.06 | 0 | 0.03 | 0.07 | 0 | 0.04 | 0.11 | 0 | 0.08 | 0.13 | 0 | 0.08 | 0.12 | 0 | 0.08 |
| 124 | 0.06 | 0 | 0.06 | 0.06 | 0 | 0.03 | 0.07 | 0 | 0.04 | 0.27 | 0 | 0.1 | 0.14 | 0 | 0.09 | 0.15 | 0 | 0.08 |
| 125 | 0.08 | 0 | 0.06 | 0.06 | 0 | 0.03 | 0.06 | 0 | 0.04 | 0.12 | 0 | 0.08 | 0.15 | 0 | 0.09 | 0.13 | 0 | 0.08 |
| 126 | 0.08 | 0 | 0.06 | 0.06 | 0 | 0.03 | 0.07 | 0 | 0.04 | 0.12 | 0 | 0.08 | 0.14 | 0 | 0.09 | 0.14 | 0 | 0.08 |
| 127 | 0.08 | 0 | 0.06 | 0.05 | 0 | 0.03 | 0.07 | 0 | 0.04 | 0.12 | 0.02 | 0.08 | 0.14 | 0 | 0.1 | 0.12 | 0 | 0.08 |
| 128 | 0.09 | 0 | 0.04 | 0.06 | 0 | 0.03 | 0.09 | 0 | 0.05 | 0.12 | 0 | 0.08 | 0.14 | 0 | 0.09 | 0.12 | 0 | 0.08 |
| 129 | 0.07 | 0 | 0.04 | 0.07 | 0 | 0.03 | 0.08 | 0.03 | 0.05 | 0.13 | 0 | 0.08 | 0.15 | 0 | 0.1 | 0.12 | 0 | 0.08 |
| 130 | 0.08 | 0 | 0.04 | 0.06 | 0 | 0.03 | 0.07 | 0.02 | 0.05 | 0.13 | 0 | 0.08 | 0.17 | 0 | 0.09 | 0.12 | 0 | 0.08 |
| 131 | 0.08 | 0 | 0.04 | 0.06 | 0 | 0.04 | 0.07 | 0 | 0.04 | 0.12 | 0 | 0.08 | 0.15 | 0 | 0.1 | 0.12 | 0 | 0.08 |
| 132 | 0.08 | 0 | 0.04 | 0.06 | 0 | 0.03 | 0.07 | 0.01 | 0.04 | 0.14 | 0 | 0.08 | 0.15 | 0 | 0.1 | 0.12 | 0.02 | 0.08 |
| 133 | 0.08 | 0 | 0.04 | 0.07 | 0 | 0.03 | 0.07 | 0 | 0.04 | 0.11 | 0 | 0.08 | 0.14 | 0 | 0.1 | 0.12 | 0 | 0.08 |
| 134 | 0.08 | 0 | 0.04 | 0.07 | 0 | 0.03 | 0.07 | 0 | 0.03 | 0.12 | 0 | 0.08 | 0.15 | 0.06 | 0.1 | 0.12 | 0.01 | 0.08 |
| 135 | 0.08 | 0 | 0.04 | 0.07 | 0 | 0.03 | 0.07 | 0 | 0.03 | 0.13 | 0 | 0.07 | 0.17 | 0 | 0.1 | 0.12 | 0 | 0.08 |
| 136 | 0.06 | 0 | 0.03 | 0.06 | 0 | 0.04 | 0.06 | 0 | 0.03 | 0.13 | 0 | 0.07 | 0.16 | 0.02 | 0.1 | 0.12 | 0 | 0.07 |
| 137 | 0.07 | 0 | 0.03 | 0.06 | 0 | 0.04 | 0.06 | 0 | 0.02 | 0.15 | 0 | 0.08 | 0.16 | 0 | 0.1 | 0.12 | 0.01 | 0.08 |
| 138 | 0.08 | 0 | 0.04 | 0.07 | 0 | 0.03 | 0.05 | 0 | 0.02 | 0.11 | 0 | 0.07 | 0.15 | 0 | 0.09 | 0.32 | 0 | 0.09 |
| 139 | 0.08 | 0 | 0.05 | 0.06 | 0 | 0.03 | 0.05 | 0 | 0.02 | 0.15 | 0 | 0.07 | 0.14 | 0 | 0.09 | 0.13 | 0 | 0.07 |
| 140 | 0.08 | 0 | 0.04 | 0.06 | 0 | 0.03 | 0.05 | 0 | 0.02 | 0.12 | 0 | 0.07 | 0.15 | 0 | 0.09 | 0.13 | 0 | 0.07 |
| 141 | 0.08 | 0 | 0.04 | 0.06 | 0 | 0.03 | 0.06 | 0 | 0.03 | 0.13 | 0 | 0.07 | 0.15 | 0 | 0.08 | 0.26 | 0.01 | 0.08 |
| 142 | 0.08 | 0 | 0.04 | 0.06 | 0 | 0.03 | 0.06 | 0 | 0.03 | 0.13 | 0 | 0.07 | 0.16 | 0 | 0.08 | 0.13 | 0.02 | 0.07 |
| 143 | 0.07 | 0 | 0.04 | 0.06 | 0 | 0.03 | 0.06 | 0 | 0.04 | 0.13 | 0 | 0.06 | 0.17 | 0 | 0.08 | 0.11 | 0 | 0.07 |
| 144 | 0.06 | 0 | 0.04 | 0.05 | 0 | 0.03 | 0.05 | 0 | 0.03 | 0.14 | 0 | 0.07 | 0.1 | 0.01 | 0.08 | 0.11 | 0 | 0.06 |
| 145 | 0.07 | 0 | 0.04 | 0.06 | 0 | 0.03 | 0.05 | 0 | 0.03 | 0.13 | 0 | 0.06 | 0.17 | 0.01 | 0.08 | 0.12 | 0 | 0.07 |
| 146 | 0.07 | 0 | 0.04 | 0.05 | 0 | 0.03 | 0.06 | 0 | 0.03 | 0.15 | 0 | 0.07 | 0.14 | 0 | 0.08 | 0.16 | 0.02 | 0.07 |
| 147 | 0.08 | 0 | 0.04 | 0.06 | 0 | 0.03 | 0.07 | 0 | 0.03 | 0.12 | 0 | 0.07 | 0.15 | 0 | 0.06 | 0.12 | 0 | 0.07 |
| 148 | 0.07 | 0 | 0.04 | 0.06 | 0 | 0.03 | 0.06 | 0 | 0.04 | 0.14 | 0 | 0.07 | 0.15 | 0 | 0.07 | 0.13 | 0 | 0.07 |
| 149 | 0.06 | 0 | 0.03 | 0.08 | 0 | 0.04 | 0.07 | 0 | 0.03 | 0.13 | 0 | 0.07 | 0.14 | 0 | 0.06 | 0.12 | 0 | 0.07 |
| 150 | 0.08 | 0 | 0.03 | 0.07 | 0 | 0.04 | 0.09 | 0 | 0.06 | 0.13 | 0 | 0.07 | 0.14 | 0 | 0.04 | 0.12 | 0.01 | 0.08 |
| 151 | 0.08 | 0 | 0.04 | 0.08 | 0 | 0.04 | 0.1 | 0 | 0.06 | 0.11 | 0 | 0.07 | 0.13 | 0 | 0.05 | 0.11 | 0 | 0.07 |
| 152 | 0.06 | 0 | 0.03 | 0.08 | 0 | 0.05 | 0.09 | 0 | 0.06 | 0.12 | 0 | 0.07 | 0.12 | 0 | 0.04 | 0.14 | 0 | 0.07 |
| 153 | 0.07 | 0 | 0.03 | 0.08 | 0 | 0.04 | 0.1 | 0 | 0.06 | 0.23 | 0.02 | 0.09 | 0.08 | 0 | 0.06 | 0.14 | 0 | 0.08 |
| 154 | 0.1 | 0 | 0.03 | 0.08 | 0 | 0.04 | 0.09 | 0 | 0.06 | 0.13 | 0 | 0.07 | 0.09 | 0 | 0.07 | 0.14 | 0 | 0.07 |
| 155 | 0.09 | 0 | 0.03 | 0.09 | 0 | 0.04 | 0.1 | 0 | 0.05 | 0.11 | 0 | 0.07 | 0.1 | 0 | 0.07 | 0.13 | 0 | 0.08 |
| 156 | 0.09 | 0 | 0.04 | 0.09 | 0 | 0.05 | 0.1 | 0 | 0.04 | 0.12 | 0 | 0.07 | 0.11 | 0 | 0.07 | 0.14 | 0.02 | 0.08 |
| 157 | 0.12 | 0 | 0.04 | 0.08 | 0 | 0.05 | 0.1 | 0.02 | 0.05 | 0.11 | 0 | 0.07 | 0.11 | 0 | 0.05 | 0.14 | 0 | 0.08 |

| | | | | | | | | | | | | | | | | | |
|---|---|---|---|---|---|---|---|---|---|---|---|---|---|---|---|---|---|
| 158 | 0.13 | 0 | 0.04 | 0.08 | 0 | 0.05 | 0.08 | 0.03 | 0.05 | 0.13 | 0 | 0.07 | 0.11 | 0 | 0.05 | 0.14 | 0.01 | 0.08 |
| 159 | 0.12 | 0 | 0.05 | 0.09 | 0 | 0.05 | 0.08 | 0 | 0.05 | 0.12 | 0 | 0.07 | 0.12 | 0 | 0.06 | 0.14 | 0 | 0.08 |
| 160 | 0.13 | 0 | 0.03 | 0.08 | 0 | 0.05 | 0.09 | 0.03 | 0.06 | 0.12 | 0 | 0.08 | 0.14 | 0 | 0.06 | 0.12 | 0.02 | 0.08 |
| 161 | 0.1 | 0 | 0.04 | 0.07 | 0 | 0.04 | 0.09 | 0.03 | 0.06 | 0.13 | 0 | 0.08 | 0.13 | 0 | 0.06 | 0.13 | 0.02 | 0.08 |
| 162 | 0.09 | 0 | 0.04 | 0.07 | 0 | 0.05 | 0.08 | 0 | 0.05 | 0.14 | 0 | 0.08 | 0.15 | 0 | 0.07 | 0.12 | 0 | 0.08 |
| 163 | 0.1 | 0 | 0.05 | 0.08 | 0 | 0.04 | 0.06 | 0 | 0.04 | 0.13 | 0 | 0.08 | 0.15 | 0 | 0.07 | 0.13 | 0 | 0.08 |
| 164 | 0.09 | 0 | 0.05 | 0.08 | 0 | 0.05 | 0.06 | 0.01 | 0.04 | 0.13 | 0 | 0.08 | 0.13 | 0 | 0.08 | 0.13 | 0 | 0.08 |
| 165 | 0.09 | 0 | 0.05 | 0.08 | 0 | 0.04 | 0.06 | 0 | 0.04 | 0.13 | 0.01 | 0.08 | 0.14 | 0 | 0.08 | 0.14 | 0 | 0.08 |
| 166 | 0.08 | 0 | 0.06 | 0.09 | 0 | 0.04 | 0.06 | 0.01 | 0.04 | 0.13 | 0 | 0.08 | 0.13 | 0 | 0.08 | 0.14 | 0.02 | 0.08 |
| 167 | 0.08 | 0 | 0.06 | 0.08 | 0 | 0.04 | 0.05 | 0 | 0.03 | 0.14 | 0 | 0.08 | 0.14 | 0 | 0.08 | 0.14 | 0.01 | 0.08 |
| 168 | 0.07 | 0 | 0.06 | 0.09 | 0 | 0.04 | 0.05 | 0 | 0.03 | 0.13 | 0 | 0.07 | 0.15 | 0 | 0.08 | 0.16 | 0 | 0.08 |
| 169 | 0.06 | 0 | 0.04 | 0.08 | 0.01 | 0.04 | 0.04 | 0 | 0.02 | 0.15 | 0 | 0.07 | 0.15 | 0 | 0.09 | 0.14 | 0 | 0.07 |
| 170 | 0.08 | 0 | 0.04 | 0.08 | 0.01 | 0.04 | 0.04 | 0 | 0.02 | 0.12 | 0 | 0.08 | 0.13 | 0 | 0.09 | 0.16 | 0 | 0.08 |
| 171 | 0.07 | 0 | 0.04 | 0.06 | 0 | 0.03 | 0.05 | 0 | 0.02 | 0.13 | 0 | 0.08 | 0.14 | 0 | 0.09 | 0.14 | 0 | 0.07 |
| 172 | 0.09 | 0 | 0.04 | 0.08 | 0 | 0.03 | 0.05 | 0 | 0.03 | 0.12 | 0 | 0.08 | 0.14 | 0 | 0.1 | 0.13 | 0 | 0.08 |
| 173 | 0.08 | 0 | 0.04 | 0.07 | 0 | 0.04 | 0.05 | 0 | 0.02 | 0.12 | 0 | 0.07 | 0.14 | 0 | 0.1 | 0.15 | 0 | 0.08 |
| 174 | 0.1 | 0 | 0.04 | 0.07 | 0 | 0.04 | 0.06 | 0 | 0.03 | 0.12 | 0 | 0.07 | 0.14 | 0.05 | 0.1 | 0.13 | 0 | 0.08 |
| 175 | 0.1 | 0 | 0.04 | 0.07 | 0 | 0.03 | 0.06 | 0 | 0.03 | 0.14 | 0 | 0.08 | 0.14 | 0.05 | 0.1 | 0.13 | 0.02 | 0.08 |
| 176 | 0.08 | 0.01 | 0.04 | 0.07 | 0 | 0.04 | 0.07 | 0 | 0.04 | 0.13 | 0 | 0.08 | 0.15 | 0.04 | 0.1 | 0.15 | 0 | 0.07 |
| 177 | 0.06 | 0 | 0.04 | 0.07 | 0 | 0.04 | 0.09 | 0 | 0.05 | 0.11 | 0 | 0.08 | 0.15 | 0.04 | 0.1 | 0.12 | 0 | 0.07 |
| 178 | 0.08 | 0 | 0.04 | 0.09 | 0 | 0.04 | 0.08 | 0 | 0.05 | 0.12 | 0 | 0.08 | 0.15 | 0.04 | 0.1 | 0.12 | 0 | 0.07 |
| 179 | 0.12 | 0 | 0.05 | 0.09 | 0 | 0.04 | 0.09 | 0 | 0.05 | 0.12 | 0 | 0.07 | 0.14 | 0.05 | 0.1 | 0.13 | 0 | 0.07 |
| 180 | 0.1 | 0 | 0.04 | 0.09 | 0 | 0.04 | 0.08 | 0 | 0.04 | 0.12 | 0 | 0.08 | 0.15 | 0.01 | 0.1 | 0.12 | 0.01 | 0.08 |
| 181 | 0.1 | 0 | 0.04 | 0.09 | 0 | 0.04 | 0.01 | 0 | 0.05 | 0.12 | 0 | 0.07 | 0.14 | 0.06 | 0.09 | 0.12 | 0 | 0.07 |
| 182 | 0.11 | 0.02 | 0.05 | 0.08 | 0 | 0.04 | 0.09 | 0 | 0.06 | 0.12 | 0 | 0.07 | 0.14 | 0 | 0.09 | 0.12 | 0 | 0.08 |
| 183 | 0.1 | 0.01 | 0.05 | 0.08 | 0 | 0.04 | 0.09 | 0 | 0.05 | 0.12 | 0.02 | 0.07 | 0.14 | 0 | 0.08 | 0.12 | 0 | 0.09 |
| 184 | 0.09 | 0.02 | 0.05 | 0.1 | 0 | 0.04 | 0.08 | 0 | 0.04 | 0.12 | 0 | 0.08 | 0.14 | 0 | 0.08 | 0.13 | 0 | 0.08 |
| 185 | 0.1 | 0.02 | 0.05 | 0.07 | 0 | 0.04 | 0.07 | 0 | 0.04 | 0.12 | 0 | 0.08 | 0.14 | 0 | 0.08 | 0.13 | 0.02 | 0.08 |
| 186 | 0.08 | 0.01 | 0.06 | 0.07 | 0 | 0.04 | 0.08 | 0 | 0.04 | 0.13 | 0 | 0.08 | 0.14 | 0 | 0.08 | 0.13 | 0 | 0.08 |
| 187 | 0.09 | 0.01 | 0.06 | 0.07 | 0 | 0.04 | 0.07 | 0 | 0.04 | 0.14 | 0 | 0.08 | 0.15 | 0.04 | 0.08 | 0.14 | 0 | 0.08 |
| 188 | 0.09 | 0 | 0.06 | 0.08 | 0 | 0.04 | 0.07 | 0 | 0.04 | 0.27 | 0 | 0.09 | 0.12 | 0.02 | 0.07 | 0.13 | 0 | 0.08 |
| 189 | 0.1 | 0.01 | 0.05 | 0.07 | 0 | 0.04 | 0.06 | 0 | 0.03 | 0.12 | 0 | 0.07 | 0.12 | 0.04 | 0.07 | 0.16 | 0 | 0.08 |
| 190 | 0.1 | 0.02 | 0.05 | 0.09 | 0.01 | 0.04 | 0.06 | 0 | 0.04 | 0.13 | 0 | 0.07 | 0.12 | 0 | 0.07 | 0.14 | 0 | 0.08 |
| 191 | 0.11 | 0 | 0.05 | 0.09 | 0.01 | 0.04 | 0.07 | 0 | 0.03 | 0.12 | 0.01 | 0.08 | 0.12 | 0 | 0.06 | 0.12 | 0 | 0.07 |
| 192 | 0.09 | 0 | 0.05 | 0.07 | 0 | 0.04 | 0.06 | 0 | 0.03 | 0.15 | 0 | 0.08 | 0.1 | 0 | 0.07 | 0.14 | 0.02 | 0.08 |
| 193 | 0.09 | 0 | 0.05 | 0.07 | 0.03 | 0.05 | 0.05 | 0 | 0.02 | 0.15 | 0.02 | 0.08 | 0.12 | 0 | 0.07 | 0.13 | 0 | 0.08 |
| 194 | 0.11 | 0.01 | 0.05 | 0.07 | 0 | 0.04 | 0.03 | 0 | 0.02 | 0.18 | 0 | 0.08 | 0.11 | 0 | 0.06 | 0.14 | 0 | 0.08 |
| 195 | 0.09 | 0 | 0.04 | 0.06 | 0 | 0.04 | 0.05 | 0 | 0.02 | 0.13 | 0 | 0.07 | 0.12 | 0 | 0.06 | 0.13 | 0 | 0.07 |
| 196 | 0.09 | 0 | 0.05 | 0.06 | 0 | 0.04 | 0.04 | 0 | 0.01 | 0.11 | 0 | 0.07 | 0.1 | 0.02 | 0.06 | 0.12 | 0.02 | 0.07 |

| | | | | | | | | | | | | | | | | | |
|---|---|---|---|---|---|---|---|---|---|---|---|---|---|---|---|---|---|
| 197 | 0.08 | 0 | 0.04 | 0.06 | 0 | 0.03 | 0.03 | 0 | 0.01 | 0.13 | 0 | 0.07 | 0.12 | 0 | 0.06 | 0.11 | 0 | 0.07 |
| 198 | 0.08 | 0 | 0.04 | 0.05 | 0 | 0.03 | 0.03 | 0 | 0.01 | 0.13 | 0 | 0.07 | 0.14 | 0 | 0.07 | 0.11 | 0 | 0.07 |
| 199 | 0.07 | 0 | 0.04 | 0.04 | 0 | 0.01 | 0.04 | 0 | 0.01 | 0.14 | 0 | 0.06 | 0.19 | 0 | 0.08 | 0.12 | 0 | 0.07 |
| 200 | 0.09 | 0 | 0.04 | 0.03 | 0 | 0.01 | 0.05 | 0 | 0.02 | 0.13 | 0 | 0.06 | 0.2 | 0 | 0.08 | 0.12 | 0 | 0.06 |

5. Tables of automated gap thickness measurements for AxC157 variety

| | Control (mm) | | | | | | | | | Infected (mm) | | | | | | | | |
|---|---|---|---|---|---|---|---|---|---|---|---|---|---|---|---|---|---|---|
| Day 2 | R1 | | | R2 | | | R3 | | | R1 | | | R2 | | | R3 | | |
| | Max | Min | Average | Max | Min | Average | Max | Min | Average | Max | Min | Average | Max | Min | Average | Max | Min | Average |
| 1 | 0.16 | 0.01 | 0.06 | 0.13 | 0 | 0.07 | 0.07 | 0 | 0.05 | 0.06 | 0 | 0.03 | 0.11 | 0.03 | 0.07 | 0.05 | 0 | 0.06 |
| 2 | 0.17 | 0 | 0.06 | 0.13 | 0 | 0.07 | 0.07 | 0 | 0.06 | 0.04 | 0 | 0.02 | 0.12 | 0 | 0.07 | 0.05 | 0 | 0.06 |
| 3 | 0.14 | 0 | 0.07 | 0.13 | 0.02 | 0.07 | 0.07 | 0.01 | 0.08 | 0.05 | 0 | 0.03 | 0.12 | 0 | 0.07 | 0.06 | 0 | 0.06 |
| 4 | 0.14 | 0 | 0.05 | 0.1 | 0 | 0.07 | 0.07 | 0 | 0.06 | 0.04 | 0 | 0.03 | 0.05 | 0 | 0.02 | 0.06 | 0 | 0.06 |
| 5 | 0.13 | 0 | 0.07 | 0.12 | 0 | 0.07 | 0.08 | 0.02 | 0.05 | 0.03 | 0 | 0.06 | 0.1 | 0 | 0.06 | 0.04 | 0 | 0.06 |
| 6 | 0.12 | 0 | 0.06 | 0.06 | 0 | 0.03 | 0.09 | 0 | 0.04 | 0.09 | 0 | 0.06 | 0.08 | 0 | 0.05 | 0.05 | 0 | 0.05 |
| 7 | 0.15 | 0 | 0.05 | 0.04 | 0 | 0.02 | 0.09 | 0 | 0.05 | 0.07 | 0 | 0.06 | 0.11 | 0 | 0.06 | 0.04 | 0 | 0.03 |
| 8 | 0.13 | 0 | 0.05 | 0.05 | 0 | 0.03 | 0.09 | 0 | 0.05 | 0.08 | 0.02 | 0.08 | 0.1 | 0 | 0.1 | 0.03 | 0 | 0.01 |
| 9 | 0.13 | 0 | 0.05 | 0.04 | 0 | 0.03 | 0.11 | 0 | 0.05 | 0.06 | 0 | 0.03 | 0.1 | 0 | 0.08 | 0.09 | 0 | 0.06 |
| 10 | 0.12 | 0 | 0.05 | 0.03 | 0 | 0.1 | 0.09 | 0 | 0.04 | 0.05 | 0 | 0.05 | 0.06 | 0 | 0.02 | 0.07 | 0 | 0.05 |
| 11 | 0.14 | 0 | 0.05 | 0.09 | 0 | 0.06 | 0.07 | 0 | 0.03 | 0.03 | 0 | 0.06 | 0.07 | 0 | 0.03 | 0.08 | 0.02 | 0.04 |
| 12 | 0.3 | 0.02 | 0.05 | 0.07 | 0 | 0.04 | 0.09 | 0 | 0.06 | 0.09 | 0 | 0.05 | 0.05 | 0 | 0.05 | 0.06 | 0 | 0.03 |
| 13 | 0.3 | 0 | 0.04 | 0.08 | 0.02 | 0.08 | 0.01 | 0 | 0.06 | 0.1 | 0 | 0.05 | 0.11 | 0 | 0.06 | 0.05 | 0 | 0.05 |
| 14 | 0.11 | 0 | 0.06 | 0.06 | 0 | 0.03 | 0.08 | 0 | 0.06 | 0.09 | 0 | 0.05 | 0.05 | 0 | 0.03 | 0.03 | 0 | 0.06 |
| 15 | 0.09 | 0 | 0.04 | 0.05 | 0 | 0.02 | 0.07 | 0 | 0.06 | 0.11 | 0 | 0.06 | 0.06 | 0 | 0.03 | 0.03 | 0 | 0.06 |
| 16 | 0.1 | 0 | 0.05 | 0.11 | 0 | 0.07 | 0.09 | 0 | 0.03 | 0.12 | 0 | 0.06 | 0.03 | 0 | 0.02 | 0.09 | 0 | 0.05 |
| 17 | 0.19 | 0 | 0.05 | 0.13 | 0.02 | 0.07 | 0.08 | 0 | 0.03 | 0.13 | 0 | 0.07 | 0.06 | 0 | 0.03 | 0.13 | 0.02 | 0.07 |
| 18 | 0.11 | 0 | 0.06 | 0.11 | 0.03 | 0.06 | 0.06 | 0 | 0.06 | 0.13 | 0 | 0.07 | 0.05 | 0 | 0.06 | 0.11 | 0 | 0.07 |
| 19 | 0.12 | 0 | 0.05 | 0.09 | 0.01 | 0.07 | 0.06 | 0 | 0.07 | 0.12 | 0.02 | 0.07 | 0.07 | 0 | 0.06 | 0.11 | 0.03 | 0.06 |
| 20 | 0.13 | 0 | 0.06 | 0.07 | 0 | 0.08 | 0.06 | 0 | 0.06 | 0.1 | 0 | 0.07 | 0.06 | 0 | 0.06 | 0.09 | 0.01 | 0.07 |

| | Control (mm) | | | | | | | | | Infected (mm) | | | | | | | | |
|---|---|---|---|---|---|---|---|---|---|---|---|---|---|---|---|---|---|---|
| Day 4 | R1 | | | R2 | | | R3 | | | R1 | | | R2 | | | R3 | | |
| | Max | Min | Average | Max | Min | Average | Max | Min | Average | Max | Min | Average | Max | Min | Average | Max | Min | Average |
| 1 | 0.1 | 0 | 0.05 | 0.8 | 0.01 | 0.05 | 0.1 | 0 | 0.06 | 0.12 | 0 | 0.08 | 0.1 | 0 | 0.06 | 0.1 | 0 | 0.08 |
| 2 | 0.09 | 0 | 0.05 | 0.08 | 0 | 0.06 | 0.12 | 0 | 0.05 | 0.13 | 0 | 0.08 | 0.1 | 0 | 0.05 | 0.11 | 0 | 0.07 |
| 3 | 0.1 | 0 | 0.04 | 0.09 | 0.01 | 0.06 | 0.1 | 0 | 0.06 | 0.12 | 0.04 | 0.08 | 0.1 | 0 | 0.05 | 0.11 | 0 | 0.06 |
| 4 | 0.1 | 0 | 0.04 | 0.1 | 0 | 0.05 | 0.1 | 0 | 0.06 | 0.13 | 0 | 0.08 | 0.09 | 0 | 0.09 | 0.1 | 0 | 0.07 |
| 5 | 0.09 | 0 | 0.04 | 0.11 | 0 | 0.06 | 0.11 | 0 | 0.06 | 0.17 | 0 | 0.08 | 0.09 | 0 | 0.08 | 0.1 | 0 | 0.06 |
| 6 | 0.12 | 0 | 0.05 | 0.11 | 0 | 0.05 | 0.1 | 0 | 0.06 | 0.12 | 0.02 | 0.07 | 0.1 | 0 | 0.05 | 0.11 | 0 | 0.06 |
| 7 | 0.11 | 0 | 0.05 | 0.1 | 0 | 0.05 | 0.1 | 0 | 0.06 | 0.12 | 0.01 | 0.07 | 0.1 | 0 | 0.06 | 0.11 | 0 | 0.06 |
| 8 | 0.1 | 0 | 0.05 | 0.09 | 0 | 0.05 | 0.12 | 0 | 0.07 | 0.12 | 0 | 0.07 | 0.13 | 0 | 0.08 | 0.09 | 0 | 0.05 |
| 9 | 0.1 | 0 | 0.06 | 0.11 | 0 | 0.06 | 0.13 | 0.03 | 0.07 | 0.13 | 0 | 0.07 | 0.13 | 0.01 | 0.08 | 0.09 | 0 | 0.09 |
| 10 | 0.1 | 0 | 0.06 | 0.11 | 0 | 0.06 | 0.12 | 0 | 0.07 | 0.12 | 0.02 | 0.08 | 0.13 | 0.01 | 0.06 | 0.1 | 0 | 0.06 |
| 11 | 0.11 | 0 | 0.05 | 0.12 | 0 | 0.06 | 0.12 | 0 | 0.06 | 0.14 | 0.03 | 0.07 | 0.14 | 0 | 0.08 | 0.09 | 0 | 0.05 |
| 12 | 0.1 | 0 | 0.05 | 0.11 | 0 | 0.05 | 0.13 | 0.03 | 0.07 | 0.17 | 0.02 | 0.08 | 0.15 | 0 | 0.07 | 0.1 | 0 | 0.07 |
| 13 | 0.1 | 0 | 0.06 | 0.11 | 0 | 0.06 | 0.13 | 0 | 0.07 | 0.16 | 0.02 | 0.07 | 0.16 | 0 | 0.06 | 0.09 | 0 | 0.07 |
| 14 | 0.11 | 0 | 0.06 | 0.12 | 0.01 | 0.06 | 0.12 | 0 | 0.06 | 0.12 | 0.01 | 0.07 | 0.14 | 0 | 0.07 | 0.09 | 0 | 0.08 |
| 15 | 0.1 | 0.01 | 0.06 | 0.11 | 0 | 0.07 | 0.12 | 0 | 0.06 | 0.12 | 0.01 | 0.07 | 0.13 | 0 | 0.07 | 0.1 | 0 | 0.1 |
| 16 | 0.09 | 0.02 | 0.06 | 0.11 | 0 | 0.07 | 0.12 | 0 | 0.06 | 0.11 | 0.01 | 0.06 | 0.15 | 0 | 0.07 | 0.11 | 0 | 0.05 |
| 17 | 0.1 | 0.01 | 0.06 | 0.13 | 0.03 | 0.08 | 0.12 | 0 | 0.06 | 0.1 | 0 | 0.06 | 0.15 | 0 | 0.08 | 0.09 | 0 | 0.06 |
| 18 | 0.1 | 0.01 | 0.06 | 0.11 | 0.03 | 0.07 | 0.12 | 0 | 0.07 | 0.11 | 0 | 0.05 | 0.15 | 0 | 0.08 | 0.1 | 0 | 0.06 |
| 19 | 0.11 | 0.02 | 0.06 | 0.12 | 0 | 0.08 | 0.12 | 0 | 0.07 | 0.12 | 0 | 0.05 | 0.15 | 0 | 0.09 | 0.09 | 0 | 0.05 |
| 20 | 0.1 | 0 | 0.05 | 0.12 | 0 | 0.09 | 0.13 | 0 | 0.07 | 0.12 | 0 | 0.05 | 0.17 | 0 | 0.08 | 0.1 | 0.01 | 0.06 |

| | Control (mm) | | | | | | | | | Infected (mm) | | | | | | | | |
|---|---|---|---|---|---|---|---|---|---|---|---|---|---|---|---|---|---|---|
| Day 6 | R1 | | | R2 | | | R3 | | | R1 | | | R2 | | | R3 | | |
| | Max | Min | Average | Max | Min | Average | Max | Min | Average | Max | Min | Average | Max | Min | Average | Max | Min | Average |
| 1 | 0.05 | 0 | 0.06 | 0.11 | 0 | 0.07 | 0.08 | 0 | 0.06 | 0.05 | 0 | 0.03 | 0.04 | 0 | 0.1 | 0.15 | 0.01 | 0.09 |
| 2 | 0.06 | 0 | 0.06 | 0.11 | 0 | 0.06 | 0.08 | 0 | 0.06 | 0.08 | 0 | 0.04 | 0.07 | 0 | 0.06 | 0.19 | 0 | 0.11 |
| 3 | 0.04 | 0 | 0.06 | 0.17 | 0 | 0.07 | 0.05 | 0 | 0.03 | 0.06 | 0 | 0.04 | 0.12 | 0 | 0.07 | 0.23 | 0 | 0.13 |
| 4 | 0.06 | 0 | 0.03 | 0.05 | 0 | 0.04 | 0.05 | 0 | 0.06 | 0.09 | 0 | 0.04 | 0.05 | 0 | 0.07 | 0.11 | 0 | 0.06 |
| 5 | 0.06 | 0 | 0.03 | 0.07 | 0 | 0.04 | 0.06 | 0 | 0.07 | 0.08 | 0 | 0.03 | 0.12 | 0 | 0.06 | 0.12 | 0.03 | 0.08 |
| 6 | 0.06 | 0 | 0.03 | 0.07 | 0 | 0.04 | 0.07 | 0 | 0.07 | 0.06 | 0 | 0.03 | 0.08 | 0 | 0.04 | 0.23 | 0 | 0.12 |

| | | | | | | | | | | | | | | | | | |
|---|---|---|---|---|---|---|---|---|---|---|---|---|---|---|---|---|---|
| 7 | 0.07 | 0 | 0.05 | 0.09 | 0.01 | 0.05 | 0.08 | 0 | 0.07 | 0.06 | 0 | 0.04 | 0.11 | 0 | 0.04 | 0.13 | 0.04 | 0.09 |
| 8 | 0.08 | 0 | 0.05 | 0.08 | 0 | 0.04 | 0.05 | 0 | 0.05 | 0.06 | 0 | 0.03 | 0.11 | 0 | 0.06 | 0.1 | 0 | 0.06 |
| 9 | 0.08 | 0.02 | 0.05 | 0.07 | 0 | 0.04 | 0.05 | 0 | 0.06 | 0.05 | 0 | 0.03 | 0.11 | 0 | 0.06 | 0.14 | 0 | 0.07 |
| 10 | 0.07 | 0.02 | 0.04 | 0.08 | 0 | 0.05 | 0.06 | 0 | 0.03 | 0.05 | 0 | 0.03 | 0.12 | 0.01 | 0.07 | 0.08 | 0 | 0.06 |
| 11 | 0.08 | 0.02 | 0.05 | 0.09 | 0 | 0.05 | 0.06 | 0 | 0.03 | 0.06 | 0 | 0.04 | 0.11 | 0 | 0.08 | 0.09 | 0 | 0.05 |
| 12 | 0.09 | 0 | 0.05 | 0.01 | 0 | 0.06 | 0.07 | 0 | 0.07 | 0.12 | 0 | 0.04 | 0.12 | 0.04 | 0.08 | 0.11 | 0 | 0.05 |
| 13 | 0.08 | 0 | 0.05 | 0.11 | 0 | 0.07 | 0.04 | 0 | 0.06 | 0.04 | 0 | 0.02 | 0.11 | 0 | 0.06 | 0.13 | 0 | 0.04 |
| 14 | 0.07 | 0 | 0.05 | 0.12 | 0 | 0.06 | 0.06 | 0 | 0.1 | 0.05 | 0 | 0.02 | 0.14 | 0.01 | 0.08 | 0.07 | 0 | 0.04 |
| 15 | 0.06 | 0 | 0.05 | 0.15 | 0 | 0.07 | 0.04 | 0 | 0.1 | 0.07 | 0 | 0.02 | 0.12 | 0 | 0.05 | 0.08 | 0 | 0.04 |
| 16 | 0.08 | 0 | 0.05 | 0.09 | 0 | 0.05 | 0.05 | 0 | 0.06 | 0.1 | 0 | 0.05 | 0.11 | 0 | 0.06 | 0.06 | 0 | 0.05 |
| 17 | 0.09 | 0.03 | 0.06 | 0.08 | 0 | 0.05 | 0.03 | 0.01 | 0.08 | 0.02 | 0 | 0.6 | 0.15 | 0 | 0.06 | 0.07 | 0 | 0.06 |
| 18 | 0.08 | 0 | 0.06 | 0.1 | 0.02 | 0.05 | 0.04 | 0 | 0.05 | 0.08 | 0 | 0.04 | 0.05 | 0 | 0.03 | 0.26 | 0 | 0.05 |
| 19 | 0.07 | 0 | 0.07 | 0.08 | 0 | 0.05 | 0.06 | 0 | 0.06 | 0.09 | 0 | 0.04 | 0.11 | 0.03 | 0.08 | 0.08 | 0 | 0.06 |
| 20 | 0.07 | 0 | 0.07 | 0.08 | 0 | 0.04 | 0.06 | 0 | 0.07 | 0.12 | 0 | 0.05 | 0.108 | 0 | 0.1 | 0.08 | 0 | 0.03 |

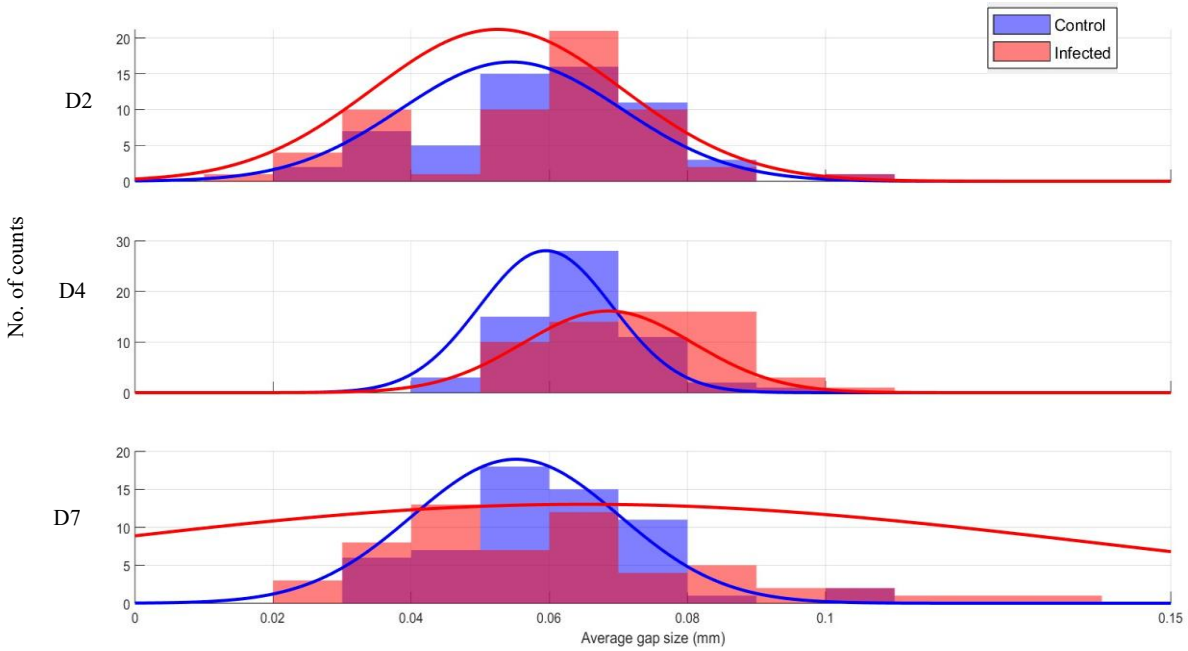


Figure 70: Average gap size distribution in control (blue) and infected (red) wheat leaves AxC157 variety extracted from automated segmentation, for D2, D4, and D6 after inoculation, with superimposed Gaussian fits. The histograms use a bin width of 0.01 mm

The data are available in Google Drive and can be exported for further analysis.

**https://docs.google.com/spreadsheets/d/1EW00Z92LVt7AvnPS3CfLGpIhW1G-Asoz/edit?usp=sharing&ouid=102742141539264065722&rtpof=true&sd=true**

Published Articles

1. Using Optical Coherence Tomography in Plant Biology Research: Review and Prospects

sensors

MDPI

*Review*

# Using Optical Coherence Tomography in Plant Biology Research: Review and Prospects

**Ghada Salem Sasi and Adrien Alexis Paul Chauvet ***

School of Mathematic and Physical Sciences, University of Sheffield, Sheffield S3 7HF, UK; gssasi1@sheffield.ac.uk
* Correspondence: a.chauvet@sheffield.ac.uk

**Abstract:** Visualizing the microscopic structure of plants in vivo, non-invasively, and in real-time is the Holy Grail of botany. Optical coherence tomography (OCT) has all the characteristics necessary to achieve this feat. Indeed, OCT provides volumetric images of the internal structure of plants without the need for histological preparation. With its micrometric resolution, OCT is commonly used in medicine, primarily in ophthalmology. But it is seldom used in the field of botany. The aim of the present work is thus to review the latest technical development in the field of OCT and to highlight its current use in botany, in order to promote the technique and further advance research in the field of botany.

**Keywords:** optical coherence tomography; plant; non-invasive; in vivo; real-time

## 1. Coming of Age

Optical coherence tomography (OCT) is, at its core, an interferometric imaging technique. One of the first uses of low-coherence interferometry induced by backscattering within soft tissues was by Fercher et al. in the 1980s [1]. In this pioneering work, Fercher et al. succeeded in measuring the optical length of the human eye in vivo. After nearly a decade of technical development, the first OCT setup was demonstrated in 1991 [2–5] by Fujimoto et al. In comparison to Fercher's single-point imaging, OCT provides cross-sectional and three-dimensional imaging of soft tissues while remaining noninvasive [6]. Five years later, the first commercial OCT instrument was launched [7] and was rapidly implemented for healthcare applications. Today, in light of its imaging capabilities and practicality, OCT is routinely used by ophthalmologists to examine patients [8]. However, using OCT imaging as a non-invasive and real-time technique to investigate plants tissue remains rare. Its first use in the field of botany was reported by Sapozhnikova et al. in 2004 [9]. In this work, the team described their ability to directly visualize the dehydration and rehydration dynamics of *Tradescantia pallida* (Rose) leaves. The penetration depth was about 1–2 mm and the spatial resolution was about 15 µm [9]. OCT techniques have, since then, greatly improved in terms of scan rates, contrast, sensitivity, and phase-stability [2,10]. For example, from an initial~400 axial scans (A-scans) per second [11], OCTs are now commonly running at hundreds of kHz [12], thus improving spatial and time resolution. These improvements in acquisition speed and precision are paving the way for real time functional imaging in all scientific fields.

Time-domain OCT (TD-OCT), which was the first type of system, was using a moving reference mirror to capture images, but it was slow and had limited resolution. Fourier-domain OCT (FD-OCT), which was later developed, instead uses Fourier transformation, thus improving speed and image quality. The development of swept-source OCT (SS-OCT), in particular, further enhanced imaging depth and speed by making use of novel tunable

check for updates

Academic Editor: Min Yong Jeon

Received: 14 February 2025
Revised: 2 April 2025
Accepted: 10 April 2025
Published: 14 April 2025

**Citation:** Sasi, G.S.; Chauvet, A.A.P. Using Optical Coherence Tomography in Plant Biology Research: Review and Prospects. *Sensors* **2025**, *25*, 2467. https://doi.org/10.3390/s25082467

lasers. All these advancements make OCT ready for agricultural applications, such as effective plant health monitoring and food quality assessment [11,13–15].

## 2. Concepts and Characteristics of OCT

The common feature of OCT systems is their ability to generate non-invasive, high-resolution, depth-resolved images of soft tissue solely by collecting backscattered light [16,17]. This backscattered light is then made to interfere with a reference light originating from the same initial light source to produce an interferogram, be it a fixed wavelength laser, a swept-source laser, or a superluminescent diode [18]. And since backscattering is the result of a variation in refraction index between differing intrinsic structural components, analysis of the interferogram allows the retrieval of this depth-resolved structural information.

In comparison to the narrow light sources and long coherence lengths typically used in Michelson interferometry [19], OCT benefits from spectrally broadband light sources with low temporal coherence and high spatial coherence, which improves the depth resolution of the resulting images [14]. The sample arm of this low coherence interferometer is often extended via an optic fiber for hand-held applications. This feature enables the OCT systems to be adapted to target samples, which is advantageous for in vivo biological applications.

OCT can be performed either in the time or spectral domain. On the one hand, as introduced earlier, TD-OCT produces tomographic images by oscillating a reference arm mirror of the interferometer to create temporal interferences. On the other hand, Fourier-domain OCT (FD-OCT) generates the spectral interferogram by mixing the broadband backscattered light from the sample with the reference light without changes in the reference arm length [20]. Because the core of FD-OCT is devoid of moving parts and because Fourier analysis of spectral interferogram is fast, the technique has the advantage of being ~100 times faster than TD-OCT [21,22] while being more robust for in-field applications. The FD-OCT family includes both the Sprrctral domain OCT (SD-OCT) as well as SS-OCT. While SD-OCT still uses a spectrometer with a dispersive element and a relatively slower detector array, the SS-OCT benefits from an optical source which rapidly sweeps a narrow linewidth over a broad range of wavelengths. In SS-OCT, each wavelength is then detected sequentially during each sweep by a high-speed photodetector. This technical feat allows SS-OCT to reach hundreds of kHz in image acquisition rates, thus increasing in reliability when monitoring moving objects [23]. Note that when it comes to scanning speed, typical TD- and SD-OCT still requires scanning of either the reference mirror or of the excitation wavelength, respectively, to produce an entire b-scan. This scanning requirement can be bypassed in "single-shot" OCT systems, which can acquire full b-scan at every shot by using a broad light source and a diffracting element to record each wavelength separately and simultaneously via photodetector arrays [24]. However, even if each b-scan is taken virtually instantaneously, the processing of each scan might take up to 140 ms [25].

In term of image quality, the axial resolution (Z-axis) typically depends on the bandwidth of the OCT light source; the lateral resolution (X-Y plane) is usually given by the numerical aperture of the microscope objective used, as depicted in Figure 1. Resolutions of both axis are typically in the order of 1–10 µm in OCT systems [26,27]. The sensitivity, on the other hand, is related to a combination of factors, including laser power (typically in the µW range to avoid damaging the tissues), scattering [28,29] (which can be enhanced with contrast agents), and scanning speed (of up to MHz for FD-OCTs).

Overall, OCTs are technically simple, compact, robust, and adaptable to various environments, which make them ideally suitable for biological applications.

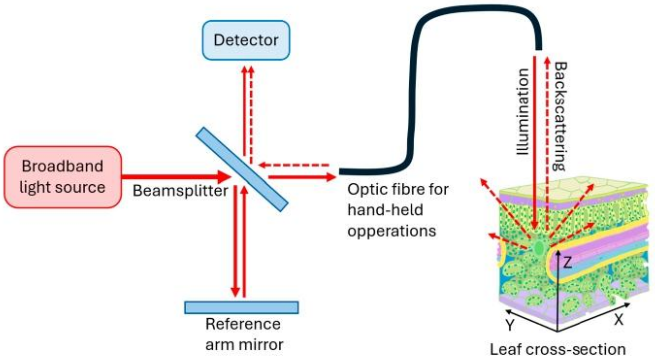


**Figure 1.** Principle of interferometry with beam propagation through optic fiber for hand-held applications. The sample is scanned laterally (X–Y) through sets of galvanometers. Created by the authors.

## 3. Popularity of OCT in Botany

Owning to its many advantages, OCT has been extensively utilized in the medical field for various health applications and, more specifically, in ophthalmology, cardiology, and dermatology. The widespread adoption of OCT is illustrated by the ever-increasing number of publications pertaining its use in the medical field, numbering in the tens of thousands every year, as shown in Figure 2. In comparison, following the same metric, the use of OCT in botany is about fifty times less prevalent. This wide disparity between the use of OCT in the medical field and in botany is actually surprising given the comparable suitability and potential impact this technique has on both fields.

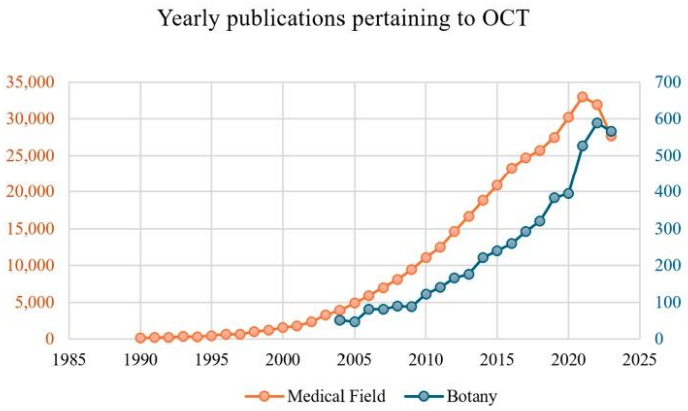


**Figure 2.** Annual number of OCT-related publications (blue) compared to the number of publications specific to the field of OCT applied to botany (In medical field: using keyword search: "optical coherence tomography" OR medical field. In botany: using keyword search: "optical coherence tomography" botany OR plant OR leaf OR seed OR plant's root).

## 4. Comparison with Alternative Techniques

To better appreciate the potentialities of OCT in plant biology research, it is useful to compare it with common imaging techniques that are readily used in the field. And beyond

the various technical characteristics of each imaging tool, the following discussion also includes practicality and ease of access, which is where OCT's primary strengths reside.

1. The highest resolution technique available is X-ray tomography (XCT). This system provides 3D rendering of the internal structures of plant tissue with nanometric resolution [30,31]. Samples can be as large as a whole plant (e.g., 40 cm tall), depending on the size of the sample chamber, but it is not field-applicable [32]. Furthermore, high X-ray dose causes ionization, which disrupts and damages the plant [33–35].
2. Hyperspectral imaging (HIS), which includes UV reflectance imaging [36,37], serves as a non-invasive and efficient tool for studying plants and whole crops. Although such spectroscopic method is in theory diffraction limited, HIS' resolution is typically low given the sensor size and its distance from the object [38]. Although HIS typically has the lowest spatial resolution [39], it is the most practical for field application, offering insights into the health, physiology, and interactions of plants with their environment.
3. Raman microscopy is often used as a convenient and non-invasive way to monitor the presence of specific molecules in tissues. Molecules are categorized by the vibrational signature of their functional groups [40]. For this technique, no sample preparation is needed; it is non-destructive and is highly sensitive, which makes it field-applicable. The past decade has seen the development of universal multiple angle Raman spectroscopy (UMRAS) for monitoring functional groups of embedded molecules, thus paving the way for 3D Raman imaging [41,42]. But to characterize tissues solely based on the functional groups of its constituting molecules is not at all trivial, and variations among research teams makes it difficult to obtain replicate measurements [43].
4. Laser-induced fluorescence (LIF) is commonly used, like HIS, to remotely assess whole leaves, plants, and even crops [44]. It allows for real-time imaging and is non-invasive [45]. LIF typically gives information about the presence of chlorophyll via its induced fluorescence [45]. Consequently, LIF is restricted to monitoring chlorophyll and other highly fluorescent molecules within tissues, without revealing direct information about the tissue's internal structure.
5. Magnetic resonance imaging (MRI) is another non-invasive, non-destructive imaging technique, which also provides three-dimensional images. It also allows for whole plant investigation [46] and is non-invasive [47]. However, MRI has a typical axial resolution of 1.5–2.0 mm [18,48] and is not field-applicable.
6. Ultrasound imaging is another 3D imaging technique which uses sound instead of radiation. It can be used to investigate plant tissue and water movement within it [49]. Ultrasound imaging benefits from a significantly higher penetration depth compared to OCT, typically up to several centimeters depending on the frequency used. However, it has lower axial and lateral resolution compared to OCT [50], often around 10 to 100 times lower, ranging from about 50 µm to 500 µm [51] while OCT's axial resolutions typically range from 1 to 15 µm [49–51]. Ultrasounds have been shown to directly affect plants, albeit in a positive way [52].

Hence, in light of the conventionally used imaging techniques, it is understood that OCT represents a powerful compromise between resolution and practicality, bringing 3D imaging into the field for real-time analysis.

## 5. The Various Variants of OCT

The suitability and potential impact of OCT in the field of botany can be further appreciated by exploring the different types of OCT systems that have already been employed in botany. Benefiting from its technical simplicity (compared to alternative imaging systems), OCT is highly suitable for a range of multimodal imaging techniques:

### 5.1. Polarization-Sensitive OCT

Polarization-sensitive OCT (PS-OCT) benefits from the ability of fibrous structures in altering the polarization of light. Because different tissues alter the polarization of light differently, this system provides an added layer of contrast, that of polarization, on top of the typical grey-scale OCT images. For example, it allows differentiation between distinct cellular layers that would otherwise appear as the same grey-shade [53]. More specifically, it measures birefringence, which reflects tissue organization by assessing how light slows differently along specific axes, with the fast axis orientation indicating the preferred direction of light propagation within the tissue, and the degree of polarization uniformity (DOPU) helping identify regions with uniform or disrupted polarization properties.

PS-OCT can be further extended by applying the Mueller matrix method to capture diattenuation, which describes how tissue differentially absorbs or transmits polarized light. This provides additional contrast for distinguishing subtle tissue characteristics [54].

### 5.2. Full-Field Optical Coherence Tomography (FF-OCT)

Full-field OCT is a technique that differs from time-domain and frequency-domain OCT by producing tomographic images without scanning a light beam using galvanometer scanners [55,56], similar to the "single-shot" OCT system discussed earlier [24,25]. Instead, the entire sample is illuminated with a light of extremely short coherence. The tomographic images are thus obtained in the en-face orientation (orthogonal to the optical axis) by a Linnik-type interferometer. Accordingly, full-field OCT is also called en-face OCT or, more commonly, full-field optical coherence microscopy (OCM). The transverse resolution of full-field OCT is similar to that of conventional microscopy (~1 µm) but has the advantage of being non-invasive and not requiring any histological treatments. The axial resolution, determined by the spectral properties of the illumination source, is also of the order of 1 µm [57].

### 5.3. Spectroscopic Optical Coherence Tomography (S-OCT)

S-OCT differs from standard OCT by further analyzing the spectrum of the backscattered light [58,59]. Analogous to the PS-OCT, S-OCT provides additional contrasts which consist of the spectral blue- or red-shift of the backscattered light's maximum amplitude. Accordingly, by monitoring the spectrum of the scattered light, structures that selectively absorb part of the incident light can thus be distinguished.

### 5.4. Biospeckle OCT (bOCT)

Biospeckle imaging consists of analyzing the backscattered light from a coherently illuminated object. Typically, for static objects, the backscattered rays interfere with themselves and create a speckle pattern that is unique to the object's surface and internal structure (depending on the penetration depth of the light used). If the objects are biological samples, the flow of their constituent parts (e.g., flow of red blood cells through veins [60]) will generate a continuously evolving speckle pattern called biospeckle. Biospeckle OCT (bOCT) is also known as "dynamic OCT" [61], as well as "OCT angiography" or "optical coherence angiography" [62]. Monitoring biospeckles over time helps assess the level of physiological activity of the sample. Thus, in comparison to OCT, bOCT provides an additional contrast which consists of the physiological activity of the sample.

### 5.5. Inverse Spectroscopic OCT (ISOCT)

In this variant of OCT, the signals are further analyzed to extract depth-dependent absorption and scattering parameters [63]. Indeed, attenuation in OCT describes the weakening of the light signal as it passes through tissue, caused by both absorption and

scattering. The more attenuation there is, the weaker the OCT signal becomes, which can affect the clarity and quality of the resulting images [64]. Thus, by monitoring the changes in scattering intensities, it then becomes possible to infer about the concentration and size of the scattering particles at various depths.

While many more types of OCT are currently employed in healthcare, the few that have been selected here are among those that have been demonstrated in botany in only the last decades, showing that the field is fast developing.

## 6. Use of OCT in Botany

As already alluded to, the use of OCT in ophthalmology has grown to the point where it is now an indispensable tool in the field. But OCT's abilities to investigate in real-time soft tissues without histological preparations, and without incurring radiation damages, are equally suited for botany. Plants, like skin and retinae, are comprised of soft tissues that can be subject to the exact same type of investigations, as demonstrated subsequently.

### *6.1. OCT for Non-Invasive Investigation of Crop Types*

Because OCT uses scattered light to probe the internal structure of tissues, the depth and overall quality of the images depend on the type of tissues investigated. For example, while OCT can image the whole cross section of a soft Arabidopsis leaf [65–67], the same equipment is barely able to image the first cell layer of a sturdy tomato leaf due to insufficient light penetration [68]. Indeed, the denser the sample, the greater the absorption and the less scattered light is collected from the sample's internal structures. This phenomena is illustrated in J.C. Clements' work on thick lupin seeds [69]. In this study, although OCT was used to distinguish between different species by looking at differences in hull thicknesses, as shown in Figure 3, the penetration depth was limited to ~200 µm with no discernable structural element within specific layers.

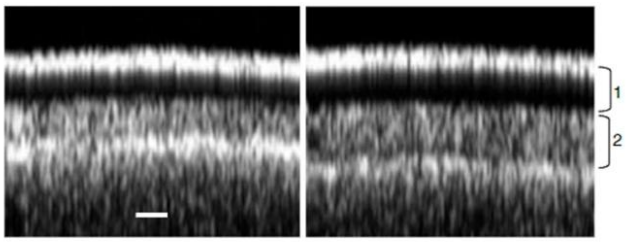


**Figure 3.** OCT images show the layers of lupin seeds. (1) is the first palisade layer. (2) is the second palisade layer. The scale bar is 50 µm. Figures were adapted from [69].

On the other hand, water-rich samples, such as onions [70], kiwi, and orange fruits, [67] allow the visualization of individual vacuoles up to 1 mm under the surface, as depicted in Figure 4. It is, however, important to note that penetration depth within tissues is wavelength-dependent. But overall, near-IR is ideally suited for plant investigations [71].

In another example, OCM has been used to investigate the soft Arabidopsis plant [72,73]. Along with the vacuoles, OCT was successful in visualizing other subcellular structures such as the trichomes' nuclei and organelles. OCT was similarly successful in distinguishing distinct stages in the senescence of leaves by monitoring texture changes at differing yellowing stages [74].

Although dense samples typically yield limited imaging depth, complementary image processing can help circumvent the limited resolution and extract additional information

such as particle size and concentrations. For example, ISOCT has been used to estimate depth-resolved concentrations of chlorophylls in corals [75].

Overall, by providing details of internal structures, OCT has been demonstrated to be a fast and reliable tool to investigate and differentiate between crop types.

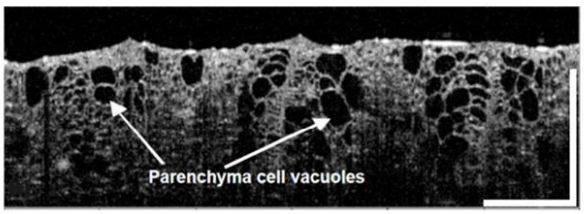


**Figure 4.** An OCT image of the kiwifruit parenchyma cell vacuoles. Figure adapted from [67]. Scale bars are 1 mm.

### *6.2. OCT to Study Plant's Responses to Biotic Stresses*

Although OCT's typical micrometric resolution does not allow for direct visualization of fungi, it can still be used to differentiate between infected and non-infected crops whenever the infection alters the plant's overall internal structure. For example, OCT has been used to study the morphological changes in response to *Anthracnose* [76], a fungal disease that typically causes dark lesions on leaves [77]. It has been used to follow the development of a progressive rind breakdown disorder in '*Nules clementine*' mandarin [65–67] via the progressive collapse of oil glands. Similarly, OCT has been used to detect pathological infections such as *Venturianashicola*, which causes pear scab disease [78–80]. It has also been used to investigate the gray leaf spot disease in *Capsicum annuum* leaves [81], to diagnose *marssonina* blotch disease in apple leave [82], to detect melon seeds infected with the Cucumber green mottle mosaic virus [83,84], to investigate fungal (*Botrytis allii*) and bacterial (*Pseudomonas* sp.) infection in onions [82,85], to detect Anthracnose fungus-infected tomato seeds [86], to investigate virus-infected orchid plant leaves [87,88], and to detect defects and rot in onions [80,85]. Considering these various applications, OCT has demonstrated to be an ideal diagnostic tool for the quality control of crops, allowing for early treatment and reducing waste.

### *6.3. OCT to Study Plant's Responses to Abiotic Stresses*

Beyond the visualization of plants' morphological changes induced by infections, OCT can effectively monitor the effects of environmental changes. For example, OCT was used to study the effect of drought and rehydration on leaf morphology [89], as well as to study the effect of ozone stress on Chinese chives (*Allium tuberosum*) leaves [90]. Similarly, the advantages of OCT over more advanced techniques, such as confocal microscopy and micro-CT, were further demonstrated while monitoring the effects of preharvest fertilization treatments and of fruit storage on fruits such as apples [91] and kiwi [92].

These last examples illustrate that OCT is also suited to studying the effects of environmental factors incurred through urbanization and industrialization.

### *6.4. OCT for Investigation of Live Responses*

Since OCT measurements are non-invasive, successive measurements can be performed at the same location without altering the plant's metabolism and physiological functions. This characteristic enables the investigation of time-resolved dynamics of structural changes within a specific section of the plant. And given the fast acquisition speed of OCT, the time laps between measurements can be easily adjusted to the process under investigation.

In this manner, the internal changes induced by the rotting of apples could be followed over the course of 25 days [80]. The spread of rot was evidenced by a gradual increase of the infected region in a lateral direction and a gradual disappearance of the cuticle, wax, epidermis, and hypodermal layers. In another instance, OCT was successfully used to monitor the emergence of roots from switchgrass seeds over a lap of 21 h [93,94]. Similarly, the effect of ozone on the internal cell structure of Chinese chives leaves was investigated via bOCT [95,96]. The technique was effective in distinguishing changes only a few hours after ozone exposure.

In faster timescales, OCT was also used to monitor modifications in the distribution and structure of chloroplasts in tobacco, only minutes after inoculation of the bacterial elicitor harpin protein [97].

Finally, through continuous monitoring, OCT was used to investigate signaling mechanisms in real time, as shown in Figure 5. It was then possible to follow the propagation of slow wave potential, induced by laser burn, across a young tomato plant [98].

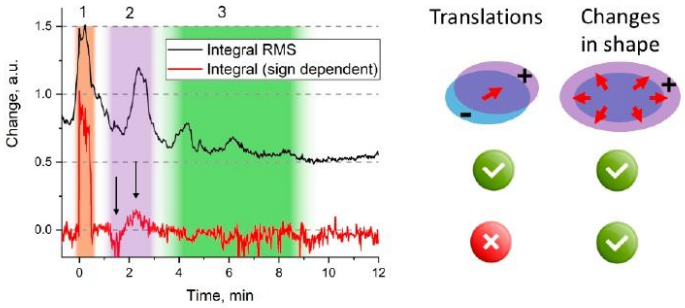


**Figure 5.** Time-resolved integrated A-scans difference image of a tomato leaf after laser burn. The red curve represents the integral accounting for changes in sign (normalized), while the black curve indicates the magnitude of the squared root of the integral (normalized and adjusted vertically for clarity). Each integral corresponds to specific cellular changes depicted to the right. The feature observed between 0 and 0.5 min is partially attributed to light scattering caused by a 30 s wounding laser pulse (zone 1). The shaded purple area (zone 2, black arrows) denotes the anticipated changes in the shape of the adjacent leaf. The shaded green area (zone 3) denotes the translational relaxation of the leaf. Adapted from [98].

## 7. The Future of OCT

Although the vast majority of research involving OCT still pertains to the medical field, this brief review demonstrates the suitability of OCT in botany as well. In comparison to current imaging tools, OCT suffers from a resolution which seems limited to ~1 µm, regardless of the equipment type. The technique, however, hugely benefits from its simplicity, real-time acquisition, and non-invasiveness. OCT is thus prone to develop in research fields that require site-specific, systematic and/or real-time monitoring. As such, OCT is ideal for systematic screening of fruits and vegetables for quality control purposes. It is also ideally suited for real-time monitoring of responses to biotic and abiotic stresses. It is noted that across the board, the quality of OCT images is often speckled, which is a common issue in coherence-based imaging techniques [99]. Fortunately, with the advent of machine learning algorithms, while speckle noise can be treated directly [100], further qualitative information can be more efficiently and effectively extracted by automated image processing such as registration and segmentation [101].

Given the simplicity and robustness of the equipment, it is a matter of time until OCT is applied for field experiments and finds its place in a farmer's toolbox for direct crop

screening. Hand-held OCT are currently being developed [93,94,102]. The impact of a portable OCT is huge and is attracting attention, as illustrated by the funding of projects aimed at its development [103], even if the vast majority of these projects are still dedicated to clinical purposes.

**Funding:** This research was funded by the Biotechnology and Biological Sciences Research Council (BBSRC), grant number BB/X005097/1, as well as the UKRI, in accordance with their Open Access Policy, for covering the article processing charges.

**Acknowledgments:** The authors thank the Embassy of Libya and The University of Sheffield for their generous funding. The authors also acknowledge the support from BBSRS (BB/X005097/1) for pump-priming the project. For the purpose of open access, the author has applied a Creative Commons Attribution (CC BY) license to any Author Accepted Manuscript version arising.

**Conflicts of Interest:** The authors declare no conflicts of interest.

## References

1. Fercher, A.; Roth, E. Ophthalmic Laser Interferometry. In Proceedings of the 1986 International Symposium, Innsbruck, Austria, 6–12 July 1986; Volume 0658.
2. Drexler, W.; Liu, M.; Kumar, A.; Kamali, T.; Unterhuber, A.; Leitgeb, R.A. Optical coherence tomography today: Speed, contrast, and multimodality. *J. Biomed. Opt.* **2014**, *19*, 071412. [CrossRef] [PubMed]
3. Fujimoto, J.G.; Puliafito, C.A.; Margolis, R.; Oseroff, A.; De Silvestri, S.; Ippen, E.P. Femtosecond optical ranging in biological systems. *Opt. Lett.* **1986**, *11*, 150–152. [CrossRef] [PubMed]
4. Huang, D.; Swanson, E.A.; Lin, C.P.; Schuman, J.S.; Stinson, W.G.; Chang, W.; Hee, M.R.; Flotte, T.; Gregory, K.; Puliafito, C.A.; et al. Optical coherence tomography. *Science* **1991**, *254*, 1178–1181. [CrossRef] [PubMed]
5. Fujimoto, J.G. Optical coherence tomography for ultrahigh resolution In Vivo imaging. *Nat. Biotechnol.* **2003**, *21*, 1361–1367. [CrossRef]
6. Drexler, W. Optical Coherence Tomography. In *Encyclopedia of the Eye*; Dartt, D.A., Ed.; Academic Press: Oxford, UK, 2010; pp. 194–204.
7. Scholtz, S.; MacMorris, L.; Langenbucher, A. The 30-Year History of Optical Coherence Tomography of the Human Eye. *Ophthalmol. Times Eur.* **2021**, *17*, 06.
8. Li, M.; Landahl, S.; East, A.R.; Verboven, P.; Terry, L.A. Optical coherence tomography—A review of the opportunities and challenges for postharvest quality evaluation. *Postharvest Biol. Technol.* **2019**, *150*, 9–18. [CrossRef]
9. Sapozhnikova, V.V.; Kamensky, V.A.; Kuranov, R.V.; Kutis, I.; Snopova, L.B.; Myakov, A.V. In Vivo visualization of Tradescantia leaf tissue and monitoring the physiological and morphological states under different water supply conditions using optical coherence tomography. *Planta* **2004**, *219*, 601–609. [CrossRef]
10. Bouma, B.E.; de Boer, J.F.; Huang, D.; Jang, I.-K.; Yonetsu, T.; Leggett, C.L.; Leitgeb, R.; Sampson, D.D.; Suter, M.; Vakoc, B.J.; et al. Optical coherence tomography. *Nat. Rev. Methods Primers* **2022**, *2*, 79. [CrossRef]
11. Gabriele, M.L.; Wollstein, G.; Ishikawa, H.; Kagemann, L.; Xu, J.; Folio, L.S.; Schuman, J.S. Optical coherence tomography: History, current status, and laboratory work. *Investig. Ophthalmol. Vis. Sci.* **2011**, *52*, 2425–2436. [CrossRef]
12. de Amorim Garcia Filho, C.A.; Yehoshua, Z.; Gregori, G.; Puliafito, C.A.; Rosenfield, P.J. Chapter 3—Optical Coherence Tomography. In *Retina*, 5th ed.; W.B. Saunders: London, UK, 2013; pp. 82–110.
13. Nanda, T.; Liang, M.C.; Duker, J.S. Optical Coherence Tomography. 2021. Available online: https://retinahistory.asrs.org/milestones-developments/history-of-oct?utm_source=chatgpt.com (accessed on 1 April 2025).
14. Zeppieri, M.; Marsili, S.; Enaholo, E.S.; Shuaibu, A.O.; Uwagboe, N.; Salati, C.; Spadea, L.; Musa, M. Optical Coherence Tomography (OCT): A Brief Look at the Uses and Technological Evolution of Ophthalmology. *Medicina* **2023**, *59*, 2114. [CrossRef]
15. Fujimoto, J.; Swanson, E. The Development, Commercialization, and Impact of Optical Coherence Tomography. *Investig. Ophthalmol. Vis. Sci.* **2016**, *57*, OCT1–OCT13. [CrossRef] [PubMed]
16. Fercher, A.F.; Drexler, W.; Hitzenberger, C.K.; Lasser, T. Optical coherence tomography—Principles and applications. *Rep. Prog. Phys.* **2003**, *66*, 239. [CrossRef]
17. Gao, W.; Wu, X. Differences between time domain and Fourier domain optical coherence tomography in imaging tissues. *J. Microsc.* **2017**, *268*, 119–128. [CrossRef]
18. Popescu, D.P.; Choo-Smith, L.-P.; Flueraru, C.; Mao, Y.; Chang, S.; Disano, J.; Sherif, S.; Sowa, M.G. Optical coherence tomography: Fundamental principles, instrumental designs and biomedical applications. *Biophys. Rev.* **2011**, *3*, 155–169. [CrossRef]

19. Comsa, G. The Coherence Length in Molecular and Electron Beam Diffraction. In *Dynamics of Gas-Surface Interaction*; Springer Series in Chemical Physics; Benedek, G., Valbusa, U., Eds.; Springer: Berlin/Heidelberg, Germany, 1982; Volume 21.
20. Nassif, N.; Cense, B.; Park, B.H.; Pierce, M.C.; Yun, S.H.; Bouma, B.E.; Tearney, G.J.; Chen, T.C.; de Boer, J.D. In Vivo high-resolution video-rate spectral-domain optical coherence tomography of the human retina and optic nerve. *Opt. Express* **2004**, *12*, 367–376. [CrossRef]
21. Leitgeb, R.; Hitzenberger, C.K.; Fercher, A.F. Performance of fourier domain vs. time domain optical coherence tomography. *Opt. Express* **2003**, *11*, 889–894. [CrossRef]
22. de Boer, J.F.; Cense, B.; Park, B.H.; Pierce, M.C.; Tearney, G.J.; Bouma, B.E. Improved signal-to-noise ratio in spectral-domain compared with time-domain optical coherence tomography. *Opt. Lett.* **2003**, *28*, 2067–2069. [CrossRef]
23. Aumann, S.; Donner, S.; Fischer, J.; Müller, F. Optical Coherence Tomography (OCT): Principle and Technical Realization. In *High Resolution Imaging in Microscopy and Ophthalmology: New Frontiers in Biomedical Optics*; Bille, J.F., Ed.; Springer International Publishing: Cham, Switzerland, 2019; pp. 59–85.
24. Torre-Ibarra, M.H.D.l.; Ruiz, P.D.; Huntley, J.M. Double-shot depth-resolved displacement field measurement using phase-contrast spectral optical coherence tomography. *Opt. Express* **2006**, *14*, 9643–9656. [CrossRef]
25. Teramura, Y.; Suekuni, M.; Kannari, F. Two-dimensional optical coherence tomography using spectral domain interferometry. *J. Opt. A Pure Appl. Opt.* **2000**, *2*, 21–26. [CrossRef]
26. Lumedica OQ Labscope 2.0. Available online: https://www.lumedicasystems.com/oq-labscope/ (accessed on 1 April 2025).
27. Sahyoun, C.C.; Subhash, H.M.; Peru, D.; Ellwood, R.P.; Pierce, M.C. An Experimental Review of Optical Coherence Tomography Systems for Noninvasive Assessment of Hard Dental Tissues. *Caries Res.* **2019**, *54*, 43–54. [CrossRef]
28. Fercher, A. Optical coherence tomography-development, principles, applications. *Z. Für Med Phys.* **2010**, *20*, 251–276. [CrossRef] [PubMed]
29. Fujimoto, J.G. Optical Coherence Tomography: Principles and Applications. *Rev. Laser Eng.* **2003**, *31*, 635–642. [CrossRef]
30. Fayad, L.M. CT Scan Versus MRI Versus X-Ray: What Type of Imaging Do I Need? Available online: https://www.hopkinsmedicine.org/health/treatment-tests-and-therapies/ct-vs-mri-vs-xray#:~:text=A%20CT%20scan,%20or%20computed,fast%20(about%20one%20minute) (accessed on 1 April 2025).
31. Staedler, Y.M.; Masson, D.; Schönenberger, J. Plant tissues in 3D via X-ray tomography: Simple contrasting methods allow high resolution imaging. *PLoS ONE* **2013**, *8*, e75295. [CrossRef] [PubMed]
32. Cnudde, V.; Boone, M.N. High-resolution X-ray computed tomography in geosciences: A review of the current technology and applications. *Earth-Sci. Rev.* **2013**, *123*, 1–17. [CrossRef]
33. Zappala, S.; Helliwell, J.R.; Tracy, S.R.; Mairhofer, S.; Sturrock, C.J.; Pridmore, T.; Bennett, M.; Mooney, S.J. Effects of X-Ray Dose on Rhizosphere Studies Using X-Ray Computed Tomography. *PLoS ONE* **2013**, *8*, e67250. [CrossRef]
34. Sasi, G.S. Responses of some plants to treatment with industrial ceramic—Waste water sludge. In *Botany*; Ain Shams University, Egyptian Universities Libraries Consortium (EULC): Cairo, Egypt, 2019; pp. 62–147.
35. Chaturvedi, A.; Jain, V. Effect of Ionizing Radiation on Human Health. *Int. J. Plant Environ.* **2019**, *5*, 200–205. [CrossRef]
36. Heath, M.; St-Onge, D.; Hausler, R. UV reflectance in crop remote sensing: Assessing the current state of knowledge and extending research with strawberry cultivars. *PLoS ONE* **2024**, *19*, e0285912. [CrossRef]
37. Liu, H.; Lee, S.-H.; Chahl, J.S. An evaluation of the contribution of ultraviolet in fused multispectral images for invertebrate detection on green leaves. *Precis. Agric.* **2016**, *18*, 667–683. [CrossRef]
38. Hyperspectral Imaging in Agriculture and Vegetation. Available online: https://www.specim.com/hyperspectral-imaging-applications/agriculture-and-vegetation/#:~:text=Crop%20Health%20Assessment,nutrient%20deficiencies,%20or%20water%20scarcity (accessed on 1 April 2025).
39. Wang, X.; Hu, Q.; Cheng, Y.; Ma, J. Hyperspectral Image Super-Resolution Meets Deep Learning: A Survey and Perspective. *IEEE/CAA J. Autom. Sin.* **2023**, *10*, 1668–1691. [CrossRef]
40. Rostron, P.; Gaber, S.; Gaber, D. Raman Spectroscopy, Review. *Int. J. Eng. Tech. Res. (IJETR)* **2016**, *6*.
41. Kuhar, N.; Sil, S.; Verma, T.; Umapathy, S. Challenges in application of Raman spectroscopy to biology and materials. *RSC Adv.* **2018**, *8*, 25888–25908. [CrossRef] [PubMed]
42. Sil, S.; Umapathy, S. Umapathy, Raman spectroscopy explores molecular structural signatures of hidden materials in depth: Universal Multiple Angle Raman Spectroscopy. *Sci. Rep.* **2014**, *4*, 5308. [CrossRef] [PubMed]
43. Dong, D.; Zhao, C. Limitations and challenges of using Raman spectroscopy to detect the abiotic plant stress response. *Proc. Natl. Acad. Sci. USA* **2017**, *114*, E5486–E5487. [CrossRef] [PubMed]
44. Saito, Y.; Saito, R.; Kawahara, T.D.; Nomura, A.; Takeda, S. Development and performance characteristics of laser-induced fluorescence imaging lidar for forestry applications. *For. Ecol. Manag.* **2000**, *128*, 129–137. [CrossRef]
45. Wan, W.; Su, J. Study of laser-induced plant fluorescence lifetime imaging technology for plant remote sensing monitor. *Measurement* **2018**, *125*, 564–571. [CrossRef]
46. Peelle, J. Introduction to MRI. Available online: http://jpeelle.net/mri/general/preliminaries.html (accessed on 1 April 2025).

47. Van As, H.; Scheenen, T.; Vergeldt, F.J. MRI of intact plants. *Photosynth. Res* **2009**, *102*, 213–222. [CrossRef]
48. Zhang, S.; Uecker, M.; Voit, D.; Merboldt, K.-D.; Frahm, J. Real-time cardiovascular magnetic resonance at high temporal resolution: Radial FLASH with nonlinear inverse reconstruction. *J. Cardiovasc. Magn. Reson.* **2010**, *12*, 39. [CrossRef]
49. Toma, M.; Vinatoru, M.; Paniwnyk, L.; Mason, T. Investigation of the effects of ultrasound on vegetal tissues during solvent extraction. *Ultrason. Sonochem.* **2001**, *8*, 137–142. [CrossRef]
50. Fujimoto, J.G.; Pitris, C.; Boppart, S.A.; Brezinski, M.E. Optical coherence tomography: An emerging technology for biomedical imaging and optical biopsy. *Neoplasia* **2000**, *2*, 9–25. [CrossRef]
51. Laschke, M.W.; Körbel, C.; Rudzitis-Auth, J.; Gashaw, I.; Reinhardt, M.; Hauff, P.; Zollner, T.M.; Menger, M.D. High-resolution ultrasound imaging: A novel technique for the noninvasive in vivo analysis of endometriotic lesion and cyst formation in small animal models. *Am. J. Pathol.* **2010**, *176*, 585–593. [CrossRef]
52. El-Sattar, A.M.A.; Tawfik, E. Effects of ultrasonic waves on seedling growth, biochemical constituents, genetic stability of fenugreek (*Trigonella foenum-graecum*) under salinity stress. *Vegetos* **2022**, *36*, 1427–1436. [CrossRef]
53. Pircher, M.; Hitzenberger, C.K.; Schmidt-Erfurth, U. Polarization sensitive optical coherence tomography in the human eye. *Prog. Retin. Eye Res.* **2011**, *30*, 431–451. [CrossRef] [PubMed]
54. Cense, B.; Chen, T.C.; Park, B.H.; Pierce, M.C.; de Boer, J.F. In Vivo depth-resolved birefringence measurements of the human retinal nerve fiber layer by polarization-sensitive optical coherence tomography. *Opt. Lett.* **2002**, *27*, 1610–1612. [CrossRef] [PubMed]
55. Aguirre, A.D.; Fujimoto, J.G. Optical Coherence Microscopy. In *Optical Coherence Tomography: Technology and Applications*; Drexler, W., Fujimoto, J.G., Eds.; Springer International Publishing: Cham, Switzerland, 2015; pp. 865–911.
56. Leitgeb, R.A. En face optical coherence tomography: A technology review [Invited]. *Biomed. Opt. Express* **2019**, *10*, 2177–2201. [CrossRef]
57. Dubois, A.; Boccara, A.C. Full-Field Optical Coherence Tomography. In *Optical Coherence Tomography: Technology and Applications*; Drexler, W., Fujimoto, J.G., Eds.; Springer: Berlin/Heidelberg, Germany, 2008; pp. 565–591.
58. Morgner, U.; Drexler, W.; Kärtner, F.X.; Li, X.D.; Pitris, C.; Ippen, E.P.; Fujimoto, J.G. Spectroscopic optical coherence tomography. *Opt. Lett.* **2000**, *25*, 111–113. [CrossRef]
59. Oldenburg, A.L.; Xu, C.; Boppart, S.A. Spectroscopic Optical Coherence Tomography and Microscopy. *IEEE J. Sel. Top. Quantum Electron.* **2007**, *13*, 1629–1640. [CrossRef]
60. Fujii, H.; Nohira, K.; Shintomi, Y.; Asakura, T.; Ohura, T. Blood flow observed by time-varying laser speckle. *Opt. Lett.* **1985**, *10*, 104–106. [CrossRef]
61. Azzollini, S.; Monfort, T.; Thouvenin, O.; Grieve, K. Dynamic optical coherence tomography for cell analysis [Invited]. *Biomed. Opt. Express* **2023**, *14*, 3362–3379. [CrossRef]
62. Spaide, R.F.; Fujimoto, J.G.; Waheed, N.K.; Sadda, S.R.; Staurenghi, G. Optical coherence tomography angiography. *Prog Retin. Eye Res.* **2018**, *64*, 1–55. [CrossRef]
63. Hope, J.; Goodwin, M.; Vanholsbeeck, F. Inverse spectroscopic optical coherence tomography (IS-OCT) for characterization of particle size and concentration. *OSA Contin.* **2021**, *4*, 2260–2274. [CrossRef]
64. Gong, P.; Almasian, M.; Van Soest, G.; De Bruin, D.M.; Van Leeuwen, T.G.; Sampson, D.D.; Faber, D.J. Parametric imaging of attenuation by optical coherence tomography: Review of models, methods, and clinical translation. *J. Biomed. Opt.* **2020**, *25*, 040901. [CrossRef] [PubMed]
65. Hettinger, J.; Mattozzi, M.d.l.P.; Myers, W.R.; Williams, M.E.; Reeves, A.; Parsons, R.L.; Haskell, R.C.; Petersen, D.C.; Wang, R.; Medford, J.I. Optical Coherence Microscopy. A Technology for Rapid, in Vivo, Non-Destructive Visualization of Plants and Plant Cells. *Plant Physiol.* **2000**, *123*, 3–16. [CrossRef] [PubMed]
66. Magwaza, L.; Ford, H.D.; Cronje, P.J.; Opara, U.L.; Landahl, S.; Tatam, R.P.; Terry, L.A. Application of optical coherence tomography to non-destructively characterise rind breakdown disorder of 'Nules Clementine' mandarins. *Postharvest Biol. Technol.* **2013**, *84*, 16–21. [CrossRef]
67. Loeb, G.; Barton, J. Imaging botanical subjects with optical coherence tomography: A feasibility study. *Trans. Am. Soc. Agric. Eng.* **2003**, *46*, 1751–1757. [CrossRef]
68. Kutis, I.; Sapozhnikova, V.V.; Kuranov, R.V.; Kamenskii, V.A. Study of the Morphological and Functional State of Higher Plant Tissues by Optical Coherence Microscopy and Optical Coherence Tomography. *Russ. J. Plant Physiol.* **2005**, *52*, 559–564. [CrossRef]
69. Clements, J.C.; Zvyagin, A.V.; Silva, K.K.M.B.D.; Wanner, T.; Sampson, D.D.; Cowling, W.A. Optical coherence tomography as a novel tool for non-destructive measurement of the hull thickness of lupin seeds. *Plant Breed.* **2004**, *123*, 266–270. [CrossRef]
70. Ullah, H.; Hussain, F.; Ahmad, E.; Ikram, M. A rapid and non-invasive bio-photonic technique to monitor the quality of onions. *Opt. Spectrosc.* **2015**, *119*, 295–299. [CrossRef]
71. Wedding, B.B.; Wright, C.; Grauf, S.; White, R.D. Wavelength variation of the depth of penetration of near infrared radiation in'Hass' avocado fruit. *Technol. Hortic.* **2024**, *4*, e008. [CrossRef]

72. Veraverbeke, E.; Van Bruaene, N.; Van Oostveldt, P.; Nicolaï, B.M. Non destructive analysis of the wax layer of apple (*Malus domestica* Borkh.) by means of confocal laser scanning microscopy. *Planta* **2001**, *213*, 525–533. [CrossRef]
73. Reeves, A.; Parsons, R.L.; Hettinger, J.W.; Medford, J.I. In Vivo three-dimensional imaging of plants with optical coherence microscopy. *J. Microsc.* **2002**, *208 Pt 3*, 177–189. [CrossRef]
74. Anna, T.; Chakraborty, S.; Cheng, C.-Y.; Srivastava, V.; Chiou, A.; Kuo, W.-C. Elucidation of microstructural changes in leaves during senescence using spectral domain optical coherence tomography. *Sci. Rep.* **2019**, *9*, 1167. [CrossRef] [PubMed]
75. Spicer, G.L.C.; Eid, A.; Wangpraseurt, D.; Swain, T.D.; Winkelmann, J.A.; Yi, J.; Kühl, M.; Marcelino, L.A.; Backman, V. Measuring light scattering and absorption in corals with Inverse Spectroscopic Optical Coherence Tomography (ISOCT): A new tool for non-invasive monitoring. *Sci. Rep.* **2019**, *9*, 14148. [CrossRef] [PubMed]
76. Wijesinghe, R.E.; Lee, S.-Y.; Ravichandran, N.K.; Shirazi, M.F.; Moon, B.; Jung, H.-Y.; Jeon, M.; Kim, J. Bio-photonic detection method for morphological analysis of anthracnose disease and physiological disorders of Diospyros kaki. *Opt. Rev.* **2017**, *24*, 199–205. [CrossRef]
77. Anthracnose Plant Disease. Science & Tech. Available online: https://www.britannica.com/science/anthracnose (accessed on 1 April 2025).
78. Wijesinghe, R.; Lee, S.-Y.; Ravichandran, N.K.; Shirazi, M.F.; Kim, P.; Jung, H.-Y.; Jeon, M.; Kim, J. Optical screening of Venturianashicola caused Pyruspyrifolia (Asian pear) scab using optical coherence tomography. *Int. J. Appl. Eng. Res.* **2016**, *11*, 7728–7731.
79. Wijesinghe, R.E.; Lee, S.-Y.; Kim, P.; Jung, H.-Y.; Jeon, M.; Kim, J. Optical sensing method to analyze germination rate of *Capsicum annum* seeds treated with growth-promoting chemical compounds using optical coherence tomography. *J. Biomed. Opt.* **2017**, *22*, 91502. [CrossRef]
80. Wijesinghe, R.E.; Lee, S.-Y.; Ravichandran, N.K.; Shirazi, M.F.; Kim, P.; Jung, H.-Y.; Jeon, M.; Kim, J. Biophotonic approach for the characterization of initial bitter-rot progression on apple specimens using optical coherence tomography assessments. *Sci. Rep.* **2018**, *8*, 15816. [CrossRef]
81. Ravichandran, N.K.; Wijesinghe, R.E.; Shirazi, M.F.; Park, K.; Lee, S.-Y.; Jung, H.-Y.; Jeon, M.; Kim, J. In Vivo Monitoring on Growth and Spread of Gray Leaf Spot Disease in Capsicum annuum Leaf Using Spectral Domain Optical Coherence Tomography. *J. Spectrosc.* **2016**, *2016*, 1–6. [CrossRef]
82. Lee, D.-H.; Back, C.-G.; Win, N.K.K.; Choi, K.-H.; Kim, K.-M.; Kang, I.-K.; Choi, C.; Yoon, T.-M.; Uhm, J.Y.; Jung, H.-Y. Biological Characterization of Marssonina coronaria Associated with Apple Blotch Disease. *Mycobiology* **2011**, *39*, 200–205. [CrossRef]
83. Lee, S.-Y.; Lee, C.; Kim, J.; Jung, H.-Y. Application of optical coherence tomography to detect Cucumber green mottle mosaic virus (CGMMV) infected cucumber seed. *Hortic. Environ. Biotechnol.* **2012**, *53*, 428–433. [CrossRef]
84. Lee, C.; Lee, S.-Y.; Kim, J.-Y.; Jung, H.-Y.; Kim, J. Optical sensing method for screening disease in melon seeds by using optical coherence tomography. *Sensors* **2011**, *11*, 9467–9477. [CrossRef]
85. Ford, H.; Tatam, R.; Landahl, S.; Terry, L. Investigation of disease in stored onions using optical coherence tomography. In Proceedings of the IV International Conference Postharvest Unlimited, Leavenworth, WA, USA, 22–26 May 2011; Volume 945, pp. 247–254.
86. Yoon, T.; Lee, B.H. Identification of Fungus-infected Tomato Seeds Based on Full-Field Optical Coherence Tomography. *Curr. Opt. Photonics* **2019**, *3*, 571–576.
87. Tzu Hao, C.; Tan, K.M.; Ng, B.K.; Razul, S.G.; Tay, C.M.; Chia, T.F.; Poh, W.T. Diagnosis of virus infection in orchid plants with high-resolution optical coherence tomography. *J. Biomed. Opt.* **2009**, *14*, 014006.
88. Meglinski, I.; Buranachai, C.; Terry, L. Plant photonics: Application of optical coherence tomography to monitor defects and rots in onion. *Laser Phys. Lett.* **2010**, *7*, 307–310. [CrossRef]
89. Sapozhnikova, V.; Kamensky, V.; Kuranov, R. Optical coherence tomography for visualization of plant tissues. In Proceedings of the International Conference on Lasers, Applications, and Technologies 2002, Moscow, Russia, 22–27 June 2002; Volume 5149.
90. Srimal, L.K.T.; Rajagopalan, U.M.; Kadono, H. Optical Coherence Tomography biospeckle signal analysis to investigate response of plant leaves to ozone. In Proceedings of the 23rd Congress of International Commission for Optics (ICO23), Santiago de Compostela, Spain, 26–29 August 2014.
91. Verboven, P.; Nemeth, A.; Abera, M.K.; Bongaers, E.; Daelemans, D.; Estrade, P.; Herremans, E.; Hertog, M.; Saeys, W.; Vanstreels, E.; et al. Optical coherence tomography visualizes microstructure of apple peel. *Postharvest Biol. Technol.* **2013**, *78*, 123–132. [CrossRef]
92. Li, M.; Verboven, P.; Buchsbaum, A.; Cantre, D.; Nicolaï, B.; Heyes, J.; Mowat, A.; East, A. Characterising kiwifruit (*Actinidia* sp.) near skin cellular structures using optical coherence tomography. *Postharvest Biol. Technol.* **2015**, *110*, 247–256. [CrossRef]
93. Wijesinghe, R.; Lee, S.-Y.; Ravichandran, N.K.; Han, S.; Jeong, H.; Han, Y.; Jung, H.-Y.; Kim, P.; Jeon, M.; Kim, J. Optical coherence tomography-integrated, wearable (backpack-type), compact diagnostic imaging modality for in situ leaf quality assessment. *Appl. Opt.* **2017**, *56*, D108–D114. [CrossRef]

94. Larimer, C.J.; Denis, E.H.; Suter, J.D.; Moran, J.J. Optical coherence tomography imaging of plant root growth in soil. *Appl. Opt.* **2020**, *59*, 2474–2481. [CrossRef]
95. Srimal, L.K.; Kadono, H.; Rajagopalan, U. Optical coherence tomography biospeckle imaging for fast monitoring varying surface responses of a plant leaf under ozone stress. In Proceedings of the 2013 SPIE, SPIE SeTBio, Yokohama, Japan, 23–26 April 2013; Volume 8881.
96. Srimal, L.K.T.; Rajagopalan, U.M.; Kadono, H. Functional optical coherence tomography (fOCT) biospeckle imaging to investigate response of plant leaves to ultra-short term exposure of Ozone. *J. Phys. Conf. Ser.* **2015**, *605*, 012013. [CrossRef]
97. Boccara, M.; Schwartz, W.; Guiot, E.; Vidal, G.; De Paepe, R.; Dubois, A.; Boccara, A. Early chloroplastic alterations analysed by optical coherence tomography during a harpin-induced hypersensitive response. *Plant J.* **2007**, *50*, 338–346. [CrossRef]
98. Williams, J.; Lin, W.C.; Li, W.; Wang, S.; Matcher, S.J.; Chauvet, A.A.P. Translating Optical Coherence Tomography Technologies from Clinical Studies to Botany: Real Time Imaging of Long-Distance Signaling in Plants. In Proceedings of the Optical Coherence Tomography, Washington, DC, USA, 20–23 April 2020.
99. Cheong, H.; Devalla, S.K.; Chuangsuwanich, T.; Tun, T.A.; Wang, X.; Aung, T.; Schmetterer, L.; Buist, M.L.; Boote, C.; Thiéry, A.H.; et al. OCT-GAN: Single step shadow and noise removal from optical coherence tomography images of the human optic nerve head. *Biomed. Opt. Express* **2021**, *12*, 1482–1498. [CrossRef]
100. Ramachandiran, R.; Gayathri, K.; Ishwariya, A.; Roopa, G. A Survey on Speckle Removal for Optical Coherence Tomography Images. In Proceedings of the 2019 IEEE International Conference on System, Computation, Automation and Networking (ICSCAN), Pondicherry, India, 29–30 March 2019.
101. Rueckert, D.; Schnabel, J.A. Registration and Segmentation in Medical Imaging. In *Registration and Recognition in Images and Videos*; Cipolla, R., Battiato, S., Farinella, G.M., Eds.; Springer: Berlin/Heidelberg, Germany, 2014; pp. 137–156.
102. Rufai, S.R. Handheld optical coherence tomography removes barriers to imaging the eyes of young children. *Eye* **2022**, *36*, 907–908. [CrossRef]
103. Handheld Optical Coherence Tomography. 2024. Available online: https://cordis.europa.eu/project/id/871312 (accessed on 1 April 2025).

2. Optical coherence tomography for early detection of crop infection

Sasi *et al. Plant Methods* (2025) 21:92
https://doi.org/10.1186/s13007-025-01411-7

Plant Methods

METHODOLOGY

Open Access

# Optical coherence tomography for early detection of crop infection

Ghada Salem Sasi[1], Stephen J. Matcher[2] and Adrien Alexis Paul Chauvet[1*]

**Abstract**

**Background** Fungal diseases are among the most significant threats to global crop production, often leading to substantial yield losses. Early detection of crop infection by fungus is the very first step to deploying a timely and effective treatment. Early and reliable detection is thus key to improving yields, sustainability, and achieving food security. Conventional diagnostic methods are however often destructive, slow, or requiring visible symptoms which appear late in the infection process. To overcome these challenges, we propose using optical coherence tomography (OCT) as an innovative imaging tool to provide cross-sectional and three-dimensional images of the plant internal microstructure non-invasively, in vivo, and in real-time.

**Results** We demonstrate the use of low-cost OCT to monitoring wheat (cultivar AxC 169) when infected by *Septoria tritici*. We show that OCT analysis can effectively detect signs of infection before any external symptoms appear. Although OCT cannot directly visualize fungal hyphae, OCT reveals apparent morphological changes of the mesophyll where the fungal filaments are expected to develop. This study thus focuses on monitoring and correlating changes within the mesophyll structural organisation with the state of infection. It results in distinct statistical difference between intact and infected wheat plants two days only after infection. We then demonstrate the use of machine learning (ML) for high throughput segmentation of OCT scans, providing a foundation for future automated fungus-detection analysis.

**Conclusions** This work highlights the potential of OCT, combined with ML tools, to enable rapid, non-invasive, and early diagnosis of crop fungal infections, opening new avenues for precision agriculture and sustainable disease management.

**Keywords** Optical coherence tomography, Wheat, *Septoria*, Machine learning

## Introduction

Wheat is cultivated in about 122 countries, with China, India, and the USA being major producers [1–3]. In the UK, wheat constitutes 58% of crops grown and yields approximately 15 million tons annually [4–6]. Its rich nutritional content makes it a key source of protein, carbohydrates, and fibers, forming the basis of foods like bread, pastries, and pasta [2, 7–10]. Wheat is, however, susceptible to various diseases amongst which the most potent are the wheat blast, *Fusarium* Head Blight, and *Zymoseptoria tritici* [11–14]. The latter especially is a devastating fungus which can cause up to 40% yield loss in wheat crops [15]. *Septoria* is thus a major concern for agriculture in the UK and Europe. Furthermore, this fungus propagates rapidly under favorable humid conditions, which is specifically relevant to the UK and continental Europe. Global efforts to help farmers anticipate *Septoria* outbreaks are being actively developed. These measures

*Correspondence:
Adrien Alexis Paul Chauvet
a.chauvet@sheffield.ac.uk
[1] School of Mathematic and Physical Sciences, University of Sheffield, Sheffield S3 7HF, UK
[2] School of Electrical and Electronic Engineering, The University of Sheffield, 3 Solly Street, Sheffield S1 4DE, UK

focus on both prophylactic and curative strategies. For example, the Agriculture and Horticulture Development Board (AHDB) [16] and UK Crop Science [17], which conducts thorough research on *Septoria*, already provides with clear guidelines on how to prevent and how to treat *Septoria* outbreak. Such outbreaks are commonly controlled using fungicides [14]. However, the key to successful fungicide treatment is the timeliness of the treatment. Delaying the treatments until external symptoms are visible can significantly decrease their efficacy [18]. Yield recovery may be limited to 10–30% compared to preventative treatment, which can save up to 70–90% of potential yield [19–21]. With respect to preventive treatments, it has been shown that triazole-based products, for example, are sustainable and effective when applied before infection. But the overuse of such prophylactic strategies nevertheless results in a decline in treatments efficacy from 60 to 90% [20]. It is then critical to detect and treat the infection as early as possible so as to limit the overuse of fungicides while preserving crop yields [22].

The fungus of concern in this study is formerly known as *Mycosphaerella graminicola* also known as *Zymoseptoria tritici* is the pathogen causing *Septoria tritici blotch* (STB), and results in yellow necrotic spots on the leaves [23]. STB life cycle is expected to last about three to four weeks in open-air fields [24, 25]; When infection occurs, spores develop into hyphae which enter through the leaves stomata and proliferate within the mesophyll as depicted in Fig. 1.

After colonizing the whole leaf, STB grows into fruiting bodies (pycnidia), through an asexual sporulation, to give fungal spores at the tip of hyphae (conidia) [27]. The symptoms, e.g. yellow spots that turn brown, usually appear on the leaves within two to three weeks only after infection [28, 29]. It is the subsequent necrosis of the leaves and the plant that causes significant yield loss every year [30]. It is important to note that the different stages coexist [26]. Since a single hyphae penetration (stage 3) suffice to initiate colonisation of the mesophyll (stage 4), it is expected that surface exploration (stage 2) of the majority of the hyphae, which have not yet "found" stomata to enter, progresses concomitantly with the first colonisation event.

There exist already various techniques to help detect and quantify STB. On the one hand, the most accurate includes imaging techniques, such as high-resolution microscopy [54], and molecular testing, such as polymerase chain reaction (PCR) [31]. However, these techniques are also the most cumbersome given the necessity to process the sample beforehand and the need to access large-scale facilities. On the other hand, more practical and field-applicable techniques often suffer from lower precision. For example, RGB Imaging [32] can be useful for plant health studies but is generally insensitive to early-stage infections [33]. In another instance, multi- or hyperspectral imaging (HSI) is increasingly used in field [34–36]. These techniques are non-invasive and field-deployable, which makes them ideal for remote evaluation of a crop's health [37, 38]. These techniques rely on the spectral changes that are either intrinsic to the plant (e.g. via changes in fluorescence [39]) or surface level (e.g. via changes in pigmentation [33]). However, spectral changes are direct consequences of molecular alteration, and thus, they occur when the plant is already prone to severe stresses, and oftentimes, already damaged [40]. However convenient and reliable, HSI thus detects the spectral signature associated with the chlorosis of wheat leaves [41]. It thus assesses the extent of infection within an already damaged crop. The same impediment is true when using other indices such as temperature and humidity, since they are primarily based of spectroscopic data [42]. Ideally, we require a technique capable of detecting early stages of infection, before the plant shows any external signs of stresses. To this end, we suggest using OCT instead, to benefit from its non-invasiveness, its real-time imaging, and potential field applicability. OCT is commonly used in the medical field, and more specifically in ophthalmology. However, given the advantages of OCT, i.e. non-invasive, in-vivo, 3D rendering, and real-time imaging [43], it is equally suitable for plants [44]. Given the practicality of the technique, OCT is increasingly used in plant imaging for various purposes. It is for example used for straightforward non-invasive assessment of plant's internal structure [45] as well as for investigation of plant's response to biotic and abiotic stressors [46, 47]. OCT can even be used for live responses to stressors, with a temporal resolution ranging from several days [48] down to hours [49, 50] and even seconds [51]. Furthermore, benefitting from a simple technical layout and robust optical components, OCT suitable to multimodal imaging [44]. Multimodal OCT variant includes for instance, polarization-sensitive OCT [52], spectroscopic OCT[53, 54], biospeckle or dynamic OCT [55, 56], and inverse spectroscopic OCT [57, 58]. In each case, the acquired data is further processed to provide an added layer of contrast, which can help differentiate structural elements that would otherwise remain indistinguishable.

We here demonstrate the suitability of standard OCT by using a low-cost compact commercial system to acquired cross-sectional images of leaves ($\sim 6 \times 2$ mm) with a $\sim 10$ µm resolution. This integrated system is considered low-cost (<£10 k) [59] compared to the better performing ones which starts at £40 k onward [60]. And although the system only resolves the first

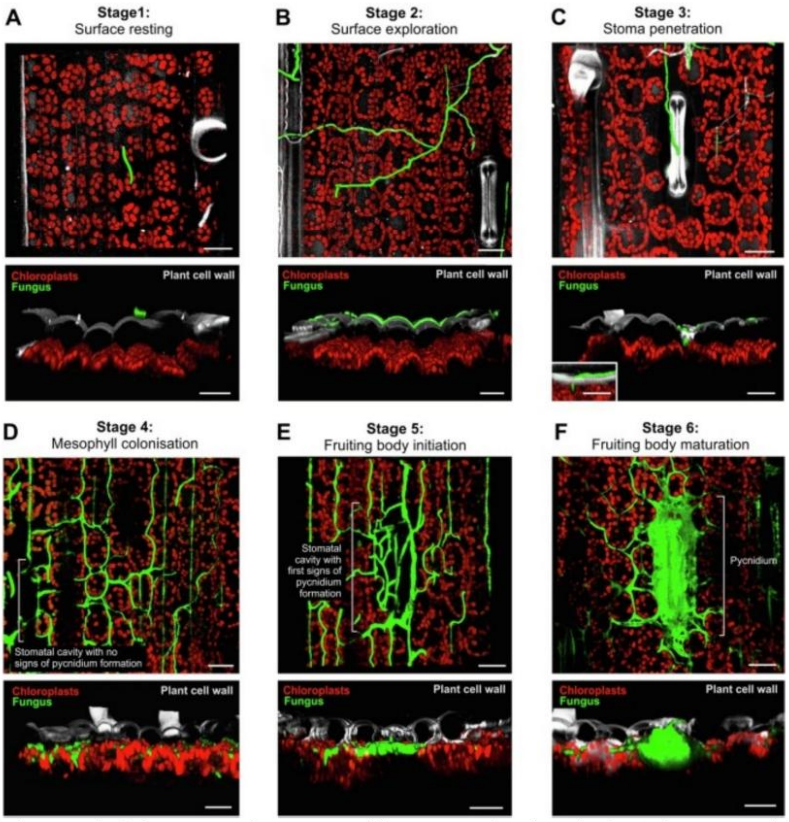


**Fig. 1** Confocal image stacks of infection process of *Septoria tritici* at different stages in wheat plants. The plants' epidermis (grey) and chloroplasts (red) are detected by their auto-fluorescence. The green fluorescence is an effect of cytoplasmic eGFP expression in the cells of the fungus. Scale bars: 20 µm. Figure reproduced from [26]. **A** Stage 1,"Surface Resting": Spores settle on the surface of leaves. **B** Stage 2,"Surface Exploration": Spores form an infectious hypha to infect leaves through stomata. **C** Stage 3,"Stoma Penetration": Penetration of the host by the hyphae through the stomata apertures. **D** Stage 4,"Mesophyll Colonization": Colonization of mesophyll by fungus, but with no visible symptoms of infection. **E** Stage 5,"Fruiting Body Initiation": The hyphae grow and fills the inner space. This is a necrotrophic phase, where signs of infection on the leaf can be seen. **F** Stage 6,"Fruiting Body Maturation": The substomatal cavity fills with filaments, fruiting body, and pycnidium, to initiate spore production

3–5 cell layers, this resolution is sufficient to monitor internal structural differences between intact and infected leaves. The project thus consists of examining the internal structure of leaves through cross-sectional OCT images. The hypothesis is to indirectly monitor the growth of the fungus within the mesophyll, which is expected to push apart the different cell layers. And although the fungus filaments are too small (~ 2 µm in diameter [61]) to be seen with the current OCT resolution, the overall structure of the mesophyll is readily monitored.

In this work, we suggest analysing differences in mesophyll structure between control and infected leaves to provide insights about the state of infection and tissue integrity. In healthy control leaves, thinner and more uniform cell layers typically indicate intact tissue structure. Conversely, in infected leaves, the monitored increase in layer thickness and irregularity of the cell layers may suggest structural degradation, possibly due to the accumulation of fungal material between the cells [62, 63].

## Material and methods

The wheat for this proof-of-concept experiment belongs to the *Avalon* and *Cadenza* (AxC) 169 variety. This variety lacks a resistance gene against *Septoria*, making it more susceptible to *Septoria*, and ensuring effective pathogenesis. The seeds are grown in M3 compost supplemented with 0.5 g osmocote. Six plants were grown for this specific experimental run: three control plants and three plants destined to be infected. The plants were incubated at 20 °C, in a 14-h:10-h a light–dark cycle, at 61% of relative humidity, and levels of carbon dioxide was kept at 455 ppm (i.e. 55 ppm above the usual ~ 400 ppm outdoors level, which enhances plant growth [64]), these adjustments were made as part of the experimental conditions set for all growth chambers. The inoculation was performed when the plants were 21-day old.

Regarding the inoculum, *Zymoseptoria tritici* IPO323 [65] was incubated during 45–60 days on potato dextrose broth (PDB) media composed of 24 g/L of PDB and 15 g/L f Agar mixed with 1000 ml of ultrapure water (resistivity 18 MΩ·cm, Type I). Inoculation was performed via spray to mimic the natural spread of spores in high humidity atmosphere. The spray solution is prepared by adding 10 mL of 0.01% Tween 20 in water to a petri dish containing black heads (pycnidia spores). The spores are then gently scraped off using a sterile spatula and poured into a Falcon tube [17, 65]. Twenty µL of the supernatant was placed onto a counting chamber, ensuring the liquid spread evenly between the chamber and the cover slip. Excess liquid was removed using tissue paper. Spores were observed at 20X magnification using a Leica microscope. After allowing the spores to settle, they were counted, and the inoculum was adjusted accordingly, using sterile Tween 20 water, to achieve a concentration of $1 \times 10^6$ spores/mL [36].

For inoculation, the plants were taken out of the growth chamber and placed inside a laminar airflow. The inoculum was sprayed on the top sides of the second newest leaf (GS31, following Zadoks system [66]). After inoculation, plants were covered with propagator lids (to maintain high humidity). The plants were then watered and placed in a sealed propagator and placed back in the growth chamber for 24 h recovery [67]. Although the control plants were left untreated, both the inoculated and controlled plants were regularly sprayed with purified water, via the control system of the growth chamber, so as to keep a high (61%) humidity level.

Scanning electron microscope (SEM) is used for high resolution imagining of surface morphology[68, 69]. In this study, it was used specifically to verify the state of infection at later stages. This study made use of a Hitachi TM3030Plus benchtop SEM.

The OCT system used is an OQ LabScope, version 2.0, from Lumedica using a superluminescent diode with central wavelength at 840 nm. The system generates 512 × 512-pixel images, with axial resolution of ~ 6 µm, and a lateral resolution of 15 µm. Daily OCT scans were collected to monitor the progression of the infection for a 14-day period after inoculation. Readings were taken from the three infected plants and from the three control plants. Scanning was performed midway along the leaf's length, beside the main vein. Incomplete scans (i.e. in which the edge of the leaf appear) are dismissed for the automated analysis. A typical volumetric (c-scan) is shown in Fig. 2.

This study focusses on analysing the extend of the dark regions appearing within the mesophyll, called "gaps", as shown in Fig. 2 (marked by arrows), by first manually processing the OCT scans using the FIJI image analysis software. Building upon the encouraging results from the manual analysis, a machine learning (ML) algorithm was developed in collaboration with Cyber Infrastructure Systems (CIS, http://www.cisin.com) to automatically segment these apparent gaps and classify the leaves. The Python code designed for OCT segmentation is a PyQt5-based GUI application that uses OpenCV, TensorFlow, NumPy, and Pandas for image processing and ML-based analysis. After training, the U-Net model (unet_masking3.keras) is used for generating segmentation masks via MaskThread class. The code is provided in supplementary information (SI), and the software is made available for download following this link:

https://drive.google.com/drive/folders/1DJm3OZHfK-P-XSRXGMtpxgSx51WnVNsF?usp=sharing

In both the manual and the automated procedure, the analysis focuses on the thickness of these apparent gaps between the second and third upper layers of the mesophyll.

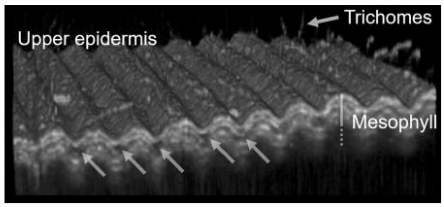


**Fig. 2** 3D OCT images (C-scan) of a control wheat leaf. Each spike above the upper epidermis represents a trichome. Only the first few cell layers of the mesophyll are distinguishable. The arrows point to the "gaps" discussed subsequently. The image has a range of 5 mm x 5 mm and is generated using 300 consecutive b-scans, each separated by ~ 0.017 mm

## Results

The effectiveness of the inoculation procedure is demonstrated in Fig. 3, where filaments can be seen emerging from the stomatal pores of infected leaves.

It is also worth noting that healthy leaves already have air gaps within their mesophyll (as shown in Fig. 2) used to facilitate gas exchange [70]. These air gaps, which are expected to appear dark in OCT B-scan, are thus indistinguishable with the low-density components of the cells (e.g. the cytoplasm). All what OCT scans shows are regions of high density (e.g. cell's nucleus and vacuole). The apparent gaps monitored in OCT images, shown in Fig. 4, thus correspond to low-density regions, which includes the air network, the surrounding of the plant cells' nucleus and vacuole, and possibly the fungus hyphae. These apparent gaps are however highly heterogeneous and not easily distinguished given the uneven leaf morphology. As such it was decided to restrict the analysis to the thickness (or height) of the apparent gap.

These apparent gaps notably increase when the plant is infected, while the leaves are still green and seemingly healthy, as shown in the subsequent Table 1. Table 1 shows the average thickness of the gaps present in a selection of 20 OCT B-scans out of each volumetric reading, for both control and infected leaves, ranging from day 0 (i.e. right before inoculation) to day 1 (i.e. 24 h after inoculation) and up to day 7. Every day, one reading was performed per plant, on the three different controlled and on the three different infected plants.

Only the first 7 days are here presented, while the leaves do not show any visual signs of infection. Images of the subsequent chlorosis and necrotic stages, from day 8 to 14, can be found in SI. When analysing the individual measurements used to compute the averages shown in the above table, the measured gap thicknesses reveal distinct trend between control and infected leaves, as depicted in Fig. 5. From day 2 after inoculation onward, infected leaves exhibit consistently larger gap thicknesses, exceeding 0.05 mm in average, while measurements on control leaves remains below or around that value. Furthermore, the width of the Gaussian-fit for the infected leaves group is typically broader (FWHM ~ 0.2 compared to that of the control group (FWHM ~ 0.15). Accordingly, the apparent gaps in infected leaves are more heterogenous than those in control leaves.

The superimposed histograms from the control and infected groups reveal distinct statistical differences in the gap size and distribution. From the average gap

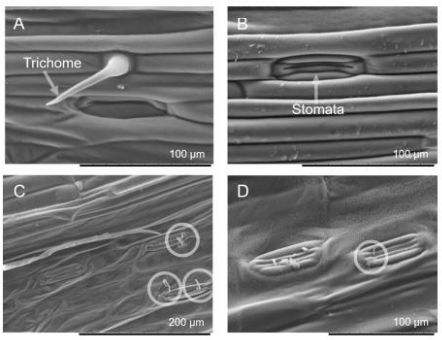


**Fig. 3** SEM images showing control wheat plant (**A**, **B**), and infected wheat plant 12 days after inoculation by *Septoria* (**B**, **C**). The circled hyphae emerging from the stomata pores illustrate an advanced colonisation (stage 4) with signs of necrosis (deflated cells, stage 5)

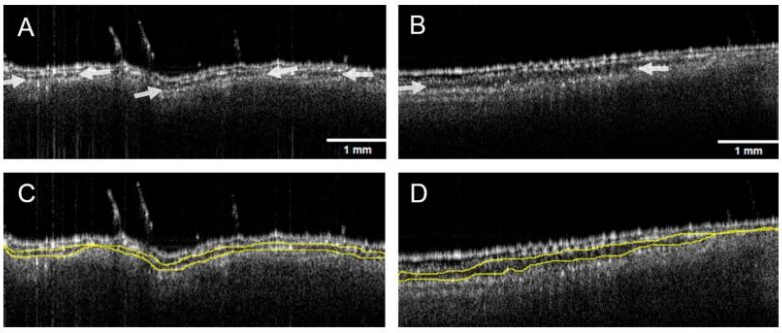


**Fig. 4** Individual OCT cross section (B-scan) of control wheat leaf (**A**, **C**) and infected wheat leaf taken 3 days after inoculation (**B**, **D**). The arrows in A and B indicate the gap between the second and third cell layers. Scale bars represent 1 mm. The yellow contour in C and D are examples of manual segmentation. Scale bar represents 1 mm.

**Table 1** Mean thickness of the gaps from day 0 (right before inoculation) to day 7 (after inoculation) of control and *Septoria*-infected wheat leaves (One reading per plant, on three different controlled and three different infected plants)

| | Control | | | Infected | | |
|---|---|---|---|---|---|---|
| | R1 | R2 | R3 | R1 | R2 | R3 |
| Day 0 | 0.055 ± 0.018 | 0.046 ± 0.016 | 0.048 ± 0.017 | 0.045 ± 0.015 | 0.0463 ± 0.015 | 0.049 ± 0.017 |
| |  | | | 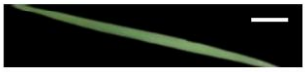 | | |
| Day 1 | 0.044 ± 0.015 | 0.038 ± 0.015 | 0.041 ± 0.014 | 0.05 ± 0.014 | 0.0543 ± 0.009 | 0.05 ± 0.015 |
| |  | | |  | | |
| Day 2 | 0.039 ± 0.014 | 0.041 ± 0.014 | 0.043 ± 0.016 | 0.051 ± 0.019 | 0.068 ± 0.026 | 0.067 ± 0.024 |
| |  | | |  | | |
| Day 3 | 0.039 ± 0.014 | 0.039 ± 0.013 | 0.042 ± 0.014 | 0.067 ± 0.024 | 0.075 ± 0.027 | 0.082 ± 0.028 |
| |  | | |  | | |
| Day 4 | 0.042 ± 0.015 | 0.049 ± 0.015 | 0.046 ± 0.013 | 0.076 ± 0.024 | 0.082 ± 0.03 | 0.073 ± 0.024 |
| |  | | |  | | |
| Day 5 | 0.049 ± 0.02 | 0.049 ± 0.02 | 0.054 ± 0.02 | 0.068 ± 0.03 | 0.069 ± 0.03 | 0.083 ± 0.03 |
| |  | | |  | | |
| Day 6 | 0.05 ± 0.017 | 0.047 ± 0.018 | 0.053 ± 0.02 | 0.082 ± 0.04 | 0.063 ± 0.024 | 0.067 ± 0.02 |
| |  | | |  | | |
| Day 7 | 0.044 ± 0.02 | 0.04 ± 0.017 | 0.046 ± 0.02 | 0.073 ± 0.024 | 0.083 ± 0.03 | 0.07 ± 0.024 |
| |  | | |  | | |

Every mean value is an average of 250 individual thickness measurements taken manually from a selection of 20 OCT B-scans out of each volumetric reading (C-scan). For each day, a single image of the leaf (out of the three available control and infected plants) is shown to appreciate the lack of external symptoms until day 7.

values, we could theoretically set a threshold value for the average gap's thickness of 0.05 mm, above which the leaf is classified as infected. If such was the case, effective assessment of infection could already be made from day 1 and affirmed from day 2 after inoculation.

To further benefit from OCT fast scanning rate and systematically processing large stacks of OCT images, a bespoke machine learning (ML)-based software for image segmentation was used instead of the manual labelling. The automated analysis is based on the same concept as the previous manual analysis: it aims to segment the apparent gap between the second and third cell layer and compute its averaged thickness. Example of the automated segmentation is shown in Fig. 6.

In comparison to the previous analysis, for each day and for each of the three OCT volumetric (C-scan) readings on control and infected plants, 200 images are selected (instead of 20 for the manual analysis) and analysed using the ML-based software. The computed average thickness of the segmented gap from each image is used to build the histograms shown in Fig. 7.

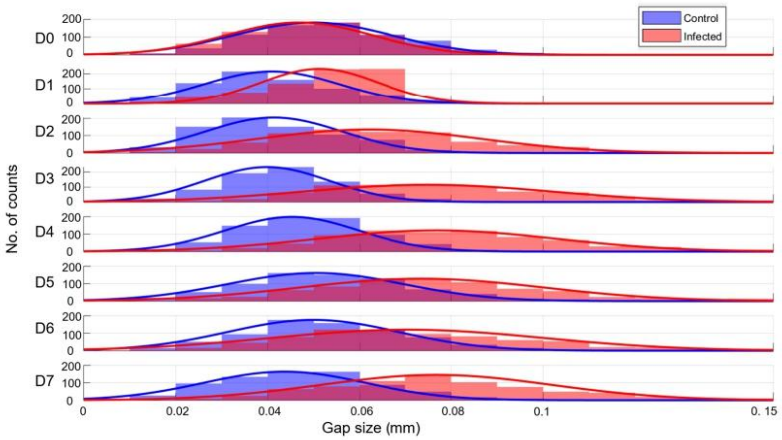


**Fig. 5** Gap size distribution for manual thickness measurements from day 0 (D0) to day 7 (D7). Superimposed histograms of control (blue) and infected leaves (red) groups with their Gaussian fits. The histograms used a bin width of 0.01 mm.

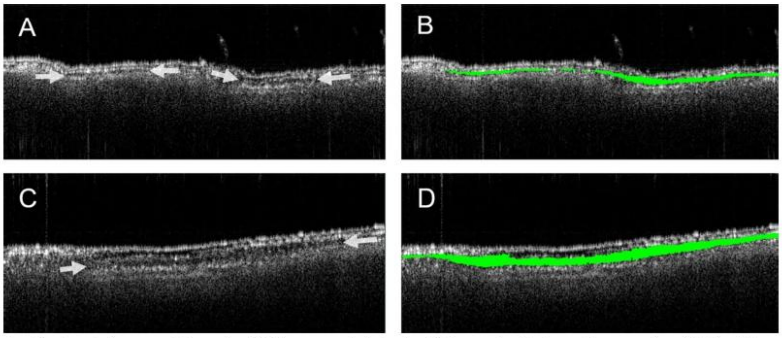


**Fig. 6** Examples of automated segmentation using OCT image analysis to classify the spacing between the second and third cell layers in a control wheat leaf (**A**) with its segmented area (**B**, green overlay), and an infected leaf (**C**) with its segmented are (**D**, green overlay), 2 days after inoculation.

The results from the ML-based image analysis appear more scattered compared to the previous manual analysis. This scattering might be a direct consequence in the apparent difficulty in adequately segmenting the OCT images, which is in part due to the uneven leaf structures, as discussed subsequently. Although histograms resulting from the automated segmentation analysis are not as consistent compared to those generated from the manual analysis, a similar pattern nonetheless emerges. Starting from day 1 after inoculation, the apparent gaps in infected leaves are statistically and consistently larger compared to those in intact leaves. And similarly, the widths of the Gaussian fits in infected leaves are also larger compared to those in controlled leaves.

It is also important to note that the ML-based segmentation software was here trained using the AxC 169 variety. The same automated procedure was used on images taken from another variety (AxC 157, same parentage but different genotype) and yielded, to a lesser extent, similar results (i.e. broader Gaussian fit and shifted Gaussian centre toward larger gap size for infected leaves, results shown in SI). One main difference between the two varieties is that intact leaves from cultivars AxC157 already have larger apparent gaps between the second and third

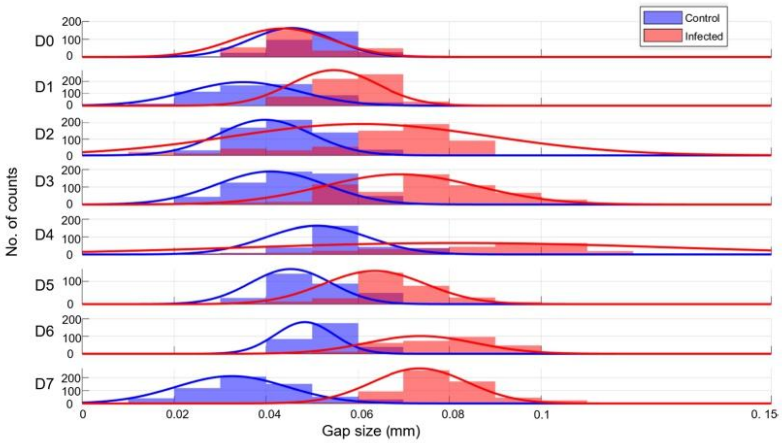


**Fig. 7** Average gap size distribution in control (blue) and infected (red) wheat leaves extracted from automated segmentation, from day 0 (D0) to day 7 (D7) after inoculation, with superimposed Gaussian fits. The histograms use a bin width of 0.01 mm

cell layers (of ~ 0.06 mm). Therefore, the distinction between infected and control became challenging when considering only the average gap size, as it will be discussed subsequently.

## Discussions

Our objective is to benefit from OCT ability to see through soft tissues to evaluate the state of infection over time. Although various features of the leaves were investigated, such as spacing between cell layers, cell appearances, number and length of trichomes, this study focuses on the former due to the absence of clear trend and difficulties to capture accurate data for the others. This study therefore solely reports on the average gap size within the mesophyll, with the aim of correlating the monitored changes with fungal growth. And while OCT cannot directly visualize fungal hyphae, this study reveals that the apparent spacing between cell layers increases where the fungal hyphae are expected to develop. Indeed, damaged tissues have a lower refractive index compared to healthy cells [71–73]. As a result, it is possible that the damaged tissues scatter less light compared to healthy ones and thus appear darker or dark (i.e. as a gap) on the OCT scans.

This increase in gap thickness and heterogeneity of the gap size is thus expected to be a direct result of the mesophyll colonisation by the hyphae (stage 4). As discussed earlier, colonisation of the mesophyll is initiated by the very first hyphae intrusion through a stoma (stage 3). The fact that we start monitoring an increase in gap thickness as early as 24 h after inoculation (instead of day 3, as per Fantozzi, E., et al. [26]) can be a result of our choice of cultivar. Indeed, AxC 169 was chosen because of its increased vulnerability to *Septoria*. It is also possible that inoculation via spray facilitates entry of the developing hyphae through the stomata. It has been shown that spore germination typically occurs within 12 h after contact with a leaf when humidity levels are high [30]. And while the presence of water droplets is not expected to trigger any direct reaction from the stomata, the overall increased humidity due to the spray implies that most stomata will be open [74], thus facilitating entry of the hyphae within the first few hours. It is important to note that our controls were only water sprayed, in accordance with previously published works, also on wheat, and similarly infected by *Septoria* [75–78]. The spraying of purified water was automatically performed within the chamber to preserve a humidity level of 61%. It is worth highlighting that both control and inoculated plants are regularly sprayed with purified water to maintain the high humidity level. Furthermore, the estimated concentration of Tween in the final spore-loaded solution is about 0.01%, which is significantly less compared to the 0.1% and 1% used in the previous works on wheat infected by *Septoria* in which water-sprayed controls were also used. While we do not expect such a low Tween concentration to trigger a systemic response, we do expect the colonisation by *Septoria* to trigger such a response. Because the response monitored (increase in gap size) seems to reach a maximum by day 2, as illustrated in Fig. 5, and

does not change until necrosis happens, we are confident that the effects measured are triggered by the pathogen rather than the surfactant or by the spraying procedure. It is, however, possible that upon the first intrusion event, before full colonisation takes place, the whole plant reacts by modifying its mesophyll structure, which might give rise to the increased in apparent gap thickness. If such is the case, this study still demonstrates that OCT can effectively be used to detect early signs of infection. This work thus demonstrated that monitoring intercellular spacing via OCT enables distinct classification between infected and intact plant from day 2 after inoculation, while visible signs of necrosis only appear on day 7.

In comparison to alternative non-invasive and similarly field-applicable methods, OCT has the advantage of being sensitive to changes that precede any discolouration or alteration of the plant's spectral signature. Indeed, the remote monitoring of the plant's pigmentation, fluorescence, temperature or water level often rely on multi- or hyperspectral data analysis [37, 38, 42]. It is difficult to directly compare our results with field applications of multi- and hyperspectral monitoring because the chosen variety is inherently more susceptible to *Spetoria*. The *Septoria* life cycle is consequently shorten compared to that in actual crops. But the fact that we can monitor infection-driven changes before any external signs appear demonstrates that detection via OCT precedes detection via multi- or hyperspectral techniques. As exemplified in Fig. 5 and 7, a distinction between infected and non-infected is monitored at least 5 to 6 days before the plant displays any yellow spots (shown in Table 1, day 7).

We concede that both methods, the manual labelling and the ML-aided labelling, are prone to biases. On the one hand, for example, manual labelling tends to focus on areas where a gap is clearly visible, thus neglecting sections of the mesophyll which may display a relatively smaller gap within the same B-scan. On the other hand, the automated segmentation is challenged with uneven leaf surfaces. The benefit of the ML-based analysis over the manual labelling is evidently its systematicity and its ability to analysed data at high throughput. Overall, whether manual or ML-based, the current analysis, with its unique distinguishing parameter, is already promising in differentiating between infected and intact plants.

We remind that our ML-based model was trained and tested on AxC 169. When the same model was applied to AxC 157, it led to more mitigated conclusions (see SI). Indeed, the fact that intact AxC 157 leaves already display gaps that are similar in size to those monitored in infected plants indicates that a single distinguishing parameter (i.e. gap thickness) might not be sufficient when assessing differing cultivars. To circumvent this limitation, it is planned to pursue such studies to include more parameters, such as to take into account the 3-dimentional shape of the gaps since it is readily available from the OCT volumetric C-scans. Additionally, we hope to improve training model by expanding our study to multiple wheat varieties. Furthermore, while the plants in our study were grown under controlled conditions, we acknowledge that field environments will introduce additional variability, such as fluctuating temperatures, humidity levels, soil composition, and pathogen exposure that cannot be fully replicated in a growth chamber. It is thus necessary to study the impact of these environmental factors onto the mesophyll to further evaluate OCT's field applicability. Nevertheless, the core physiological and structural responses observed in this work (e.g., mesophyll disruption detectable by OCT as early as two days after infection) are expected to manifest similarly in field-grown plants.

## Conclusions

In this proof-of-concept experiment, we demonstrate low-cost OCT to be ideally suited to monitor minute structural changes within the mesophyll. OCT is here used to effectively detect the increased intercellular spacing induced by the inoculation of pathogens. The monitored changes, taken as direct indication that the leaf is being colonized by the pathogen, demonstrate that OCT can be used to detect infections even before any visible signs appear on the plant. Systematic analysis of several thousands of images acquired, over time and non-invasively, is made possible by using bespoke ML-based analysis. And although the analysis currently relies on a single parameter (apparent gap thickness), statistical differences between controlled and infected leaves is established from day 2 after inoculation. Accordingly, OCT imaging holds the promise for quick and accurate identification of infection, even at an asymptomatic stage. The application of OCT coupled with ML analysis thus presents a valuable opportunity to effectively assess crop health. By harnessing and combining these cutting-edge technologies, this work contributes to advancing agricultural practices by providing with a tool that may enable timely treatments, help reduce crop losses, and achieve global food security.

This work also highlights current limitations of using OCT for detection of infection. OCT cannot directly visualize fungal hyphae, and its penetration depth may be insufficient for imaging thicker plant tissues. Furthermore, ML-based segmentation models require further validation to ensure it is applicable across different plant species and can distinguish between the various biotic and abiotic stressors. Despite these challenges, this research highlights the promise that OCT holds, when combined with ML analysis, as a non-destructive,

real-time imaging technique to transform precision agriculture and promote sustainable crop disease management.

## Future work

While the resolution of the OCT images is set by the system optoelectronic components, the current software used for image segmentation can be readily improved. The ML based analysis software was trained specifically on a single wheat variety (AxC 169). Future work will expand the dataset to include multiple wheat varieties and potentially correlate with other plant species to improve the robustness of the model. Further experimental runs are also required to disentangle the morphological responses triggered by environmental factors such as variability in temperature and in humidity, as well as variability in soil and atmospheric composition. Additionally, to differential between multiple stressors, it may become required to incorporate other measurables, such as gap density, gap volume and overall structural heterogeneity of the leaf. Including multiple parameters in the analysis could significantly advance the technique's precision. Given these necessary improvements, the path to make OCT an integral item in a farmer's toolbox is still long but is definitively underway.

## Supplementary Information

The online version contains supplementary material available at https://doi.org/10.1186/s13007-025-01411-7.

Supplementary File 1

**Acknowledgements**
The authors acknowledge support from BBSRS (BB/X005097/1) for pump-priming the project as well as NERC's (NE/X01827X/1) Cross-disciplinary research for Discovery Science for the acquisition of the Labscope OCT system, through the discipline hopping opportunity it provided. The ML-base analysis software was developed in collaboration with Cyber Infrastructure (http://www.cisin.com). The authors thank the Libyan Embassy-London/Academic attaché for their financial support.

**Authors contributions**
GS has acquire, analysed, interpretated the data, drafted the work and revised it. SM has made substantial contributions to the conception and design of the work, as well as to the interpretation of data. AC has made substantial contributions to the conception and design of the work, as well as to the analysis and interpretation of data, and has substantively revised it.

**Funding**
This research was supported by Biotechnology and Biological Sciences Research Council (BB/X005097/1,BB/X005097/1) and Natural Environment Research Council (NE/X01827X/1,NE/X01827X/1).

**Data availability**
Analysed data is provided within the manuscript or supplementary information files. The ML-base segmentation software is accessible via Google Drive: https://drive.google.com/drive/u/0/folders/1DJm3OZHfK-P-XSRXGMtpxg-Sx51WnVNsF The raw data (OCT B-scans of wheat leaves) is provided upon request.

## Declarations

**Competing interests**
The authors declare no competing interests.

Received: 19 May 2025 Accepted: 28 June 2025
Published online: 06 July 2025

**References**

1. Rastogi K. *Which countries produce the most wheat?* 2022 [cited 2021. https://www.visualcapitalist.com/cp/visualizing-global-wheat-production-by-country/.
2. Jaenisch BR, et al. Modulation of wheat yield components in response to management intensification to reduce yield gaps. Front Plant Sci. 2022;13:772232.
3. G, P. Wheat: Origin, Distribution and Importance | Agronomy. cited 2023. https://www.agricultureinindia.net/agronomy/wheat-cultivation/wheat-origin-distribution-and-importance-agronomy/11973#:~:text=Wheat%20is%20cultivated%20in%20about,Federation%2C%20Canada%2C%20Australia%20etc.
4. Shewry PR. Wheat. J Exp Bot. 2009;60(6):1537–53.
5. *Wheat*. 2024. cited 2024. https://www.agricentre.basf.co.uk/en/Crop-Solutions/Cereals/Wheat/.
6. Imports & exports: wheat & flour. cited 2022 Aug. https://www.ukflourmillers.org/importsexports.
7. Arvanitoyannis IS, Tserkezou P. 10—Cereal waste management: treatment methods and potential uses of treated waste. In: Arvanitoyannis IS, editor. Waste management for the food industries. Amsterdam: Academic Press; 2008. p. 629–702.
8. Hansen M, et al. Enzyme affinity to cell types in wheat straw (*Triticum æstivum* L.) before and after hydrothermal pretreatment. Biotechnol Biofuels. 2013;6:54.
9. Bishaw Z, et al. Political economy of the wheat sector in Turkey: seed systems, varietal adoption, and impacts. 2021.
10. Overend A. Shifting food facts: dietary discourse in a post-truth culture. 2020.
11. Goodwin SB. Instant Insights Septoria tritici blotch in cereals. Disease affecting wheat: Septoria tritici blotch. Burleigh Dodds Science Publishing Limited; 2019, p. 158.
12. Nizolli VO, et al. Wheat blast: the last enemy of hunger fighters. Genet Mol Biol. 2023;46:e20220002.
13. Darino M, et al. Identification and functional characterisation of a locus for target site integration in *Fusarium graminearum*. Fungal Biol Biotechnol. 2024;11(1):2.
14. Figueroa M, Hammond-Kosack KE, Solomon PS. A review of wheat diseases-a field perspective. Mol Plant Pathol. 2018;19(6):1523–36.
15. Impey L. Guide to tackling septoria disease in wheat. 2021 [cited 2022. https://www.fwi.co.uk/arable/crop-management/disease-management/a-guide-to-tackling-septoria-in-wheat.
16. Septoria tritici in winter wheat. 2024 [cited 2024]. https://ahdb.org.uk/knowledge-library/septoria-tritici-in-winter-wheat.
17. Septoria tritici in wheat. cited 2024. https://cropscience.bayer.co.uk/agronomy-id/diseases/wheat-diseases/septoria-tritici-in-wheat.
18. Zubrod JP, et al. Fungicides: an overlooked pesticide class? Environ Sci Technol. 2019;53(7):3347–65.
19. Sisson A. Fungicide use in field crops web book. The Crop Protection Network (CPN)
20. Fungicide efficacy for control of wheat diseases. 2024.
21. Cook, Hims, and Vaughan. Effects of fungicide spray timing on winter wheat disease control. Plant Pathol 2002; 48: 33–50.
22. Jacquet F, et al. Pesticide-free agriculture as a new paradigm for research. Agron Sustain Dev. 2022;42:8.
23. Verkley GJM, et al. A new approach to species delimitation in Septoria. Stud Mycol. 2013;75(1):213–305.
24. Gohari A. Identification and functional characterization of putative (a) virulence factors in the fungal wheat pathogen Zymoseptoria tritici. 2015.
25. Das S, Pattanayak S. Over view of septoria diseases on different crops and its management. Int J Agric Environ Biotechnol. 2020;13:351–70.

26. Fantozzi E, et al. Asynchronous development of Zymoseptoria tritici infection in wheat. Fungal Genet Biol. 2021;146: 103504.
27. Quaedvlieg W, et al. *Zymoseptoria* gen. nov.: a new genus to accommodate Septoria-like species occurring on graminicolous hosts. Persoonia. 2011;26:57–69.
28. Toropova EY, Kazakova OA, Piskarev VV. Septoria blotch epidemic process on spring wheat varieties. Vavilovskii zhurnal genetiki i selektsii. 2020;24(2):139–48.
29. Chaudhary R, Pujari M. *Major diseases of wheat and their management: a review.* Plant Arch 2021; 21.
30. Mirzadi Gohari A, et al. Effector discovery in the fungal wheat pathogen Zymoseptoria tritici. Mol Plant Pathol. 2015;16(9):931–45.
31. Yang S, Rothman RE. PCR-based diagnostics for infectious diseases: uses, limitations, and future applications in acute-care settings. Lancet Infect Dis. 2004;4(6):337–48.
32. Pinhero A, et al. Malware detection employed by visualization and deep neural network. Comput Secur. 2021;105: 102247.
33. Kior A, et al. RGB imaging as a tool for remote sensing of characteristics of terrestrial plants: a review. Plants. 2024;13(9):1262.
34. Mathieu L, et al. SeptoSympto: a precise image analysis of Septoria tritici blotch disease symptoms using deep learning methods on scanned images. Plant Methods. 2024;20(1):18.
35. Yu K, et al. Hyperspectral canopy sensing of wheat septoria tritici blotch disease. Front Plant Sci. 2018;9:1195.
36. Anderegg J, et al. In-Field detection and quantification of Septoria tritici blotch in diverse wheat germplasm using spectral-temporal features. Front Plant Sci. 2019;10:1355.
37. Giakoumoglou N, et al. Early detection of Botrytis cinerea symptoms using deep learning multi-spectral image segmentation. Smart Agric Technol. 2024;8: 100481.
38. García-Vera YE, et al. Hyperspectral image analysis and machine learning techniques for crop disease detection and identification: a review. Sustainability. 2024;16(14):6064.
39. Park B, et al. Chlorophyll fluorescence imaging for environmental stress diagnosis in crops. Sensors. 2024;24(5):1442.
40. Zhang K, Yan F, Liu P. The application of hyperspectral imaging for wheat biotic and abiotic stress analysis: a review. Comput Electron Agric. 2024;221: 109008.
41. Mahlein AK. Plant disease detection by imaging sensors—parallels and specific demands for precision agriculture and plant phenotyping. Plant Dis. 2016;100(2):241–51.
42. Ghazal S, Munir A, Qureshi WS. Computer vision in smart agriculture and precision farming: techniques and applications. Artif Intell Agric. 2024;13:64–83.
43. Fercher A. Optical coherence tomography-development, principles, applications. Z Med Phys. 2010;20:251–76.
44. Sasi GS, Chauvet AAP. Using optical coherence tomography in plant biology research: review and prospects. Sensors (Basel). 2025;25(8):2467.
45. Saleah SA, et al. Optical coherence tomography as a non-invasive tool for plant material characterization in agriculture: a review. Sensors. 2024;24(1):219.
46. He J, et al. Technological advances on imaging and modelling of leaf structural traits: a review on heat stress in wheat. J Exp Bot 2025.
47. Banerjee A, et al. Multimodal RGB and optical coherence tomography imaging for enhanced machine learning classification of crop diseases and stress phenotyping. Instrum Sci Technol 2025: 1–24.
48. Wijesinghe RE, et al. Biophotonic approach for the characterization of initial bitter-rot progression on apple specimens using optical coherence tomography assessments. Sci Rep. 2018;8(1):15816.
49. Wijesinghe R, et al. Optical coherence tomography-integrated, wearable (backpack-type), compact diagnostic imaging modality for in situ leaf quality assessment. Appl Opt. 2017;56:D108.
50. Larimer CJ, et al. Optical coherence tomography imaging of plant root growth in soil. Appl Opt. 2020;59(8):2474–81.
51. Williams J, et al. Translating optical coherence tomography technologies from clinical studies to botany: real time imaging of long-distance signaling in plants. Washington DC: White Rose Research Online; 2020.
52. de Boer JF, Hitzenberger CK, Yasuno Y. Polarization sensitive optical coherence tomography—a review [Invited]. Biomed Opt Express. 2017;8(3):1838–73.
53. Morgner U, et al. Spectroscopic optical coherence tomography. Opt Lett. 2000;25(2):111–3.
54. Oldenburg A, Xu C, Boppart S. Spectroscopic optical coherence tomography and microscopy. IEEE J Select Top Quantum 2007.
55. Azzollini S, et al. Dynamic optical coherence tomography for cell analysis [Invited]. Biomed Opt Express. 2023;14:3362–79.
56. de Wit J, et al. Revealing real-time 3D in vivo pathogen dynamics in plants by label-free optical coherence tomography. Nat Commun. 2024;15(1):8353.
57. Gong P, et al. Parametric imaging of attenuation by optical coherence tomography: review of models, methods, and clinical translation. J Biomed Opt. 2020;25(4):1–34.
58. Hope J, Goodwin M, Vanholsbeeck F. Inverse spectroscopic optical coherence tomography (ISOCT) for characterization of particle size and concentration. 2021.
59. Barrington N. Affordable Optical Coherence Tomography (OCT) Imaging System provides high resolution imaging. Features axial resolutions of 5µm and lateral resolutions of 15µm 2017. cited 2025. https://www.edmundoptics.com/company/press-releases/products/affordable-optical-coherence-tomography-oct-imaging-system-provides-high-resolution-imaging/.
60. Ganymede™ Series SD-OCT Systems. cited 2025. https://www.thorlabs.com/newgrouppage9.cfm?objectgroup_id=8214.
61. Zitter TA. Septoria Leaf Spot. APS 1992. cited 2024. https://www.apsnet.org/edcenter/apsnetfeatures/Pages/SeptoriaLeafSpot.aspx.
62. Steinberg G. Cell biology of Zymoseptoria tritici: pathogen cell organization and wheat infection. Fungal Genet Biol. 2015;79:17–23.
63. Haueisen J, et al. Highly flexible infection programs in a specialized wheat pathogen. Ecol Evol. 2018;9:275–94.
64. Shriram S, Ramamurthy K, Ramakrishnan S. Effect of occupant-induced indoor CO2 concentration and bioeffluents on human physiology using a spirometric test. Build Environ. 2018;149:58–67.
65. Zain M, et al. Influence of growth medium on diagnostic characters of Aspergillus and Penicillium species. Afr J Microbiol Res. 2009;3:280–6.
66. Growth stages. cited 2024; www.wheat-training.com.
67. Gupta S, Saxena A. Experimental comparison: methods for the preservation of fungal cultures. Curr Res Environ Appl Mycol. 2019;9:208–12.
68. Halahlaha A, et al. Chapter 14—Techniques for internal and surface structure characterisation of food powders. In Bhandari B, et al., editors. Handbook of food powders (second edition). Woodhead Publishing; 2024. p. 219–248.
69. Salouti M, Derakhshan FK. Chapter 3—Phytosynthesis of nanoscale materials. In: Ghorbanpour M, Wani SH, editors. Advances in phytonanotechnology. Cambridge: Academic Press; 2019. p. 45–121.
70. Lundgren MR, et al. Mesophyll porosity is modulated by the presence of functional stomata. Nat Commun. 2019;10(1):2825.
71. Fones H, Gurr S. The impact of Septoria tritici Blotch disease on wheat: an EU perspective. Fungal Genet Biol. 2015;79:3–7.
72. Sankaran S, et al. A review of advanced techniques for detecting plant diseases. Comput Electron Agric. 2010;72(1):1–13.
73. Cairós C, et al. Refractive index estimation in biological tissues by quantitative phase imaging. Opt Mater. 2023;142: 114087.
74. Pantin F, Blatt MR. Stomatal response to humidity: blurring the boundary between active and passive movement. Plant Physiol. 2018;176(1):485–8.
75. Odilbekov F, et al. Proximal phenotyping and machine learning methods to identify Septoria tritici blotch disease symptoms in wheat. Front Plant Sci. 2018;9:685.
76. Yang F, et al. Battle through signaling between wheat and the fungal pathogen Septoria tritici revealed by proteomics and phosphoproteomics. Mol Cell Proteomics. 2013;12(9):2497–508.
77. Cerón-Bustamante M, et al. Effect of different light wavelengths on Zymoseptoria tritici development and leaf colonization in bread wheat. J Fungi (Basel). 2023;9(6):670.
78. Yang F, et al. Unraveling incompatibility between wheat and the fungal pathogen Zymoseptoria tritici through apoplastic proteomics. BMC Genom. 2015;16(1):362.


## Publisher's Note